

12415

# RESULTS OF THE TEAR GAS FATE AND EFFECTS STUDY

Volume II of II



*Prepared for*  
**U.S. ARMY ENVIRONMENTAL CENTER**  
**Pollution Prevention and Environmental Technology Division**  
***Aberdeen Proving Ground, Maryland 21010-5401***

**DISTRIBUTION STATEMENT A**  
Approved for Public Release  
Distribution Unlimited

*Prepared by*  
**Tennessee Valley Authority**  
**Environmental Research Center**  
***Muscle Shoals, Alabama 35662-1010***

**June 1999**

**TVA Contract No. RG-99802V**  
**Report No. SFIM-AEC-ET-CR-98027**

**Results of the  
Tear Gas Fate and Effects Study**

**Volume II of II**

*Prepared for*

**U.S. Army Environmental Center  
Pollution Prevention and Environmental Technology Division  
Aberdeen Proving Ground, Maryland 21010-5401  
POC: A. J. Walker**

*Prepared by*

**Tennessee Valley Authority  
Tennessee Valley Authority Resource Management  
Environmental Research Center  
Muscle Shoals, Alabama 35662-1010**

**June 1999**

**20030221 160**



REPORT DOCUMENTATION PAGE				Form Approved OMB No. 0704-0188	
1a. REPORT SECURITY CLASSIFICATION <b>Unclassified</b>			1b. RESTRICTIVE MARKINGS		
2a. SECURITY CLASSIFICATION AUTHORITY			3. DISTRIBUTION/AVAILABILITY OF REPORT  <b>Unlimited</b>		
2b. DECLASSIFICATION/DOWNGRADING SCHEDULE					
4. PERFORMING ORGANIZATION REPORT NUMBER(S)			5. MONITORING ORGANIZATION REPORT NUMBER(S) <b>SFIM-AEC-ET-CR-98027</b>		
6a. NAME OF PERFORMING ORGANIZATION  <b>Tennessee Valley Authority</b>		6b. OFFICE SYMBOL <i>(if applicable)</i> <b>CEB 4C-M</b>		7a. NAME OF MONITORING ORGANIZATION  <b>U.S. Army Environmental Center Pollution Prevention and Environmental Technology Division</b>	
6c. ADDRESS (City, State, and ZIP Code) <b>TVA Reservation Post Office Box 1010 Muscle Shoals, Alabama 35662-1010</b>			7b. ADDRESS (City, State, and Zip Code) <b>USAEC Attn: SFIM-AEC-ETD Aberdeen Proving Ground, MD 21010-5401</b>		
8a. NAME OF FUNDING /SPONSORING ORGANIZATION  <b>U.S. Army Environmental Center</b>		8b. OFFICE SYMBOL <i>(if applicable)</i> <b>SFIM-AEC-ETD</b>		9. PROCUREMENT INSTRUMENT IDENTIFICATION NUMBER  <b>TVA Contract No. RG-99802V</b>	
8c. ADDRESS (City, State, and ZIP Code)			10. SOURCE OF FUNDING NUMBERS		
			PROGRAM. ELEMENT NO	PROJECT NO.	TASK NO.
			WORK UNIT ACCESSION NO.		
11. TITLE (Include Security Classification) <b>Results of the Tear Gas Fate and Effects Study</b>					
12. PERSONAL AUTHOR(S) <b>M. F. Broder, M. J. Beck, J. M. Boggs, R. A. Almond, J. J. Hoagland, H. Julian, D. A. Kelly, W. J. Rogers, and A. J. Walker</b>					
13a. TYPE OF REPORT <b>Final</b>		13b. TIME COVERED FROM <b>_/_/</b> TO <b>_/_/</b>		14. DATE OF REPORT (Year, Month, Day) <b>1999, June</b>	
15. PAGE COUNT					
16. SUPPLEMENTARY NOTATION					
17. COSATI CODES			18. SUBJECT TERMS (Continue on reverse if necessary and identify by block number) <b>Fate, transport, and effects of CNS Tear gas in contaminated soils.</b>		
FIELD	GROUP	SUB-GROUP			
19. ABSTRACT (Continue on reverse if necessary and identify by block number) <b>This document describes the results of a study examining the environmental processes which effect of CNS tear gas and fate of the tear gas as it moves through soil. The study examines both the general properties of CNS tear gas as well as how these properties effected a CNS burial site at the Federal Laboratories No. 3 Plant near Saltsburg, Pennsylvania. The report also provides specific recommendations for remediating the Saltsburg site.</b>					
20. DISTRIBUTION/AVAILABILITY OF ABSTRACT <input checked="" type="checkbox"/> UNCLASSIFIED/UNLIMI <input type="checkbox"/> SAME AS RPT <input type="checkbox"/> DTIC USERS <b>TED</b>				21. ABSTRACT SECURITY CLASSIFICATION <b>Unclassified</b>	
22a. NAME OF RESPONSIBLE INDIVIDUAL  <b>A. J. Walker</b>			22b. TELEPHONE (Include Area Code) <b>(410) 612-6863</b>		22c. OFFICE SYMBOL  <b>SFIM-AEC-ETD</b>

**TABLE OF CONTENTS**  
**(Volume II Only)**

<b>SECTION</b>	<b>TITLE</b>	<b>PAGE NUMBER</b>
<b>Volume II</b>		
D	RAPID DETECTION OF CNS TEAR GAS COMPONENTS USING DSITMS	
D-1	DSITMS FINAL REPORT	
D-2	DSITMS METHOD SUMMARY	
E	BOREHOLE FLOWMETER TESTS	
F	SIMULATION OF NATURAL RESTORATION	
G	REMEDIATION STRATEGY SELECTION	
H	INJECTION AND RECOVERY SYSTEM DESIGN	

## ABBREVIATIONS

C	Carbon
°C	Degrees Centigrade
<sup>14</sup> C	Carbon 14
CaCl <sub>2</sub>	Calcium Chloride
μCi	
Cl <sup>-</sup>	Chloride
cm/s	Centimeters per Second
CN	Phenacyl Chloride
CNS	The term CNS tear gas refers to the military version of tear gas with a composition of 24% phenacyl chloride, 38% chloropicrin, and 38% chloroform by weight. The origin of the abbreviation CNS could not be determined but is thought to stand for the mixture of the two active ingredients phenacyl chloride (CN) and chloropicrin (PS) with the symbols combined. It is believed that the symbol for chloroform is not present because this component is not an active component and is present only to promote volatility.
CO <sub>2</sub>	Carbon Dioxide
CS	O-Chlorbenzylidene Malononitrile
CWS	Army's Chemical Warfare Service
DoD	Department of Defense
DNAPL	Dense Non-Aqueous Phase Liquids
DSITMS	Direct Sampling Ion Trap Mass Spectrometry
EPA	Environmental Protection Agency
ERC	Environmental Research Center
°F	Degrees Fahrenheit
FTE	Fate, Transport, and Effects
g	grams
μg	Microgram
g/cm <sup>3</sup>	Grams per Cubic Centimeter
μg/L	Microgram per Liter
GC	Gas Chromatography
GC/MS	Gas Chromatography - Mass Spectrometry
°K	Degrees Kelvin
kPa	Kilopascal
L	Liter
μL	Microliter
lb.	Pounds
M	Molar
M <sup>2</sup> /day	Meters Squared per Day
μL	Micrometer
MDL	Method Detection Limit
mg	Milligram
mg/Kg	Milligrams per Kilogram

ABBREVIATIONS (Continued)

mg/L	Milligrams per Liter
ml	Milliliters
mm	Millimeter
mM	Millimole
NaOH	Sodium Hydroxide
NO <sub>3</sub> <sup>-</sup>	Nitrate
ORNL	Oak Ridge National Laboratory
ppb	Parts Per Billion
PETG	Polyethylene Terephthalate
QA	Quality Assurance
QC	Quality Control
rpm	Revolutions per Minute
TOC	Total Organic Carbon
TVA	Tennessee Valley Authority
SL	Specialty Laboratory
SVE	Soil Vapor Extraction
UL	Uniformly Labeled
U.S.	United States
USAEC	United States Army Environmental Center
USEPA	United States Environmental Protection Agency
VOA	Volatile Organic Analysis
VOC	Volatile Organic Compounds

**APPENDIX D**  
**RAPID DETECTION OF CNS TEAR GAS COMPONENTS USING DSITMS**

**APPENDIX D-1**  
**DSITMS FINAL REPORT**

**Analysis of Water and Soil for the Presence of Chloropicrin, Chloroform,  
2-Chloroacetophenone and 3-Chloroacetophenone by  
Direct Sampling Ion Trap Mass Spectrometry**

Roosevelt Merriweather, Marcus Wise, and Michael Guerin  
Chemical and Analytical Sciences Division

Oak Ridge National Laboratory  
P.O. Box 2008  
4500-S, MS-6120  
Oak Ridge, Tennessee 37831-6120

**Final Report**

Prepared for Submission to:

The Tennessee Valley Authority  
Muscle Shoals, Alabama

Revised  
September 11, 1998

## Contents

	<u>Page</u>
Table of Contents.....	i
List of Tables.....	iv
List of Figures.....	v
Executive Summary.....	1
Introduction.....	3
Background.....	4
General Description of DSITMS.....	4
Applications and Instrument Cost.....	6
Instrumentation.....	7
Direct Sampling Inlet System.....	7
Analytical Methods Development.....	9
Purpose.....	9
Apparatus: Ion Trap Mass Spectrometers.....	9
Reagents and Solutions.....	10
External Standard Calibration Solutions.....	10
Internal Standard Solutions.....	11
Basic Procedure for the Analysis of 40-ml Samples.....	11
Sparging Module for 40-ml Samples of Water and Soil.....	11
Monitoring of Purge Flow Rate and Sample Temperature.....	12
Tuning of the Ion Trap Mass Spectrometer.....	12
General Operating Conditions of the Ion Trap MS.....	13



## Contents (continued)

	<u>Page</u>
Quantitation of Targeted Analytes.....	14
Analysis of Blank Water Samples.....	15
Generation of External Standard Calibration Curves.....	16
Analysis of Unknown Samples.....	17
Analysis of Soil Samples.....	17
In-Situ Sparge Procedure for Analysis of Groundwater in Wells.....	18
In-Situ Sparge Probe for Groundwater Analysis.....	18
Monitoring of Purge Flow Rate and Sampling Rate.....	19
Tuning of the Ion Trap Mass Spectrometer.....	19
General Operating Conditions of the Ion Trap MS.....	19
Quantitation of Targeted Analytes.....	20
Analysis of Blank Water Samples.....	20
Generation of External Standard Calibration Curves.....	21
Analysis of Unknown Samples.....	21
Results and Discussion.....	22
Mass Spectra.....	22
2-Chloroacetophenone and 3-Chloroacetophenone.....	23
Chloropicrin.....	25
Chloroform.....	27
Composite Mass Spectrum.....	28

## Contents (continued)

	<u>Page</u>
Results for 40-ml Sparge Analysis of Water Samples.....	28
Chloropicrin.....	28
Chloroform.....	29
2-Chloroacetophenone and 3-Chloroacetophenone.....	30
Ambient Temperature Purge From Water at 25°C....	31
Heated Purge from Water at 60°C.....	32
Results for 40-ml Sparge Analysis of Soil Samples.....	33
Chloroform and Chloropicrin.....	33
2-Chloroacetophenone and 3-Chloroacetophenone.....	33
Effect of Water on Purgability.....	34
Results for In-Situ Sparge of Groundwater Samples.....	35
Chloropicrin.....	35
Chloroform.....	35
2-Chloroacetophenone and 3-chloroacetophenone.....	35
Analysis of Field Samples From the Federal Laboratories Site.....	36
Performance Data.....	37
Detection Limits.....	37
Precision and Accuracy.....	38
Analysis of Performance Samples for Water.....	38
Analysis of Performance Samples for Soil.....	39
In-situ Sparge Performance.....	39

## Contents (continued)

	<u>Page</u>
Conclusion.....	40
References.....	41

## List of Tables

	<u>Page</u>
Table 1: Water and Soil Samples From the Federal Laboratories Site (DSITMS Results).....	42
Table 2: Precision Results for Chloropicrin and Chloroform in Water.....	43
Table 3a: Accuracy (% recovery) Results for Chloropicrin and Chloroform in Blind QC Water Samples.....	44
Table 3b: Recovery Results for Chloropicrin and Chloroform in Soil Samples Spiked at Know Concentrations.....	44

## List of Figures

	<u>Page</u>
Figure 1: Schematic Diagram of DSITMS.....	45
Figure 2: Capillary Restrictor Interface and Sample Splitter.....	46
Figure 3: Example DSITMS Sample Inlets.....	47
Figure 4: Photograph of a DSITMS Instrument.....	48
Figure 5: 40-ml VOA Vial Sparging Module.....	49
Figure 6: Example Purge Profiles for VOCs in Water.....	50
Figure 7: In-Situ Sparging Probe for VOCs in Groundwater Wells.....	51

## List of Figures (continued)

	<u>Page</u>
Figure 8: Response Profiles for In-Situ Sparge of Chloropicrin in Water...	52
Figure 9: In-Situ Sparge Profiles for Chloroform and Chloropicrin .....	53
Figure 10: EI Mass Spectrum of 3-Chloroacetophenone.....	54
Figure 11: EI Mass Spectrum of 2-Chloroacetophenone.....	55
Figure 12: EI Mass Spectrum of Chloropicrin.....	56
Figure 13: EI Mass Spectrum of Chloroform.....	57
Figure 14: Composite EI Mass Spectrum of Chloroform, Chloropicrin, 2-Chloroacetophenone, and 3-Chloroacetophenone.....	58
Figure 15: Calibration Curve for Chloropicrin in Water: 40-ml VOA Vial Sparge at Ambient Temperature (5-100 ppb).....	59
Figure 16: Calibration Curve for Chloropicrin in Water: 40-ml VOA Vial Sparge at Ambient Temperature (100-8,000 ppb).....	60
Figure 17: Calibration Curve for Chloroform in Water: 40-ml VOA Vial Sparge at Ambient Temperature (5-500 ppb).....	61
Figure 18: Purge Profile for 100 ppb of 2-Chloroacetophenone in Water: 40-ml VOA Vial Sparge at Ambient Temperature.....	62
Figure 19: Purge Profile for 100 ppb of 3-Chloroacetophenone in Water: 40-ml VOA Vial Sparge at Ambient Temperature.....	63
Figure 20: Calibration Curve for 2-Chloroacetophenone in Water: 40-ml VOA Vial Sparge at Ambient Temperature (100-1,000 ppb)...	64
Figure 21: Calibration Curve for 3-Chloroacetophenone in Water: 40-ml VOA Vial Sparge at Ambient Temperature (10-500 ppb).....	65
Figure 22: Purge Profile for 100 ppb of 2-Chloroacetophenone in Water: 40-ml VOA Vial Sparge at 60°C.....	66
Figure 23: Purge Profile for 100 ppb of 3-Chloroacetophenone in Water: 40-ml VOA Vial Sparge at 60°C.....	67

## List of Figures (continued)

	<u>Page</u>
Figure 24: Calibration Curve for 2-Chloroacetophenone in Water: 40-ml VOA Vial Sparge at 60°C (5-1,000 ppb).....	68
Figure 25: Calibration Curve for 3-Chloroacetophenone in Water: 40-ml VOA Vial Sparge at 60°C (5-1,000 ppb).....	69
Figure 26: Purge Profile for 100 ppb of 2-Chloroacetophenone in Soil: 40-ml VOA Vial Sparge of Slurry at 60°C.....	70
Figure 27: Purge Profile for 100 ppb of 3-Chloroacetophenone in Soil: 40-ml VOA Vial Sparge of Slurry at 60°C.....	71
Figure 28: Calibration Curve for 2-Chloroacetophenone in Soil: 40-ml VOA Vial Sparge of Slurry at 60°C (250-1,000 ppb).....	72
Figure 29: Calibration Curve for 3-Chloroacetophenone in Soil: 40-ml VOA Vial Sparge of Slurry at 60°C (10-1,000 ppb).....	73
Figure 30: Purge Profile for 4 µg of 2-Chloroacetophenone in a 40-ml VOA Vial: Headspace Purge at Ambient Temperature.....	74
Figure 31: Purge Profile for 4 µg of 3-Chloroacetophenone in a 40-ml VOA Vial: Headspace Purge at Ambient Temperature.....	75
Figure 32: EI Mass Spectrum of Chloroform and Chloropicrin in Water Using the In-Situ Sparging Probe.....	76
Figure 33: Calibration Curve for Chloropicrin in Water: In-Situ Sparge at Ambient Temperature (5-500 ppb).....	77
Figure 34: Calibration Curve for Chloroform in Water: In-Situ Sparge at Ambient Temperature (5-500 ppb).....	78

# **Analysis of Water and Soil for the Presence of Chloropicrin, Chloroform, 2-Chloroacetophenone, and 3-Chloroacetophenone by Direct Sampling Ion Trap Mass Spectrometry**

## **Executive Summary**

A fast, cost-effective method has been developed at the Oak Ridge National Laboratory for the screening of groundwater and soil samples for the major components of CNS tear gas, including chloroform, chloropicrin, and 2-chloroacetophenone (phenacyl chloride) using Direct Sampling Ion Trap Mass Spectrometry (DSITMS). This method was also extended to 3-chloroacetophenone due to its possible presence as a contaminant in very old CNS tear gas. This method involves either the direct purge of discrete 40-ml samples of water or soil or the direct (in-situ) analysis of water samples in groundwater wells using a specially designed sampling probe.

Compounds that are purged from a water or soil sample are transported through a fixed-ratio splitter arrangement into a deactivated micro-bore fused-silica capillary restrictor that permits a small amount of the sample to directly enter the ion trap mass spectrometer. Analytes that are present in the ion trap can be ionized either by electron ionization (EI) or by chemical ionization (CI) if they have a sufficiently high proton affinity.

A major advantage of DSITMS methods is that they involve little or no sample preparation and the analytes are detected in real-time. The primary disadvantage is that no chromatographic separation of the individual components is performed prior to their injection into the ion trap. This can result in interferences (peak overlap) in complex samples or ambiguity in compound identification if the mass spectra of two or more analytes in a sample are very similar.

In most cases, DSITMS permit samples can be analyzed in less than 3 minutes with compound detection limits in the low part-per-billion range. Although the DSITMS method works very well for the quantitative analysis of chloroform and chloropicrin in water and soil, it has been determined that both 2-chloroacetophenone and 3-chloroacetophenone interact strongly with water and soil. As a result, these compounds are difficult to purge from either water or soil, even at elevated

temperatures. In practice, this means that it is not possible to accurately quantitate either 2-chloroacetophenone or 3-chloroacetophenone by DSITMS purge techniques using an analysis time of less than 15 minutes. Furthermore, the performance of both 2-chloroacetophenone and 3-chloroacetophenone is also negatively affected by interaction of these compounds with the deactivated fused silica surfaces in the sample interface and in the sample transfer line that is used for in-situ sampling. This surface interaction causes a significant lag time (from the start of an analysis cycle) in observing a stable signal for the chloroacetophenones and can also result in unacceptable levels of analyte carryover from one sample to the next. In fact, this interaction is so severe with the in-situ sampler transfer line that neither of the chloroacetophenone compounds can be practically measured by that technique.

In spite of the difficulties in the rapid *quantitative analysis* of both 2-chloroacetophenone and 3-chloroacetophenone, each of these compounds does produce a *measurable* signal at low to mid part-per-billion concentration levels within a 3 minute analysis time using the technique for the analysis of 40-ml discrete samples. From a qualitative standpoint, observation of the chloroacetophenones (especially 2-chloroacetophenone) in a sample concurrently with chloroform and chloropicrin is strong evidence for the presence of CNS tear gas.

At the Federal Laboratories site in Saltsburg, PA, where the DSITMS method was to be used, the primary groundwater contaminants are chloroform and chloropicrin. At this particular site, DSITMS should be useful as a technique for generating rapid field analytical data to map the concentration gradient of the tear gas plume in the groundwater. The speed of the method would enable results to be generated onsite to guide sampling strategy and monitoring well placement.

# **Analysis of Water and Soil for the Presence of Chloropicrin, Chloroform, 2-Chloroacetophenone, and 3-Chloroacetophenone by Direct Sampling Ion Trap Mass Spectrometry**

## **Introduction**

Chloropicrin, chloroform, and 2-chloroacetophenone (phenacyl chloride) are the primary components of a form of tear gas (CNS) that was buried at the Federal Laboratories site located in Saltsburg, PA. Over the years, leakage of storage containers resulted in seepage of the tear gas components into the soil and groundwater. Once in the groundwater, the tear gas components (particularly chloroform and chloropicrin) migrated onto adjacent property and into nearby surface waters down-gradient from the original burial site.

Under the direction of the U.S. Army Environmental Center (AEC), Oak Ridge National Laboratory was requested to participate in a remedial investigation of the Federal Laboratories site by demonstrating an innovative technology, Direct Sampling Ion Trap Mass Spectrometry (DSITMS), for the rapid analysis of CNS tear gas components in water and soil. In the past, AEC has provided much of the support for the development of DSITMS and has continually supported field demonstrations and deployments of the technology for numerous applications at different sites across the United States. However, because the Federal Laboratories site investigation (fate and transport study) was actually being conducted by the Tennessee Valley Authority (TVA), work on this project by ORNL was performed under contract to TVA.

The purpose of this project was to perform a laboratory evaluation of DSITMS as a technique for the rapid analysis of chloropicrin, chloroform, 2-chloroacetophenone, and 3-chloroacetophenone in water and soil. Methods to be investigated included direct purge of discrete 40-ml samples of water or soil slurries and in-situ sparge analysis of water in groundwater wells.

At the beginning of this project, a couple of representative samples of soil and water were collected by TVA personnel at the Federal Laboratories site and provided to ORNL to aid in the development and optimization of the DSITMS analytical procedures. Analytical figures of merit that were to be determined as part of this effort included



detection limits, linearity, reproducibility, and possible interferences from other chemicals that might be present at the Federal Laboratories site. Additionally, blind performance samples were to be analyzed to verify the quantitative capabilities of the technique.

In the event that the results of the laboratory-based methods development work were satisfactory, a second phase of this project was planned in which DSITMS would be demonstrated in the field at the Federal Laboratories site in Saltsburg, PA. The plan for the field work was to perform onsite analysis of groundwater in existing monitoring wells, analysis of surface water collected from nearby streams, and depth profile analysis (analyte concentration vs. depth) in one or two deep monitoring wells that were to be installed at the site.

As the result of project redirection, TVA decided not to conduct the field analysis portion of the DSITMS project. Under the suggestion of AEC, the commercial analytical laboratory that is responsible for the analysis of samples at the Federal Laboratories site was contacted to determine if they were interested in employing DSITMS for some of their analytical work. However, they did not express any interest in using any analytical technique, including DSITMS, that was outside of their standard analytical procedures.

## **BACKGROUND**

### *General Description of DSITMS*

Direct Sampling Ion Trap Mass Spectrometry (DSITMS) (1,2) is defined as the technique of introducing the components of a sample directly into an ion trap mass spectrometer by means of a simple capillary restrictor interface (**Figure 1**). Very little, if any, sample preparation is required and no chromatographic separation of the constituents in a sample is performed prior to their introduction into the ion trap mass spectrometer. This means that the response of the instrument to the analytes in a sample is nearly instantaneous and that analytical methods based on DSITMS are likewise very fast.

By keeping the interface hardware simple, the interaction of the analytes with active surfaces is minimized. This generally helps to reduce analyte losses due to surface adsorption or decomposition, particularly for polar and labile compounds. Even so,

there are some polar and/or semi-volatile compounds, such as alcohols and the chloroacetophenones, that are especially difficult to extract from a sample by DSITMS techniques. This diminishes the detection limits relative to the detection limits of most non-polar compounds and/or increases the overall time required for quantitative analysis.

Initial development of DSITMS was co-funded by the US Army Environmental Center and the US Department of Energy as an innovative technique for rapid site characterization. Their applications have primarily focused on the rapid detection of common organic pollutants in water and soil. During the last ten years, DSITMS has become increasingly practical as an analytical technique for a number of environmental applications. This is the result of dramatic improvements in the reliability and ruggedness of ion trap mass spectrometers, as well as the development of versatile sample inlets, which permit the measurement of volatile organic compounds (VOCs) and some semi-volatile organic compounds (SVOCs) in air, water, soil, and sludges. These inlets are mechanically simple devices that extract the analytes from a sample and present them efficiently to the direct sampling interface of the mass spectrometer. Some of the inlets provide the capability of real-time, in-situ monitoring, while others are designed for the rapid analysis of discrete samples such as water collected in standard 40-ml volatile organic analysis (VOA) vials. The simplicity of the sample inlets and capillary direct interface, combined with the advances in ion trap hardware, has greatly facilitated the development of practical instruments for onsite field applications.

The major benefits of DSITMS include versatility, fast analysis, high sample throughput, and very low analyte detection limits. Sample analysis times typically range from real-time to less than 5 minutes and up to 30 water samples per hour can be analyzed in the field for VOC contamination. Detection limits range from  $< 1$  ppb for non-polar VOCs in water to 100 ppbv (parts-per-billion by volume) or better for targeted organics in air. Once again, there are exceptions to these figures of merit since there are some compounds that tend to interact strongly with their matrix or with the interface components.

In general, the primary analytical limitation of DSITMS arises from the fact that there is no chromatographic separation of the analytes in a sample prior to their introduction into the mass spectrometer. In contrast with GC/MS (combined gas chromatography/mass spectrometry), this means that it is not possible to obtain "pure" mass spectra of each compound in a mixture. For many real-world environmental

applications, however, this is not a significant problem. In the case of samples which are contaminated with fewer than 20 compounds, it is often possible to deconvolute the combined mass spectra using spectral subtraction techniques or multiple linear regression and matrix algebra to provide accurate quantitation of the individual components. If an ion trap is equipped with mass spectrometry/mass spectrometry (MS/MS) capability, it is also possible to quantitatively measure trace levels of specific targeted compounds even in highly complex samples. Both the qualitative and quantitative data generated under these conditions can rival the quality of standard GC/MS methods at a fraction of the cost per sample and with much faster turnaround than standard analytical techniques.

There are, however, situations where DSITMS cannot distinguish all of the constituents of interest in a sample due to excessive complexity or presence of multiple compounds that have indistinguishable mass spectra such as cis and trans isomers of dichloroethylene. Another example would be chloropicrin and carbon tetrachloride. Although these two compounds are quite different chemically, they produce nearly identical mass spectra under electron ionization conditions. Fortunately, the likelihood of encountering interfering compounds at a specific site can often be evaluated from existing site characterization data or from historical records. For example, it is not expected that carbon tetrachloride was disposed of at the Federal Laboratories site in Saltsburg, PA, indicating that it should not be an interference in the determination of chloropicrin.

#### *Applications and Instrument Cost*

Sophisticated field analytical techniques, such as DSITMS, typically have a high cost associated with the instrumentation. For example, a commercial ion trap that has been modified for DSITMS applications will cost approximately \$80K. However, the high sample throughput capacity of DSITMS can reduce the cost of sample analysis (both sample handling and labor) by 75% or more relative to the cost of conventional laboratory analysis. This means that in situations where DSITMS is an acceptable alternative to traditional laboratory methods, the initial capital investment can be recovered after the analysis of several hundred samples.

Even in situations where DSITMS is used primarily for screening purposes, it can provide significant cost savings. For example, at many sites in the US, it is not uncommon for 70% or more of the groundwater samples that are submitted to a laboratory for analysis to have non-detectable levels of contamination. Based on the

current price for laboratory analysis of VOCs in water, it is possible to save \$100 or more for each "non-detect" sample that is identified by DSITMS screening and not submitted to a laboratory for full analysis.

In addition to the cost savings which can be documented relative to traditional laboratory analysis, DSITMS can provide further economic benefits by reducing sample handling costs, enabling more thorough (higher resolution) characterization of a site, and providing immediate results to sampling and remediation crews. For example, DSITMS instruments that are equipped with in-situ probes for measuring VOCs in groundwater can eliminate the cost of sample collection and handling while producing analytical results that are immediately available.

### *Instrumentation*

Ion trap mass spectrometers are especially well suited for direct sampling field applications because of their small size, rugged construction, reliable performance, and ease of operation. In addition, these instruments can be equipped for EI, CI, and MS/MS applications. Furthermore, the ion storage capability of the ion trap provides considerably more sensitivity than conventional mass spectrometers such as linear quadrupoles. This is an especially important factor in the ability of DSITMS to reduce or eliminate the need for sample preparation and analyte preconcentration steps.

Because the capillary restrictor interface of the DSITMS instrument continuously introduces approximately 0.5 ml/min (at standard temperature and pressure) of helium into the ion trap, the pumping capacity of the vacuum system must be sufficient to handle this gas load and maintain the ion trap operating pressure in the range  $10^{-4}$  torr. In practice, this means that the vacuum pump must have a rated pumping speed of at least 60 l/sec. The DSITMS instruments used for this study are equipped with 70 l/sec turbo-drag pumps. Instead of using an oil-filled roughing pump to back the turbo-drag pump, small DC-powered diaphragm pumps are used. This significantly reduces the power consumption and also produces a much cleaner background in the mass spectrometer since back-streaming of vacuum pump oil into the ion trap has been eliminated.

Since DSITMS instruments are intended for field use as well as laboratory use, they are designed to have a power consumption of less than 400 Watts during normal operation. This permits approximately 8 hours of operation in the field using a portable power supply that consists of four deep-cycle, lead-acid storage batteries and a DC-to-AC

voltage inverter. To further support field applications, the DSITMS instruments employ a vacuum system that permits mobile operation. This can save considerable time in the field by enabling rapid relocation of the instrument from one location to another without having to shut down and restart the equipment.

#### *Direct Sampling Inlet System*

The direct sampling interface that is used with the DSITMS instruments is comprised of a short length of microbore deactivated fused silica capillary restrictor (**Figure 2**). The purpose of the capillary restrictor is to convey analytes into the mass spectrometer ion source quickly and efficiently while simultaneously restricting the flow of gas into the vacuum chamber to a level that can be easily handled by the vacuum pumps. The capillary restrictor consists of a 25-cm length of 100- $\mu$ m, ID-deactivated fused silica tubing that extends from the mass spectrometer ion source to the outside of the vacuum chamber where the other end is open to atmospheric pressure. Because atmospheric pressure is nearly constant, the rate of gas flow through the capillary restrictor into the ion source is primarily a function of the inside diameter and the length of the capillary.

Because the transport time of analytes through the capillary restrictor is typically less than 100 msec, the ion trap responds almost instantly to the presence of analytes when they are presented to the atmospheric pressure end of the restrictor. In some instances however, strong interaction of a compound with the fused silica surface greatly increases the transport time through the restrictor. This can significantly delay the response of the DSITMS instrument to a period of several seconds, or even a few minutes, in a few severe cases. In order to reduce surface interaction problems, the fused silica restrictor can be heated to 250°C. Unfortunately, there are still some semi-volatile compounds such as TNT, 2-chloroacetophenone, and 3-chloroacetophenone that may exhibit noticeable interaction with the capillary restrictor. Regardless of some limitations, the capillary restrictor sample inlet is a good choice for fast and efficient introduction of many different volatile and semi-volatile organic compounds into the DSITMS instrument.

In order to enable the measurement of both VOCs and SVOCs in a full range of environmental samples, it is necessary to employ various sample-handling modules in conjunction with the capillary restrictor inlet. The function of the sample-handling modules is to extract, vaporize, and convey the analytes from a sample into the capillary restrictor. For water and soil samples, this is typically accomplished by

sparging a sample with a controlled flow of helium. Samples may be heated in order to increase the partitioning of organics from the sample matrix into the helium. By employing a gas flow splitter in between the sample module and the atmospheric pressure end of the capillary restrictor (see **Figure 2**), it is possible to sparge samples with a flow of helium that is in excess of 100 ml/min. This provides very efficient sample sparging and fast recovery to baseline at the completion of sample analysis. Variations of the sample-handling modules (**Figure 3**) have been developed that permit a wide range of analytical capabilities, including the analysis of discrete samples, as well as real-time, continuous monitoring of process streams and bulk samples which include groundwater wells, surface water, and soil gas.

## **ANALYTICAL METHODS DEVELOPMENT**

### *Purpose*

The purpose of the analytical methods development was to evaluate DSITMS for the detection and quantification of CNS tear gas components in water and soil. Using baseline performance data, the methods were to be optimized to provide the best combination of analytical speed, detection limits, and quantitative capability. Methods were to be developed for the analysis of discrete samples collected in 40-ml VOA vials and also for bulk water samples in groundwater wells using an in-situ sparging probe. The analysis method for samples in 40-ml VOA vials was to include groundwater, surface water, and soil samples. The in-situ sampling method was intended strictly for the analysis of groundwater samples.

### *Apparatus: Ion Trap Mass Spectrometers*

The ion trap mass spectrometers used for this study included a 3D-Q (**Figure 4**) manufactured by Teledyne Electronics Technologies (Mountain View, CA) and a Magnum ITMS manufactured by Finnigan MAT (San Jose, CA). Both instruments had identical direct-sampling interfaces and each was capable of being operated in electron ionization (EI) or chemical ionization (CI) mode. Additionally, each of these instruments had been previously modified at ORNL for field applications, which meant that either one could be used in the field at the Federal Laboratories site in Saltsburg, PA, for this project.

Although the initial methods development (40-ml VOA vial sparge) work was performed using the Finnigan Magnum ion trap, guidance from AEC project officers in July 1997



specified that the Teledyne 3D-Q was to be used for all of the remaining methods development work. They also recommended that the Teledyne 3D-Q was to be used as the primary instrument for the field studies at the Federal Laboratories site. The Finnigan Magnum ion trap was to be used in the field only as a backup unit or if multiple instruments were needed at the same time to handle the work load. The reason for emphasizing the use of the Teledyne 3D-Q ion trap was to demonstrate and highlight the advanced analytical capabilities of that instrument. This was especially important because the Teledyne ion trap was an innovative analytical technology that was being developed as part of the DARPA Technology Reinvestment Program with both AEC and ORNL as two of the partners.

#### *Reagents and Solutions*

Reagents for the preparation of analytical standards were purchased from commercial sources and used without additional purification. Chloropicrin, 2-chloroacetophenone, and 3-chloroacetophenone were purchased from Chem Service (West Chester, PA) and chloroform was purchased from Burdick and Jackson (Muskegon, MI). HPLC-grade methanol for the preparation of the stock and working standards was purchased from J.T. Baker, Inc. (Phillipsburg, NJ). Pure 1,4-difluorobenzene (for use as the internal standard) was purchased from Aldrich Chemical Company (Milwaukee, WI). Helium was used as the purge gas for sparging the water and soil samples. Compressed cylinders of helium were obtained from Aphagaz (Walnut Creek, CA) with a stated purity of 99.9999%. Simulated groundwater for the preparation of calibration standards was produced in our laboratory by adding 148 mg/l of sodium sulfate and 165 mg/l of sodium chloride (100 mg/l each of  $\text{SO}_4^{2-}$  and  $\text{Cl}^-$  ions) to ASTM Type II water that was obtained from a Milli-Q<sup>®</sup> water purification unit.

#### *External Standard Calibration Solutions*

Stock and working standards for quantitative calibration were prepared in 5-ml Pyrex<sup>®</sup> volumetric flasks (Corning, NY) using precalibrated variable-volume pipets compatible with methanol and other common organic solvents. These pipets were purchased from Polymerase Chain Reaction Tri-Continent Scientific, Inc. (Gross Valley, CA). After stock and working standards were prepared, they were stored in 5-ml capacity screw-cap amber vials purchased from I-Chem Research (New Castle, DE) and capped with solid caps containing fixed Teflon<sup>®</sup> liners. A 25- $\mu\text{l}$  capacity syringe manufactured by Precision Sampling (Baton Rouge, LA) was used to spike the standard solutions into water and soil samples. Spiked samples of water and soil were prepared in 40-ml

capacity screw-cap VOA vials that were purchased from I-Chem Research (New Castle, DE).

Individual stock solutions of each of the targeted CNS tear gas analytes (chloropicrin, chloroform, 2-chloroacetophenone, and 3-chloroacetophenone) were prepared at a concentration of 5,000 µg/ml in HPLC-grade methanol. Individual working standards of each analyte at a concentration of 100 µg/ml were prepared by diluting 100 µl of the previously described stock solutions to a volume of 5 ml using HPLC-grade methanol. The working and stock solutions were stored in a freezer that was maintained between -10°C and -20°C to preserve their integrity. Fresh working standards were to be prepared every two weeks in order to minimize possible analytical bias due to loss of analyte or solvent from the working standards.

#### *Internal Standard Solutions*

A stock solution of the 1,4-difluorobenzene internal standard was prepared at a concentration of 5,000 µg/ml by adding 21.4 µl of neat 1,4-difluorobenzene to a 5-ml capacity volumetric flask and diluting it to final volume with HPLC-grade methanol. This solution was transferred to a 5-ml capacity screw-cap vial. A working solution of the internal standard at a concentration of 200 µg/ml was prepared by diluting 200 µl of the stock solution to a final volume of 5 ml with HPLC-grade methanol. This solution was also transferred to a 5-ml capacity screw-cap vial. Both the stock and working solutions were stored in a freezer that was maintained between -10°C and -20°C to preserve the sample integrity. Fresh solutions of the working standard were to be prepared every two weeks.

The reason for using 1,4-difluorobenzene as the internal standard is that it responds well under both EI and CI conditions and it does not produce any peaks in the mass spectrum that overlap with any of the peaks in the mass spectrum that result from the CNS tear gas compounds.

### **Basic Procedure for the Analysis of 40-ml Samples**

#### *Sparging Module for 40-ml Samples of Water and Soil*

Water samples in 40-ml VOA vials were analyzed using a custom sparging module designed and built at the Oak Ridge National Laboratory (ORNL). This sparging module couples directly with the capillary restrictor interface of the ion trap mass



spectrometer and is designed to accept standard 40-ml VOA sample vials, as shown in **Figure 5**. In order to increase the recovery of analytes from a sample, an optional sleeve heater can be placed around the VOA vial in order to heat the sample during sparging.

Soil samples were analyzed using the same 40-ml VOA vial sparging module that was used for the analysis of water samples. However, for the analysis of soil samples, the sleeve heater was always used. In addition, a stir bar was placed in the sample vial along with the soil sample so that the soil could be stirred while being sparged. The purpose of the stirring was to increase the interaction of the purge gas with the soil particles for more uniform sparging.

The operating principle of the 40-ml VOA vial sample sparging module is very simple. A standard 40-ml-VOA vial containing the sample is attached to the module by means of a threaded collar. A stainless steel sparging needle projects into the bottom of the VOA vial and a flow of  $100 \pm 5$  ml/min of helium purges the volatile (and some semi-volatile) organics from the sample. The VOCs that are purged from the sample are conveyed by the helium directly into the ion trap mass spectrometer through a fixed-ratio sample splitter and the fused silica capillary restrictor. The sample splitter arrangement directs approximately 0.5% of the gas flow into the ion trap while the remaining 99.5% exits through a vent port. Start and stop of the helium flow through the VOA vial is controlled by a 3-way solenoid valve. In one position, this valve directs the flow of helium through the VOA vial during sparging of the sample. In the other position, the valve diverts the helium directly into the capillary restrictor interface, completely bypassing the sample vial.

If desired, sorbent tubes can be attached to the vent port of the splitter for sample archival purposes. Archival samples can be collected at the same time that a DSITMS analysis is being performed without affecting the quality of the DSITMS results or the speed of the analysis.

#### *Monitoring of Purge Flow Rate and Sample Temperature*

Calibration of the helium flow rate through the 40-ml VOA vial sparging device was performed using a Model M-5 Flow Calibration Meter manufactured by A.P. Buck (Orlando, FL). This flow meter was capable of measuring helium flow in the range of 100 ml/min and it was attached to the vent port of the sample splitter during the flow adjustment procedure.

A small 110-vac heating element capable of reaching a temperature of up to 100°C was used to heat the samples during heated purge experiments. The heating element consisted of a small cartridge heater that was attached to an aluminum sleeve 6.5 cm in length and 2.8 cm ID. The aluminum sleeve was manufactured at Oak Ridge National Laboratory (Oak Ridge, TN) and was designed to slide over the outside of standard 40-ml VOA vials. An Omega Engineering proportional heater controller was used to control the temperature of the heating element. The temperature of the aluminum sleeve was monitored with a Model HH81 temperature meter and a thermocouple, both manufactured by Omega Engineering (Stamford, CT).

#### *Tuning of the Ion Trap Mass Spectrometer*

The mass axis calibration of the ion trap mass spectrometer was checked daily using perfluorotributylamine (PFTBA) which is a compound that is widely used for this purpose. If mass axis recalibration was necessary, it was performed according to the procedure described in the Operator's Manual for the appropriate ion trap. Other daily operational checks for the ion trap mass spectrometer included checking and tuning the radio frequency (RF) drive circuit, checking and nulling the signal electrometer, and checking for air leaks in the vacuum chamber, as indicated by excessive air and water background in the mass spectrum. Details of the basic instrument tuning procedures are described in the Operator's Manual produced by the ion trap manufacturers for their specific instruments.

#### *General Operating Conditions of the Ion Trap Mass Spectrometer*

During sample analysis, the operating conditions of the ion trap mass spectrometer during data acquisition were completely controlled by the instrument control computer using parameters stored in an "Acquisition Method" file. The specific parameters in the "Acquisition Method" file, such as scan range and ionization mode, were input into the data file by the instrument operator prior to the start of data acquisition. For the analysis of CNS tear gas compounds, the ion trap mass spectrometer was set to acquire mass spectra over a range of at least 45-200 Daltons (atomic mass units). A minimum of four mass spectra (microscans) were signal-averaged for every mass spectrum that was displayed or acquired to computer disk. This helped to reduce electronic noise and random signal fluctuations in the mass spectrum. Approximately one signal-averaged mass spectrum was generated per second.

Although the ion trap mass spectrometer responds almost instantaneously to the analytes that are purged from a sample by the 40-ml VOA vial sparging module, quantitative precision is improved if a sample is sparged and data are continuously collected for a period of 2-3 minutes. This tends to average out instrument noise and also minimizes the effects of slight differences between the sparging conditions of replicate samples. During the 2-3 minute analysis time, a series of mass spectra is continuously generated and saved to the computer disk in the form of an "Acquisition Data File." Assuming that one mass spectrum per second is generated, a 3-minute-long "Acquisition Data File" will consist of 180 individual mass spectra stored in sequence according to when they were acquired.

The ionization mode of the ion trap mass spectrometer is normally set so that either EI or CI data only are acquired during the 2- to 3-minute analysis time. This operating mode requires the sequential analysis of duplicate samples, one using EI conditions and the other using CI conditions, if both types of data are required. Alternatively, the Teledyne 3D-Q ion trap has a unique mode of operation that permits the simultaneous generation of both EI and CI data during a single 2- to 3-minute analysis without significant loss of quantitative performance. This is accomplished by continuously alternating between EI and CI conditions once every second. A 3-minute-long data file generated under these conditions will consist of 90 EI spectra and 90 CI spectra stored on disk as a sequence of alternating EI and CI spectra. Software for extracting both the EI and CI spectra from a combined data file is included in the commercial data reduction software provided with the Teledyne 3D-Q instrument. The alternating EI/CI mode of operation can provide considerable time savings by eliminating the need for sequential sample analysis.

#### *Quantitation of Targeted Analytes*

A plot of the response of the mass spectrometer (ion current) versus analysis time is referred to as a "purge profile." Purge profiles can be plotted using the total ion current (the response for all masses summed together) or they can be a plot of the ion current for specific mass values (**Figure 6**). Quantitation of targeted analytes is performed by integrating purge profiles that have been plotted using specific quantitation masses (referred to as  $m/z$  values) that are characteristic of the analytes of interest. The quantitation masses for DSITMS methods are normally selected by choosing the largest peak in the mass spectrum of a particular analyte that is not expected to overlap with the peak from another compound in the sample. For the analysis of samples that contain CNS tear gas compounds, the quantitation masses (electron ionization

conditions) are as follows: chloroform ( $m/z$  83), chloropicrin ( $m/z$  119), 2-chloroacetophenone ( $m/z$  105), and 3-chloroacetophenone ( $m/z$  139). In situations where peak overlap is a significant problem, spectral subtraction routines or other deconvolution techniques must be applied to the mass spectrum in order to recover the quantitative information for individual analytes. The samples analyzed for this project did not require spectral subtraction or special deconvolution techniques.

For the analysis of samples in 40-ml VOA vials, the data integration window normally includes all but the first 15 seconds of the 2- to 3-minute purge profile. The data from the first 15 seconds of data acquisition are not usually integrated due to possible artifacts, such as charge exchange peaks, that can be present in the mass spectra during the first few seconds of the sparging process. These artifacts arise from traces of air that are trapped in the void volume of the sparging module and sample interface.

If the same integration limits (time window) are consistently used to integrate all purge profiles for a set of samples, the integrated area of each quantitation mass will be directly proportional to the concentration of the corresponding analytes in a particular sample. Because of this, linear calibration curves can readily be generated from a series of standards of known concentration. Unknown samples can then be quantitated by comparison of the integrated response for the targeted analytes with the corresponding calibration data. Automated quantitation software included with the ion trap mass spectrometers provides the capability to generate calibration curves and calculate analyte concentrations for unknown samples.

#### *Analysis of Blank Water Samples*

Blank water samples were routinely analyzed throughout this project to check for possible analyte carryover in the sample interface and to check for contamination of the ion trap mass spectrometer. The blank water samples consisted of simulated groundwater that had been transferred into 40-ml VOA vials. All of the blank water samples were spiked with a 10- $\mu$ l aliquot of 1,4-difluorobenzene internal standard solution, producing a final concentration of approximately 50 ppb of 1,4-difluorobenzene in the sample. The function of the internal standard in the blank samples was to verify that the ion trap was functioning properly in terms of mass calibration and expected signal response (ion counts).

At the beginning of the sample analysis, the helium flow through the stainless steel sparging needle was started, purging VOCs from the water. The sample was sparged

for a total of 2-3 minutes during which mass spectra were continually recorded at 1-second intervals, as previously described.

At the end of data acquisition, the helium flow through the sample vial was stopped and the acquisition of mass spectra was terminated. The sample vial was then removed and replaced with an empty 40-ml VOA vial. The flow of helium was then again permitted to pass through the sparging needle and into the empty VOA vial. This was performed after every sample in order to remove analyte carryover from the sparging module prior to the analysis of the next sample.

The 2- to 3-minute-long "purge profiles" for the blank water samples were examined for the presence of anomalous peaks in the mass spectrum. Mass peaks that could not be accounted for by the internal standard or by background air were generally an indication of contamination in either the blank water sample or in the sample interface hardware.

In addition to checking for anomalous peaks in the mass spectrum, the response for the 1,4-difluorobenzene internal standard was checked to verify that the signal intensity (ion counts) was sufficient to enable detection of this compound at a concentration of less than 5 ppb. Assuming that a signal-to-noise ratio of 5:1 is needed to reliably detect a sample containing 5 ppb of the targeted analyte, the signal-to-noise ratio for the  $m/z$  114 peak of the 1,4-difluorobenzene at a concentration of 50 ppb needed to be at least 50:1.

#### *Generation of External Standard Calibration Curves*

External standard calibration curves were used for the quantitation of unknown samples. These calibration curves were generated by sparging 40-ml samples of water that were spiked with known amounts of the targeted analytes.

The calibration samples were prepared by using a syringe to add appropriate aliquots of the external standard "working" solutions to 40-ml VOA vials that were completely filled with simulated groundwater. Calibration samples of chloropicrin and chloroform were prepared over a concentration range from 5-8,000 ppb and 5-500 ppb, respectively. Calibration samples of both 2-chloroacetophenone and 3-chloroacetophenone were prepared at concentrations ranging from 5-1,000 ppb. Each calibration sample was also spiked with the 1,4-difluorobenzene internal standard "working" solution to produce a final concentration of 50 ppb.

The concentrations of the chloropicrin and chloroform calibration samples were selected based on the expected relative abundances of these two compounds in the groundwater at the Federal Laboratories site in Saltsburg, PA. Although it was not anticipated that either 2-chloroacetophenone or 3-chloroacetophenone would be detected in the groundwater at this site, it was an objective of this project to demonstrate method detection limits in the low part-per-billion range for all of the targeted analytes.

Each calibration sample was prepared immediately prior to analysis. After spiking each sample with the appropriate standards, the sample vial was attached to the purge module and data acquisition was started. The calibration samples were each sparged for a total of 3 minutes during which mass spectra were continually acquired and stored in the form of an "Acquisition Data File."

Example 40-ml VOA vial purge profiles for chloroform, chloropicrin, 2-chloroacetophenone, and 3-chloroacetophenone are shown in **Figure 6**. These purge profiles were generated at ambient temperature (approximately 25°C). As can be seen by these examples, both chloroform and chloropicrin respond readily by the 40-ml sparging method at ambient temperature. The chloroacetophenones, however, respond very slowly and do not reach a steady-state signal for approximately 15 minutes. This is most likely due to strong interaction of the chloroacetophenones with water, as well as the adsorption of these compounds on the surfaces of the sample interface. Because of this, calibration curves for the chloroacetophenones could not be generated using the same analytical conditions that were used for the chloroform and chloropicrin. Instead, in order to accumulate sufficient signal to produce calibration curves for the chloroacetophenones, it was necessary to perform a heated purge and to acquire data for at least 15 minutes instead of 2-3 minutes.

The heated purge for 2-chloroacetophenone and 3-chloroacetophenone was performed the same as previously described, except that a sleeve heater was used to heat the sample vial to approximately 60°C during the sparging process. Because most organic compounds can be purged from water faster and more efficiently at higher temperatures, the measured response will be greater for a sample that is purged at elevated temperature compared with the same sample purged at ambient temperature. In other words, heated purge can help to speed up the analysis time and improve detection limits for compounds, such as the chloroacetophenones, that do not purge easily at ambient temperature.



### *Analysis of Unknown Samples*

Samples of unknown water from the Federal Laboratories site in Saltsburg, PA were carefully transferred from their original container into 40-ml VOA vials for analysis. Using a syringe, each 40-ml water sample was spiked with 1,4-difluorobenzene internal standard "working solution" to a final concentration of 50 ppb in the sample. Immediately after adding the internal standard, the sample vial was attached to the purge module and data acquisition was started. Each sample was sparged for a total of 2-3 minutes during which time mass spectra were continually acquired and stored in the form of an "Acquisition Data File."

Upon completion of data acquisition, a quantitation program was used to automatically integrate the purge profiles for the response of the target compound quantitation masses. The concentrations of the targeted analytes were calculated by substituting the integrated responses into the external standard calibration equation and solving for concentration.

### *Analysis of Soil Samples*

The procedure for the analysis of soil samples is basically the same as that previously described for the analysis of water samples, except that heated sparging at 60°C was employed. The soil samples were prepared in the form of a water slurry by transferring 5 gr of soil to a 40-ml VOA vial and then adding sufficient distilled water to fill the vial to the bottom of the cap threads. The 1,4-difluorobenzene internal standard was added to the sample with a syringe to produce a final concentration of 50 ppb in the slurry. A small magnetic stir bar was added to the slurry immediately prior to analysis so that the soil slurry could be continuously stirred during the sparging process.

### **In-situ Sparge Procedure for Analysis of Groundwater in Wells**

There are a number of groundwater monitoring wells at the Federal Laboratories site in Saltsburg, PA. One of the analytical capabilities that was to be demonstrated at this site was the ability to measure VOCs directly in the groundwater using a special in-situ sparging probe that was developed at ORNL (3). In addition, this probe was to be used to measure concentration gradients of VOCs in a couple of groundwater wells (depth profiling) in order to help locate sources of contaminant influx into the groundwater such as rock fracture zones.

### *In-situ Sparging Probe for Groundwater Analysis*

The in-situ sparging probe (**Figure 7**) consists of a 1/2-inch-diameter sampling head that is inserted into the groundwater through a well casing or drive point. The probe head is attached to a 1/16-inch OD Teflon<sup>®</sup> tube that supplies helium to the sparger. It is also attached to a Silco-steel<sup>®</sup>-lined, 1/8-inch OD stainless steel tube that is used to transport the analyte vapors from the headspace chamber on the sampling probe to the mass spectrometer. The sample transfer line of the in-situ sparger connects directly with the capillary restrictor interface of the ion trap mass spectrometer. Analyte vapors are pulled through the transfer line and across the end of the capillary restrictor interface by means of a sampling pump attached to the vent port of the sample splitter. At the present, there is no provision for heating the sample transfer line or the probe head. Unfortunately, this restricts the range of compounds that can be analyzed using this probe to those that are highly volatile at ambient temperature.

The operating principle of the in-situ sparging probe is very simple. During sample analysis, the in-situ sparging probe uses a flow of helium in the range of 20-100 ml/min to purge VOCs from the water. The differential in the density of the water column that is being sparged and the density of the surrounding water creates a pumping action that continually draws a fresh sample into the sparger. Electronic flow controllers maintain a slight excess of helium in the sparger relative to the flow of gas through the transfer line and into the MS. This maintains a nearly constant volume of helium in the headspace chamber and also prevents water from flowing into the sample transfer line. For depth profiling applications, this probe can be used at any depth below the water surface, provided that the helium flow controllers are rated for use at a pressure that is greater than the maximum water pressure that will be encountered.

The standard length of the in-situ sparge transfer line is 150-200 feet. Because TVA and AEC expressed interest in depth profiling, a well at the Federal Laboratories' site that was 90-100 feet deep, it was decided that a 150-ft transfer line should be used for the field work. An added benefit of using a transfer line of this length is that it would also be possible to analyze water samples in wells located in close proximity to one another without having to relocate the DSITMS instrument each time.

### *Monitoring of Purge Flow Rate Sampling Rate*

The flow of helium into the sparging probe is controlled by an electronic flow controller. Potentiometer adjustments permit the flow rate to be varied from 10-100 ml/min. A digital readout provides a direct indication of the flow rate. The same type of flow



controller is used to maintain a constant flow of helium through the sample transfer line and into the mass spectrometer interface. For proper operation, it is necessary for the flow rate of the helium into the sparging probe to always be 1%-2% greater than the flow through the sample transfer line into the mass spectrometer. This maintains a slight positive pressure of helium inside the sampling head and prevents water from entering the transfer line.

Prior to adjusting the flow rate of helium, the in-situ sparging probe must be immersed in a container of water. The flow rate of helium through the sample transfer line is adjusted to 0 ml/min and the flow rate of helium through the sparging tube is adjusted to approximately 40 ml/min. If properly adjusted, a steady stream of bubbles will be observed exiting the bottom of the sparging probe. At this point, the flow rate through the sample transfer line is slowly increased to 39 ml/min. If the flow rates are set properly, approximately one bubble should exit the bottom of the sparging probe every 5 seconds.

#### *Tuning of the Ion Trap Mass Spectrometer*

The tuning procedure for the ion trap mass spectrometer is identical to that performed when analyzing 40-ml samples of water using the VOA vial-sparging device. Refer to the appropriate instrument Operator's Manual for details.

#### *General Operating Conditions of the Ion Trap Mass Spectrometer*

As previously described for the analysis of 40-ml VOA vial samples, the operating conditions of the ion trap mass spectrometer during the acquisition of in-situ sparge data were also controlled by the data acquisition computer. The parameters stored in the "Acquisition Method" file, such as scan range and ionization mode, were also the same as those used for the analysis of 40-ml VOA vials.

#### *Quantitation of Targeted Analytes*

In general, the analytical procedure using the in-situ sparging probe is similar to that used for the analysis of 40-ml sample vials. However, because there is a constant flow of water into the in-situ sparger (as opposed to a fixed 40-ml volume), a steady-state signal is generated provided that the concentration of the analytes in the bulk sample does not change significantly. The steady-state response is directly proportional to the concentration of the analytes in the sample, as shown in **Figure 8**.

As with the 40-ml VOA vial samples, the analyte concentration in an unknown sample is determined by integrating the response profile over a fixed time window. The integrated value is compared with a calibration working curve generated from standards of a known concentration that were also integrated over the same time window.

#### *Analysis of Blank Water Samples*

Blank water samples were analyzed prior to every sample analysis in which the in-situ sparging probe was used. This was done to ensure that the sampling probe and mass spectrometer were functioning properly and that there was little or no sample carryover between samples. This was especially important because the long sample transfer line that was used with the in-situ sparging probe has a tendency to retain some of the higher boiling point VOCs.

Blank water samples were prepared, as needed, by adding 250 ml of simulated groundwater to a 500-ml graduated cylinder. A 63- $\mu$ l aliquot of the 1,4-difluorobenzene internal standard was added to the sample to produce a final concentration of 50 ppb. The in-situ sparging probe (with flow rates already adjusted) was then inserted into the graduated cylinder and data acquisition was started. Typically, the probe was left in the container of water for 3 to 5 minutes until the signal level had stabilized for at least 30 seconds. Data acquisition was then terminated and the probe was removed from the water sample.

The 3- to 5-minute-long in-situ sparge "purge profiles" for the blank water samples were examined for the presence of anomalous peaks in the mass spectrum. Mass peaks that could not be accounted for by the internal standard or by background air were generally an indication of contamination in either the blank water sample, in the sample interface hardware, or more likely, in the sample transfer line.

In addition to checking for anomalous peaks in the mass spectrum, the response for the 1,4-difluorobenzene internal standard was checked to verify that the signal intensity (ion counts) was sufficient to enable detection at a concentration of less than 5 ppb. Assuming that a signal-to-noise ratio of 5:1 is needed to reliably detect a sample containing 5 ppb of the targeted analyte, the signal-to-noise ratio for the  $m/z$  114 peak of the 1,4-difluorobenzene at a concentration of 50 ppb is needed to be at least 50:1.

### *Generation of External Standard Calibration Curves*

Calibration of the in-situ sparging probe for quantitation was accomplished through the use of external standards. This procedure involved adjusting the in-situ sparging probe to the proper flow rates and acquiring a satisfactory spectrum from a blank water sample as previously described. The probe was then placed in a 500-ml graduated cylinder that was filled with 250 ml of simulated groundwater. A 63- $\mu$ l aliquot of the 1,4-difluorobenzene internal standard was added to the sample to produce a final concentration of 50 ppb. A syringe was then used to add the appropriate amounts of the analyte "working" standard solutions to the water sample to produce the desired final concentration. Data acquisition was then started and the in-situ sparging probe was left in the sample container for at least 3 to 5 minutes or until the signal had stabilized for 30 seconds. The probe was then removed from the graduated cylinder and rinsed with distilled water. The calibration sample was then discarded into a waste container and the entire process was repeated using a sample with a different concentration of analytes.

Calibration curves were produced by integrating the flat portion of the purge profile over a fixed time window (typically 30-seconds wide) using the response for targeted ions in the mass spectrum. The integrated area was directly proportional to the concentration of the analytes in the sample.

### *Analysis of Unknown Samples*

Blank samples and probe calibration are typically performed prior to the analysis of unknown groundwater samples. Immediately prior to inserting the probe into the groundwater, it is cleaned with distilled water and inserted into a glass container of clean water in order to obtain a background spectrum. Once a satisfactory background has been obtained, the probe is removed from the container of clean water and slowly lowered into the groundwater well. A conductivity detector mounted on the in-situ sparging probe indicates when the probe is at the proper level in the water.

Once the probe is in the proper position in the groundwater well, data acquisition is started. Mass spectra are continuously generated at 1-second intervals for a period of 3-5 minutes or until a stable signal has been obtained for at least 30 seconds. Data acquisition is then terminated and the probe is withdrawn from the well. It is immediately decontaminated by rinsing with clean water.

The quantitation of targeted analytes in the groundwater well is accomplished by plotting the purge profiles for the appropriate quantitation ions and then integrating these profiles using the same limits as applied to the calibration samples. Typical data for the in-situ sparging probe are shown in **Figure 9**.

## **Results and Discussion**

### *Mass Spectra*

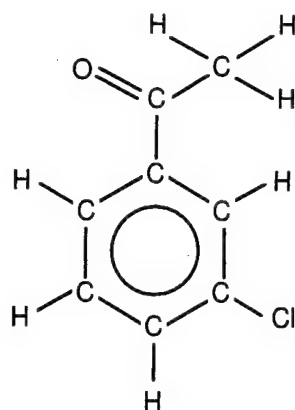
Individual mass spectra of pure samples of chloroform, chloropicrin, 2-chloroacetophenone, and 3-chloroacetophenone were generated using the direct sampling ion trap mass spectrometer. Both electron ionization (EI) and proton transfer chemical ionization (CI) were evaluated. Under EI conditions, each of the four compounds studied produced characteristic fragmentation spectra with little or no observable molecular ion.

Proton transfer CI was investigated to determine if either chloropicrin or the chloroacetophenones would produce quasi-molecular ions that could be used to help identify these compounds in unknown samples. Unfortunately, it was found that none of the four compounds produced a significant response under CI conditions, although a range of CI reagents were tested (water, methanol, and benzene). This was especially a problem for chloropicrin since the base peak in the EI mass spectrum corresponds to a loss of the nitrate group, producing an ion that has the same mass and structure as the primary ion in the EI mass spectrum of carbon tetrachloride. Similarly, 2-chloroacetophenone produces a fragmentation spectrum under EI conditions that could be confused with some of the aromatic components in a gasoline sample. The EI response and mass spectra for each compound are described below.

### 2-Chloroacetophenone and 3-chloroacetophenone

Both 2-chloroacetophenone and 3-chloroacetophenone have eight carbon atoms, seven hydrogen atoms, one oxygen atom, and one chlorine atom, giving a nominal molecular weight of 154 for those molecules having the most abundant isotope ( $^{12}\text{C}$  and  $^{35}\text{Cl}$ ). These two molecules differ in the position of where the chlorine atom is located on the molecule. In the case of 3-chloroacetophenone, the chlorine atom is located on the benzene ring in the meta position relative to the ketone substituent as shown in **Structure I**.

**Structure I**

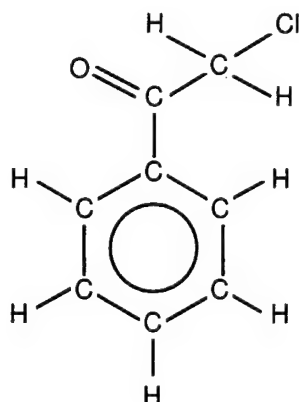


3-Chloroacetophenone  
mw=154\*

\*Based on Chlorine-35

The structure of 2-chloroacetophenone actually has the chlorine atom located on the methyl group of the substituent (**Structure II**) as opposed to the ortho position on the ring as one might assume. For this reason, 2-chloroacetophenone is also called phenacyl chloride.

**Structure II**

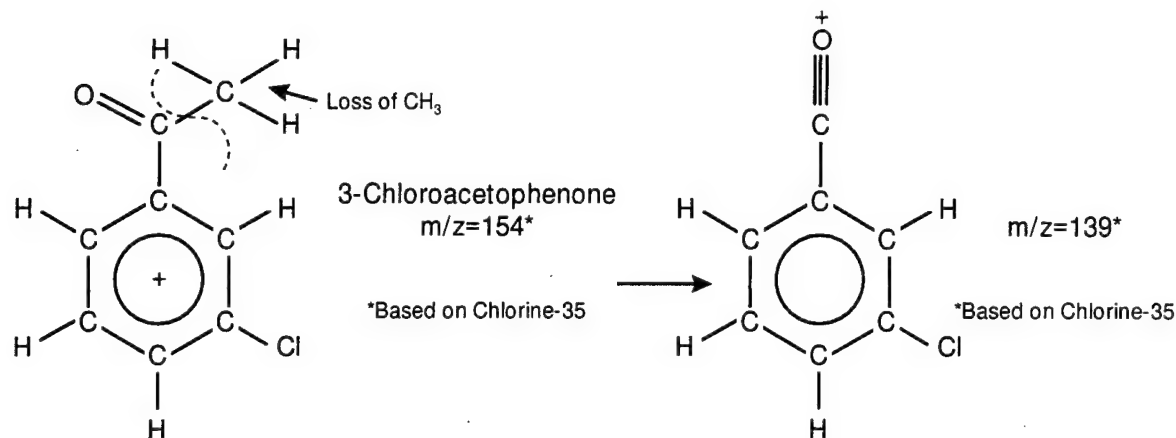


2-Chloroacetophenone  
mw=154\*

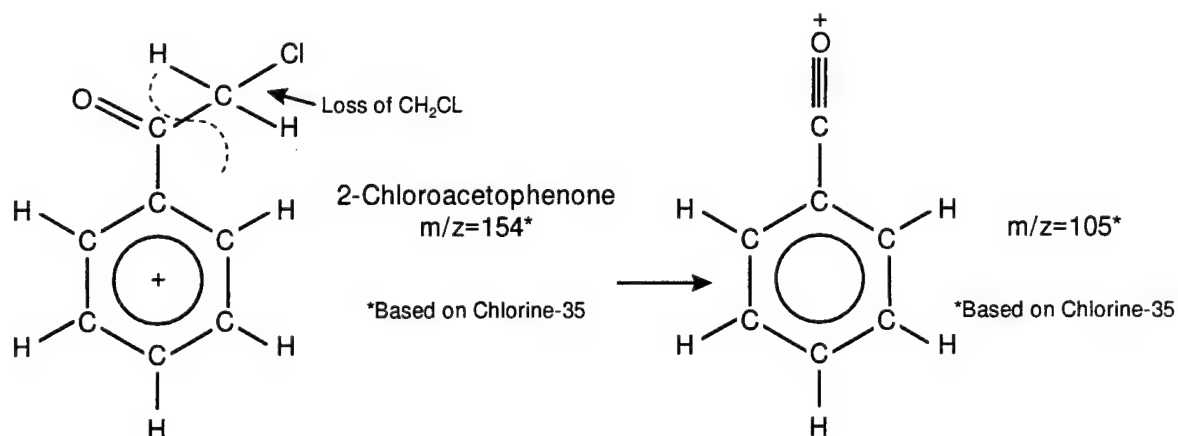
\*Based on Chlorine-35

The mass spectra of both 2-chloroacetophenone and 3-chloroacetophenone are dominated by a base peak that is the result of a cleavage at the bond beta to the aromatic ring, leaving a characteristic  $\text{ArCO}^+$  ion. This is well known to be the most facile cleavage for aryl alkyl ketones under electron ionization conditions. These are shown below.

### El fragmentation of 3-chloroacetophenone to produce the base peak at m/z 139



### El fragmentation of 2-chloroacetophenone to produce the base peak at m/z 105



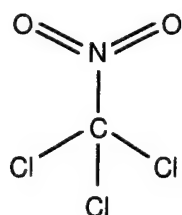
The  $m/z$  105 ion from 2-chloroacetophenone may also undergo a loss of  $\text{CO}$ , giving rise to an ion at  $m/z$  77. The corresponding loss from the  $m/z$  139 ion of 3-chloroacetophenone may produce an ion at  $m/z$  111. Additional losses and rearrangements can occur giving rise to other minor peaks in the mass spectrum. Although there is a small but measurable molecular ion for 3-chloroacetophenone at  $m/z$  154, the corresponding molecular ion for 2-chloroacetophenone is barely detectable. Example electron ionization (EI) mass spectra of 3-chloroacetophenone and 2-chloroacetophenone are shown in **Figures 10 and 11**, respectively.

As can be seen from the mass spectrum in **Figure 10**, the fragmentation pattern in the EI mass spectrum for 3-chloroacetophenone is reasonably diagnostic, especially with the presence of abundant ion intensity at  $m/z$  139 and the  $^{37}\text{Cl}$  isotope peak at  $m/z$  141. The EI mass spectrum of 2-chloroacetophenone, however, is considerably less diagnostic due to a very low abundance of the molecular ion and loss of the chlorine atom in the primary fragmentation pathway. Although some ion intensity has been observed at  $m/z$  139 and  $m/z$  141 for this compound, it is possible that these ions may be the result of contamination by 3-chloroacetophenone or the result of a complex rearrangement reaction during the ionization event. In either case, no significant abundance of ion intensity at  $m/z$  139 is observed at concentrations of 2-chloroacetophenone in a sample of less than 1 ppm. Instead, the primary ions in the mass spectrum of 2-chloroacetophenone occur at  $m/z$  105 (base peak) and  $m/z$  77. Unfortunately, both of these ions are frequently observed in environmental samples that have been contaminated with fuels that contain alkyl aromatic compounds. Although chemical ionization (CI) can be used to help rule out fuel contamination in a sample, it does not help confirm the identity of 2-chloroacetophenone. At sites known to be contaminated only with tear gas, however, the mass spectra should provide the necessary information to distinguish between 2-chloroacetophenone and 3-chloroacetophenone and to permit their relative concentration to be measured.

### Chloropicrin

Chloropicrin (nitrotrichloromethane) is a molecule that contains 1 carbon, 3 chlorine atoms, 1 nitrogen atom, and 2 oxygen atoms (**Structure III**). It is considered to be a substituted methane in which the three chlorine atoms and the nitrogen are bound directly to the carbon atom. The two oxygen atoms are bound to the nitrogen in the form of a nitro group. The nominal molecular weight is 163 based on the most abundant isotopes ( $^{12}\text{C}$ ,  $^{35}\text{Cl}$ ).

**Structure III**

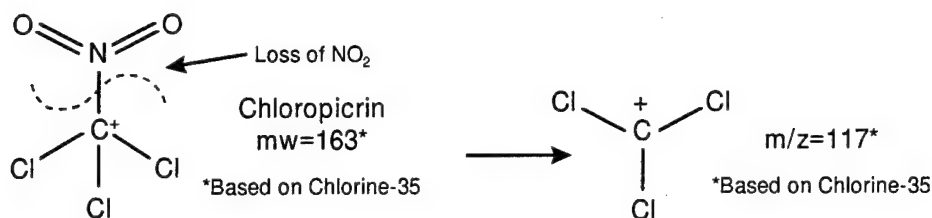


Chloropicrin  
mw=163\*

\*Based on Chlorine-35

The mass spectrum of chloropicrin is dominated by the presence of ions that result from the cleavage of the bond between the nitrogen atom and the carbon atom. This results in loss of the nitro group ( $\text{NO}_2$ ), leaving the  $\text{CCl}_3^+$  ion as shown below.

## El fragmentation of chloropicrin to produce the base peak at m/z 117



An example EI mass spectrum of chloropicrin is shown in **Figure 12**. The spectrum primarily consists of a group of peaks at  $m/z$  117,  $m/z$  119,  $m/z$  121, and  $m/z$  123. Although each of these peaks correspond to  $\text{CCl}_3^+$ , there are four unique peaks due to the natural occurrence of both  $^{35}\text{Cl}$  and  $^{37}\text{Cl}$  isotopes (75% and 25% abundance, respectively). The peak at  $m/z$  117 ( $M^+$ ) contains three  $^{35}\text{Cl}$  atoms, the peak at  $m/z$  119 ( $M+2$ )<sup>+</sup> contains two  $^{35}\text{Cl}$  atoms and one  $^{37}\text{Cl}$  atom, and the peak at  $m/z$  121 ( $M+4$ )<sup>+</sup> contains one  $^{35}\text{Cl}$  atom and two  $^{37}\text{Cl}$  atoms. The peak corresponding to the presence of three  $^{37}\text{Cl}$  atoms ( $M+6$ )<sup>+</sup> at  $m/z$  123 is only a few percent of the intensity of the largest peak in the cluster and may be difficult to detect.

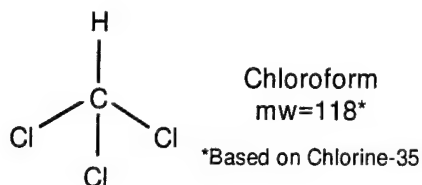
The abundance ratio of the chlorine isotope peaks is diagnostic for confirming the presence of chlorine in this molecule. Unfortunately, the molecular ion for chloropicrin cannot be detected by this technique, making it difficult to distinguish the mass spectrum of chloropicrin from other compounds, such as carbon tetrachloride, that also form  $\text{CCl}_3^+$  under EI conditions. Although one might expect to observe other diagnostic peaks in the mass spectrum of chloropicrin such as  $m/z$  30 ( $\text{NO}^+$ ) or  $m/z$  46 ( $\text{NO}_2^+$ ), interferences in the mass spectrum due to the presence of air make these particular ions difficult to distinguish from background gases.

### Chloroform

Chloroform (trichloromethane) is a molecule that contains one carbon, three chlorine atoms, and one hydrogen atom (**Structure IV**). Chloroform is also considered to be a substituted methane in which the three chlorine atoms and the hydrogen are bound directly to the carbon atom. The nominal molecular weight is 118 based on the most abundant isotopes ( $^{12}\text{C}$ ,  $^{35}\text{Cl}$ ).

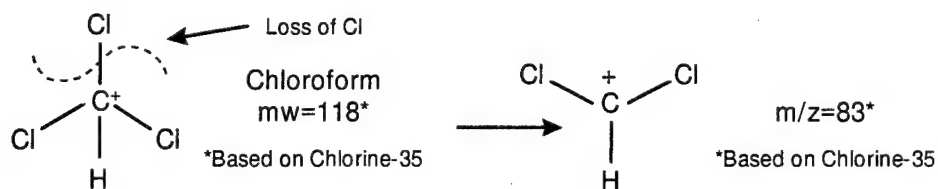


**Structure IV**



The mass spectrum of chloroform is dominated by the presence of ions that result from the cleavage of the bond between one of the chlorine atoms and the carbon atom. This results in loss of a chlorine radical ( $\text{Cl}^\cdot$ ), leaving the  $\text{CHCl}_2^+$  ion as shown below.

**EI fragmentation of chloroform to produce the base peak at m/z 83**



An example of EI mass spectrum of chloroform is shown in **Figure 13**. The principal peaks in the mass spectrum of chloroform are at m/z 83, m/z 85, and m/z 87. Each of these peaks corresponds to  $\text{CHCl}_2^+$ , with the m/z 85 and m/z 87 peaks being the  $(\text{M}+2)^+$  and  $(\text{M}+4)^+$  chlorine isotope peaks, as previously explained for chloropicrin.

Composite Mass Spectrum

As shown in **Figure 14**, there are no major overlapping mass spectral peaks in a sample containing all four of the targeted analytes. As a result, it was possible to use the base peak (most intense ion) in the individual mass spectra for each compound as a unique quantitation mass for that compound. The quantitation mass was m/z 105 for 2-chloroacetophenone, m/z 139 for 3-chloroacetophenone, m/z 119 for chloropicrin, and m/z 83 for chloroform.

*Results for 40-ml Sparge Analysis of Water Samples*

The primary objective of this phase of the project was to evaluate DSITMS for measuring chloropicrin, chloroform, 2-chloroacetophenone, and 3-chloroacetophenone in groundwater. This work was conducted in the laboratory using simulated groundwater samples that were spiked with known amounts of each of the targeted

analytes. All of the work during this phase of the project was conducted using the 40-ml VOA vial-sparging inlet. Each analyte was studied over a range of concentrations in order to permit an estimation of detection limits and linear dynamic range.

#### Chloropicrin

Calibration plots for chloropicrin in 40-ml VOA vial samples of simulated groundwater were generated as previously described. Examples of these plots are shown in **Figures 15 and 16**. Chloropicrin was easily detected in water at a concentration of 5 ppb and the response was found to be linear over a range of 5-8,000 ppb. The calibration plots in **Figures 15 and 16** have been divided into low level and high level range, respectively, for greater visual clarity.

One concern regarding the analysis of chloropicrin by DSITMS techniques was the potential for interference from carbon tetrachloride if it were present as a co-contaminant in a sample. The reason for this is that under EI conditions, the quantitation mass for chloropicrin at  $m/z$  119 overlaps with the principal peaks in the mass spectrum of carbon tetrachloride ( $m/z$  117,  $m/z$  119, and  $m/z$  121). In fact, the ion that gives rise to these peaks is the same for both compounds ( $CCl_3^+$ ). Although the mass spectrum of chloropicrin should exhibit some measurable ion intensity at  $m/z$  46 ( $NO_2^+$ ) that potentially could be used to distinguish it from carbon tetrachloride, we were unable to reliably detect this ion by the DSITMS method.

One possible approach to circumventing the potential interference of chloropicrin with carbon tetrachloride was to determine if these two compounds had different purge efficiencies from water. If so, the "shape" of the purge profiles would be different and mathematical deconvolution techniques could be used to distinguish the individual contributions to the mass spectrum. Unfortunately, it was determined that both compounds had very similar purge profiles, despite the presence of the  $NO_2$  group on the chloropicrin. In fact, the only significant difference that was observed between chloropicrin and carbon tetrachloride using the 40-ml VOA vial sparge technique was that carbon tetrachloride exhibited a response that was approximately twice that of chloropicrin for the same concentration in water.

Another possible approach to distinguishing chloropicrin from carbon tetrachloride was to use chemical ionization as a means of selectively ionizing chloropicrin in the presence of carbon tetrachloride. It was known from previous work that carbon tetrachloride will not undergo proton transfer reactions in the ion trap; however,

because of the presence of the nitro group on the chloropicrin, it was thought that this compound might undergo proton transfer or at least produce a characteristic adduct ion with the CI reagent. As previously indicated, though, no response could be generated for chloropicrin under proton transfer CI conditions, even though a wide range of proton transfer reagents were examined.

Because of the fact that chloropicrin and carbon tetrachloride cannot be distinguished by DSITMS techniques, they will interfere with one another if they are both present in the same sample. Fortunately, for tear gas analysis, CNS tear gas contains chloropicrin but not carbon tetrachloride. Conversely, CNB tear gas contains carbon tetrachloride but not chloropicrin. At the Federal Laboratories site in Saltsburg, PA, it is believed that CNS tear gas only was disposed of at this site; therefore, carbon tetrachloride is not expected to be an interference in the samples.

#### Chloroform

Chloroform is easily detected in simulated groundwater using the 40-ml VOA sparging technique. It can be readily detected at a concentration of less than 5 ppb and it exhibits a linear dynamic range of at least three orders of magnitude. A typical calibration curve for chloroform in water is shown in **Figure 17**. Although the quantitation mass for chloroform ( $m/z$  83) does have some potential interferences from higher molecular weight chlorinated hydrocarbons under EI fragmentation conditions, these compounds are not frequently encountered in environmental samples. Aliphatic hydrocarbons may also interfere with the  $m/z$  83 quantitation ion; however, the presence of the characteristic chlorine isotope peaks at  $m/z$  85 and  $m/z$  87 can be used to distinguish chloroform from aliphatic hydrocarbons. In fact, the chlorine isotope peaks can be used as alternative quantitation ions for chloroform in the event that aliphatic hydrocarbons may also be present in a sample.

#### 2-Chloroacetophenone and 3-Chloroacetophenone

Even though both 2-chloroacetophenone and 3-chloroacetophenone are not soluble in water at high concentrations, both of these compounds can be dissolved in water at part-per-million concentrations and lower. In spite of the poor solubility of these compounds in water, trace levels of 2-chloroacetophenone and 3-chloroacetophenone are very difficult to purge from water compared with most VOCs, even at elevated temperatures.

Based on the preliminary results of this laboratory study, it was our opinion that the poor purgability of the 2-chloroacetophenone and 3-chloroacetophenone was due primarily to strong interaction of these compounds with the sample matrix (water or soil slurry). However, because the boiling points of 2-chloroacetophenone and 3-chloroacetophenone (247°C and 241°C, respectively) are higher than the boiling points of most compounds that are classified as "volatile organics" (generally less than 200°C), it was suggested by project managers that the poor purgability from water may simply be the result of the high boiling point of the analytes and not a matrix interaction effect.

In order to evaluate the relative effects of matrix interaction versus the boiling point of the chloroacetophenones, several experiments were performed. First, an experiment was performed at ambient temperature (approximately 25°C) in which 40-ml VOA vials of simulated groundwater spiked with either 2-chloroacetophenone or 3-chloroacetophenone were analyzed by DSITMS. Second, the same experiment was performed at elevated temperature (60°C) using the heated purge method. Both the ambient temperature and heated purge experiments were conducted at analyte concentrations in water ranging from 5-1,000 ppb. Finally, a set of experiments was conducted in which a 4-µg aliquot of either 2-chloroacetophenone or 3-chloroacetophenone (in 40 µl of methanol) was added to an empty 40-ml VOA vial, followed by purging of the headspace of the VOA vial. The first two experiments were conducted to evaluate the effects of the boiling point of the analytes and the last experiment was conducted to evaluate the effect of the sample matrix.

#### Ambient temperature purge from water at 25°C

At ambient temperature, the 2-chloroacetophenone and 3-chloroacetophenone were very difficult to purge from water. As shown by the purge profiles in **Figures 18** and **19**, there was very little response at all for the 2-chloroacetophenone (100 ppb) and there was only a very slight response for 3-chloroacetophenone (100 ppb) that slowly increased over a 15-minute time window. For comparison, both **Figures 18** and **19** show the purge profiles corresponding to the analyte of interest (chloroacetophenone), as well as the purge profile for the internal standard, 1,4-difluorobenzene (m/z 114). Note that the purge profile for the 1,4-difluorobenzene is very characteristic of a typical VOC that is easily purged from water.

As can be seen by the 40-ml VOA vial purge profiles for the 1,4-difluorobenzene, VOCs that are easily purged from water typically produce a response that rapidly increases

during the first few seconds of the analysis followed by a rapid decay of the signal over a period of several minutes as the concentration of the VOC in the sample decreases. Because a significant percentage of the total analyte is purged out of the sample during the first few minutes of the analysis, it is usually possible to perform accurate quantitative analysis by this technique using a 3-minute analysis time. For the chloroacetophenones, however, this is not the case. As shown by the purge profile for 3-chloroacetophenone in **Figure 19**, only a very small percentage of the analyte was actually purged from the sample during the first 3 minutes of the sample analysis. Attempts to quantitate the analyte within a 3-minute analysis time would lead to unacceptable error, diminished detection limits, and very poor reproducibility.

In order to perform quantitative analysis of 2-chloroacetophenone or 3-chloroacetophenone in water at ambient temperature, it is necessary to generate purge profiles that span an analysis time of at least 15 minutes. In this case, it is possible to generate reasonably linear response curves for both 2-chloroacetophenone and 3-chloroacetophenone (**Figures 20 and 21**).

Unfortunately, the detection limits under ambient temperature purge conditions are relatively poor. In fact, it appears that the detection limits using ambient temperature purge DSITMS are approximately in the range of 50 ppb for 3-chloroacetophenone and >200 ppb for 2-chloroacetophenone. It should be noted that the response curves shown in **Figures 20 and 21** are plots of background subtracted data that were normalized relative to the integrated response for the 1,4-difluorobenzene internal standard. As can also be seen by these plots, the relative response factor for 2-chloroacetophenone (using  $m/z$  105) compared with 3-chloroacetophenone (using  $m/z$  139) is approximately 0.1. Since it is expected that the response of the ion trap mass spectrometer should be similar for both 2-chloroacetophenone and 3-chloroacetophenone, the measured relative response factor suggests that it is more difficult to purge 2-chloroacetophenone from water than it is to purge the 3-chloroacetophenone from water.

**Note:** The relative response factor is the normalized response for 2-chloroacetophenone divided by the normalized response for 3-chloroacetophenone. The normalized response is the integrated area for the quantitation mass (either  $m/z$  105 or  $m/z$  139) divided by the integrated area of the quantitation mass ( $m/z$  114) for 50 ppb of the internal standard.

#### Heated Purge from Water at 60°C

Heating of water samples to 60°C while sparging greatly increases the response for both 2-chloroacetophenone and 3-chloroacetophenone relative to the response obtained at ambient temperature. However, as shown by the purge profiles for 2-chloroacetophenone and 3-chloroacetophenone in **Figures 22** and **23**, both compounds exhibit a slow increase in response over a 15-minute analysis time, even with heating. As was the case with ambient temperature 40-ml VOA vial sparge analysis, only a small percentage of the analyte was actually purged from the water during the initial 3 minutes of the analysis. By comparison, the internal standard 1,4-difluorobenzene is almost completely purged from the sample during the first 3 minutes of the analysis. Note the difference in the purge profiles for 1,4-difluorobenzene in **Figures 22** and **23** at 60°C versus the purge profiles shown in **Figures 18** and **19** at ambient temperature.

Response curves for 2-chloroacetophenone and 3-chloroacetophenone generated under heated purge conditions are shown in **Figures 24** and **25**, respectively. As can be seen by the normalized response relative to the internal standard, the relative response factor for the 2-chloroacetophenone ( $m/z$  105) compared with 3-chloroacetophenone ( $m/z$  139) is again approximately 0.1. By comparing the response data shown in **Figures 24** and **25** with the response data shown in **Figures 20** and **21**, it can be seen that heating the sample provides up to a factor of 15 increase in response compared with ambient temperature sparging.

Under heated purge conditions at 60°C, the detection limit for 3-chloroacetophenone in water is approximately 5 ppb (or less) and for 2-chloroacetophenone, it is in the range of 50 ppb (or less). Although it should be possible to use heated purge DSITMS to quantitatively analyze water samples for 2-chloroacetophenone or 3-chloroacetophenone, a sample analysis time of at least 15 minutes would be required. This would ensure that a sufficient mass of the analyte has been purged from the sample to produce a stable and reproducible response by the mass spectrometer. Conversely, if one attempted to quantitate these two compounds in water within the typical 2-3 minute DSITMS analysis time, the result would be a loss of accuracy, poor precision, and higher diminished detection limits.

#### *Results for 40-ml Sparge Analysis of Soil Samples*

All soil samples were analyzed using the 40-ml VOA sparging technique. The samples were all prepared as water slurries, as previously described, and heated to 60°C during

the sparging process. All other conditions were the same, as previously described, for the analysis of water samples.

#### Chloroform and Chloropicrin

Both chloroform and chloropicrin were easily detected in soil samples using the 40-ml VOA vial sparging technique. The purge profiles, detection limits, and linear dynamic range were very similar to those for chloroform and chloropicrin in water.

#### 2-Chloroacetophenone and 3-Chloroacetophenone

As can be seen by the purge profiles for 2-chloroacetophenone and 3-chloroacetophenone in **Figures 26** and **27**, they are surprisingly similar to those that were produced by heated purge analysis of water samples. This suggests that the analyte-matrix interactions with the standard soil that was used are less than the analyte-water interactions. These results could also suggest that the way in which the soil samples were prepared did not provide sufficient time for the analyte to bind with the soil particles prior to analysis. Regardless, these results for soil can be considered to be a "best case scenario" and it is likely that the performance for real-world soil samples contaminated with either analyte will be worse. As was shown to be the case for the water samples, it is also true for the soil slurry samples that insufficient analyte is purged from the sample during the first 3 minutes of the analysis to permit accurate quantitation. Over a 10- to 15-minute analysis window, however, it is possible to generate linear response curves with detection limits for soil in the range of 50-80  $\mu\text{g/kg}$  for 3-chloroacetophenone and 500-800  $\mu\text{g/kg}$  for 2-chloroacetophenone. As can be seen by the response curves in **Figures 28** and **29**, the relative response factor for the 2-chloroacetophenone ( $m/z$  105) relative to 3-chloroacetophenone ( $m/z$  139) in a soil slurry is approximately 0.15. These data suggest that both the absolute and relative response for a soil slurry is similar to those for heated purge analysis of plain water samples.

#### *Effect of Water on Purgability*

As demonstrated by the example DSITMS purge profiles for both 2-chloroacetophenone and 3-chloroacetophenone in water, neither compound can be quickly or easily purged, even with moderate heating. This could primarily be due to the relatively high boiling points of 2-chloroacetophenone and 3-chloroacetophenone (247°C and 241°C, respectively) or it could be due to interaction of the analytes with the water matrix (or a combination of both).



In order to try to assess these effects, a set of experiments was performed in which 4 µg of either 2-chloroacetophenone or 3-chloroacetophenone were added to an empty 40-ml VOA vial by injecting 40 µl of a 100-ng/µl solution of the compound in methanol into a clean vial. The vial was then analyzed at ambient temperature (25°C) by purging the headspace of the VOA vial with 100 ml/min of helium directly into the ion trap mass spectrometer.

As shown by the example purge profiles in **Figures 30** and **31**, both 2-chloroacetophenone and 3-chloroacetophenone were completely purged from the sample vial within 4 minutes of the start of the analysis. It can also be seen from these data that the shape of the purge profiles for the 2-chloroacetophenone and 3-chloroacetophenone are not significantly different from those for the 1,4-difluorobenzene internal standard. The anomaly during the first 30 seconds of the purge profiles was likely due to the rapid evaporation of the methanol that was used as the solvent for the chloroacetophenones.

The data shown by the purge profiles in **Figures 30** and **31** suggest that in the absence of the water matrix, both 2-chloroacetophenone and 3-chloroacetophenone can be easily and efficiently purged from a sample vial, even at ambient temperature. These data further suggest that when purging microgram quantities or less of the chloroacetophenones from a sample container in the absence of a matrix, the high boiling points of these compounds are not a significant factor in their detectability using the 40-ml VOA vial sparging method. In fact, these data suggest that the poor analytical performance of 2-chloroacetophenone and 3-chloroacetophenone is almost entirely due to strong analyte-matrix interactions.

#### *Results for In-situ Sparge of Groundwater Samples*

No actual groundwater samples were analyzed by in-situ sparge as part of this work. All of the methods development work was performed in the lab using glass containers filled with simulated groundwater that was spiked with known amounts of the targeted analytes. A standard in-situ sparging probe and 150-ft sample transfer line were used for this study. The transfer line was not heated and was coiled up except for a few feet of the ends that were attached to the ion trap and the probe head. An example mass spectrum of an in-situ sparge experiment is shown in **Figure 32**. Results for each analyte are described below.



### Chloropicrin

Chloropicrin was easily detected in water at less than 5 ppb using the in-situ probe. No significant carryover problems were observed for this compound. As was the case with the 40-ml VOA vial sparging method, there is the same potential for interference from carbon tetrachloride if it is also present in the sample. An example calibration curve for chloropicrin in water by in-situ sparge is shown in **Figure 33**.

### Chloroform

Chloroform is also easily detected by the in-situ sparge method. It is possible to detect this compound at a concentration of less than 5 ppb. As was the case with chloropicrin, no significant sample carryover problems were encountered and no significant interferences were identified. An example calibration curve for chloroform in water by in-situ sparge is shown in **Figure 34**.

### 2-Chloroacetophenone and 3-Chloroacetophenone

As demonstrated by the results of the 40-ml VOA vial sparging method, it is very difficult to purge 2-chloroacetophenone and 3-chloroacetophenone from water. This problem is even worse for the in-situ sparge method because groundwater is typically at a temperature of approximately 15°C, which is even lower than the ambient temperature purge conditions used in the laboratory. Because there is currently no means of heating the in-situ sparging probe and sample transfer line, it is virtually impossible to use this probe to efficiently purge 2-chloroacetophenone and 3-chloroacetophenone from water. In addition, the extreme length of the sample transfer line in itself represents a major challenge to the transport of chloroacetophenone vapors into the mass spectrometer.

Attempts to analyze 2-chloroacetophenone and 3-chloroacetophenone by in-situ sparge were basically unsuccessful. It was found that there was approximately a 30-minute delay between the start of an analysis and the time at which a response for the compounds could be measured with the ion trap mass spectrometer. Even worse, once the in-situ sparging probe had been removed from the sample and decontaminated, carryover in the transfer line was severe enough to produce a background signal from the chloroacetophenones for more than 1 hour.

Because of these problems, it has been determined that the in-situ sparging probe is not suitable for the analysis of 2-chloroacetophenone or 3-chloroacetophenone.

However, if a heated version of this probe is eventually developed, it is possible that the performance for these two compounds will improve considerably.

*Analysis of Field Samples From the Federal Laboratories Site in Saltsburg, PA*

In order to assist ORNL in optimizing the methods for CNS tear gas components in water and soil, TVA provided ORNL with a couple of representative water and soil samples that were collected at the Federal Laboratories site in Saltsburg, PA. The main objective of analyzing the field samples was to identify any contaminants in the samples other than CNS tear gas that might have caused an interference with the quantitation of the targeted analytes.

ORNL was provided with two replicates of water samples in 1-liter containers from two different monitoring wells (a total of four samples). The groundwater samples were simply identified as "sample 1" and "sample 2." Information provided with the samples indicated that "sample 1" was suspected of being clean while "sample 2" was suspected of being contaminated with CNS tear gas compounds.

The water samples were analyzed by the 40-ml VOA vial sparge method using a heated purge at 60°C. The results of the analyses indeed confirmed that "sample 1" was clean and that "sample 2" was contaminated with chloropicrin, chloroform, and a few other common VOCs. Each sample was analyzed in duplicate and the results of the two analyses were averaged. As shown in **Table 1**, "sample 2" was found to be contaminated with approximately 100 ppm of chloropicrin, 13 ppm benzene, 2 ppm total xylenes, 600 ppb toluene, and 500 ppm of chloroform. It is feasible that the benzene, xylenes, and possibly toluene are the result of breakdown of 2-chloroacetophenone; however, their presence in the sample is more likely the result of contamination by gasoline.

In addition to the water samples, ORNL was provided with two soil samples that were identified as "sample 1A" and "sample 9." Both of these soil samples were analyzed by the 40-ml VOA vial sparging method using a heated purge at 60°C. For the analysis of these samples, 5-g aliquots of the soil were prepared as water slurries as previously described.

The results for the DSITMS analysis indicated that neither "sample 1A" or "sample 9" was contaminated with chloropicrin, 2-chloroacetophenone, or 3-chloroacetophenone. Interestingly, "sample 9" was found to be contaminated with 66 ppb of chloroform.

Neither soil sample was found to have contamination from benzene, toluene, or xylenes as was observed in the water samples. These results are also summarized in **Table 1**.

Because the results of the DSITMS analysis indicated that the water and soil samples were either clean or contaminated with only a few compounds, it was determined that GC/MS analysis of these samples would not provide any significant additional qualitative or quantitative information that would be helpful in optimizing the DSITMS method. Therefore, it was decided that the high cost of GC/MS analysis of these samples could not be justified and was not performed.

### *Performance Data*

#### Detection Limits

Experiments using authentic standards of chloroform and chloropicrin clearly demonstrate that these two compounds can be detected at ambient temperature in water at concentrations of less than 5 ppb using either the 40-ml VOA vial sparging method or the in-situ sparging probe. Using the 40-ml VOA sparging method, both of these compounds can be quantitated in water or soil samples using a 3-minute analysis time. The total time required to quantitate these compounds by the in-situ sparging method is approximately 5-15 minutes per groundwater well. If depth profiling is performed, it currently requires approximately 1 minute per foot of depth over the interval that is profiled.

In order to detect 2-chloroacetophenone in water at a concentration of less than 50 ppb and 3-chloroacetophenone in water at a concentration of less than 5 ppb, it is necessary to use the 40-ml VOA vial sparging method while heating the sample to 60°C. The time required for quantitation of these two compounds is approximately 15 minutes. Neither 2-chloroacetophenone nor 3-chloroacetophenone is suitable for in-situ sparge analysis.

#### Precision and Accuracy

The precision and accuracy of the 40-ml VOA vial sparge method were only evaluated for chloroform and chloropicrin. Because of the difficulties with purging 2-chloroacetophenone and 3-chloroacetophenone from water within a 3-minute analysis, we do not consider this method to be quantitative for these two compounds. As a result, both 2-chloroacetophenone and 3-chloroacetophenone were excluded from the P&A study.

The P&A study involved the analysis of four replicate samples of water that were spiked with 25 ppb each of chloropicrin and chloroform in 40-ml VOA vials of water. These samples were analyzed, as previously described, and the concentration of chloroform and chloropicrin was determined in each sample.

The results of these samples permitted calculation of mean and standard deviation (SD) for the concentration of the two analytes. For chloropicrin, the mean value was determined to be 23 ppb and the standard deviation was determined to be  $\pm 0.71$ . For chloroform, the mean concentration was found to be 23 ppb and the standard deviation was determined to be  $\pm 1.5$ . These results are also summarized in Table 2 and indicate that the precision and accuracy for these two compounds is within 10% which compares favorably with the performance of DSITMS for many other non-polar VOCs.

#### Analysis of Performance Samples for Water

In order to evaluate the quantitative accuracy of the 40-ml direct sparge method, we analyzed two 40-ml blind spiked water samples (high and low concentration) for each individual analyte (chloroform and chloropicrin). These samples were prepared by internal lab personnel.

For chloropicrin, the recovery was found to be in the range of 97% to 106% and for chloroform, the recovery ranged between 89% and 91%, as shown in **Table 3a**. The low-level chloropicrin and chloroform samples were spiked with 12.5 ppb of analyte. The concentrations that were found were 12.2 ppb and 11.1 ppb, respectively, corresponding to an error of 3% and 11%. The high-level performance samples were spiked with chloropicrin and chloroform to produce a solution concentration of 62.5 ppb for each analyte. The found concentrations by DSITMS were 66.3 ppb for the chloroform and 56.7 ppb for the chloropicrin. This corresponds to an error of 6% and 9%, respectively, relative to the known concentration.

#### Analysis of Performance Samples for Soil

Performance for soil was determined by analyzing soil samples that had been spiked with chloropicrin and chloroform. For this experiment, 5-g aliquots of a standard soil sample were spiked with 400 ppb of chloropicrin and chloroform.

Because soil matrices are far more complicated than water in terms of the interaction with analytes, many compounds are not easily purged from soil or soil slurries.

Therefore, the results showed a significantly lower recovery than the water results. For chloropicrin, the percent recovery ranged between 48% and 58% and for chloroform, the percent recovery ranged between 24% and 30%, as shown in **Table 3b**. For this reason, calibration curves for soil analysis should be generated using a soil type that is very similar in composition to the soil from the site where the samples are collected.

Interestingly, the soil recovery study indicates that the percent recovery for chloropicrin is approximately twice that for chloroform. This is a bit surprising since it would have been expected that the interaction of the chloropicrin with soil would be greater than that of the chloroform. Although these results suggest that the chloroform interacts more strongly with the sample matrix than the chloropicrin, it is also possible that the lower recovery for chloroform may simply be due to faster evaporation of chloroform from the sample.

#### In-situ Sparge Performance

Detection limits for chloroform and chloropicrin were found to be less than 5 ppb and both compounds exhibited good linearity over a dynamic range of at least  $10^3$ . As expected, neither 2-chloroacetophenone nor 3-chloroacetophenone could be observed by this method due to the fact that the probe head and sample transfer line could not be heated.

Because of the nature of this type of analysis, replicate samples are not typically analyzed. Therefore, figures of merit such as mean and precision cannot be determined. Additionally, since no field work was actually performed, no comparative data was generated between the performance of the in-situ probe and the 40-ml VOA vial sparger for a real groundwater sample at the Federal Laboratories site in Saltsburg, PA.

## **CONCLUSION**

The results of this study clearly demonstrate that DSITMS has significant potential for the rapid analysis of water samples contaminated with chloroform and chloropicrin, which are two of the components of CNS tear gas. Because of difficulties in the purging and transport of 2-chloroacetophenone and 3-chloroacetophenone from water and soil, these compounds are considerably more difficult and time consuming to quantitatively determine by DSITMS. However, the qualitative identification of these

compounds in a sample that also is contaminated with chloropicrin and chloroform is good evidence for the presence of CNS tear gas contamination.

For laboratory-based screening and quantitative analysis applications, 40-ml discrete sample sparging can be used effectively. In the field, it is also possible to utilize the in-situ sparging probe for the analysis of chloroform and chloropicrin in groundwater wells. Detection limits are in the range of 5 ppb for water samples and the precision is typically better than  $\pm 10\%$ . Soil samples are more difficult to analyze than water samples and have a recovery of as little as 25% of that for the same compounds in water. Detection limits are in the low ppb range for chloroform and chloropicrin in soil, but are expected to vary with the specific type of soil.

Work has continued at ORNL on the further development of DSITMS instruments and methods for the rapid analysis of water and soil samples. A general method (8265) is currently under consideration by EPA for inclusion in the SW-846 manual (4). Work performed under this task has been compiled into a shorter method that is specific to the analysis of chloroform, 2-chloroacetophenone, 3-chloroacetophenone and chloropicrin and water and soil. A copy of this method has also been submitted to TVA and AEC for their use.

## References

1. Marcus B. Wise and Michael R. Guerin, "Direct Sampling MS for Environmental Screening," *Analytical Chemistry*, 1997, 69,26A-32A.
2. Marcus B. Wise, Cyril V. Thompson, Roosevelt Merriweather, and Michael R. Guerin, "Review of Direct MS Analysis of Environmental Samples," *Field Analytical Chemistry and Technonogy*, 1997, 1(5), 251-276.
3. W. M. Davis, M. B. Wise, J. S. Furey, and C. V. Thompson, "Rapid Detection of Volatile Organic Compounds in Groundwater by In-Situ Purge and Direct Sampling Ion Trap Mass Spectrometry," *Field Analytical Chemistry and Technonogy*, 1998, 2(2), 89-96.
4. Marcus B. Wise, Michael R. Guerin, Roosevelt Merriweather, and Cyril V. Thompson, "Direct Sampling Ion Trap Mass Spectrometry For the Measurement of Volatile Organic Compounds in Water, Soil, and Air," Proposed Method 8265 for US EPA SW-846 Manual, Oak Ridge National Laboratory, 1997.

**Table 1**

**Water and Soil Samples From the Federal Laboratory Site  
(DSITMS Results)**

<b>Sample ID</b>	<b>Chloropicrin</b>	<b>Chloroform</b>	<b>Benzene</b>	<b>Toluene</b>	<b>Xylenes</b>
GW1 #1	<5 ppb	<5 ppb	<5 ppb	<5 ppb	<5 ppb
GW1 #2	<5 ppb	<5 ppb	<5 ppb	<5 ppb	<5 ppb
GW2 #1	89 ppm	459 ppm	13 ppm	557 ppb	2.5 ppm
GW2 #2	100 ppm	493 ppm	13 ppm	+	1.7 ppm
Soil 1A	ND	ND	ND	ND	ND
Soil 9	ND	66 ppb	ND	ND	ND

ND = Not Detected

+ = Detected but not quantitated



**Table 2**

**Precision Results for Chloropicrin and Chloroform in Water**

Replicate #	Chloropicrin (ppb)	Chloroform (ppb)
1	23	22
2	23	23
3	24	25
4	22	21
Mean	23	23
Standard Deviation	0.71	1.5

**Table 3a**

**Accuracy (% Recovery) Results for Chloropicrin and Chloroform  
in Blind QC Water Samples**

Sample #	Chloropicrin			Chloroform		
	Known Conc.	Found Conc.	% Recovery	Known Conc.	Found Conc.	% Recovery
1	12.5 ppb	12.2 ppb	97%	12.5 ppb	11.1 ppb	89%
2	62.5 ppb	66.3 ppb	106%	62.5 ppb	56.7 ppb	91%

**Table 3b**

**Recovery Results for Chloropicrin and Chloroform  
in Soil Samples Spiked at Known Concentrations**

Sample #	Chloropicrin			Chloroform		
	Known Conc.	Found Conc.	% Recovery	Known Conc.	Found Conc.	% Recovery
1	400 ppb	192 ppb	48%	400 ppb	120 ppb	30%
2	400 ppb	232 ppb	58%	62.5 ppb	96 ppb	24%

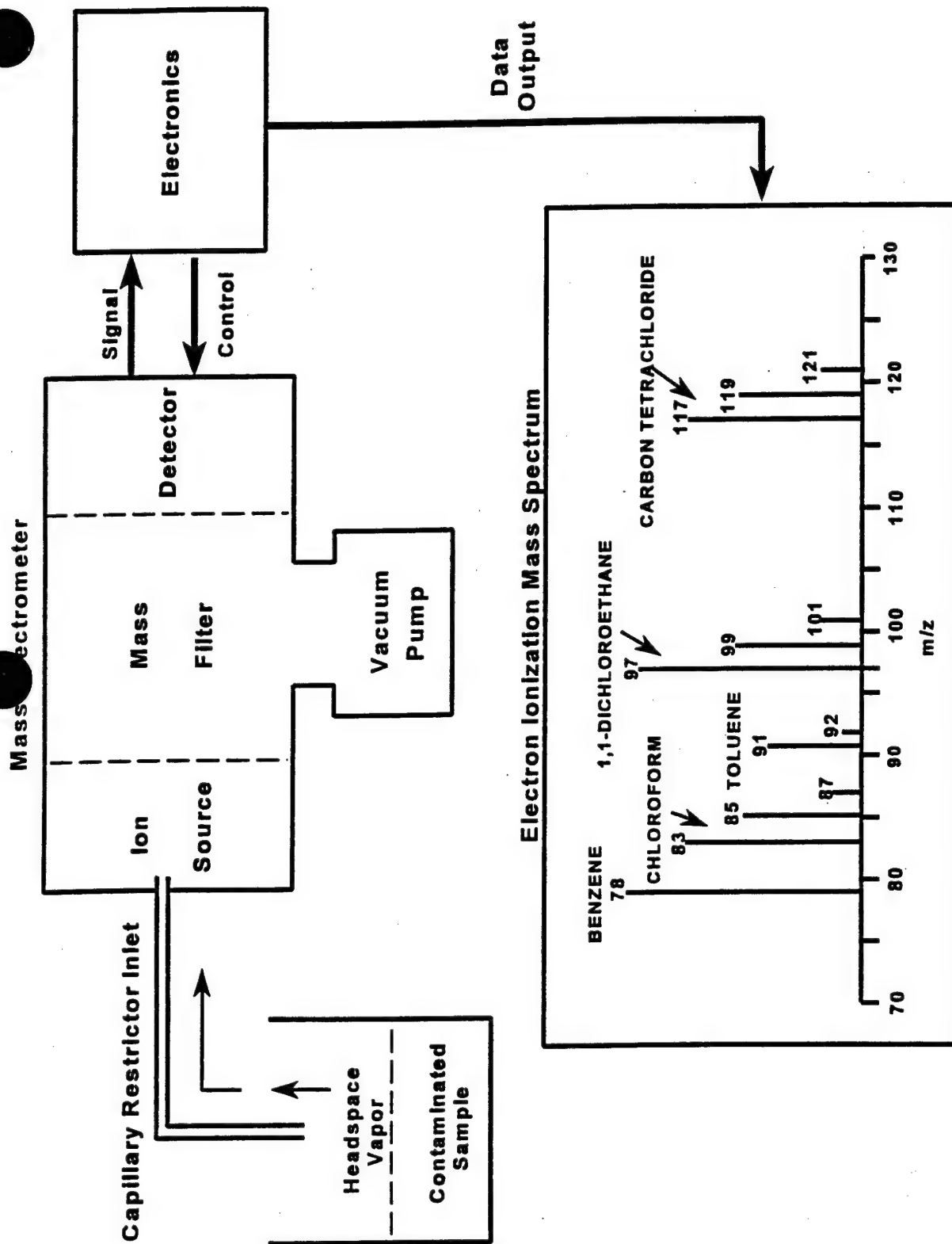


Figure 1: Schematic Diagram of DSITMS

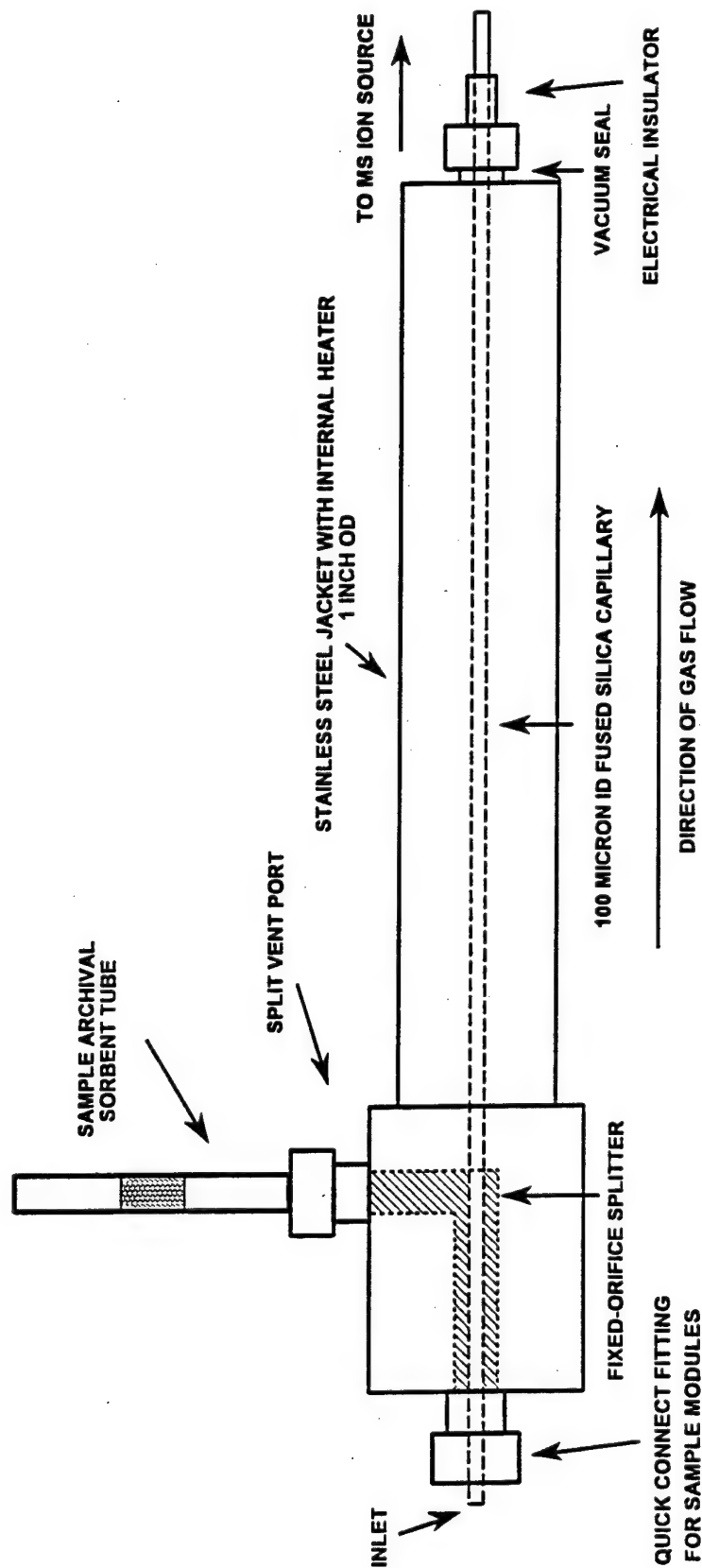


Figure 2: Capillary Restrictor Interface and Sample Splitter

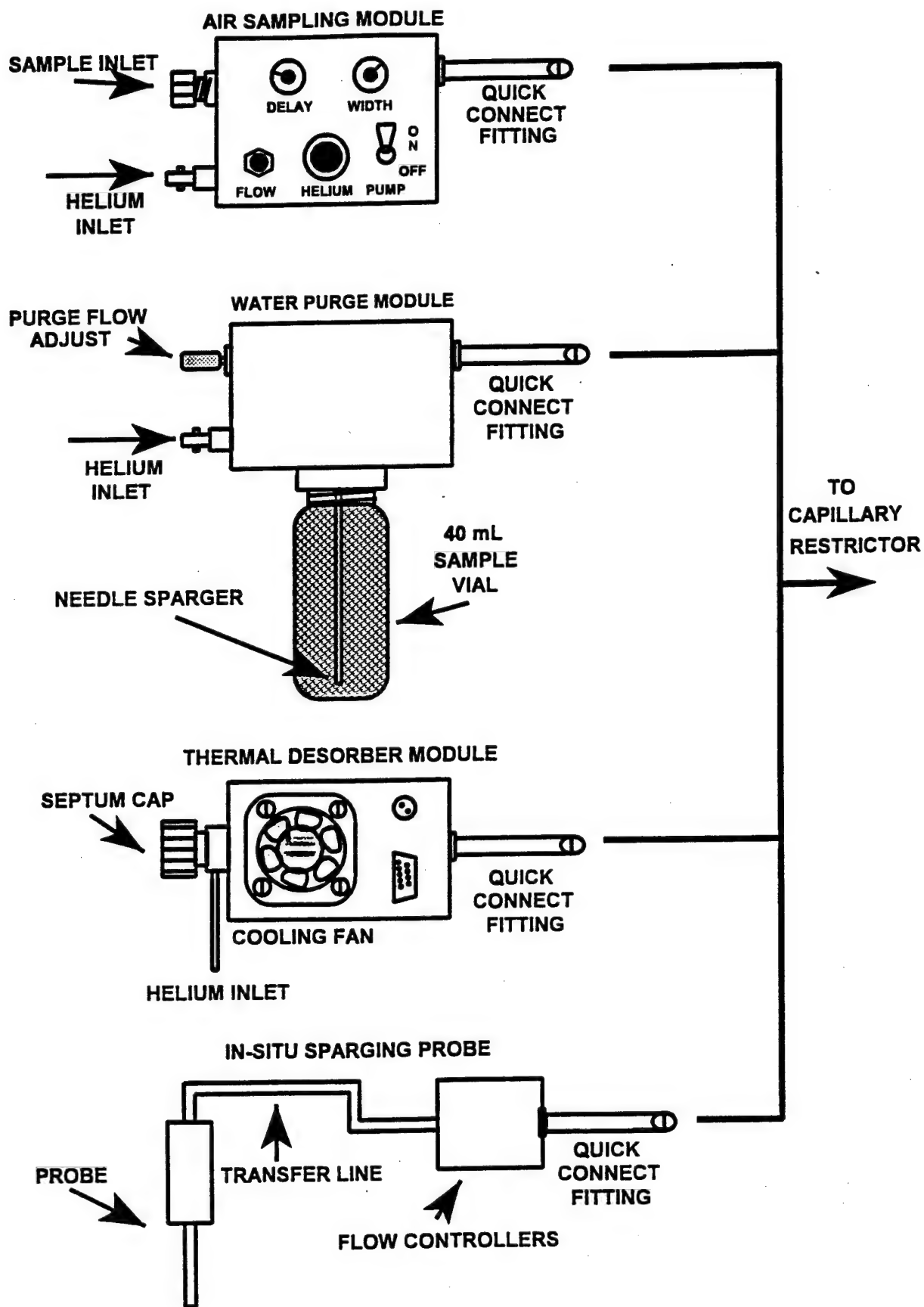


Figure 3: Example DSITMS Sample Inlets



Figure 4: Photograph of a DSITMS Instrument

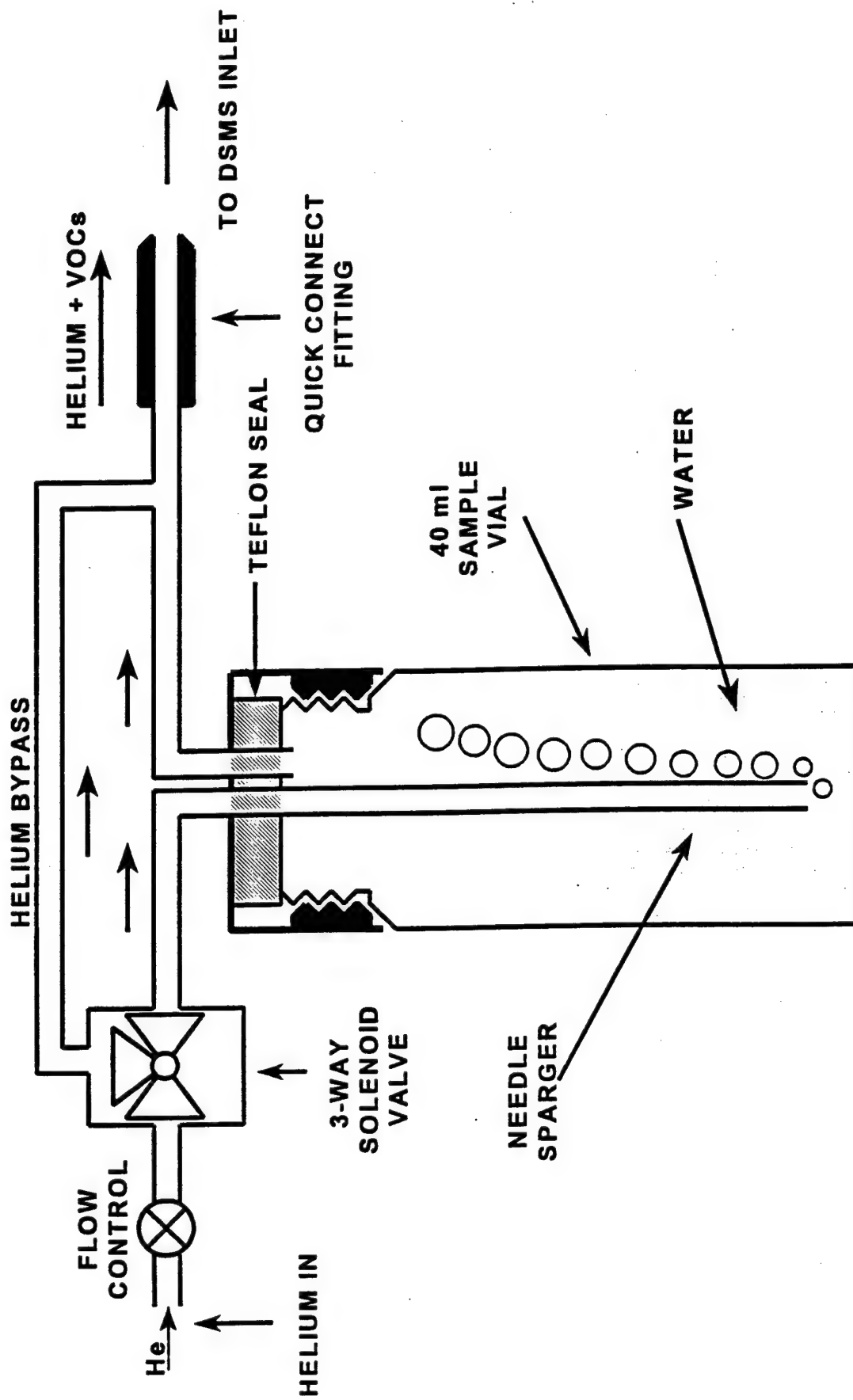


Figure 5: 40 ml VOA Vial Sparging Module

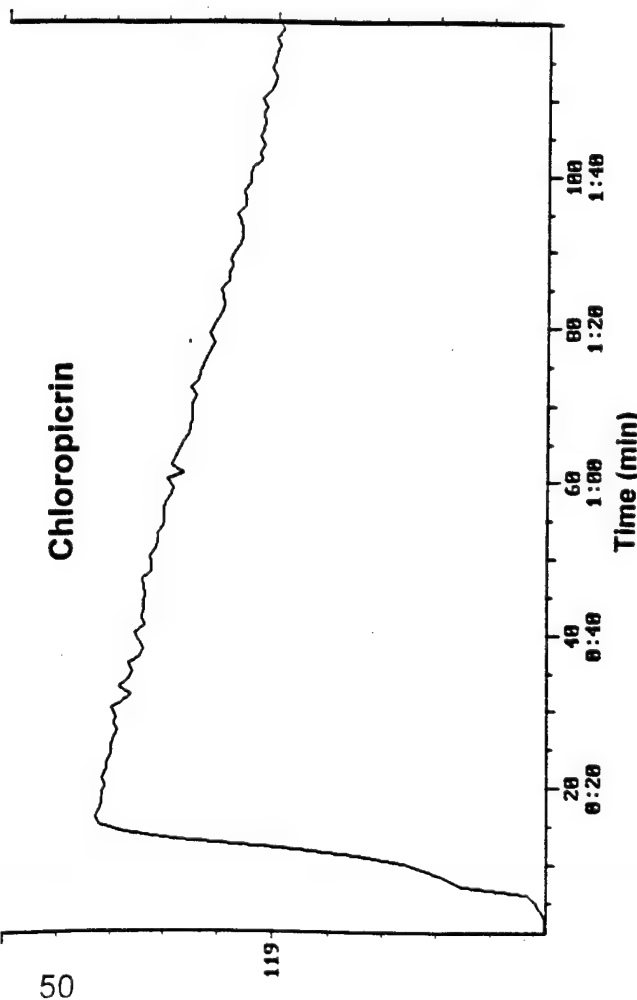
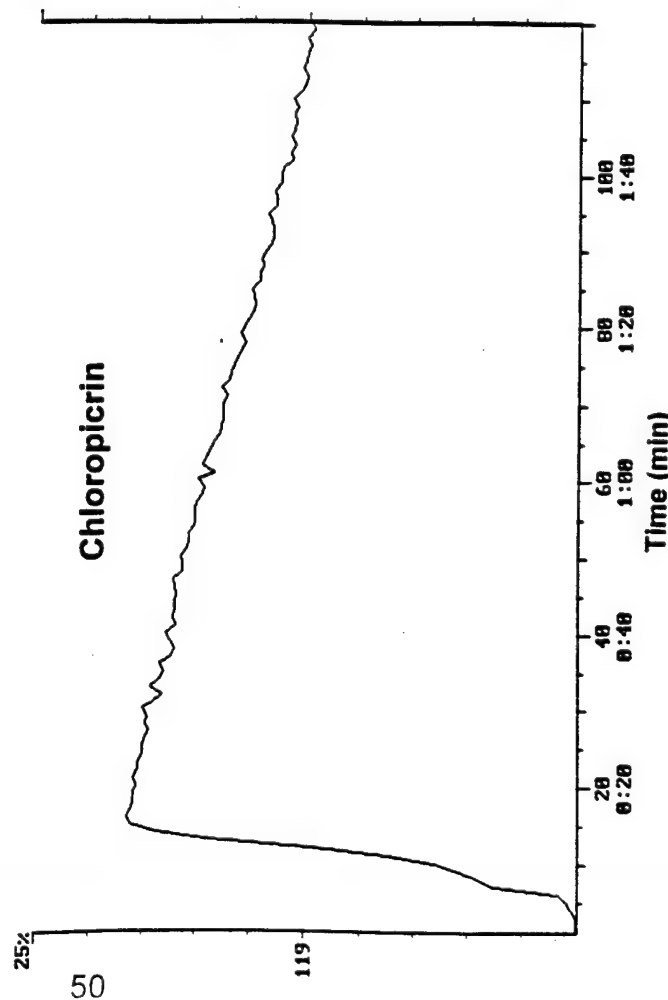
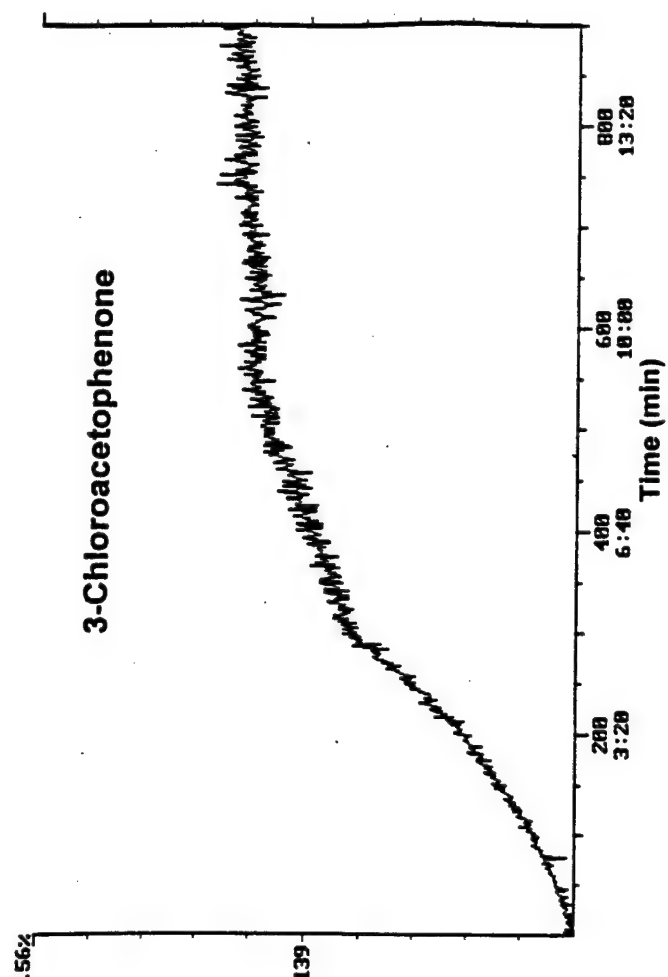
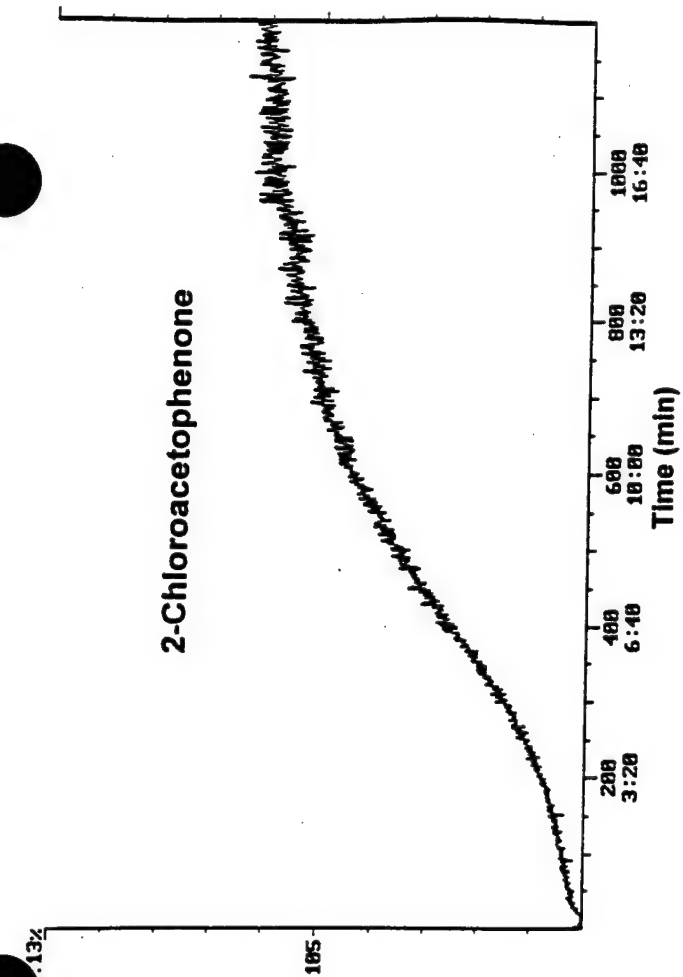


Figure 6: Example Purge Profiles for VOCs in Water



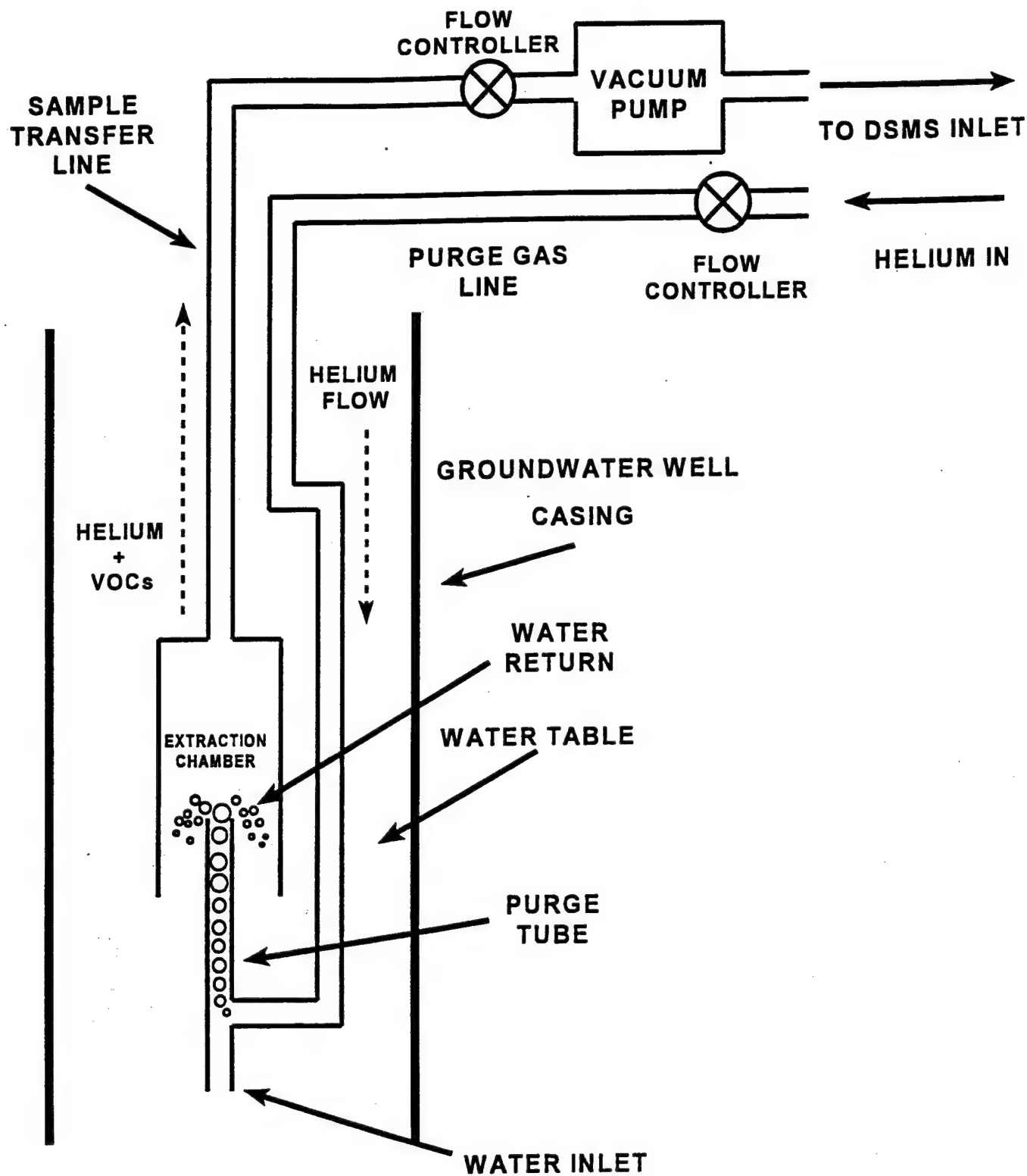


Figure 7: In-Situ Sparging Probe for VOCs in Groundwater Wells

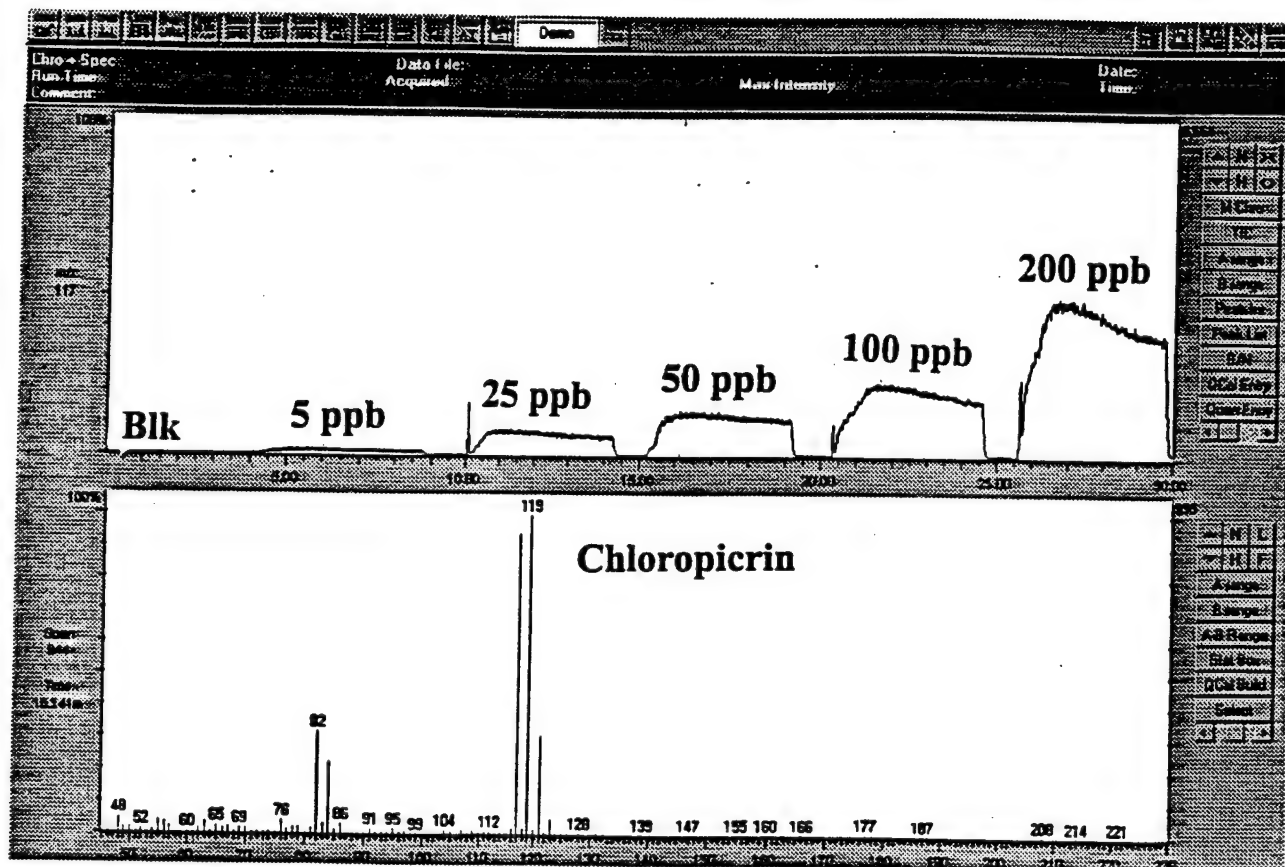


Figure 8: Response Profiles for In-Situ Sparge of Chloropicrin in Water

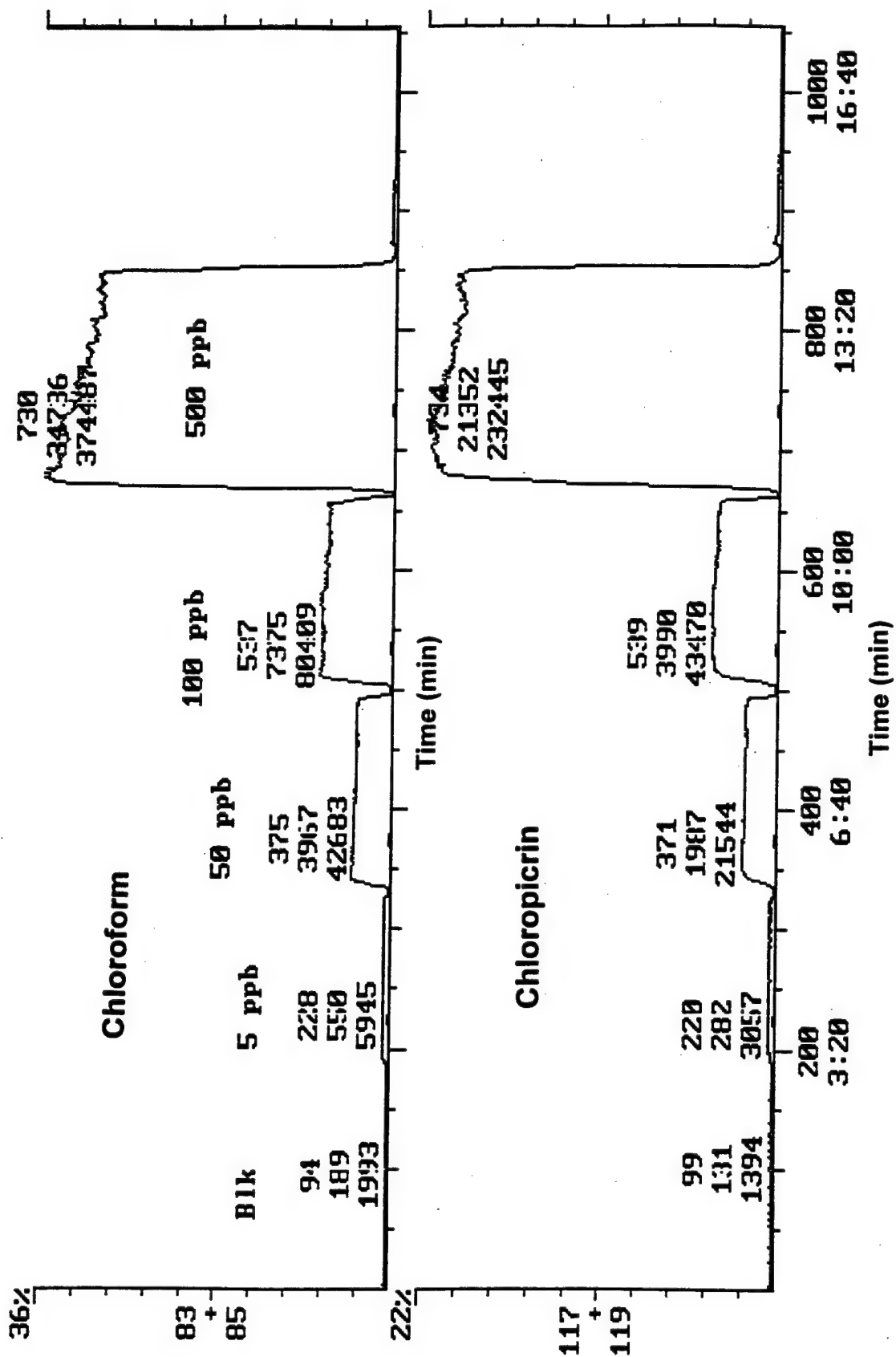


Figure 9: In-Situ Sparge Profiles for Chloroform and Chloropicrin

# Electron Ionization Mass Spectrum

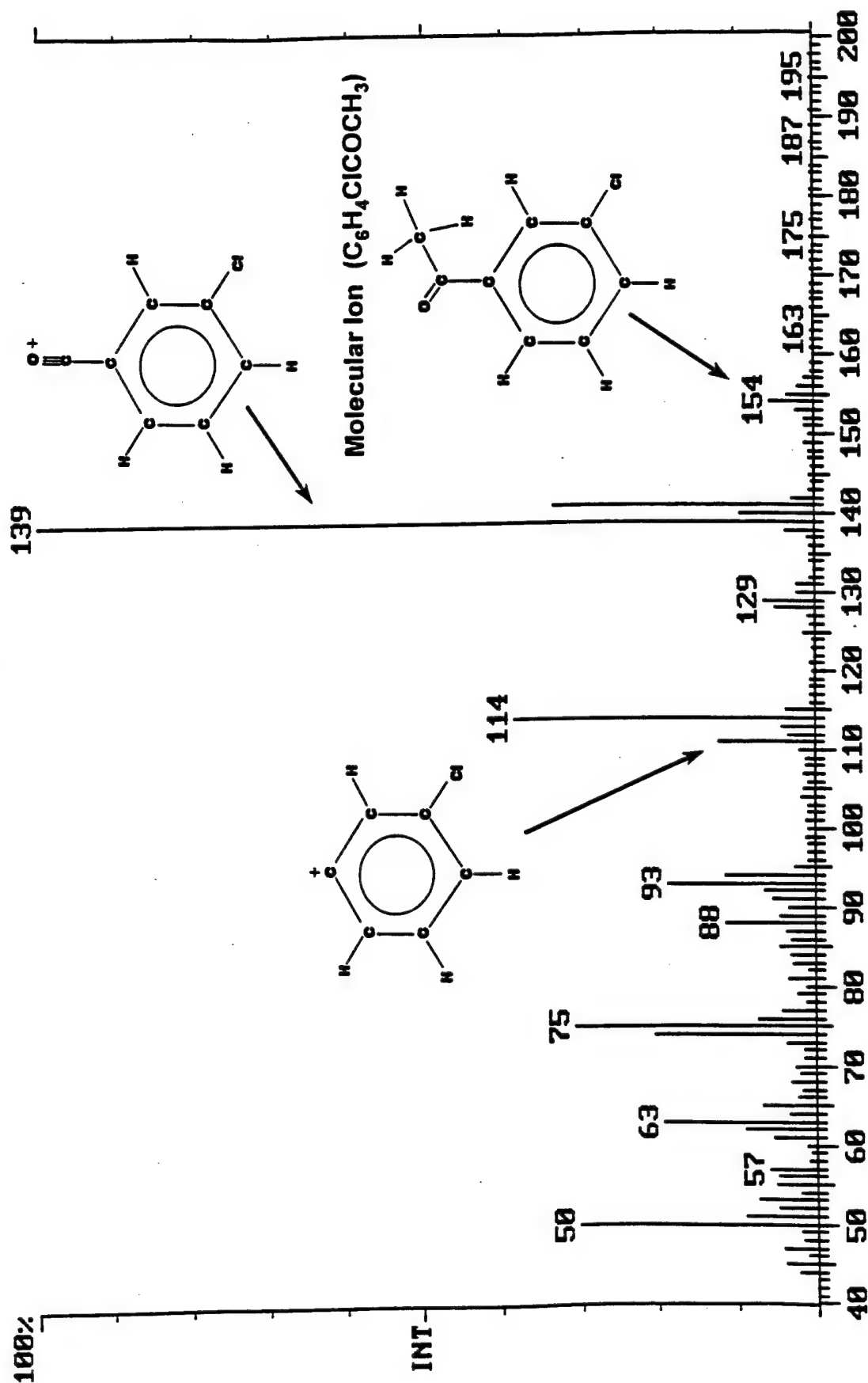


Figure 10: EI Mass Spectrum of 3-Chloroacetophenone

# Electron Ionization Mass Spectrum

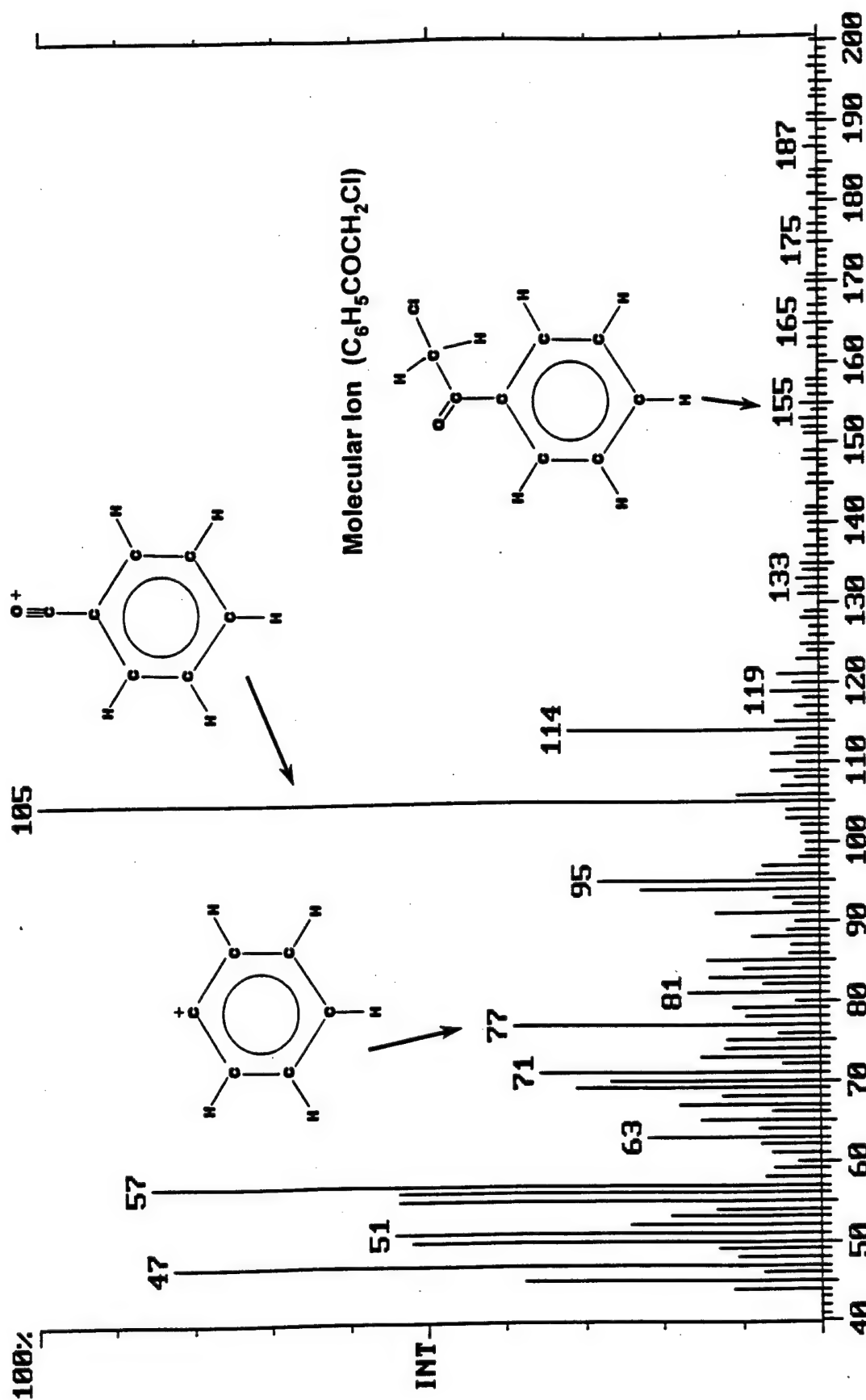


Figure 11: EI Mass Spectrum of 2-Chloroacetophenone

# Electron Ionization Mass Spectrum

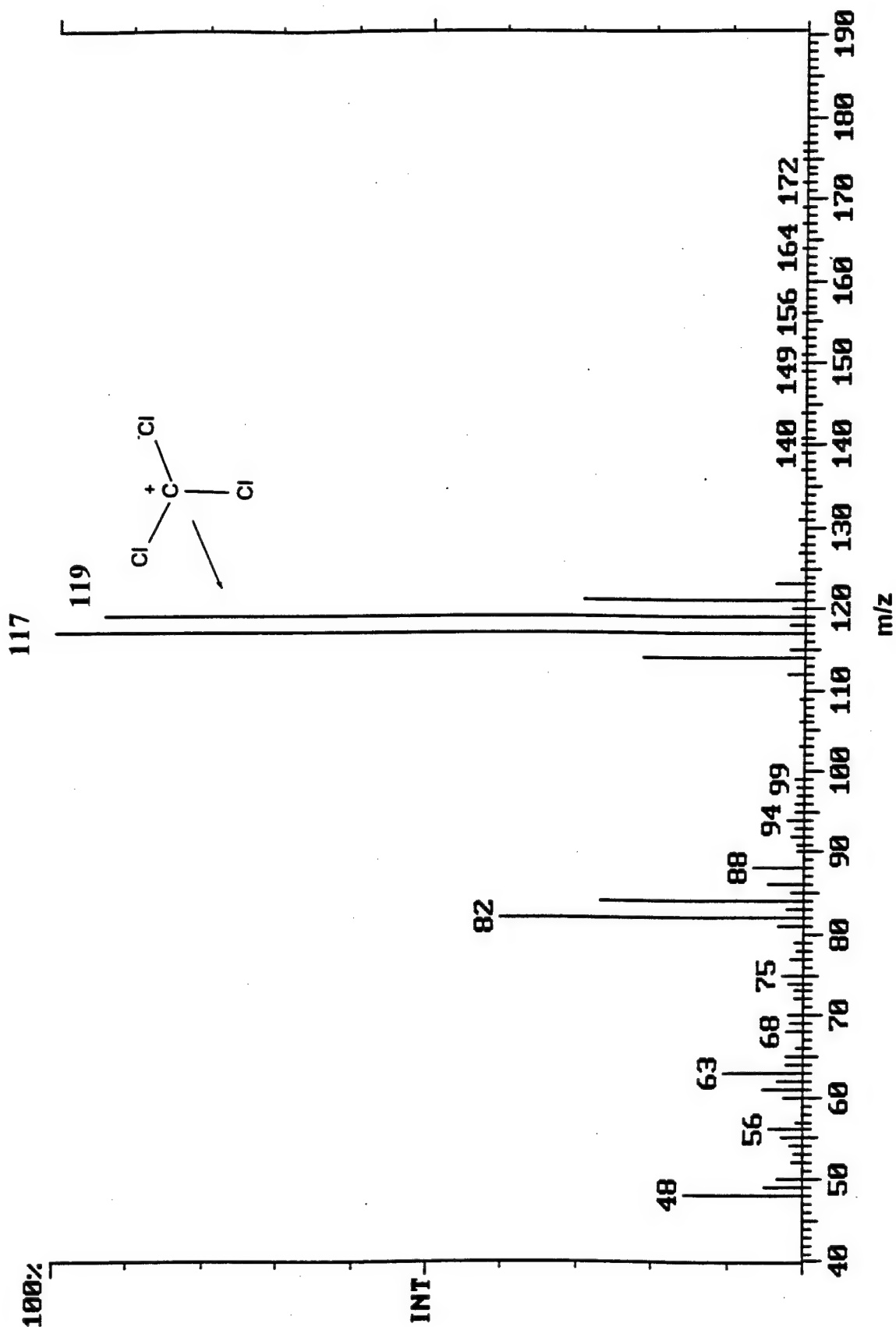


Figure 12: EI Mass Spectrum of Chloropicrin

# Electron Ionization Mass Spectrum

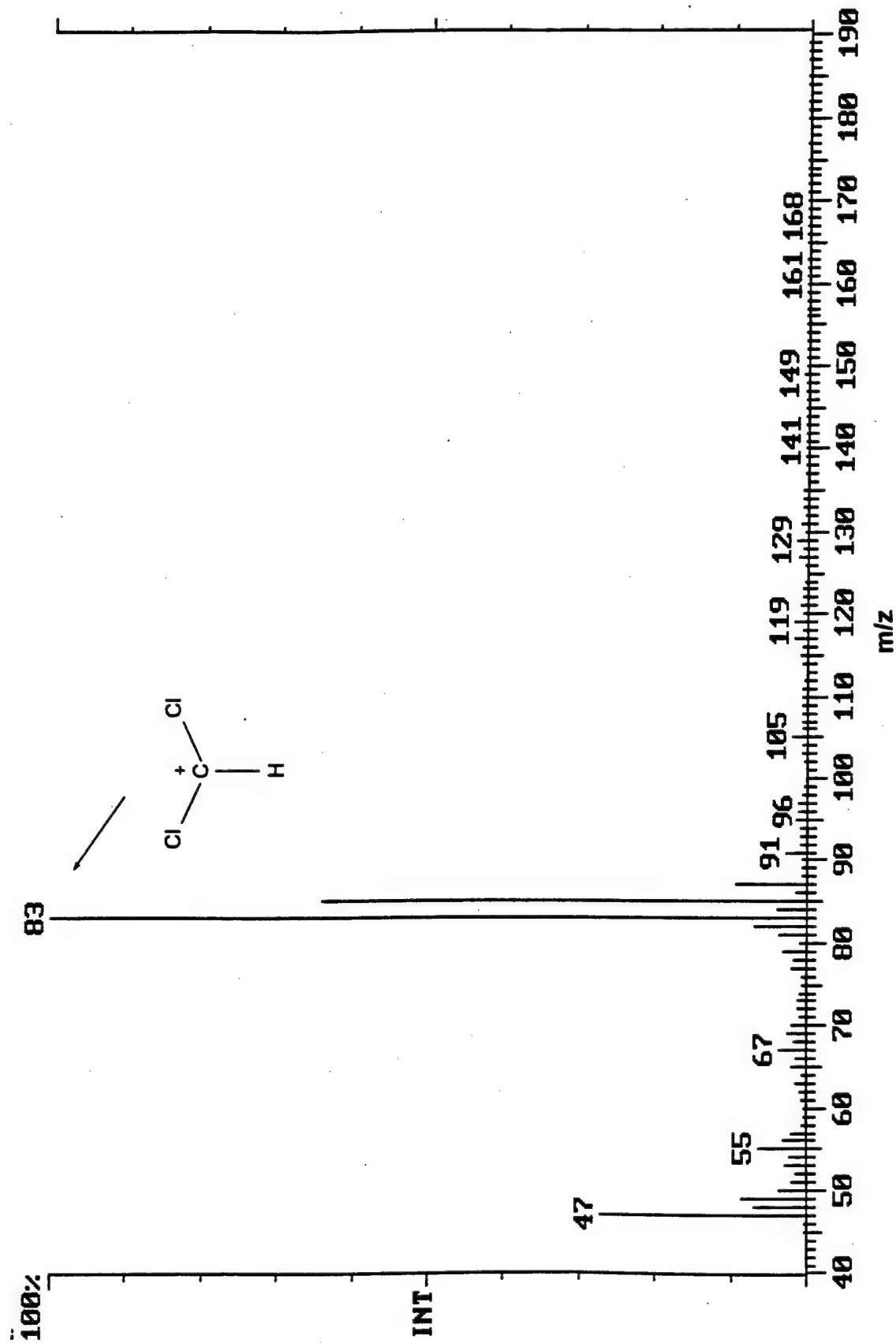


Figure 13: EI Mass Spectrum of Chloroform

# Electron Ionization Mass Spectrum

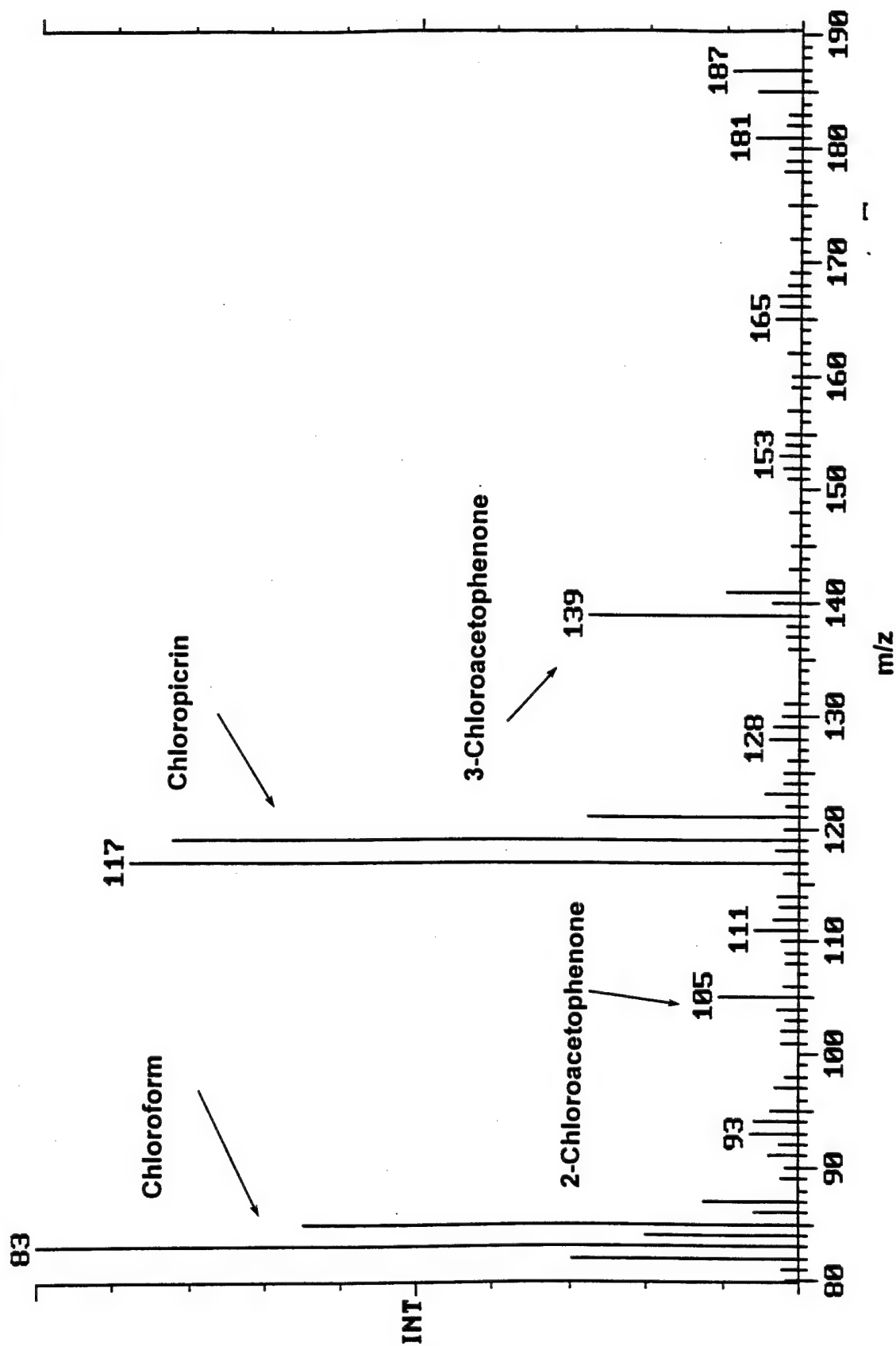


Figure 14: Composite EI Mass Spectrum of Chloroform, Chloropicrin, 2-Chloroacetophenone, and 3-Chloroacetophenone



Chloropicrin in Water  
Ambient Temperature Purge

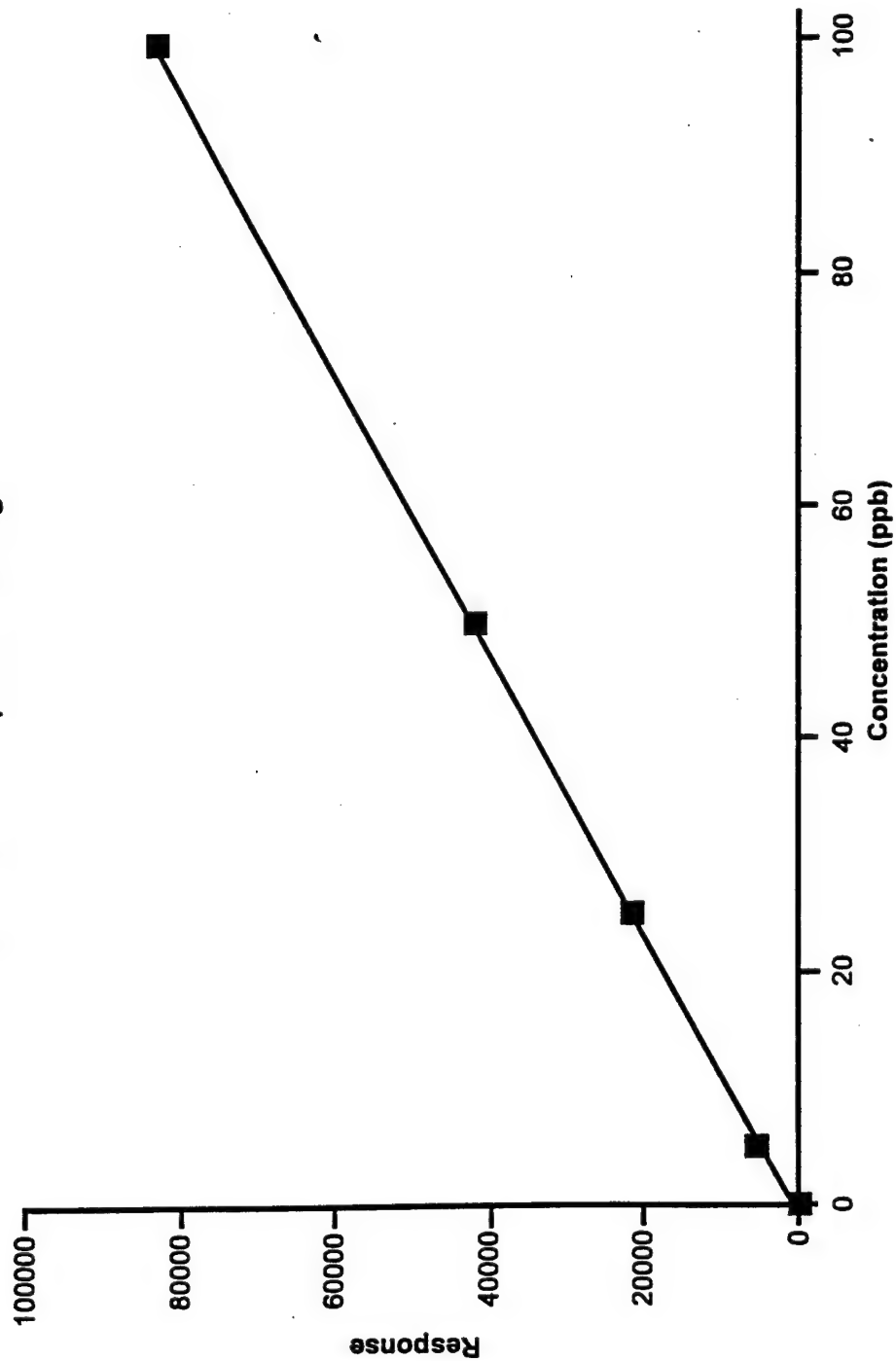


Figure 15: Calibration Curve for Chloropicrin in Water: 40 ml VOA Vial  
Spurge at Ambient Temperature (5 - 100 ppb)

Chloropicrin in Water  
Ambient Temperature Purge

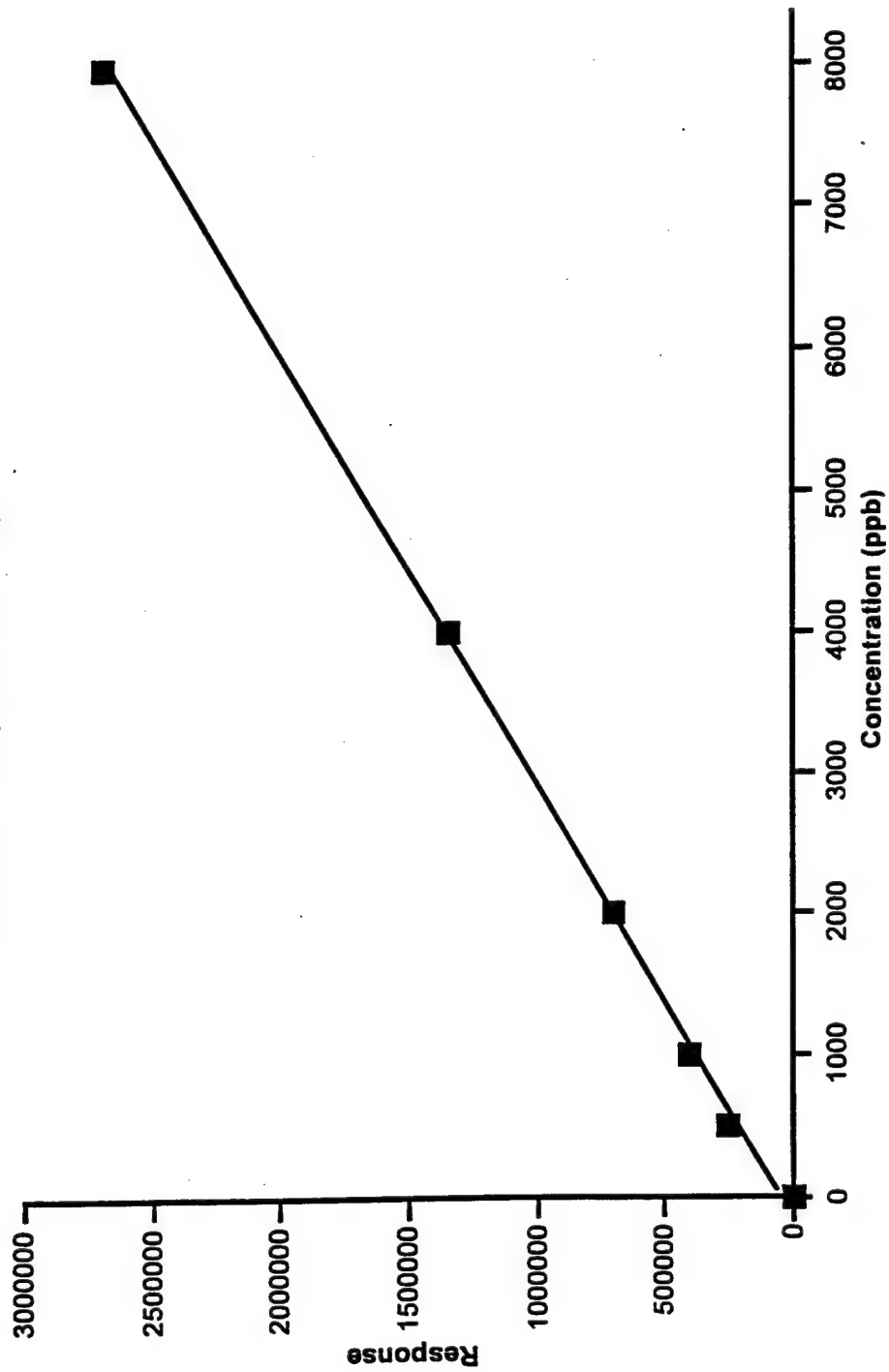


Figure 16: Calibration Curve for Chloropicrin in Water: 40 ml VOA Vial  
Spurge at Ambient Temperature (100 - 8000 ppb)

Chloroform in Water  
Ambient Temperature Purge

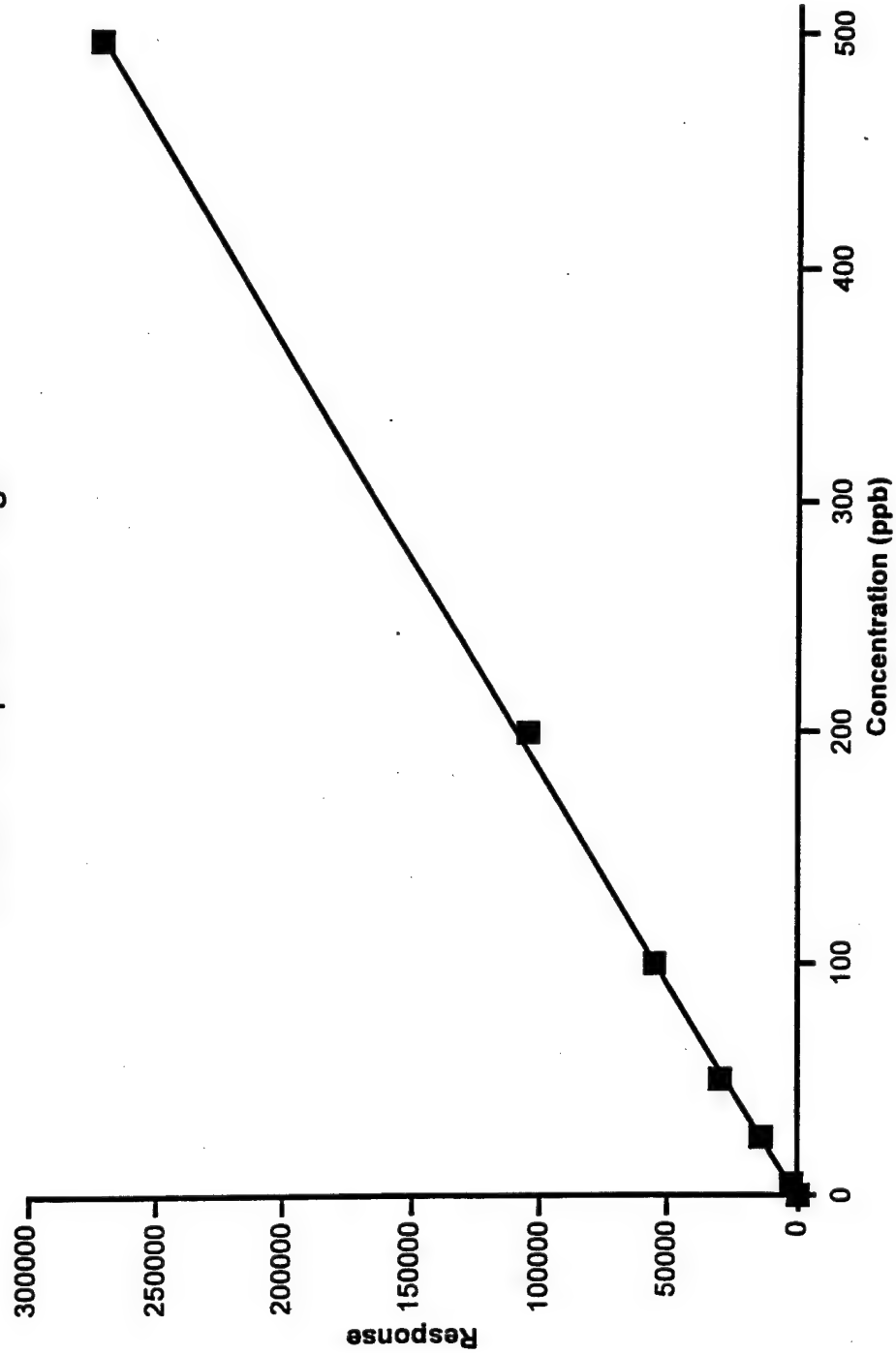


Figure 17: Calibration Curve for Chloroform in Water: 40 ml VOA Vial  
Spurge at Ambient Temperature (5 - 500 ppb)

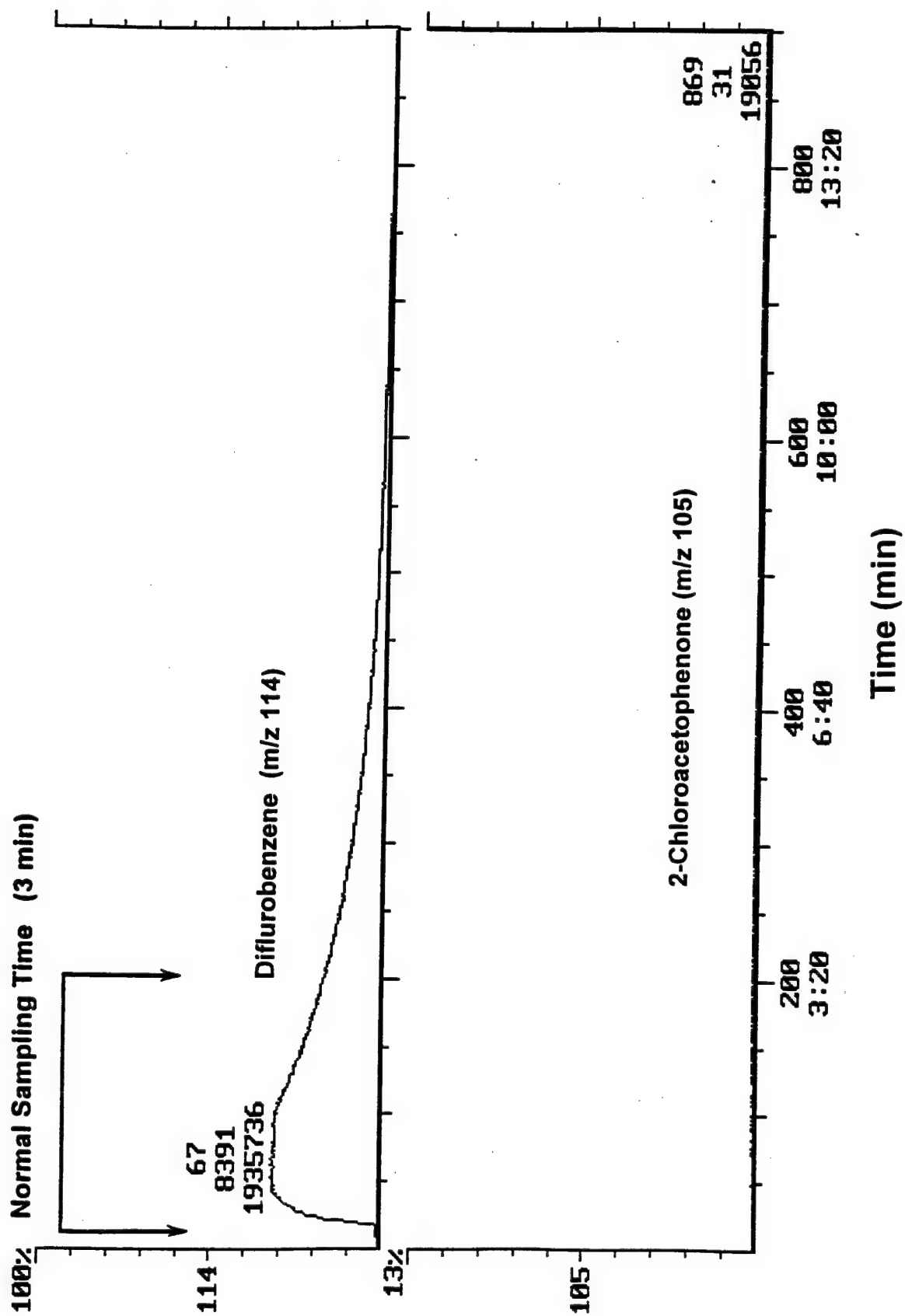


Figure 18: Purge Profile for 100 ppb of 2-Chloroacetophenone in Water:

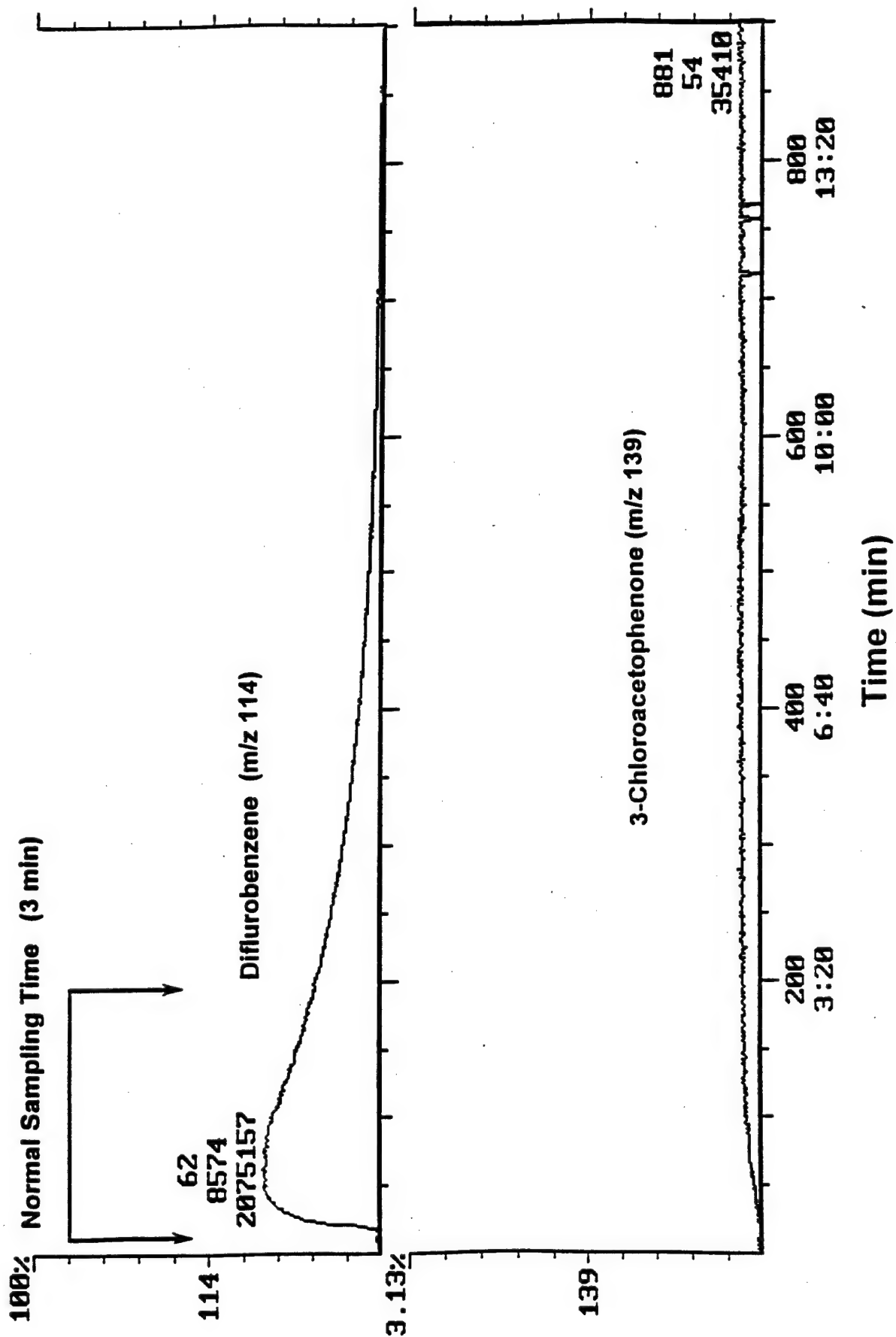


Figure 19: Purge Profile for 100 ppb of 3-Chloroacetophenone in Water:  
40 ml VOA Vial Spurge at Ambient Temperature

## 2-Chloroacetophenone in Water Ambient Temperature Purge

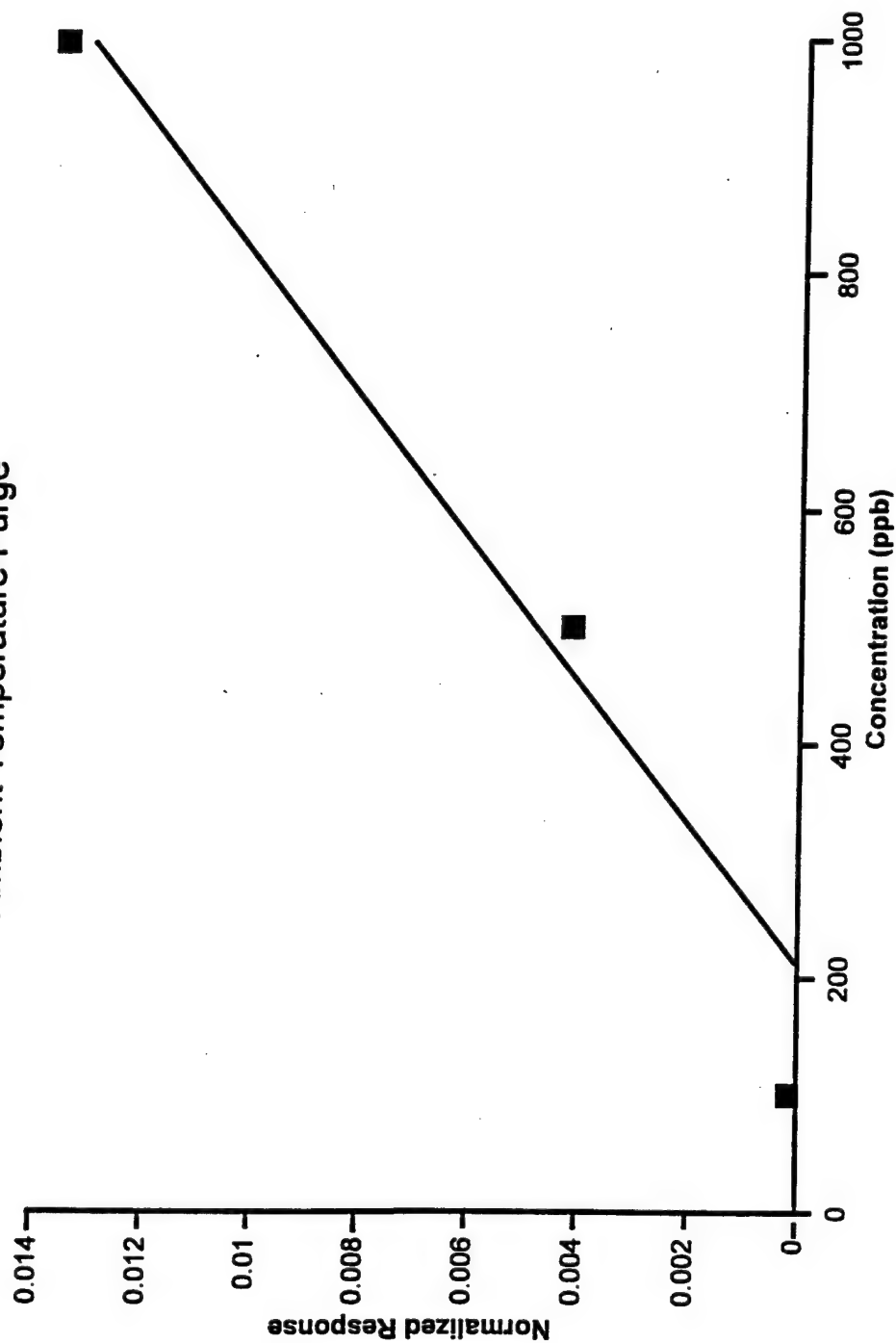


Figure 20: Calibration Curve for 2-Chloroacetophenone in Water: 40 ml  
VOA Vial Spurge at Ambient Temperature (100 -1000 ppb)

### 3-Chloroacetophenone in Water Ambient Temperature Purge

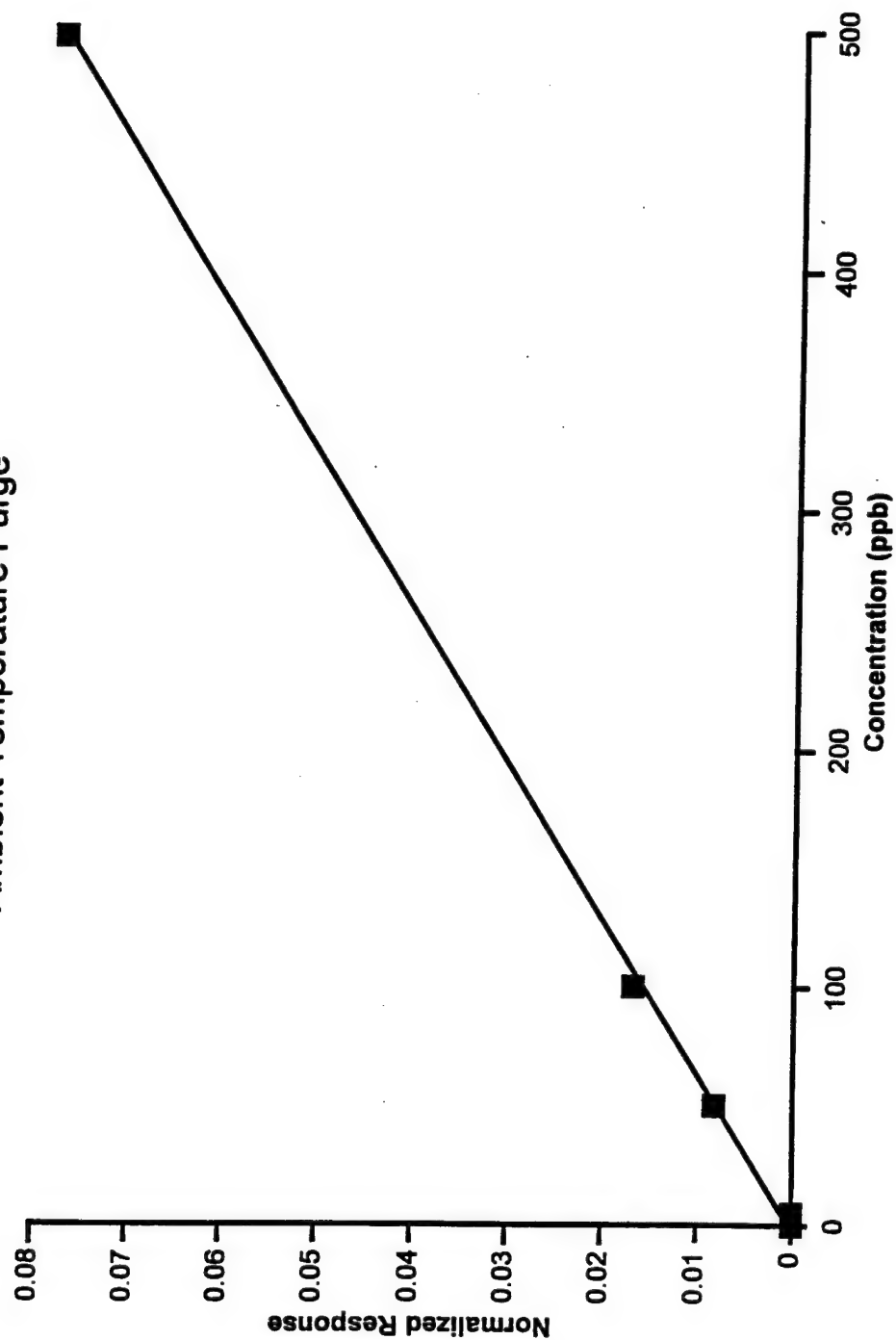


Figure 21: Calibration Curve for 3-Chloroacetophenone in Water: 40 ml  
VOA Vial Spurge at Ambient Temperature (10 -500 ppb).

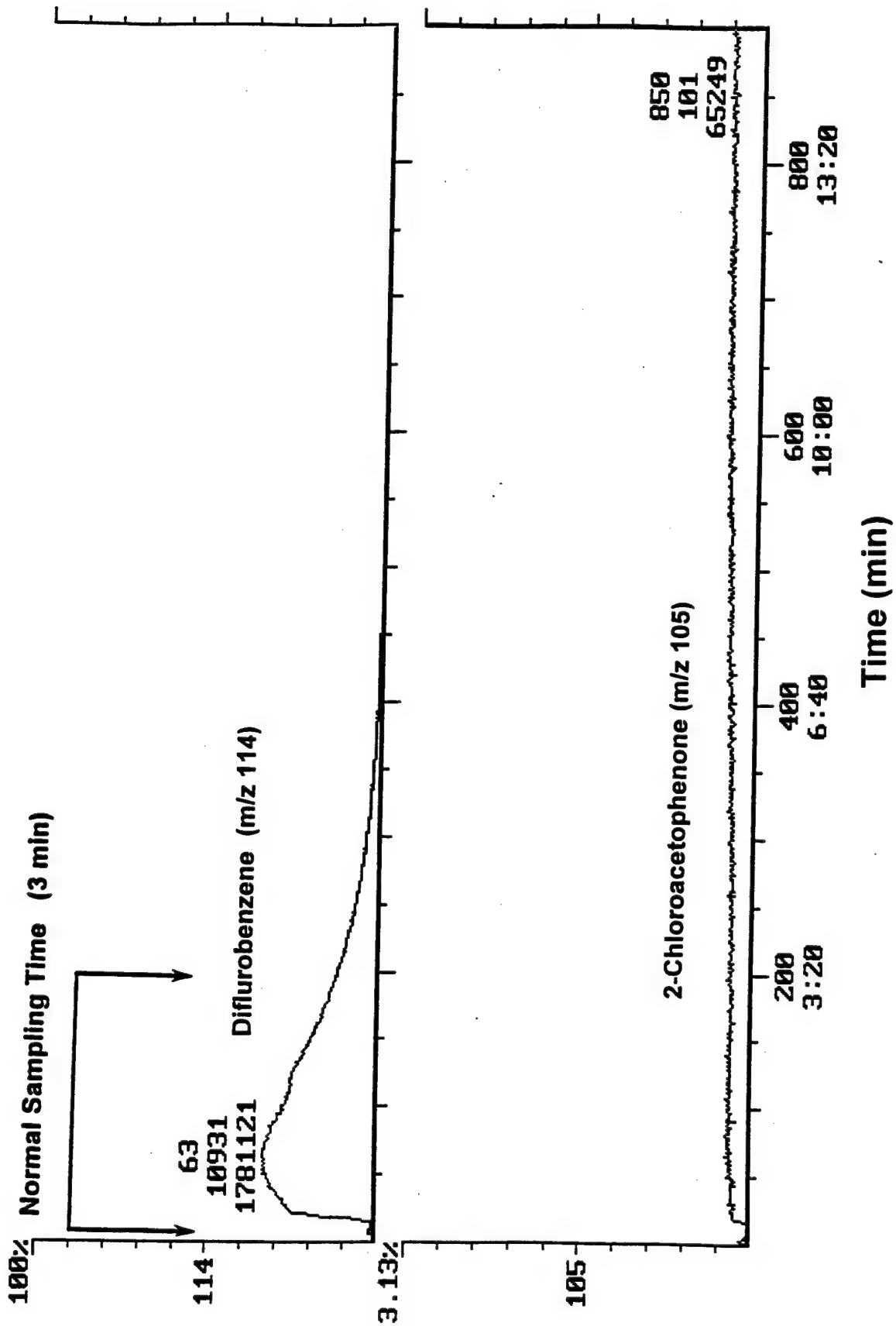


Figure 22: Purge Profile for 100 ppb of 2-Chloroacetophenone in Water:  
40 ml VOA Vial Sparge at 60 C



Page 67 Figure 23 is unavailable for "Results of the Tear Gas Fate and Effects Study (Volume I and II)"

# 2-Chloroacetophenone in Water Heated Purge at 60 C

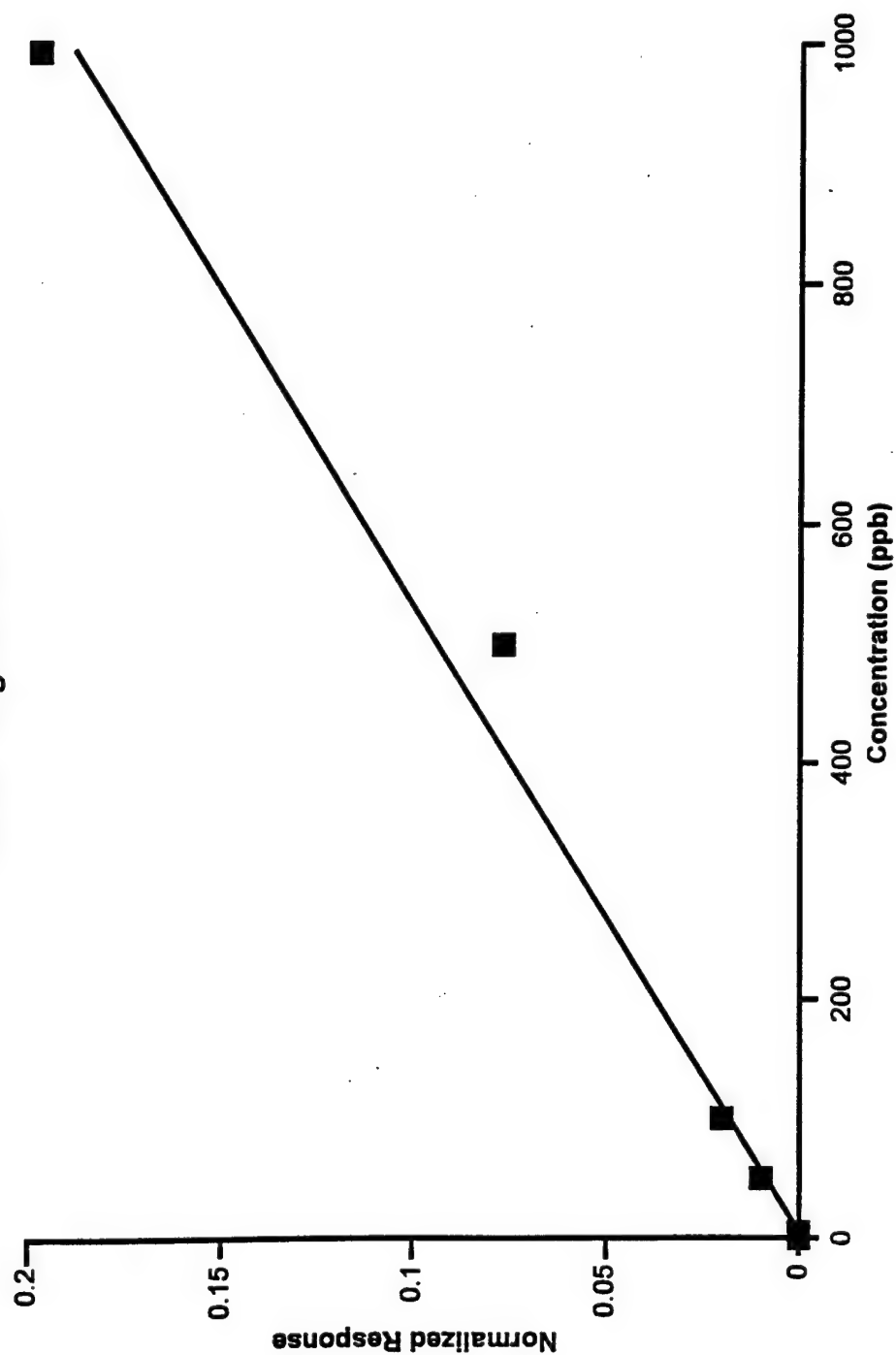


Figure 24: Calibration Curve for 2-Chloroacetophenone in Water: 40 ml  
VOA Vial Sparge at 60 C (5 - 1000 ppb)

3-Chloroacetophenone in Water  
Heated Purge at 60 C

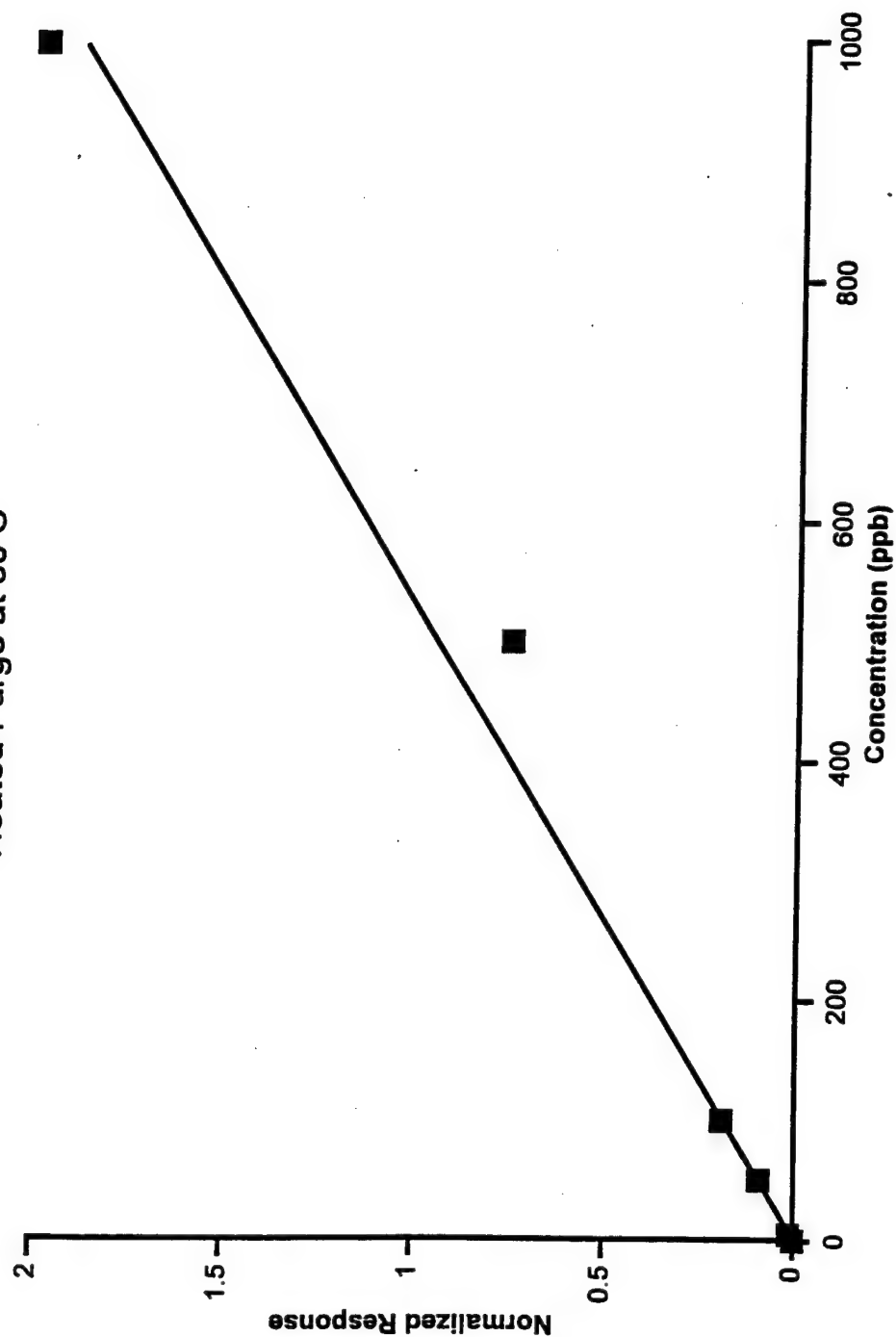


Figure 25: Calibration Curve for 3-Chloroacetophenone in Water: 40 ml  
VOA Vial Sparge at 60 C (5 - 1000 ppb)

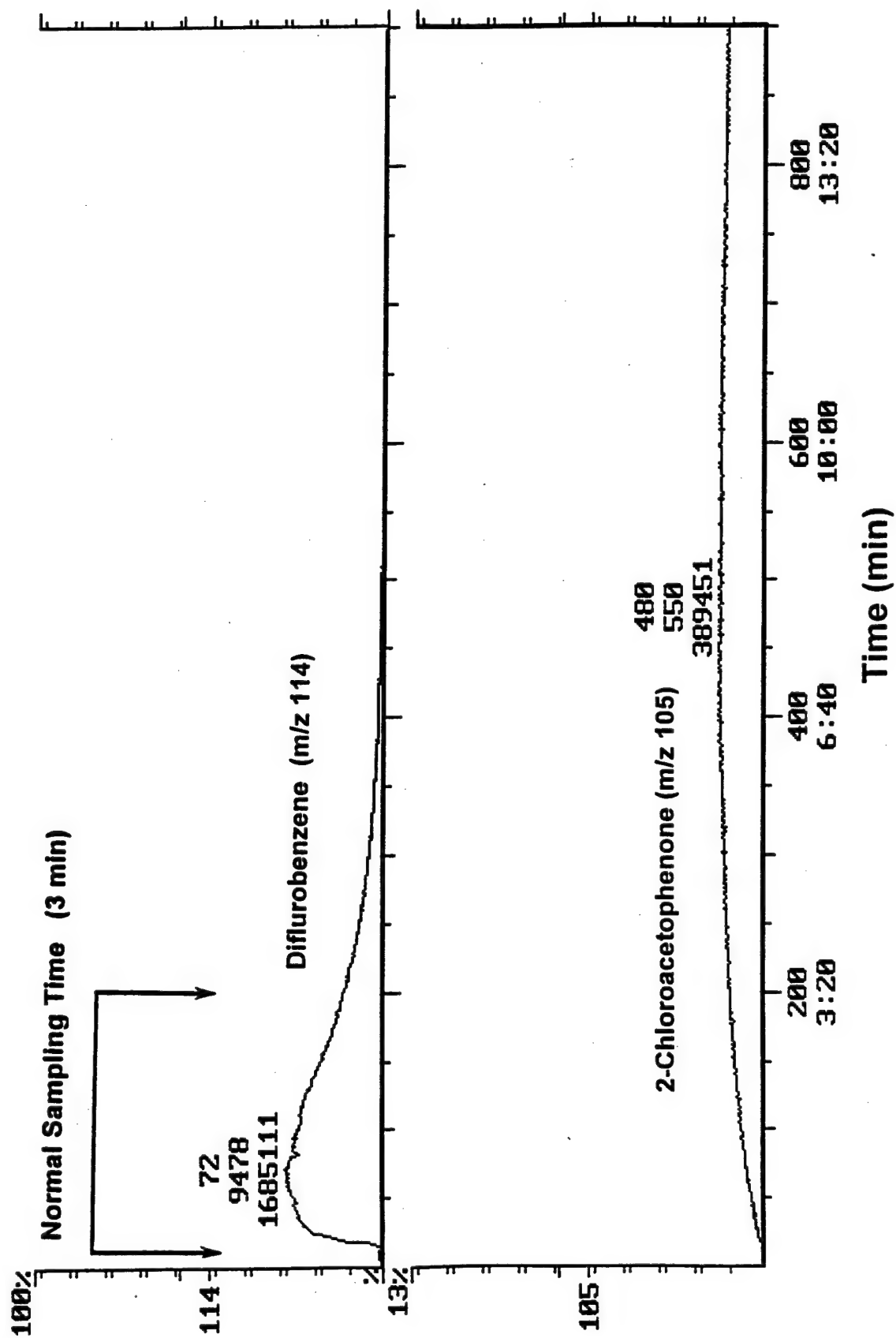


Figure 26: Purge Profile for 100 ppb of 2-Chloroacetophenone in Soil:  
40 ml VOA Vial Spurge of Slurry at 60 C

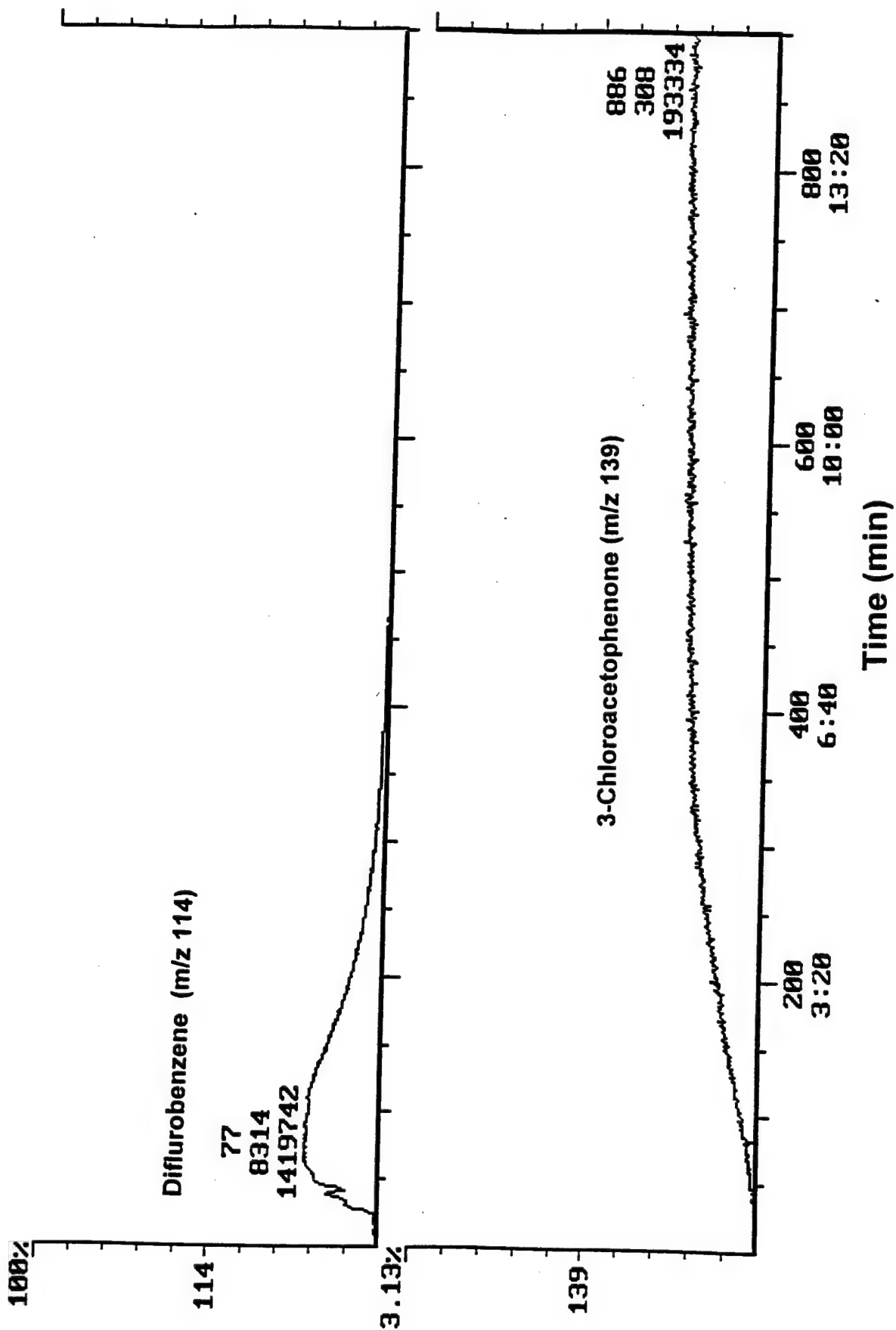


Figure 27: Purge Profile for 100 ppb of 3-Chloroacetophenone in Soil:  
40 ml VOA Vial Spurge of Slurry at 60 C

2-Chloroacetophenone in Soil  
Heated Purge at 60 C

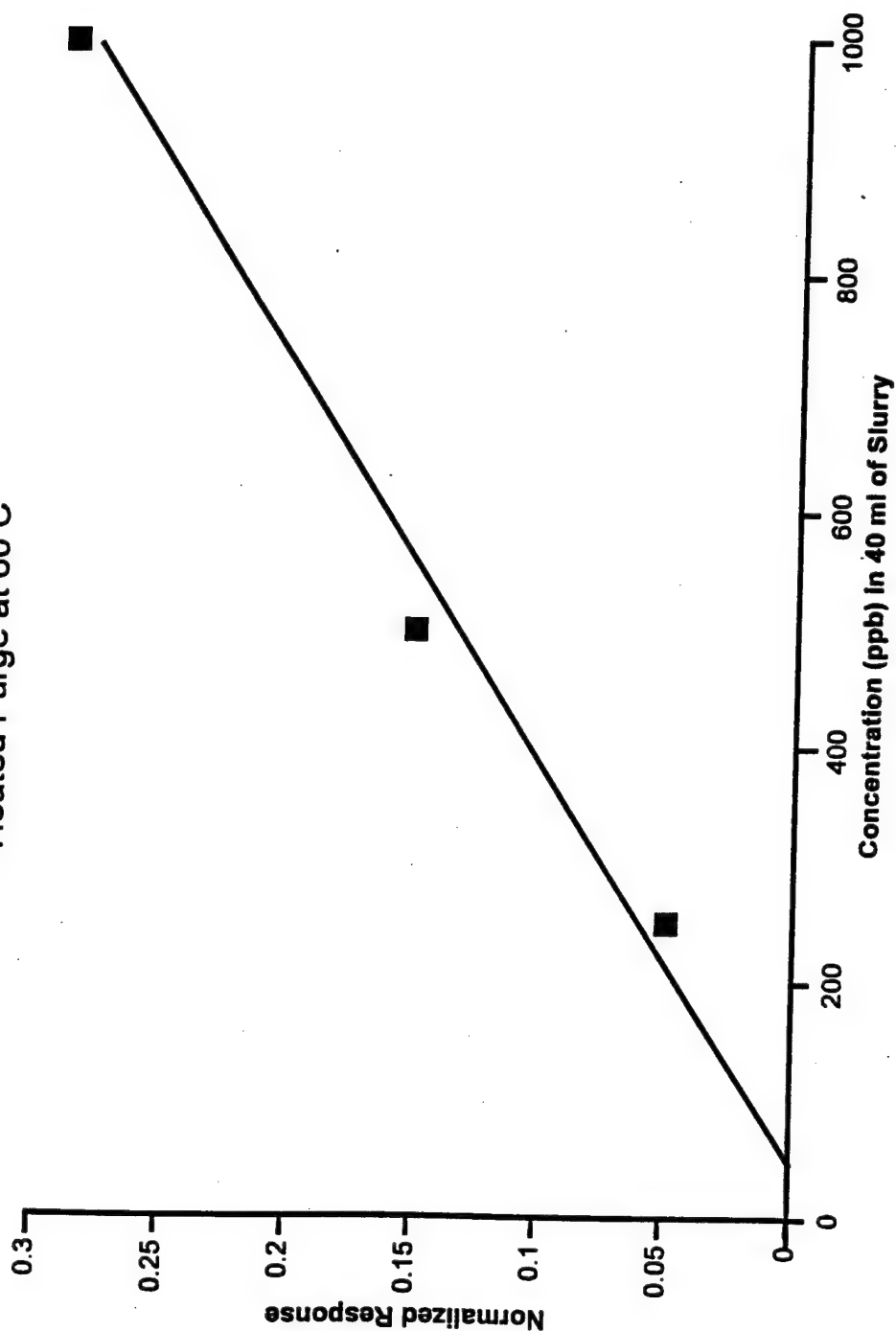


Figure 28: Calibration Curve for 2-Chloroacetophenone in Soil: 40 ml  
VOA Vial Spurge at 60 C (250 - 1000 ppb)

3-Chloroacetophenone in Soil  
Heated Purge at 60 C

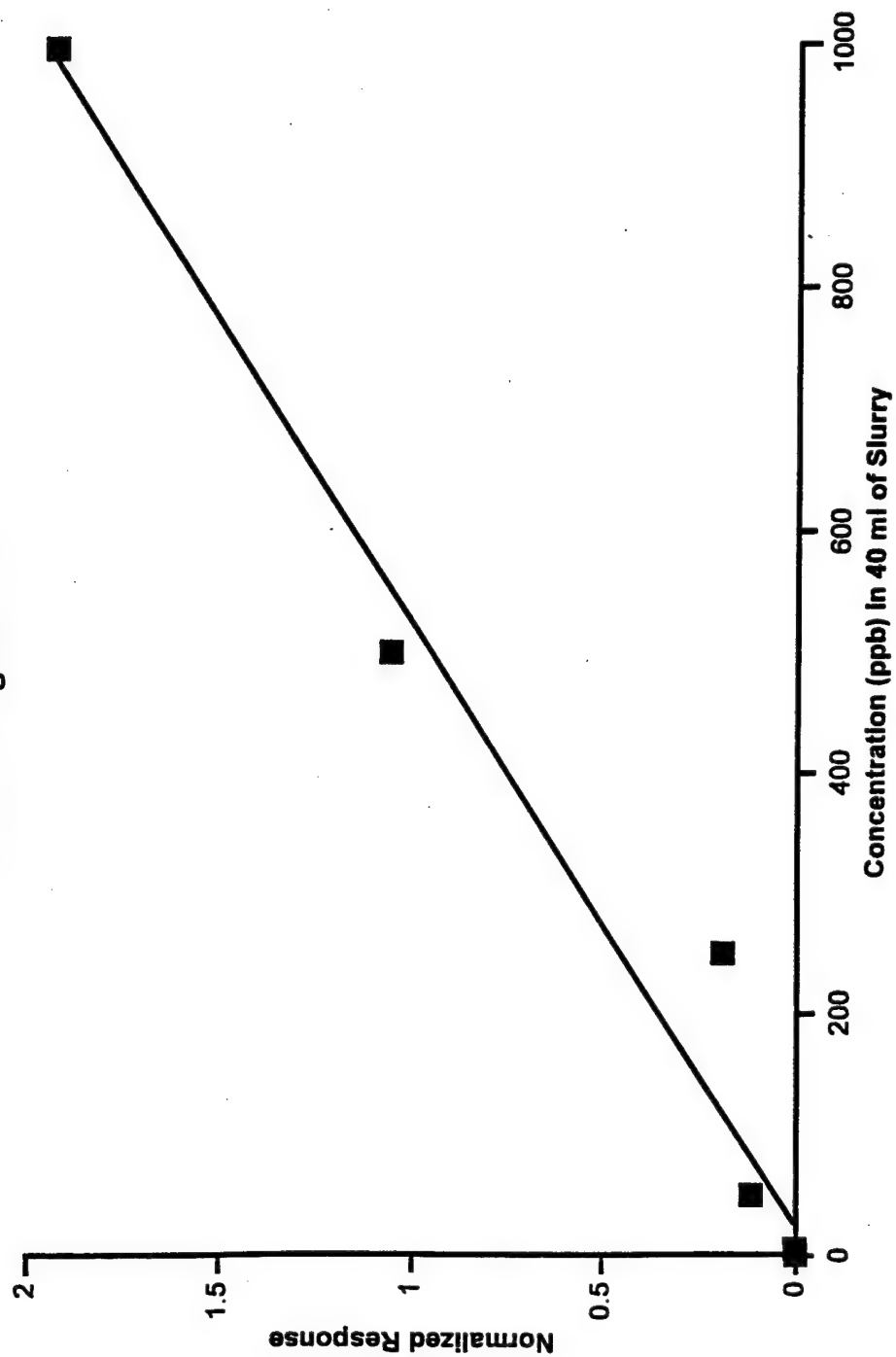


Figure 29: Calibration Curve for 3-Chloroacetophenone in Soil: 40 ml

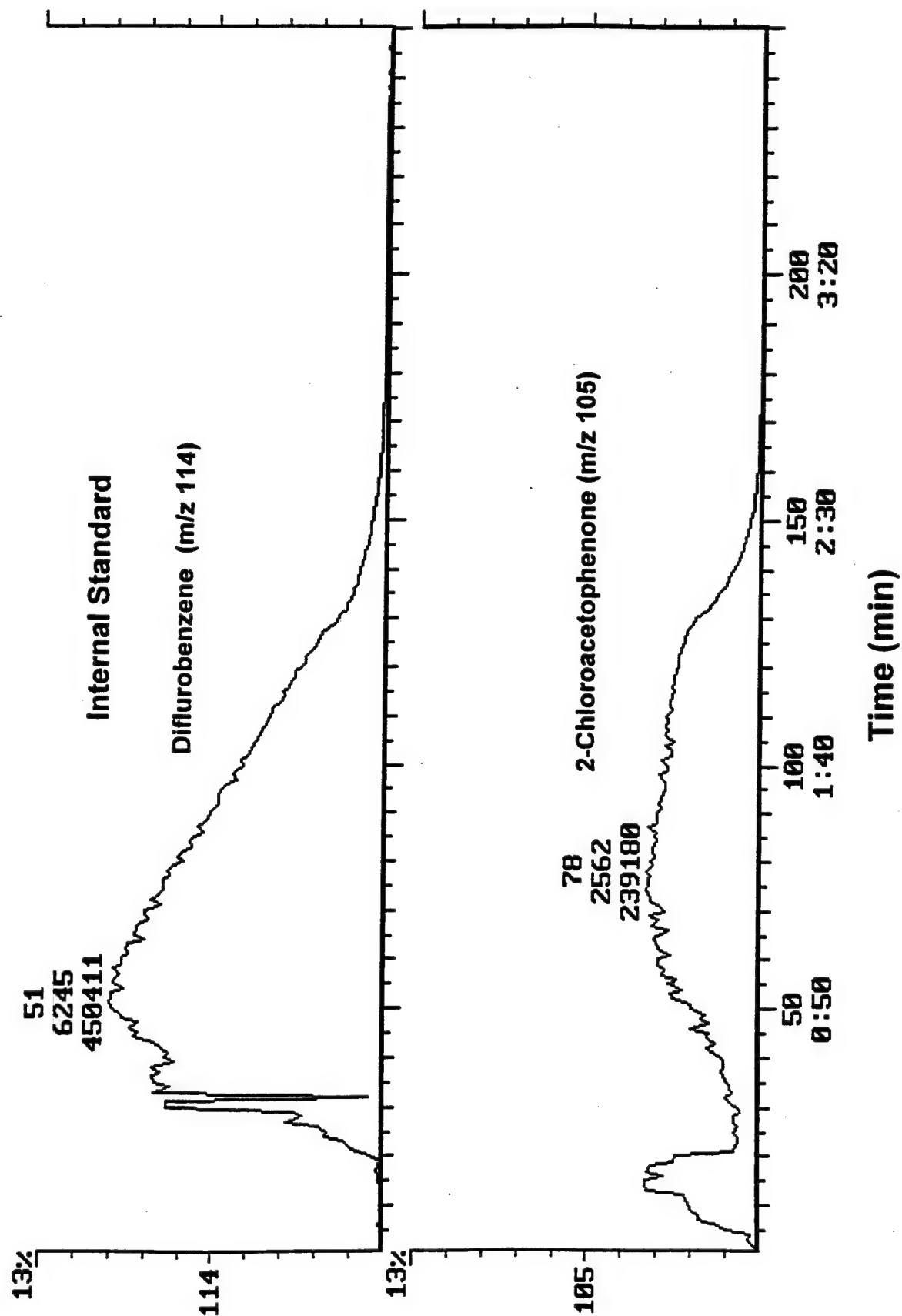


Figure 30: Purge Profile for 4  $\mu$ g of 2-Chloroacetophenone in a 40 ml VOA Vial: Headspace Purge at Ambient Temperature



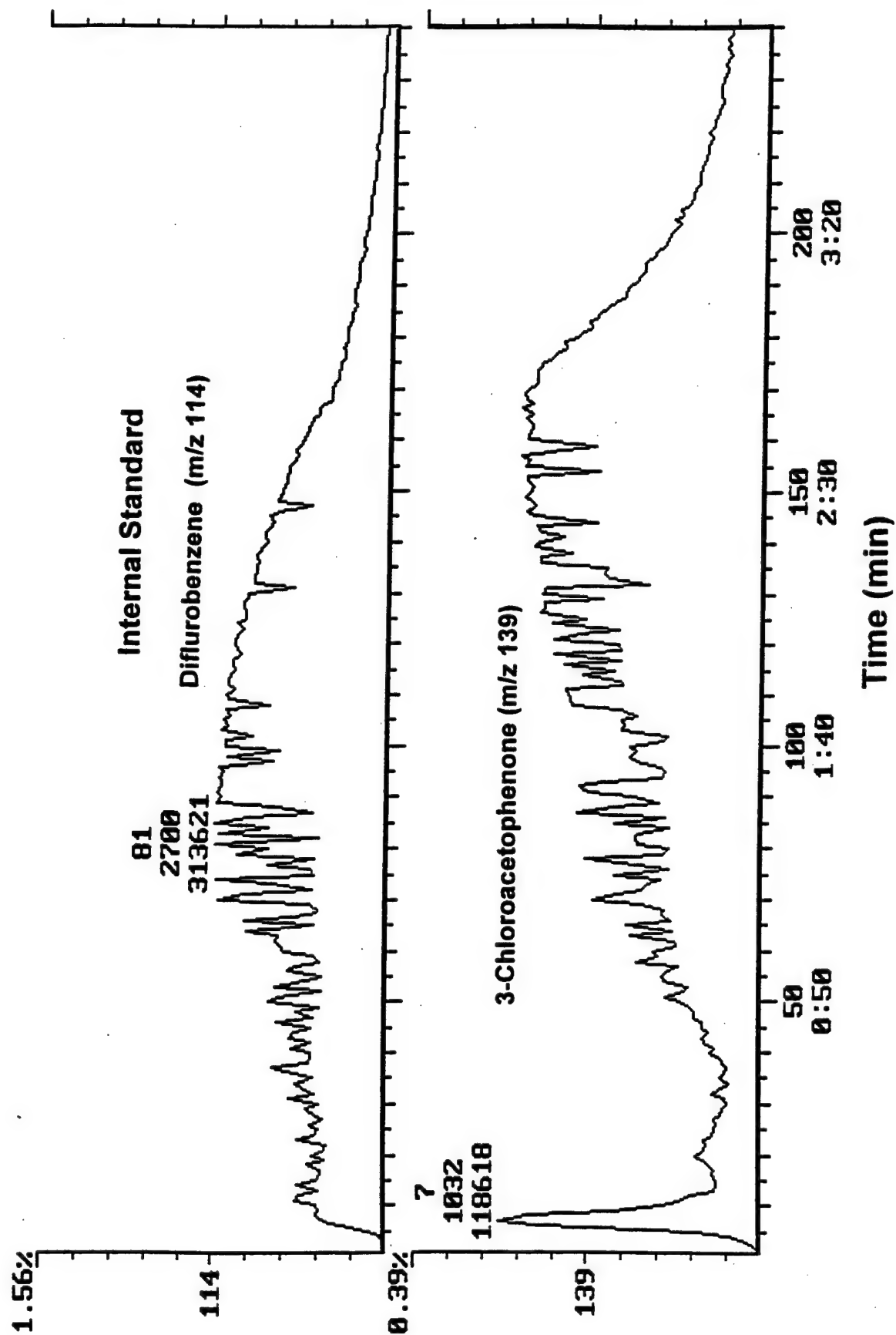


Figure 31: Purge Profile for 4  $\mu$ g of 3-Chloroacetophenone in a 40 ml  
VOC/Volatile Hydrocarbon Purge at Ambient Temperature

# In-situ Sparge

## Mass Spectrum of Chloroform and Chloropicrin

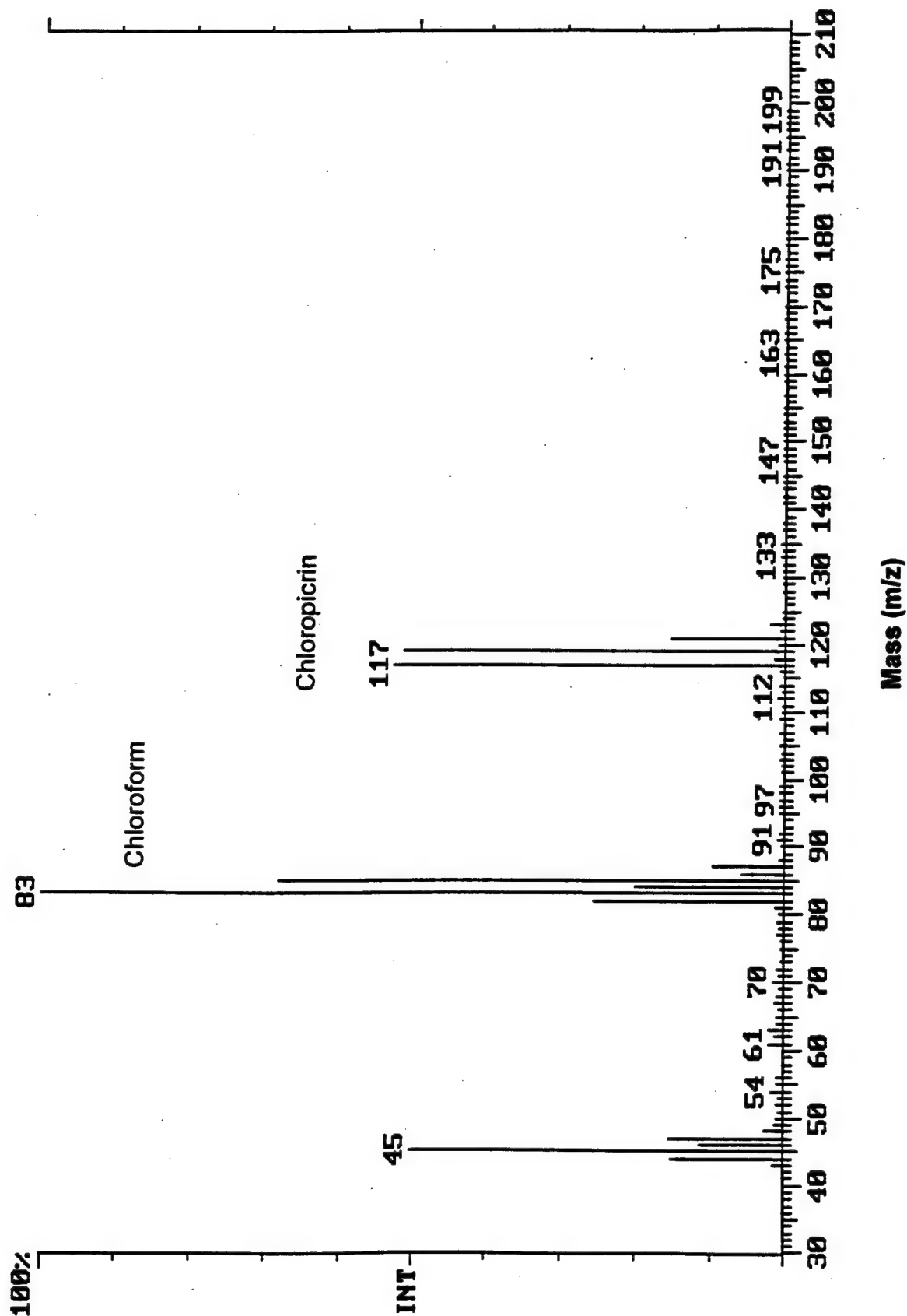


Figure 32: EI Mass Spectrum of Chloroform and Chloropicrin in Water

# Chloropicrin in Water In-Situ Sparge

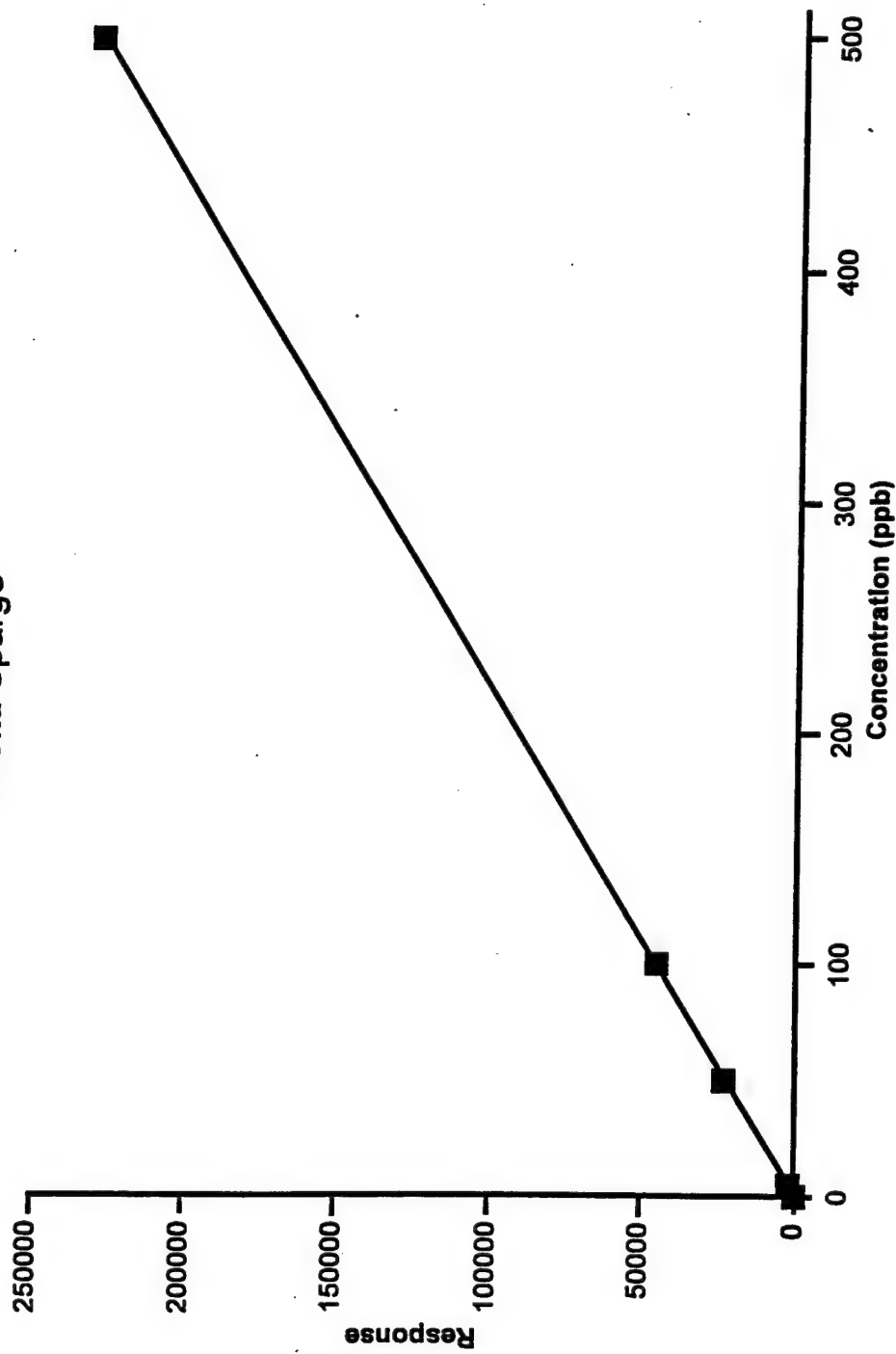


Figure 33: Calibration Curve for Chloropicrin in Water: In-Situ Sparge  
at Ambient Temperature (5 - 500 ppb)

# Chloroform in Water In-Situ Sparge

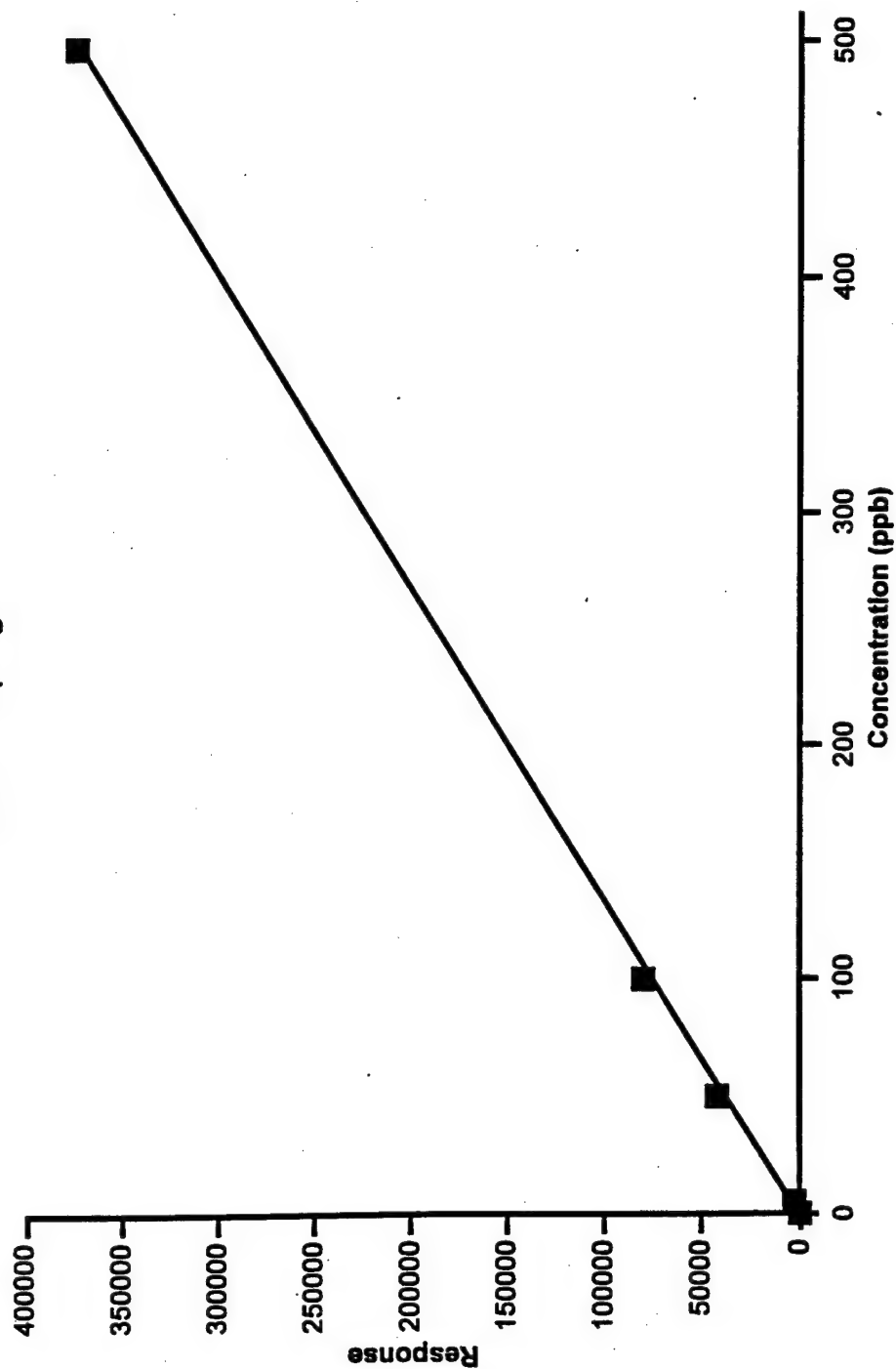


Figure 34: Calibration Curve for Chloroform in Water: In-Situ Sparge  
at Ambient Temperature (5 - 500 ppb)

**APPENDIX D-2**  
**DSITMS METHOD SUMMARY**

**DIRECT SAMPLING ION TRAP MASS SPECTROMETRY (DSITMS) SCREENING  
METHODS FOR CHLOROPICRIN, CHLOROFORM, 2-CHLOROACETOPHENONE  
AND 3-CHLOROACETOPHENONE IN WATER AND SOIL**

Roosevelt Merriweather, Marcus Wise, and Michael Guerin  
Chemical and Analytical Sciences Division

Oak Ridge National Laboratory  
P.O. Box 2008  
4500-S, MS-6120  
Oak Ridge, Tennessee 37831-6120

**Analytical Method Summary**

Prepared for Submission to:

The Tennessee Valley Authority  
Muscle Shoals, Alabama

Revised  
October 1998

## Contents

	<u>Page</u>
Table of Contents.....	i
List of Tables.....	ii
List of Figures.....	ii
1.0 Scope and Application.....	1
1.1 Principle of Operation.....	1
2.0 Summary of Method.....	2
3.0 Interferences.....	3
4.0 Apparatus and Materials.....	3
4.1 Apparatus for the Analysis of Water.....	3
4.2 Apparatus for the Analysis of Soil.....	6
5.0 Reagents.....	8
5.1 Reagents for the Analysis of Water and Soil.....	8
5.2 Standard Solutions of Chloropicrin, Chloroform, 2-Chloroacetophenone, and 3-Chloroacetophenone.....	9
6.0 Sample Handling and Preservation.....	11
7.0 Procedure.....	12
7.1 General Operation Conditions of the Ion Trap Mass Spectrometer.....	12
7.2 Data Processing.....	14
7.3 Analysis of Water Samples in 40-ml VOA Vials.....	16

## Contents (continued)

	<b><u>Page</u></b>
7.4 Analysis of Soil Samples in 40-ml VOA Vials.....	20
7.5 Analysis of Groundwater by In-Situ Sparge.....	24
8.0 Quality Control.....	28
8.1 Instrument Performance.....	28
8.2 Calibration Curve Statistics.....	28
8.3 Quality Control Samples.....	29
8.4 Detection Limits.....	29
9.0 References.....	30
Appendix 1.....	A-1

## List of Tables

	<b><u>Page</u></b>
Table I: Physical Properties of Targeted Analytes.....	A-2
Table II: Quantity of Analyte Required to Produce a 5,000-µg/ml Stock Solution of Each Analyte in a Total of 5 ml of Methanol..	A-4

## List of Figures

	<b><u>Page</u></b>
Figure 1: 40-ml VOA Vial Sparging Module.....	A-3
Figure 2: In-Situ Sparging Probe for VOCs in Groundwater Wells.....	A-3



# **DIRECT SAMPLING ION TRAP MASS SPECTROMETRY (DSITMS) SCREENING METHODS FOR CHLOROPICRIN, CHLOROFORM, 2-CHLOROACETOPHENONE, AND 3-CHLOROACETOPHENONE IN WATER AND SOIL**

## **1.0 SCOPE AND APPLICATION**

This document describes quick, cost-effective procedures for the detection and quantification of the CNS tear gas components: 2-chloroacetophenone, chloropicrin, and chloroform in water and soil samples using Direct Sampling Ion Trap Mass Spectrometry (DSITMS) (see References 1-4). This analytical method has also been extended to the detection of 3-chloroacetophenone, which may be present as a contaminant in very old CNS tear gas.

The DSITMS method permits both screening or accurate quantitative analysis of samples containing chloropicrin and chloroform at a solution concentration of approximately 5 ppb (5 ng/ml) in 3 minutes. Because 3-chloroacetophenone and 2-chloroacetophenone interact strongly with water and soil, they can only be qualitatively analyzed during a 3-minute analysis time. Detection limits are typically in the range of 10 to 100 ppb for these two compounds. Although it is possible to accurately quantitate 2-chloroacetophenone and 3-chloroacetophenone using DSITMS, the analysis time must be extended from 3 minutes to at least 15 minutes, significantly reducing the speed advantage of the DSITMS technique.

### **1.1 Principle of Operation**

This method employs two different custom-built sparging units that are interfaced directly to the ITMS by means of a capillary restrictor interface. One of the sparging units is designed to accept standard 40-ml VOA vials for the analysis of discrete samples of water or soil (**Figure 1**). The other sparging inlet is designed as a sampling probe that is intended for in-situ analysis of VOCs in groundwater wells (**Figure 2**).

As a sample is sparged with a flow of helium, the analytes are conveyed into the ion trap where they are ionized by electron ionization (EI). Alternatively, the ion trap may be operated in a mode that continuously alternates between the EI and chemical ionization (CI) modes, providing greater qualitative information for a sample without increasing the time required for sample analysis. For example, although chloroform and chloropicrin respond only in the EI mode, the CI data may provide useful information for the determination of other compounds, such as benzene or toluene, that may be present as co-contaminants in a real-world sample.

During the sparging process, full scan mass spectra are acquired continuously and stored in data file. Characteristic ions that are unique to the target analytes are used to identify the targeted compounds. Quantitation is performed by integrating the response for the most intense characteristic ions and comparing the integrated response to that from a comparably generated calibration curve.

## **2.0 SUMMARY OF THE METHOD**

Batch (discrete) samples of water and soil are analyzed for VOCs by purging them with a stream of helium in a manner comparable to that performed in standard purge-and-trap gas chromatography/mass spectrometry (GC/MS) methods (e.g., EPA 8260) (see Reference 5). However, the VOCs are monitored continuously in real-time with the ion trap mass spectrometer rather than being collected on a sorbent trap for subsequent analysis by GC/MS.

This method involves the sparging of VOCs from samples contained in standard 40-ml volatile organic analysis (VOA) vials using a specially designed purge module that was developed and produced at the Oak Ridge National Laboratory (Oak Ridge, TN) (see References 1 and 4). This device connects directly to a sample splitter which allows approximately 0.5% of the analyte vapor to enter a microbore-fused silica transfer line whereby the analytes are conveyed directly into the quadrupole ion trap mass spectrometer. The remaining 99.5% of the analyte vapor is directed to a split port where it is either vented to a fume hood or collected on a sorbent trap for sample archival purposes (see Section 6.2). Normally, the flow of helium through the sample is approximately 100 ml/min. This means that approximately 0.5 ml/min enters the ion trap mass spectrometer and the remaining 99.5 ml/min are vented or archived.

As soon as the sample enters the inside of the mass spectrometer, the analytes are ionized either by electron ionization (EI) or chemical ionization (CI). The ion trap analyzer cell provides a means of storing and mass analyzing ions and an electron multiplier is used to detect and amplify the resulting signal.

Using the 40-ml VOA vial purge module with an ion trap mass spectrometer, the data for a complete DSITMS VOC analysis can be generated in 3 minutes. This compares to approximately 45 minutes to an hour using EPA-accepted purge-and-trap GC/MS methods (see Reference 5). Qualitative analysis is performed by matching the spectrum of known target ions and quantitation analysis is performed by integrating the extracted ion current for specific marker masses that correspond to the target compounds. The integrated response is then compared to working curves generated from known standards using the same analytical conditions and data integration limits as those of the unknown sample.

In-situ measurement of VOCs is performed using a sampling probe that transfers the VOCs from their matrix into the gas phase. The VOCs are delivered to the mass spectrometer by an inert transfer line that is equipped with an air sampling pump. The in-situ probe may be deployed using site characterization tools such as cone penetrometry and hydropunch or it may be deployed by hand in existing monitoring wells and piezometers. The in-situ probe is connected to the ion trap mass spectrometer by means of a fused-silica line stainless steel tube that has an outside diameter of 1/8 in. This transfer line is normally 150-200 ft in length. Longer transfer lines could be used in principle; however, the void volume of a longer length of tubing would result in a delay of 1 minute or more between the start of analysis and the time that analytes reach the mass spectrometer.

### 3.0 INTERFERENCES

Samples containing VOCs which yield molecular or fragment ions with the same  $m/z$  values as the characteristic ions of interest will give a false positive result. For example, carbon tetrachloride gives the same basic fragmentation pattern as chloropicrin and, therefore, is a known interference. In some instances, secondary ions in the mass spectrum of the targeted compound can be used for quantitation.

### 4.0 APPARATUS AND MATERIALS

#### 4.1 Apparatus for the Analysis of Water

##### 4.1.1 ITMS (ion trap mass spectrometer) capable of being operated in EI or CI mode.

An acceptable unit is the Teledyne 3DQ ion trap mass spectrometer that was manufactured by Teledyne Electronic Technologies (Mountain View, CA). Other acceptable ion traps are available from Finnigan MAT (San Jose, CA) and Varian (Palo Alto, CA).

##### 4.1.2 Custom-built sparging unit

The sparging unit (**Figure 1**) can be obtained from Oak Ridge National Laboratory, Oak Ridge, TN. This sparging module couples directly with the capillary restrictor interface of the ion trap mass spectrometer and is designed to accept standard 40-ml VOA sample vials. In order to increase the recovery of analytes from a sample, an optional sleeve heater can be placed around the VOA vial in order to heat the sample during sparging.

The operating principle of the 40-ml VOA vial sample sparging module is very simple. A standard 40-ml VOA vial containing the

sample is attached to the module by means of a threaded collar. A stainless steel sparging needle projects into the bottom of the VOA vial and a flow of  $100 \pm 5$  ml/min of helium purges the volatile (and some semi-volatile) organics from the sample. The VOCs that are purged from the sample are conveyed by the helium directly into the ion trap mass spectrometer through a fixed-ratio sample splitter and the fused-silica capillary restrictor. The sample splitter arrangement directs approximately 0.5% of the gas flow into the ion trap while the remaining 99.5% exits through a vent port. Start and stop of the helium flow through the VOA vial is controlled by a 3-way solenoid valve. In one position, this valve directs the flow of helium through the VOA vial during sparging of the sample. In the other position, the valve diverts the helium directly into the capillary restrictor interface, completely bypassing the sample vial.

If desired, sorbent tubes can be attached to the vent port of the splitter for sample archival purposes. Archival samples can be collected at the same time that a DSITMS analysis is being performed without affecting the quality of the DSITMS data or the speed of the analysis.

#### 4.1.3 In-situ sparging probe assembly

The in-situ sparging probe can be obtained from Oak Ridge National Laboratory, Oak Ridge, TN. This probe (**Figure 2**) consists of a sampling head (1/2-in. OD) that is inserted into the groundwater through a well casing or drive point. The probe head is attached to a 1/16-in. OD Teflon<sup>®</sup> tube that supplies helium to the sparger. It is also connected to a Silco-steel<sup>®</sup>-lined 1/8-in. OD stainless steel tube that is used to transport the analyte vapors from the extraction chamber on the sampling probe to the mass spectrometer. The sample transfer line interfaces directly with the capillary restrictor inlet of the ion trap mass spectrometer. Sample is pulled through the transfer line and across the end of the capillary restrictor by means of an air-sampling pump that is attached to the vent port of the sample splitter. At the present, there is no provision for heating the sample transfer line or the probe head. This means that the range of compounds that can be analyzed using this probe is restricted to those compounds that are highly volatile at ambient temperature.

The operating principle of the in-situ sparging probe is very simple. During sample analysis, the in-situ sparging probe uses a flow of helium in the range of 20-100 ml/min to purge VOCs from

the water. The differential in the density of the water column that is being sparged and the density of the surrounding water creates a pumping action that continually draws a fresh sample into the sparger. Electronic flow controllers maintain a slight excess of helium in the sparger relative to the flow of gas through the transfer line and into the MS. This maintains a nearly constant volume of helium in the extraction chamber and also prevents water from flowing into the sample transfer line. For depth profiling applications, this probe can be used at any depth below the water surface, provided that the helium flow controllers are rated for use at a pressure that is greater than the maximum water pressure that will be encountered.

4.1.4 Heater sleeve for 40-ml VOA vials (used for heated purge)

The heater sleeve is manufactured by Oak Ridge National Laboratory (Oak Ridge, TN).

4.1.5 Heater controller for 40-ml VOA vial heater sleeve capable of controlling temperature up to 100°C

An acceptable heater controller is the Model CN9000A manufactured by Omega Engineering (Stamford, CT). Equivalent controllers are available from other manufacturers.

4.1.6 Thermocouple and digital thermometer for 40-ml VOA vial heater sleeve

An acceptable unit is the Model HH81 digital thermometer manufactured by Omega Engineering (Stamford, CT). Equivalent units are available from other vendors.

4.1.7 Syringe, 25- $\mu$ L capacity

These syringes can be purchased from Precision Sampling (Baton Rouge, LA). Equivalent units are available from other vendors.

4.1.8 Precalibrated variable volume pipets compatible with methanol

These pipets can be purchased from Polymerase Chain Reaction Tri-Continent Scientific, Inc. (Gross Valley, CA). Equivalent units may be available from other vendors.

- 4.1.9 Screw cap amber vials (pre-cleaned) with solid caps and fixed Teflon<sup>®</sup> liners (5-ml capacity)

These vials can be purchased from I-Chem Research (New Castle, DE). Equivalent units may be available from other vendors.

- 4.1.10 Screw cap VOA vials (pre-cleaned) (40-ml capacity)

These vials can be purchased from I-Chem Research (New Castle, DE). Equivalent units may be available from other vendors.

- 4.1.11 Flow meter capable of measuring 100 mL/min

An example is Calibration Meter Model M-5, A.P. Buck (Orlando, FL). Other acceptable flow meters are available from equivalent vendors.

- 4.1.12 Pyrex<sup>®</sup> volumetric flask (5-ml capacity)

These flasks can be purchased from most laboratory supply companies.

- 4.1.13 Graduated cylinder (500-ml capacity)

These items can be purchased from most laboratory supply companies.

- 4.1.14 Waste disposal jug (4-liter capacity)

Any appropriate container, such as an empty methanol jug, may be used for the collection of waste samples.

## 4.2 Apparatus for the Analysis of Soil

- 4.2.1 Ion trap mass spectrometer, as described in Section 4.1.1

- 4.2.2 Purge module, as described in Section 4.1.2

- 4.2.3 Syringe, 10- $\mu$ l capacity

These syringes can be purchased from Precision Sampling (Baton Rouge, LA). Equivalent units are available from other vendors.

4.2.4 Heater sleeve for 40-ml VOA vials

The heater sleeve was manufactured by Oak Ridge National Laboratory, (Oak Ridge, TN).

4.2.5 Heater controller for 40-ml VOA vial heater sleeve capable of controlling temperature up to 100°C

An acceptable heater controller is the Model CN9000A manufactured by Omega Engineering (Stamford, CT). Equivalent controllers are available from other manufacturers.

4.2.6 Thermocouple and digital thermometer for 40-ml VOA vial heater sleeve

An acceptable unit is the Model HH81 digital thermometer manufactured by Omega Engineering (Stamford, CT). Equivalent units are available from other vendors.

4.2.7 Vortex Mixer

An acceptable vortex mixer is the Maxi Mix 1, Model M16715 manufactured by Thermolyne Corporation (Dubuque, IA). Other equivalent units may be available from other manufacturers.

4.2.8 Electronic balance with 0.1-g resolution or better

An acceptable balance is the Model 8301A manufactured by Allied Fisher Scientific (Denver, CO). Equivalent units are available from other vendors.

4.2.9 Magnetic stirrer

An acceptable unit is the Model 15 manufactured by Arthur Thomas Co. (Philadelphia, PA). Equivalent units are available from other vendors.

4.2.10 Stirring bar, approximately 0.8 cm in thickness and 1 cm in length

Acceptable stir bars are available from most laboratory supply companies.

#### 4.2.11 Syringe, 25- $\mu$ L capacity

These syringes can be purchased from Precision Sampling (Baton Rouge, LA). Equivalent units are available from other vendors.

#### 4.2.12 Precalibrated variable volume pipettes compatible with methanol

These pipettes can be purchased from Polymerase Chain Reaction Tri-Continent Scientific, Inc. (Gross Valley, CA). Equivalent units may be available from other vendors.

#### 4.2.13 Screw cap amber vials (pre-cleaned) with solid caps and fixed Teflon<sup>®</sup> liners (5-ml capacity)

These vials can be purchased from I-Chem Research (New Castle, DE). Equivalent units may be available from other vendors.

#### 4.2.14 Screw cap VOA vials (pre-cleaned) (40-ml capacity)

These vials can be purchased from I-Chem Research (New Castle, DE). Equivalent units may be available from other vendors.

#### 4.2.15 Flow meter capable of measuring 100 mL/min

An example is Calibration Meter Model M-5, A.P. Buck (Orlando, FL). Other acceptable flow meters are available from equivalent vendors.

#### 4.2.16 Pyrex<sup>®</sup> volumetric flask (5-ml capacity)

These flasks can be purchased from most laboratory supply companies.

## 5.0 REAGENTS

### 5.1 Reagents for the Analysis of Water and Soil

#### 5.1.1 Methanol, HPLC or "purge and trap" grade.

This product may be purchased from J. T. Baker, Inc. (Phillipsburg, NJ). Equivalent products are available from other vendors.



5.1.2 Water for preparation of standards (simulated groundwater)

Simulated groundwater is prepared by adding 148 mg/L of sodium sulfate and 165 mg/L of sodium chloride (100 mg/L each of  $\text{SO}_4^{2-}$  and  $\text{Cl}^-$  ions) to ASTM Type II water obtained from a Millipore Milli-Q<sup>®</sup> unit, or equivalent water purifier.

5.1.3 Helium 99.9999% minimum purity (compressed gas cylinder)

Acceptable helium is available from Alphagaz (Walnut Creek, CA). Equivalent product is available from other vendors.

5.1.4 Chloroform (neat)

This product can be obtained from Burdick and Jackson (Muskegon, MI). Equivalent product is available from other vendors.

5.1.5 Chloropicrin (neat)

This product can be purchased from Chem Service (West Chester, PA). Equivalent product may be available from other vendors.

5.1.6 2-Chloroacetophenone (solid)

This product can be purchased from Chem Service (West Chester, PA). Equivalent product may be available from other vendors.

5.1.7 3-Chloroacetophenone (neat)

This product can be purchased from Chem Service (West Chester, PA). Equivalent product may be available from other vendors.

5.2 Standard Solutions of Chloropicrin, Chloroform, 2-Chloroacetophenone, and 3-Chloroacetophenone

5.2.1 Analyte Master Stock Solution (from neat liquid or pure solid)

5.2.1.1 Dilute an appropriate quantity of chloropicrin chloroform, or 3-chloroacetophenone in a 5-ml volumetric flask with HPLC grade methanol to yield a final concentration of

5,000 µg/ml in the solution (see **Table II** for the appropriate quantities). For 2-chloroacetophenone, dissolve the appropriate amount of crystals in a 5-ml volumetric flask with HPLC grade methanol to yield a final concentration of 5,000 µg/ml in the solution (see **Table II**).

5.2.1.2 Transfer the solutions prepared in Section 5.2.1.1 to 5-ml-capacity screw-cap amber vials. Seal the vial with a Teflon<sup>®</sup>-lined cap and store in a freezer maintained between -20°C and -10°C. These are the analyte *Master Stock Solutions*. The storage life of the Master Stock Solutions is about six months. For this method, Master Stock Solutions may be prepared separately for each analyte or can be combined in a single mixture as they are added to the calibration samples at the same time.

5.2.2 Analyte Working Solution (from *Master Stock Solution*)

5.2.2.1 Dilute exactly 100 µl of the *Master Stock Solution* prepared in Section 5.2.1.1 to 5 ml in a volumetric flask with HPLC grade methanol. The final solution concentration is 100 µg/ml.

5.2.2.2 Transfer the solution in 5.2.2.1 to a 5-ml capacity screw-cap amber vial. Seal the vial with a Teflon<sup>®</sup>-lined cap and store in a freezer maintained between -20°C and -10°C. These are the analyte *Working Solutions*. The storage life for the *Working Solutions* is about two weeks.

5.2.3 Internal Standard Master Stock Solution

5.2.3.1 Dilute 21.5 µl of neat 1,4-difluorobenzene to exactly 5 ml with HPLC grade methanol in a volumetric flask to make a final solution concentration of 5,000 µg/ml. This is the internal standard *Master Stock Solution*.

5.2.3.2 Transfer the Internal Standard *Master Stock Solution* to a 5-ml capacity screw-cap vial with a Teflon<sup>®</sup>-lined cap. Store in a freezer maintained between -20°C and -10°C. The storage life of the Master Stock Solution is about six months.

#### 5.2.4 Internal Standard Working Solution

5.2.4.1 Dilute exactly 200 µl of the *Master Stock Solution* prepared in Section 5.2.3.1 in a 5-ml volumetric flask with HPLC grade methanol. The final solution concentration is 200 µg/ml.

5.2.4.2 Transfer the solution prepared in Section 5.2.4.1 to a 5-ml capacity screw-cap amber vial. Seal the vial with a Teflon®-lined cap and store in a freezer maintained between -20°C and -10°C. The storage life is about two weeks.

### 6.0 SAMPLE HANDLING AND PRESERVATION

6.1 Water samples should be collected in clean 40-ml VOA vials in the absence of headspace. Soil samples should be collected using a non-disruptive sampling procedure and stored in glass containers with minimal headspace. Both water and soil samples should be immediately stored in a cooler packed with ice until they can be transferred to a sample storage refrigerator (see Reference 5). Holding times for samples are dependent on the specific QA/QC requirements for a site. Holding times are specified for VOCs in EPA Method 624 (water) and EPA Method 8260 (soil).

6.2 Procedure for collection of a split vent sample on sorbent trap for sample archival purposes

6.2.1 Remove sealed end-caps from a clean triple sorbent trap (0.25-in. diameter, 3-in. long)

6.2.2 Insert sorbent trap in the o-ring seal fitting on the split-vent port of the interface and tighten the o-ring

6.2.3 Start sample analyses

6.2.4 At the completion of sample analyses, remove the triple sorbent trap from the o-ring fitting on the sample interface

6.2.5 Replace the end-caps on the sorbent trap and tighten them

6.2.6 Store sorbent traps in a cooler or sample refrigerator until analysis

## **7.0 PROCEDURE**

### **7.1 General Operating Conditions of the Ion Trap Mass Spectrometer**

Specific details of the operation of an ion trap mass spectrometer will vary from one instrument model to another. The Instrument Operator's Manual for a particular ion trap should be consulted for this information (see Reference 6). General operating conditions described in this section apply to all ion trap instruments, regardless of the manufacturer or specific model used.

#### **7.1.1 Instrument Tuning**

The mass axis calibration of the ion trap mass spectrometer is checked on a daily basis using perfluorotributylamine (PFTBA), which is a compound that is commonly used for this application. Other daily operational checks include adjustment of the radio frequency (RF) drive circuit and nulling of the signal amplifier output. In addition, the ion trap is checked for an excessive background of air or water, which may be an indication of a leak in the vacuum system.

#### **7.1.2 General Parameters for Data Acquisition**

During sample analysis, the operating conditions of the ion trap mass spectrometer are controlled by the data acquisition computer using the parameters stored in an "Acquisition Method" file. The individual parameters in the "Acquisition Method" file, such as scan range and ionization mode, are entered into the data file by the instrument operator prior to start of data acquisition.

##### **7.1.2.1 Mass Scan Range**

For the analysis of the compounds in CNS tear gas, the ion trap mass spectrometer must acquire mass spectra over a range of at least 45-200 Daltons (atomic mass units). A minimum of 4 mass spectra (microscans) must be signal-averaged for every mass spectrum that is displayed or acquired to computer disk. This is necessary in order to reduce electronic noise and random signal fluctuations in the mass spectrum. As a general rule, as many microscans should be signal-averaged as possible to produce approximately 1 signal-averaged mass spectrum per second. This will vary from

one instrument to another because of differences in the mass scan rate.

#### 7.1.2.2 Analysis "Run Time"

##### 7.1.2.2.1 40-ml VOA Vial Analysis of Water and Soil

Although the ion trap mass spectrometer responds almost instantaneously to the analytes that are purged from a sample by the 40-ml VOA vial-sparging module, quantitative precision is improved if a sample is sparged and data are collected for a period of 2-3 minutes. This tends to average out instrument noise and also minimizes the effects of slight differences between the sparging conditions of replicate samples. During the 2- to 3-minute analysis time, a series of mass spectra is continuously generated and saved to the computer disk in the form of an "Acquisition Data File." Assuming that 1 mass spectrum per second is generated, a 3-minute-long "Acquisition Data File" will consist of 180 individual mass spectra stored in sequence according to when they were acquired. *Note: If it is desired to quantitatively measure either 2-chloroacetophenone or 3-chloroacetophenone in water or soil, the analysis run time must be extended to at least 15 minutes.*

##### 7.1.2.2.2 In-situ Sparge Analysis of Groundwater

When using the in-situ sparging probe in conjunction with a 150-200-ft sample transfer line, there is a lag time of 30-45 seconds between the time that the sparging process is started and the time that a signal is actually observed with the ion trap mass spectrometer. This is due to the void volume of the transfer line that must be cleared from the line before the sample reaches the instrument. Once the analytes reach the mass spectrometer, a steady-state signal is usually observed within 60 seconds. Data are usually acquired for at

least another 60 seconds after a steady-state signal is reached. This means the minimum "run time" for data acquisition should be 3 minutes.

#### 7.1.2.3 Ionization Mode of the Mass Spectrometer

The ionization mode of the ion trap mass spectrometer is normally set so that either EI or CI data are exclusively acquired during the 2- to 3-minute analysis time. This means that it is necessary to perform sequential analysis of duplicate samples, one using EI conditions and the other using CI conditions, if both types of data are required. Alternatively, some of the more advanced ion trap mass spectrometers, such as the Teledyne 3D-Q, have a mode of operation that permits the simultaneous generation of both EI and CI data during a single 2- to 3-minute analysis without significant loss of quantitative performance. This is accomplished by having the data acquisition computer continuously alternate between the EI and CI modes once every second. A 3-minute-long data file generated under these conditions will consist of 90 EI spectra and 90 CI spectra stored on disk as a sequence of alternating EI and CI spectra. The alternating EI/CI mode of operation can provide considerable time savings by eliminating the need for sequential sample analysis.

### 7.2 Data Processing

#### 7.2.1 Quantitation Masses for Targeted Analytes

The quantitation masses for DSITMS methods are normally selected by choosing the largest peak in the mass spectrum of a particular analyte that is not expected to overlap with the peak from another compound in the sample. For the analysis of samples that contain CNS tear gas compounds, the quantitation masses (EI conditions) that are used include: chloroform ( $m/z$  83), chloropicrin ( $m/z$  119), 2-chloroacetophenone ( $m/z$  105), and 3-chloroacetophenone ( $m/z$  139). In situations where peak overlap is a significant problem, spectral subtraction routines or other deconvolution techniques must be applied to the mass spectrum in order to recover the quantitative information for individual analytes.

## 7.2.2 Purge Profiles

A plot of the response of the mass spectrometer (ion current) versus analysis time is referred to as a "purge profile". Purge profiles can be plotted using the total ion current (the response for all masses summed together) or they can be plotted using the ion current for specific mass values. Quantitation of targeted analytes is performed by integrating purge profiles that have been plotted using specific quantitation masses that are characteristic of the analytes of interest.

## 7.2.3 Data Integration Limits

### 7.2.3.1 Analysis of Water and Soil in 40-ml VOA Vial Samples

For the analysis of samples in 40-ml VOA vials, the data integration window normally includes all but the first 15 seconds of the 3-minute purge profile. The data from the first 15 seconds of data acquisition are not usually integrated due to possible artifacts, such as charge exchange peaks, that can be present in the mass spectra during the first few seconds of the sparging process. These artifacts arise from traces of air that are trapped in the void volume of the sparging module and sample interface.

### 7.2.3.2 Analysis of Groundwater using the In-situ Sparging Probe

In general, the analytical procedure using the in-situ sparging probe is similar to that used for the analysis of 40-ml sample vials. However, because there is a constant flow of water into the in-situ sparger (as opposed to a fixed 40-ml volume), a steady-state signal is generated provided that the concentration of the analytes in the bulk sample does not change significantly. Data are usually integrated over a time interval of 30 seconds covering a portion of the response profile that is flat (steady-state signal).

## 7.2.4 Quantitation of Targeted Analytes

If the same integration limits (time window) are consistently used to integrate all purge profiles for a set of samples, the integrated area of each quantitation mass will be directly proportional to the concentration of the corresponding analytes in a particular

sample. Because of this, linear calibration curves can readily be generated from a series of standards of known concentration. Unknown samples can then be quantitated by comparison of the integrated response for the targeted analytes with the corresponding calibration data. Automated quantitation software included with the ion trap mass spectrometers provides the capability to generate calibration curves and calculate analyte concentrations for unknown samples.

### 7.3 Analysis of Water Samples in 40-ml VOA Vials

This section describes the procedure for the analysis of CNS tear gas compounds in water samples that have been collected in 40-ml VOA vials.

#### 7.3.1 Set-up of Purge Module

The 40-ml VOA vial purge module described in Section 4.1.2 is used for these analyses. The device is attached to the capillary restrictor interface and the flow rate of helium is adjusted to 100 +/- 5 ml/min. If heated purge is required, the sleeve heater described in Section 4.2.4 is used.

#### 7.3.2 Monitoring of Purge Flow Rate and Sample Temperature

Calibration of the helium flow rate through the 40-ml VOA vial sparging device is performed using a flow meter capable of measuring helium flow in the range of 100 ml/min. It is attached to the vent port of the sample splitter during the flow adjustment procedure.

*Note: If the sleeve heater is used, the temperature is monitored with a digital thermometer, as described in Section 4.2.6.*

#### 7.3.3 Blank Water Samples

Blank water samples are to be routinely analyzed to check for possible analyte carryover in the sample interface and to check for contamination of the ion trap mass spectrometer.

##### 7.3.3.1 Preparation of Blank Water Samples

Blank water samples are prepared by completely filling a 40-ml VOA vial with simulated groundwater. The water samples are then spiked with a 10- $\mu$ l aliquot of 1,4-difluorobenzene internal standard solution, producing a final concentration of approximately 50 ppb of



1,4-difluorobenzene in the sample. The function of the internal standard in the blank samples is to verify that the ion trap is functioning properly in terms of mass calibration and expected signal response (ion counts).

#### 7.3.3.2 Analysis of Blank Water Samples

Immediately after the water sample is spiked with the internal standard solution, the sample vial is attached to the sparging module. The helium flow is then permitted to pass through the sample and data acquisition is begun. The sample is sparged for a total of 3 minutes during which mass spectra are continually recorded at 1-second intervals.

At the end of 3 minutes, the helium flow through the sample vial is stopped and the acquisition of mass spectra is terminated. The sample vial is then removed and replaced with an empty 40-ml VOA vial. Helium is permitted to pass through the empty VOA vial. This is performed after every sample in order to remove analyte carryover from the sparging module prior to the analysis of the next sample.

The 3-minute-long "purge profiles" for the blank water samples are examined for the presence of anomalous peaks in the mass spectrum. Mass peaks that cannot be accounted for by the internal standard or by background air are generally an indication of contamination in either the blank water sample or in the sample interface hardware.

In addition to checking for anomalous peaks in the mass spectrum, the response for the 1,4-difluorobenzene internal standard must be checked to verify that the signal intensity is sufficient to enable detection of this compound at a concentration of less than 5 ppb. This means that the signal-to-noise ratio for the  $m/z$  114 peak of the 1,4-difluorobenzene at a concentration of 50 ppb needs to be at least 50:1. This assumes that the response of the mass spectrometer is linear and a signal-to-noise ratio of 5:1 is needed to reliably detect a sample containing 5 ppb of the targeted analyte.

#### 7.3.4 External Standard Calibration

External standard calibration curves are used for the quantitation of unknown samples. These calibration curves are generated by sparging 40-ml samples of water that are spiked with known amounts of the targeted analytes.

##### 7.3.4.1 Preparation of Calibration Samples

The calibration samples are prepared by using a syringe to add appropriate aliquots of the external standard "working" solutions to 40-ml VOA vials that are completely filled with simulated groundwater. *Refer to data in **Tables I and II** and **Equation 1** to determine the quantities of the analyte "Working Solutions" to add to the water for a desired final concentration.* Each calibration sample is also spiked with 10  $\mu$ l of the 1,4-difluorobenzene internal standard "working" solution to produce a final concentration of 50 ppb in the sample. Each calibration sample should be prepared immediately prior to analysis.

After spiking a calibration sample with the appropriate standards, the sample vial is attached to the purge module and data acquisition is started. The calibration samples are each sparged for a total of 3 minutes during which mass spectra are continually acquired and stored in the form of an "Acquisition Data File."

*Note: Special conditions must be used for 2-Chloroacetophenone and 3-Chloroacetophenone.*

*Due to the strong matrix interaction of both 2-chloroacetophenone and 3-chloroacetophenone with water, they respond very poorly at ambient temperature and the samples must be heated for quantitative analysis. In addition, the response is very slow and the ion current signals do not reach a steady-state for approximately 15 minutes. Therefore, in order to accumulate sufficient signal to generate reliable calibration curves for the chloroacetophenones, it is necessary to perform a heated purge and to acquire data for at least 15 minutes instead of 3 minutes. The analytical procedure for the heated purge for 2-chloroacetophenone and 3-chloroacetophenone is the same as described in this section except that the sleeve*

heater described in Section 4.1.4 was used to heat the sample vial to approximately 60°C during the sparging process.

#### 7.3.4.2 Generation of Calibration Curves

The "Acquisition Data Files" generated in Section 7.3.4.1 are subjected to the data reduction process described in Section 7.2. Automated software provided by the ion trap manufacturers is available for the integration of the purge profiles and plotting of the calibration curves.

#### 7.3.5 Analysis of Unknown Samples

A sample of unknown water in a 40-ml VOA vial is spiked with a 10µl aliquot of 1,4-difluorobenzene internal standard "Working Solution" to produce a final concentration of 50 ppb in the sample. Immediately after adding the internal standard, the sample vial is attached to the purge module and data acquisition is started. Each sample is sparged for a total of 3 minutes during which time mass spectra are continually acquired and stored in the form of an "Acquisition Data File."

Upon completion of data acquisition, the "Acquisition Data File" is subjected to the data analysis procedure described in Section 7.2. An automated quantitation program provided by the ion trap instrument manufacturer can be used to integrate the purge profiles for the response of the quantitation masses for the targeted compounds. The concentrations of the targeted analytes can also be automatically calculated by this software by substituting the integrated responses into the external standard calibration equation and solving for concentration.

*Note: Special conditions must be used for 2-Chloroacetophenone and 3-Chloroacetophenone.*

*Due to the strong matrix interaction of both 2-chloroacetophenone and 3-chloroacetophenone with water, they respond very poorly at ambient temperature and the samples must be heated for quantitative analysis. In addition, the response is very slow and the ion current signals do not reach a steady state for approximately 15 minutes. Therefore, in order to accumulate sufficient signal to produce reliable quantitation of the chloroacetophenones, it is necessary to perform a heated purge and to acquire data for at least 15 minutes instead of the normal 3 minutes. The analytical procedure for the heated purge for*

*2-chloroacetophenone and 3-chloroacetophenone is the same as previously described, except that the sleeve heater described in Section 4.1.4 was used to heat the sample vial to approximately 60°C during the sparging process.*

#### 7.4 Analysis of Soil Samples in 40-ml VOA Vials

##### 7.4.1 Set-up of Purge Module

The 40-ml VOA vial purge module described in Section 4.1.2 is used for these analyses. The device is attached to the capillary restrictor interface and the flow rate of helium is adjusted to 100 +/- 5 ml/min. For the analysis of soil samples, heated purge is required. This is accomplished through the use of the sleeve heater described in Section 4.2.4.

##### 7.4.2 Monitoring of Purge Flow Rate and Sample Temperature

Calibration of the helium flow rate through the 40-ml VOA vial sparging device was performed using a flow meter capable of measuring helium flow in the range of 100 ml/min. It is attached to the vent port of the sample splitter during the flow adjustment procedure.

Using the sleeve heater controller described in Section 4.2.5, the temperature of the heater is set to 60°C. The actual temperature is monitored with a digital thermometer, as described in Section 4.2.6.

##### 7.4.3 Blank Soil Samples

Blank soil samples are to be routinely analyzed to check for possible analyte carryover in the sample interface and to check for contamination of the ion trap mass spectrometer.

###### 7.4.3.1 Preparation of Blank Soil Samples

A 5-g aliquot of an appropriate standard soil (certified to be clean) is weighed and placed in a 40-ml VOA vial. A small magnetic stir bar is placed in the vial along with the soil and simulated groundwater is added to completely fill the vial. The sample is then spiked with a 10-μl aliquot of the 1,4-difluorobenzene internal standard solution, producing a final concentration of approximately 50 ppb of 1,4-difluorobenzene in the sample. The cap is then placed on the vial and the sample is stirred for 30

seconds using a vortex stirrer in order to create a slurry of the soil and water.

#### 7.4.3.2 Analysis of Blank Soil Samples

Immediately after vortexing the sample, the cap is removed from the VOA vial and the vial is attached to the sparging module. The heater sleeve is placed over the vial and the magnetic stirrer is placed beneath the vial. The sample is heated to 60°C while it is stirred at a medium speed.

After allowing the sample to heat for 1 minute, the helium flow is permitted to pass through the sample and data acquisition is begun. The sample is sparged for a total of 3 minutes during which mass spectra are continually recorded at 1-second intervals.

At the end of 3 minutes, the helium flow through the sample is stopped and the acquisition of mass spectra is terminated. The sample vial is then removed and replaced with an empty 40-ml VOA vial. Helium is permitted to pass through the empty VOA vial. This is performed after every sample in order to remove analyte carryover from the sparging module prior to the analysis of the next sample.

The 3-minute-long "purge profiles" for the blank soil samples are examined for the presence of anomalous peaks in the mass spectrum. Mass peaks that cannot be accounted for by the internal standard or by background air are generally an indication of contamination in either the blank water sample or in the sample interface hardware.

Decontamination of the sample interface is corrected by heating the interface to a temperature of 100°C while purging the sample lines with a flow of clean helium at a rate of 100 ml/min until the background contamination is eliminated. The sample interface can usually be decontaminated in less than 15 minutes. Persistent contamination may require switching the sample-handling module with a clean sample-handling module if it is available.

In addition to checking for anomalous peaks in the mass spectrum, the response for the 1,4-difluorobenzene internal standard must be checked to verify that the signal intensity is sufficient to enable detection of this compound at a concentration of less than 5 ppb. This means that the signal-to-noise ratio for the  $m/z$  114 peak of the 1,4-difluorobenzene at a concentration of 50 ppb needs to be at least 50:1. This assumes that the response of the mass spectrometer is linear and a signal-to-noise ratio of 5:1 is needed to reliably detect a sample containing 5 ppb of the targeted analyte.

#### 7.4.4 External Standard Calibration

External standard calibration curves are used for the quantitation of unknown samples. These calibration curves are generated by sparging 40-ml samples of soil slurries that are spiked with known amounts of the targeted analytes.

##### 7.4.4.1 Preparation of Calibration Samples

A 5-g aliquot of an appropriate standard soil (certified to be clean) is weighed and placed in a 40-ml VOA vial. A small magnetic stir bar is placed in the vial along with the soil. The calibration samples are then prepared by using a syringe to add appropriate aliquots of the external standard "working" solutions to the soil. *Refer to the data in **Tables I and II** and **Equation 1** to determine the quantities of the analyte "Working Solutions" to add to the soil slurry for a desired final solution concentration.*

Once the standards have been added to the soil sample, it should be allowed to equilibrate for several minutes, allowing the standards to soak into the soil. The cap is then removed from the vial and simulated groundwater is added to the vial until it is completely filled. The sample is then spiked with a 10 $\mu$ l aliquot of the 1,4-difluorobenzene internal standard solution, producing a final concentration of approximately 50 ppb of 1,4-difluorobenzene in the sample. The cap is then replaced on the vial and the sample is stirred for 30 seconds using a vortex stirrer in order to create a slurry of the soil and water. Each calibration sample should be prepared immediately prior to analysis.

Immediately after spiking the calibration sample with the appropriate standards, the sample vial is attached to the purge module and data acquisition is started. The calibration samples are each sparged for a total of 3 minutes during which mass spectra are continually acquired and stored in the form of an "Acquisition Data File."

*Note: Special conditions must be used for the DSITMS analysis of samples that contain either 2-Chloroacetophenone or 3-Chloroacetophenone.*

*Due to the strong matrix interaction of 2-chloroacetophenone and 3-chloroacetophenone with water and soil, they respond very slowly and the ion current signals do not reach a steady state for approximately 15 minutes. Therefore, in order to accumulate sufficient signal to generate reliable calibration curves for the chloroacetophenones, it is necessary to acquire data for at least 15 minutes instead of the normal 3 minutes. Otherwise, the analytical procedure for the heated purge for 2-chloroacetophenone and 3-chloroacetophenone in a soil slurry is the same as previously described.*

#### 7.4.4.2 Generation of Calibration Curves

The "Acquisition Data Files" generated in Section 7.4.4.1 are subjected to the data reduction process described in Section 7.2. Automated software provided by the ion trap manufacturers is available for the integration of the purge profiles and plotting of the calibration curves.

#### 7.4.5 Analysis of Unknown Samples

A 5-g aliquot of an unknown soil sample is weighed and placed in a 40-ml VOA vial. *Note: Extra care must be taken with the sample to minimize the loss of volatile organics.* A small magnetic stir bar is placed in the vial along with the soil and simulated groundwater is added to the vial until it is completely filled. The sample is then spiked with a 10- $\mu$ l aliquot of the 1,4-difluorobenzene internal standard solution, producing a final concentration of approximately 50 ppb of 1,4-difluorobenzene in the slurry.

Once the internal standard has been added to the soil sample, the cap is replaced on the vial and the sample is stirred for 30 seconds using a vortex stirrer in order to create a slurry of the soil and water. Each sample should be prepared immediately prior to analysis.

Immediately after vortexing the unknown sample, the sample vial is attached to the purge module and data acquisition is started. The unknown samples are sparged for a total of 3 minutes during which mass spectra are continually acquired and stored in the form of an "Acquisition Data File."

*Note: Special conditions must be used for 2-Chloroacetophenone and 3-Chloroacetophenone.*

*Due to the strong matrix interaction of both 2-chloroacetophenone and 3-chloroacetophenone with water and soil, they respond very poorly at ambient temperature. In particular, the response is very slow and the ion current signals do not reach a steady state for approximately 15 minutes. Therefore, in order to accumulate sufficient signal to produce reliable quantitation of the chloroacetophenones, it is necessary to acquire data for at least 15 minutes instead of the normal 3 minutes. Otherwise, the analytical procedure for the heated purge for 2-chloroacetophenone and 3-chloroacetophenone is the same as previously described.*

## 7.5 Analysis of Groundwater by In-situ Sparge

This section describes the procedure for the analysis of CNS tear gas compounds in groundwater samples using an in-situ sampling probe. Because this probe is not heated, it can only be used for the determination of organics that are volatile at ambient temperature. In the case of CNS tear gas, this means that only chloroform and chloropicrin can be determined. Neither 2-chloroacetophenone nor 3-chloroacetophenone can be effectively determined by this technique.

### 7.5.1 Set-up of the In-situ Sparging Probe Assembly

The sample transfer line for the in-situ probe is connected to the capillary restrictor inlet of the ion trap mass spectrometer and the inlet of the air-sampling pump is attached to the split vent of the capillary restrictor. The helium line is connected to a cylinder of helium and the pressure is set to 30 psi.



The flow of helium into the sparging probe is controlled by an electronic flow controller. Potentiometer adjustments permit the flow rate to be varied from 10-100 ml/min. A digital readout provides a direct indication of the flow rate.

A flow controller identical to the one used to control the sparge helium is used to maintain a constant flow of helium through the sample transfer line and into the mass spectrometer interface. For proper operation, it is necessary for the flow rate of the helium into the sparging probe to always be 1% to 2% greater than the flow through the sample transfer line into the mass spectrometer. This maintains a slight positive pressure of helium inside of the sampling head and prevents water from entering the transfer line.

Prior to adjusting the flow rate of helium, the in-situ sparging probe must be immersed in a container of water. The flow rate of helium through the sample transfer line is adjusted to 0 ml/min and the flow rate of helium through the sparging tube is adjusted to approximately 40 ml/min. If properly adjusted, a steady stream of bubbles will be observed exiting the bottom of the sparging probe. At this point, the flow rate through the sample transfer line is slowly increased to 39 ml/min. If the flow rates are set properly, approximately one bubble should exit the bottom of the sparging probe every 5 seconds.

#### 7.5.2 Monitoring of Purge Flow

The purge flow rate is continuously monitored using the digital readout of the flow controller. Care must be exercised to make certain that the flow of helium into the sparging probe is always greater than the flow of gas out of the probe.

#### 7.5.3 Blank Water Samples

Blank water samples are analyzed prior to every sample analysis in which the in-situ sparging probe is used. This is done to ensure that the sampling probe and mass spectrometer are functioning properly and that there is little or no sample carryover between samples. This is especially important because the long sample transfer line that is used with the in-situ sparging probe has a tendency to retain some of the higher boiling point VOCs.

#### 7.5.3.1 Preparation of Blank Water Samples

Blank water samples are prepared by adding 250 ml of simulated groundwater to a 500-ml graduated cylinder. A 63- $\mu$ l aliquot of the 1,4-difluorobenzene internal standard is added to the sample to produce a final concentration of 50 ppb.

#### 7.5.3.2 Analysis of Blank Water Samples

The in-situ sparging probe (with flow rates already adjusted) is inserted into the graduated cylinder containing the water blank and data acquisition is started. Typically, the probe is left in the container of water for at least 1 or 2 minutes or until the signal level has stabilized for at least 30 seconds. Data acquisition is then terminated and the probe is removed from the water sample.

The 1- or 2-minute-long in-situ sparge "purge profiles" for the blank water samples are then examined for the presence of anomalous peaks in the mass spectrum. Mass peaks that cannot be accounted for by the internal standard or by background air are generally an indication of contamination in either the blank water sample, in the sample interface hardware, or more likely, in the sample transfer line.

Contamination of the ion trap mass spectrometer is corrected by heating the mass analyzer to a temperature of 150°C for a period of at least 8 hours until the contamination is eliminated.

In addition to checking for anomalous peaks in the mass spectrum, the response for the 1,4-difluorobenzene internal standard is checked to verify that the signal intensity is sufficient to enable detection of this compound at a concentration of less than 5 ppb. This means that the signal-to-noise ratio for the  $m/z$  114 peak of the 1,4-difluorobenzene at a concentration of 50 ppb needs to be at least 50:1. This assumes that the response of the mass spectrometer is linear and that a signal-to-noise ratio of 5:1 is needed to reliably detect a sample containing 5 ppb of the targeted analyte.

#### 7.5.4 External Standard Calibration

Calibration of the in-situ sparging probe for quantitation is accomplished through the use of external standards. This procedure first involves adjusting the in-situ sparging probe to the proper flow rates and acquiring a satisfactory spectrum from a blank water sample as previously described.

##### 7.5.4.1 Preparation of Calibration Standards

As soon as a satisfactory blank has been run, the in-situ probe is placed in a 500 ml graduated cylinder that is filled with exactly 250 ml of simulated groundwater. A 63- $\mu$ l aliquot of the 1,4-difluorobenzene internal standard is added to the sample to produce a final concentration of 50 ppb. A syringe is then used to add the appropriate amounts of the analyte "working" standard solutions to the water sample to produce the desired final concentration (see **Equation 2**).

##### 7.5.4.2 Generation of Calibration Curves

After letting the standard mix with the water for 60 seconds, data acquisition is started. The in-situ sparging probe is left in the sample container for at least 1 to 2 minutes or until the signal stabilizes for at least 30 seconds. The probe is then removed from the graduated cylinder and rinsed with distilled water. The calibration sample is then discarded into a waste container and the entire process is repeated using a sample with a different concentration of analytes.

Calibration curves are produced by integrating the flat portion of the purge profile over a fixed time window (typically 30-second intervals) using the response for targeted ions in the mass spectrum. The integrated area is directly proportional to the concentration of the analytes in the sample. Automated software for calibration and quantitation is provided by the ion trap instrument manufacturers.

#### 7.5.5 Analysis of Unknown Samples

Blank samples and probe calibration are typically performed prior to the analysis of unknown groundwater samples. Immediately

prior to inserting the probe into the groundwater, it is cleaned with distilled water and inserted into a glass container of clean water in order to obtain a background spectrum. Once a satisfactory background has been obtained, the probe is removed from the container of clean water and slowly lowered into the groundwater well. A conductivity detector mounted on the in-situ sparging probe indicates when the probe is at the proper level in the water.

Once the probe is in the proper position in the groundwater well, data acquisition is started. Mass spectra are continuously generated at 1-second intervals for a period of 3-5 minutes or until a stable signal has been obtained for at least 30 seconds. Data acquisition is then terminated and the probe is withdrawn from the well. It is immediately decontaminated by rinsing with clean water.

The quantitation of targeted analytes in the groundwater well is accomplished by plotting the purge profiles for the appropriate quantitation ions and then integrating these profiles using the same limits as applied to the calibration samples. Automated software for data integration and quantitation is available from the ion trap instrument manufacturers.

## **8.0 QUALITY CONTROL**

### **8.1 Instrument Performance**

Each sample that is analyzed is spiked with 1,4 difluorobenzene internal standard to produce a final concentration of 50 ppb. The response of the instrument is considered acceptable if the ion count for  $m/z$  114 is plus or minus three times the standard deviation of the mean response for the internal standard based on at least four previous measurements under the same operating conditions. If the response for the internal standard falls outside of this range, the analysis should be repeated. If the response again falls outside of the acceptable range, the instrument must be tuned and recalibrated.

### **8.2 Calibration Curve Statistics**

Calibration curves should be generated using at least three replicate measurements at each point. Full statistical information should then be determined for the calibration data, including the mean, standard deviation, and coefficient of variation. This information can be calculated using a spreadsheet or the data reduction software supplied by the vendors of the ion trap mass spectrometers.

### 8.3 Quality Control Samples

- 8.3.1 Blank samples should be run at the beginning of every set or group of analytical samples and at least once for every 20 analytical samples. If instrument contamination or analyte carryover is suspected, blank samples should be run prior to each analytical sample.
- 8.3.2 Check standards should be prepared by QC personnel and must be analyzed after the initial blank sample and at least once for every ten analytical samples. If the measured concentration of the check standard deviates from the known concentration  $\pm 20\%$ , then the instrument must be recalibrated before additional samples are analyzed.
- 8.3.3 Re-analysis of calibration solutions should be performed at least once every two days. If instrument repairs have been performed that result in replacement of the filament assembly or electron multiplier, re-calibration must be performed prior to the analysis of samples.
- 8.3.4 Matrix spikes, trip blanks, and blind QC samples should be run on a regular basis. The specific requirements for the number and types of samples to be run will depend on the level of QA and QC that is specified for a particular project.

### 8.4 Detection Limits

The Method Detection Limit (MDL) over a target concentration range was calculated by plotting the regression line representing the relationship between the "instrument response" vs "target concentrations" with appropriate one-sided upper 99% confidence limits for a predicted observation (see **Appendix 1**). After locating the intercept of the upper 99% predictive confidence limits with the y-axis "instrument response," a horizontal line is drawn from the intercept until it intersects the regression line. Finally, a vertical line is drawn from the intercept to the x-axis "target concentrations." This intersection with the x-axis is the MDL. It should be noted that EPA provides a different procedure (**Reference 7**) for determining detection limits. EPA's method was not used in this project, however, the method described above should produce similar results.

The MDLs for chloropicrin and chloroform were determined using a concentration range of 0-15 ppb with four replicate measurements each at 0, 2, 5, 10, and 15 ppb. The calculated MDL for chloroform is 0.15 ppb and the calculated MDL for chloropicrin is 0.20 ppb.

Calculation of the MDL can be performed using a standard spreadsheet program such as Microsoft EXCEL.

## 9.0 REFERENCES

1. Marcus B. Wise and Michael R. Guerin, "Direct Sampling MS for Environmental Screening," *Analytical Chemistry*, 1997, 69, 26A-32A.
2. Marcus B. Wise, Cyril V. Thompson, Roosevelt Merriweather, and Michael R. Guerin, "Review of Direct MS Analysis of Environmental Samples," *Field Analytical Chemistry and Technology*, 1997, 1(5), 251-276.
3. W. M. Davis, M. B. Wise, J. S. Furey, and C. V. Thompson, "Rapid Detection of Volatile Organic Compounds in Groundwater by In Situ Purge and Direct Sampling Ion Trap Mass Spectrometry," *Field Analytical Chemistry and Technology*, 1998, 2(2), 89-96.
4. Marcus B. Wise, Michael R. Guerin, Roosevelt Merriweather, and Cyril V. Thompson, "Direct Sampling Ion Trap Mass Spectrometry for the Measurement of Volatile Organic Compounds in Water, Soil, and Air," Proposed Method 8265 for US EPA SW-846 Manual, Oak Ridge National Laboratory, 1997.
5. Test Methods for Evaluating Solid Waste, Volume IB: Laboratory Manual Physical Chemical Methods, US EPA SW-846 Manual, November 1986.
6. Teledyne Electronic Technologies 3DQ Discovery Reference Manual, May 17, 1995, Mountain View, California.
7. Code of Federal Regulations, 1990 "Definition and Procedure for the Determination of the Method Detection Limit," Code of Federal Regulations, Part 136, Appendix B, pp. 537.

## **Appendix 1**

### **Method Detection Limit (MDL) Calculation Procedure**

- (1) Calculate and plot the regression line representing the relationship between the "instrument response" vs. "target concentration" with appropriate one-sided upper 99% confidence limits for a predicted observation.
- (2) Locate the intercept of the upper 99% predictive confidence limits with the y-axis "instrument response."
- (3) Draw a horizontal line from the intercept described in (2) until it intersects the regression line.
- (4) Draw a vertical line from the intercept described in (3) to the x-axis "target concentrations." This intersection with the x-axis is the MDL.

**Table I**  
Physical Properties of the Targeted Analytes

Analyte	Molecular Weight	Density	MP	BP
Chloropicrin	164.38 g/mole	1.6566 g/ml	-64 C	112 C
Chloroform	119.38 g/mole	1.4832 g/ml	-63 C	62 C
3-Chloroacetophenone	154.60 g/mole	1.2130 g/ml	.....	241 C
2-Chloroacetophenone	154.60 g/mole	1.2016 g/ml	56 C	247 C

**Table II**  
Quantity of Analyte Required to Produce a 5,000 ug/ml Stock Solution of Each Analyte  
in a Total of 5 ml of Methanol

Analyte	Weight of Analyte Required	Liquid Equivalent
Chloropicrin	25 mg	15.1 µl
Chloroform	25 mg	16.8 µl
3-Chloroacetophenone	25 mg	20.6 µl
2-Chloroacetophenone	25 mg	(solid)

**Equation 1**

Equation for producing a known concentration of targeted analyte in a 40-ml water sample using a 100-µg/ml stock solution of analyte.

$$\text{Total } \mu\text{l of stock solution} = \text{Desired Final Concentration (ppb)} \div 2.5 \text{ ppb}/\mu\text{l}$$

**Equation 2**

Equation for producing a known concentration of targeted analyte in a 250-ml water sample using a 100-µg/ml stock solution of analyte.

$$\text{Total } \mu\text{l of stock solution} = \text{Desired Final Concentration (ppb)} \div 0.4 \text{ ppb}/\mu\text{l}$$



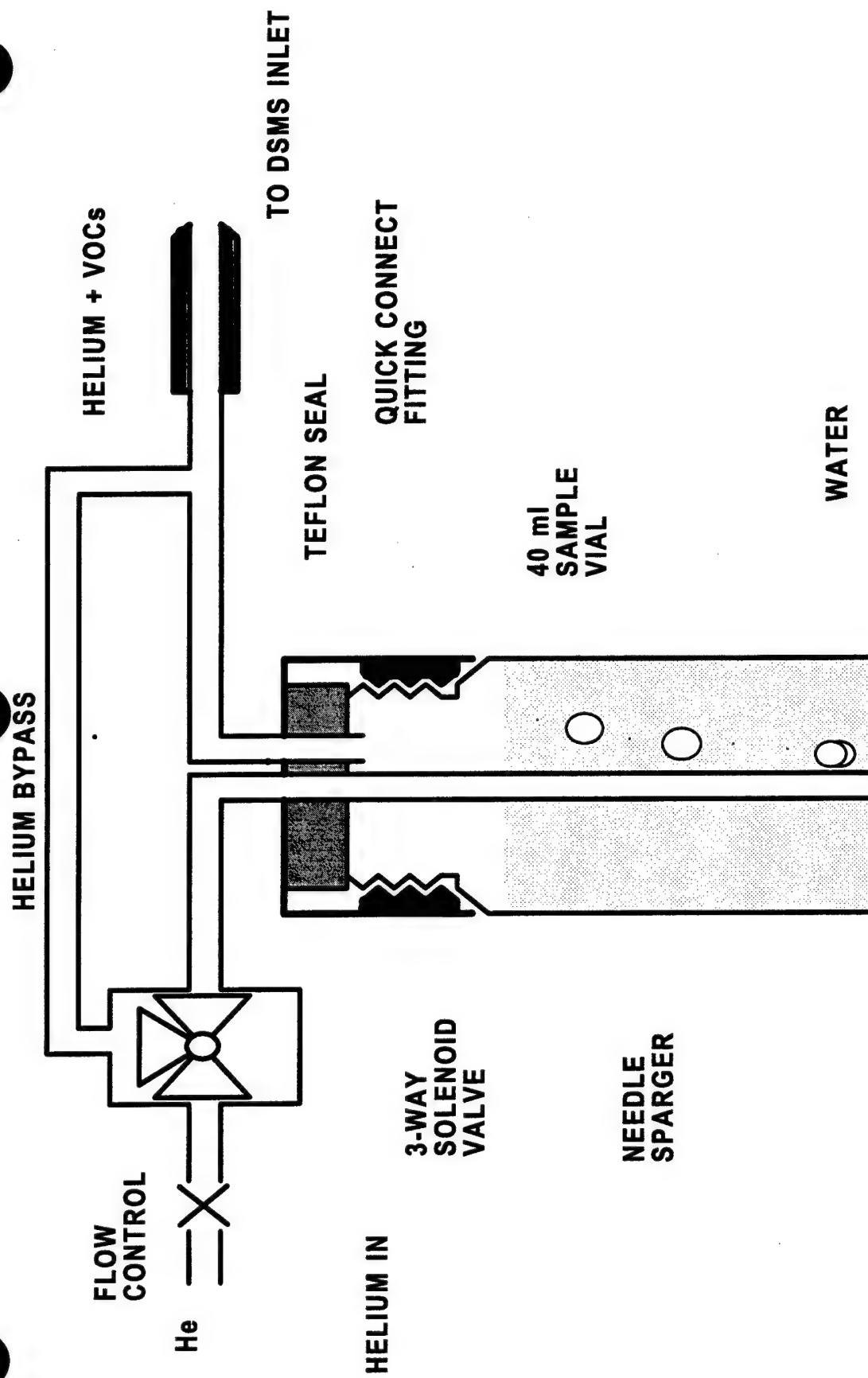


Figure 1: Purge module for analysis of VOCs in water. This apparatus is intended for use in conjunction with standard 40-ml VOA sample vials.

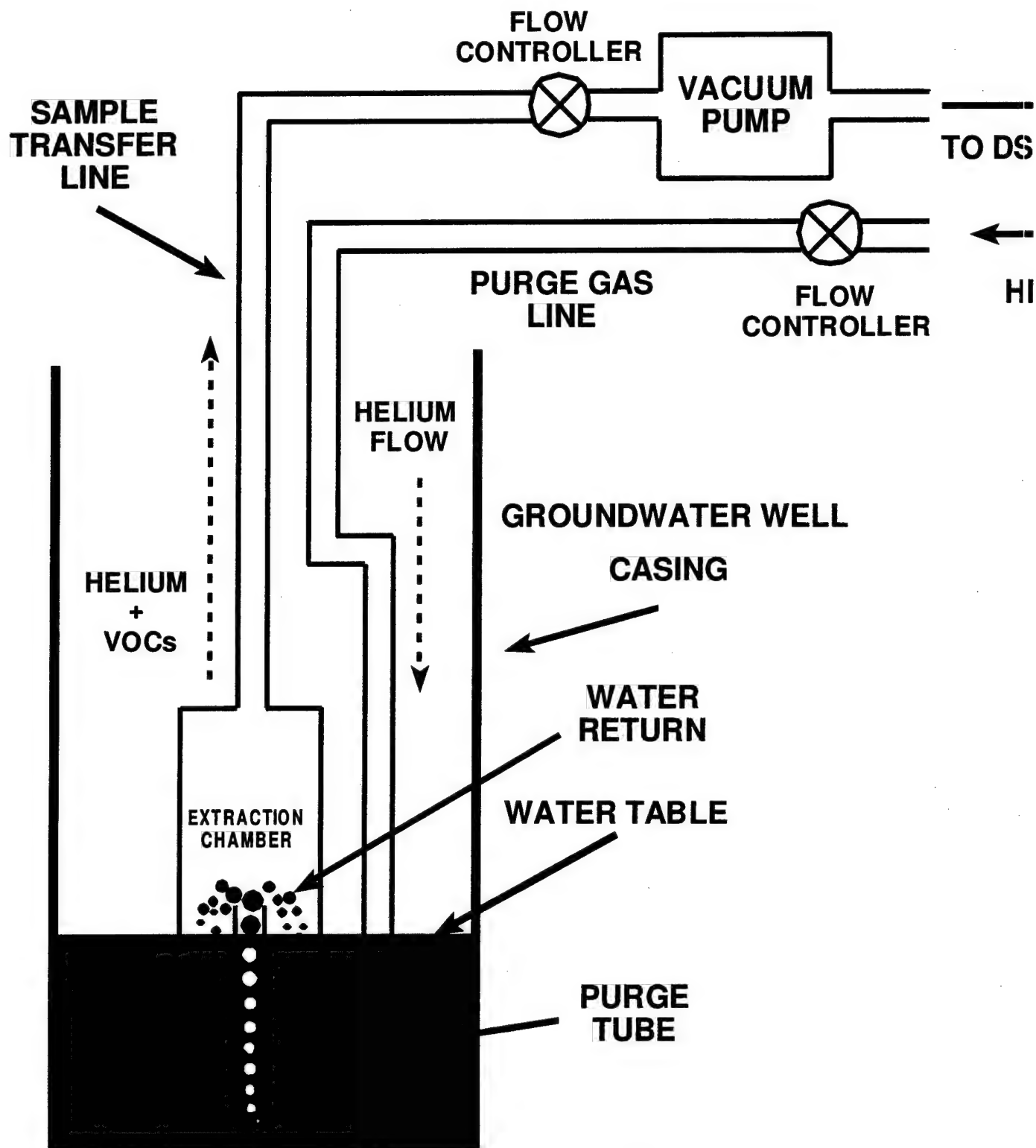


Figure 2: In-situ probe for the continuous measurement of VOCs in surface water and groundwater.

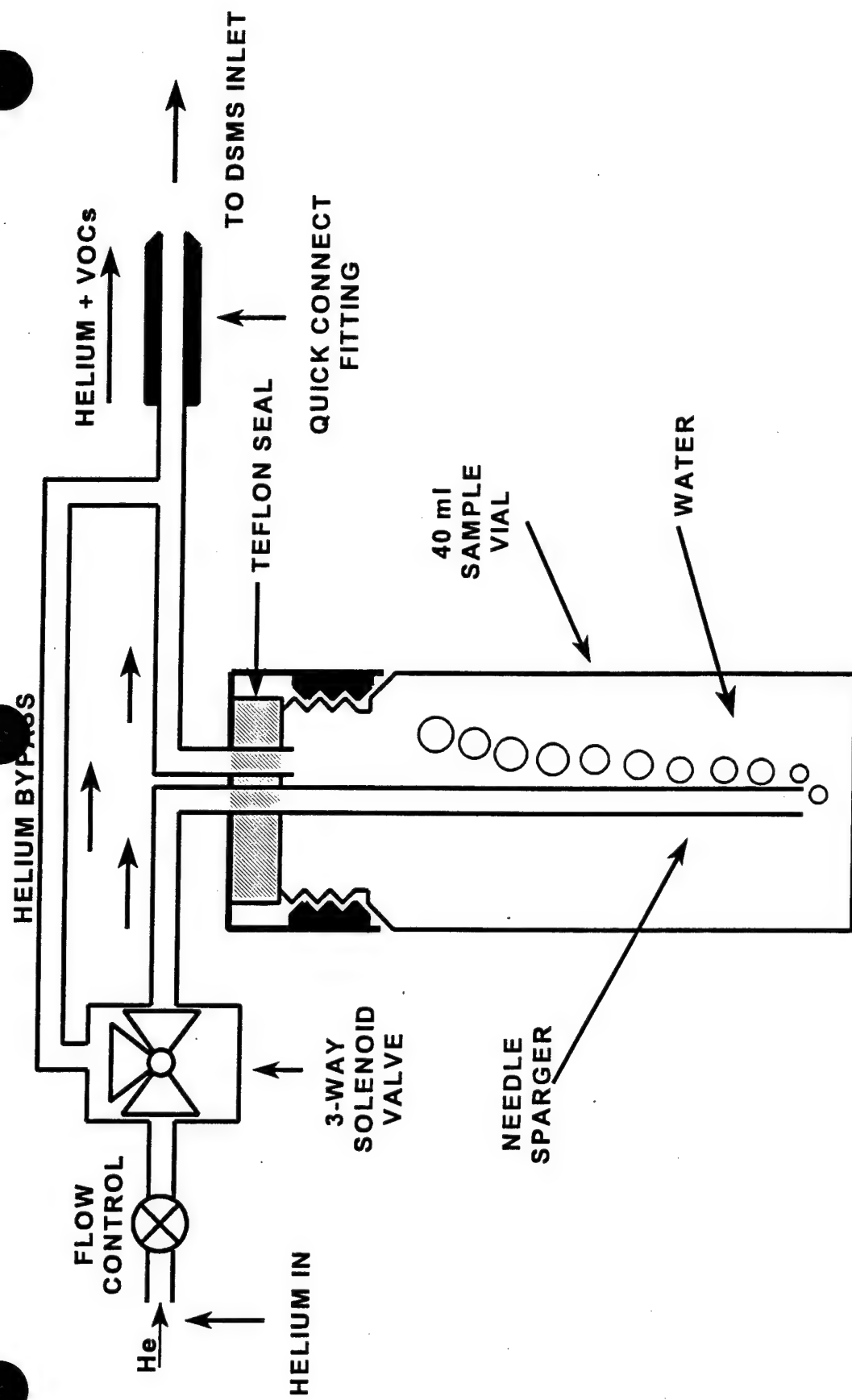


Figure 1: Purge module for analysis of VOCs in water. This apparatus is intended for use in conjunction with standard 40 ml VOA sample vials.

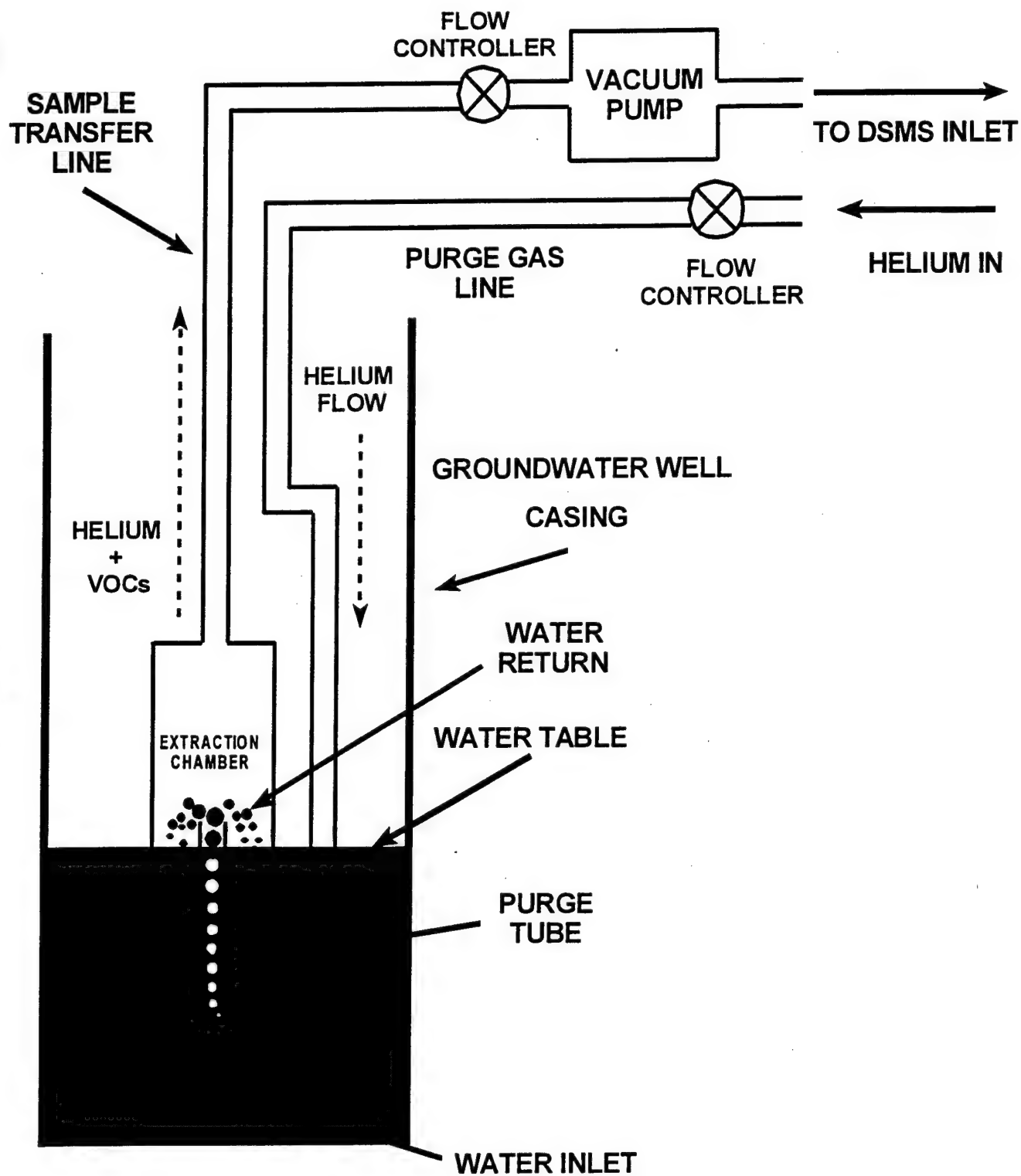


Figure 2: In-situ probe for the continuous measurement of VOCs in surface water and groundwater.



**APPENDIX E**  
**BOREHOLE FLOWMETER TESTS**

**TENNESSEE VALLEY AUTHORITY  
RESOURCE GROUP, WATER MANAGEMENT  
ENGINEERING LABORATORY**

**DEMONSTRATION OF THE ELECTROMAGNETIC BOREHOLE FLOWMETER AT  
FEDERAL LABORATORIES AREA 15A, SALTSBURG, PENNSYLVANIA**

**WR98-1-520-200**

**Prepared by**

**J. Mark Boggs  
and  
Hank E. Julian**

**Norris, Tennessee  
February 1998**

## TABLE OF CONTENTS

	Page
Acronyms and Abbreviations .....	iii
Executive Summary .....	S-1
Introduction .....	1-1
Site Description .....	2-1
Flowmeter Description .....	3-1
Background .....	3-1
Instrument Design .....	3-2
Calibration .....	3-7
Sensitivity and Accuracy .....	3-8
Limitations .....	3-10
Methodology for Collection and Analysis of Flowmeter Data .....	4-1
Flowmeter Testing Procedure .....	4-1
Data Analysis .....	4-3
Flowmeter Applications at Federal Laboratories Area 15 .....	5-1
Methods .....	5-1
Results and Interpretation .....	5-5
Implications .....	5-11
References .....	6-1
Appendix A - Geologic Logs and Well Construction Diagrams .....	A-1
Appendix B - EM Borehole Flowmeter Surveys .....	B-1

## LIST OF FIGURES

2.1 Structural Contours on Upper Freeport Coal .....	2-2
2.2 West-East Hydrostratigraphic Section Through Area 15A .....	2-3



## TABLE OF CONTENTS (continued)

	Page
2.3 Potentiometric Levels in Saltsburg (upper box) and Buffalo (lower box) Aquifers as Measured on 11/20/97 .....	2-5
3.1 EM Borehole Flowmeter System Showing Above-Ground Electronic and Flowmeter .....	3-4
3.2 Schematic Diagram of EM Flowmeter .....	3-5
3.3 EM Flowmeter with (a) Mechanical Collar (left), and (b) Pneumatic Packer (right) .....	3-6
3.4 Precalibration (November 1997) Data for 1.0-Inch Flowmeter .....	3-9
3.5 Laboratory Calibration Data for 1.0-Inch Flowmeter at Lower Threshold .....	3-10
4.1 Concept of Borehole Flowmeter Test .....	4-2
4.2 Assumed Layered Geometry Within Which Flowmeter Data are Collected and Analyzed .....	4-4
5.1 Well Location Map .....	5-2
5.2 West-East Stratigraphic Section Showing Well Flow Profiles .....	5-6
5.3 North-South Stratigraphic Section Showing Well Flow Profiles .....	5-7
5.4 Surface Elevation of Upper Preferential Flow Zone .....	5-8
5.5 Surface Elevation of Lower Preferential Flow Zone .....	5-8
5.6 Hydraulic Conductivity Profiles for Test Wells (Arithmetic Scales) .....	5-9
5.7 Hydraulic Conductivity Profiles for Test Wells (Logarithmic Scales) .....	5-10
5.8 Probability Distribution of Log K Data .....	5-12
5.9 Example of Three Stochastically-Generated Fracture Realizations .....	5-14

## LIST OF TABLES

3.1 Potential Field Problems That May Produce Errors in EM Flowmeter Measurements .....	3-11
4.1 Summary of Borehole Flowmeter Testing Procedures .....	4-3
5.1 Summary of Single-Well Pumping and Injection Tests .....	5-1

## ACRONYMS AND ABBREVIATIONS

AFB	Air Force Base
CNS	Chloroacetophenone, Chloropicrin, and Chloroform
DC	Direct Current
DNAPL	Dense Nonaqueous Phase Liquid
EM	Electromagnetic
EPA	Environmental Protection Agency
K	Hydraulic Conductivity
K <sub>i</sub>	Incremental (Layer) Hydraulic Conductivity
MSL	Mean Sea Level
NAPL	Nonaqueous Phase Liquid
PVC	Polyvinyl Chloride
RCRA	Resource Conservation and Recovery Act
T	Transmissivity
S	Storage Coefficient
SS	Stainless Steel
TVA	Tennessee Valley Authority

# **DEMONSTRATION OF THE ELECTROMAGNETIC BOREHOLE FLOWMETER AT FEDERAL LABORATORIES AREA 15A, SALTSBURG, PENNSYLVANIA**

## **EXECUTIVE SUMMARY**

Eight borehole flowmeter tests were performed in November 1997, at the Area 15A CNS tear gas disposal site located at the Federal Laboratories Facility near Saltsburg, Pennsylvania. The purpose of the investigation was to obtain quantitative information regarding the spatial distribution of hydraulic properties of shallow geologic materials that underlie the site. These data will be used in numerical models to evaluate remedial strategies for the disposal site.

Previous investigations have shown that the residual soil overburden beneath Area 15A consists primarily of clay and ranges from 10 to 18 ft in thickness. Some 300 to 1700 steel drums containing CNS tear gas were reportedly buried in the basal section of the overburden. The underlying bedrock consists of sandstone and shale units of the Glenshaw formation. The Saltsburg sandstone member of the Glenshaw formation represents the shallowest aquifer beneath the site. Thickness of this unit, in the site vicinity, is generally 50 ft or less. Flowmeter testing in seven existing monitoring wells was limited to the lower few feet of soil overburden and the upper 10 to 20 ft of sandstone and shale bedrock. A new test well installed as part of this investigation allowed testing over deeper intervals of the Saltsburg aquifer.

A sensitive electromagnetic (EM) flowmeter capable of measuring flow rates as low as 20 mL/min was used to measure flow in each well during a constant-rate pumping or injection test. Flow measurements were generally performed at intervals of 0.5 to 1.0 ft along the full length of the well screen. Discrete estimates of hydraulic conductivity (K), corresponding to the flow measurement intervals for each well, were subsequently computed from the flow data. A total of 165 discrete K estimates were obtained from the eight well tests. K estimates ranged from 0.04 to 560 ft/d. K data are log-normally distributed with a mean log K of 0.61 and standard deviation of 0.83. The field measurement thresholds for K varied by well, ranging from 0.04 to 3 ft/d. Approximately 55 percent of the total data were below field threshold limits.

Results indicate that a few thin preferential flow zones dominate shallow groundwater movement. For the most part, these features are believed to be hydraulically active bedrock fractures. Collective examination of well flow profiles indicates two preferential flow zones which appear to be continuous over most of the site. The shallowest of these features lies within

the upper bedrock or, in the case of wells MWU-14, -19, and -20, in the lower part of the soil overburden. The second preferential flow feature was observed some 8 to 12 ft below the first. Contaminants released in NAPL form from the corroded containers will tend to move downward through the underlying bedrock in response to density and natural hydraulic gradients. Once in the bedrock, their movement may be largely controlled by the orientation and connectivity of hydraulically active fractures.

While groundwater circulation within the bedrock matrix was not detectable in the flowmeter logs, it is likely that there is limited porosity and permeability associated with the rock matrix that may be important in the ultimate fate and transport of the tear gas contaminants. Past experience at other fractured rock sites indicates that NAPL contaminants migrating through fractures may quickly disappear due to dissolution and subsequent diffusion into the rock matrix. Under such conditions, clean-up times may be extremely long as contaminants slowly diffuse out of the rock matrix.

The flowmeter results suggest that fractured porous media type flow and transport models would best represent the bedrock aquifer system present beneath Area 15A. Although existing models of this type are incapable of handling multiphase (aqueous, nonaqueous, vapor) flow and transport, a reasonable approximation is possible by treating the nonaqueous phase implicitly in the model (e.g., as a boundary condition). Such models can be used to simulate the ultimate fate of tear gas contaminants in the bedrock underlying Area 15A under assumptions of (1) future removal of the buried source material, or (2) no source removal. In view of the infeasibility of completely characterizing the bedrock fracture network at the site, a stochastic approach to fate and transport predictions is recommended. Porous media models capable of complete multiphase simulations are available for evaluation of in situ treatment system options focused on the drum-burial site.

## Chapter 1

### Introduction

The U.S. Army Environmental Center contracted, in 1996, with the Tennessee Valley Authority Resource Management to conduct a scientific study of the fate of tear gas in soils. The study is primarily intended to develop quantitative data regarding the behavior of CNS tear gas in soils that can be applied to future environmental investigations at other tear gas contaminated sites. A second study objective is to evaluate technologies for remediation of CNS tear gas contaminants (i.e., chloroform, chloropicrin, and chloroacetophenone) at a tear gas disposal facility located at the Federal Laboratories Plant No. 3 near Saltsburg, Pennsylvania. During the mid-1950s between 300 and 1700 55-gallon drums of surplus CNS tear gas were buried in the southwestern portion of the plant property at a disposal site known as Area 15A. Corrosion of the steel storage drums has occurred over time, and contamination consistent with CNS has been detected in groundwater beneath Area 15A and in springs located on adjoining property.

As part of the process of evaluating remedial options for Area 15A, a groundwater flow/transport model of the site will be developed to assess the fate of contaminants under natural conditions and under conditions of active remediation. Limited subsurface characterization of the site has been performed to support model development. A relatively new technology, known as the electromagnetic (EM) borehole flowmeter, has been applied at the site to characterize the groundwater flow field and the hydraulic properties of the underlying geologic media. Demonstration of the EM flowmeter at the Area 15A site is the subject of this report.

Characterization of the hydraulic properties of geologic media underlying a contaminated site is fundamental to any remediation effort. Local heterogeneities in the hydraulic conductivity of geologic materials in the vicinity of a contaminant source strongly influence the groundwater transport of contaminants away from the source. Contaminated groundwater migrates quickly through zones of high hydraulic conductivity, but lags behind in regions of low hydraulic conductivity. To accurately predict the movement and spreading of the contaminant plume requires detailed measurements of the spatial distribution of hydraulic conductivity. Conventional methods of characterizing aquifers and other geologic media commonly involve single or multiple-well aquifer tests. These tests involve pumping a well at a constant rate while monitoring the water level response in the pumped well and, in the case of multiple-well tests, in surrounding

observation wells. Conventional aquifer tests produce estimates of the transmissivity and average hydraulic conductivity for the aquifer, but reveal little about the spatial variations in aquifer properties which invariably exist in geologic media. Unfortunately, the underestimation of aquifer heterogeneity through the application of conventional aquifer characterization methods has significantly contributed to the improper design and, consequently, inadequate performance of many types of remediation systems [U.S. EPA, 1990; Haley et al., 1991; National Research Council, 1995].

The EM flowmeter is a highly sensitive instrument that allows direct estimation of the spatial distribution of hydraulic conductivity. The flowmeter test is similar to a conventional aquifer test except that measurements of flow entering (or exiting) the well are made at discrete intervals while the well is pumped (or injected) at a constant rate. The hydraulic conductivity of each measurement interval (and corresponding layer of the aquifer) is proportional to the measured flow. By performing flowmeter tests in a network of wells at a particular site, one can develop a three-dimensional representation of the hydraulic conductivity distribution. The flowmeter method is particularly useful for characterizing complex fractured bedrock aquifers such as that at the Area 15A site. Vertical flow logs can be used to readily identify hydraulically active fractures. The EM flowmeter is also capable of measuring the natural (ambient) vertical flow often present in wells or boreholes. Knowledge of ambient flow allows one to infer the direction of the vertical component of the hydraulic gradient in the vicinity of the test well.

Previous investigations of the Area 15A site have focused largely on delineation and monitoring of the contaminant plumes in the site vicinity [Earth Sciences Consultants, Inc., 1992]. The only attempt at characterizing the hydraulic properties of the geologic materials in the immediate vicinity of Area 15A involved a multiple-well pumping test conducted in 1995 by Conestoga-Rovers & Associates on behalf of TransTechnology, Inc., the present operators of the Federal Laboratories facility. The test was intended to provide data for designing a network of interceptor wells to prevent further off-site migration of tear gas contaminants. The test produced estimates of the average transmissivity of the shallow sandstone aquifer at the site ranging from 44 to 179 ft<sup>2</sup>/d [Conestoga-Rovers & Associates, 1995]. While these test results may be useful for determining the number of interceptor wells required and for estimating well pumping rates, they do not provide the type of data required for predicting the fate and transport of contaminants under natural or remediation conditions.

This report presents background theory and documents application of the EM flowmeter at Federal Laboratories Area 15A tear gas disposal facility. Chapter 2 presents a brief description of the hydrogeologic conditions at the disposal site. A comprehensive description of the EM flowmeter instrument is given in Chapter 3 of the report along with a discussion of meter calibration, sensitivity, and limitations. The theoretical basis for estimating layer hydraulic conductivities from well (or borehole) flow measurements is given in Chapter 4 along general field testing protocols. The application of the flowmeter technique to the Area 15A site is described in Chapter 5. Site-specific testing methods and results are presented in this chapter. Preliminary implications of the flowmeter testing results for groundwater modeling and remedial strategy selection for Area 15A are discussed at the conclusion of Chapter 5.

## Chapter 2

### Site Description

The Federal Laboratories facility is located in the Conemaugh Township of Indiana County, Pennsylvania. The facility is physiographically situated in the Pittsburgh Plateaus section of the Appalachian Plateau Physiographic Province. The primary geologic unit of interest relative to Area 15A is the Pennsylvanian age Glenshaw formation of the Conemaugh Group. The Glenshaw is comprised of sequence of interbedded sandstone, shale, and coal units. Aquifers within the Glenshaw include (in order of increasing depth) the Saltsburg sandstone, Buffalo sandstone, and Mahoning sandstone. The Upper Freeport Coal lies at the base of the Glenshaw formation and provides a marker bed which serves to define shallow geologic structure. Figure 2.1 shows elevation contours on the top of the Upper Freeport Coal and indicates that Area 15A lies just west of the crest of a northeast-southwest trending anticline which plunges to the southwest. Geologic strata directly beneath Area 15A dip gently to the northwest.

Area 15A is topographically situated in the uplands along the north side of the Conemaugh River. In the immediate vicinity of the disposal site, land surface slopes gently to the west toward Elders Run, a tributary to the Conemaugh River. Ground elevation ranges from approximately 1170 to 1200 ft mean sea level across the site. Just west and south of the site the ground elevation declines steeply toward Elders Run and the Conemaugh River.

A generalized west-east hydrostratigraphic section through the Area 15A site is presented on Figure 2.2. The unconsolidated soil overburden beneath the site is derived from weathering of the underlying shale and sandstone bedrock. These residual soils primarily consist of sandy clay with occasional weathered rock fragments. Soil deposits range from about 10 to 18 ft in thickness across the disposal area. The saturated hydraulic conductivity of six soil samples collected at Area 15A, in November 1997, range from  $7 \times 10^{-9}$  to  $5 \times 10^{-6}$  cm/s [D.B. Stephens & Associates, 1997]. Based on geologic logs for monitoring wells in the site vicinity, it appears that shale lies directly below the eastern two-thirds of the disposal area with the Saltsburg sandstone directly underlying the remaining area. The Saltsburg is a gray fine-to-coarse grained sandstone with thin interbedded shale and coal seams. Thickness is on the order of 50 ft or less in the site vicinity. A shale zone some 20 to 40 ft thick separates the Saltsburg sandstone from



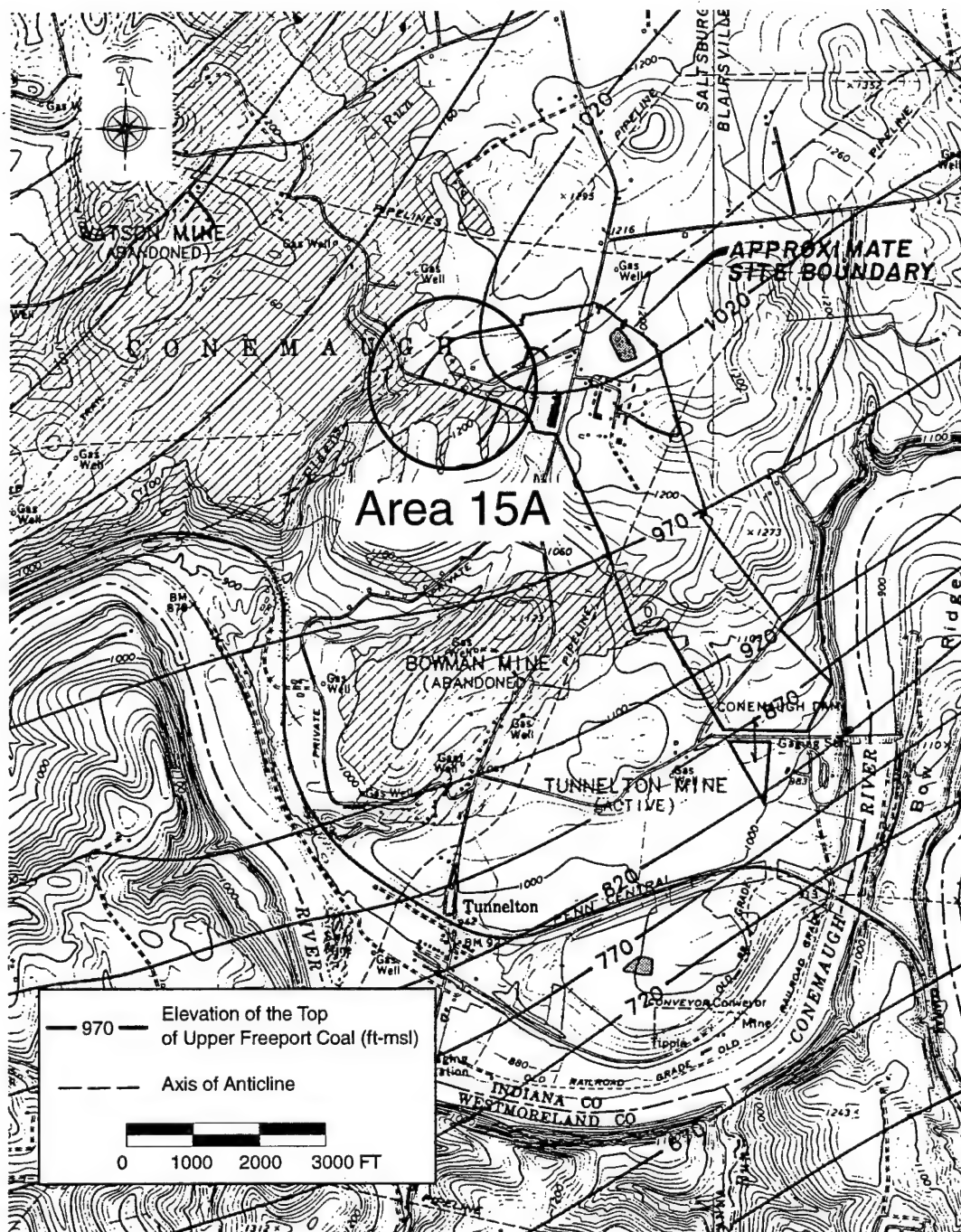


Figure 2.1 Structural Contours on Upper Freeport Coal

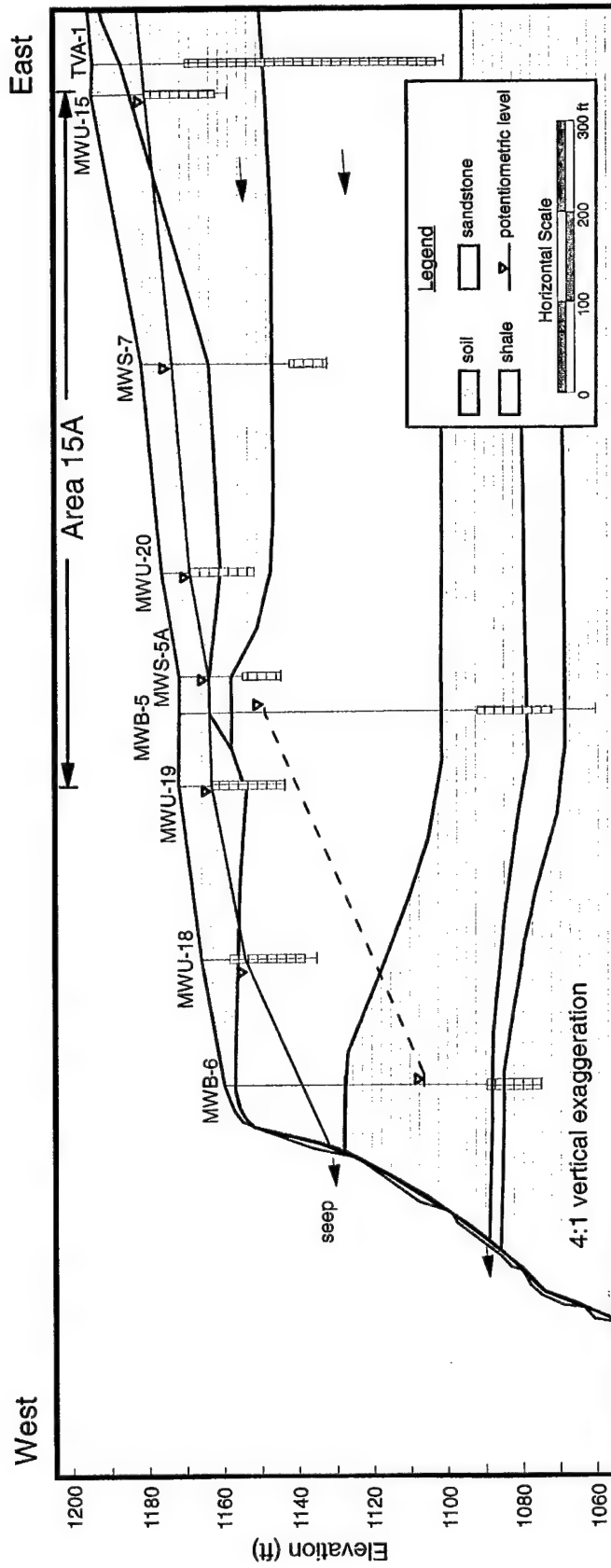


Figure 2.2 West-East Hydrostratigraphic Section Through Area 15A

the underlying Buffalo sandstone. Although considered an aquifer in the site region, the water-bearing capacity of the Buffalo is locally doubtful. It consists of gray shaly sandstone and ranges from 3 to 12 ft in thickness. The Saltsburg and Buffalo sandstones dip to the west and northwest at gradients of about 2 percent and outcrop along the Elders Run valley wall just west of the site. To our knowledge, no subsurface investigations below the Buffalo sandstone have been performed at Area 15A.

Figure 2.3 shows the potentiometric surfaces in both the upper Saltsburg sandstone and in the Buffalo sandstone based on water level measurements in site monitor wells made in June 1995. The gradient of the potentiometric surface in the Saltsburg is approximately 2 to 3 percent to the west and southwest, whereas that of the Buffalo is about 14 percent west-northwest. A roughly west-to-east direction of groundwater movement across the disposal site is indicated by both potentiometric maps. Based on the prevailing horizontal hydraulic gradients in these aquifers and on geologic considerations, it appears that groundwater originating on-site, or passing beneath the site, ultimately discharges at the aquifer outcrop areas west of the site. The vertical component of the hydraulic gradient at the site is downward. This is evident in comparisons of the potentiometric surfaces for the Saltsburg and Buffalo aquifers (Figure 2.3) and in comparisons of the water levels in staged monitoring wells such as MWS-5A and MWB-5 (Figure 2.2). The magnitude of the hydraulic gradient between the two aquifers is approximately 20 percent. The relatively large downward gradient at the site is thought to be produced by the downward convergence of groundwater flow toward the aquifer discharge zones along the steep valley wall just west of the site. The presence of the abandoned mine in the Upper Freeport coal seam, some 160 ft below the site, may also contribute to the downward hydraulic gradient.

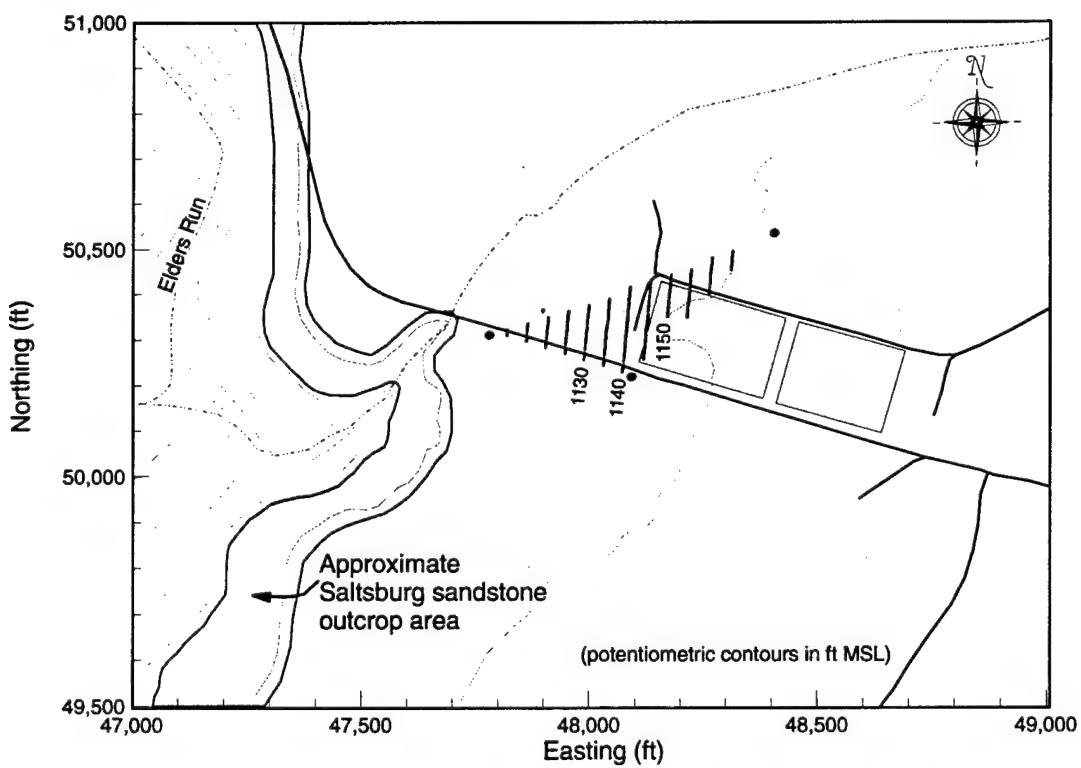
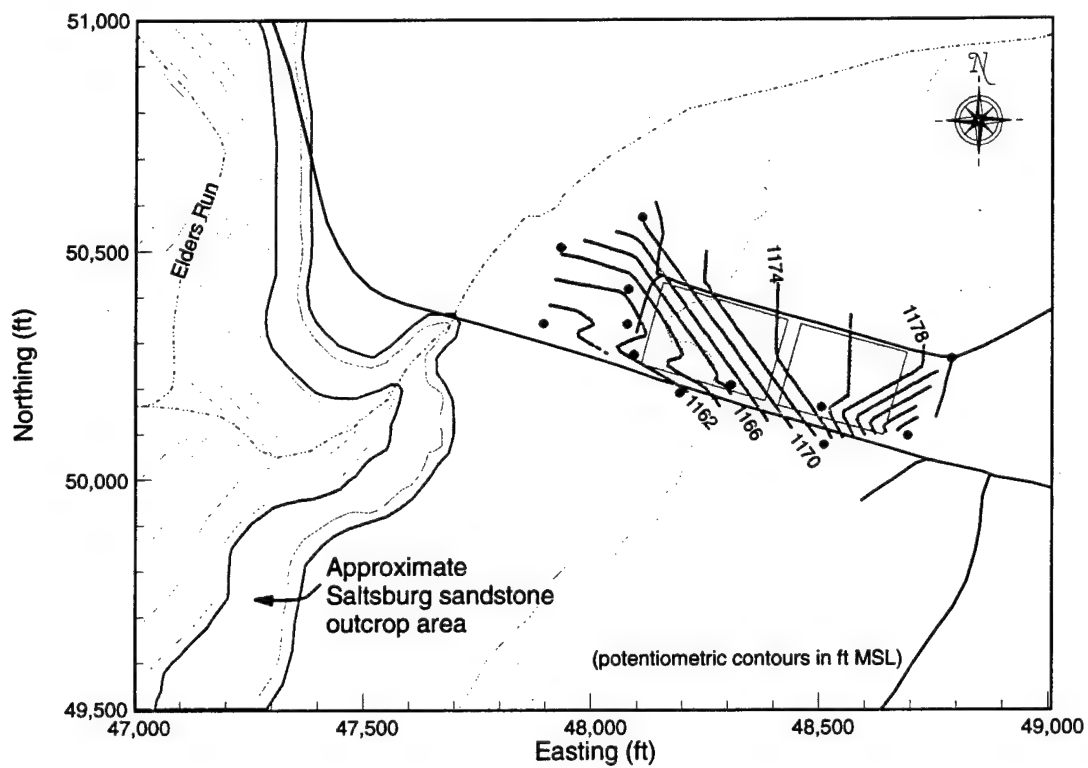


Figure 2.3 Potentiometric Levels in Saltzburg (upper box) and Buffalo (lower box) Aquifers as Measured on 11/20/97

## Chapter 3

### Flowmeter Description

#### Background

Development of borehole flowmeters for environmental and hydrogeological applications resulted from a growing recognition beginning in the 1960s that transport and dispersion of groundwater contaminants are controlled by the spatial variability of hydraulic conductivity [Skibitzke and Robertson, 1963; Dagan, 1982, 1984; Gelhar and Axness, 1983]. The theoretical advancements of these researchers in dispersive transport modeling necessitated development of practical methods for characterizing the hydraulic conductivity distributions of aquifers to support modeling of contaminant transport and remediation. A theoretical model for estimating vertical variations in hydraulic conductivity from borehole flowmeter data by Hufschmied [1983] represented a major step towards the development of such methods. Flowmeters had long been recognized by the petroleum industry as a practical tool for delineating productive oil-bearing zones in tests wells. However, mechanical impeller flowmeters available before the early 1980s lacked sufficient sensitivity and precision for the relatively low well flow rates typical of environmental applications. One of the first sensitive impeller flowmeters designed for environmental and hydrogeological applications was developed by INTEGRO (Zug, Switzerland) as reported by Hufschmied [1983, 1986] and Rehfeldt et al. [1989a, 1989b]. A series of papers by Hess [1982, 1986], Morin et al. [1988], and Hess and Paillet [1989, 1990] describe advancements in heat-pulse type flowmeters and their application to fractured rock hydrology. Late in the eighties, the EM flowmeter was developed and patented by the TVA Engineering Laboratory [Young and Waldrop, 1989].

Taylor et al. [1990] reviewed various techniques, both direct and indirect, for developing flow or hydraulic conductivity information in screened wells and/or boreholes. They concluded that methods relying on direct hydraulic measurements of some type, such as transient pressure changes or flowrates, offer the most promising methodologies for determining accurate logs of horizontal K and/or fracture locations in aquifers. Boggs et al. [1989], Rehfeldt et al. [1989a, 1989b], and Molz et al. [1989a, 1989b, 1990] also evaluated alternative methods for measuring the vertical variation of hydraulic conductivity. Among the different methods are small-scale tracer

tests, multilevel slug tests, laboratory permeameter tests, equations based on grain-size distributions, and borehole flowmeter tests. All three groups concluded that the borehole flowmeter test is the most promising method for measuring the spatial variability in an aquifer's hydraulic conductivity field.

EM borehole flowmeter logging has been successfully conducted at several research facilities, RCRA, and Superfund sites. Initial applications of the EM flowmeter were targeted at characterizing the heterogeneous alluvial aquifer of the groundwater research facility at Columbus AFB, Mississippi [Rehfeldt et al., 1989b, 1992]. Well development and performance testing with the EM flowmeter have been conducted by Julian and Young [1994] to gauge development requirements of wells used for hydraulic characterization of aquifers. Field demonstration of the prototype EM flowmeter was conducted at three Superfund sites selected by the EPA [Young et al., 1997b]. Further demonstrations of the EM flowmeter include applications at Oak Ridge National Laboratories [Moore and Young, 1992; Julian, 1996b], the Paducah Gaseous Diffusion Plant [Young et al., 1993], and numerous other TVA facilities [Julian et al., 1993, 1994b, 1996a].

The most sensitive types of meters have been based on heat-pulse or tracer-dilution technology [Hess, 1986], and more recently, on electromagnetic field technology. In the past, only prototypes of these high sensitivity meters have been available. However, in the case of heat-pulse and electromagnetic flowmeters, this situation is changing. Subsequently, EPA contracted with TVA and Auburn University to: (1) develop a field-worthy, reliable, and versatile EM borehole flowmeter; (2) provide guidelines on drilling boreholes and developing wells for borehole flowmeter testing [Young et al., 1997a]; (3) evaluate interpolation methodologies for generating hydraulic conductivity distributions from measured data [Molz et al., 1997 and Boman, et al., 1997]; (4) provide computer programs to analyze borehole flowmeter data [Young et al., 1997c]; and (5) document application of the EM flowmeter at several sites [Young et al., 1997a, 1997b].

### **Instrument Design**

The EM borehole flowmeter system can measure vertical flow in various types of wells and boreholes. The system has three main components: the downhole flowmeter, the collar or

packer assembly, and the above-ground electronics (Figure 3.1). The flowmeter provides accurate flow measurements up to a four order-of-magnitude range and fits snugly into 2-inch diameter schedule-40 PVC well screen/casing. The packer assembly can be one of several units that attaches to the flowmeter to ensure that water passes through the flowmeter orifice during testing. The above-ground electronics operate the hardware in the flowmeter and process the flowmeter signal to a discharge reading.

The flowmeter contains an electromagnet, a pair of chloride electrodes mounted at right angles to the pole pieces of the electromagnet, and a buffer amplifier that are cast in a ceramic epoxy within a stainless steel shell (Figure 3.2a). The flowmeter orifice is molded into a cylindrical shape to minimize turbulence associated with water being channeled past the electrodes. Having no movable parts, the flowmeter operates according to Faraday's law of induction, which states that the voltage induced across a conductor moving at right angles through a magnetic field is directly proportional to the translational velocity of the conductor. During operation, the electromagnet creates a strong magnetic field across the flow passage. As water (the conductor) flows through the magnetic field, a voltage gradient is generated. The voltage is proportional to the average velocity of the water across the magnetic field and is detected by the electrodes. Theoretically, and verified by laboratory tests, the magnitude of the voltage is unaffected by the groundwater's electrical conductivity. The polarity of the voltage generated is dependent on the direction of flow. Upward flow is generally designated as a positive voltage and downward flow as a negative voltage.

Presently, EM flowmeters are designed with an outer diameter of approximately 1.9 inches, and with inner (orifice) diameters of either 0.5 or 1.0 inch (Figure 3.2b). A standard length is 11.8 inches, but flowmeters as short as 4 inches have been used successfully. EM flowmeters are designed to operate under a maximum hydraulic head of approximately 2,000 ft. The 0.5- and 1.0-inch flowmeters are typically used to measure low flow rates and high flow rates, respectively. In wells or boreholes with relatively large diameters ( $> 2$  inches), flow is directed through the orifice of the flowmeter using a mechanical collar or inflatable packer assembly (Figure 3.3).

The mechanical collar (Figure 3.3a) consists of rubberized gasket material sandwiched between two Plexiglas or stainless steel rings that slip over the flowmeter and are held in place with set screws. The mechanical collar is easily used but its application can be tedious because

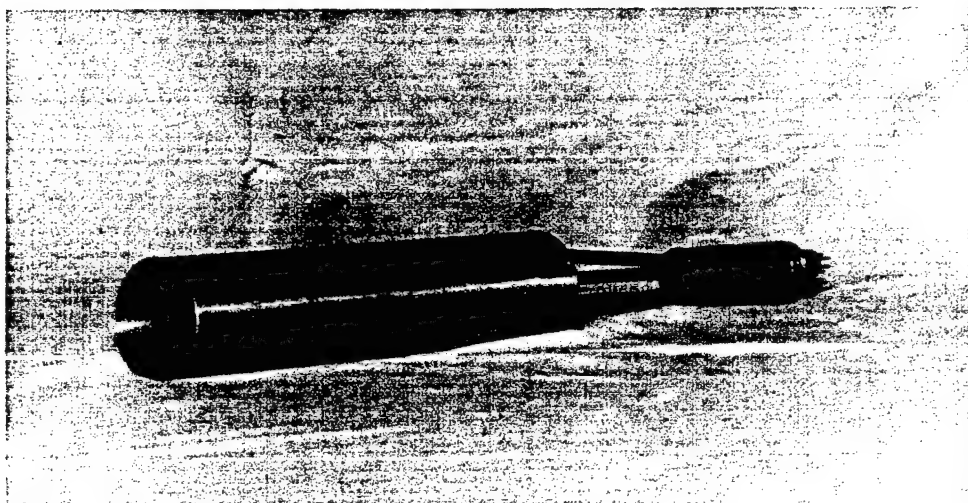
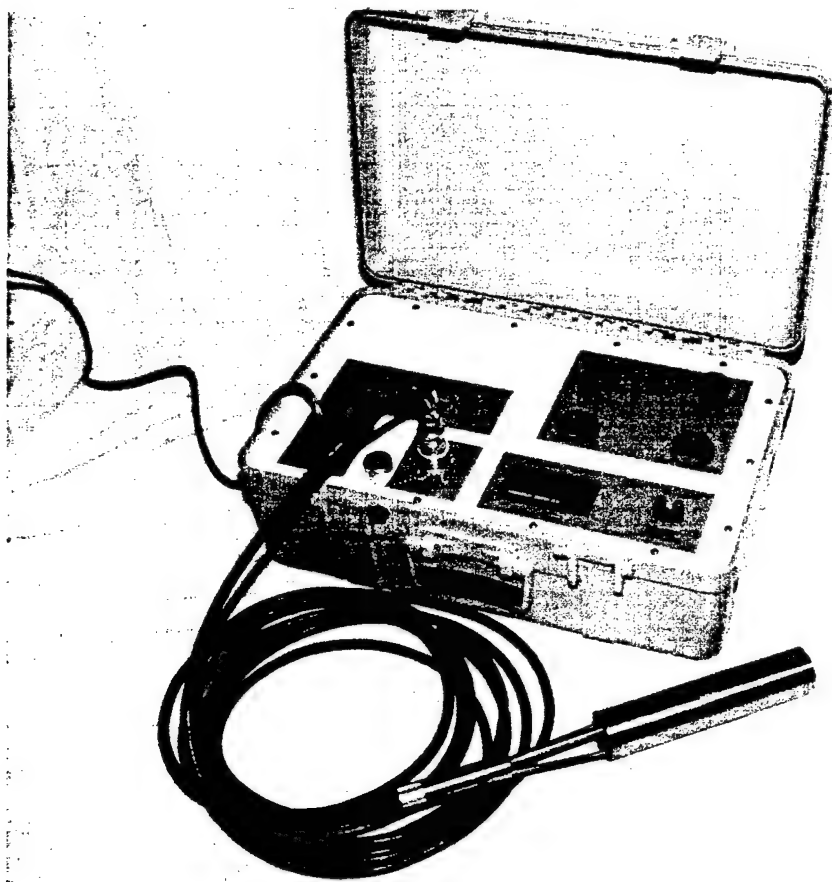


Figure 3.1 EM Borehole Flowmeter System Showing Above-Ground Electronics and Flowmeter



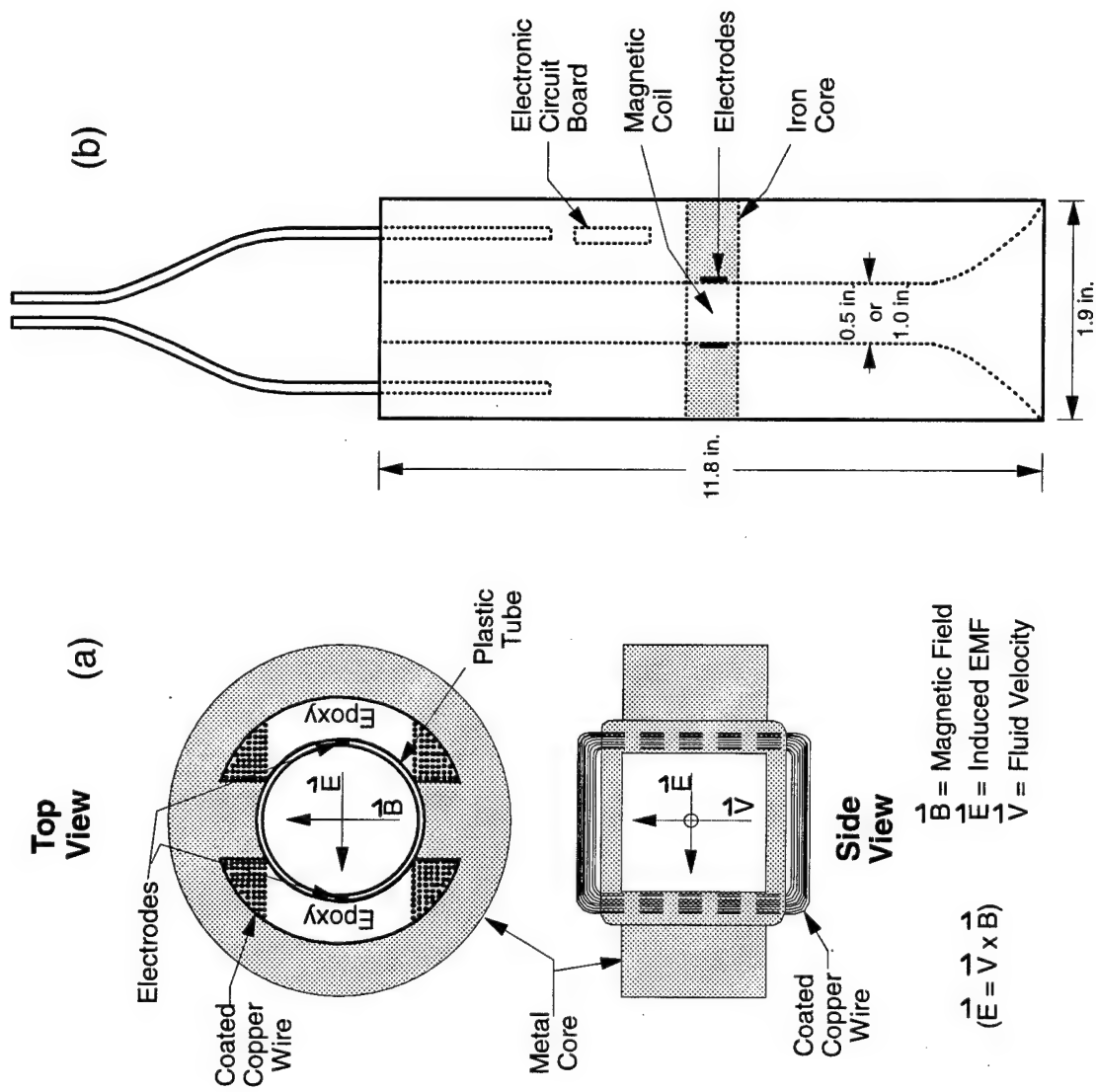


Figure 3.2 Schematic Diagram of EM Flowmeter

Needs typed  
"Page 3-6"

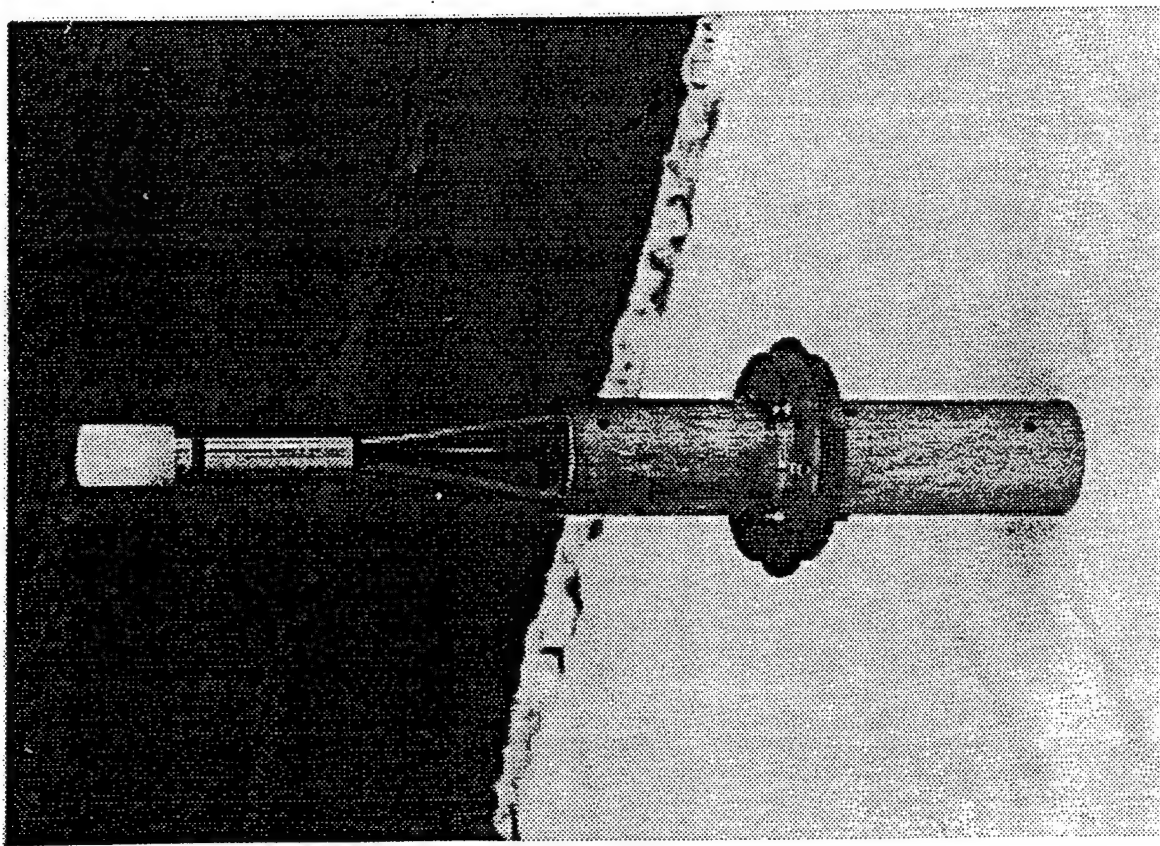


Figure 3.3 EM Flowmeter with (a) Mechanical Collar (left), and (b) Pneumatic Packer (right)

of friction between the collar and well. In situations where the well screen or borehole is uneven, the collar design may not provide an adequate seal and is not used.

The inflatable packer assembly (Figure 3.3b) slips onto the flowmeter and seals with "O" rings. Inflation of the packer is achieved by injecting water or air through a tube in the flowmeter. Either a pressurized chamber at the ground surface or a submersible pump can be used to inject air or water, respectively, into the packer. For most applications, the submersible pump is the method of choice. However, at shallow depths (<20 meters) where only a few flowmeter measurements are desired, the pressurized chamber has an advantage in its simplicity and relatively short set-up time.

The above-ground electronics includes an electromagnet drive, circuitry to measure the voltage generated by flow through the meter, and computer hardware to output the discharge reading. The electromagnetic drive consists of alternating positive and negative pulses. The signal produced by the electrodes is in the microvolt range and will typically be several orders-of-magnitude less than background noise. Because of the large noise level, synchronous demodulation is used to extract the signal. Synchronous demodulation has the effect of canceling noise out of phase with the electromagnetic drive. With additional amplification and filtering, a DC signal proportional to the water velocity through the flowmeter is generated. The electronics collect and process signals from the flowmeter every second. Readout is on a digital display with an analog voltage output for external devices. At the end of a preset time interval or upon keyboard command, the signals are averaged and the standard deviation is calculated. This average and standard deviation is displayed, stored on disk, and alternately printed to a hard copy device.

## **Calibration**

Before and after any field measurements, calibration checks are generally performed at a range of flow rates using the same EM flowmeter system (above-ground electronics, packer system, cable, and flowmeter) used in the field. Calibrations are simple and consist primarily of establishing a constant uniform flow through a vertical PVC pipe and comparing the EM flowmeter measurements to other flow measurements at the intake and/or the outlet of the PVC

pipe. Flow rates greater than 0.5 L/min are maintained by throttling a pressure valve on the public waterline and measuring the generated flow rate near the PVC pipe intake with an in-line commercial flowmeter. Flow rates less than 0.5 L/min are established using a peristaltic pump. For all flow rates, the baseline flow rate is determined by measuring the time required for the discharge to fill a calibrated container.

Figure 3.4 shows laboratory calibration data for the 1.0-inch flowmeter obtained just prior to field testing at Area 15A. For each point on the calibration curve, flowmeter measurements were taken every second over an interval of several minutes (several hundred values) to acquire a mean value and standard deviation of the voltage signal. As shown in Figure 3.4, twelve data points were collected across the flow range of interest (0 to ~20 L/min). The calibration data were then used to express a linear relationship between volts and flow. For most field applications, the reproduction of absolute flow measurements across several different calibration periods is not as important as the linearity of flowmeter response during a particular set-up. Previous calibration studies [Young et al., 1997a] and field applications indicate that errors associated with measuring very low (threshold) flow rates are more significant than temporal changes in the response characteristics of the flowmeter. For many types of flowmeter tests, laboratory and field conditions in a well differ; however, refinement in a calibration equation would not necessarily provide greater accuracy in the measurement values.

### **Sensitivity and Accuracy**

Laboratory data shows that the original (prototype) 0.5-inch flowmeter has excellent repeatability from ~30 mL/min to 10 L/min. Over this range, the 0.5-inch flowmeter produces a signal that is linearly proportional to the flow. Below 30 mL/min, the repeatability of data declines for the 0.5-inch flowmeter. The low flow values that deviate from the apparent linear trend in the data are attributed to the difficulty and error of measuring low flows and shifts in the flowmeter's electronic response over time. Recent improvements to the 0.5-inch flowmeter suggest that its operating range is more extensive than reported herein. This increase in sensitivity is primarily due to amendments in above-ground electronics (constant current source) and signal amplification in the flowmeter probe.

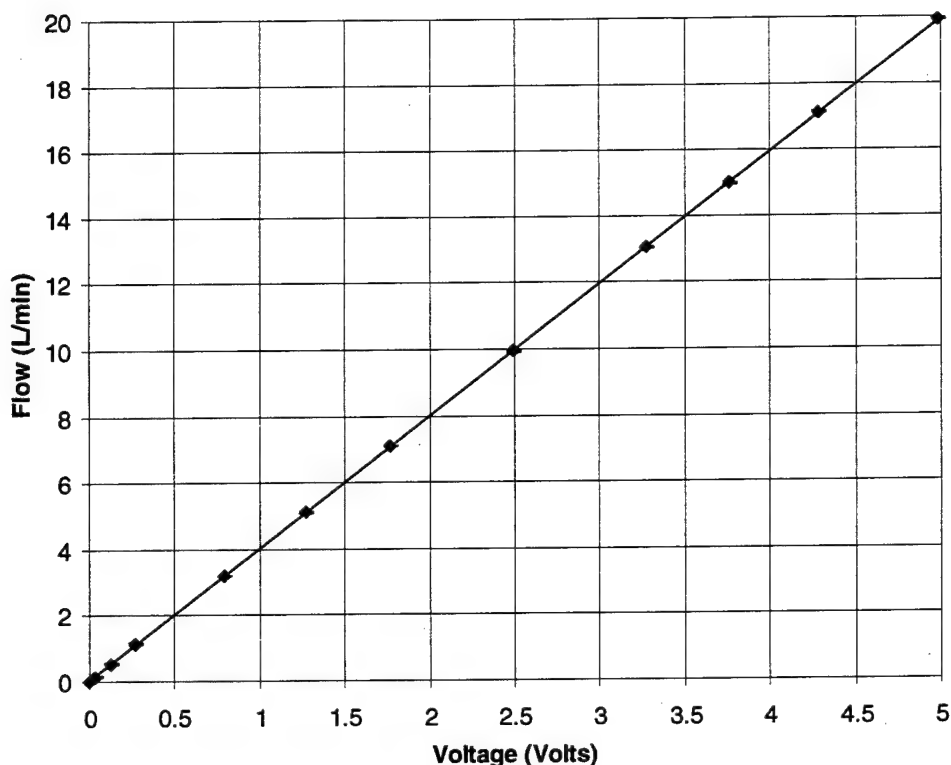


Figure 3.4 Precalibration (November 1997) Data for 1.0-inch Flowmeter

At flow rates above 10 L/min, two concerns exist with regard to application of the 0.5-inch flowmeter: (1) headlosses through the orifice, and (2) a flowmeter signal that will exceed the capacity of the electronics. To avoid these potential problems at the Area 15A site, the 1.0-inch flowmeter was used for testing.

The 1.0-inch flowmeter exhibits excellent repeatability from ~20 mL/min to 40 L/min. The flowmeter signal over this range is linearly proportional to flow and any deviation in the data is attributed to the same difficulties described for the 0.5-inch flowmeter. Figure 3.5 shows laboratory calibration data for the 1.0-inch flowmeter at low flow rates (0 to 74 mL/min). As shown in the figure, the 1.0-inch flowmeter signal is linearly proportional to flow with data repeatability diminishing near its lower threshold of 20 mL/min ( $5.3 \times 10^{-3}$  gal/min). This value is significantly lower than that reported for early prototypes of the 1.0-inch flowmeter. As with the 0.5-inch flowmeter, the superiority of the newer 1.0-inch flowmeter can be attributed to advancements in above-ground electronics and signal amplification.

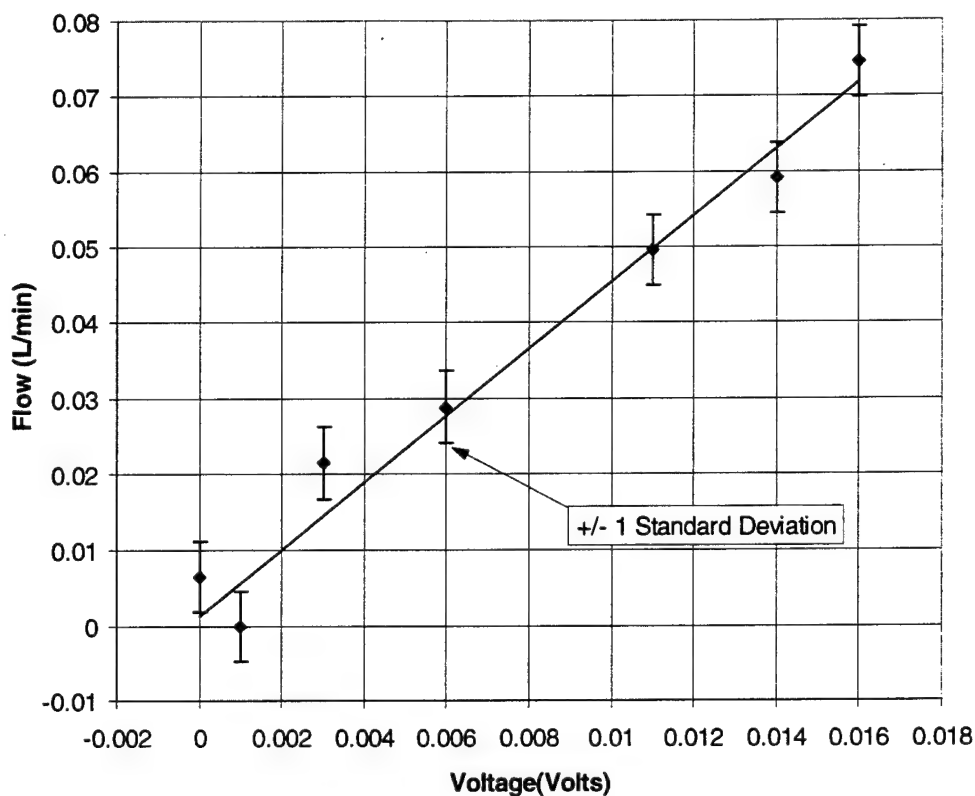


Figure 3.5 Laboratory Calibration Data for 1.0-inch Flowmeter at Lower Threshold

### Limitations

Although the EM flowmeter almost always produces accurate measurements, there are potential field problems that can result in errors. The majority of these problems are rarely encountered during flowmeter logging and the remainder can be prevented by following guidelines [Young et al., 1997] developed for flowmeter applications. Table 3.1 lists problems that have been encountered during field use of the EM flowmeters are listed below, with a description of each following.

Problem 1 usually occurs in low permeability aquifers (e.g., clay or unfractured bedrock) due to the initial displacement of water in a well or borehole by the flowmeter and telemetry cable. To prevent errors associated with this problem, accurate water level

measurements and spot checking of ambient flows are conducted prior to beginning flowmeter measurements to assure that the aquifer has returned to equilibrium.

Table 3.1. Potential Field Problems That May Produce Errors in EM Flowmeter Measurements

1. Insufficient time allowed for dissipation of flow in well caused by initial flowmeter movement.
2. Coating on the electrodes.
3. Signal interference by gas bubbles.
4. Large variations in air temperature.
5. Variations in pumping rate.
6. Water turbulence and bypass produced by high flow rate entering/exiting well at location of flowmeter.
7. Inadequate packer or collar seal resulting in flow bypass.
8. High electromagnetic background currents. (Overhead or underground powerlines or power sources in vicinity of well or boreholes.)

To prohibit errors associated with problems 2 and 3, the flowmeter is cleaned and rinsed between well or borehole test locations. In contaminated settings, decontamination procedures are followed to assure that all materials in contact with water (i.e., flowmeter and cable) are free of contaminants. Should the electrodes become coated after lowering the flowmeter into the well or borehole, they can usually be cleaned by rapidly moving the flowmeter up and down several times.

Field testing has shown that meter calibration may drift up to 10 millivolts (0.1 percent full-scale) during several hours if large temperature changes ( $> 10^{\circ}\text{C}$ ) occur (problem 4). As a result, the flowmeter output is checked at a location of zero flow before, after, and during the testing period. The temperature sensitivity is a property of the electronic components. In most instances, this sensitivity is not a concern because of the relative short time needed to obtain a flow log.

The problems associated with maintaining a constant flow rate (problem 5) are particularly acute where large drawdowns occur. Changes in drawdown affect the lift



requirements on a pump. If no adjustments are made to the pump as the drawdown increases, the pumping rate will decrease until the drawdown stabilizes. In regions of low transmissivity, the problems associated with a constant flow rate can be severe because of large drawdowns. Although data analysis methods can be adjusted to compensate for changes in the pumping rate, these changes are not desirable. Whenever possible, injection tests should be considered as an alternative to pumping tests if large drawdowns are expected.

One of the possible sources for error in borehole flowmeter measurements results from water turbulence and/or bypass produced by high flow rates entering or exiting a well at a given test interval (problem 6). The turbulence and/or bypass is produced by blockage of a high flow (permeable horizon or fracture) zone by the body of the flowmeter probe and is usually represented by high standard deviations in the flowmeter signal. These potential errors can be avoided by raising or lowering the flowmeter slightly above or below the high flow zone.

The bypass of water around the flowmeter can also be caused by poor packer or collar seal along a well or borehole wall (problem 7). This problem is most acute in uncased boreholes and wire-wound stainless steel (SS) well screens, and is rarely a source of error in PVC well screen. The most appropriate method for minimizing errors associated with this problem is to calibrate the flowmeter in the laboratory before and after field testing. Calibration should be conducted with the same packer or collar assembly used in the field, within a well screen of identical diameter and material, and at a flow range anticipated to be used in the field.

The flowmeter's exterior and cables are shielded against ground currents, but the flowmeter's inlet and outlet are not. As a result, background voltage gradients (problem 8) can affect the flowmeter's circuitry. Although the flowmeter is designed to reject noise, the flow signal is in the microvolt range and large voltage gradients could mask the signal. Past experience has shown that testing in the vicinity of either overhead or underground high voltage power lines can influence EM flowmeter readings.



## Chapter 4

### Methodology for Collection and Analysis of Flowmeter Data

#### Flowmeter Testing Procedure

The concept of borehole flowmeter testing is illustrated in Figure 4.1. First, a caliper log is recorded to ascertain that the screen/borehole diameter is known and constant. After measuring the static groundwater level in the well/borehole, a flowmeter log may then be recorded before pumping in an attempt to measure any natural (ambient) flow in the well/borehole, which (if detected) is recorded and saved for later data analysis. This step is most important if ambient flow is expected to be a significant fraction of the flow induced by pumping or injection.

Following the ambient flow test, a pump is placed in the test well and operated at a constant flow rate ( $QP$ ). After the water level drawdown in the well has approximately stabilized, the flowmeter is lowered to near the bottom of the well and a measurement of discharge rate at the flowmeter depth is obtained. The meter is then raised a distance  $\Delta z$  and another flow measurement is taken; the meter is raised another distance  $\Delta z$  and a flow measurement recorded. This is repeated along the saturated thickness of the well screen/borehole. As illustrated in Figure 4.1, the result is a series of data points giving cumulative vertical discharge,  $Q$ , within the well screen or borehole as a function of vertical position  $z$ . Just above the top of the well screen, the meter reading should be equal to  $QP$ , the steady pumping rate that is measured independently at the surface.

One of the most important aspects of the well test is the pumping rate,  $QP$ . The rate must be high enough to have a measurable influence but low enough for the water level to stabilize in a timely fashion. In addition, considerations need to include methods for maintaining a constant flow rate throughout the test and for managing the discharged groundwater. Whenever possible, injection tests should be considered as an alternative to pumping tests if large drawdown changes are expected or problems might exist in managing discharged groundwater.

The borehole flowmeter technique relies on the capability to accurately measure the drawdown rate and the vertical flow distribution in a screened well or borehole. Table 4.1

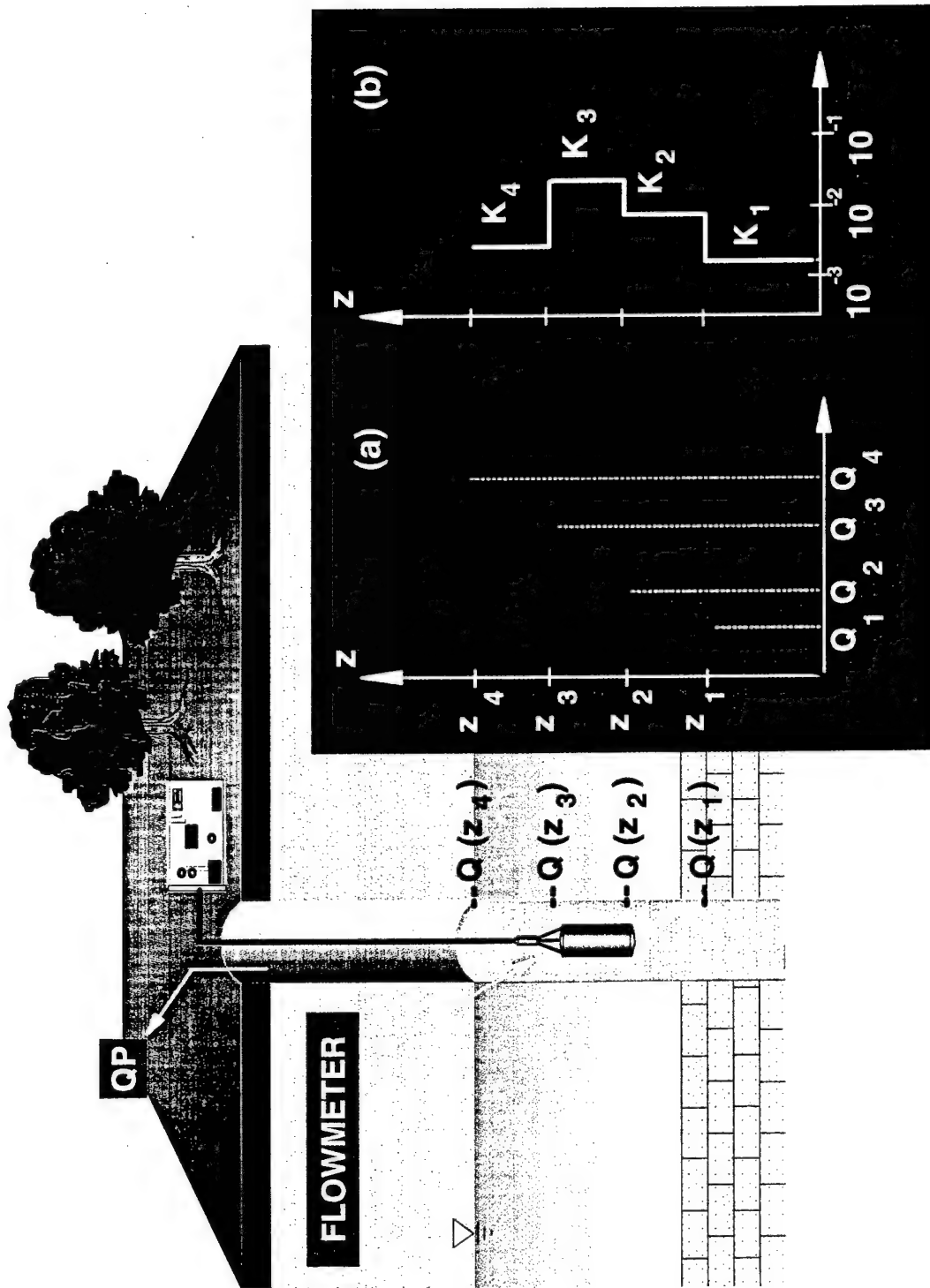


Figure 4.1 Concept of Borehole Flowmeter Test

provides a simplified overview of the procedures used to implement the technique at the test site discussed in this report.

TABLE 4.1 Summary of Borehole Flowmeter Testing Procedures

1. Measure water elevation in the well relative to a fixed datum.
2. Attach mechanical collar to flowmeter and lower to bottom of well.
3. Install pressure transducer and set up data logger to record drawdown and recovery at 2-second intervals.
4. Lower pump or injection hose into well.
5. Re-measure the water elevation in the well (pumping test).
6. Start pumping and check flow rate with stopwatch and a volumetric container.
7. Record drawdown with the pressure transducer system until the water elevation in the well stabilizes (occasionally take manual drawdown measurements).
8. Record discrete measurements of vertical flow along full length of well bore using flowmeter.
9. Turn-off pump and allow well to recover.

### Data Analysis

One assumes that the aquifer is composed of a series of  $n$  horizontal layers as shown on Figure 4.2 and takes the difference between two successive meter readings, which yields the net flow,  $\Delta Q_i$ , entering the screen segment between the elevations where the readings were taken, which are assumed to bound layer  $i$  ( $i = 1, 2, \dots, n$ ). If detected, the  $\Delta q_i$  from the ambient flow log are computed in an identical manner. One could argue that many, perhaps most, aquifers are not composed of horizontal, homogeneous layers. This may be so, but the  $n$ -layer case is a lot closer to reality than the single layer case of classical pumping test analysis.

At this point, the data may be analyzed further using two options. The first option is based on the Cooper-Jacob [1946] equation relating drawdown to pumping rate in a fully-penetrating well in a confined aquifer, while the second, and probably superior, option is based

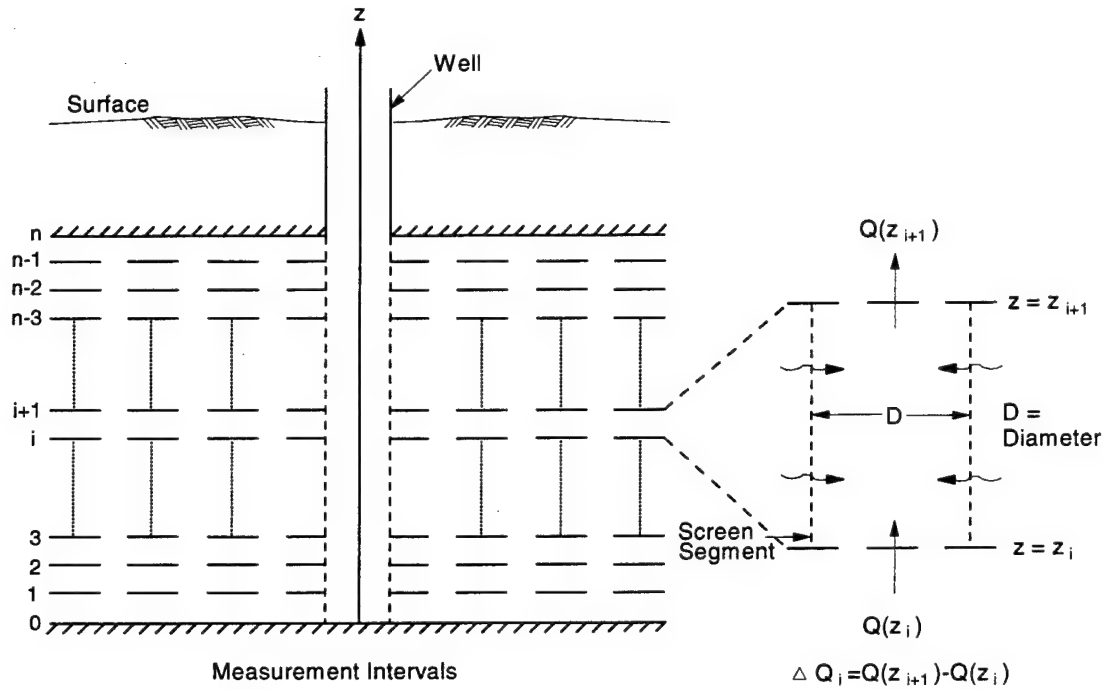


Figure 4.2 Assumed Layered Geometry Within Which Flowmeter Data are Collected and Analyzed

on a study by Javandel and Witherspoon [1969]. The Cooper-Jacob method is presented first. Both methods assume that flow in the aquifer is horizontal.

In the Cooper-Jacob method, one treats the assumed horizontal flow in each layer as if it were coming from an aquifer of infinite horizontal extent and thickness  $\Delta z_i$ . Then for each layer,  $i$ , one can write

$$\Delta H_i(r_w, t) = \frac{(\Delta Q_i - \Delta q_i)}{2\pi K_i \Delta z_i} \ln \left[ \frac{15}{r_w} \sqrt{\frac{K_i \Delta z_i t}{S_i}} \right] \quad (4.1)$$

where;

$\Delta H_i$  = drawdown in  $i$ th layer

$\Delta Q_i$  = flow from  $i$ th layer into the well

$\Delta q_i$  = ambient flow from  $i$ th layer

$K_i$  = horizontal hydraulic conductivity of the  $i$ th layer

$\Delta z_i$  =  $i$ th layer thickness

$r_w$  = effective well radius

$t$  = time since pumping started

$S_i$  = storage coefficient for the  $i$ th layer.

At this point questions arise as to how  $\Delta H_i$  and  $S_i$  should be specified. If one assumes that headlosses associated with flow within the well are negligible, and with many screen diameter/pumping-rate combinations such an assumption is reasonable, then all the  $\Delta H_i = \Delta H$ , the measured drawdown in the test well. If such an assumption cannot be made, then one must measure the pressure drop opposite each layer associated with pumping the test well. For further discussion of various possible headlosses, see Rehfeldt et al. [1989b].

Normally, a value for the storativity of the aquifer being studied will be known or estimated, and the question is how to use this information to obtain  $S_i$  for each layer. In the past, two assumptions have been made. The most obvious is to assume that  $S_s$ , the specific storage, is constant, in which case  $S_i = S_s \Delta z_i$  [Morin et al., 1988; Molz et al., 1989a]. An alternate assumption used by Rehfeldt et al. [1989b] is that  $S_s$  varies in such a way that the hydraulic diffusivity of each layer,  $K_i \Delta z_i / S_i$ , remains constant and equal to the hydraulic diffusivity ( $T/S$ ) for the aquifer, where  $T$  is transmissivity and  $S$  is storage coefficient. If the latter assumption is made, Equation (4.1) may be solved for  $K_i$  yielding

$$K_i = \frac{(\Delta Q_i - \Delta q_i)}{2\pi H_i \Delta z_i} \ln \left[ \frac{1.5}{r_w} \sqrt{\frac{Tt}{S}} \right] \quad (4.2)$$

If the constant  $S_s$  assumption is made, one can solve Equation (4.1) for  $K_i$  outside the ln term to yield

$$K_i = \frac{(\Delta Q_i - \Delta q_i)}{2\pi \Delta H_i \Delta z_i} \ln \left[ \frac{1.5}{r_w} \sqrt{\frac{K_i \Delta z_i t}{S_i}} \right] \quad (4.3)$$

which can be solved iteratively to obtain a value for  $K_i$ . Further details may be found in Morin et al. [1988], Molz et al. [1989a] or Rehfeldt et al. [1989b].

An alternative method for obtaining a distribution that requires fewer assumptions is based on the study of flow in a layered, stratified aquifer by Javandel and Witherspoon [1969]. Their work showed that in idealized, layered aquifers, flow at the well-bore radius,  $r_w$ , rapidly

becomes horizontal even for relatively large permeability contrasts between layers. As the writers point out, under such conditions, the radial gradients along the well bore are constant and uniform, and flow into the well from a given layer, due to pumping, is proportional to the transmissivity of that layer. That is:

$$(\Delta Q_i - \Delta q_i) = \alpha \Delta z_i K_i \quad (4.4)$$

where  $\alpha$  is a constant of proportionality. This condition occurs when the dimensionless time  $t_D = \bar{K} t / S_s r_w^2$  is  $\geq 100$ . (In this expression  $\bar{K}$  is the average aquifer hydraulic conductivity defined as  $\Sigma K_i \Delta z_i / b$ , where  $b$  is aquifer thickness,  $S_s$  is the aquifer specific storage,  $t$  is time since pumping started, and  $r_w$  is wellbore radius.)

To solve for  $\alpha$ , sum the  $(\Delta Q_i - \Delta q_i)$  over the aquifer thickness, to obtain

$$\sum_{i=1}^n (\Delta Q_i - \Delta q_i) = QP = \alpha \sum_{i=1}^n \Delta z_i K_i \quad (4.5)$$

Multiplying the right-hand side of Equation (4.5) by  $b/b$  and solving for  $\alpha$  yields

$$\alpha = \frac{QP}{b \bar{K}} \quad (4.6)$$

Finally, substituting for  $\alpha$  in Equation (4.5) and solving for  $K_i / \bar{K}$  gives

$$\frac{K_i}{\bar{K}} = \frac{(\Delta Q_i - \Delta q_i) / \Delta z_i}{QP / b}; i = 1, 2, \dots, n \quad (4.7)$$

To obtain Equation (4.7), it was assumed that  $(\Delta Q_i - \Delta q_i)$  and  $QP$  do not change with time (i.e., pseudo-steady conditions apply). This will occur when  $r_w^2 S / 4 T t < 0.01$ , where  $S$  and  $T$  are aquifer storage coefficient and transmissivity, respectively. Thus, from the basic data it is quite easy to get a plot of  $K / \bar{K}$  versus elevation. If one then has the value of  $\bar{K}$  from a fully-penetrating pumping test, one can easily obtain dimensional values for  $K$  by multiplying  $K / \bar{K}$  by the pumping test result. The  $K / \bar{K}$  approach has practical appeal because one does not have to know values for  $r_w$  or  $S_i$ , which are impossible to specify precisely. Also, errors in flowmeter readings involving constant multipliers are canceled out, and the meter does not have to be

calibrated as long as its response is linear. However, a fully-penetrating pumping test or slug test must be performed along with each flowmeter test.

## Chapter 5

### Flowmeter Applications at Federal Laboratories Area 15

#### Methods

During the fourth week of November 1977, eight flowmeter tests were performed during single-well pumping and injection tests at Area 15. Test locations (Figure 5.1) included seven existing wells screened through the lower overburden and upper Saltsburg sandstone, and a new well (TVA-1) which was screened over the entire thickness of the Saltsburg sandstone to a depth of 93.2 ft. Table 5.1 presents a summary of information related to the single-well tests including the estimated transmissivity (T) and average hydraulic conductivity ( $\bar{K}$ ) for each test site. Well construction diagrams and geologic logs of the test wells are provided in Appendix A. Flowmeter data for each well test is presented in Appendix B.

TABLE 5.1. Summary of Single-Well Pumping and Injection Tests

Well	Test Type	Q(gal/min)	D(ft)*	T (ft <sup>2</sup> /d)	$\bar{K}$ (ft/d)
MWS-8	Injection	1.57	15.5	62	4.0
MWS-9	Pumping	1.57	15.2	85	5.6
MWU-14	Injection	1.05	15.0	50	3.3
MWU-15	Injection	0.62	14.3	14	1.0
MWU-16	Pumping	0.41	15.0	6.2	0.4
MWU-19	Pumping	0.48	19.0	4.7	0.2
MWU-20	Injection	0.94	14.3	120	8.4
MWU-20	Pumping	1.15	14.3	29	2.0
TVA-1	Injection	1.56	74.2	920	12

D(ft)\* = Saturated Screened Interval

In making flowmeter measurements it is generally advantageous to measure vertical flows that occur under natural (ambient) hydraulic-head conditions, as well as flows that are induced by pumping or injection. However, initial flow logging under ambient conditions at Area 15A indicated that the sensitivity of the flow measurements was severely limited by the stainless steel well screens present in most site wells. The wire-wound stainless steel screen contains vertical support rods along the inside of the screen which make it impossible to obtain



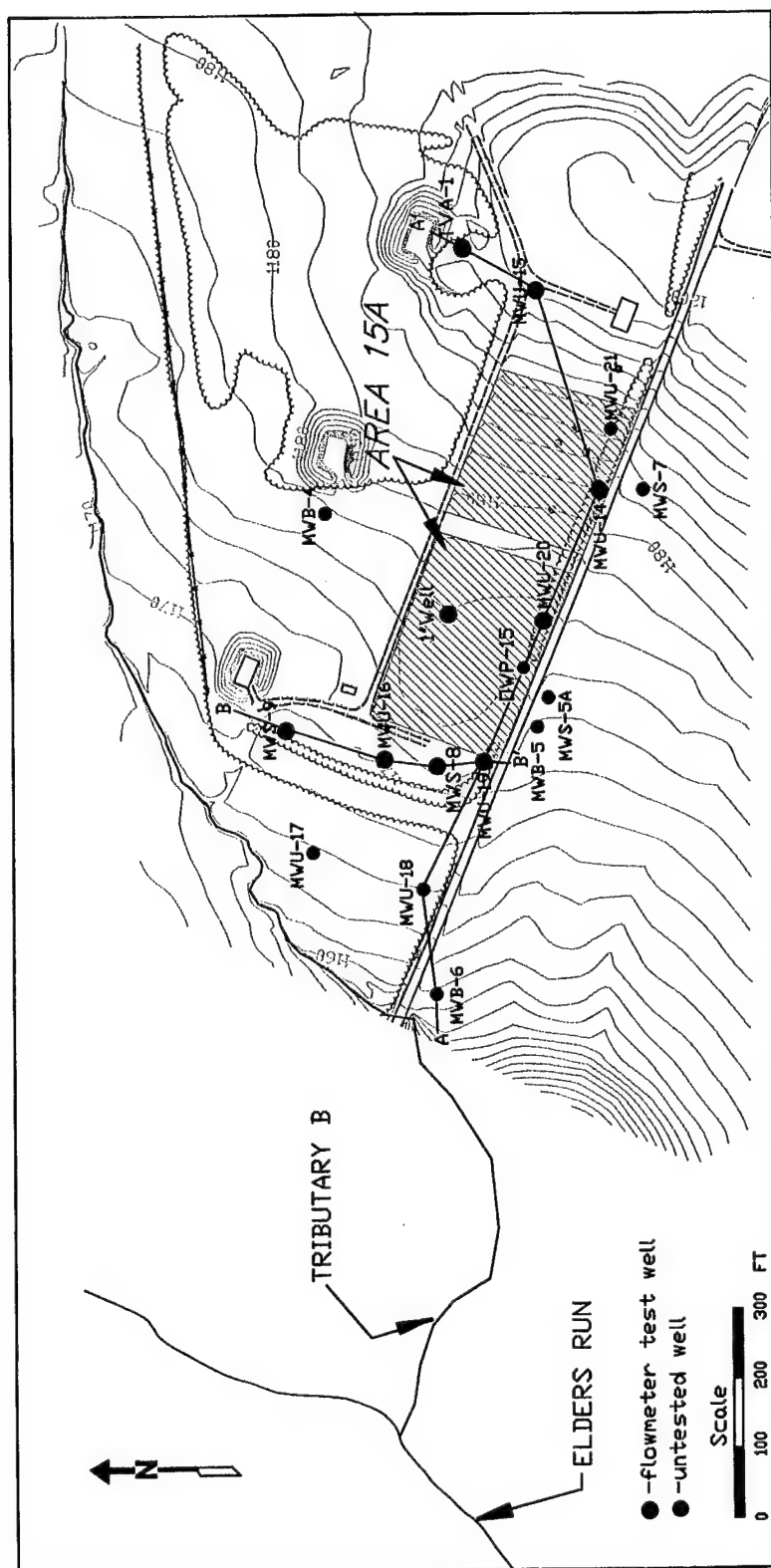


Figure 5.1 Well Location Map

an integral seal between the flowmeter and screen. Therefore, no ambient flow data are available for monitoring wells at Area 15A.

Selection of pumping and injection rates for site test wells involved several criteria which included: (1) a rate high enough to stress the entire screened interval of the aquifer but low enough such that the groundwater level was able to stabilize in a timely fashion (usually after 30 to 45 minutes); (2) considerations for maintaining a constant flow rate throughout the test (i.e., injection water was limited to 300 gallons per test); and (3) managing discharged groundwater. A RediFlow™ pump and variable frequency Grundfos™ controller were used to obtain well pumping rates of 0.41 to 1.57 gal/min. Potable water for injection was obtained from the town of Saltsburg, Pennsylvania. The set-up for injection included a 300-gallon plastic container and assorted Teflon tubing to maintain injection rates of 0.62 to 1.57 gal/min. Drawdown measurements during pumping and injection tests were collected at 2-second intervals using 5-psi pressure transducers connected to Telog™ dataloggers. Drawdown during testing was monitored and recorded manually using an electric water level detector, and visually using a laptop computer connected to the datalogger.

Drawdown data for pumping and injection tests were analyzed using the Cooper-Jacob [1946] straight-line method (Equation 5.1). T values were estimated from late-time drawdown data for each test. Transmissivity values and resulting average hydraulic conductivity values are provided in Table 5.1. The average T (46 ft<sup>2</sup>/d) from all single-well tests (excluding well TVA-1) is about half of the average T (89 ft<sup>2</sup>/d) estimated by Conestoga-Rovers & Associates [1995] based on their Theis curve-matching analysis of a seven-hour multi-well pump test at the site. Disparity between the average T estimates can be related to a combination of several factors which include: (1) scale of tests - tens of feet versus hundreds of feet, (2) duration of tests - one hour opposed to seven hours, (3) pumping rates - less than 1.6 gal/min compared to 4.5 gal/min, (4) analytical method - Cooper-Jacob method versus Theis curve-matching, and (5) conditions during testing - groundwater levels, etc.

$$T = \frac{2.3Q}{4\pi \frac{ds}{d(\log t)}} \quad (5.1)$$

where: T = transmissivity (ft<sup>2</sup>/d)  
Q = total discharge rate (ft<sup>3</sup>/d)

$ds/d(\log t)$  = derivative of drawdown (s) with respect to the logarithm of time (t).

Flowmeter testing was performed at all wells listed in Table 5.1 after they had reached a pseudo-steady condition and in accordance with methods outlined in Chapter 4 of this report. Flowmeter measurements were generally made at 1-ft intervals except where relatively transmissive flow zones were observed. At these locations, 0.5-ft intervals were surveyed. Another exception is well TVA-1, where logging intervals of 3 ft were sometimes used in sections of the well where flow changes were negligible. Analysis of the flowmeter data was conducted in accordance with Chapter 4 of this report.

One of the possible sources for error in borehole flowmeter measurements at Area 15 results from water turbulence and/or bypass produced by high flow rates entering or exiting the well at a given test interval. The turbulence and/or bypass can be produced by blockage of a high flow (permeable horizon or fracture) zone by the body of the flowmeter probe and is usually represented by high standard deviations in the flowmeter signal. During flowmeter testing at Area 15, this potential error was avoided by rigorous monitoring of standard deviations in the flowmeter's signal response. If anomalous variations were observed in signal response, the flowmeter was raised and lowered above and below high permeability zones to obtain additional flow measurements. The result is a higher resolution data set along zones of high flow such as those shown at well TVA-1 between elevations 1133.5 to 1135.5 ft and 1146 to 1148 ft (Appendix B).

The bypass of water around the flowmeter can also be caused by poor packer or collar in wire-wound stainless steel (SS) well screens. Many of the wells at Area 15A possess 4-inch diameter wire-wound SS well screens and this is probably the largest source of error in flowmeter measurements at the site. Additionally, these errors are most likely to be associated with lower flow measurements (i.e., smaller, less transmissive fracture zones). To minimize such errors, the 1.0-inch flowmeter was precalibrated at TVA's Engineering Laboratory just prior to field testing (see Chapter 3). Additionally, the minimum flow values used for hydraulic conductivity estimates are never less than the lower threshold of the 1.0-inch flowmeter (20 mL/min). Although this method may result in lower hydraulic conductivity values being precluded from the K profiles, much of the uncertainty associated with low flow errors is removed.

## Results and Interpretation

Figures 5.2 and 5.3 present the interval flow logs derived from the flowmeter tests superimposed on two stratigraphic cross-sections of the site. Section A-A' (Figure 5.2) trends roughly west-east along stratigraphic dip, whereas section B-B' (Figure 5.3) trends north-south approximately along strike. These figures indicate that, except for well TVA-1, flowmeter testing was generally limited to the lower few feet of soil overburden and the upper 10 to 20 feet of sandstone and shale associated with the Saltsburg formation. In general, the flowmeter profiles indicate that a few thin flow zones dominate shallow groundwater movement. This is common in fractured sedimentary rock in which groundwater moves preferentially through a few hydraulically active fractures with only minor flow through the porous rock matrix.

Flow profiles for the shallow test wells typically indicate two preferential flow zones. The shallowest of these features lies within the upper bedrock or, in the case of wells MWU-14, -19, and -20, in the lower part of the soil overburden. A transitional zone of variably-weathered bedrock, undoubtedly exists between unconsolidated soils and competent bedrock, although it cannot be confirmed with available geologic logs. The presence of a shallow preferential flow zone, within what appears to be soil overburden, may be a permeable soil layer or possibly a relic bedding fracture which has been preserved in the weather rock. A contour map showing the approximate elevation of this feature is given on Figure 5.4. The feature appears to be roughly planar, dipping west-north-west at a gradient of approximately 4 percent. Its dip is generally consistent with local bedrock dip and with the shallow groundwater potentiometric surface gradient in the Saltsburg formation (Figure 2.3). Some 8 to 12 ft below this feature another preferential flow zone was observed at most test sites. Based on geologic logs this zone may represent a bedding fracture and may be correlated with a thin fractured coal seam. As indicated on Figure 5.5, the gradient of this flow feature is similar to that of the shallow zone, although the general direction of dip is more westerly. Other deeper (and possibly more transmissive) preferential flow zones are evident in well TVA-1; however, the continuity of these features is unknown since no other testing was performed at comparable elevations.

Horizontal hydraulic conductivity profiles derived from flowmeter logs are presented on Figures 5.6 and 5.7. Data are plotted using arithmetic K scales on Figure 5.6 in order

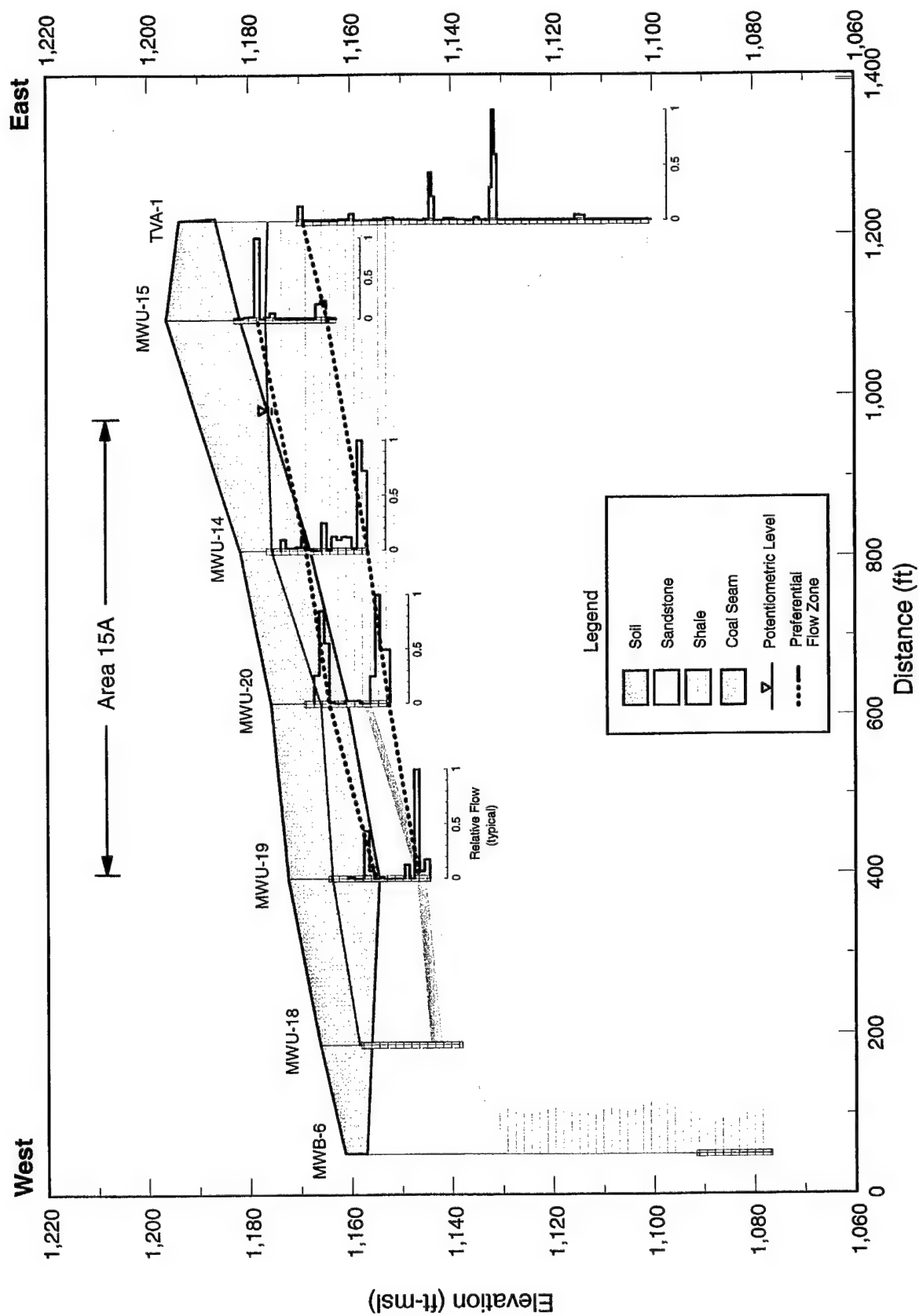


Figure 5.2 West-East Stratigraphic Section Showing Well Flow Profiles

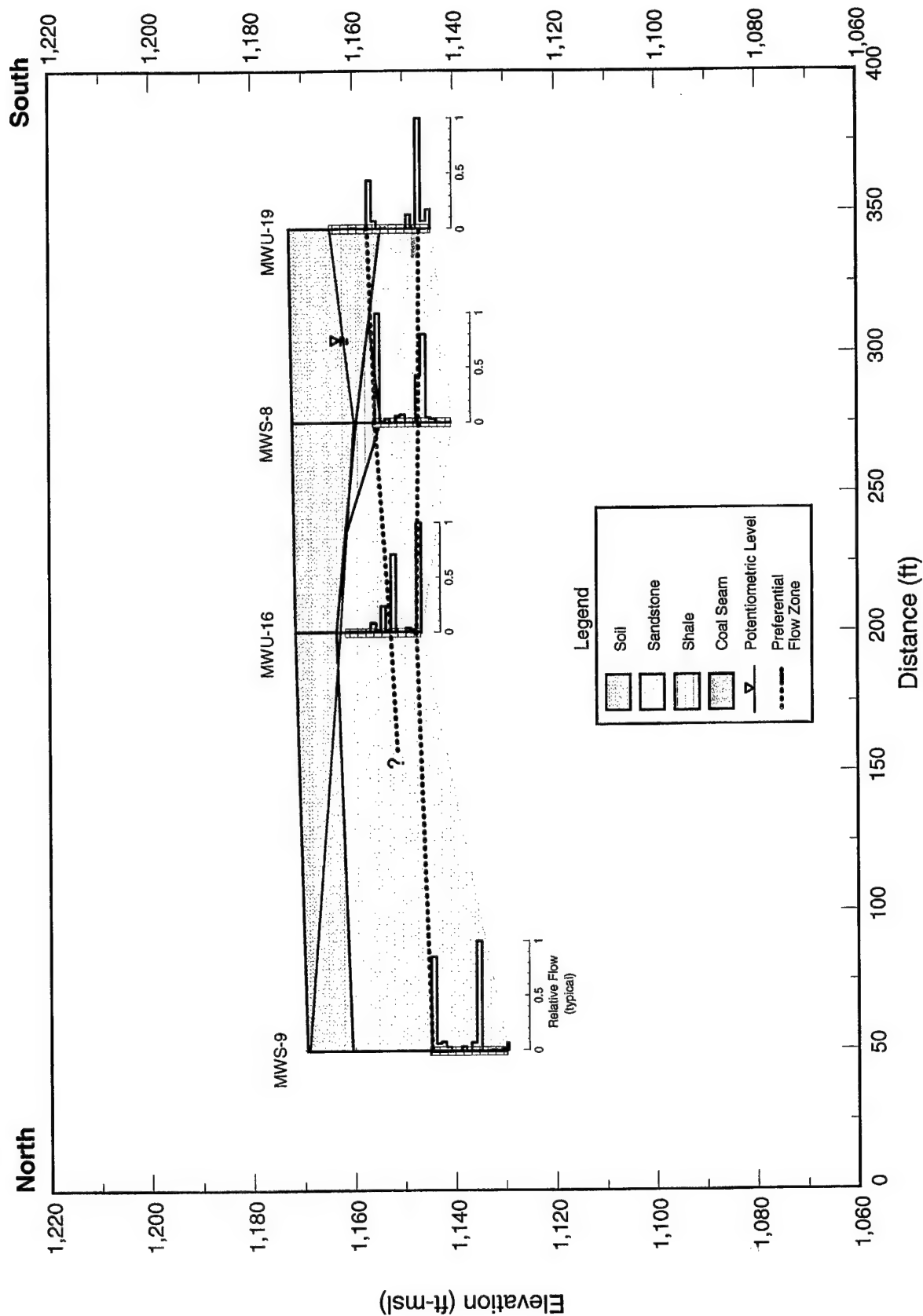


Figure 5.3 North-South Stratigraphic Section Showing Well Flow Profiles

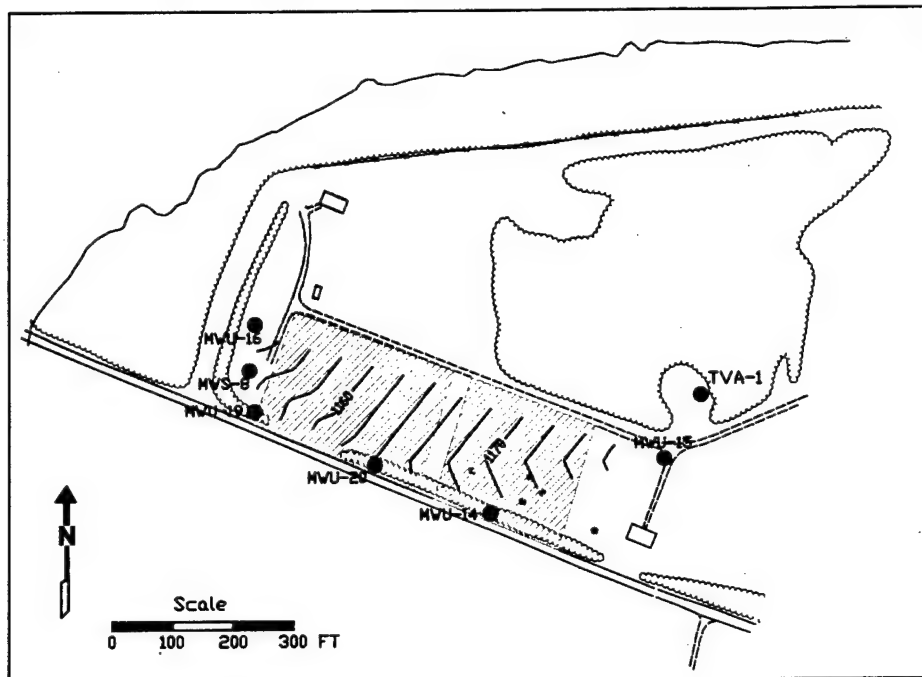


Figure 5.4 Surface Elevation of Upper Preferential Flow Zone

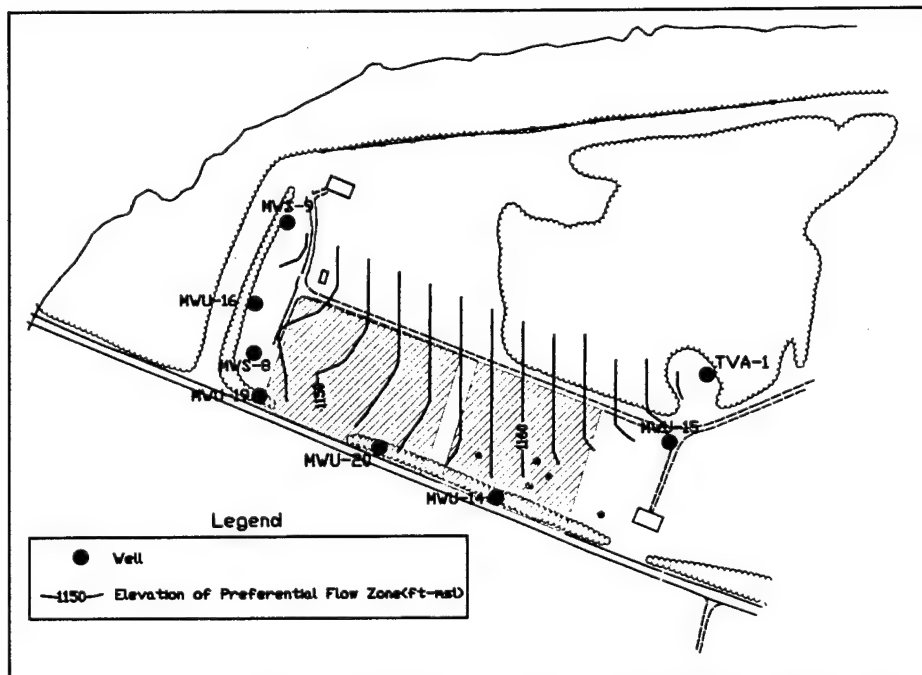
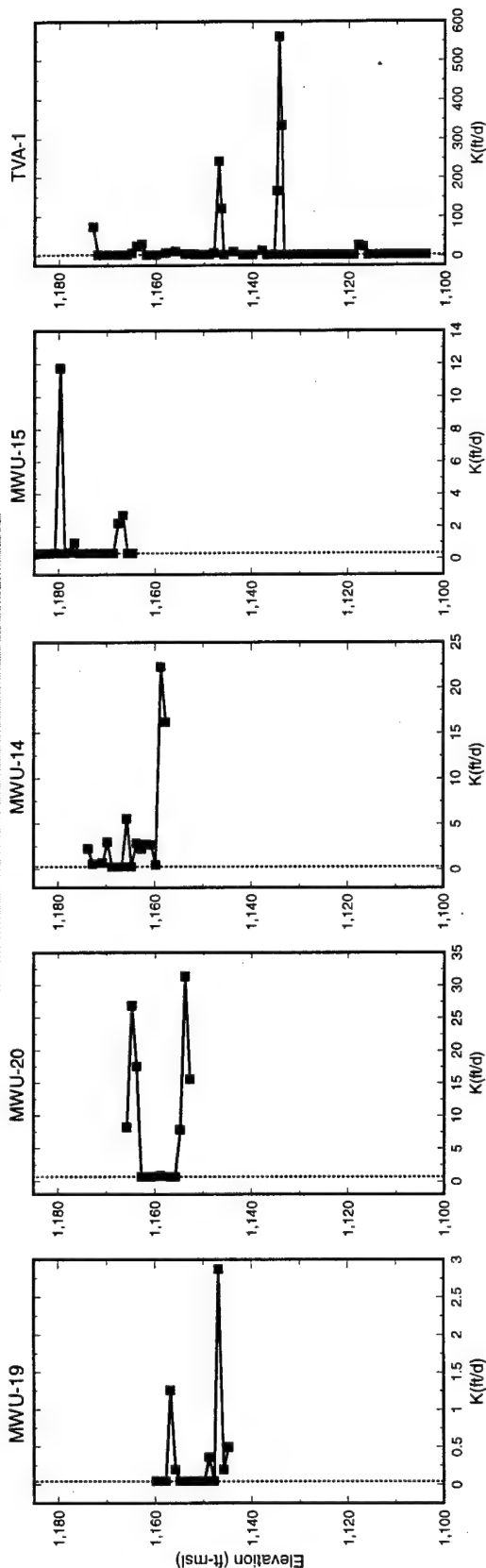


Figure 5.5 Surface Elevation of Lower Preferential Flow Zone

# West - East Section A-A'



# North - South Section B-B'

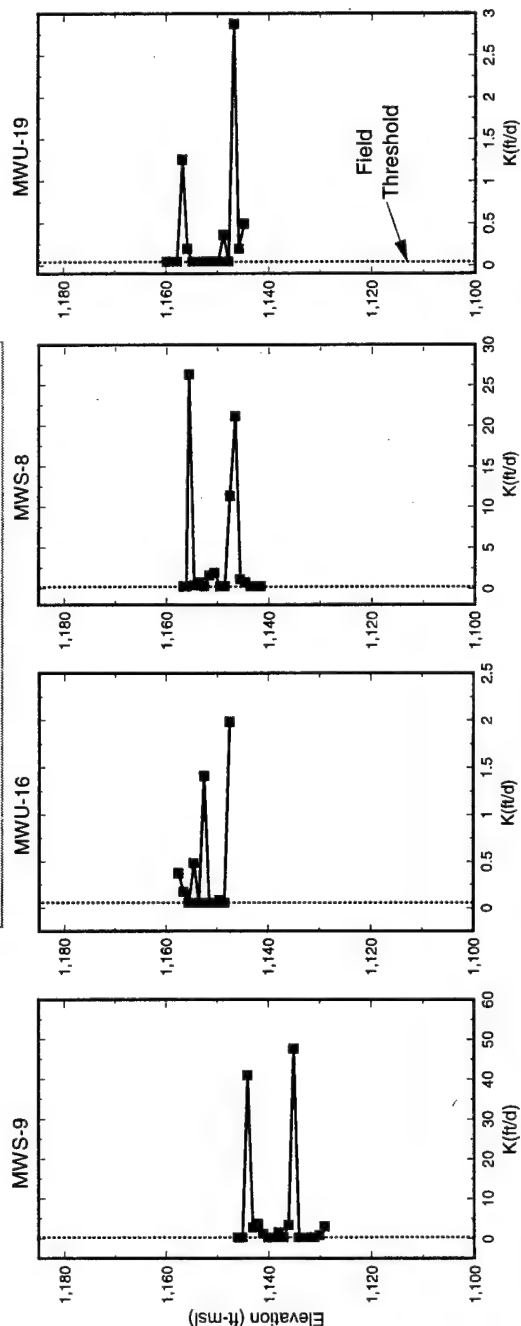


Figure 5.6 Hydraulic Conductivity Profiles for Test Wells (Arithmetic Scales)



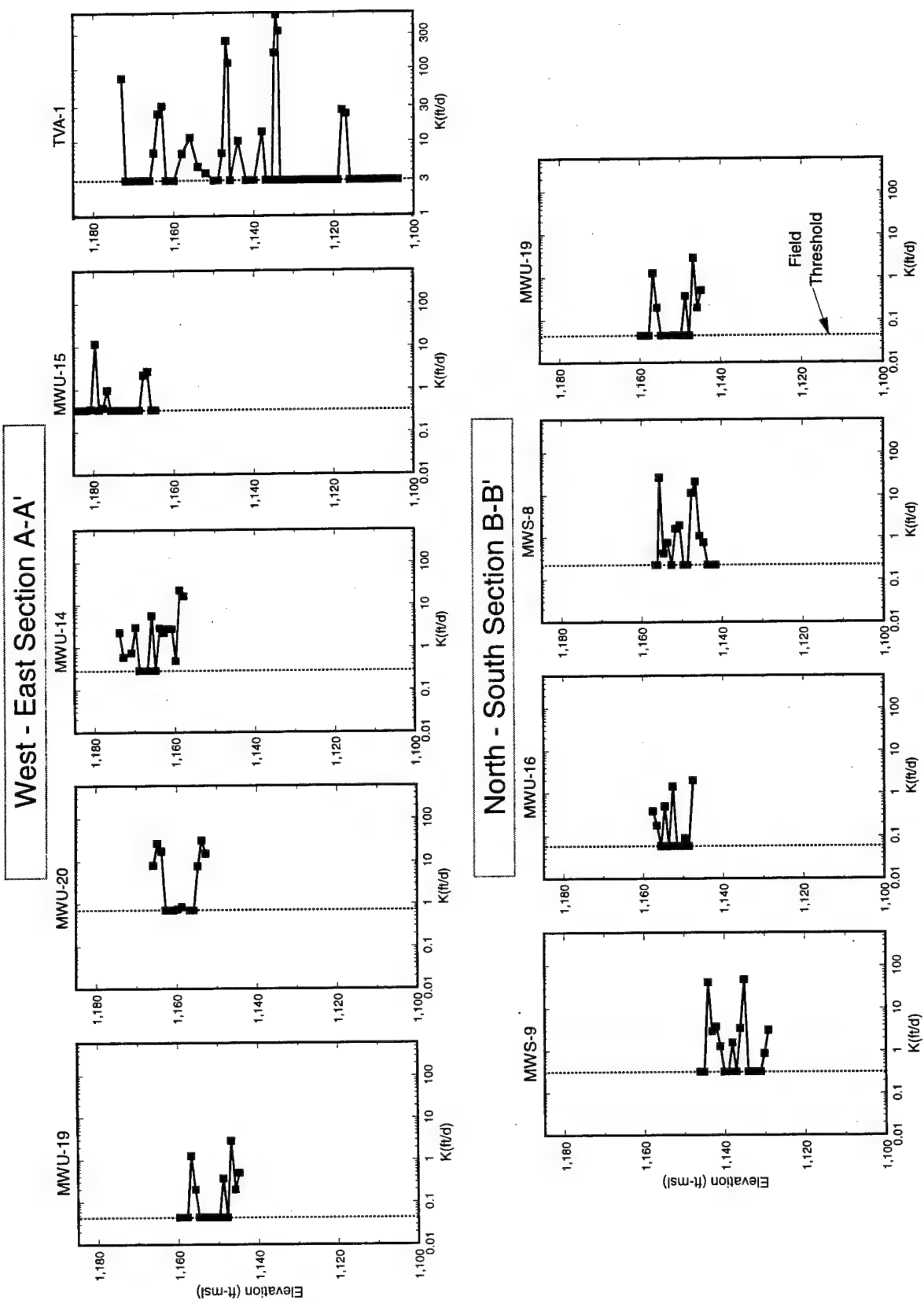


Figure 5.7 Hydraulic Conductivity Profiles for Test Wells (Logarithmic Scales)

to emphasize contrasts in the estimated K values at each test site. Logarithmic K scales are used in Figure 5.7 graphs to better display the full range of K measurements. The lower K measurement threshold for these tests varies from 0.04 to 3 ft/d. The hydraulic conductivity of the unfractured matrix of sandstone and shale is generally well below the 1 ft/d measurement threshold, i.e., the matrix K values for shales rarely exceed  $3 \times 10^{-4}$  ft/d ( $10^{-7}$  cm/s) while values less than  $3 \times 10^{-2}$  ft/d ( $10^{-5}$  cm/s) are typical of sandstones [Freeze and Cherry, 1979]. Therefore, the measured hydraulic conductivities for the sandstone and shale bedrock can largely be attributed to fractures and openings along bedding planes.

Since all of the test wells are vertically oriented, we can infer that the measured K values are primarily associated with horizontal fractures intersected by the wells. However, vertical fracture sets undoubtedly exist at the site as a result of past tectonic activity. The anticlinal structure of the bedrock underlying Area-15A suggests the likelihood of vertical tension fracture sets, even though this cannot be confirmed with either the flowmeter tests or geologic logs derived from vertical wells.

A total of 165 discrete K estimates were obtained from the eight well tests. K estimates ranged from 0.04 to 560 ft/d. A normal probability distribution of the pooled interval K measurements from all test wells is shown on Figure 5.8. Note that the base 10 logarithm of K is plotted rather than actual K since hydraulic conductivity has generally been found to be a log-normal process [Freeze and Cherry, 1979]. Approximately 55 percent of the measurements fall in the "censored data" category, i.e., data which is less than the measurement threshold. The remaining data exhibit an approximately linear trend consistent with a log-normal distribution. Data have a mean log K of 0.61 and standard deviation of 0.83. Visual inspection reveals no major differences between the overall magnitude of K data for the sandstones and shales.

## Implications

The flowmeter test results suggest several refinements to the conceptual hydrogeologic model of the site with implications for numerical modeling and site remediation. Prior to the flowmeter testing, it was recognized that tear gas contaminants released from containers buried in basal overburden deposits tend to move downward through the underlying bedrock in response

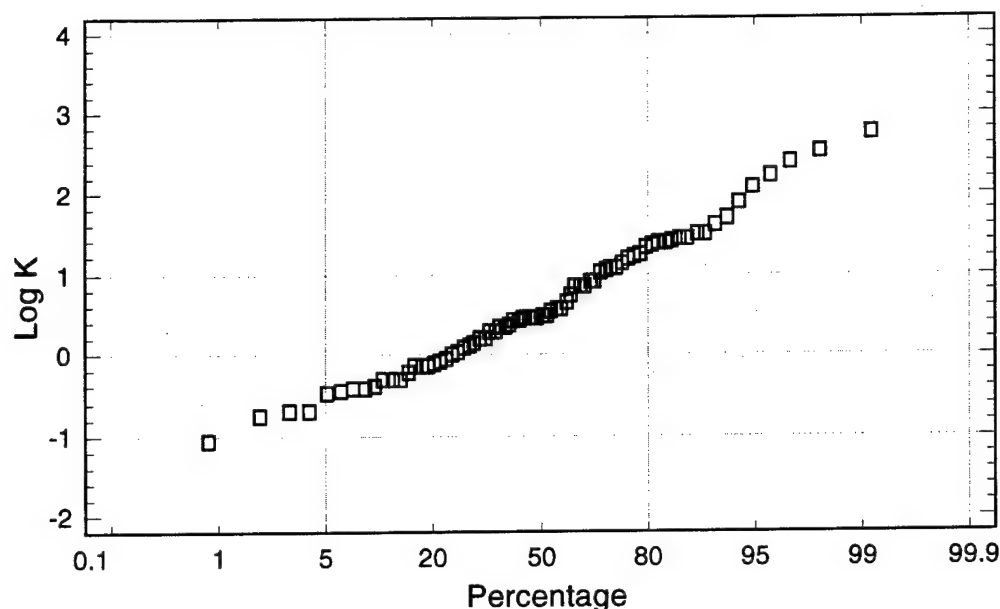


Figure 5.8 Probability Distribution of Log K Data

to density and natural hydraulic gradients. Based on flowmeter tests, we now know that a few thin, sparsely-distributed fractures dominate shallow groundwater contaminant movement in the bedrock aquifer. While groundwater circulation within the bedrock matrix was not detectable in the flowmeter logs, it is likely that there is limited porosity and permeability associated with the rock matrix that may be important in the ultimate fate and transport of the tear gas contaminants. If contaminants enter the bedrock in NAPL form, their movement will be largely controlled by the orientation and connectivity of the hydraulically active fractures. Past experience at other fractured rock sites indicates that NAPL contaminants migrating through fractures may quickly disappear due to dissolution and subsequent diffusion into the rock matrix [Pankow and Cherry, 1996]. Under such conditions, clean-up times may be extremely long as contaminants slowly diffuse out of the rock matrix.

There are two basic approaches that can be taken in modeling fractured porous media such as the sandstone-shale bedrock system underlying Area 15A. First, a dual-porosity model can be applied in which flow/transport is simulated in discrete fractures and in the surrounding rock matrix. Conceptually, this is the preferred approach, although currently only single (dissolved) phase models are available for dual-porosity systems. The second approach would be to apply porous media approximation to the fractured porous system by representing fractures as

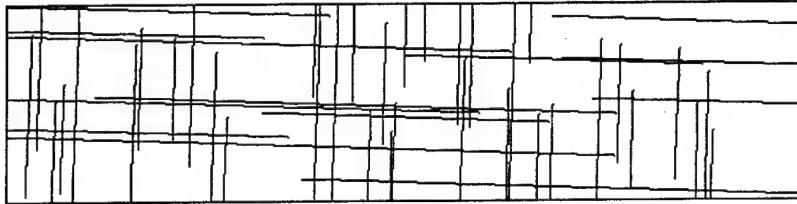
thin zones of high K relative to the rock matrix. In either case, complete three-dimensional spatial characterization of the active fractures in the site vicinity would be technically and economically infeasible. The primary limitation to complete fracture characterization is the risk associated with well construction directly below the disposal area which might open direct pathways for downward migration of DNAPL contaminants.

In the absence of complete fracture characterization, stochastic modeling represents the best approach for simulating contaminant fate and transport in the bedrock underlying Area 15A. Stochastic modeling is generally more complicated than the more traditional deterministic approach because it involves multiple simulations and statistical analysis of modeling results. First, multiple realizations of the bedrock fracture network are generated using the Monte Carlo method. The method requires the spatial statistics of the fracture system including the mean and variance of fracture length, aperture dimensions (or permeability if porous media models are applied), and fracture density. These parameters can be estimated from flowmeter data, geologic logs, local rock exposures, and/or from literature for similar rock types. As an example, three realizations of a fractured rock aquifer are presented on Figure 5.9. All three realizations were stochastically generated using the same set of fracture statistics, i.e., (1) two fracture sets having angles of -2 degrees and 88 degrees counter-clockwise from horizontal; (2) a Poisson fracture length distribution having mean and minimum lengths of 12 m and 7 m for the first set of fractures, and 3 m and 2 m for the second set; and (3) a total of 50 randomly located fractures with 30 percent of the fractures associated with the first fracture set and 70 percent with the second set.

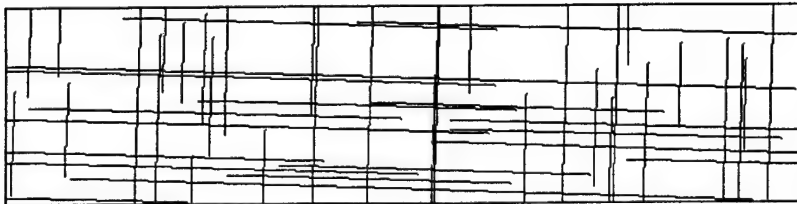
The next step in the process involves flow and transport simulations for each fractured aquifer realization. Results of the multiple simulations are presented as a probability density function of possible outcomes, as opposed to the single prediction of a deterministic model.

Application of fractured porous media models to the tear gas contaminant site is subject to certain limitations. As noted above, models for simulation of multi-constituent, multiphase flow and transport in fractured systems are currently unavailable. Of the existing fractured porous media models, *FRAC3DVS* [Thierren et al., 1994] and *FRACDENS* [Shikaze et al., 1995] appear most promising. *FRAC3DVS* is capable of simulating three-dimensional flow and transport of multiple, dissolved constituents subject to sorption and oxygen-limited biodegradation in a dual porosity, variably-saturated aquifer. Application of this model would

realization 1



realization 2



realization 3

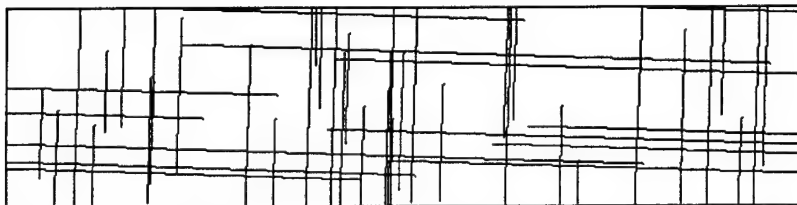


Figure 5.9 Example of Three Stochastically-Generated Fracture Realizations

require implicit treatment of the NAPL phase. *FRACDENS* simulates two-dimensional density-dependent flow and contaminant transport of a single dissolved constituent in discretely-fractured fully-saturated porous media. The solute may be subject to linear equilibrium sorption and first-order biotransformation. As with *FRAC3DVS*, the NAPL phase would have to be handled implicitly, but the potentially-important density effects associated with the tear gas constituents could be largely accounted for with *FRACDENS*. Either of these models could be used to simulate the ultimate fate of tear gas contaminants in the bedrock underlying Area 15A under assumptions of (1) future removal of the buried source material, or (2) no source removal.

Several porous-media type multiphase flow and contaminant codes are available for potential application to Area 15A. *MOTRANS* [Kaluarachchi and Parker, 1990] represents one of the more versatile of these models. The code simulates multiphase (aqueous, nonaqueous, and vapor) flow and transport of up to five constituents subject to sorption and first-order biotransformation in two dimensions. This code would be applicable to the evaluation of in situ treatment systems focused on the overburden drum-burial site.

## Chapter 6

### References

- Boggs, J. M., S. C. Young, D. J. Benton, and Y. C. Chung, "Hydrogeologic Characterization of the MADE Site," Electric Power Research Institute Interim Report, EN-6915, Palo Alto, CA, 1989.
- Bowman, G. K., F. J. Molz, and K. D. Boone, "Borehole Flowmeter Application in Fluvial Sediments: Methodology, Results, and Assessment," Ground Water, 35(3):443-450, 1997.
- Butler, J. J., Jr., "Pumping Tests in Nonuniform Aquifers: A Deterministic and Stochastic Analysis," (Ph.D. Dissertation), Stanford Univ., Stanford, CA, 1990.
- Butler, James A., "The Role of Pumping Tests in Site Characterization: Some Theoretical Considerations," Ground Water, 28(3):394-402, 1990.
- Cooper, H. H., and C. E. Jacob, "A Generalized Graphical Method for Evaluations Formation Constants and Summarizing Well-Field History," Trans. of the Am. Geophys. Union, 217, pp 676-634, 1946.
- Conestoga-Rovers & Associates, "Area 15A Groundwater Pumping Evaluation," Report Ref. No. 6099 (13), November 1995.
- D. B. Stephens & Associates, Inc., "Labor Analysis of Soil Hydraulic Properties of Tennessee Valley Authority Soil Samples," Letter Report, December 30, 1997.
- Dagan, G., "Analysis of Flow through Heterogeneous Random Aquifers, 2: Unsteady Flow in Confined Formation," Water Resources Research, 18(5):1571-85, 1982.
- Dagan, G., "Solute transport in heterogeneous porous formations," Fluid Mechanics, 145(3):241-248, 1984.
- Earth Sciences Consultants, Inc., "Summary of Site Characterization Studies, Federal Laboratories, Saltsburg, Pennsylvania," 1992.
- Freeze, R. A., and J. A. Cherry, Groundwater, Prentice-Hall, Inc., New Jersey, 600 pp, 1979.
- Gelhar, L. W. and C. L. Axness, "Three-dimensional stochastic analysis of macrodispersion in aquifers," Water Resources Research, 19(1):161-180, 1983.
- Haley, J. L., B. Hanson, C. Enfield, and J. Glass, "Evaluating the Effectiveness of Groundwater Extraction Systems," Ground Water Monitoring Review, pp 119-124, 1991.

- Hess, A. E., "A Heat-Pulse Flowmeter for Measuring Low Velocities in Boreholes," U.S. Geological Survey Open-File Report 82-699, 40 pp, 1982.
- Hess, A. E., "Identifying Hydraulically Conductive Fractures with a Slow-Velocity Borehole Flowmeter," Canadian Geotechnical Journal, 23, pp 69-78, 1986.
- Hess, A. E., and F. L. Paillet, "Applications of the Thermal-Pulse Flowmeter in the Hydraulic Characterization of Fractured Rocks," in ASTM STP 1101, pp 99-112, 1990.
- Hess, A. E., and F. L. Paillet, "Characterizing Flow Paths and Permeability Distribution in Fractured Rock Aquifers Using a Sensitive Thermal Borehole Flowmeter," in Proceedings of the Conference on New Field Techniques for Quantifying the Physical and Chemical Properties of Heterogeneous Aquifers, F. J. Molz, O. Güven, and J. G. Melville, ed., Water Resources Research Institute, Auburn University, AL, 1989.
- Hufschmied, P., Ermittlung der Durchlässigkeit von Lockergesteins-Grundwasserleitern, eine vergleichende Untersuchung verschiedener Feldmethoden, Ph.D. Dissertation 7397, Eidgenössische Technische Hochschule, Zurich, Switzerland, 1983.
- Hufschmied, P., "Estimation of Three-Dimensional Statistically Anisotropic Hydraulic Conductivity Field by Means of a Single Well Pumping Test Combined with Flowmeter Measurements," Hydrogeologie, 2, 163-174, 1986.
- Julian, H. E., S. C. Young, C. Lu, J. C. Herwiejer, and K. E. Richter, "NFERC - Regional Groundwater Investigation," TVA Engineering Lab Report WR28-1-520-191, April 1993.
- Julian, H. E., and S. C. Young, "Measuring Well Development With an Electromagnetic Borehole Flowmeter," Proceedings of the Eight National Outdoor Action Conference, NGWA, Minneapolis, Minnesota, May 1994a.
- Julian, H. E., "Site Assessment and Remediation Plan for TVA Centerville 161 kV Substation, Centerville, Tennessee," Tennessee Valley Authority, Resource Group, Chattanooga, Tennessee, November 1994b.
- Julian, Hank E., "Assessment of Groundwater Impacts from Releases of Diesel Fuel Oil at Bellefonte Nuclear Plant," TVA Engineering Lab Report WR28-1-88-120, June 1996a.
- Julian, H. E., "Electromagnetic Borehole Flowmeter Application at Solid Waste Storage Area 5-North, Oak Ridge National Laboratory," TVA Engineering Laboratory Data Report, March 1996b.
- Javandel, I., and P. A. Witherspoon, "A Method of Analyzing Transient Fluid Flow in Multilayered Aquifers," Water Resources Research, Vol. 5, pp 856-869, 1969.



- Kaluarachchi, J. J. and J. C. Parker, "Modeling multicomponent organic chemical transport in three fluid phase porous media," J. Contaminant Hydrology, 5:349-374, 1990.
- Molz, F. J., O. Güven, and J. G. Melville (with contributions by I. Javandel, A. E. Hess and F. L. Paillet), "A New Approach and Methodologies for Characterizing the Hydrogeologic Properties of Aquifers," Robert S. Kerr Environmental Research Laboratory, Ada, OK, Report EPA/600-2-90/002, 205 pp, 1990.
- Molz, F. J., O. Güven, J. G. Melville, and C. Cardone, Hydraulic Conductivity Measurement at Different Scales and Contaminant Transport Modeling: Dynamics of Fluids in Hierarchical Porous Media, J. H. Cushman, ed., Academic Press, New York, pp 37-59, 1989b.
- Molz, F. J., R. H. Morin, A. E. Hess, J. G. Melville, and O. Güven, "The Impeller Meter for Measuring Aquifer Permeability Variations: Evaluations and Comparison With Other Tests," Water Resources Research, Vol. 25, pp 1677-1683, 1989a.
- Moore, G. K., and S. C. Young, "Borehole Flowmeter Data and Interpretation," ORNL/ER-91, Oak Ridge, Tennessee, 1992.
- Morin, R. H., A. E. Hess, and F. L. Paillet, "Determining the Distribution of Hydraulic Conductivity in Fractured Limestone Aquifers by Simultaneous Injection and Geophysical Logging," Ground Water, Vol. 26, pp 587-595, 1988.
- National Research Council, Alternatives for Ground Water Cleanup, National Academy Press, Washington, D.C., 1995.
- Pankow, J. F. and J. A. Cherry, Dense Chlorinated Solvents and Other DNAPLs in Groundwater, Waterloo Press, Portland, Oregon, 1996.
- Rehfeldt, K. R., L. W. Gelhar, J. B. Southard, and A. M. Dasinger, "Estimates of Macrodispersivity Based on Analysis of Hydraulic Conductivity Variability at the MADE Site," EPRI Interim Rep. EN-6405, Electric Power Research Institute, Palo Alto, California, 1989a.
- Rehfeldt, K. R., P. Hufschmied, L. W. Gelhar, and M. E. Schaefer, "Measuring Hydraulic Conductivity with the Borehole Flowmeter," EPRI Top. Rep. EN-6511, Electric Power Research Institute, Palo Alto, California, 1989b.
- Rehfeldt, K. R., J. M. Boggs, and L. W. Gelhar, "Field study of dispersion in a heterogeneous aquifer, 3: Geostatistical analysis of hydraulic conductivity," Water Resources Research, 28(12):3309-3325, 1992.
- Shikaze, S. G., E. A. Sudicky, R. G. McLaren, and J. E. VanderKwaak, "User's guide for FracDen: A two-dimensional numerical model for transient, density-dependent flow and

solute transport in discretely-fractured, saturated porous media," Waterloo Centre for Groundwater Research, Waterloo, Ontario, 1995.

Skibitzke, H. E. and G. M. Robertson, "Dispersion in groundwater flowing through heterogeneous materials," U.S. Geological Survey Prof. Paper 386-B, 1963.

Taylor, K., S. W. Wheatcraft, J. Hess, J. S. Hayworth, and F. J. Molz, "Evaluation of Methods for Determining the Vertical Distribution of Hydraulic Conductivity," Ground Water, 27, pp 88-98, 1990.

Therrien, R., E. A. Sudicky, and R. G. MacLaren, "User's guide for FRAC3DVS: An efficient simulator for three-dimensional, saturated-unsaturated groundwater flow and chain-decay solute transport in porous or discretely-fractured porous formations," Waterloo Centre for Groundwater Research, Waterloo, Ontario, 1994.

U.S. EPA, Basics of Pump-and-Treat Remediation Technology, EPA/600/8-90/003, prepared by GeoTrans, Inc., Herndon, Virginia, 1990.

Young, S. C., H. E. Julian, and M. J. Neton, "Application of the Electromagnetic Borehole Flowmeter and Evaluation of Previous Pumping Tests at Paducah Gaseous Diffusion Plant," TVA Engineering Laboratory, Report No. WR28-1-520-187, January 1993.

Young, S. C., and W. R. Waldrop, "An Electromagnetic Borehole Flowmeter for Measuring Hydraulic Conductivity Variability," in Proceedings of the Conference on New Field Techniques for Quantifying the Physical and Chemical Properties of Heterogeneous Aquifers, F. J. Molz, O. Güven, and J. G. Melville, eds., Water Resources Research Institute, Auburn University, AL, 1989.

Young, S. C., H. E. Julian, H. S. Pearson, F. J. Molz, and J. K. Bowman, "User's Guide for Application of the Electromagnetic Borehole," U.S. EPA report, Robert S. Kerr Environmental Research Laboratory, Ada, OK, Report in Press, 1997a.

Young, S. C., H. S. Pearson, F. J. Molz, and J. K. Bowman, "Field Demonstration of the Electromagnetic Borehole Flowmeter Technology," U.S. EPA report, Robert S. Kerr Environmental Research Laboratory, Ada, OK, Report in Press, 1997b.

## **APPENDIX A**

### **Geologic Logs and Well Construction Diagrams**

Geologic logs and well construction diagrams for all wells except TVA-1 were obtained from "Groundwater Monitoring Report: 1995 Quarterly Groundwater Monitoring, 1995 Monthly Seep Sampling, Federal Laboratories Facility, Saltsburg, Pennsylvania," Conestoga-Rovers & Associates Report Ref. No. 6099 (15), February 1996.

# STRATIGRAPHIC AND INSTRUMENTATION LOG (OVERBURDEN)

(L-13)

PROJECT NAME: FEDERAL LABS FACILITY

HOLE DESIGNATION: MWU-8

PROJECT NO.: 6099


(Page 1 of 3)  
DATE COMPLETED: AUGUST 19, 1994

CLIENT: TRANSTECHNOLOGY

DRILLING METHOD: 6 1/4" ID HSA/WR

LOCATION: SALTSBURG, PA

CRA SUPERVISOR: A. KISIEL

DEPTH ft BGS	STRATIGRAPHIC DESCRIPTION & REMARKS	ELEVATION ft AMSL	MONITOR INSTALLATION	SAMPLE			
				NUMBER	STATE	VALUE	PID
	REFERENCE POINT (Top of Riser) GROUND SURFACE	1216.60 1213.8					
	VEGETATION, some silt, brown	1213.5					
	ML-SILT, trace clay, roots, soft, brown, moist	1213.0					
1.0	CL-CLAY, firm, slightly plastic, orange brown, brown and gray			1SS		5	0
2.0	- trace gravel						
3.0		1210.8		2SS		17	0
4.0	CL-CLAY(NATIVE), trace gravel, firm, slightly plastic, laminated, orange brown, brown and gray, mottled, moist						
5.0	- some silt, trace sand, fissile			3SS		31	0
6.0	- very stiff						
7.0				4SS		52	0
8.0	BEDROCK - augered to 8.0 ft BGS	1206.2					
	END OF OVERBURDEN HOLE @ 8.0 FT BGS	1205.8					
9.0							
10.0							
11.0							
12.0							
13.0							

NOTES: MEASURING POINT ELEVATIONS MAY CHANGE; REFER TO CURRENT ELEVATION TABLE

CHEMICAL ANALYSIS



WATER FOUND



STATIC WATER LEVEL



# STRATIGRAPHIC AND INSTRUMENTATION LOG (BEDROCK)

(L-14)

PROJECT NAME: FEDERAL LABS FACILITY

PROJECT NO.: 6099

CLIENT: TRANSTECHNOLOGY

LOCATION: SALTSBURG, PA

HOLE DESIGNATION: MWJ-8  
(Page 2 of 3)

DATE COMPLETED: AUGUST 16, 1994

DRILLING METHOD: 6 1/4" ID HSA/WR

CRA SUPERVISOR: A. KISIEL

DEPTH	DESCRIPTION OF STRATA	ELEVATION	MONITOR INSTALLATION	BI EN DT RE OR CY KAL	RN UN MB ER	CR OE RE CO VE RY	R OD	WR AE TT EU RN
ft BGS		ft. AMSL				%	%	%
7.0	OVERBURDEN							
8.0	SHALE: black, carbonaceous, thinly bedded	1206.2			1			
9.0	- highly broken, black to gray - dark gray to gray to green gray, clayey, graphite like texture, numerous thin weathered horizontal fractures							
10.0								
11.0								
12.0	SILTSTONE: gray, hard, dipping to near vertical fractures (approximately 45° from horizontal)	1202.0						
13.0	SHALE: dark gray to gray to green gray, clayey graphite like texture, numerous thin weathered horizontal fractures	1201.2			1	86	41.0	100
14.0								
15.0	- completely weathered fracture (● 17.6 ft BGS)							
16.0								
17.0								
18.0	- occasional silty shale to siltstone interbeds - weathered fracture (● 17.7 ft BGS)							

NOTES: MEASURING POINT ELEVATIONS MAY CHANGE; REFER TO CURRENT ELEVATION TABLE

Σ WATER FOUND

Σ STATIC WATER LEVEL

NM - NOT MEASURED

# STRATIGRAPHIC AND INSTRUMENTATION LOG (BEDROCK)

(L-14)

PROJECT NAME: FEDERAL LABS FACILITY

HOLE DESIGNATION: MWU-8  
(Page 3 of 3)

PROJECT NO.: 6099

DATE COMPLETED: AUGUST 16, 1994

CLIENT: TRANSTECHNOLOGY

DRILLING METHOD: 6 1/4" ID HSA/WR

LOCATION: SALTSBURG, PA

CRA SUPERVISOR: A. KISIEL

DEPTH	DESCRIPTION OF STRATA	ELEVATION	MONITOR INSTALLATION	BI EN DT RE OR CV KA L	RN UN NM BER	CR OE RE CO VE RY	ROD	WR AT T E UR N
ft BGS		ft. AMSL				%	%	%
19.0			2" PVC PIPE					
20.0			WELL SCREEN		2	100	84.0	100
21.0								
22.0			4" HQ COREHOLE					
23.0	END OF HOLE • 23 FT. BGS	1190.8						
24.0			SCREEN DETAILS: Screened Interval: 7.5 to 22.5' BGS Length -15.0' Diameter -2.0" Slot # 20 Material -SCH 40 PVC Sand pack Interval: 5.5 to 21.5' BGS Material -# 1 Sand					
25.0								
26.0								
27.0								
28.0								
29.0								
30.0								

NOTES: MEASURING POINT ELEVATIONS MAY CHANGE; REFER TO CURRENT ELEVATION TABLE

W WATER FOUND

S STATIC WATER LEVEL

NM - NOT MEASURED

# STRATIGRAPHIC AND INSTRUMENTATION LOG (OVERBURDEN)

(L-15)

PROJECT NAME: FEDERAL LABS FACILITY

PROJECT NO.: 6099

CLIENT: TRANSTECHNOLOGY


LOCATION: SALTSBURG, PA

HOLE DESIGNATION: MWU-9

DATE COMPLETED: (Page 1 of 3)  
AUGUST 15, 1994

DRILLING METHOD: 6 1/4" ID HSA/WR

CRA SUPERVISOR: A. KISIEL

DEPTH ft BGS	STRATIGRAPHIC DESCRIPTION & REMARKS	ELEVATION ft AMSL	MONITOR INSTALLATION	SAMPLE			
				NUMBER	STATE	VALUE	PID
	REFERENCE POINT (Top of Riser) GROUND SURFACE	1198.80 1195.9					
1.0	ML-SILT, some vegetation, some fine sand, trace charred wood, brown, moist CL-CLAY, some silt, some fine sand, little fine gravel, stiff, no plasticity, mottled, orange brown, gray and dark brown, moist	1195.5	13" CONCRETE PAD	1SS		7	
2.0	- variable amounts of sand and fine gravel		10" BOREHOLE				
3.0	ML/CL-SILT and CLAY, interbedded, some fine gravel, trace fine sand, very stiff, brown, orange brown and gray, moist	1192.9	CEMENT/ BENTONITE GROUT	2SS		18	
4.0			2" PVC PIPE				
5.0				3SS		28	
6.0	CL-CLAY, some silt, sand and fine gravel, stiff, orange brown and gray, moist	1189.9	BENTONITE PELLET SEAL				
7.0	SM-SAND, some silt, trace coarse friable sandstone gravel, loose to medium dense, orange brown and gray, moist	1188.9		4SS		26	
8.0	- trace to little coarse gravel, medium dense to dense		SAND PACK				
9.0				5SS		27	
10.0	BEDROCK END OF OVERBURDEN HOLE @ 9.6 FT BGS	1186.3	WELL SCREEN				
11.0			4" HQ COREHOLE				
12.0							
13.0							

NOTES: MEASURING POINT ELEVATIONS MAY CHANGE; REFER TO CURRENT ELEVATION TABLE

CHEMICAL ANALYSIS



WATER FOUND



STATIC WATER LEVEL



# STRATIGRAPHIC AND INSTRUMENTATION LOG (BEDROCK)

(L-16)

PROJECT NAME: FEDERAL LABS FACILITY

PROJECT NO.: 6099

CLIENT: TRANSTECHNOLOGY

LOCATION: SALTSBURG, PA

HOLE DESIGNATION: MWU-9  
(Page 2 of 3)

DATE COMPLETED: AUGUST 15, 1994

DRILLING METHOD: 6 1/4" ID HSA/WR

CRA SUPERVISOR: A. KISIEL

DEPTH	DESCRIPTION OF STRATA	ELEVATION	MONITOR INSTALLATION	BENTHIC RECOVERIAL	RUN NUMBER	RECOVERY	ROD	WEATHER
ft BGS		ft. AMSL				%	%	%
9.0	OVERBURDEN		SAND PACK					
10.0	SANDSTONE: light gray, fine grained, massive, hard, highly weathered irregular fractures infilled with stiff clay and gravel - Irregular near vertical weathered fracture with limonitic staining (9.6 to 10.0 ft BGS)	1186.3 1185.3						
11.0	INTERBEDDED SILTSTONE and fine SANDSTONE: orange brown and gray sand and clay seams, light gray and brown, thin to medium bedded, highly weathered, limonitic staining		WELL SCREEN		1	102	0.0	100
12.0								
13.0								
14.0								
15.0	SANDSTONE: silty, highly broken, fine grained, crossbedded, moderately to highly weathered limonitic staining	1181.2	2" PVC PIPE					
16.0	- vertical fracture (16.0 to 17.0 ft BGS)							
17.0								
18.0					2	96	32.0	100
19.0	- abundant horizontal and vertical fractures with limonitic staining (18.4 to 20.0 ft BGS) - clay infilled horizontal fractures (18.4 to 19.5 ft BGS)							
20.0	END OF HOLE 20 FT. BGS NOTES: 1.	1175.9	4" HQ COREHOLE					

NOTES: MEASURING POINT ELEVATIONS MAY CHANGE; REFER TO CURRENT ELEVATION TABLE

WATER FOUND

STATIC WATER LEVEL

NM - NOT MEASURED



# STRATIGRAPHIC AND INSTRUMENTATION LOG (BEDROCK)

(L-16)

PROJECT NAME: FEDERAL LABS FACILITY

HOLE DESIGNATION: MWJ-9  
(Page 3 of 3)

PROJECT NO.: 6099

DATE COMPLETED: AUGUST 15, 1994

CLIENT: TRANSTECHNOLOGY

DRILLING METHOD: 6 1/4" ID HSA/WR

LOCATION: SALTSBURG, PA

CRA SUPERVISOR: A. KISIEL

DEPTH	DESCRIPTION OF STRATA	ELEVATION	MONITOR INSTALLATION	B I E N D R E O R C Y K A L	R N U U M B E R	C R O C E O V E R Y	R O D	W R E T T E R N
ft BGS		ft AMSL				%	%	%
21.0			SCREEN DETAILS: Screened Interval: 9.5 to 19.5' BGS Length -10.0' Diameter -2.0" Slot # 20 Material -SCH 40 PVC Sand pack interval: 7.4 to 21.5' BGS Material -# 1 Sand					
22.0								
23.0								
24.0								
25.0								
26.0								
27.0								
28.0								
29.0								
30.0								
31.0								
32.0								

NOTES: MEASURING POINT ELEVATIONS MAY CHANGE; REFER TO CURRENT ELEVATION TABLE

W WATER FOUND

X STATIC WATER LEVEL

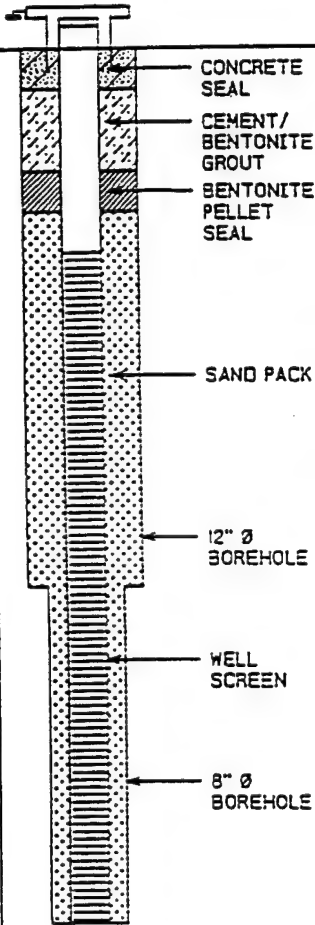
NM - NOT MEASURED

# STRATIGRAPHIC AND INSTRUMENTATION LOG (OVERBURDEN)

(NL-28)  
Page 1 of 1

PROJECT NAME: FEDERAL LABORATORIES FACILITY  
PROJECT NUMBER: 6099  
CLIENT: TRANS TECHNOLOGY  
LOCATION: SALTSBURG, PA

HOLE DESIGNATION: MWU-14  
DATE COMPLETED: AUGUST 31, 1995  
DRILLING METHOD: 8 X" ID HSA/WR  
CRA SUPERVISOR: A.P. KISIEL

DEPTH ft. BGS	STRATIGRAPHIC DESCRIPTION & REMARKS	ELEV. ft. BGS	MONITOR INSTALLATION	SAMPLE			
				NUMBER	STATE	'N' VALUE	PID (ppm)
	REFERENCE POINT (Top of Riser) GROUND SURFACE	.00 .0					
	ML-SILT, some clay			1SS	X	13	-
-2.5	CL-CLAY, some silt, some shale fragments, mottled gray and orange	-2.0		2SS	X	18	-
-5.0	- stiff, mottled brown and gray, slight chemical odor			3SS	X	14	106.0
-7.5	- moist			4SS	X	35	-
-10.0	- slightly plastic to plastic			5SS	X	20	190.0
-12.5	ML-SILT, weathered shale fragments, brown, dry to slightly moist	-12.0		6SS	X	35	-
	BEDROCK	-13.2		7SS	X	>50	163.0
-15.0							
-17.5							
-20.0	END OF OVERBURDEN HOLE @ 19.5ft BGS	-19.5					
-22.5							
-25.0							
-27.5							
-30.0							
-32.5							


NOTES: MEASURING POINT ELEVATIONS MAY CHANGE; REFER TO CURRENT ELEVATION TABLE  
WATER FOUND ↓ STATIC WATER LEVEL ↓

## (BEDROCK)

(WL-28)  
Page 1 of 1

PROJECT NAME: FEDERAL LABORATORIES FACILITY  
 PROJECT NUMBER: 6099  
 CLIENT: TRANS TECHNOLOGY  
 LOCATION: SALTSBURG, PA

HOLE DESIGNATION: MWU-14  
 DATE COMPLETED: AUGUST 31, 1995  
 DRILLING METHOD: 4 1/2" ID HSA/WR  
 CRA SUPERVISOR: A.P. KISIEL

DEPTH ft. BGS	DESCRIPTION OF STRATA	ELEV. ft. AMSL	MONITOR INSTALLATION	BEDROCK INTERVAL	RUN NUMBER	CORE RECOVERY %	ROD %	WATER RETURN %
	Overburden							
-20.0	INTERBEDDED SHALE, gray, soft, with SILTSTONE: gray, sandy, clayey, fine bedded, occasional cross bedded, some contorted bedding	-19.5	 <p>SAND PACK</p> <p>WELL SCREEN</p> <p>8" Ø BOREHOLE</p>					
-22.5	- occasional ripup clasts, composed of brown gray siltstone, claystone, and fine gravel, occasional fossiliferous horizontal bedding plane fractures and microfractures, weathered, no visible oxidation, easily broken	-23.0			1	80	0	-100
-25.0	- broken rock	-25.0						
-27.5	SHALE: dark gray to black, soft, platy, bedding plane partings, occasional siltstone intraclasts, trace pyrite		<p><u>SCREEN DETAILS</u>          Screened interval:          5.0 to 25.0ft BGS          Length: 20ft          Diameter: 4"          Slot Size: #20          Material: SCH 40 PVC          Sand Pack:          4.0 to 25.0ft BGS          Material: #1 Silica Sand</p>					
-30.0	END OF HOLE @ 25.0ft BGS							
-32.5								
-35.0								
-37.5								
-40.0								
-42.5								
-45.0								
-47.5								
-50.0								

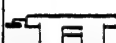

NOTES: MEASURING POINT ELEVATIONS MAY CHANGE; REFER TO CURRENT ELEVATION TABLE  
 WATER FOUND ▼ STATIC WATER LEVEL ▼

# STRATIGRAPHIC AND INSTRUMENTATION LOG (OVERBURDEN)

(WL-21)  
Page 1 of 1

PROJECT NAME: FEDERAL LABORATORIES FACILITY  
PROJECT NUMBER: 6099  
CLIENT: TRANS TECHNOLOGY  
LOCATION: SALTSBURG, PA

HOLE DESIGNATION: MWU-15  
DATE COMPLETED: MAY 11, 1995  
DRILLING METHOD: 4 1/2" ID HSA/WR  
CRA SUPERVISOR: A.P. KISIEL

DEPTH ft. BGS	STRATIGRAPHIC DESCRIPTION & REMARKS	ELEV. ft. AMSL	MONITOR INSTALLATION	SAMPLE			
				NUMBER	STATE	'N' VALUE	PID (ppm)
	REFERENCE POINT (Top of Riser) GROUND SURFACE	1198.70 1198.3					
	ML-SILT, some clay, roots, brown, moist	1195.9		1SS	X	16	0
	CL-CLAY, some silt, red sandy siltstone fragments (0 to 1.0ft BGS)	1194.3		2SS	X	39	0
-2.5	CL/ML-CLAY and SILT, trace sand and gravel, soft to stiff, non plastic, brown and gray, mottled, slightly moist to dry	1192.3		3SS	X	45	0
-5.0	CL-CLAY, some silt, trace to little sand, trace gravel, silt lenses, occasional black organic residue, stiff to very stiff, non plastic, brown and gray, slightly moist to dry			4SS	X	34	0
-7.5	- trace weathered shale fragments			5SS	X	>100	0
	- weathered shale, dark gray, silty shale in spoon tip, dry	1187.3	8" Ø BOREHOLE				
-10.0	SHALE: gray, soft, dry						
-12.5							
-15.0	- silty	1181.8		6SS	X	>100	0.3
	END OF OVERBURDEN HOLE @ 14.5ft BGS		WELL SCREEN 4" Ø BOREHOLE				
-17.5							
-20.0							
-22.5							
-25.0							
-27.5							
-30.0							
-32.5							

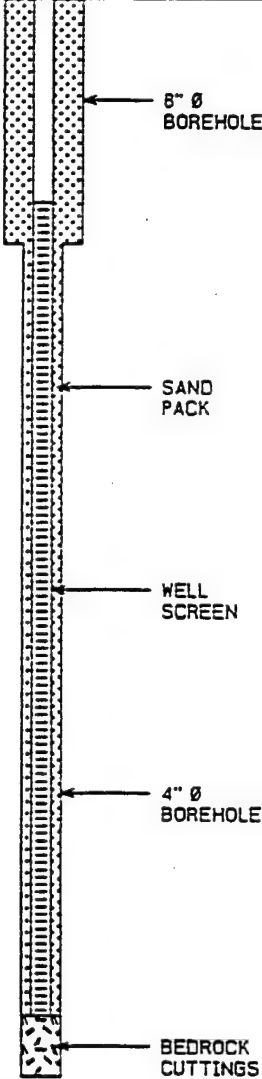
NOTES: MEASURING POINT ELEVATIONS MAY CHANGE; REFER TO CURRENT ELEVATION TABLE  
WATER FOUND ▼ STATIC WATER LEVEL ▼

# STRATIGRAPHIC AND INSTRUMENTATION LOG (BEDROCK)

(WL-21)  
Page 1 of 1

PROJECT NAME: FEDERAL LABORATORIES FACILITY  
PROJECT NUMBER: 6099  
CLIENT: TRANS TECHNOLOGY  
LOCATION: SALTSBURG, PA

HOLE DESIGNATION: MWU-15  
DATE COMPLETED: MAY 11, 1995  
DRILLING METHOD: 4 1/2" ID HSA/WR  
CRA SUPERVISOR: A.P. KISIEL

DEPTH ft. BGS	DESCRIPTION OF STRATA	ELEV. ft. AMSL	MONITOR INSTALLATION	BEDROCK INTERVAL	RUN NUMBER	CORE RECOVERY %	ROD %	WATER RETURN %
	Overburden							
11.0	SHALE: gray, soft, dry	1187.3						
13.5	- silty	1181.8						
16.0	SHALE: gray, fissile, weathered							
18.5	- clayey, highly to extremely weathered, soft, some bedding plane and irregular near horizontal fractures				1	90	50	100
21.0								
23.5								
26.0	SILTSTONE: gray, hard	1172.1 1171.5						
28.5	SHALE: gray, silty, moderately weathered, occasional bedding plane fractures							
31.0	- interbedded with silty shale and cross bedded fine sandstone, slightly weathered, some horizontal bedding plane fractures				2	97	70	100
33.5								
36.0	END OF HOLE @ 35.0ft BGS	1161.3						
38.5			SCREEN DETAILS Screened Interval: 13.5 to 33.5ft BGS Length: 20ft Diameter: 2" Slot Size: #20 Material: SCH 40 PVC Sand Pack: 12.0 to 33.5ft BGS Material: #1 Silica Sand					
41.0								

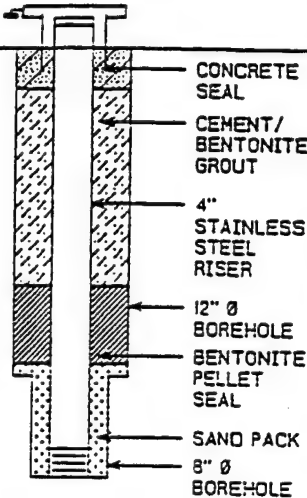
**NOTES:** MEASURING POINT ELEVATIONS MAY CHANGE; REFER TO CURRENT ELEVATION TABLE  
WATER FOUND ▼ STATIC WATER LEVEL ▼

# STRATIGRAPHIC AND INSTRUMENTATION LOG (OVERBURDEN)

(WL-22)  
Page 1 of 1

PROJECT NAME: FEDERAL LABORATORIES FACILITY  
PROJECT NUMBER: 6099  
CLIENT: TRANS TECHNOLOGY  
LOCATION: SALTSBURG, PA

HOLE DESIGNATION: MWU-16  
DATE COMPLETED: MAY 19, 1995  
DRILLING METHOD: 8 1/4" ID HSA/WR  
CRA SUPERVISOR: A.P. KISIEL

DEPTH ft. BGS	STRATIGRAPHIC DESCRIPTION & REMARKS	ELEV. ft. AMSL	MONITOR INSTALLATION	SAMPLE			
				NUMBER	STATE	"N" VALUE	PID (ppm)
	REFERENCE POINT (Top of Riser) GROUND SURFACE	1173.62 1171.4					
2.5	ML/CL-SILT and CLAY, trace sand and gravel, roots, brown, very moist	1170.4		1SS	X	6	0
5.0	CL-CLAY, some silt, trace to little sand, trace roots, oxidized, slightly plastic to plastic, soft, orange brown, moist - no roots - trace to little fine to coarse gravel, friable sandstone fragments, oxidized, slightly plastic, stiff, orange brown and gray			2SS	X	18	0
7.5				3SS	X	58	0
10.0	CL-CLAY, trace to little silt, very stiff, plastic, gray, moist END OF OVERBURDEN HOLE @ 8.0ft BGS	1163.7 1163.4		4SS	X	49	0
12.5							
15.0							
17.5							
20.0							
22.5							
25.0							
27.5							
30.0							
32.5							

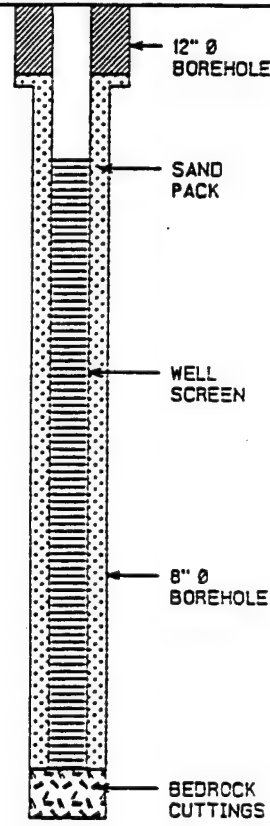
NOTES: MEASURING POINT ELEVATIONS MAY CHANGE; REFER TO CURRENT ELEVATION TABLE  
WATER FOUND ▼ STATIC WATER LEVEL ▼

# STRATIGRAPHIC AND INSTRUMENTATION LOG (BEDROCK)

(WL-22)  
Page 1 of 1

PROJECT NAME: FEDERAL LABORATORIES FACILITY  
PROJECT NUMBER: 6099  
CLIENT: TRANS TECHNOLOGY  
LOCATION: SALTSBURG, PA

HOLE DESIGNATION: MWU-16  
DATE COMPLETED: MAY 19, 1995  
DRILLING METHOD: 8 X" ID HSA/WR  
CRA SUPERVISOR: A.P. KISIEL

DEPTH ft. BGS	DESCRIPTION OF STRATA	ELEV. ft. AMSL	MONITOR INSTALLATION	BEDROCK INTERVAL	RUN NUMBER	CORE RECOVERY %	RQD %	WATER RETURN %
	Overburden							
-8.5	<b>SANDSTONE:</b> light gray and brown, fine to medium grained, fine to medium bedded, slightly weathered to weathered, oxidized, solution pits, irregular vugs, occasionally carbonaceous, many near horizontal irregular fractures, occasional ripup clasts - vertical fractures - gray and dark gray, cross bedded, highly fractured, oxidized - conglomerate beds, approximately 0.3ft thick, weathered fractures (@ 14.7 and 21.1ft BGS)	1163.4			1	105	0	-100
-11.0								
-13.5					2	95	48	-100
-16.0								
-18.5	- fine grained, slightly weathered, light gray	1145.4			3	110	86	-100
-21.0								
-23.5								
-26.0								
-26.0	END OF HOLE @ 26.0ft BGS							
-28.5								
-31.0								
-33.5								
-36.0								
-38.5								

**SCREEN DETAILS**  
Screened Interval:  
9.8 to 24.8ft BGS  
Length: 15ft  
Diameter: 4"  
Slot Size: #20  
Material: Stainless Steel  
Sand Pack:  
7.7 to 24.8ft BGS  
Material: #1 Silica Sand

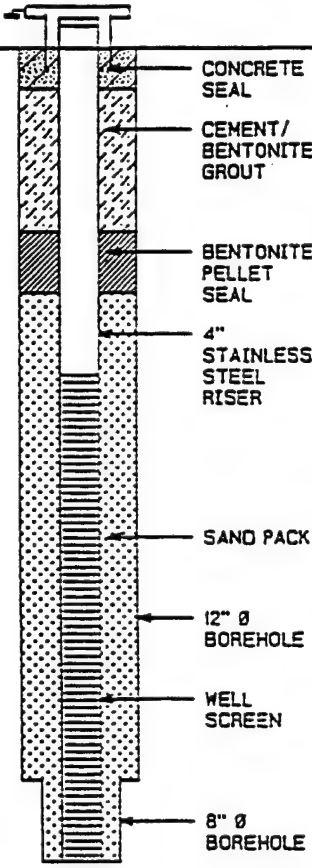
**NOTES:** MEASURING POINT ELEVATIONS MAY CHANGE; REFER TO CURRENT ELEVATION TABLE  
WATER FOUND ▽ STATIC WATER LEVEL ▽

# STRATIGRAPHIC AND INSTRUMENTATION LOG (OVERBURDEN)

(WL-25)  
Page 1 of 1

PROJECT NAME: FEDERAL LABORATORIES FACILITY  
PROJECT NUMBER: 6099  
CLIENT: TRANS TECHNOLOGY  
LOCATION: SALTSBURG, PA

HOLE DESIGNATION: MWU-19  
DATE COMPLETED: MAY 22, 1995  
DRILLING METHOD: 8" ID HSA/WR  
CRA SUPERVISOR: A.P. KISIEL

DEPTH ft. BGS	STRATIGRAPHIC DESCRIPTION & REMARKS	ELEV. ft. AMSL	MONITOR INSTALLATION	SAMPLE			
				NUMBER	STATE	"N" VALUE	PID (ppm)
	REFERENCE POINT (Top of Riser) GROUND SURFACE	1174.83 1172.5					
	ML-SILT, roots, organic matter, trace gravel, wood, brown, very moist	1171.5		1SS	X	8	0
-2.5	CL-CLAY, some silt, trace gravel and sand, oxidized, slightly plastic, soft, cohesive, orange brown, moist	1170.5 1170.1		2SS	X	57	0
	SM-SAND, sandstone fragments, some silt, oxidized, gray, slightly moist to dry	1168.5		3SS	X	>100	0
-5.0	ML/SM-SILT and SAND, trace clay, some to little gravel, sandstone, slightly laminated, black, carbonaceous streaks, orange brown and gray, moist	1166.5		4SS	X	70	0
-7.5	CL-CLAY, some silt, sand and gravel, orange brown and gray, wet, no odor	1164.5		5SS	X	>100	0
-10.0	ML-SILT, weathered sandstone, clay, oxidized, orange brown and gray, dry			6SS	X	45	0.8
	SM-SAND, some silt, sandstone fragments, carbonaceous streaks, gray, dry			7SS	X	17	8.3
-12.5	- weathered sandstone, trace to little silt, non cohesive, loose to dense, oxidized to non oxidized, gray and orange brown, dry to moist	1159.5		8SS	X	>100	28.1
-15.0	CL-CLAY, trace to some silt and sand, hard, thin oxidized layers, gray, moist, chemical odor	1158.5		9SS	X	>100	18.3
	SM/ML/CL-SAND, SILT and CLAY, hard, laminated, fissile, oxidized to non oxidized, gray, dry, chemical odor						
-17.5	- trace to little clay						
	END OF OVERBURDEN HOLE @ 18.0ft BGS	1154.5					
-20.0							
-22.5							
-25.0							
-27.5							
-30.0							
-32.5							

NOTES: MEASURING POINT ELEVATIONS MAY CHANGE; REFER TO CURRENT ELEVATION TABLE  
WATER FOUND ↓ STATIC WATER LEVEL ↓

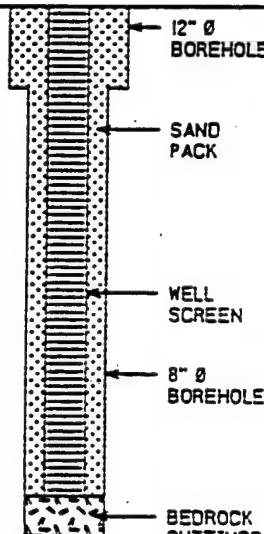


(BEDROCK)

(WL-25)  
Page 1 of 1

PROJECT NAME: FEDERAL LABORATORIES FACILITY  
PROJECT NUMBER: 6099  
CLIENT: TRANS TECHNOLOGY  
LOCATION: SALTSBURG, PA

HOLE DESIGNATION: MWU-19  
DATE COMPLETED: MAY 22, 1995  
DRILLING METHOD: 4 1/2" ID HSA/WR  
CRA SUPERVISOR: A.P. KISIEL

DEPTH ft. BGS	DESCRIPTION OF STRATA	ELEV. ft. AMSL	MONITOR INSTALLATION	BEDROCK INTERVAL	RUN NUMBER	CORE RECOVERY %	ROD %	WATER RETURN %
	Overburden							
18.5	SANDSTONE: gray, medium to coarse grained, fine to medium bedded, moderately to well cemented, occasional shale and ripup clasts, slightly inclined bedding, trace small irregular to oblong vugs, irregular horizontal to near horizontal fractures, weathered, oxidized  - coal streaks (25.1 to 25.9ft BGS)  - fine grained, well cemented, cross bedded, occasional near horizontal to horizontal slightly weathered fractures	1154.5	 <p>12" Ø BOREHOLE SAND PACK WELL SCREEN 8" Ø BOREHOLE BEDROCK CUTTINGS</p>					
21.0								
23.5					1	100	92	-100
26.0								
28.5	END OF HOLE @ 29.0ft BGS	1143.5	<p><u>SCREEN DETAILS</u> Screened interval: 8.0 to 28.0ft BGS Length: 20ft Diameter: 4" Slot Size: #20 Material: Stainless Steel Sand Pack: 8.0 to 28.0ft BGS Material: #1 Silica Sand</p>					
31.0								
33.5								
36.0								
38.5								
41.0								
43.5								
46.0								
48.5								

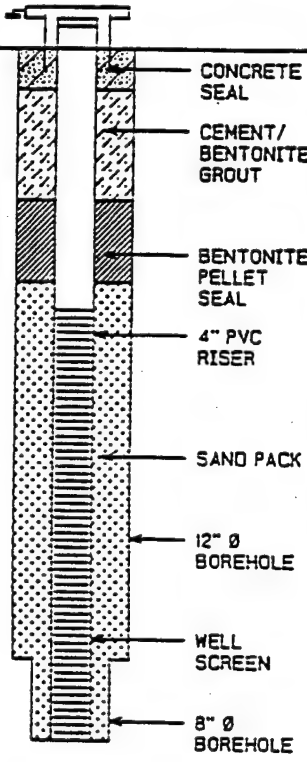
NOTES: MEASURING POINT ELEVATIONS MAY CHANGE; REFER TO CURRENT ELEVATION TABLE  
WATER FOUND ∇ STATIC WATER LEVEL ∇

# STRATIGRAPHIC AND INSTRUMENTATION LOG (OVERBURDEN)

(WL-28)  
Page 1 of 1

PROJECT NAME: FEDERAL LABORATORIES FACILITY  
PROJECT NUMBER: 6099  
CLIENT: TRANS TECHNOLOGY  
LOCATION: SALTSBURG, PA

HOLE DESIGNATION: MWU-20  
DATE COMPLETED: MAY 24, 1995  
DRILLING METHOD: 8 1/2" ID HSA/WR  
CRA SUPERVISOR: A.P. KISIEL

DEPTH ft. BGS	STRATIGRAPHIC DESCRIPTION & REMARKS	ELEV. ft. AMSL	MONITOR INSTALLATION	SAMPLE			
				NUMBER	STATE	'N' VALUE	PID (ppm)
	REFERENCE POINT (Top of Riser) GROUND SURFACE	1177.79 1175.6					
	ML-SILT, trace to some clay, trace gravel, roots, sand, brown, moist	1174.6		1SS	X	8	0
-2.5	CL-CLAY, some silt, trace gravel, soft, slightly plastic, orange brown, moist			2SS	X	10	0
-5.0	- rootlets, organic residue, mottled, orange brown and gray, no gravel			3SS	X	20	0
-7.5	- decreased silt content, slightly plastic to plastic, stiff			4SS	X	33	0
-10.0	- slightly mottled, no roots			5SS	X	53	17.4
-12.5	- trace to little sand, trace gravel			6SS	X	20	48.1
-15.0	- coal streaks, slightly moist to moist			7SS	X	27	23.0
-17.5	- highly to completely weathered shale, oxidized, fissile, stiff, black, brown, gray, and orange brown, wet spoon			8SS	X	>100	17.4
-20.0	- chemical odor, moist						
-22.5	END OF OVERBURDEN HOLE @ 15.0ft BGS	1160.6					
-25.0							
-27.5							
-30.0							
-32.5							

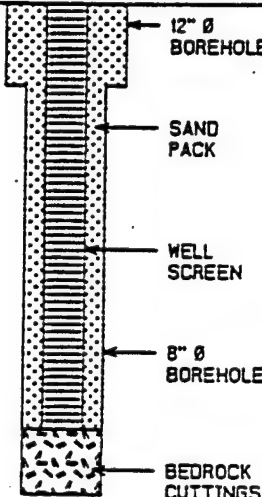
NOTES: MEASURING POINT ELEVATIONS MAY CHANGE; REFER TO CURRENT ELEVATION TABLE  
WATER FOUND ∇ STATIC WATER LEVEL ∇

# (BEDROCK)

(WL-26)  
Page 1 of 1

PROJECT NAME: FEDERAL LABORATORIES FACILITY  
PROJECT NUMBER: 6099  
CLIENT: TRANS TECHNOLOGY  
LOCATION: SALTSBURG, PA

HOLE DESIGNATION: MWU-20  
DATE COMPLETED: MAY 24, 1995  
DRILLING METHOD: 4 X" ID HSA/WR  
CRA SUPERVISOR: A.P. KISIEL

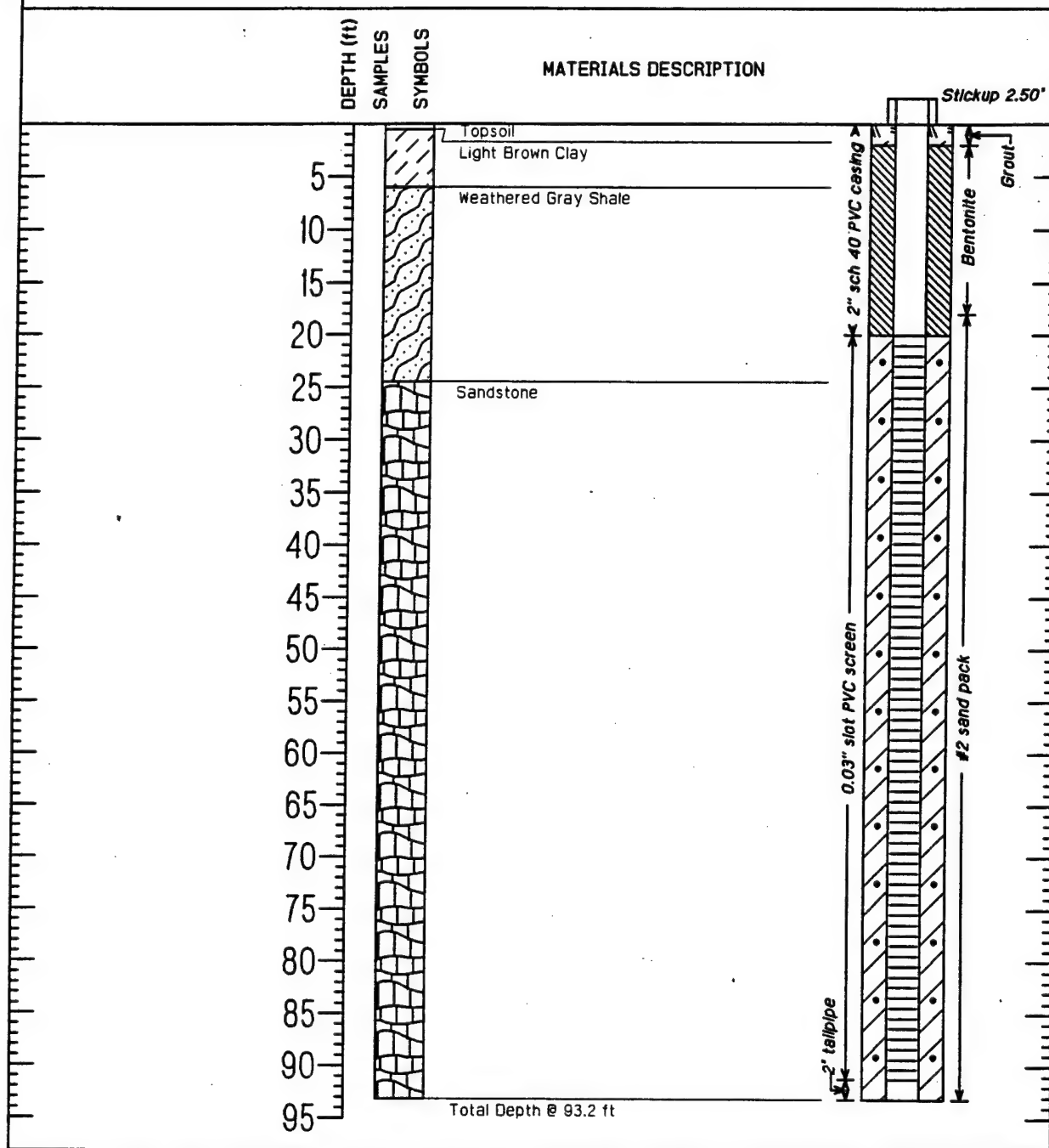
DEPTH ft. BGS	DESCRIPTION OF STRATA	ELEV. ft. AMSL	MONITOR INSTALLATION	BEDROCK INTERVAL	RUN NUMBER	CORE RECOVERY %	RQD %	WATER RETURN %
	Overburden							
15.5	SHALE: gray, silty to clayey, siltstone, weathered, broken, soft to medium hard, oxidized	1160.6						
18.0	- dark gray to black, slightly weathered, fissile - abundant clay ripup clasts, thin coal seams							
20.5					1	69	0	-100
23.0								
25.5	END OF HOLE @ 25.0ft BGS	1150.6						
28.0			<b>SCREEN DETAILS</b> Screened Interval: 6.4 to 23.4ft BGS Length: 17ft Diameter: 4" Slot Size: #20 Material: SCH 40 PVC Sand Pack: 5.7 to 23.4ft BGS Material: #1 Silica Sand					
30.5								
33.0								
35.5								
38.0								
40.5								
43.0								
45.5								

NOTES: MEASURING POINT ELEVATIONS MAY CHANGE; REFER TO CURRENT ELEVATION TABLE  
WATER FOUND ∇ STATIC WATER LEVEL ∇

Tennessee Valley Authority

## MONITORING WELL TVA-1

## WELL CONSTRUCTION DETAIL

PROJECT SALTSBURG - AREA-15DRILLING COMPANY Law EngineeringLOCATION Saltsburg, PA - Federal LaboratoryDATE DRILLED 11/19/97DRILL RIG 4 1/4" ID HS Auger Soil, HQ BedrockSURFACE ELEVATION 1193.9 feet-mslLOGGER/ENGINEER DraperT.O.C. ELEVATION 1196.4 ft feet-mslEAST 8942.0 ftNORTH 10564.0 ft

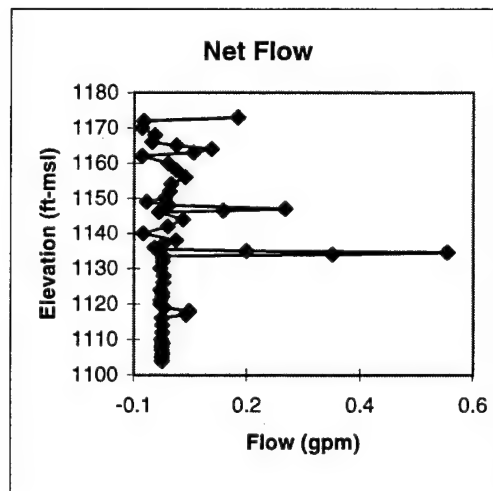
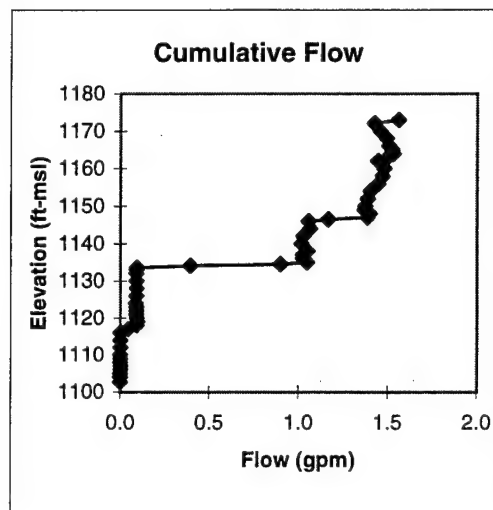
## **APPENDIX B**

### **EM Borehole Flowmeter Surveys**

# Well TVA1, Injection

Top of Casing Elev. = 1197 ft-msl  
K<sub>avg</sub> = 12.346 ft/d

Depth (ft)	Elevation (ft-msl)	Flow (gpm)	Net Flow (gpm)
94.3	1102.7	0.00025	
93	1104.0	0.00025	0.00000
92	1105.0	0.00025	0.00000
91	1106.0	0.00125	0.00100
90	1107.0	0.00125	0.00000
89	1108.0	0.00050	-0.00075
88	1109.0	0.00150	0.00100
87	1110.0	0.00050	-0.00100
85	1112.0	0.00100	0.00050
83	1114.0	0.00125	0.00025
81	1116.0	0.00100	-0.00025
80	1117.0	0.04375	0.04275
79	1118.0	0.09175	0.04800
78	1119.0	0.09550	0.00375
77	1120.0	0.09275	-0.00275
76	1121.0	0.09000	-0.00275
75	1122.0	0.09075	0.00075
74	1123.0	0.09100	0.00025
73	1124.0	0.08800	-0.00300
71	1126.0	0.09025	0.00225
69	1128.0	0.09325	0.00300
67	1130.0	0.09025	-0.00300
65	1132.0	0.09125	0.00100
64	1133.0	0.09225	0.00100
63.5	1133.5	0.09375	0.00150
63	1134.0	0.39500	0.30125
62.5	1134.5	0.89975	0.50475
62	1135.0	1.04875	0.14900
61.5	1135.5	1.03875	-0.01000
61	1136.0	1.02525	-0.01350
60	1137.0	1.02725	0.00200
59	1138.0	1.05175	0.02450
57	1140.0	1.01825	-0.03350
55	1142.0	1.02825	0.01000
53	1144.0	1.06500	0.03675
51	1146.0	1.05950	-0.00550
50.5	1146.5	1.16800	0.10850
50	1147.0	1.38550	0.21750
49	1148.0	1.39800	0.01250
48	1149.0	1.37050	-0.02750
47	1150.0	1.37525	0.00475
45	1152.0	1.38850	0.01325
43	1154.0	1.40475	0.01625
41	1156.0	1.44575	0.04100
39	1158.0	1.47050	0.02475



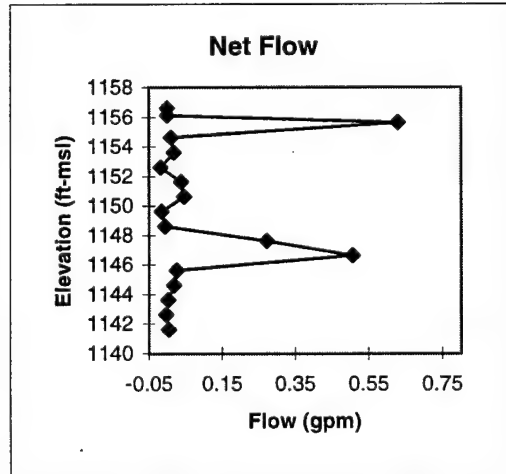
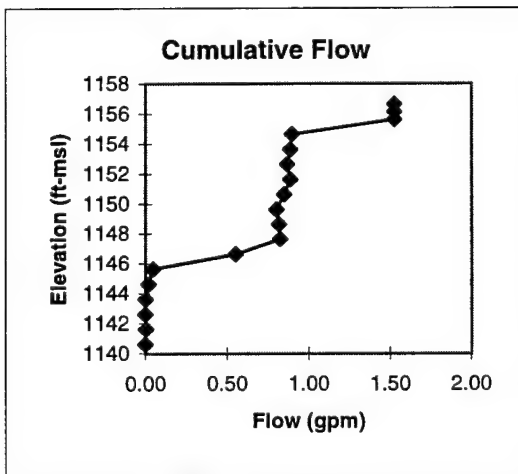
**Well TVA1, Injection**

<b>Depth (ft)</b>	<b>Elevation (ft-msl)</b>	<b>Flow (gpm)</b>	<b>Net Flow (gpm)</b>
37	1160.0	1.48100	0.01050
35	1162.0	1.44500	-0.03600
34	1163.0	1.50025	0.05525
33	1164.0	1.53225	0.08725
32	1165.0	1.52550	0.02525
31	1166.0	1.50775	-0.01775
29	1168.0	1.49475	-0.01300
27	1170.0	1.45900	-0.03575
25	1172.0	1.42625	-0.03275
24	1173.0	1.56050	0.13425

# Well MWS-8, Injection

Top of Casing Elev. = 1173.62 ft-msl  
 $K_{avg} = 3.987$  ft/d

Depth (ft)	Elevation (ft-msl)	Flow (gpm)	Net Flow (gpm)
33	1140.62	0.0000	
32	1141.62	0.0040	0.0040
31	1142.62	0.0000	-0.0040
30	1143.62	0.0020	0.0020
29	1144.62	0.0200	0.0180
28	1145.62	0.0460	0.0260
27	1146.62	0.5520	0.5060
26	1147.62	0.8240	0.2720
25	1148.62	0.8180	-0.0060
24	1149.62	0.8020	-0.0160
23	1150.62	0.8480	0.0460
22	1151.62	0.8860	0.0380
21	1152.62	0.8680	-0.0180
20	1153.62	0.8860	0.0180
19	1154.62	0.8960	0.0100
18	1155.62	1.5260	0.6300
17.5	1156.12	1.5260	0.0000
17	1156.62	1.5260	0.0000

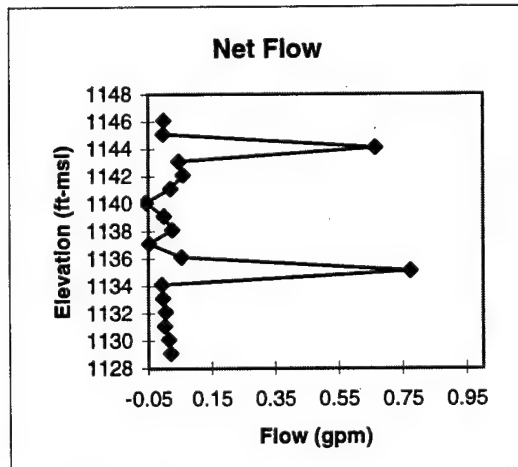
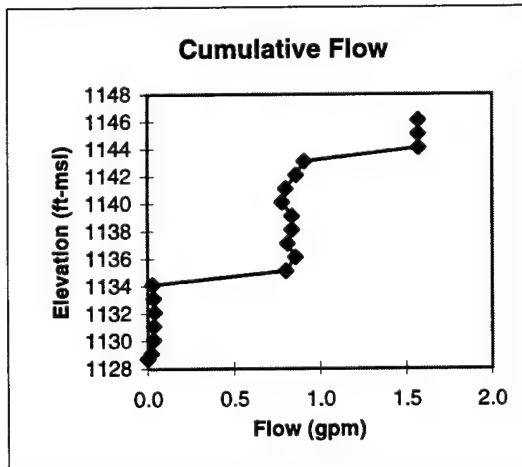




# Well MWS-9, Pumping

Top of Casing Elev. = 1171.1 ft-msl  
 $K_{avg}$  = 5.564 ft/d

Depth (ft)	Elevation (ft-msl)	Flow (gpm)	Net Flow (gpm)
42.4	1128.7	0.0000	
42	1129.1	0.0200	0.0200
41	1130.1	0.0342	0.0142
40	1131.1	0.0356	0.0014
39	1132.1	0.0400	0.0044
38	1133.1	0.0356	-0.0044
37	1134.1	0.0285	-0.0071
36	1135.1	0.8021	0.7736
35	1136.1	0.8577	0.0556
34	1137.1	0.8107	-0.0470
33	1138.1	0.8363	0.0256
32	1139.1	0.8363	0.0000
31	1140.1	0.7793	-0.0570
30	1141.1	0.8000	0.0207
29	1142.1	0.8605	0.0605
28	1143.1	0.9075	0.0470
27	1144.1	1.5729	0.6653
26	1145.1	1.5700	-0.0028
25	1146.1	1.5700	0.0000

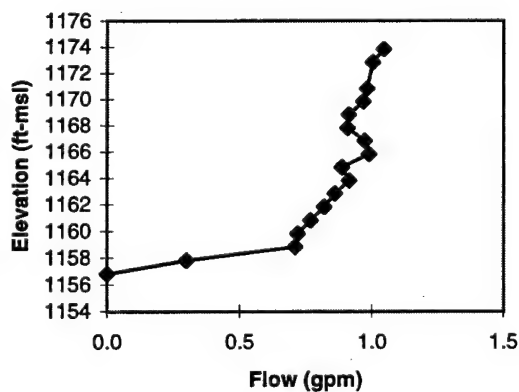


# Well MWU-14, Injection

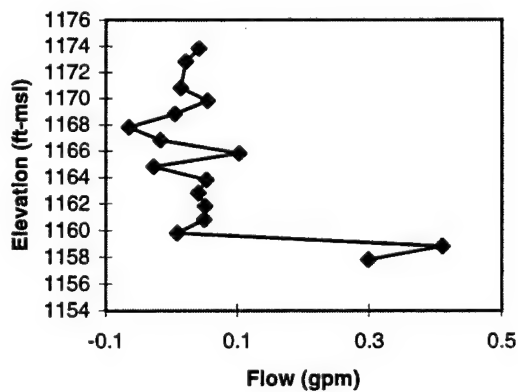
Top of Casing Elev. = 1183.81 ft-msl  
 $K_{avg}$  = 3.337 ft/d

Depth (ft)	Elevation (ft-msl)	Flow (gpm)	Net Flow (gpm)
27	1156.81	0.000	
26	1157.81	0.299	0.299
25	1158.81	0.710	0.411
24	1159.81	0.719	0.009
23	1160.81	0.769	0.050
22	1161.81	0.820	0.051
21	1162.81	0.861	0.041
20	1163.81	0.914	0.053
19	1164.81	0.887	-0.027
18	1165.81	0.990	0.103
17	1166.81	0.973	-0.017
16	1167.81	0.908	-0.065
15	1168.81	0.913	0.005
14	1169.81	0.968	0.055
13	1170.81	0.982	0.014
11	1172.81	1.004	0.022
10	1173.81	1.046	0.042

Cumulative Flow



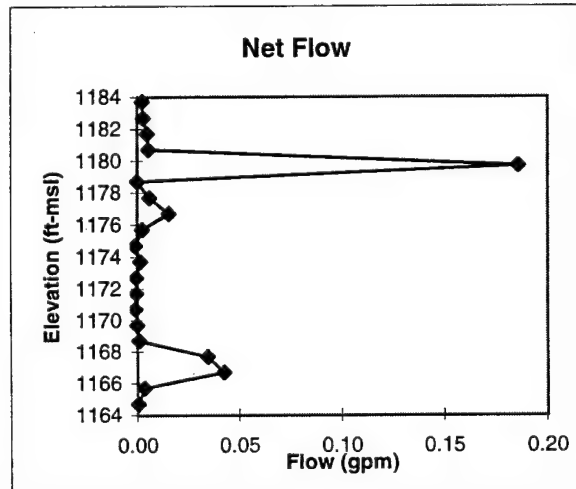
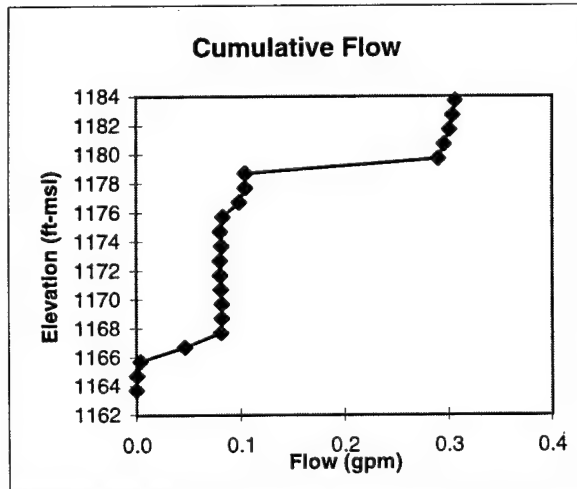
Net Flow



# Well MWU-15, Injection

Top of Casing Elevation = 1198.7 ft-msl  
 $K_{avg} = 0.973 \text{ ft/d}$

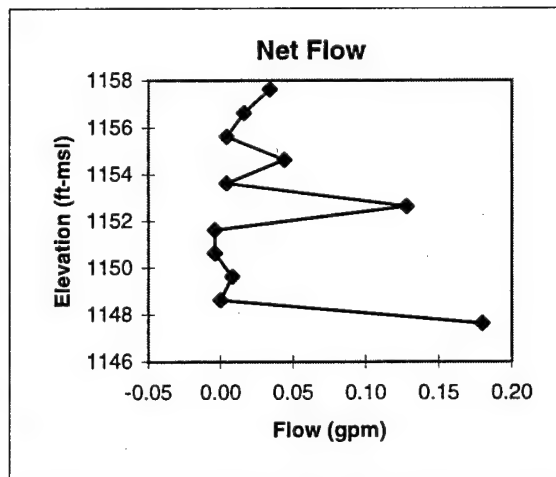
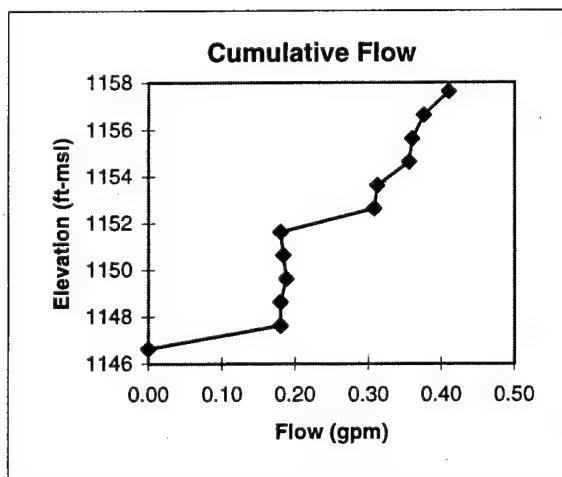
Depth (ft)	Elevation (ft-msl)	Flow (gpm)	Net Flow (gpm)
35	1163.7	0.00000	
34	1164.7	0.00050	0.00050
33	1165.7	0.00400	0.00350
32	1166.7	0.04650	0.04250
31	1167.7	0.08100	0.03450
30	1168.7	0.08200	0.00100
29	1169.7	0.08200	0.00000
28	1170.7	0.08100	-0.00100
27	1171.7	0.08050	-0.00050
26	1172.7	0.08000	-0.00050
25	1173.7	0.08150	0.00150
24	1174.7	0.08050	-0.00100
23	1175.7	0.08300	0.00250
22	1176.7	0.09850	0.01550
21	1177.7	0.10450	0.00600
20	1178.7	0.10450	0.00000
19	1179.7	0.29050	0.18600
18	1180.7	0.29600	0.00550
17	1181.7	0.30100	0.00500
16	1182.7	0.30400	0.00300
15	1183.7	0.30650	0.00250



# Well MWU-16, Pumping

Top of Casing Elev. = 1173.62 ft-msl  
 $K_{avg}$  = 0.412 ft/d

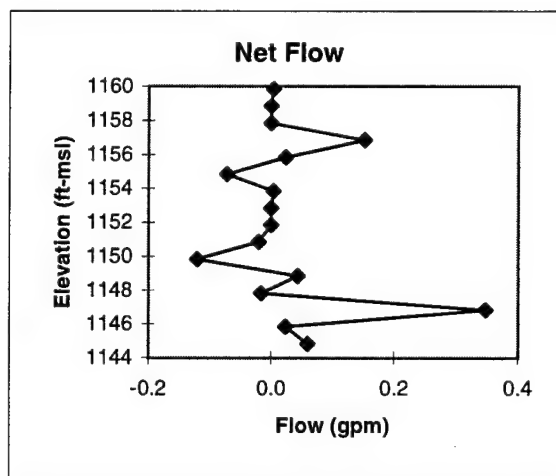
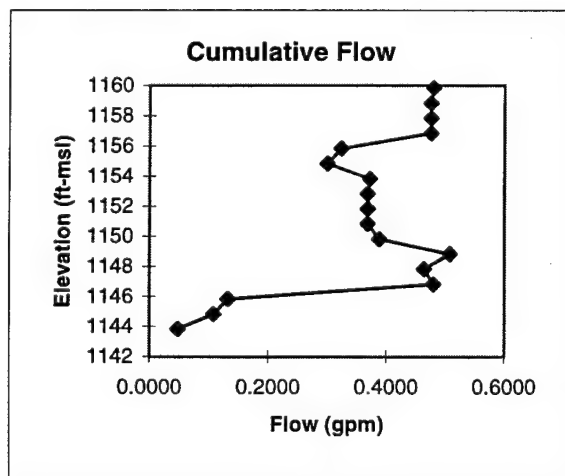
Depth (ft)	Elevation (ft-msl)	Flow (gpm)	Net Flow (gpm)
27	1146.62	0.0000	
26	1147.62	0.1800	0.1800
25	1148.62	0.1800	0.0000
24	1149.62	0.1880	0.0080
23	1150.62	0.1840	-0.0040
22	1151.62	0.1800	-0.0040
21	1152.62	0.3080	0.1280
20	1153.62	0.3120	0.0040
19	1154.62	0.3560	0.0440
18	1155.62	0.3600	0.0040
17	1156.62	0.3760	0.0160
16	1157.62	0.4100	0.0340



# Well MWU-19, Pumping

Top of Casing Elev. = 1174.83 ft-msl  
 $K_{avg} = 0.248$  ft/d

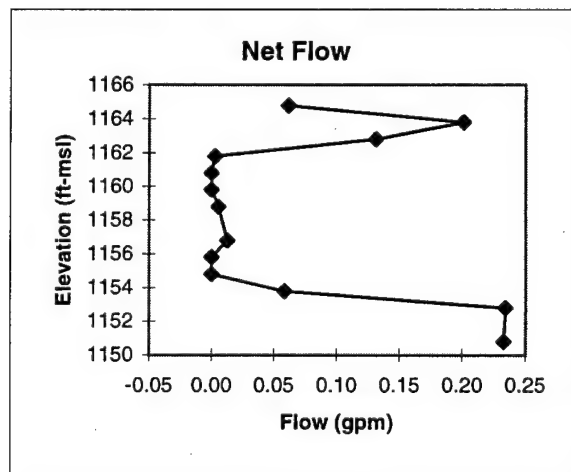
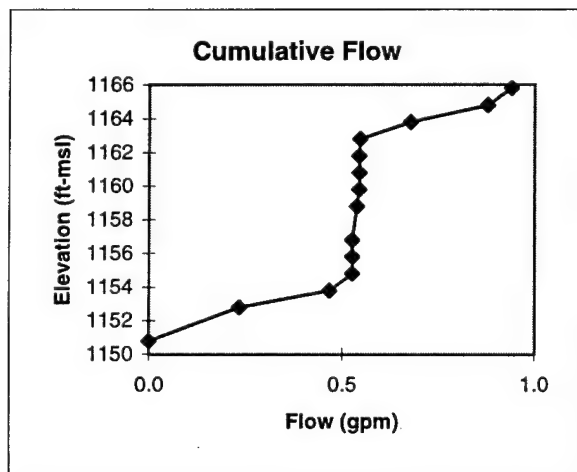
Depth (ft)	Elevation (ft-msl)	Flow (gpm)	Net Flow (gpm)
31	1143.83	0.0480	
30	1144.83	0.1080	0.0600
29	1145.83	0.1320	0.0240
28	1146.83	0.4800	0.3480
27	1147.83	0.4640	-0.0160
26	1148.83	0.5080	0.0440
25	1149.83	0.3880	-0.1200
24	1150.83	0.3680	-0.0200
23	1151.83	0.3680	0.0000
22	1152.83	0.3680	0.0000
21	1153.83	0.3720	0.0040
20	1154.83	0.3000	-0.0720
19	1155.83	0.3240	0.0240
18	1156.83	0.4760	0.1520
17	1157.83	0.4760	0.0000
16	1158.83	0.4760	0.0000
15	1159.83	0.4800	0.0040



# Well MWU-20, Injection

Top of Casing Elev. = 1177.79 ft-msl  
 $K_{avg}$  = 8.391 ft/d

Depth (ft)	Elevation (ft-msl)	Flow (gpm)	Net Flow (gpm)
27	1150.79	0.00000	
25	1152.79	0.23297	0.23297
24	1153.79	0.46733	0.23436
23	1154.79	0.52592	0.05859
22	1155.79	0.52592	0.00000
21	1156.79	0.52592	0.00000
19	1158.79	0.53847	0.01256
18	1159.79	0.54405	0.00558
17	1160.79	0.54405	0.00000
16	1161.79	0.54405	0.00000
15	1162.79	0.54684	0.00279
14	1163.79	0.67797	0.13113
13	1164.79	0.87885	0.20088
12	1165.79	0.94023	0.06138



**APPENDIX F**  
**SIMULATION OF NATURAL RESTORATION**

**DRAFT**

April 28, 1999

EFFECT OF AREA 15A SOIL REMEDIATION ON NATURAL  
RESTORATION OF BEDROCK AQUIFER  
FEDERAL LABORATORIES FACILITY NO. 3  
SALTSBURG, PENNSYLVANIA

*Prepared for*

U.S. Army Environmental Center  
*Aberdeen Proving Ground, Maryland*

*Prepared by*

Tennessee Valley Authority  
Environmental Research Center  
*Muscle Shoals, Alabama*

April 1999

TVA Contract No. RG-99802V  
Report No. \_\_\_\_\_



## Table of Contents

<b>Acronyms and Abbreviations .....</b>	<b>vi</b>
<b>Executive Summary .....</b>	<b>vii</b>
<b>1. Introduction.....</b>	<b>1</b>
1.1 Background .....	1
1.2 Purpose and Scope.....	2
<b>2. Site Description .....</b>	<b>4</b>
2.1 Location and Setting.....	4
2.2 Physiography .....	7
2.3 Geology .....	9
2.3.1 Depositional Environment .....	9
2.3.2 Bedrock .....	11
2.3.3 Soil Overburden.....	14
2.3.4 Local Coal Mines.....	14
2.4 Hydrostratigraphy.....	17
2.5 Hydraulic Properties.....	24
2.5.1 Soil Properties.....	24
2.5.2 Bedrock Properties.....	24
<b>3. Simulation Methods.....</b>	<b>28</b>
3.1 Conceptual Model .....	28
3.2 Model Selection and Limitations .....	30
3.3 Code Description.....	31
3.4 Model Domain.....	31
3.5 Soil and Bedrock Matrix Properties .....	32
3.6 Fracture Characteristics.....	35
3.7 Chloroform Degradation Rate.....	37

3.8 Flow Boundary Conditions .....	38
3.9 Transport Boundary Conditions .....	38
3.10 General Approach.....	41
<b>4. Results and Discussion.....</b>	<b>44</b>
4.1 Flow Simulations.....	44
4.2 Transport Simulations .....	46
4.2.1 Base Case .....	46
4.2.2 Chloroform Degradation Sensitivity Analysis.....	54
4.2.3 Fracture Network Sensitivity Analysis .....	57
<b>5. Conclusions and Recommendations.....</b>	<b>61</b>
<b>References .....</b>	<b>63</b>
Supplement F-1. Bedrock Fracture Aperture Estimates .....	66
Supplement F-2. DNAPL Entry Calculations.....	68
Supplement F-3. Parameter Estimates for Container Failure Distribution .....	70

## List of Figures

2-1 Site Location Map.....	5
2-2 Topography in the Vicinity of Area 15A (Contours in ft-msl).....	6
2-3 Regional Physiography Maps (Adapted from Pennsylvania Department of Conservation and Natural Resources Maps 13 and 64) .....	8
2-4 Structural Map of the Region Surrounding Area 15A Using Base of the Upper Freeport Coal as Lithologic Marker (Adapted from Williams and McElroy, 1997) .....	13
2-5 Soil Sampling Map for (a) May 1997 and (b) November 1997.....	15
2-6 Approximate Aerial Extent of the Upper Freeport Coal Underground Tunnel System for the Abandoned Watson Mine in the Vicinity of Area 15A.....	16

2-7	Temporal Plots of Groundwater Levels at Wells Developed in the Saltsburg Sandstone .....	18
2-8	Continuous Groundwater Levels Versus Precipitation at Wells MWU-15, MWU-19, MWU-20, and OWP-15 for the Period December 1997 through July 1998 (Dashed Lines Indicate Artificially Generated Data) .....	20
2-9	Temporal Plots of Groundwater Levels at Wells Developed in the Buffalo Sandstone ....	21
2-10	Potentiometric Maps for the Saltsburg Sandstone During (a) March 1997 - Wet Period, and (b) December 1998 - Dry Period (Contours in m-msl) .....	22
2-11	Potentiometric Maps for the Buffalo Sandstone During (a) March 1997 - Wet Period, and (b) December 1998 - Dry Period (Contours in m-msl) .....	23
2-12	Fracture Aperture Frequency Distribution .....	27
3-1	Generalized Hydrogeologic Profile Through Disposal Site Following Approximate Groundwater Streamline (upper box), Model Domain (lower box) .....	33
3-2	(a) Assumed Normal Distribution of Container Failures Over Time, (b) Approximation of Container Failure Distribution Applied in Simulations .....	40
3-3	Example of Time-Dependent Specified Concentration Boundary Conditions Representing Randomly Located Contaminant Releases .....	42
4-1	Fracture Network and Steady-State Hydraulic Head Field for Six Fracture Models .....	45
4-2	Predicted Versus Observed Hydraulic Heads for Six Fracture Models .....	47
4-3	Predicted Chloroform Concentration Distribution at Year 1968.8 .....	49
4-4	Predicted Chloroform Concentration Distribution at Year 1989.6 .....	50
4-5	Predicted Chloroform Concentration Distribution at Year 2000 .....	51
4-6	Predicted Chloroform Mass Storage, Boundary Discharge, Boundary Concentrations for No-Action and Soil-Remediation Cases Assuming No Chloroform Degradation .....	52
4-7	Initial Chloroform Breakthrough Predicted at Western (Seep) Boundary of Model Assuming No Chloroform Degradation .....	53
4-8	Predicted Chloroform Mass Storage, Boundary Discharge, Boundary Concentrations for No-Action and Soil-Remediation Cases Assuming CF Degradation Half Life of 1800 Days .....	55

4-9	Predicted Chloroform Mass Storage, Boundary Discharge, Boundary Concentrations for No-Action and Soil-Remediation Cases Assuming CF Degradation Half Life of 277 Days .....	56
4-10	Predicted Chloroform Mass Storage for Six Fracture Models (No CF Degradation) .....	59
4-11	Summary of Predicted Chloroform Mass Storage Fractions at Year 2200 for Six Fracture Models (No CF Degradation) .....	60

## List of Tables

2-1	Classification, Grain-Size Fractions, Organic Carbon, and pH Data for Soils .....	17
2-2	Physical and Hydraulic Properties of Soils .....	24
2-3	Summary of Transmissivity and Hydraulic Conductivity Estimates Associated with Upper Zone Wells from Constant-Rate Pumping Test .....	26
3-1	Minimum DNAPL Pool Heights Required for Entry into Fractures .....	28
3-2	Soil and Bedrock Matrix Properties Applied to Model .....	34
3-3	Literature Estimates of Matrix Properties of Sandstone, Shale, and Related Sedimentary Rocks .....	34
3-4	Fracture Length and Density Characteristics .....	37
4-1	Predicted Net Infiltration and Groundwater Discharge Rates .....	46

## Acronyms and Abbreviations

CNS	Mixture of 2-Chloroacetophenone (CN), Chloroform (CF), and Chloropicrin (CP)
DNAPL	Dense, Non-aqueous Phase Liquid
CN	2-Chloroacetophenone
CF	Chloroform
CP	Chloropicrin
MCL	Maximum Concentration Limit
MSL	Mean Sea Level
ESC	Environmental Sciences Consultants, Inc.
UF	Upper Freeport
TOC	Total Organic Carbon
K	Hydraulic Conductivity
$K_h$	Horizontal Hydraulic Conductivity
$K_v$	Vertical Hydraulic Conductivity
CJSL	Cooper Jacob Straight-Line
T	Transmissivity
$P_c$	Capillary Pressure
$P_e$	Entry Pressure
b	Fracture Aperture
$K_d$	Distribution Coefficient
$R_f$	Retardation Factor
$K_{oc}$	Octonal-Water Partitioning Coefficient
$f_{oc}$	Organic Carbon Fraction
$D_d$	Diffusion Coefficient

## Executive Summary

A numerical modeling analysis was performed to assess whether remediation of the soil drum burial zone at the Area 15A CNS tear gas disposal facility will significantly reduce the time required for natural restoration of the remaining contamination within the underlying bedrock aquifer. The site is characterized by a thin layer of silty, sandy clay soil of residual origin averaging approximately 3 m in thickness in the disposal area. Fractured and interbedded sandstones, shales, and thin coal seams of the Glenshaw Formation lie below the soil overburden. Groundwater originating at the site as incident precipitation migrates downward through the drum burial zone into the underlying bedrock. Subsequent groundwater movement in the bedrock is both downward and westerly, occurring primarily in a sparse network of hydraulically active fractures with only limited flow in the low permeability rock matrix. Groundwater ultimately discharges along bedrock outcrops forming surface seeps some of which are located less than 200 m west of Area 15A.

CNS tear gas is a dense, non-aqueous phase liquid (DNAPL) composed of chloroform (CF), chloropicrin (CP), and 2-chloroacetophenone (CN). The migration behavior of DNAPLs in the subsurface is complex and strongly affected by the density gradient created by their high specific gravities. DNAPLs can be particularly problematic in aquifers dominated by fracture flow, such as the Glenshaw Formation. Rapid contaminant movement may occur through a complex network of discrete fractures in the formation and is accompanied by diffusion of contaminants into the adjacent rock matrix. The present study focuses on CF, the least reactive and the most environmentally persistent of the three CNS tear compounds.

For the analysis, a finite element model is used for predicting flow and transport of dissolved-phase contaminants subject to adsorption and first-order degradation in fractured porous media. The random release of contaminants from the disposal area due to corrosive failure of the presumed 1700 buried, 55-gallon metal drums is represented in the model by a normal distribution. Overall characteristics of the normal distribution were estimated from investigations conducted in 1985 that showed 90% failure of sampled drums. The resulting distribution predicts that 100% of container failures occur between year 1948 (the assumed year of drum disposal) and year 2000. Time-dependent, randomly-located specified concentration

boundary conditions are used to represent regions of residual DNAPL which are expected to form in the drum burial soil zone and in restricted fractures in the underlying rock following the initial release and redistribution of CF from corroded containers. Hydrogeologic data for the model, including bedrock fracture characteristics, were obtained from borehole flowmeter tests conducted as part of this study and from previous site investigations by others. The sorptive and degradative characteristics of CF were largely derived from the fate and effects laboratory studies. Literature estimates were used where site-specific data were unavailable. The sensitivity of model predictions to the natural CF degradation rate at the site was examined using CF half lives of 0, 277, and 1800 days. A similar analysis was performed to examine the sensitivity of model results to variations in random bedrock fracture distributions. Rigorous calibration of the six fracture models was not attempted. However, the predicted hydraulic head fields for all models are in general agreement with observed heads in site monitoring wells. In addition, net surface infiltration rates predicted by these models ranged from 8.0 to 11.5 cm/yr which are consistent with the 20-yr average net infiltration rate of 11.6 cm/yr estimated independently from a hydrologic water balance simulation for the site.

Two site restoration scenarios were evaluated: (1) a *no-action* scenario in which natural restoration of the site was allowed to occur without remediation of contaminated soil at the disposal site, and (2) a *soil-remediation* case which assumed complete removal of all soil contamination at Area 15A in the year 2000 followed by natural restoration of bedrock contamination. All simulations were performed for the period 1948 to 2200 in order to examine the long-term effects of each restoration scenario.

Predictions of long-term natural restoration of the contaminated region affected by Area 15A were shown to be highly sensitive to the assumed CF degradation rate. Of the decay parameters considered, TVA's mineralization study half-life estimate of 277 days provided the best agreement with observed CF concentrations in downgradient seep and groundwater samples. Therefore, predictions using this degradation value may be the best indicators of future conditions. Predictions using moderate degradation rates generally showed better comparisons with observed data than those assuming no degradation thereby supporting assertions by Castro [1986] and others that active microbial degradation of CF has been occurring at the site. Significantly, comparisons of the *no-action* and *soil-remediation* cases using the 277-day CF half

life showed essentially no difference in predicted mass storage and discharge boundary breakthrough concentrations. In both *no-action* and *soil-remediation* cases, degradation of all CF mass was predicted by year 2050 and concentrations at the discharge boundary were below the CF MCL ( $10^{-4}$  g/L) by about year 2010.

Predictions of temporal variations of CF mass storage for six distinct fracture models, all of which assumed no CF degradation, exhibited similar overall mass storage trends with peak storage estimates differing by only about 30%. These findings indicate only minor sensitivity of predictions to fracture distribution. They also suggest that, even without significant CF degradation, remediation of overburden contamination will not significantly reduce the time required for natural restoration of the bedrock system. Although removal of overburden contamination results in a substantial decrease in predicted CF mass storage at year 2000, the mass storage curves for both site restoration cases tended to converge over time and showed little difference by year 2200. This suggests that mobilization of contaminants in the overburden by infiltrating precipitation and their removal from the system through active fractures is relatively rapid compared with the slow diffusion and advection of contaminants from the rock matrix into fractures. So while overburden remediation may provide certain environmental benefits, it will not substantially reduce the time needed for natural restoration of the bedrock.

All simulations considered in the modeling analysis indicated that the highest CF levels have already been observed at the site and that improving conditions can be expected in the future. That is, time-series predictions of CF mass storage and breakthrough at the discharge boundary all peak prior to year 2000, followed by declining mass storage and concentration levels. These trends are a direct consequence of the contaminant release function applied in model simulations which produces failure of all tear gas containers by year 2000. This finding, coupled with the earlier conclusion that remediation of soils in the drum burial area will not significantly reduce the time required for natural restoration of the bedrock, suggests that Area 15A may be a viable candidate for monitored natural attenuation.



# 1. Introduction

## 1.1 Background

The Army Environmental Center contracted with TVA Resource Management to conduct a scientific study of the fate, transport, and effects of CNS tear gas in soils. The goal of this study was to obtain basic information regarding the behavior of soil-borne CNS tear gas components for use in predicting their transport and fate in soil and groundwater. A CNS tear gas disposal facility operated by the U.S. Army following World War II near Saltsburg, Pennsylvania, was selected as the study site. The original project goal was expanded to include development of a remedial strategy for the disposal facility, known as Area 15A, now owned by TransTechnology Corporation. The primary focus of this report is on the hydrogeologic aspects of remedial strategy development.

CNS tear gas is composed of chloroform (CF), chloropicrin (CP), and 2-chloroacetophenone (CN) in relative proportions of 38%, 38%, and 24%, respectively. CF and CP are dense, non-aqueous phase liquids (DNAPLs). CF serves as a solvent for CN which is a solid at standard temperature and pressure. The migration behavior of DNAPLs in the subsurface is complex and is strongly affected by the density gradient they create by virtue of their higher density compared with water. Unlike neutrally buoyant compounds, their migration is often influenced as much by geologic conditions as by ambient groundwater movement. Because of their complex migration behavior, characterizing the subsurface spatial distribution of DNAPLs is problematic. Care must be taken in exploratory drilling and well installation not to create pathways for further downward migration of DNAPL contaminants. For this reason, there has been no characterization of the CNS contaminant plumes directly beneath Area 15A.

In general, the Area 15A site is underlain by a relatively thin soil overburden layer followed by fractured sandstone and shale bedrock. Some 300 to 1700 metal drums containing CNS tear gas were buried in the soil sometime in the late 1940s. Subsequent corrosion of the metal containers has lead to contamination of both the soil and underlying bedrock aquifer. The focus of remedial strategies development in the present study has been on restoration of the contaminated soil overburden. Severe technical difficulties associated with treatment or removal of DNAPL contaminants in fractured porous media render active remediation of the bedrock

aquifer infeasible from a practical standpoint. Containment is generally the only practical means of dealing with such situations, and TransTechnology is currently considering installation of interceptor wells to control contaminant migration. The central question addressed in this report is whether overburden remediation at Area 15A will significantly reduce the overall time required for natural restoration of the remaining contamination within the bedrock aquifer in the site vicinity.

### ***1.2 Purpose and Scope***

The primary objective of this study is to assess the environmental benefit of remediation of overburden contamination in terms of its impact on the overall time required for natural restoration of the bedrock aquifer at the site. Numerical groundwater modeling methods are applied in evaluating the two basic site restoration scenarios. The first case, referred to as the "*no-action*" scenario, considers natural restoration of the site without remediation or removal of CNS tear gas contamination in the soil overburden at Area 15A. The *no-action* case would likely involve institutional controls regarding future use of the site in conjunction with long-term monitoring of groundwater and surface water downgradient of the facility. Containment of tear gas contaminants by an interceptor well system can be part of this scenario, although such a system was not considered in this modeling analysis. The "*soil-remediation*" case evaluates future conditions at the site assuming that all tear gas contamination within the soil overburden at Area 15A is treated or removed. For purposes of this analysis, soil remediation is assumed to occur in the year 2000. This restoration scenario allows flexibility regarding future use of the site, but requires long-term monitoring downgradient of the former disposal facility since bedrock contamination remains unaddressed. The primary basis for evaluating the relative benefits of one restoration scenario over another was the comparison of the predicted contaminant mass stored in the subsurface for each case during the post-remediation period. This evaluation provides a sense of whether soil remediation results in a significant decrease in the time required for natural restoration of the bedrock aquifer. Other evaluation measures include the predicted contaminant concentrations and cumulative contaminant mass at the model discharge boundary corresponding to the region of groundwater discharge seeps (located less than 200 m west of Area 15A).

Hydrogeologic data used in the modeling analysis were obtained from previous site investigations conducted by others and from borehole flowmeter tests performed at the site in November 1997 as part of this study (see Appendix E). The fate and effects laboratory studies conducted by TVA (see Section 4 of main report) provided most of the required information pertaining to the sorptive and degradative properties of the CNS tear gas compounds. Literature data were used where gaps existed in the site-specific hydrogeologic and chemical information. The modeling analysis was performed as a parametric study to address uncertainties regarding key model parameters including contaminant degradation rate and bedrock fracture distribution. Consequently, model predictions are presented for a range of expected parameters in order to bound possible future site conditions for each site restoration alternative. The analysis aids in the identification of the important processes affecting transport of the tear gas contaminants and provides insights regarding their migration rates, spatial distribution, and ultimate fate that may prove useful in decision making regarding the final disposition of the site.

## 2. Site Description

### *2.1 Location and Setting*

The Federal Laboratories facility is located in Conemaugh Township, Indiana County, Pennsylvania. Historical operations of the Federal Laboratory are described in previous site investigation reports [ESC, 1985; ESC, 1992a and 1992b]. The facility is approximately 4.5 km east of the town of Saltsburg, and 2.0 km north of the town of Tunnelton (Figure 2-1). Manufacturing activities currently exist on 14.2 ha adjacent to State Route 3003 (Tunnelton Road).

Area 15A resides on the western portion of the Federal Laboratories property within a 60.7-ha area referred to as Drainage Basin I [ESC, 1992a]. The site is topographically situated in the uplands along the north side of the Conemaugh River. In the immediate vicinity of the disposal site, the land surface slopes gently to the west toward Elders Run, a tributary to the Conemaugh River.

According to ESC [1992a], the approximate contaminated surface area of Area 15A is 1.52 ha. Based upon surface geophysical investigations, test pits, borings, and monitoring wells, the contaminant source area (~1 ha) is depicted by a rectangle with approximate dimensions of 60 m by 170 m (Figure 2-1). As shown in Figure 2-2, Area 15A is bounded on the immediate northwest by Tributary B, and Tributary A is located approximately 240 m east of the site. A public gravel road is proximal to the southern boundary of the site, and a small gravel roadway provides access to the site from the east. The ground surface of Area 15A is grassed, and elevation ranges from approximately 1170 to 1200 ft-msl (3 to 4 percent westerly slope). Just west and south of the site, the ground elevation declines steeply toward Elders Run and the Conemaugh River.

Surface geophysical investigations, test pits, and interviews with plant personnel were used to estimate the approximate extent and alignment of buried drums in Area 15A. During test pits investigations conducted in 1985, drums were judged to be lying on their sides in rows oriented NE-SW, perpendicular to the gravel roadway south of the site. The conditions of the 55-gallon, heavy gauge steel drums ranged from slightly to extremely deteriorated. The occurrence of aqueous fluids in the eleven drums investigated and the stained soil adjacent to the

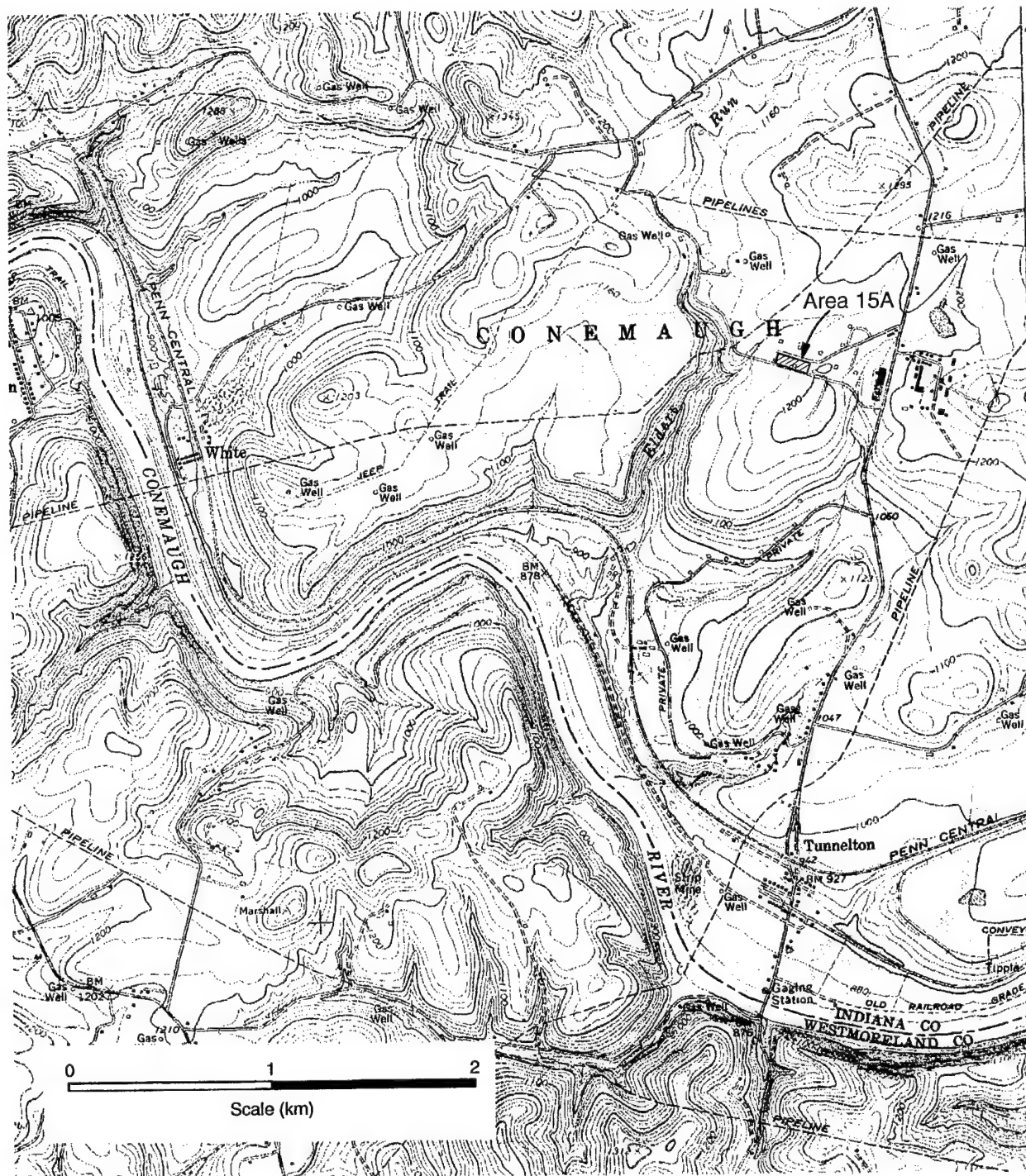


Figure 2-1 Site Location Map

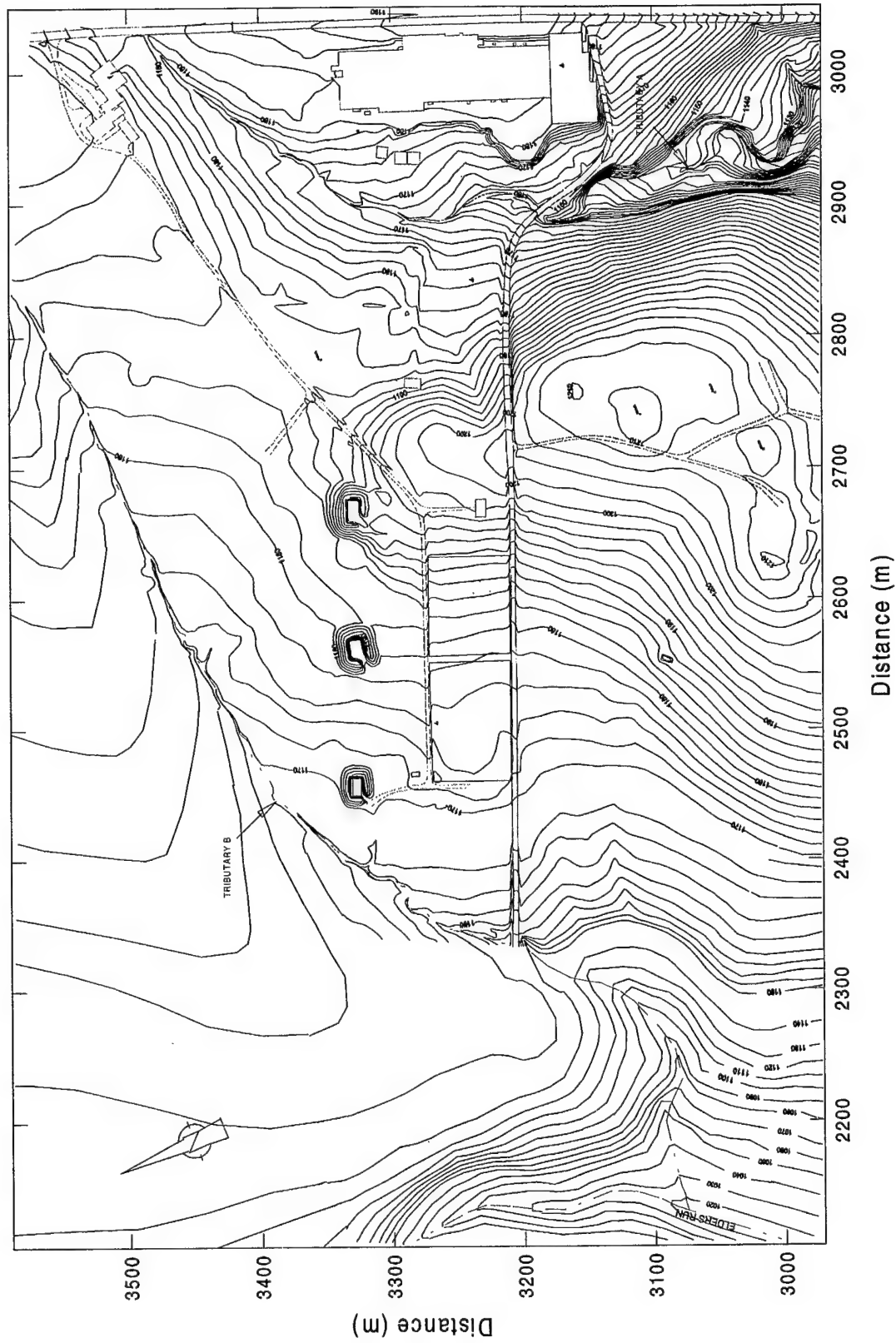


Figure 2-2 Topography in the Vicinity of Area 15A (Contours in ft-msl)

drums indicate leakage over time. Data from test pits suggest that CNS comprises about ten percent of the total volume of drums investigated. Consequently, the vast majority of CNS originally in the drums at the time of burial has leaked into the adjacent soils [ESC, 1985]. This has been confirmed by soil sampling at the site.

## *2.2 Physiography*

The site resides in the Pittsburgh Low Plateau Section of the Appalachian Plateaus Physiographic Province within the Appalachian Basin (Figure 2-3). Like parts of the Reading Prong and the Valley and Ridge Province, the northern part of the Appalachian Plateaus Province in Pennsylvania has been glaciated. However, the study site resides in the unglaciated section of the Appalachian Plateaus Province. Historically, this section has been referred to as the Unglaciated Allegheny Plateau Section [Fenneman, 1938]. The Appalachian Plateaus Physiographic Province extends over more than one-half of Pennsylvania. The province is bounded on the east and southeast by the Valley and Ridge Province and by a narrow strip of the Central Lowland Province in Erie County, Pennsylvania. The Appalachian Plateaus Province is underlain by rocks that are continuous with those of the Valley and Ridge Province, but in the Appalachian Plateaus the layered rocks are nearly flat-lying or gently tilted and warped, rather than being intensively folded and faulted. The eastern boundary of the Appalachian Plateaus is marked by a prominent southeast-facing scarp called the Allegheny Front in Pennsylvania. A northward-facing erosional escarpment forms the boundary between the Appalachian Plateaus and the Central Lowland Provinces. The altitude of the Appalachian Plateaus Province is higher than that of the Valley and Ridge Province as well as the Central Lowland Province.

The Pittsburgh Low Plateau Section consists of a smooth undulating upland surface that is maturely dissected by numerous, narrow relatively shallow valleys. The uplands are developed on rocks containing the bulk of the significant bituminous coal in Pennsylvania. The landscape reflects this by the presence of some operating surface and subsurface mines, many old stripping areas, and many reclaimed stripping areas [PTGS, 1998]. Ground surface elevations in the Pittsburgh Low Plateau Section range from 200 to 520 m-msl. Local relief between valley bottoms and upland surfaces may be as much as 120 m. Valley sides are usually moderately



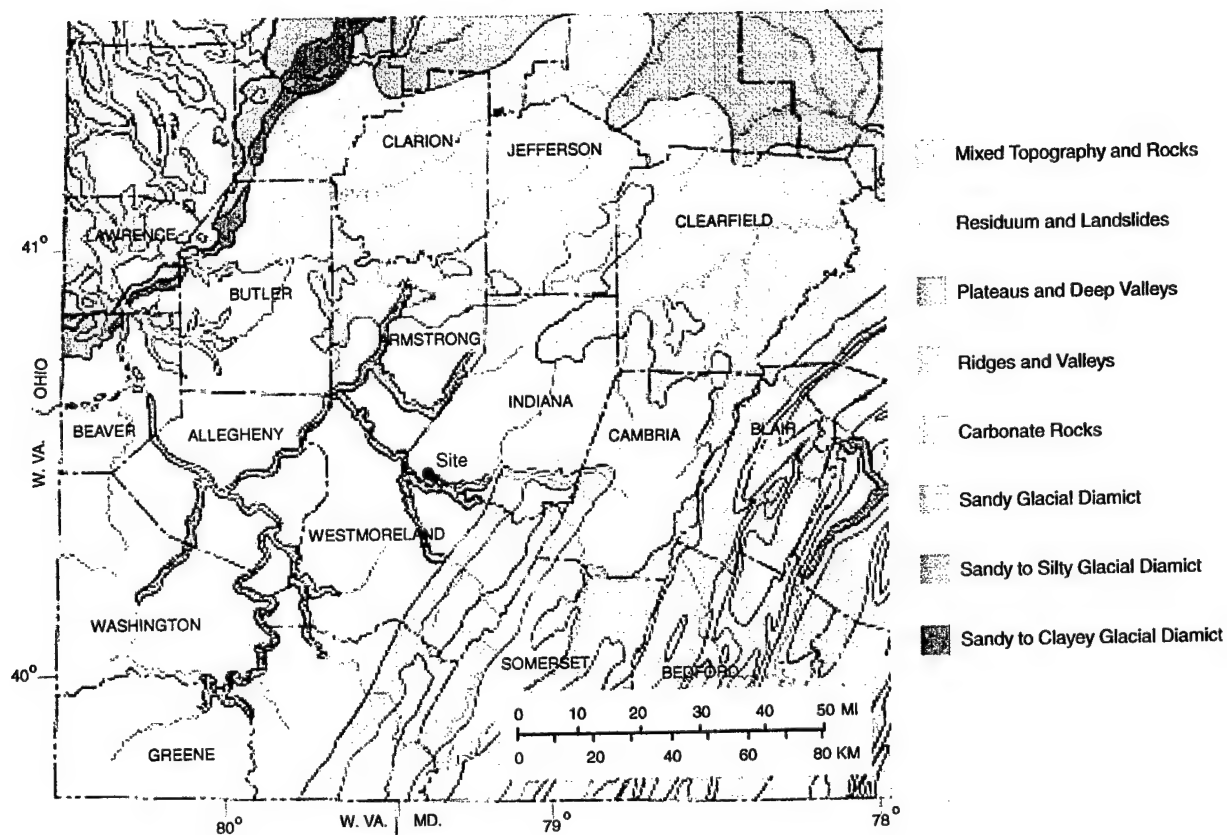
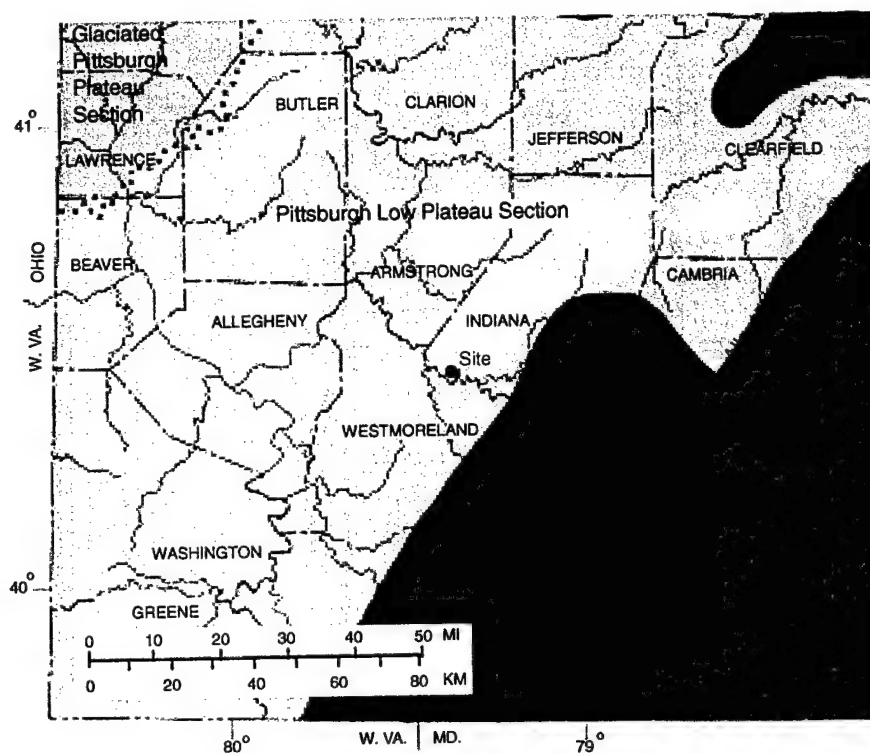


Figure 2-3 Regional Physiography Maps (Adapted from Pennsylvania Department of Conservation and Natural Resources Maps 13 and 64)



steep except in the upper reaches of streams where the side slopes are fairly gentle. Ground surface elevations in the vicinity of the site range from about 270 to 340 m-msl.

Geologic structure in this section of the Appalachian Plateaus Province consists of a series of NE-SW trending anticlines and synclines which resulted from compressional forces from the southeast during episodic mountain building. The intensity of structural deformation decreases progressively to the west from the Appalachian structural front. Hence, the rocks of the Appalachian Plateaus are characterized by the general absence of thrust faults intersecting the surface, and by gentle, approximately symmetric, surface folds [Colton, 1970].

## **2.3 Geology**

### **2.3.1 Depositional Environment**

The Appalachian Basin is an oblong sedimentary basin extending from the Canadian shield southwestward to Alabama, approximately parallel to the Atlantic coastline. This basin is an elongated down-warped segment of the earth's crust in which a great thickness of sediment accumulated, mostly from shallow marine deposition of tectonic source sediments, during long periods throughout the Paleozoic era. To some extent concurrently with deposition, but largely after the bulk of sediments had been deposited, the mass of sedimentary rock was uplifted and deformed. Finally, erosional processes, which are still active, created the present topography [Colton, 1970].

The study site resides on the western margin of the Appalachian geosyncline, a narrow zone of maximum subsidence oriented NE-SW within the Appalachian Basin. The western margin is a transitional zone of the geosyncline to a broad stable platform area (foreland). Thick wedges of nonmarine clastics were deposited at three times during the filling of the Appalachian geosyncline, once in the late Ordovician and early Silurian and twice in the late Devonian through Pennsylvanian. Each sequence is associated with a major source area orogeny (mountain building episode of the Appalachians) and terminated a period of widespread marine deposition. These thick, dominantly alluvial accumulations of lithologies, ranging from conglomerate to coal, thin markedly away from the source and intertongue basinward (W-NW) with shallow marine sections. Lithologically, Pennsylvanian formations show similar regional patterns. The clastics are coarsest in the eastern areas and become progressively finer to the

W-NW. In the westernmost areas, shale predominates over sandstone. The Pennsylvanian sequence originally constituted a much thicker and more extensive wedge of clastic rocks, much of which has been removed since Paleozoic time [Meckel, 1970].

The uppermost sequence of rocks at the site belong to the Conemaugh Formation. Approximately 120 to 150 m thick, the Conemaugh was deposited in late Paleozoic time, primarily during the Upper Pennsylvanian Period (290 to 300 Ma). During this interval, the Appalachian Orogeny (Revolution) occurred intermittently with periods of widespread alluvial deposition from the E-SE. Regionally, the sediments represent a variety of depositional environments, all of which are elements of a broad coastal plain flanking a marine embayment. Along the western margin of the geosyncline (Foreland), the sediments are low-gradient deltaic and intertidal planes derived from a broad emergent alluvial apron. According to Meckel [1970], the depositional pattern of the tectonically derived sediments is one of thick alluvial clastics in the east which thin and intertongue westward with thinner time-equivalent marine strata.

Facies of the arenaceous upper bedrocks at the site suggest basal lacustrine and flood plain deposition accompanied by episodic progradation by meandering stream deposits. The source of the sediment was probably a combination of clastics from both the tectonic source to the east and cratonic sources to the north. The light gray to dark gray mudrocks (shales and siltstones) and sandstones are highly carbonaceous and suggest deposition in an anoxic environment with little water circulation. Low granularity also implies deposition via turbidity currents or geostrophic flows. Such conditions are indicative of ancient lacustrine facies. However, paleontologic studies to distinguish fossils as marine or non-marine are lacking. Observations of fissility and thin bedding in the mudrock cores suggest a fresh water depositional environment. There were likely periods of emergence during deposition of the site upper bedrocks since thin coal seams were produced by autochthonous swamp deposits. The site setting during periods of basal rock deposition, therefore, may be described as a subaerial swamp bordering the lacustrine basin during low water periods.

The presence of thin conglomerate (rounded gravel) beds and clasts (i.e., rip-up and detrital) in the upper bedrocks at the site also indicate time intervals of relatively fast moving waters (fluvial activity) across the site during pluvial times. Lithologic evidence of progradation and/or fluvial activity is also displayed by large lateral facies variations and bedding (i.e., thin to

massive). The source of conglomerate-containing sediment is likely cratonic material originating from the north. Ferm's [1970] depositional model for Pennsylvanian rocks in Indiana County is one of an actively prograding deltaic wedge from the north. This model is supported, to some degree, by fluvial strata in upper bedrock at the site. It is possible that fluvial-dominated deltaic deposits from the north periodically drowned and reworked swampy flood plain and lacustrine sediments at the site during several periods. However, the position of the site relative to the vertical and lateral facies of the prograding delta is undetermined.

### 2.3.2 *Bedrock*

The primary geologic unit of interest relative to Area 15A is the Pennsylvanian age Glenshaw Formation of the Conemaugh Group. It is the uppermost lithologic unit at Area 15A. The Glenshaw is comprised of a sequence of interbedded sandstone, shale, and thin coal units. The top of the Upper Freeport Coal marks the base of the Conemaugh Group and Glenshaw Formation.

Based upon a review of the site assessment literature, ESC [1985] was the first to delineate stratigraphic units of interest beneath the site. Typical of strata within this geologic sequence, the arenaceous members of the Glenshaw are described by ESC [1985] as fine- to medium-grained, micaceous, thin to massively bedded, and commonly displaying large lateral facies variation. Argillaceous strata are depicted as fissile and typically thin bedded. Coal seams are thin and discontinuous or may be represented by bony coal, possibly the Brush Creek Coal horizon. ESC [1985] indicates that the lithologic units of interest beneath the site are, from youngest to oldest, the Saltsburg Sandstone, Buffalo Sandstone, Brush Creek Coal, Mahoning Coal, Mahoning Sandstone, and Upper Freeport Coal. This stratigraphic description has been echoed in subsequent reports [ESC, 1992a, b] dealing with Federal Laboratories site investigations.

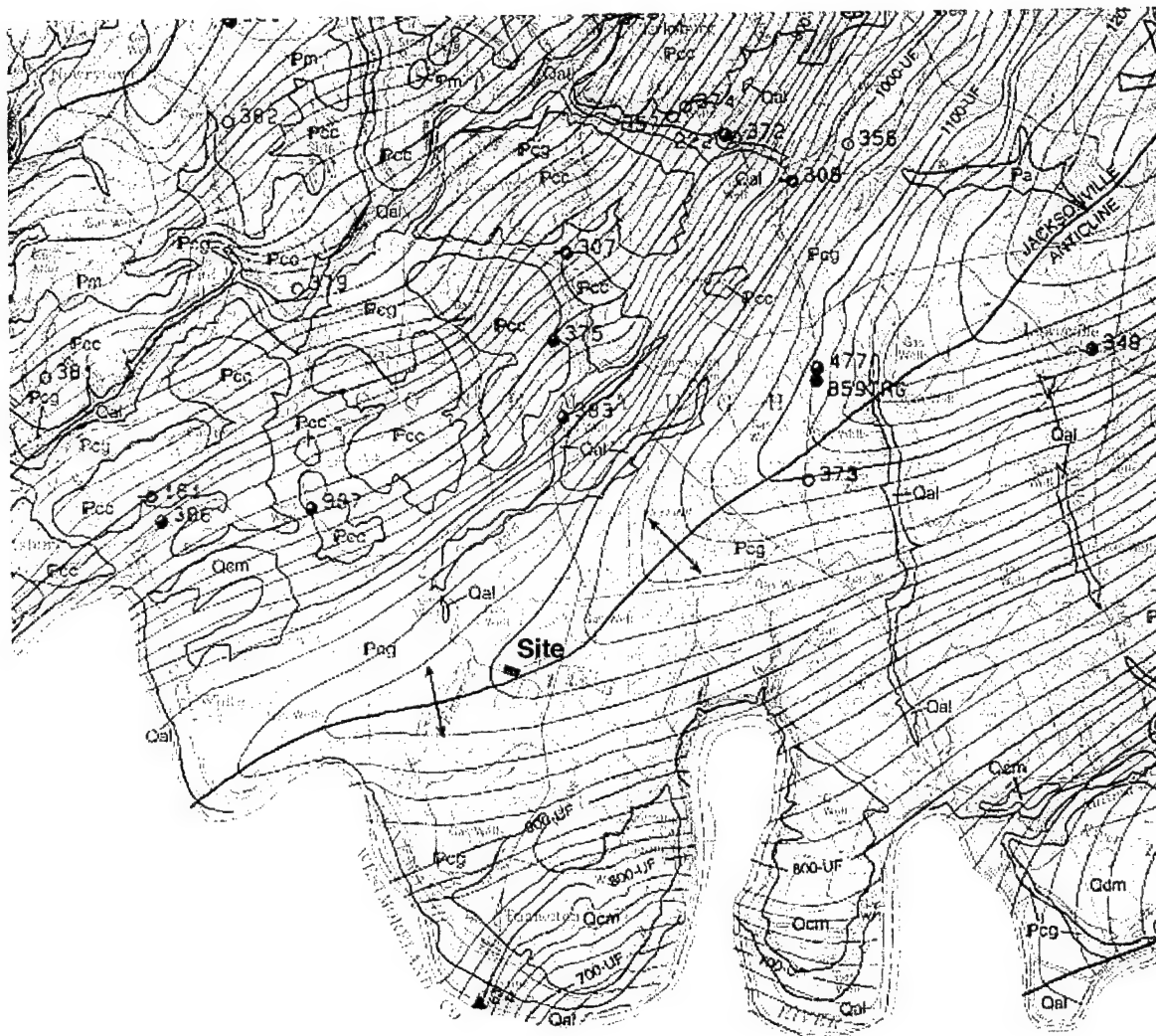
The names of many stratigraphic units, particularly coal-beds and sandstone units, have arisen from local nomenclature, particularly by coal companies. The names have been taken from geographic locations within relatively small mining districts or within coherent drainage basins. Rice et al. [1994] provide a comprehensive glossary for the central Appalachian basin which expands on older stratigraphic glossaries and includes the joint SEAMS database of the

University of Kentucky's Energy Center for Applied Energy Research and the Kentucky Geological Survey. Informal rock units contained in the glossary and present at the site include the Buffalo and Saltsburg Sandstones. According to the glossary of Rice et al. [1994], the Saltsburg Sandstone is exposed along Conemaugh and Loyalhanna Rivers near Saltsburg, Indiana County, Pennsylvania, in the Conemaugh Formation between the Harlem Coal or Pittsburgh Redbeds and Upper Bakerstown Coal [Keroher et al., 1966]. The Buffalo Sandstone is a massive sandstone member cropping out in Buffalo Creek, Buffalo Township, eastern Butler County, Pennsylvania; in lower part of Conemaugh Formation between Cambridge or Meyersdale limestone (above) and Brush Creek limestone [Wanless, 1939].

The glossary of Rice et al. [1994] indicates that the original designation of lithologic units at the site by ESC [1985] may be the result of convenience rather than true stratigraphic identity since these formations exhibit significant lateral facies variability. Regardless, this nomenclature is sufficient for purposes of lithologic description, and the stratigraphic time correlation is approximately correct. For the sake of continuity, therefore, this report will adhere to the lithologic nomenclature prescribed by previous site investigation reports.

Based on geologic logs for monitoring wells in the site vicinity, it appears that shale or saprolite lies directly below the eastern two-thirds of the disposal area with the Saltsburg Sandstone directly underlying the remaining area. According to ESC [1992a], the Saltsburg Sandstone outcrops along tributary B at an approximate elevation of 344 m-msl. The Saltsburg is a fine- to medium-grained sandstone containing fissile shale sequences and very thin coal seams. Thickness is on the order of 15 m or less in the site vicinity. A predominantly shale zone some 6 to 12 m thick separates the Saltsburg Sandstone from the underlying Buffalo Sandstone. The Buffalo consists of gray shaly sandstone and ranges from 1 to 4 m in thickness. To our knowledge, no subsurface investigations have been performed below the Buffalo sandstone at Area 15A.

Figure 2-4, adapted from Williams and McElroy [1997], depicts the shallow geologic structure near Area 15A constructed from well and boring logs in the area. The elevation contours in the figure represent the base of the Upper Freeport (UF) Coal, an excellent marker bed residing at the base of the Glenshaw Formation. As shown in Figure 2-4, Area 15A resides



on the western flank of the Jacksonville Anticline which plunges gently (about three percent near the site) to the southwest. Geologic strata directly beneath Area 15A dip gently to the northwest.

### *2.3.3 Soil Overburden*

A generalized east-west hydrostratigraphic section through the Area 15A site is presented in Figure 3-1(a). The unconsolidated soil overburden beneath the site is derived from weathering of the underlying shale and sandstone bedrock. Five test pits in Area 15A indicated silty-clay soil thickness ranging from 1.1 to 2.4 m [ESC, 1985]. However, well installation and soil borings suggest that soil thickness ranges from about 2.7 to 3.4 m within the immediate vicinity of the disposal area. Shallower soil depths occur on the eastern side of the site gradually increasing in depth to the west.

In May 1997, eight soil samples were collected from four areas in the vicinity of the Area 15A disposal site (Figure 2-5) and analyzed for selected properties by TVA's Environmental Research Center. As shown in Table 2-1, residual soils are primarily silty to sandy clay with occasional weathered rock fragments. Total organic carbon (TOC) and pH average 0.42 percent and 5.13, respectively. The TOC of soil sample 8 is considered anomalously high due to its sampling location within the contaminated source.

### *2.3.4 Local Coal Mines*

Figure 2-6 shows the approximate aerial extent of the Upper Freeport coal underground tunnel system for the abandoned Watson Mine in the vicinity of Area 15A. This figure is based on a plat obtained from the Pennsylvania Department of Environmental Protection's District Mining Office in McMurray, Pennsylvania. Figure 4 from ESC [1985] indicates that the abandoned underground tunnel system extends beneath Area 15A at a depth of about 55 m below ground surface [ESC, 1992a]. The representation of the tunnel system in Figure 2-6 is slightly different from that of ESC [1985] and indicates that mining excavations may be limited to the southern boundary of Area 15A. Both figures, however, indicate that the abandoned tunnel system resides below the contaminated horizons of Area 15A.

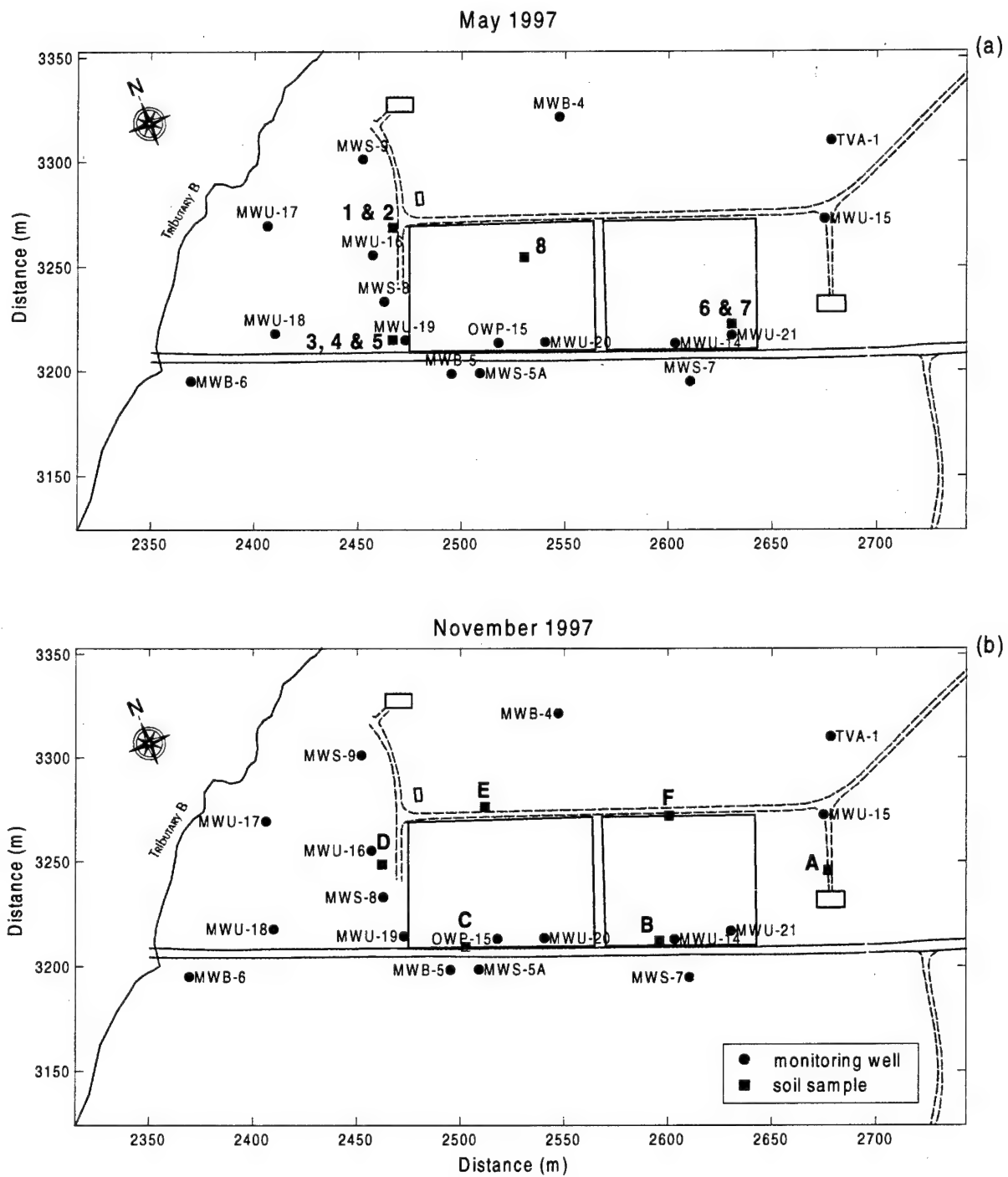


Figure 2-5 Soil Sampling Map for (a) May 1997 and (b) November 1997



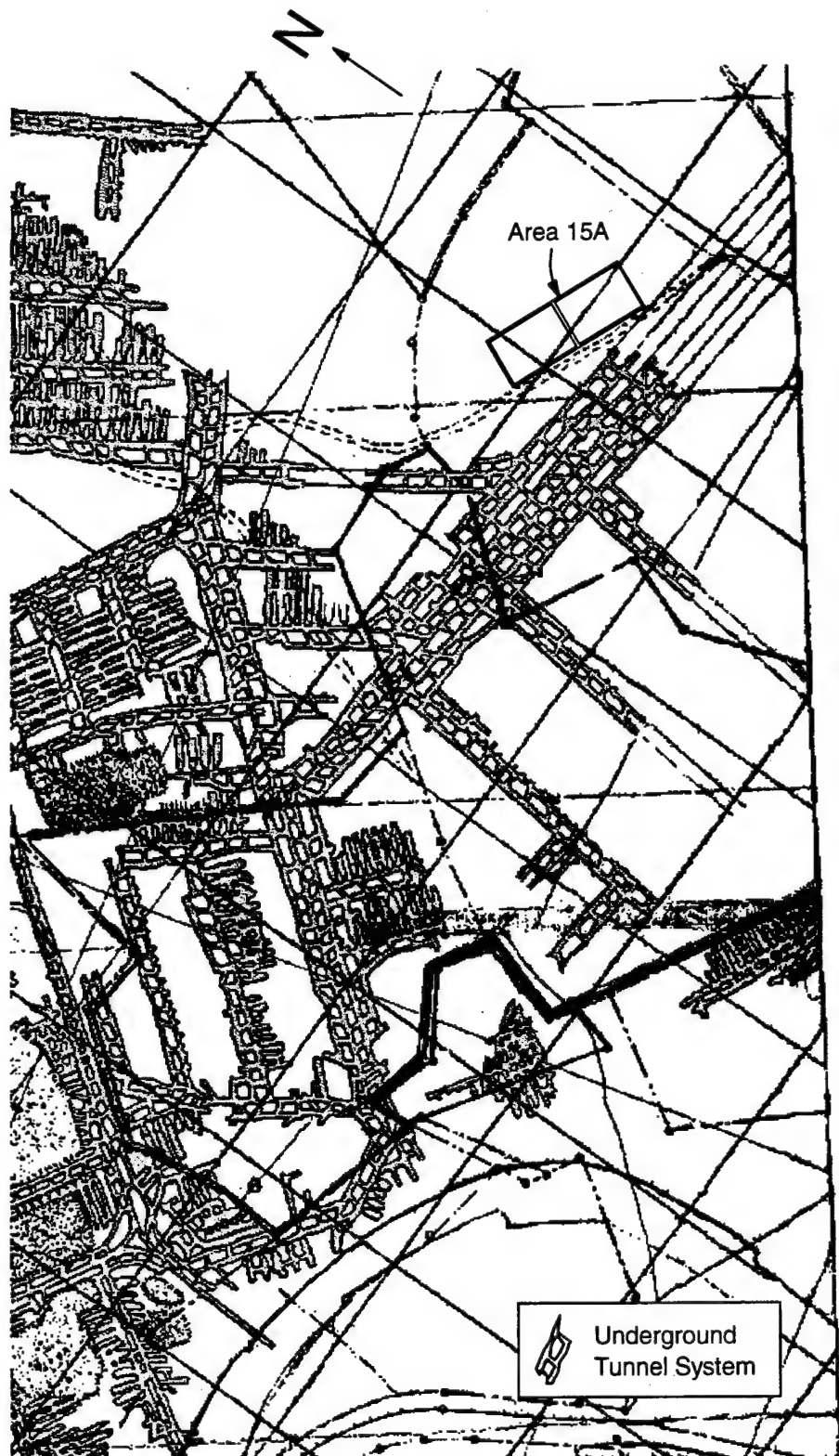


Figure 2-6 Approximate Aerial Extent of the Upper Freeport Coal Underground Tunnel System for the Abandoned Watson Mine in the Vicinity of Area 15A



Table 2-1

## Classification, Grain-Size Fractions, Organic Carbon, and pH Data for Soils

Sample ID	Sample Interval (m)	Grain Size			Organic Carbon (%)	pH	Classification
		Sand (%)	Silt (%)	Clay (%)			
1	0.2 to 0.6	18.2	57.7	24.1	0.62	5.72	silt loam
2	0.6 to 1.2	33.6	39.4	27.0	0.23	5.01	loam
3	0.2 to 0.6	48.3	34.0	17.7	0.34	4.94	loam
4	0.6 to 1.2	43.9	34.1	22.0	0.22	4.96	loam
5	1.2 to 1.8	56.6	24.5	18.9	0.18	4.78	sandy loam
6	0.0 to 0.9	14.1	56.2	29.7	0.74	4.94	silty clay loam
7	0.9 to 1.8	8.2	61.0	30.8	0.62	5.38	silty clay loam
8	1.8 to 2.4	11.8	59.1	29.1	3.85	5.27	silty clay loam
Averages:		29.3	45.8	24.9	0.42*	5.13	

\*Average excluding sample 8

## 2.4 Hydrostratigraphy

Aquifers within the Glenshaw include, in order of increasing depth, the Saltsburg Sandstone, Buffalo Sandstone, and Mahoning Sandstone [ESC, 1985]. Although considered an aquifer in the site region, the water-bearing capacity of the Buffalo is locally doubtful.

It is expected that the potentiometric surface within the soil horizon at the site generally follows topographic trends. Only one soil well, OWP-15, has been installed at Area 15A. Groundwater level measurements at site wells indicate that soil groundwater levels (Figure 2-7) follow temporal trends that are very similar to shallow bedrock (MWS wells) at the site. According to ESC [1985], high and low chroma mottling (alternating oxidizing and reducing conditions) of the soil observed during test pit investigations suggests the occurrence of a fluctuating seasonal perched water table. The fluctuation of groundwater levels is supported by water level data from OWP-15 which indicate groundwater levels ranging from 0.70 m to >2.43 m below ground surface at the site. During dry periods (e.g., 12/98), groundwater levels may reside below the top of bedrock beneath all, or parts, of the disposal site. It is possible that

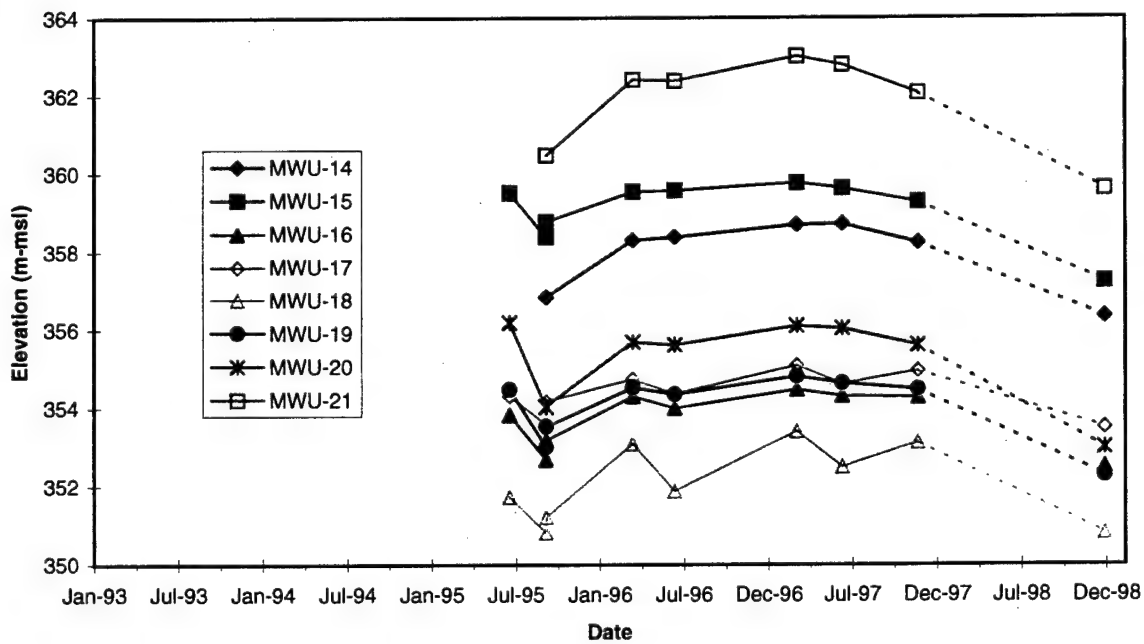
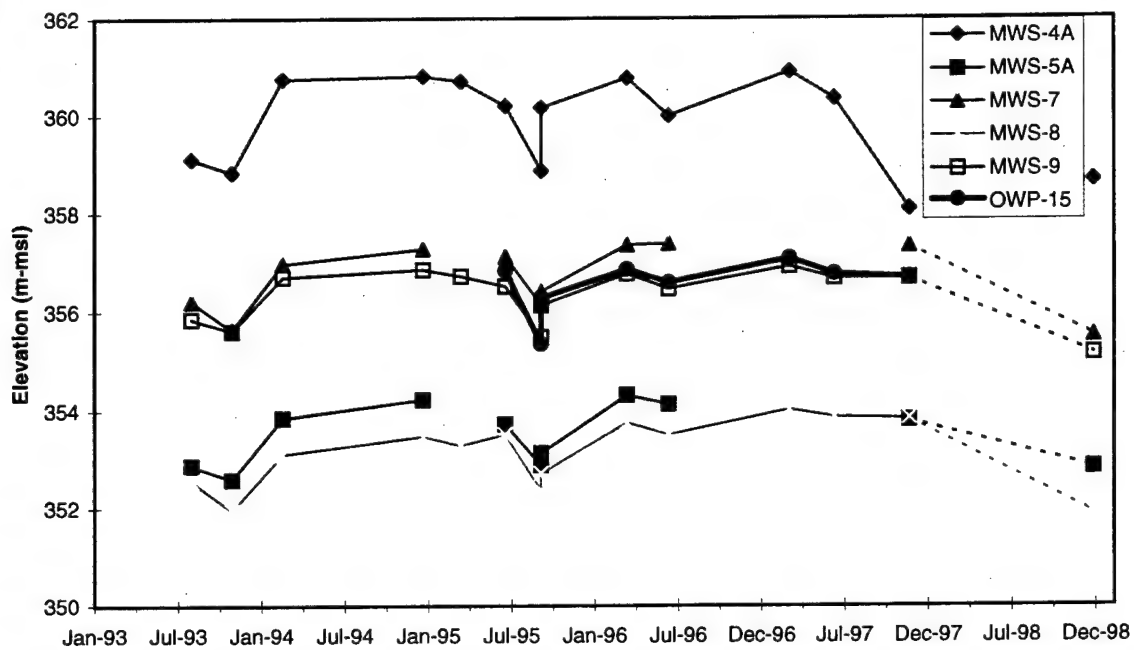


Figure 2-7 Temporal Plots of Groundwater Levels at Wells Developed in the Saltsburg Sandstone

perched groundwater conditions can occur in soil horizons underlain by relatively permeable bedrock fractures, or in zones possessing high K soil and voids from drum burial. However, there have been no quantitative field measurements to assess this situation.

Of interest in Figure 2-7 is the strong correlation in groundwater level measurements between well OWP-15 and MWS-9. Well MWS-9, a shallow bedrock well over 35 m north of the disposal area (Figure 2-5b), has exhibited anomalous groundwater levels since its installation. It has been described as occasionally artesian by some field investigators. Based upon groundwater level observations shown in Figure 2-7, it is likely that well MWS-9 intersects a transmissive vertical or horizontal fracture interval that is well-interconnected with the disposal facility.

Groundwater levels of shallow bedrock wells MWU-14 through MWU-21 are shown in Figure 2-8. This plot indicates nothing remarkable, and the general trend in hydraulic gradients is from east to west across the site. Based upon wells MWU-15 and MWU-16, the average horizontal gradient in the upper bedrock ranges from about 2.2 to 2.6 percent across the disposal site. Continuous precipitation and groundwater level measurements from selected wells at the site are shown in Figure 2-8. Based on the period of measurement (12/97 through 7/98), it can be inferred from Figure 2-8 that there is little variability between groundwater levels of soil well OWP-15 and shallow bedrock wells (MWU-15, MWU-19, and MWU-20) in response to precipitation events. Hydraulic communication between the soil overburden and underlying bedrock is indicated by these data.

Figure 2-9 shows groundwater levels collected at wells MWB-4, MWB-5, and MWB-6 (Buffalo Sandstone wells) since 1993. With little exception, potentiometric levels in these site wells exhibit little temporal variability. Figures 2-10 and 2-11 show the potentiometric surface of the upper Saltsburg Sandstone and the Buffalo Sandstone for periods of high (3/97) and low (12/98) groundwater conditions. The gradient of the potentiometric surface in the Saltsburg is approximately 2 to 3 percent to the W-SW, whereas that of the Buffalo ranges from 16 to 19 percent W-SW. A roughly east-to-west direction of groundwater movement across the disposal site is indicated by both potentiometric maps. Based on the prevailing horizontal hydraulic gradients in these aquifers and on geologic considerations, it appears that groundwater

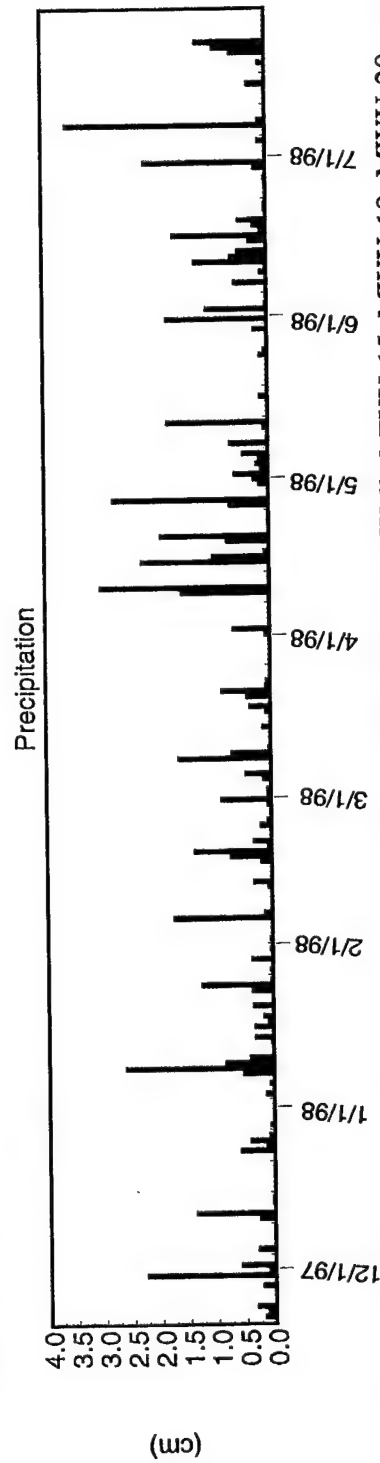
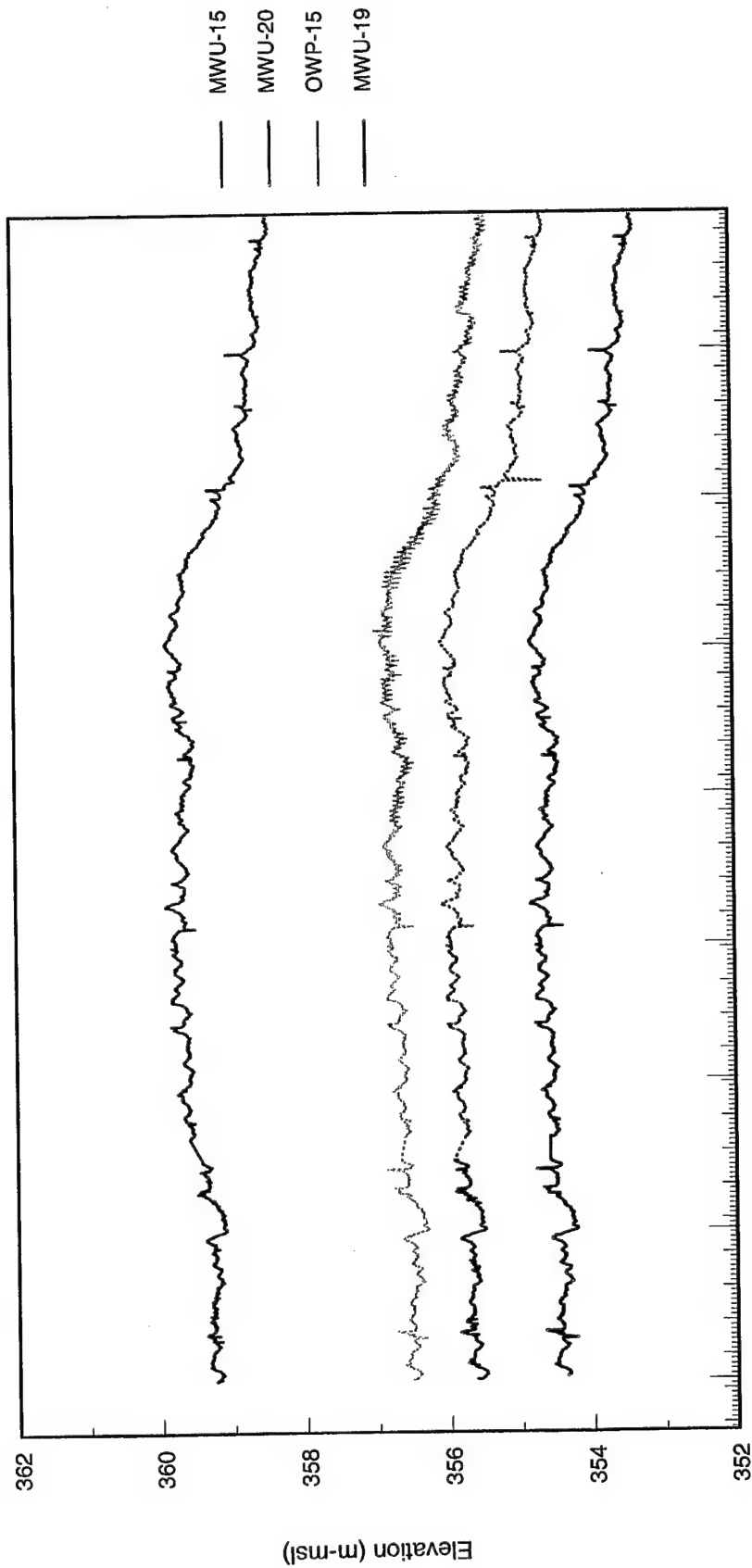


Figure 2-8 Continuous Groundwater Levels Versus Precipitation at Wells MWU-15, MWU-19, MWU-20, and OWP-15 for the Period December 1997 through July 1998 (Dashed Lines Indicate Artificially Generated Data)

originating on site, or passing beneath the site from areas to the west, ultimately discharges at the aquifer outcrop areas west of the site.

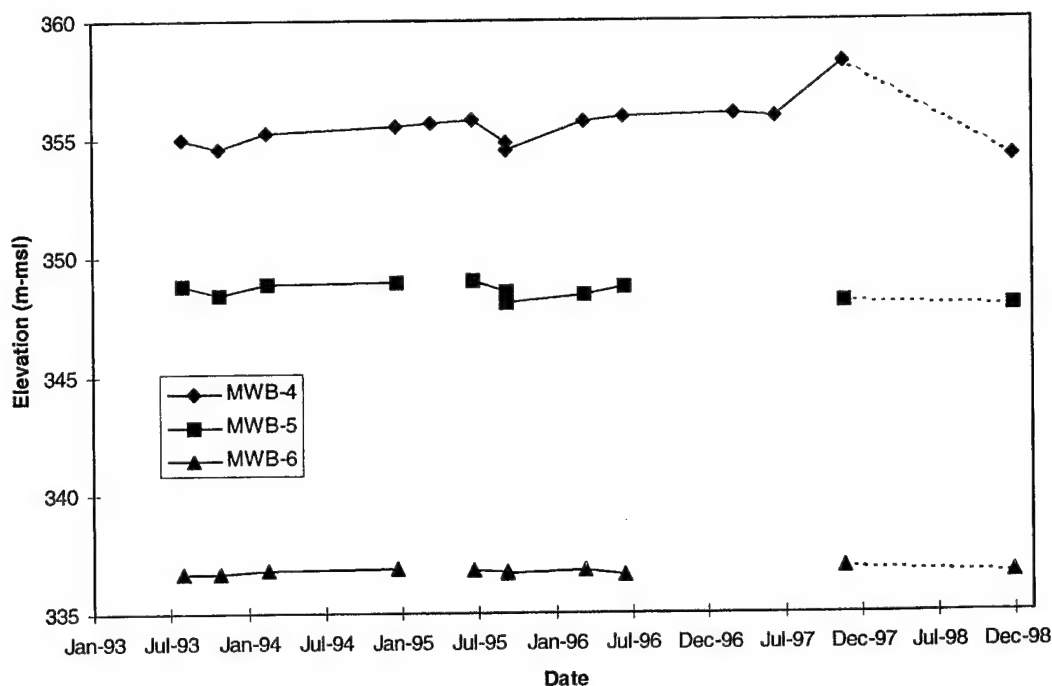


Figure 2-9 Temporal Plots of Groundwater Levels at Wells Developed in the Buffalo Sandstone

The vertical component of the hydraulic gradient at the site is downward. This is evident in comparisons of the potentiometric surfaces for the Saltsburg and Buffalo aquifers (Figures 2-10 and 2-11) and in comparisons of the water levels in staged monitoring wells such as MWS-5A and MWB-5 (Figures 2-7 and 2-9). The magnitude of the hydraulic gradient between the two aquifers averages approximately 30%. The relatively vertical hydraulic gradient at the site may be produced by poor vertical hydraulic interconnectivity between the Saltsburg and Buffalo Sandstones. This suggests that the shale zone separating the Saltsburg and Buffalo Sandstones may be expected to exhibit low vertical hydraulic conductivity. The presence of the abandoned mine in the Upper Freeport Coal seam, some 55 m below the site, may also contribute to the downward hydraulic gradient.

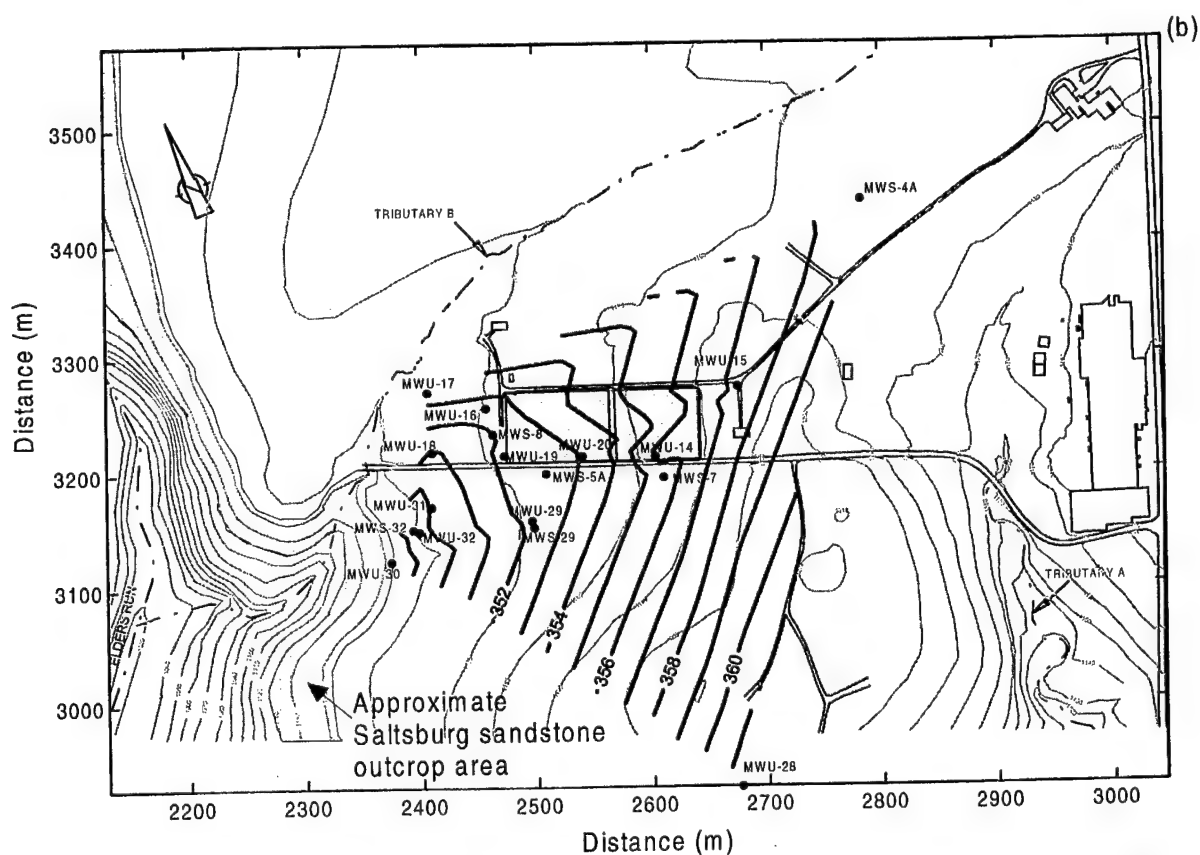
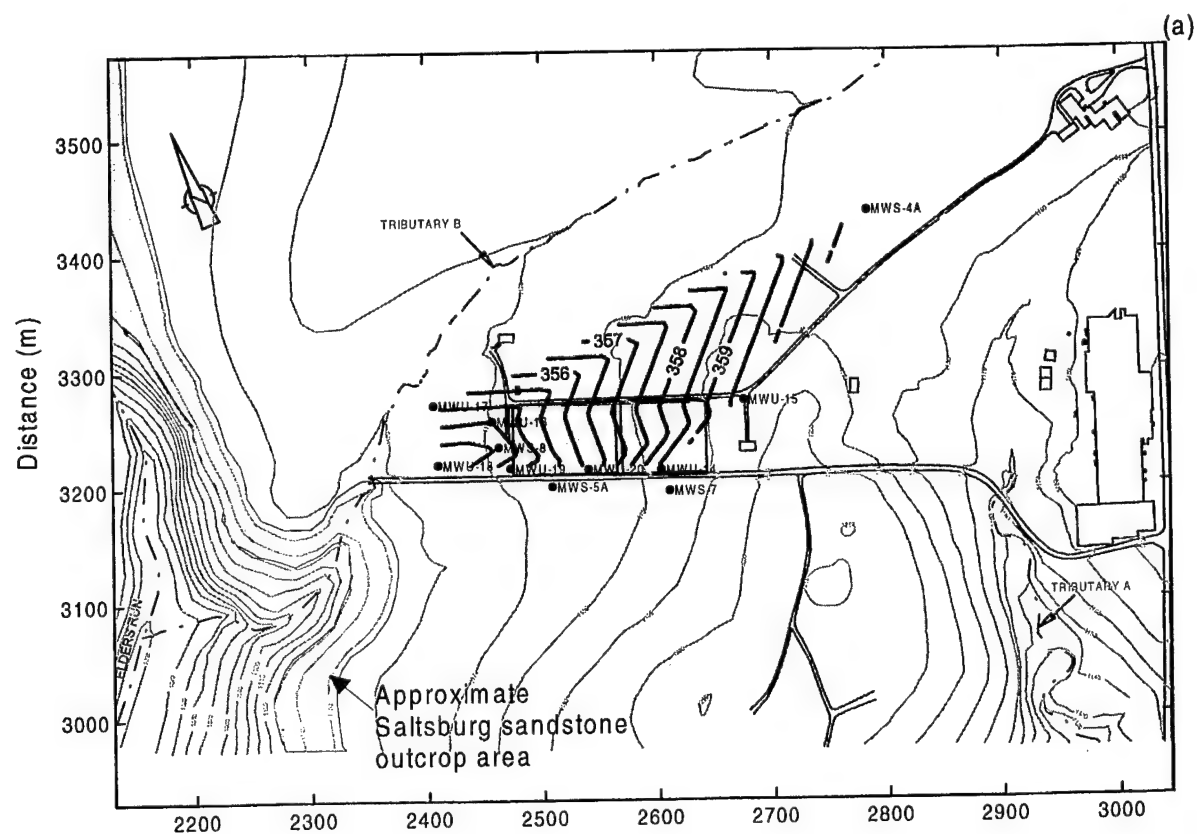


Figure 2-10 Potentiometric Maps for the Saltsburg Sandstone During (a) March 1997 - Wet Period, and (b) December 1998 - Dry Period (Contours in m-msl)

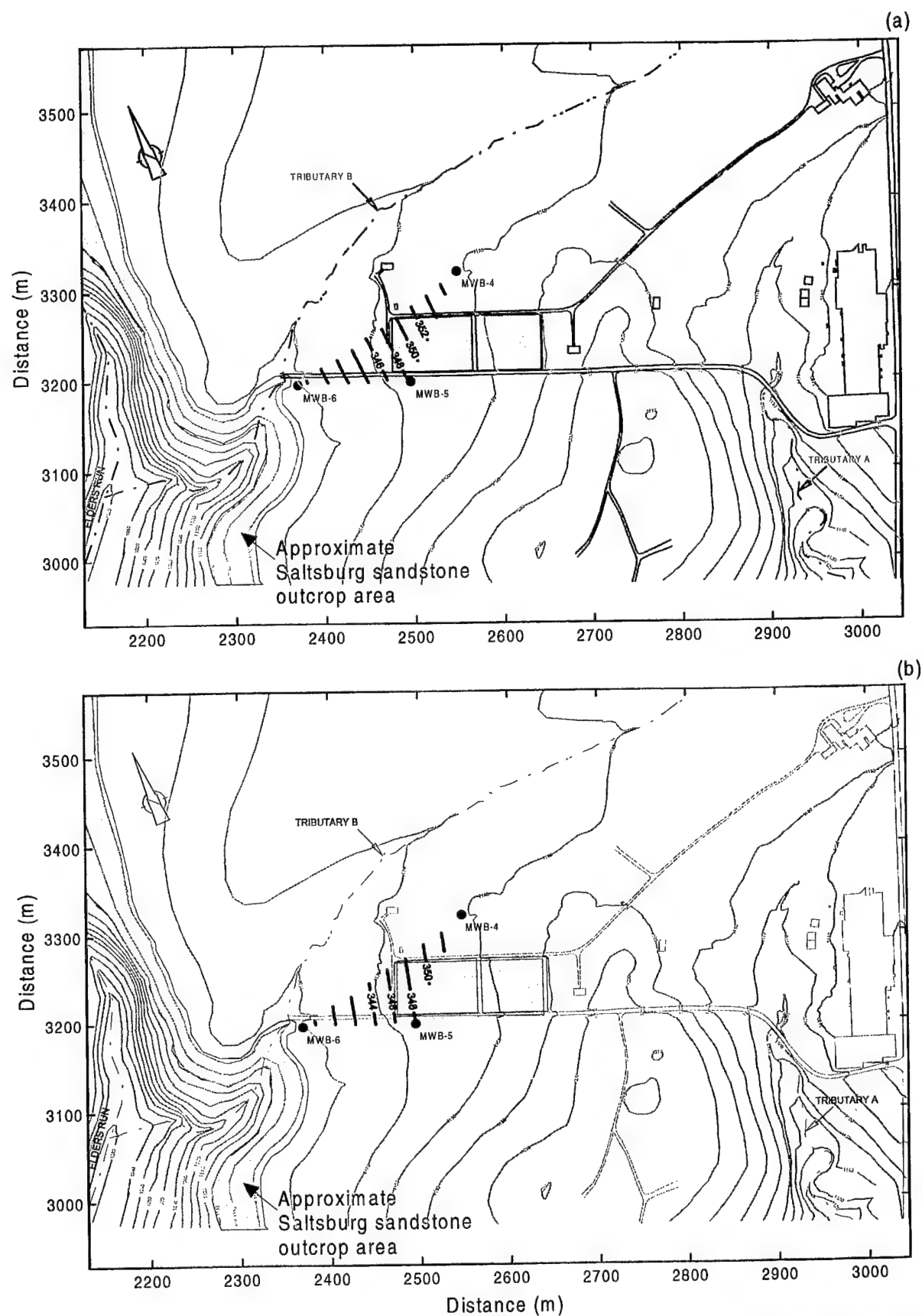


Figure 2-11 Potentiometric Maps for the Buffalo Sandstone During (a) March 1997 - Wet Period, and (b) December 1998 - Dry Period (Contours in m-msl)

## 2.5 Hydraulic Properties

### 2.5.1 Soil Properties

It is expected that the soil/bedrock interface is gradational at many locations. Previous site investigation reports do not indicate measurements of soil hydraulic properties. Soil samples were obtained as part of this study to gauge hydraulic properties necessary to support numerical modeling. At the request of the site owner, and for health and safety reasons, soil samples were collected outside of the designated disposal area. Hence, these results are not necessarily representative of soils used to backfill the disposal area.

In November 1997, six soil samples were collected from the perimeter of the Area 15A disposal site (Figure 2-5b) and analyzed for specific hydraulic properties by D.B. Stephens & Associates [1997]. As shown in Table 2-2, saturated hydraulic conductivity of the soil samples from falling head permeameter tests range from  $7 \times 10^{-9}$  to  $5 \times 10^{-6}$  cm/s, and average about  $10^{-6}$  cm/s. The average calculated porosity of the samples is 34.4 percent.

**Table 2-2**  
**Physical and Hydraulic Properties of Soils**

Sample ID	Ground Elevation (m-msl)	Sample Interval (m)	Initial Moisture Content		Dry Bulk Density (g/cm <sup>3</sup> )	Wet Bulk Density (g/cm <sup>3</sup> )	Calculated Porosity (%)	K <sub>sat</sub> (cm/s)
			Gravimetric (%)	Volumetric (%)				
A	364.85	2.3 to 3.4	19.4	33.2	1.71	2.04	35.5	2.7E-08
B	359.85	2.1 to 3.4	18.1	32.2	1.78	2.10	32.9	7.0E-09
C	357.57	2.3 to 3.5	16.6	29.3	1.77	2.06	33.3	7.8E-08
D	357.02	1.8 to 3	14.6	27.2	1.86	2.13	29.9	8.6E-09
E	357.66	1.8 to 3	15.4	25.8	1.67	1.93	36.8	2.9E-07
F	360.43	1.8 to 3	8.4	13.7	1.64	1.78	38.1	5.2E-06
Averages:			15.4	26.9	1.74	2.01	34.4	9.4E-07

### 2.5.2 Bedrock Properties

Bedrock hydraulic properties (i.e., mean K, matrix K, and fracture K), fracture orientation, density, and dimensions were estimated or inferred from borehole flowmeter testing, geologic core logs, and reports regarding regional geologic structure. Site-specific fracture data are limited to horizontal fractures since all test wells and core holes completed to date have been vertically oriented.



To our knowledge, the first on-site pumping test at Area 15A was conducted in June 1985 by CRA [1995]. Subsequent to a step test, a constant rate pumping test was conducted for a period of seven hours. This was followed by a recovery period of 43 hours. Well MWS-8 was pumped at an initial flow rate of 15.1 L/min for 30 minutes. Following a brief (6-minute) shut down due to pump malfunction, pumping resumed at an average flow rate of 17 L/min. Fifteen observation wells at the site were monitored before, during, and after (recovery) pumping.

Drawdown during the pumping test was relatively symmetrical, indicating approximately radial groundwater flow to the pumping well. All upper zone observation wells monitored during the test responded to pumping at MWS-8 except for wells MWU-20, MWU-15, and MWS-4A. The latter wells are the most remote of the upper zone wells monitored and are located at distances of 80, 215, and 380 m, respectively, from MWS-8. Table 2-3 shows transmissivity and hydraulic conductivity values estimated for the upper zone based on the Theis [1935] method of analysis by CRA [1995] and the Cooper-Jacob straight-line analysis [Cooper and Jacob, 1946] by the authors.

As shown in Table 2-3, the geometric mean K estimates ( $1.7 \times 10^{-3}$  and  $8.4 \times 10^{-3}$  cm/s) differ by a factor of about five. The results of single-well pumping tests conducted during borehole flowmeter measurements at the site (Appendix E; Table 5-2) indicate mean and geometric mean K values of  $1.5 \times 10^{-5}$  and  $8 \times 10^{-6}$  cm/s, respectively, for shallow bedrock.

A total of 165 discrete horizontal hydraulic conductivity ( $K_h$ ) estimates were obtained during eight flowmeter tests (Appendix E) in shallow bedrock at Area 15A. Except for well TVA-1, flowmeter testing was generally limited to the lower meter or so of soil overburden and the upper 3 to 6 m of sandstone and shale associated with the Saltsburg Formation. In general, the flowmeter profiles indicate that a few thin flow zones dominate shallow groundwater movement. This is typical of fractured sedimentary rock aquifers in which groundwater moves preferentially through a few hydraulically active fractures with only minor flow through the porous rock matrix. Approximately 55% of these data were censored measurements; i.e., data which are less than the measurement threshold.  $K_h$  estimates for the 74 uncensored data ranged from  $1.4 \times 10^{-5}$  to 0.2 cm/s. Visual inspection reveals no major differences between the overall magnitude of K data for the sandstones and shales.

**Table 2-3**  
**Summary of Transmissivity and Hydraulic Conductivity Estimates Associated with Upper**  
**Zone Wells from Constant-Rate Pumping Test**

Well	Well Type	CJSL Analyses <sup>1</sup>		Theis Analyses <sup>2</sup>	
		T (m <sup>2</sup> /d)	K (cm/s)	T (m <sup>2</sup> /d)	K (cm/s)
MWS-8	Pumping	1.9	4.6E-04		
MWS-5A	Observation	2.7	7.0E-04	5.0	5.8E-03
MWS-9	Observation	17.7	4.4E-03		
MWU-16	Observation	13.2	3.3E-03	4.1	4.7E-03
MWU-17	Observation	5.8	1.1E-03	16.6	1.9E-02
MWU-18	Observation	2.4	4.5E-04	5.7	6.6E-03
MWU-19	Observation	5.8	1.1E-03	9.9	1.2E-02
MWU-20	Observation	9.1	2.0E-03		
OWP-15	Observation	28.4	2.2E-02		
<b>Mean:</b>		<b>9.7</b>	<b>3.9E-03</b>	<b>8.3</b>	<b>9.6E-03</b>
<b>Geometric Mean:</b>		<b>6.6</b>	<b>1.7-03</b>	<b>7.2</b>	<b>8.4E-03</b>

<sup>1</sup>Cooper-Jacob Straight-Line Analyses

<sup>2</sup>Theis Method of Analyses

The measured hydraulic conductivities for the sandstone and shale bedrock can largely be attributed to fractures. The hydraulic conductivity of the unfractured matrix of sandstone and shale is generally well below the measurement threshold of the flowmeter; i.e., the matrix K values for shales rarely exceed 10<sup>-7</sup> cm/s while values less than 10<sup>-5</sup> cm/s are typical of sandstones [Freeze and Cherry, 1979].

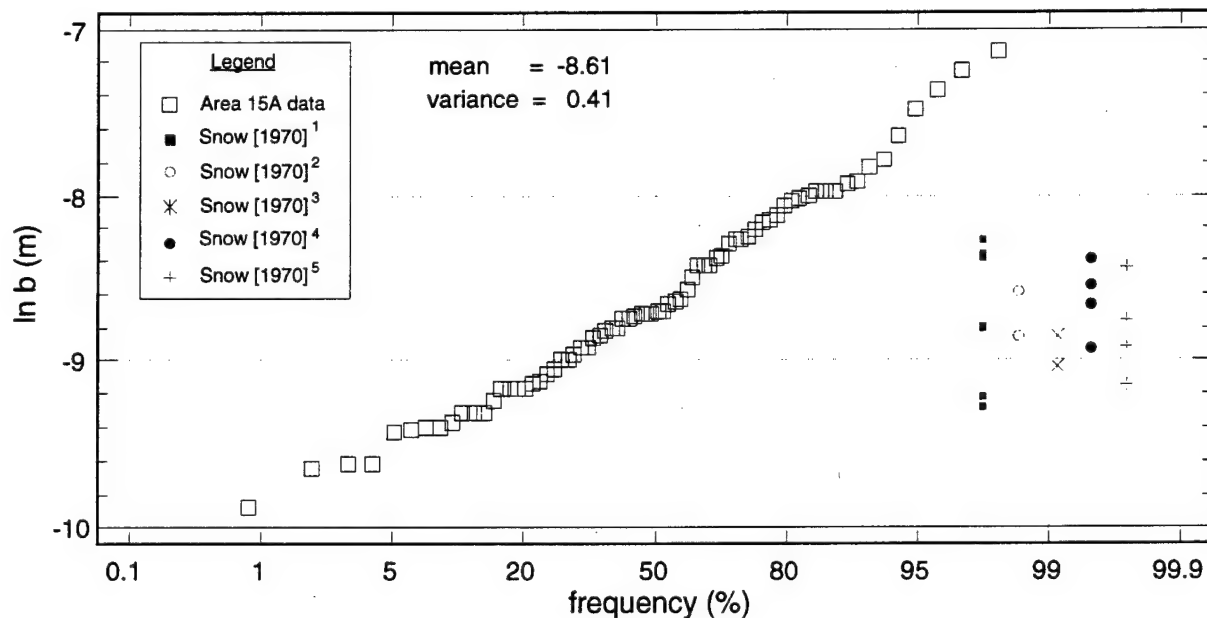
Fracture aperture estimates were computed from the uncensored K<sub>f</sub> measurements given in Appendix E using the relationship [Freeze and Cherry, 1979],

$$K = \rho g N b^3 / 12 \mu \quad (2.1)$$

where  $\rho$  is fluid density,  $g$  is gravitational constant,  $N$  is the number of fractures per unit length of rock face,  $b$  is fracture aperture, and  $\mu$  is absolute fluid viscosity. Solving for  $b$  we have,

$$b = (12 K \mu / \rho g N)^{1/3} \quad (2.2)$$

Supplement F-1 provides the computed fracture aperture data along with the  $K$  data and physical constants used in calculations. A normal probability graph of these data is presented in Figure 2-12. The aperture data exhibit a log-normal frequency distribution having a mean  $\ln b$  of -8.61 (m) and variance of 0.41. The magnitude of estimated fracture apertures for bedrock beneath Area 15A are similar to those reported by Snow [1968] for sandstones and shales investigated at five other sites. The log-normality of the data is also consistent with results reported by other investigators; e.g., Nelson [1985] and Snow [1969]. Since all of the test wells were vertically oriented, we can infer that the measured  $K$  values are primarily associated with horizontal fractures intersected by the wells. However, vertical fracture sets undoubtedly exist at the site as a result of past tectonic activity. The anticlinal structure of the bedrock underlying Area 15A suggests the likelihood of vertical tension fracture sets. However, this cannot be confirmed with data derived from vertical wells.



<sup>1</sup> Pacheco Tunnel, CA, metamorphic sandstone; <sup>2</sup> Paskenta Damsite, CA, sandstone and shale; <sup>3</sup> Newville Reservoir, CA, conglomerate and sandstone; <sup>4</sup> Monticello Damsite, CA, sandstone and shale; <sup>5</sup> Newville Damsite, CA, sandstone and shale

Figure 2-12 Fracture Aperture Frequency Distribution

### 3. Simulation Methods

#### 3.1 Conceptual Model

Metal drums containing CNS tear gas are believed to have been deposited at or near the soil-bedrock interface over the base of the disposal area excavation. The tear gas liquids released from corroded containers would initially tend to move primarily downward through fractures in the underlying bedrock in response to both the natural downward hydraulic gradient and the density gradient produced by its higher density relative to groundwater. Some lateral movement of these DNAPLs within the basal overburden soils in and below the drum burial zone is also expected, particularly in areas where hydraulically active fractures are absent in the underlying bedrock. In order for DNAPLs to enter a bedrock fracture, the capillary pressure ( $P_c$ ) at the base of the DNAPL pool must exceed the entry pressure ( $P_e$ ) of the fracture [Kueper and McWhorter, 1991]. Conservative estimates of the minimum DNAPL pool height required to overcome  $P_e$  for the range of measured fracture apertures at the site are given in Table 3-1 with calculations presented in Supplement F-2. Results indicate that DNAPL pool heights of 25 cm or less will induce downward DNAPL movement in fractures having apertures covering more than 95% of the estimated size range for bedrock fractures at the site. Once the entry pressure of a vertical fracture has been exceeded, downward movement of DNAPL can be sustained by the increasing height of DNAPL accumulating in the fracture, even after the overlying pool drops below the critical entry height. Where vertical fractures are present directly below release points, downward migration can be rapid. For example, the time required for a 55-gallon drum to fully drain into a single fracture is roughly estimated to range from a few hours to a few months for the fracture aperture sizes encountered at the site (see Supplement F-2 for calculations).

**Table 3-1**  
**Minimum DNAPL Pool Heights Required for Entry into Fractures**

$b$ (m)	$\ln b$	Minimum Pool Height (cm)	Relative Aperture Size
5.1E-05	-9.88	27.9	minimum
5.7E-05	-9.77	25.0	≈5 percentile
1.8E-04	-8.61	7.9	mean
9.4E-04	-6.96	1.5	maximum

Transport of DNAPL within the bedrock aquifer will be controlled by the aperture size, orientation, and connectivity of fractures and by prevailing hydraulic gradients. Shallow fluid movement in the bedrock will occur primarily through a relatively sparse network of hydraulically active fractures as indicated by flowmeter testing. Only limited flow is expected in the sandstone-shale rock matrix due its low hydraulic conductivity. On entering fractures, the relatively soluble DNAPL compounds such as CF may dissolve and subsequently diffuse into and out of the rock matrix as they are transported with ambient groundwater. Migrating DNAPL may also become disconnected or trapped by capillary forces in narrow fractures forming zones of residual product. These regions of residual product and rock matrix contamination result in persistent sources of dissolved-phase contamination within the bedrock and are important factors in the fate and transport of the tear gas contaminants.

Limited upward diffusion of volatile contaminants may also occur through the soil vadose zone above the drum burial zone. Volatile losses are most likely for CF and, to a lesser extent, CP and CN. Overall vapor losses are expected to be small since the vapor densities of these compounds (which range from approximately 4.9 to 6.8 g/L at 20°C ) greatly exceed that of ambient air (approximately 1.2 g/L) indicating a tendency for vapors to sink rather than rise in the vadose zone. Vapor losses may be enhanced by seasonal water table fluctuations which may force vapors to the surface as rising water displaces soil vapors.

All of the CNS tear gas constituents are subject to natural attenuation by microbiological and chemical transformation processes [Castro, 1986, 1998]. CP and CN are more susceptible to degradation than CF because of their high reactivity. The batch sorption studies described in Section 4 of the main report showed that these compounds readily sorb to soils of the site. Sorption on the bedrock matrix is also expected given the highly carbonaceous nature of the sandstones and shales underlying the site. CP and CN may be degraded by several reductive and oxidative reactions with iron and iron oxides associated with the corroded metal containers [Castro, 1986]. They are also highly susceptible to hydrolytic reactions with hydroxyl groups present in clay soils as well as hydroxide ions in groundwater. Evidence of these pathways is generally suggested by low soil groundwater pH and soil discoloration [Castro, 1986] and, specifically, by analytical data for groundwater samples from well MWS-5A which showed the presence of benzoyl chloride and benzaldehyde. The latter two are expected by-products of CN

hydrolysis [ESC, 1992a]. Castro [1986] describes biodegradative pathways for CP, which is known to be readily degraded by several common soil bacteria, and for CN which has been less studied but should be amenable to reductive dehalogenation on the basis of its chemical characteristics. Rapid aerobic biodegradation of CP and CN was indicated in the laboratory mineralization studies performed on soil samples from Area 15A using  $^{14}\text{C}$ -labelled compounds with reported half lives of 0.21 and 6.3 days (see Section 4 of main report).

CF is the least reactive of three tear gas compounds and consequently the most environmentally persistent [Castro, 1986]. This is consistent with historical monitoring data which indicates relatively frequent and wide-spread occurrence of CF in groundwater and surface seeps downgradient of Area 15A but very limited evidence of CP and CN [ESC, 1992a]. CF is subject to environmental attenuation at the site by many of the same processes affecting CP and CN, but to a lesser degree. The sorption studies reported in Section 4 of the main report show moderate sorption of CF on soil samples from the site, and, as with CP and CN, sorption on the underlying bedrock can be expected. Castro [1986] reports that CF is less susceptible to hydrolysis and iron reduction reactions than the other two compounds. A half life of 277 days was estimated for CF from the aerobic mineralization studies performed using site soils (see Section 4 of main report), indicating the likelihood of field microbial degradation of this compound. Potential anaerobic microbiological degradative pathways for CF have also been proposed by [Castro, 1986].

For purposes of evaluating the long-term natural restoration of the bedrock aquifer at the site, the focus of the contaminant transport analysis will be limited to CF. The persistence and mobility of CF in the subsurface environment relative to CP and CN clearly indicate that CF is the principal contaminant of concern.

### ***3.2 Model Selection and Limitations***

The tear gas contaminant transport conceptual model described above for Area 15A can be generally characterized as multiphase (dissolved and NAPL) transport through discretely fractured porous media. The relatively small problem scale associated with Area 15A (i.e., transport distances from the western edge of the disposal area to the seep discharge area are less than 200 meters) requires explicit treatment of the dual porosity bedrock system in the transport

analysis. If the problem scale was larger, say on the order of several hundred meters to kilometers, the bedrock beneath the site might be justifiably approximated as strictly porous media. Numerical models capable of simulating multiphase contaminant transport in dual-porosity systems are the subject of current research and development [Slough et al., 1999; Keller, 1996], but are unavailable outside of the research community at this time. Single-phase models for such systems are available that can be used to quantitatively evaluate the long-term fate and transport of tear gas contaminants from the facility under the two proposed site restoration scenarios. The presence of DNAPL contaminants can be treated implicitly in the single-phase model using internal boundary conditions as discussed in Section 3.9.

### ***3.3 Code Description***

The FRACTRAN code [Sudicky and MacLaren, 1998] was selected for simulation of the fate and transport of tear gas contaminants released from Area 15A. The code simulates advection, hydrodynamic dispersion, and molecular diffusion in both fractures and the porous matrix within a two-dimensional rectangular domain. Reactive solutes subject to linear equilibrium sorption and first-order decay are accommodated [Sudicky and MacLaren, 1998]. The model offers an efficient numerical approach for the solution of long-term flow and transport of aqueous-phase contaminants in discretely fractured porous media. A conventional Galerkin finite element scheme is used to solve the advection-dispersion equation in Laplace transform space with subsequent numerical inversion of nodal concentrations. The method avoids time-stepping associated with traditional numerical schemes and permits the use of a relatively coarse grid without compromising accuracy. Because the numerical scheme does not involve time steps, it is well-suited to the long time frames characteristic of contaminant transport in fractured porous media. A complete discussion of the FRACTRAN numerical algorithm can be found in Sudicky and MacLaren [1992], while code documentation is given in Sudicky and MacLaren [1998].

### ***3.4 Model Domain***

A 375-m long by 48-m thick, northeast-southwest trending vertical section through the disposal area was selected for evaluating the fate and transport of tear gas contaminants from

Area 15A (Figure 3-1). The trajectory of the cross section generally follows the southwesterly direction of groundwater flow across the site from a point just upgradient of the disposal area to the seep discharge area. The model consists of a soil overburden layer underlain by a layer representing the fractured sandstone and shale bedrock associated with the Glenshaw Formation. Across the eastern half of the domain, the soil zone is approximated as a 3-m thick layer corresponding to the mean soil thickness in the vicinity of the disposal area. The soil thickness increases to 6 m in the western portion of the model to account for the decrease in the elevation of the soil-rock interface to the west. This approximation is necessary because the code does not permit irregular domain geometry. On the basis of the borehole flowmeter testing, no hydrostratigraphic distinction is made between the sandstone and shale units in the model.

The finite element grids used in simulations vary with each fracture realization, but generally contain approximately 150 nodes in the horizontal dimension and 280 nodes in the vertical dimension for a total of about 42,000 nodes. Maximum allowable grid intervals of 12 m and 0.25 m were specified for the horizontal and vertical directions in the generating of numerical grids for each model.

### ***3.5 Soil and Bedrock Matrix Properties***

A summary of the soil and bedrock matrix properties incorporated in the model is given in Table 3-2. Laboratory measurements of hydraulic conductivity ( $K$ ) for re-compacted soil samples collected at the site ranged from  $7 \times 10^{-9}$  to  $5.2 \times 10^{-6}$  cm/s (see Table 2-2). A calibrated soil  $K_v$  of  $10^{-6}$  cm/s was found to provide reasonable head fits during initial simulations. No soil anisotropy was assumed since the soil has been disturbed over much of the area. Rock matrix hydraulic conductivity at the site has not been specifically measured. However, a literature survey of matrix properties for sandstones, shales, and other closely related sedimentary rocks is summarized in Table 3-3. Bedrock matrix hydraulic conductivity was adjusted within the limits of the literature estimates during initial model calibrations resulting in calibrated values of  $10^{-7}$  cm/s for both  $K_h$  and  $K_v$ .



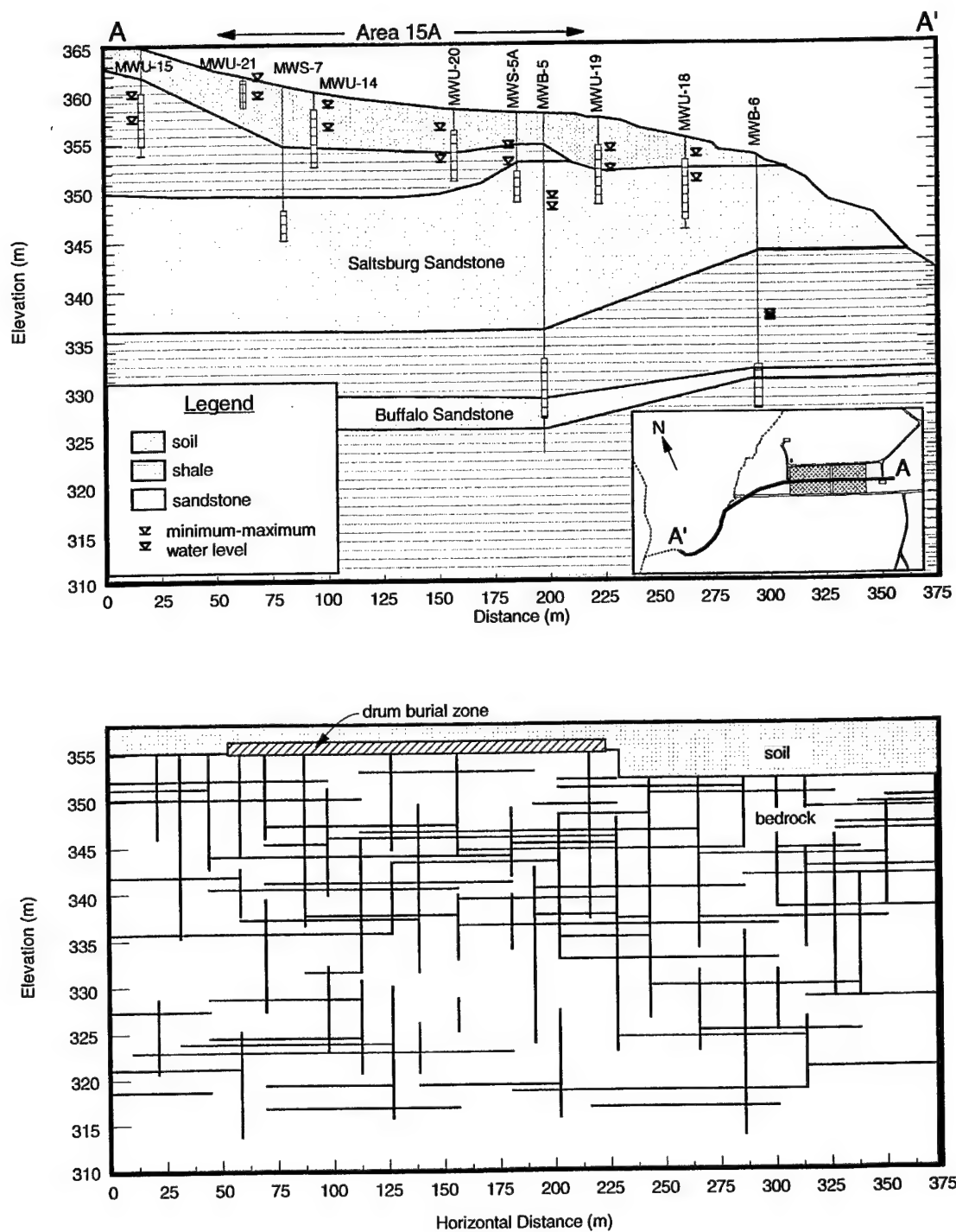


Figure 3-1 Generalized Hydrogeologic Profile Through Disposal Site Following Approximate Groundwater Streamline (upper box), Model Domain (lower box)

Table 3-2

## Soil and Bedrock Matrix Properties Applied to Model

Property	Soil	Rock Matrix
Horizontal hydraulic conductivity ( $K_h$ ), cm/s	$10^{-6}$	$10^{-7}$
Vertical hydraulic conductivity ( $K_v$ ), cm/s	$10^{-6}$	$10^{-7}$
Effective porosity	0.34	0.05
Dry bulk density, g/cm <sup>3</sup>	1.74	2.40
Longitudinal dispersivity, m	0.1	0.1
Transverse dispersivity, m	0.01	0.01
Effective diffusion coefficient, m <sup>2</sup> /yr	$9.5 \times 10^{-3}$	$2.9 \times 10^{-3}$
Distribution coefficient, mL/g	1.84	0.087
Retardation factor	10.4	5.2

Table 3-3

Literature Estimates of Matrix Properties of Sandstone, Shale,  
and Related Sedimentary Rocks

Rock Type	$K_h$ (cm/s)	$K_v$ (cm/s)	$K_r$ (cm/s)	Effective Porosity (%)	N	Reference
Sandstone	$3 \times 10^{-6}$ to $1 \times 10^{-4}$	$2 \times 10^{-6}$ to $2 \times 10^{-4}$	--	--	41	Nelson [1985]
"	$1.4 \times 10^{-7}$ to $7.7 \times 10^{-4}$	$4.5 \times 10^{-5}$ to $5.2 \times 10^{-4}$	--	--	6	De Wiest [1969]
"	$1 \times 10^{-5}$ to $5 \times 10^{-4}$	--	--	--	(?)	Carr [1969]
"	$5 \times 10^{-5}$	--	--	--	1	Francis [1981]
"	--	--	--	0.5 to 10	(?)	Domenico and Schwartz [1990]
Shale	--	--	$4 \times 10^{-9}$	--	1	De Wiest [1969]
"	--	--	$8 \times 10^{-11}$	--	1	De Wiest [1969]
"	--	--	--	0.5 to 5	(?)	Domenico and Schwartz [1990]
Siltstone/ Claystone	$1.1 \times 10^{-7}$	$1.5 \times 10^{-7}$	--	--	1	De Wiest [1969]
"	--	$1.4 \times 10^{-11}$	--	--	1	De Wiest [1969]
"	$10^{-8}$	--	--	--	1	Francis [1981]

Model values of soil porosity and bulk density presented in Table 3-1 are computed means for six soil samples collected from Area 15A (see Table 2-2). Bedrock matrix porosity is based on the literature data given in Table 3-2, while density is an average value from a literature survey of sandstones and shales as reported by Parker et al. [1997]. The model dispersivity parameters for the soil and rock matrix listed in Table 3-1 are consistent with values commonly reported for these media (e.g., Harrison et al., 1992; Gelhar et al., 1992). The effective diffusion coefficients ( $D_e$ ) for CF in soil and rock matrix were estimated from the relationship [Parker et al., 1997],

$$D_e = \tau D_d \quad (3.1)$$

using the free solution diffusion coefficient ( $D_d$ ) for CF of  $9.1 \times 10^{-6}$  cm<sup>2</sup>/s (0.0287 m<sup>2</sup>/yr) [Cohen and Mercer, 1993] and representative apparent tortuosities ( $\tau$ ) of 0.33 and 0.10 for clay soil and sandstone/shale, respectively [Parker et al., 1997].

The soil distribution coefficient ( $K_d$ ) for CF listed in Table 3-1 was measured using soil collected at Area 15A (refer to Section 4 of main report for discussion of sorption studies). The CF retardation factor ( $R_f$ ) for soil was estimated from the expression [Freeze and Cherry, 1979],

$$R_f = 1 + \rho K_d / \theta \quad (3.2)$$

where  $\rho$  is bulk density and  $\theta$  is porosity. The rock matrix distribution coefficient for CF was estimated from the relationship,

$$K_d = K_{oc} f_{oc} \quad (3.3)$$

where  $K_{oc}$  is the octanol-water partitioning coefficient and  $f_{oc}$  is the organic carbon fraction of the rock matrix [Lyman et al., 1982]. The reported  $\log K_{oc}$  of 1.64 mL/g for CF of Cohen and Mercer [1993] and a representative  $f_{oc}$  of 0.002 for sandstone and shale based on the literature data of Parker et al. [1997] were used to estimate the bedrock  $K_d$  and  $R_f$  for the model.

### 3.6 Fracture Characteristics

Horizontal and vertical fractures within the sandstone and shale bedrock beneath the site are assumed, for modeling purposes, to be discrete planar features intersecting at right angles. Each fracture possesses smooth parallel walls and uniform aperture. No bedrock exposures of sufficient size are known to exist in the site vicinity for direct observation of fracture orientation,

density, and spacing. Hence, these parameters were estimated or inferred from borehole flowmeter testing, geologic core logs, and reports regarding regional geologic structure. Site-specific fracture data are limited to horizontal fractures since all test wells and core holes are vertically oriented.

The flowmeter-derived fracture aperture estimates shown in Figure 2-12 and listed in Supplement F-1 were utilized in the modeling analysis. Data exhibit a log-normal frequency distribution having a mean  $\ln b$  of -8.61 (m) and variance of 0.41. These aperture statistics were used to randomly generate fracture apertures for each model. Given the vertical orientation of the flowmeter test wells, we can infer that these aperture data are primarily associated with horizontal fractures. However, in the absence of vertical fracture aperture data, the horizontal fracture statistics were also used to generate vertical fracture apertures for the model. The presence of vertical fractures has not been directly observed at the site, but can be inferred from the anticlinal structure of the underlying bedrock. The tectonic forces which created the anticline likely produced a network of more-or-less vertically oriented tension fractures. In the horizontal dimension, these fracture sets are likely oriented parallel and at angles to the axis of the anticline [Nelson, 1985].

FRACTRAN also requires the minimum and maximum fracture lengths and overall fracture density characteristics. Correlation of high flow zones between flowmeter test wells suggests that hydraulically active horizontal fractures might be continuous over distances in excess of 100 m (see Appendix E), thus providing an estimate for the upper limit of horizontal fracture length. However, no estimate of the minimum length of horizontal fractures is possible with existing site information. Nor are sufficient data available from which reliable estimates of vertical fracture lengths and fracture density (i.e., the number of fractures per unit area) can be made. Consequently, model fracture characteristics were treated as calibration parameters during early flow simulation trials to produce reasonable overall hydraulic head fits and net surface recharge estimates. Since other studies (e.g., Snow, 1968 and 1970; Nelson, 1985) have consistently shown that fracture density decreases with depth, higher overall fracture density was assumed for the upper portion of the bedrock corresponding to the Saltsburg unit than for the lower bedrock. The final estimates for these parameters used in subsequent simulations are given in Table 3-4.

**Table 3-4**  
**Fracture Length and Density Characteristics**

	Horizontal Fractures	Vertical Fractures
<i>Upper Bedrock (elevation 335 to 358 m)</i>		
Minimum length, m	15	3
Maximum length, m	100	15
Density (m <sup>-2</sup> )	0.009	0.010
<i>Lower Bedrock (elevation 310 to 335 m)</i>		
Minimum length, m	15	3
Maximum length, m	100	15
Density (m <sup>-2</sup> )	0.003	0.003

### **3.7 Chloroform Degradation Rate**

Laboratory studies designed to quantify the overall rates of natural degradation of the CNS tear gas compounds are presented in Section 4 of the main report. Both total degradation and mineralization tests were performed using soil samples collected from Area 15A. In general, the total degradation test, as its name implies, provides a rate estimate representing the combined effects of all chemical and biological processes acting to attenuate a particular compound. For this reason, rate estimates derived by this method are generally less useful for modeling because sorption and bio-decay are treated as separate terms in the governing transport equations. On the other hand, the mineralization study specifically measures the rate of aerobic biodegradation of a <sup>14</sup>C-labeled compound based on recovery of <sup>14</sup>CO<sub>2</sub> and can be directly applied to the model.

The total degradation and mineralization studies yielded first-order rate constant estimates for CF of 0.13 and 0.0025 day<sup>-1</sup>, corresponding to half lives of 5.3 and 277 days. The rate constant derived from the mineralization study is consistent with half-life estimates of 56 to 1800 days presented by Howard et al. [1991] for aerobic biodegradation of CF in groundwater. Given the uncertainty regarding the representativeness of the laboratory rate estimate to field conditions, a sensitivity analysis was performed for the CF degradation constant. First-order degradation rate constants of 0.0, 0.0025, and 0.00039 day<sup>-1</sup> (corresponding to half lives of 0, 277, and 1800 days) were applied to the model in an attempt to bracket predictions.

### ***3.8 Flow Boundary Conditions***

Hydraulic head boundary values were specified along the upper surface of the model which decrease linearly from elevation 360 m at the upper left corner of the domain to elevation 352.5 m on the upper right corner. Over the lower 20 m of left and right ends of the domain, hydraulic heads of 351.6 m and 344.4 m, respectively, were assigned. These head specifications produce a mean horizontal (westerly) hydraulic gradient of two percent consistent with average site conditions. They also create a mean downward vertical gradient of 30% through the soil and upper bedrock zone as observed at the site. A no-flow boundary condition was assumed on the lower model boundary to represent a lower limit for downward migration of contaminants. Although somewhat arbitrary, the lower boundary condition is consistent with the lack of evidence of significant contamination below the Saltsburg Sandstone. The imposed boundary conditions produce inflow along the upper boundary of the model representing net infiltration of precipitation. A relatively small lateral inflow typically occurs at the left (eastern) boundary, and outflow is produced on the right (western) boundary corresponding to groundwater discharge at the seep area. Steady-state flow conditions were assumed for all simulations.

### ***3.9 Transport Boundary Conditions***

Model boundary conditions representing the spatial and temporal release of CF were developed on the basis of the site conceptual model described in Section 3.1, historical information regarding tear gas disposal operations, and subsurface investigations at Area 15A. What is known concerning disposal operations at Area 15A can be summarized as follows: (1) 300 to 1700, 55-gallon drums of CNS tear gas were buried within the soil overburden at Area 15A in the late 1940s, (2) tear gas contaminants were first observed in groundwater and seeps downgradient of Area 15A during site investigations in 1985, and (3) test pit investigations within the disposal area in 1985 indicated that only about 10% of the original volume of CNS tear gas remained in Area 15A [ESC, 1985]. From these facts one can infer that, although CNS containers were all buried at about the same time, corrosion rates were not the same for all containers, and tear gas releases occurred progressively over time. In the absence of specific information concerning the temporal distribution of drum failures, we assume the corrosive failure of drums was a random process following a normal (or Gaussian) distribution. This

assumption has also been employed by others (e.g., Golder Associates, 1998) to represent buried container failure distributions. The mean and standard deviation of the drum-failure distribution were estimated from the historical information. Referring to Figure 3-2(a), we arbitrarily define the lower end point of the distribution as year 1948, the assumed year containers were buried. We also know that by 1985 approximately 90% of the containers had failed. This corresponds to 90% of the total area under the normal curve. From this we estimate a standard deviation of 8.65 years and mean of year 1974 for the failure distribution (see Supplement F-3 for calculation). The resulting distribution indicates that 100% of container failures occur between years 1948 and 2000.

The conceptual model of Area 15A developed in Section 3.1 suggests that vertical fractures present below contaminant release points will produce relatively rapid initial downward migration and redistribution of DNAPL in the bedrock aquifer system, perhaps within a period of a few months. Moreover, the redistributed DNAPL will create persistent sources of dissolved-phase contamination in the form of zones of residual product trapped in fractures as well as in the basal overburden soils within the drum burial zone. Simulation of the temporally and spatially-varying release of CF in the drum burial zone during the 52-year period between 1948 and 2000 was performed in five 10.4-year time increments as shown in Figure 3-2(b). Residual DNAPL contaminated regions in the drum burial zone and in the underlying bedrock were represented in the model by time-dependent specified concentration boundary conditions. The effective solubility of CF from the tear gas mixture (3.4 g/L) was assigned to the internal boundary nodes representing the approximate concentration acquired by groundwater migrating through DNAPL contaminated zones. This assumption is supported by laboratory experiments which suggest that groundwater passing through residual DNAPL zones acquires saturated dissolved concentrations when the residual zones are at least several centimeters in length and groundwater velocities are less than about 1 m/d [Pankow and Cherry, 1996]. By comparison, the estimated groundwater velocities through the soil drum burial zone are expected to be less than  $10^{-3}$  m/d (i.e.,  $v = K_v J / \theta = 10^{-6} * 0.3 / 0.34 = 8.8 \times 10^{-7}$  cm/s  $\approx 8 \times 10^{-4}$  m/d). All of the specified concentration nodes within the drum burial region of the model were pooled and randomly selected to form five groups. Each group represents spatially random releases occurring during one of the five contaminant release periods. The fraction of the total number of nodes in each group corresponds to the

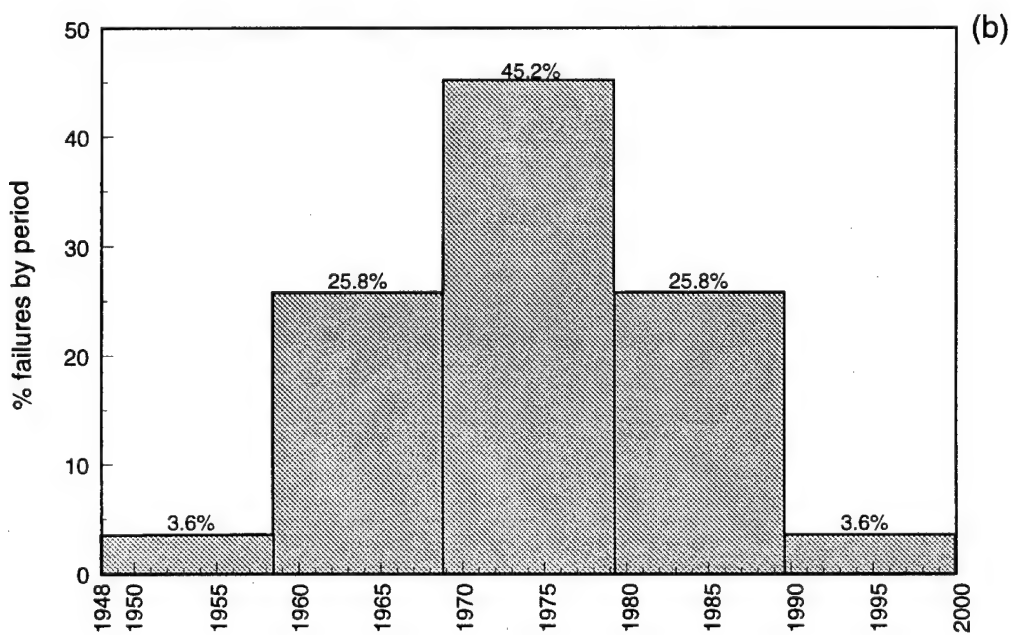
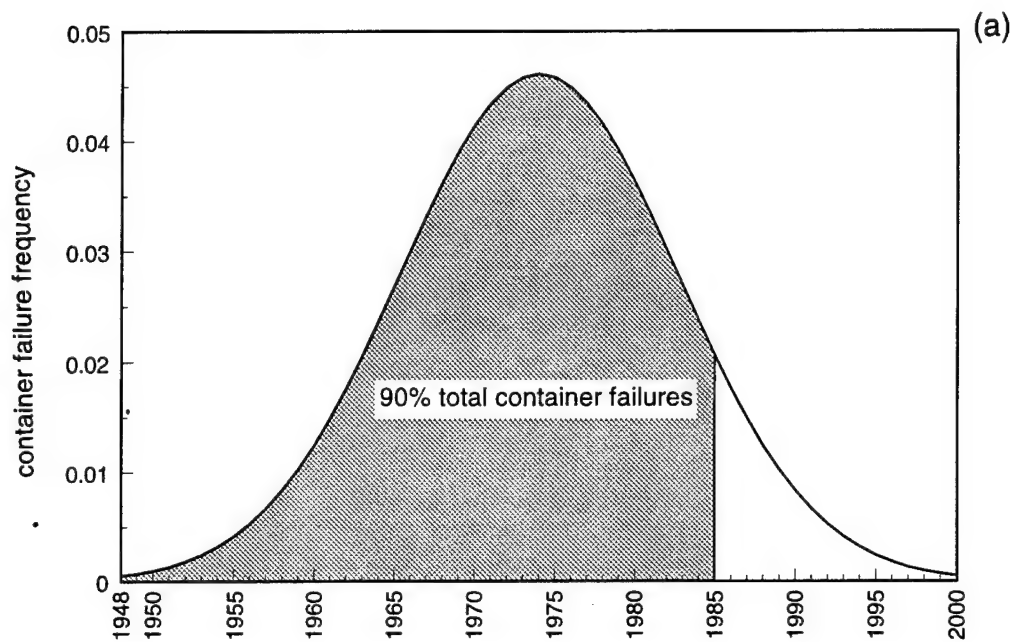


Figure 3-2 (a) Assumed Normal Distribution of Container Failures Over Time,  
(b) Approximation of Container Failure Distribution Applied in Simulations



release fractions shown in Figure 3-2(b). Specified concentration nodes representing zones of residual product in bedrock were handled in a similar manner. Fifty nodes were randomly selected from the pool of nodes within hydraulically active regions of the bedrock portion of the model below the disposal area on the basis of a preliminary simulation. The grouping and time-dependent activation of the bedrock residual nodes followed the same protocol as the drum burial zone nodes.

To illustrate the numerical implementation of these boundary conditions, one can consider the example sequence of specified concentration boundary specifications presented in Figure 3-3. This figure shows the spatial locations of random release points within the model domain for each of the five time steps. During the first time interval (1948 to 1958.4), three specified concentration nodes are activated within the drum burial zone, denoting drum failure sites along with three corresponding nodes in the underlying bedrock representing residual product sites. The residual product nodes appear directly below drum failure points in order to represent the rapid formation of zones of residual product below release sites, as previously discussed. Twenty new specified concentration nodes are added in the drum burial zone during the second time interval (1958.4 to 68.8) along with six bedrock residual nodes. Data for this period illustrate that residual product nodes are not associated with every drum burial zone release point. This is simply due to the limit on the total number of bedrock residual nodes and, in some instances, the absence of active fracture sites below a particular drum burial zone release point. For consistency, all specified concentration nodes were activated for the same fixed time period. A fixed activation period of 20.8 years (i.e., two 10.4-year time intervals) was established through trial and error during early model trials. For example, as shown in Figure 3-3, the specified concentration nodes in the first group are active from 1948 to 1968.8; nodes in the second group are active from 1958.4 to 1979.2; and so on.

### 3.10 General Approach

A parametric study was performed to evaluate the relative benefits of *no-action* and *soil-remediation* site restoration options under conditions of model parameter uncertainty. The sensitivity of model predictions to the natural CF degradation rate at the site was examined using CF half lives of 0, 277, and 1800 days. A similar analysis was performed to examine the

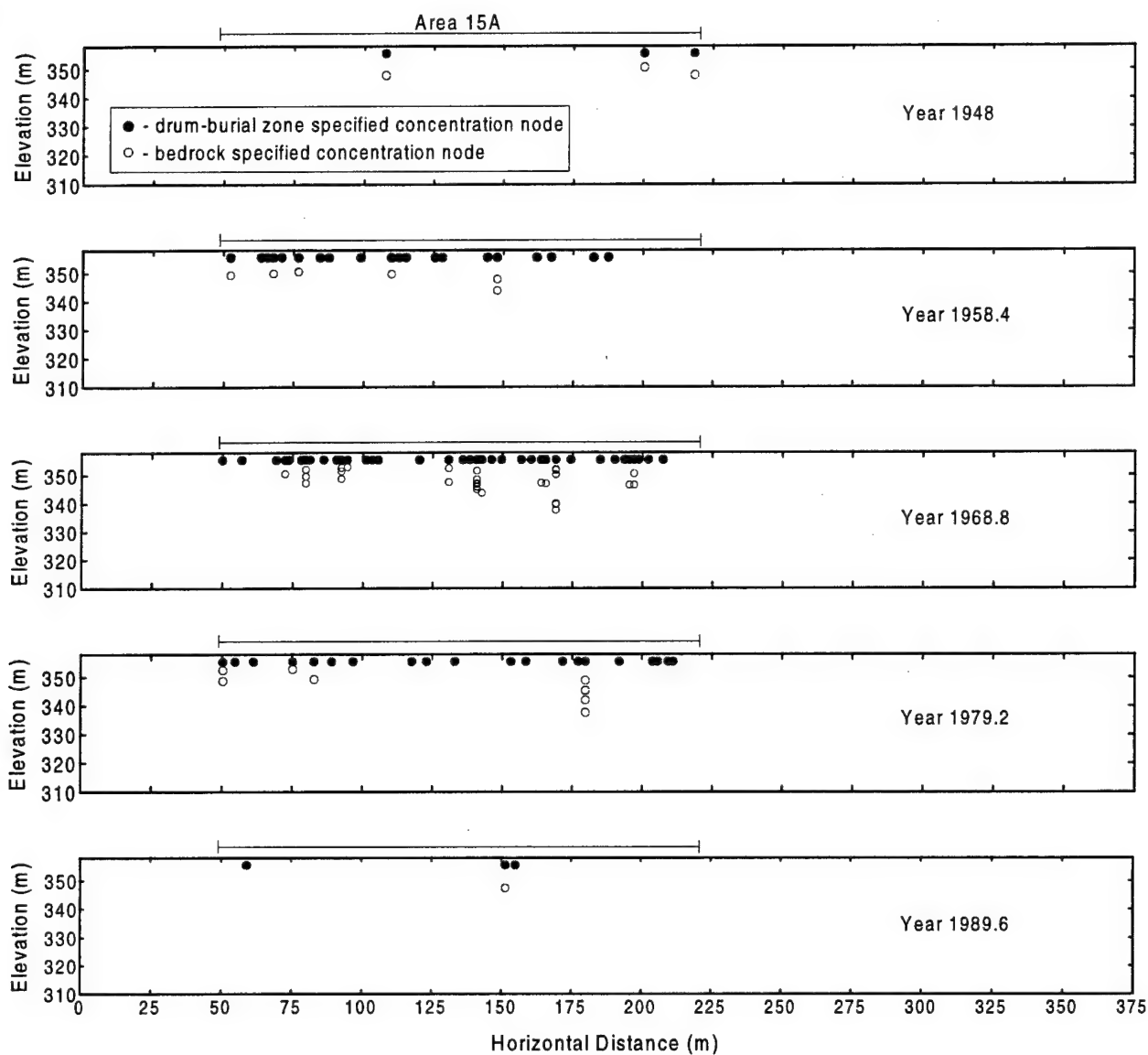


Figure 3-3 Example of Time-Dependent Specified Concentration Boundary Conditions Representing Randomly Located Contaminant Releases

sensitivity of model results to variations in the randomly generated fracture distributions in the bedrock below the site. All simulations were performed for the period 1948 to 2200 in order to examine the long-term effects of each restoration scenario.

In simulating the contaminant release period for cases involving the *no-action* case, the predicted CF mass balance was monitored from one modeling time increment to the next to determine when to deactivate specified concentration nodes representing contaminant release points. The total CF mass associated with the assumed 1700 55-gallon containers of CNS tear gas deposited at the site is estimated to be approximately 203,000 kg. Once the cumulative mass generated by specified concentration nodes within the drum burial and bedrock zones was approximately equal to the assumed initial mass, the internal boundary nodes were deactivated. This generally occurred in year 2000 or, in a few cases, the year 2010. For simulations associated with the *soil-remediation* scenario, internal boundary nodes were deactivated at year 2000 (the assumed date of soil remediation) regardless of the CF mass generated. Subsequent post-release simulations for the *no-action* cases were initiated with the CF concentration distribution from the previous run assigned as the initial condition. On the other hand, *soil-remediation* cases were restarted using CF concentrations in the drum burial zone set equal to zero in order to represent total removal of CF from the disposal site. All other areas of the model domain were assigned CF concentrations from the previous run as the initial condition.

The primary basis for evaluating the relative benefits of the two restoration scenarios was a comparison of the predicted CF mass stored in the aquifer system during the post-release period for each case. Such comparisons provide a sense of whether soil remediation results in a significant difference in the time required for natural restoration of the bedrock aquifer. Other results useful in the comparative evaluations include the predicted CF concentrations and cumulative CF mass discharge at the western seep boundary of the model.

## 4. Results and Discussion

### 4.1 Flow Simulations

The fracture distribution and steady-state hydraulic head distribution for each of the six fracture realizations considered in the analysis are shown in Figure 4-1. All fracture networks were stochastically generated using the model parameters and flow boundary conditions described in Section 3. It is evident that the distribution of fractures within the profile has a significant affect on the hydraulic head field and, in turn, on the groundwater flow field. The presence of fractures produces complex flow patterns, particularly near the soil-bedrock interface, which are unique for each realization. Table 4-1 illustrates that the fracture geometry also influences the overall rate of net infiltration over the upper model surface. Infiltration rates range from approximately 8.0 to 11.5 cm/yr , and are in general agreement with the 20-yr average net infiltration rate of 11.6 cm/yr predicted by the HELP hydrologic water balance simulation for the site (see Appendix G). The net infiltration rate of 1.6 cm/yr is approximately 13% of total mean annual precipitation. The agreement between the model and HELP net infiltration is important because the rate of percolation of infiltrating water through the overburden soils in the drum burial zone largely controls the rate at which tear gas contaminants are mobilized and transported through the subsurface.

Estimates of total groundwater discharge at the western boundary of the model integrated over the approximate 60-m width of the disposal area are also provided in Table 4-1. No measured flow data for Tributary B and associated seeps are available for comparison to model estimates. Even if data were available, comparisons are problematic because the contributing area of the seeps may differ from that of the model. Nevertheless, model discharge rates appear qualitatively consistent with the limited seep discharges observed in the field.

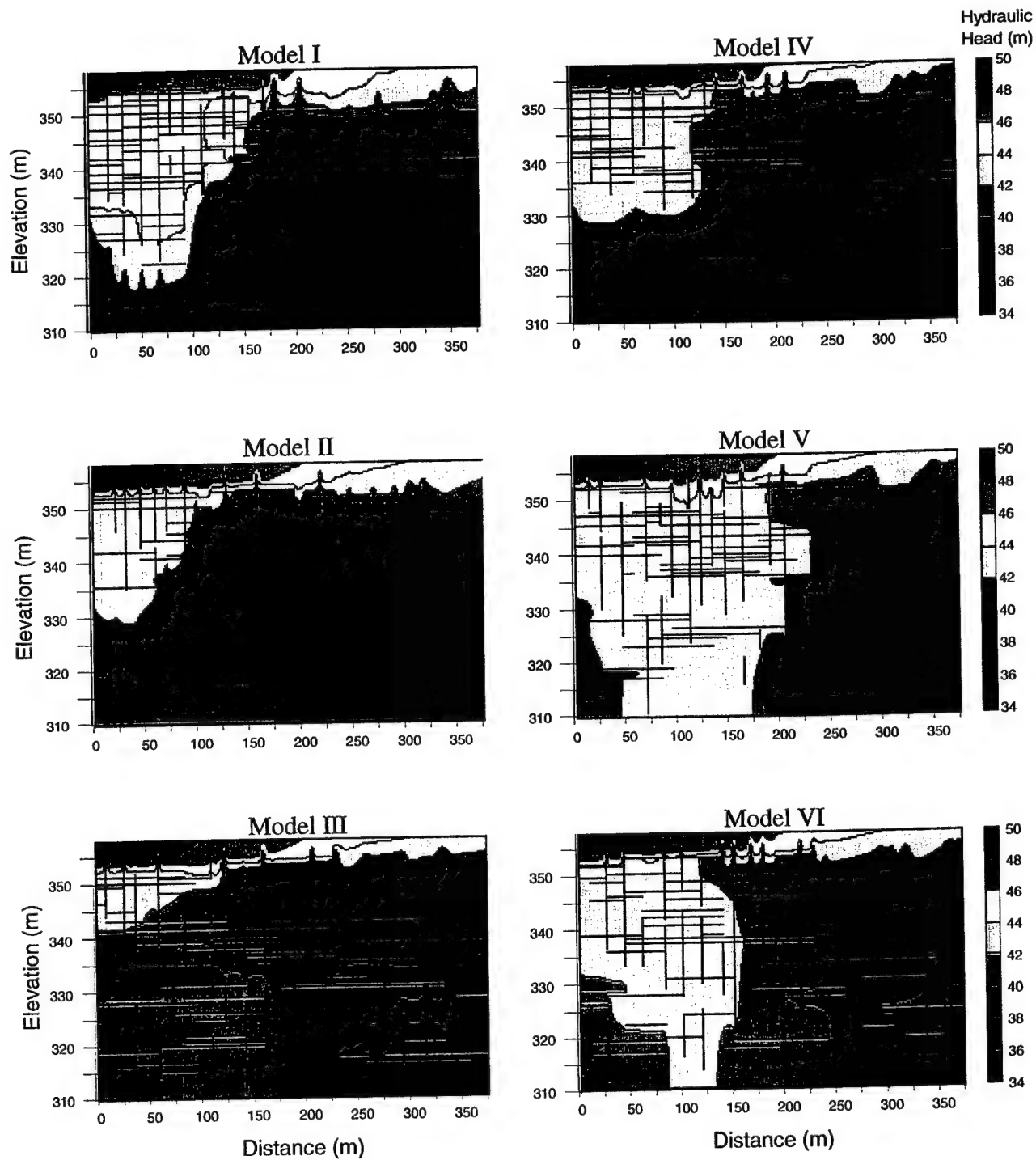


Figure 4-1 Fracture Network and Steady-State Hydraulic Head Field for Six Fracture Models

**Table 4-1**  
**Predicted Net Infiltration and Groundwater Discharge Rates**

Model	Net Infiltration	Groundwater Discharge
	(cm/yr)	(L/min)
I	9.1	3.9
II	10.0	4.3
III	11.5	4.9
IV	11.3	4.8
V	8.0	3.4
VI	10.9	4.7

Scatter plots comparing the predicted heads to observed heads in site monitoring wells for each fracture realization are shown in Figure 4-2. Comparisons of this type can be problematic because the presence or absence of fractures in the screened interval of the well can greatly affect the predicted head. Nevertheless, with the exception of well MWB-6 for which head is over-predicted in every case, reasonable overall comparisons are indicated for most fracture models. The poor head predictions at MWB-6 are unavoidable with model constraints on boundary geometry. The rectangular model domain requirement of FRACTRAN does not permit accurate spatial representation of head boundary conditions on the western end of the model in the region where the topography drops off sharply toward the Conemaugh River Valley.

## **4.2 Transport Simulations**

### **4.2.1 Base Case**

Detailed results of a base case simulation are presented to illustrate some of the important features of contaminant migration through the fractured porous aquifer present below the site. Results provide additional insight into the method of simulating contaminant releases using time-dependent internal boundary conditions and the overall effect of this approach on predicted contaminant distributions. In order to make the base case as representative as possible, the Model-II fracture realization was used since the overall groundwater system flow rate for this

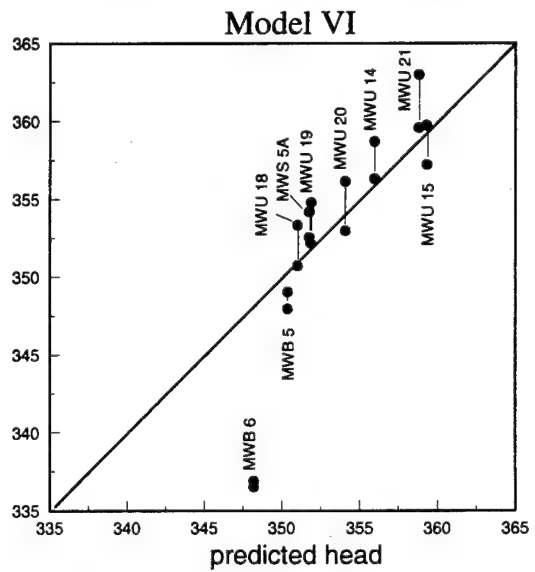
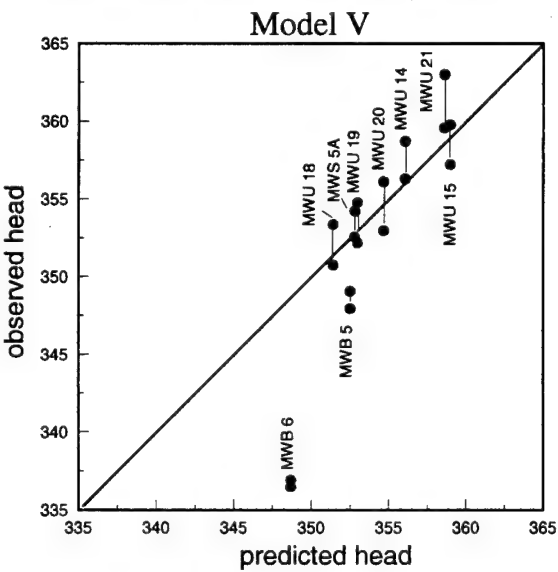
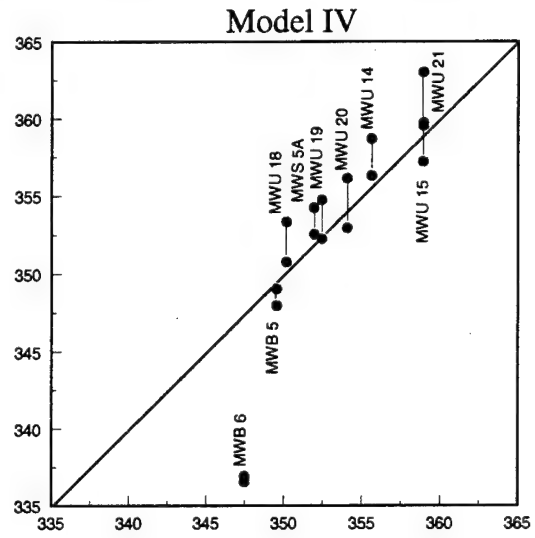
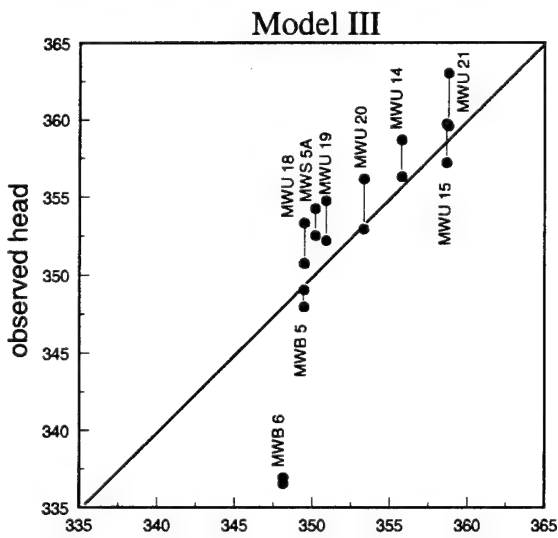
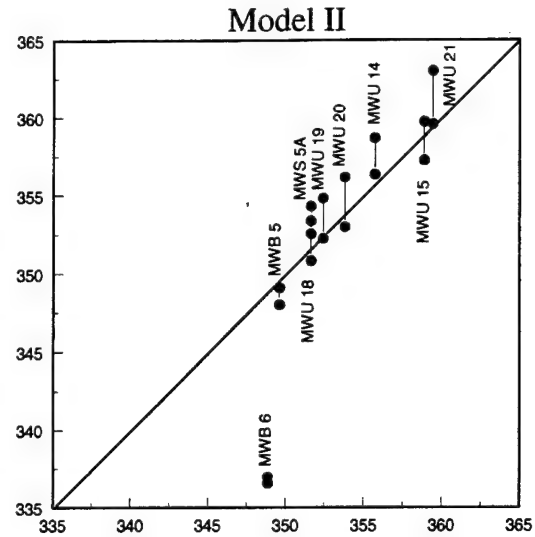
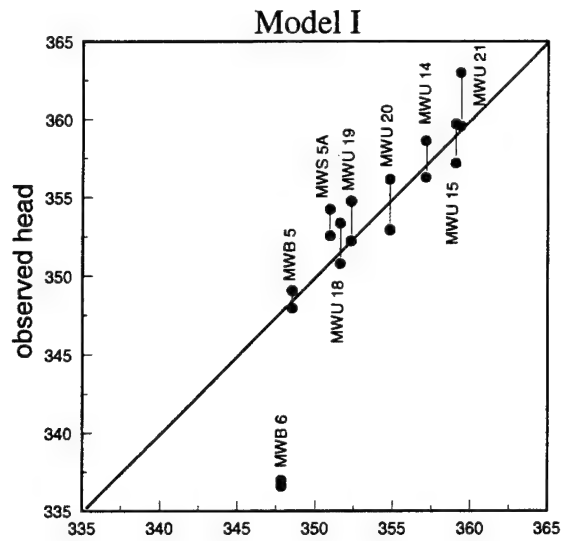


Figure 4-2 Predicted Versus Observed Hydraulic Heads for Six Fracture Models

model was mid-range among the six fracture models considered. No CF decay was assumed for the base case; otherwise all model parameters are as defined in Section 3.

Figures 4-3 through 4-5 show the predicted CF concentration distributions associated with the no-decay case for three time steps. Figure 4-3 represents the CF distribution at year 1968.8, the end of the second 10.4-yr release period. The randomly located release points in the drum burial zone correspond to the isolated concentration 'hot spots' at approximate elevation 355 m. Similarly, residual product sites are evident at several locations below the drum burial area, for example at approximate coordinates [128, 347], [144, 347], and [217, 353]. It is evident from the relatively high concentrations along fracture pathways that transport is dominated by advection along hydraulically active fractures. The concentration halo surrounding these active fractures suggests diffusion and/or advection of CF into the adjacent rock. Where shallow vertical fractures lie directly below the release points in the drum burial zone, CF migration is enhanced, for example the release point at coordinates [127, 355]. On the other hand, downward migration from the drum burial zone is limited where only low-permeability bedrock matrix is present directly beneath release sites. The time-series graph of CF mass storage shown in Figure 4-6(a) indicates that the amount of CF stored in the aquifer system is relatively low at this stage of the simulation (i.e., approximately 20,000 kg); however, the predicted average concentration at the downgradient boundary has reached approximately 0.7 g/L [Figure 4-6(c)]. The relatively high boundary concentration is the result of rapid advection through fractures with little attenuation by sorption and dispersion. Closer examination of boundary concentration data indicates that the initial CF arrival at the discharge boundary occurs less than 0.4 year (150 days) after the initial release (Figure 4-7). These breakthrough data apply to a boundary node at approximate coordinates [375, 321] associated with an active fracture contributing over 80% of the total boundary discharge. Based on these results, an average intra-fracture groundwater velocity of about 1.5 m/d is indicated between the release point and the discharge boundary.

By year 1989.6, approximately 96% of the tear gas containers are estimated to have failed, producing a nearly continuous source of CF over the burial zone (Figure 4-4). A diffuse region of CF lies below virtually the entire burial zone extending down to the shallowest horizontal fractures. Inspection of the CF distribution adjacent to active horizontal fractures indicates greater penetration of CF in the rock matrix on the lower side of fractures than on the



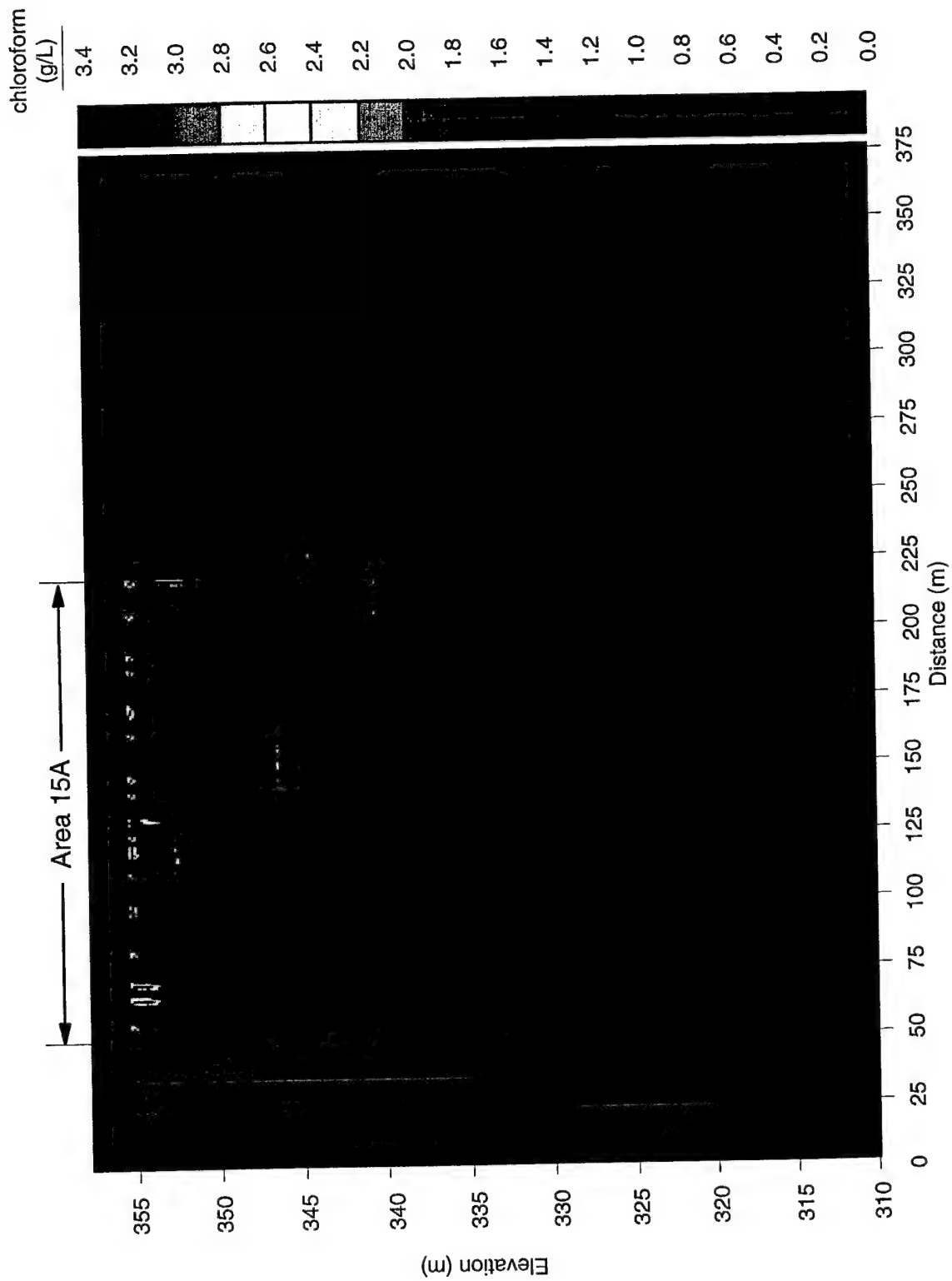


Figure 4-3 Predicted Chloroform Concentration Distribution At Year 1968.8

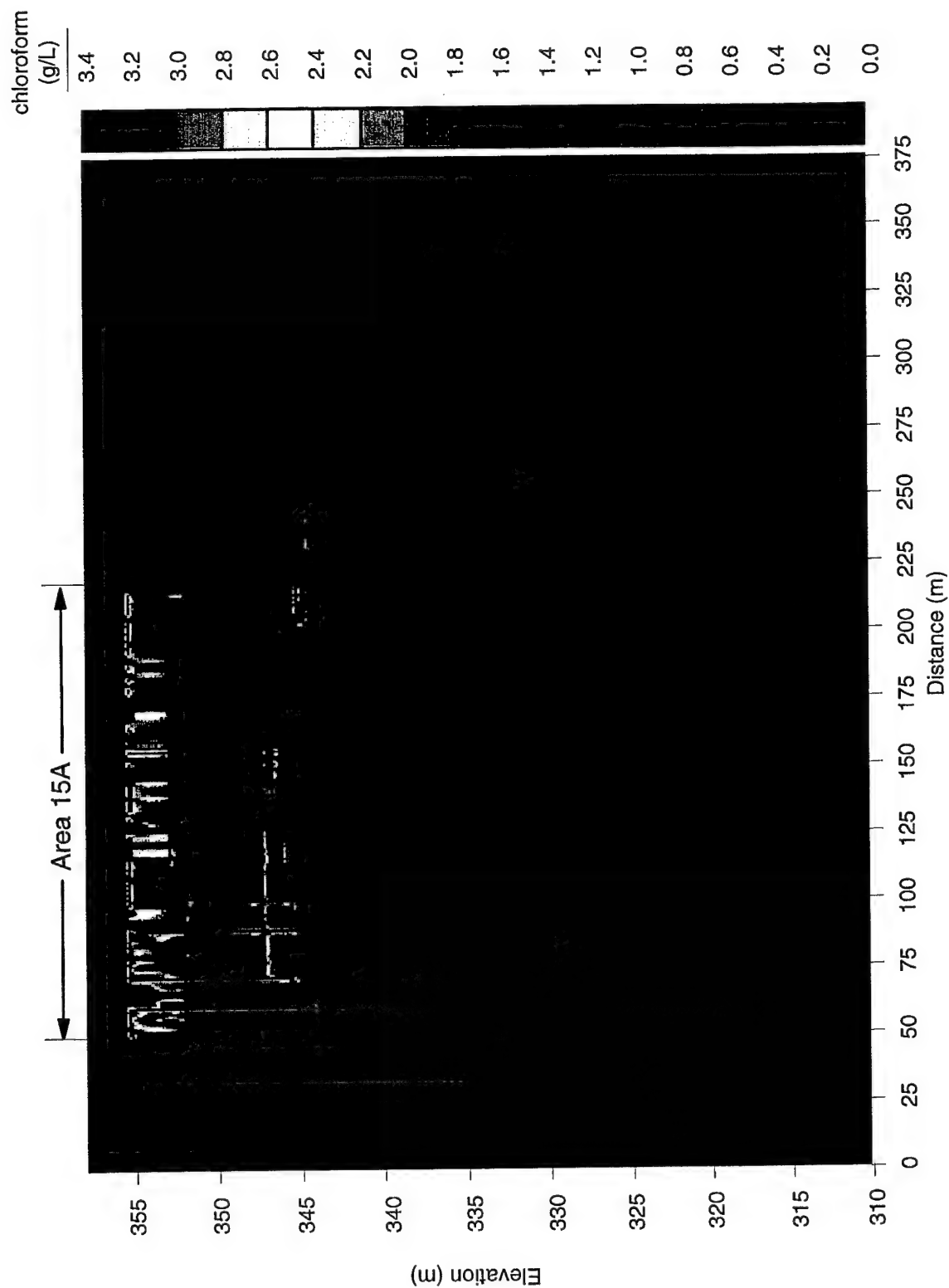


Figure 4-4 Predicted Chloroform Concentration Distribution At Year 1989.6

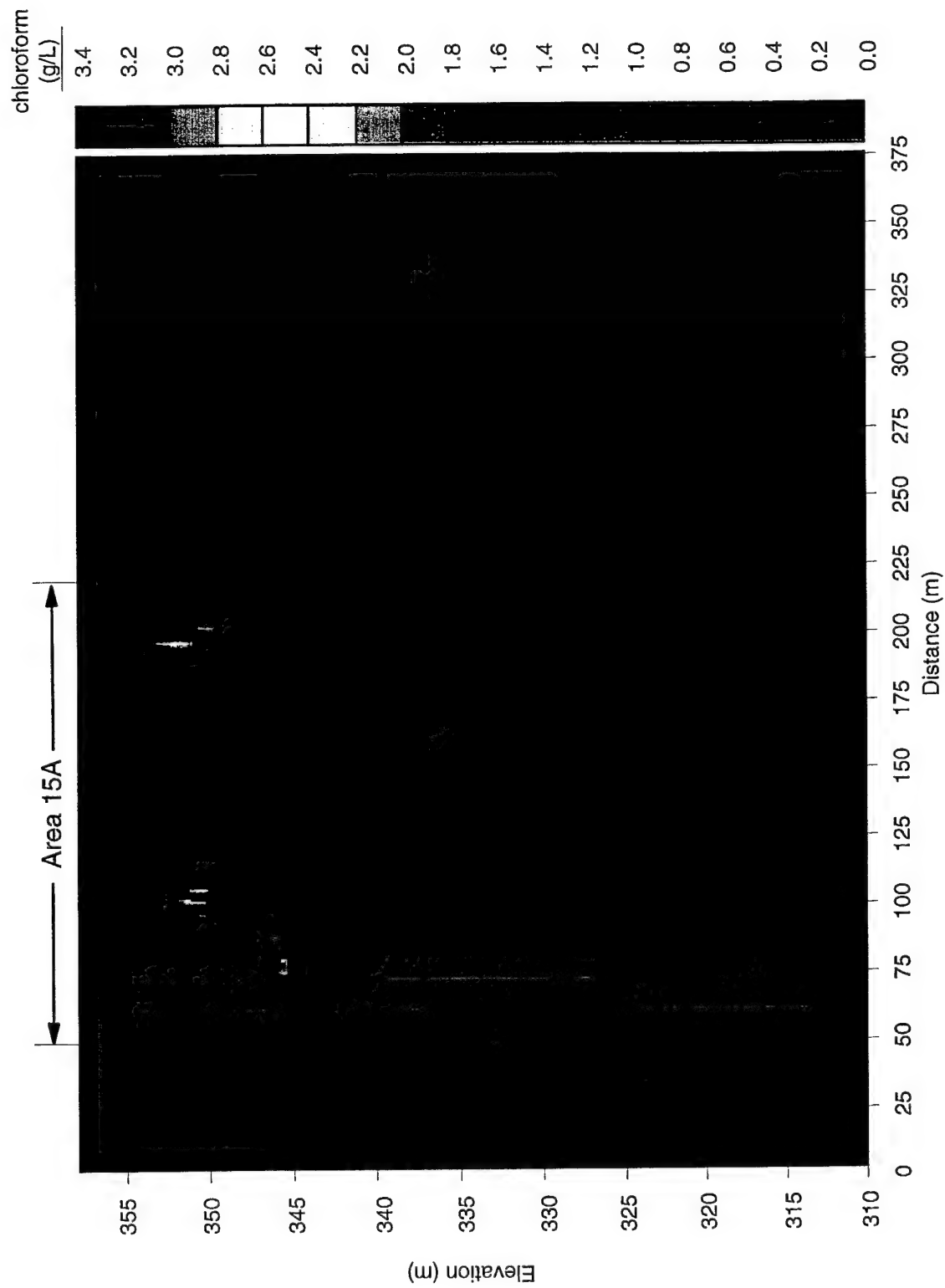


Figure 4-5 Predicted Chloroform Concentration Distribution At Year 2000

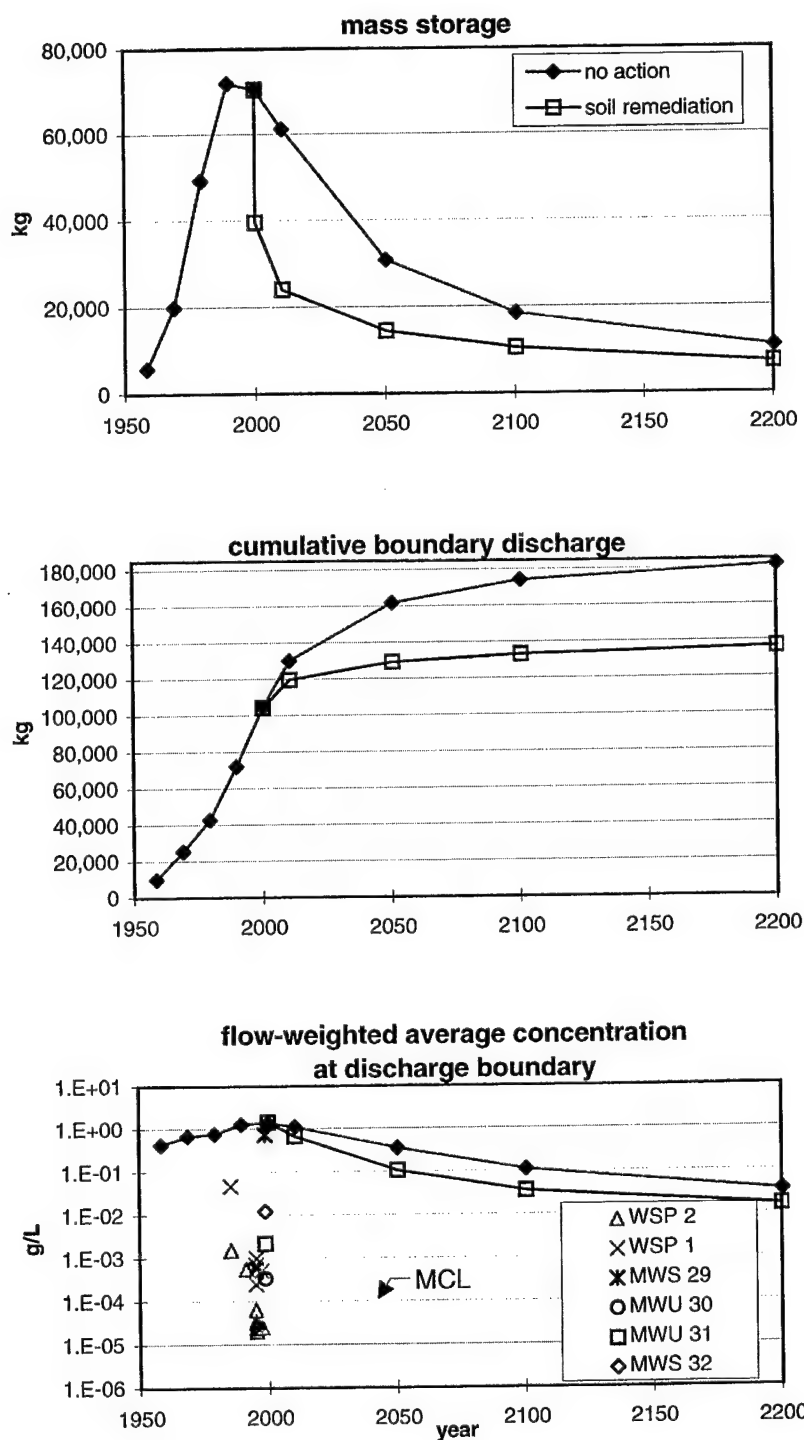


Figure 4-6 Predicted Chloroform Mass Storage, Boundary Discharge, Boundary Concentrations For No-Action and Soil-Remediation Cases Assuming No Chloroform Degradation

upper side in response to the natural downward hydraulic gradient. As indicated in Figure 4-6(a), the estimated CF mass storage has reached a maximum for the simulation, and the average downgradient concentration is approaching the peak of the breakthrough curve [Figure 4-6(c)].

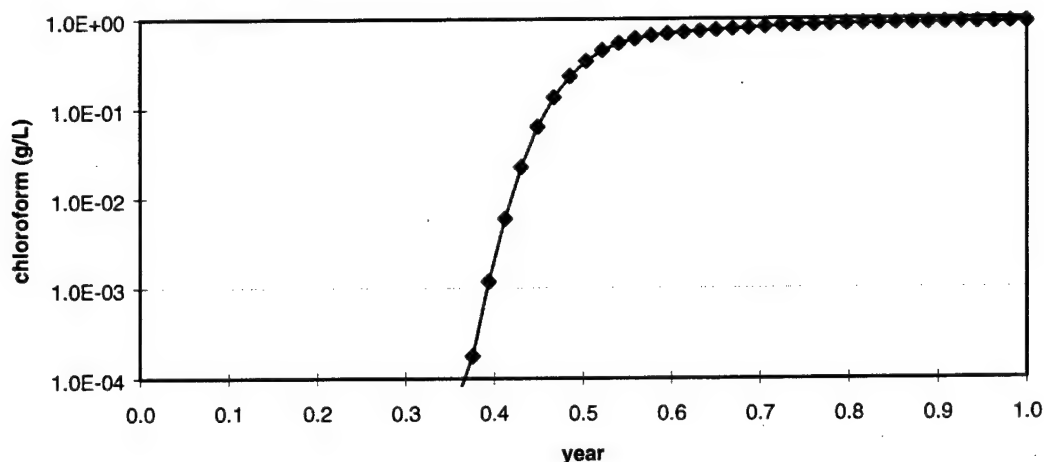


Figure 4-7 Initial Chloroform Breakthrough Predicted at Western (Seep) Boundary of Model Assuming No Chloroform Degradation

Fifty years after the assumed failure of all containers (year 2050.4) the highest observed CF concentrations are found in the basal soil deposits, shallow bedrock matrix below the burial area, and in the rock matrix adjacent to assumed residual product bedrock nodes (Figure 4-5). The process of downward percolation of fresh, uncontaminated surface infiltration through the depleted burial area has reduced overall CF concentrations in the soil and significantly lowered concentrations in fractures. In fact, CF concentrations in the fractures are now generally lower than in the adjacent rock matrix, the reverse of earlier concentrations gradients observed during periods of simulated CF release. During the post-release period, CF stored in the rock matrix diffuses back into fractures in response to reversed concentration gradients. This slow re-entry of contaminants into the fractures is responsible for the gradual decline in CF mass storage [Figure 4-6(a)] and the slow rate of decrease in the predicted concentrations at the downgradient boundary [Figure 4-6(c)].

In comparing the predicted long-term CF mass storage curves for the *no-action* and *soil-remediation* scenarios, a large decrease in stored mass is observed in year 2000 for the *soil-*

*remediation* case corresponding to the assumed removal of all contaminants from the soil overburden. The removal of overburden contamination reduces the ultimate quantity of contaminant mass discharged at the downgradient boundary shown in Figure 4-6(b) by an estimated 25%. However, it does not significantly affect the period of time required for natural restoration of contaminated bedrock. Figure 4-6(a) indicates that after the year 2000, mass storage curves for both scenarios gradually converge as they decline exponentially over time. A simple visual extrapolation of these curves beyond year 2200 is sufficient to recognize that several hundred additional years will be required to completely purge contaminants from the system by natural processes. This result is worthy of consideration in evaluating the relative environmental benefits of overburden contaminant removal.

The predicted CF concentrations at the discharge boundary are generally higher than the limited historical data for the seeps in this region as well as for most of the downgradient well sample data. Given the likelihood of natural CF degradation (see Section 3), the over-predicted concentrations in this region may be due to the assumption of no CF decay applied to this simulation. However, the disparity can also be due, in part, to the limited extent of spatial and temporal sampling and, perhaps, to bias produced by sampling methods, such as grab sampling of pooled seepage, that fail to prevent the CF losses due to volatilization and photolysis.

#### *4.2.2 Chloroform Degradation Sensitivity Analysis*

Evidence suggests that CF decay is occurring at the site due to microbiological transformation and/or abiotic processes such as iron reduction and hydrolysis [Castro, 1986]. However, considerable uncertainty exists regarding a representative field-average decay rate for CF. A sensitivity analysis was performed for the CF first-order decay constant used in transport simulations in an attempt to bracket the predictions. The fracture distribution of Model-II was used for the sensitivity analysis. First-order rate constants of 0.000, 0.913, and 0.141 yr<sup>-1</sup>, corresponding to half lives of 0, 277, and 1800 days, were applied to Model-II. Figures 4-8 and 4-9 show simulation results for CF half lives of 1800 days and 277 days, respectively. Results for the zero-decay case, (base case) discussed earlier are given in Figure 4-6.

The simulation using the 277-day half life estimated from the <sup>14</sup>C mineralization study shows the best agreement with observed CF concentrations in downgradient seep and

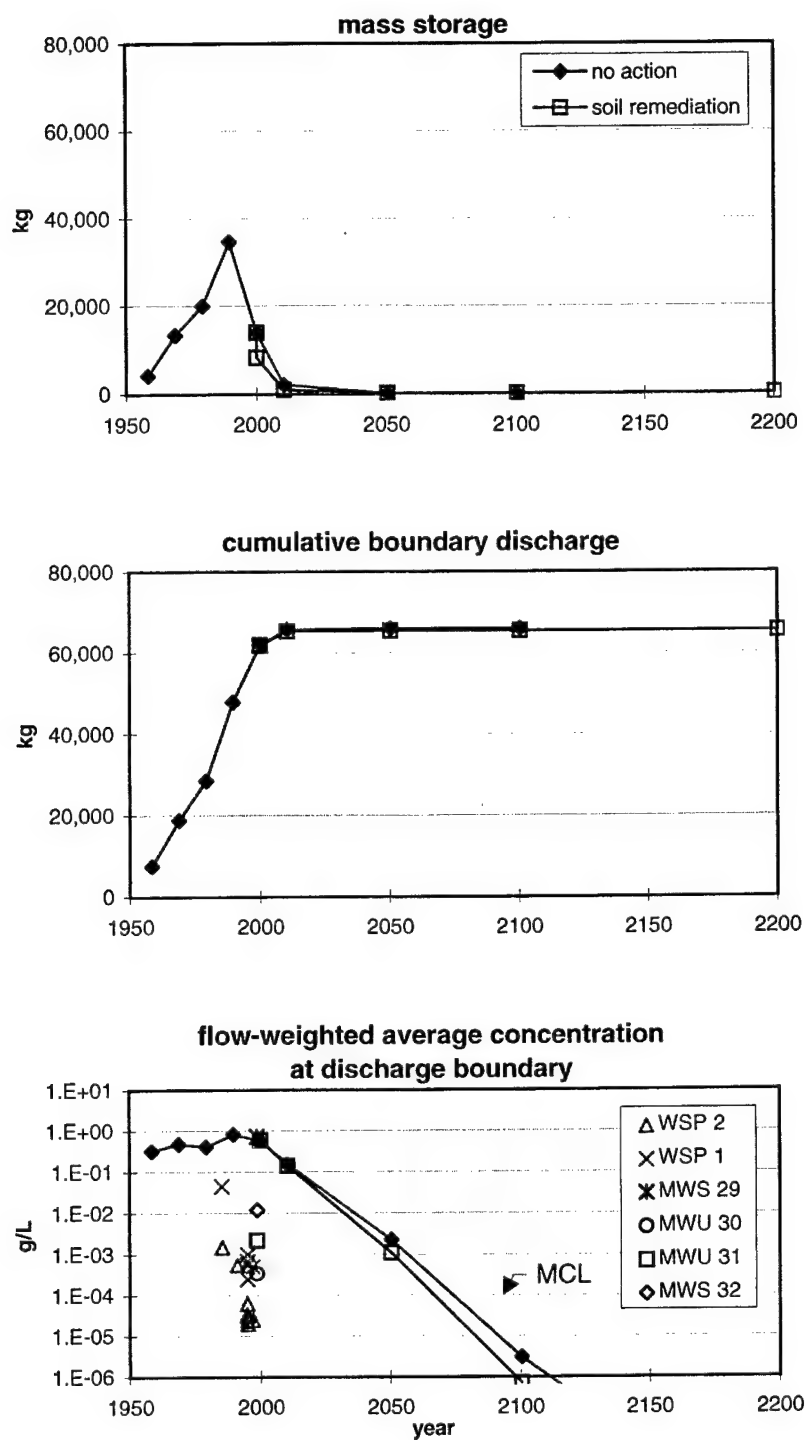


Figure 4-8 Predicted Chloroform Mass Storage, Boundary Discharge, Boundary Concentrations For No-Action and Soil-Remediation Cases Assuming CF Degradation Half Life of 1800 Days

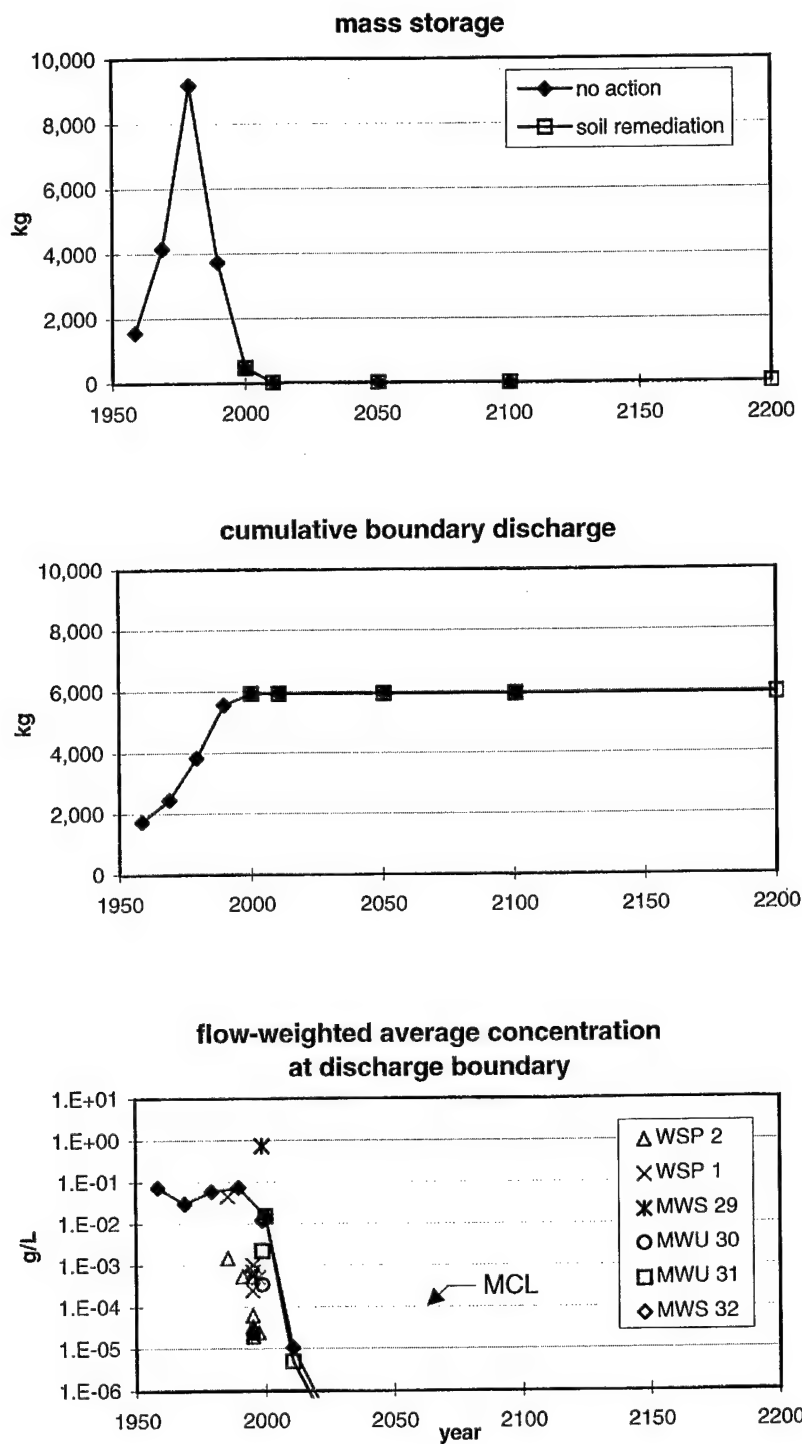


Figure 4-9 Predicted Chloroform Mass Storage, Boundary Discharge, Boundary Concentrations For No-Action and Soil-Remediation Cases Assuming CF Degradation Half Life of 277 Days



groundwater samples, although predicted concentrations still tend to be higher than most seep observations [Figure 4-9(c)]. Predicted CF concentration in groundwater discharge from the downgradient model boundary drop below the EPA MCL ( $10^{-4}$  g/L) by approximately year 2010. Figure 4-9(a) indicates that CF mass stored within the system peaks at just under 10,000 kg by year 1989.2, and, by the year 2050, virtually all mass has been removed through degradation and physical transport. It is important to note that the relatively rapid decay produced by the 277 day CF half life results in essentially no difference between the *no-action* and *soil-remediation* cases in terms of predicted mass storage and boundary breakthrough concentrations. This observation also applies to the results for the 1800-day half-life simulations (Figure 4-8). In this case, essentially all stored CF mass is depleted by about year 2100 for both site restoration scenarios, and predicted discharge boundary breakthrough concentrations fall below the CF MCL by about year 2075.

Sensitivity results indicate that predictions of long-term natural restoration of the Area 15A site are highly sensitive to the assumed CF degradation rate. Of the decay parameters considered, the mineralization study half-life estimate of 277 days appears to provide the best representation of historical conditions at the site and, thus, the best estimate of what is likely to occur in the future. In general, these findings support the previous evidence and suggestions that active microbial degradation of CF is occurring at the site. Better understanding of degradation processes and rates combined with more reliable and complete data regarding CF concentrations in seep discharges downgradient of the site can significantly improve the reliability of predictions of the long-term natural restoration of the site.

#### 4.2.3 Fracture Network Sensitivity Analysis

In order to assess the effect of random fracture geometry on simulation results, a sensitivity study was performed for six fracture realizations. Based on the dominating effect of CF decay on model results indicated by the decay sensitivity study, fracture sensitivity simulations assumed no CF decay so as to maximize differences between the *no-action* and *soil-remediation* cases. The only model parameters changed in the fracture sensitivity study were the two numerical seeds used to randomly generate fracture locations and apertures.

Predicted temporal variations in the CF mass storage to year 2200 are shown in Figure 4-10 for each fracture realization. Although peak mass storage estimates differ by as much as 30%, the overall mass storage trends for all realizations are similar, indicating only modest sensitivity to fracture geometry. This is particularly true for the long-term results which are of primary interest in comparative evaluations of site restoration alternatives. Curves for the *no-action* case all peak toward the end of the simulated release period followed by a gradual exponential decline to year 2200. As shown in Figure 4-11, estimates of the CF mass storage at year 2200 for the *no-action* case, expressed in terms of original mass fraction, range from 5.2 to 12% and average approximately 7%. Mass storage curves for the *soil-remediation* case exhibit a sharp drop at year 2000, corresponding to the assumed removal of contamination from the soil overburden, followed by gradual exponential decline. The CF mass remaining at year 2200 averages approximately 5% of original mass. As observed earlier, even though removal of overburden contamination produces a significant decrease in stored mass at year 2000, the mass curves for both cases tend to converge during the latter phase of simulations, resulting in little difference in stored mass by year 2200. This apparent paradox can be explained by recognizing that the difference between the two mass curves represents the amount of mass stored in the overburden. The mass curves associated with the *no-action* scenario reflect the simultaneous effects of natural restoration processes in the soil and bedrock, whereas, the *soil-remediation* curves relate only to bedrock restoration processes. The mass storage trends suggest that rates of natural restoration in the soil and bedrock are different. That is, the natural process by which contaminants in the soil overburden are mobilized by infiltrating precipitation and transported out of the system through active fractures is relatively fast compared to the slow advection and diffusion of contaminants from the rock matrix into fractures. These findings suggest that, without significant natural CF degradation, removal of overburden contamination in Area 15A will not significantly decrease the time required for natural restoration of the bedrock aquifer below the site. The transport properties of the bedrock matrix, such as porosity, hydraulic conductivity, effective matrix diffusion coefficient, and distribution coefficient assume more importance in forecasting long-term natural restoration of the bedrock under conditions of limited natural CF degradation.

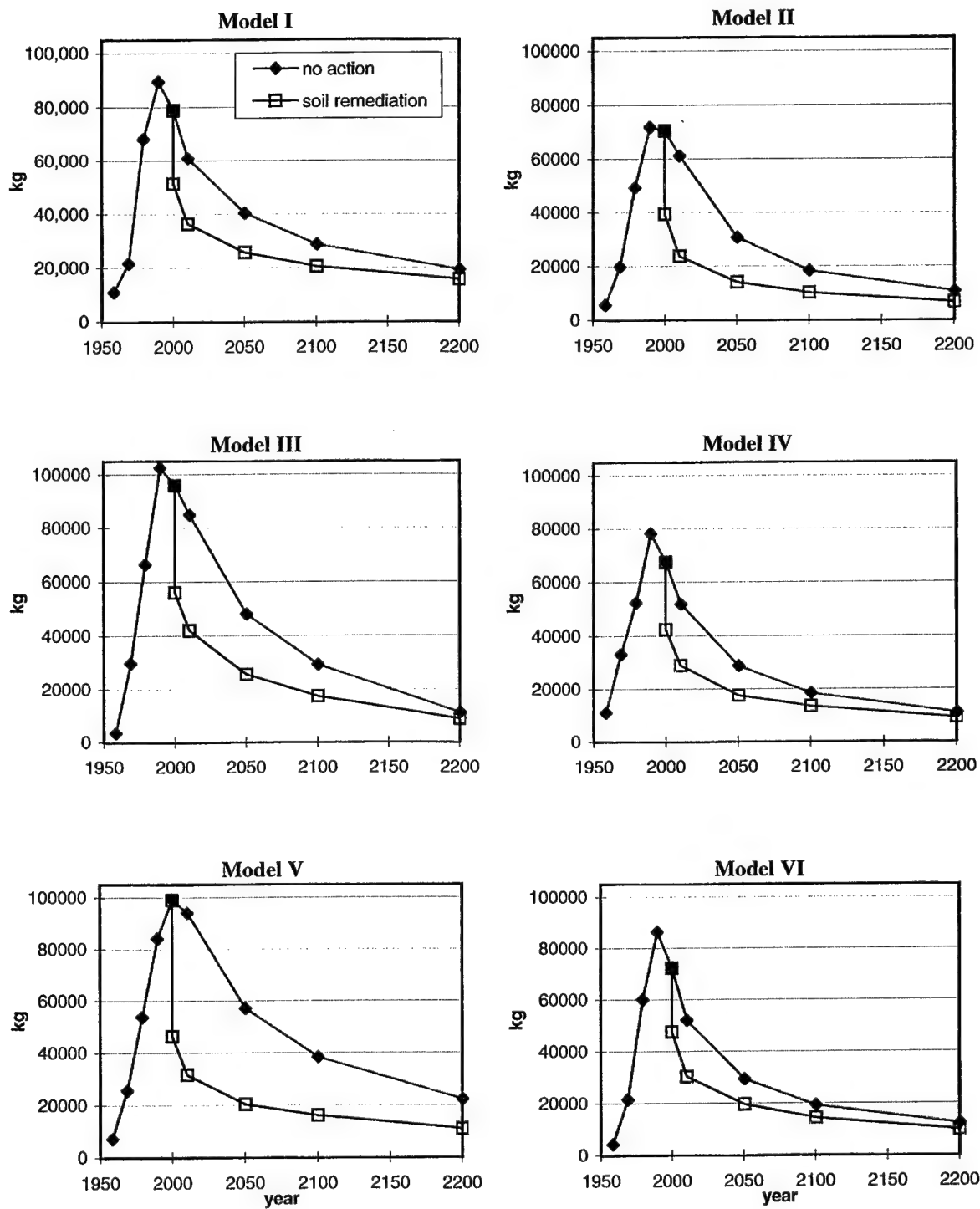


Figure 4-10 Predicted Chloroform Mass Storage For Six Fracture Models (No CF Degradation)

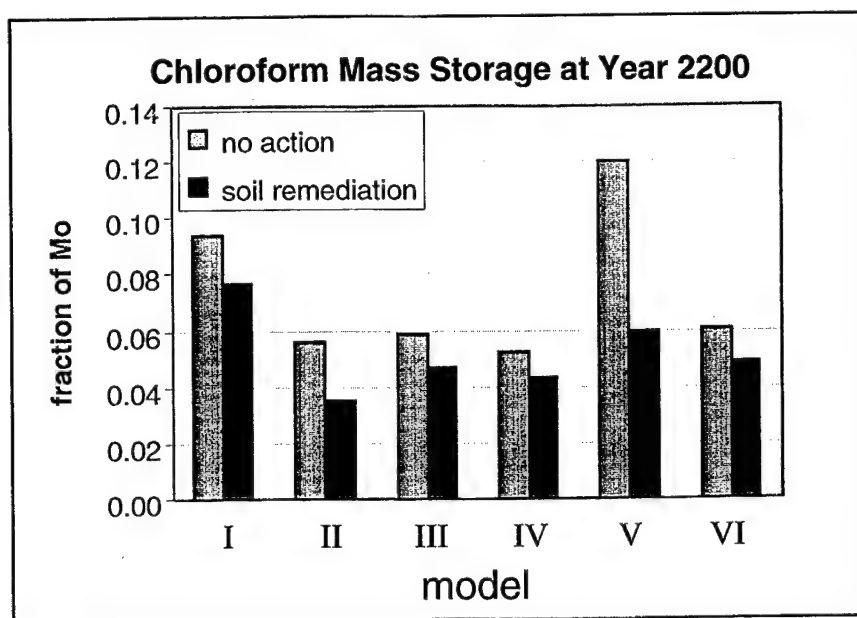


Figure 4-11 Summary of Predicted Chloroform Mass Storage Fractions at Year 2200 For Six Fracture Models (No CF Degradation)

## 5. Conclusions and Recommendations

The two-dimensional fractured porous media models developed for the parametric study provide reasonable representations of the hydrogeologic system present at Area 15A upon which to base evaluations of long-term natural restoration of the site. The predicted hydraulic head fields associated with the six fracture models were all in general agreement with observed heads in site monitoring wells. Net surface infiltration rates predicted by these models ranged from 8.0 to 11.5 cm/yr and were consistent with the 20-yr average net infiltration rate of 11.6 cm/yr estimated from a hydrologic water balance simulation for the site. Model-predicted average discharge rates of about 4 Lpm in the seep area of the site also appear consistent with visual observations of seep flow. Flow model calibrations appear adequate in view of the inherent difficulties in calibrating models involving randomly-generated fracture networks.

Predictions of long-term natural restoration of the contaminated region affected by Area 15A are highly sensitive to the assumed CF degradation rate. Of the decay parameters considered, TVA's mineralization study half-life estimate of 277 days provided the best agreement with observed CF concentrations in seep and downgradient groundwater samples and, therefore, may be most indicative of future conditions. Predictions using moderate degradation rates showed better comparisons with observed data than those assuming no degradation, thereby supporting assertions of Castro [1986] and others that active microbial degradation of CF has been occurring at the site. Comparisons of the *no-action* and *soil-remediation* cases using the 277-day CF half life showed essentially no difference in predicted mass storage and discharge boundary breakthrough concentrations. In both cases, degradation of all CF mass was predicted by year 2050, and concentrations at the discharge boundary were below the CF MCL by about year 2010. Better understanding of CF degradation processes and rates, combined with more complete data regarding CF concentrations in seep discharges downgradient of the site, can significantly improve the reliability of predictions of the long-term natural restoration of the site.

Predictions of temporal variations of CF mass storage for six distinct fracture models, all of which assumed no CF degradation, exhibited similar overall mass storage trends with peak storage estimates differing by only about 30%. These findings indicate only minor sensitivity of predictions to fracture distribution. They also suggest that, even without significant CF

degradation, remediation of overburden contamination will not significantly reduce the time required for natural restoration of the bedrock system. Although removal of overburden contamination resulted in a substantial decrease in predicted CF mass storage at year 2000, the mass storage curves for both cases tended to converge over time and showed little difference by year 2200. These results illustrate that mobilization of contaminants in the overburden by infiltrating precipitation and removal from the system through active fractures is relatively fast compared with the slow advection and diffusion of contaminants from the rock matrix into fractures. So while overburden remediation may have other environmental benefits, it will not substantially reduce the time needed for natural restoration of the bedrock.

All simulations considered in the modeling analysis indicated that the worst conditions with respect to CF levels have already occurred and that improving conditions can be expected in the future. That is, time-series predictions of CF mass storage and breakthrough at the discharge boundary all peak prior to year 2000, followed by declining mass storage and concentration levels. These trends are a direct consequence of the contaminant release function applied in model simulations which produces failure of all tear gas containers by year 2000. This finding, coupled with the earlier conclusion that remediation of soils in the drum burial area will not significantly reduce the time required for natural restoration of the bedrock, suggests that Area 15A may be a viable candidate for monitored natural attenuation.

## References

- Benjamin, J. R., and C. A. Cornell, 1970, Probability, statistics, and decision for civil engineers, McGraw-Hill, New York.
- Carr, P. A., 1969, "Salt-water intrusion in Prince Edward Island," *Canadian J. of Earth Sciences*, 6(63): 63-74.
- Castro, C. E., 1986, "Chemical and microbiological transformations at the 15A site, Report to Alan E. Opel, Trans Technology, Inc.
- Castro, C. E., 1998, "The remediation of Site 15A", report to Michael Broder, Tennessee Valley Authority.
- Cohen, R. M., and J. W. Mercer, 1993, "DNAPL site evaluation," Environmental Protection Agency Report No. EPA/600/R-93/022.
- Colton, G. W., 1970, "The Appalachian Basin - Its Depositional Sequences and Their Geologic Relationships," in *Studies of Appalachian Geology: Central and Southern*, ed. G. W. Fisher, F. J. Pettijohn, J. C. Reed, Jr., and K. N. Weaver, Interscience Publishers, pp 5-47.
- Cooper, H. H. Jr., and C. E. Jacob, 1946, "A Generalized Graphical Method for Evaluations of Formation Constants and Summarizing Well Field History," *Transactions of the American Geophysical Union*, 27:526-534.
- CRA, 1995, "Area 15A Groundwater Pumping Evaluation, Federal Laboratories, Saltsburg, Pennsylvania," Ref. No. 6099 (13), Conestoga-Rovers & Associates, Niagara Falls, New York.
- De Wiest, R.J.M., 1969, Flow Through Porous Media, Academic Press, New York.
- D.B. Stephens & Associates, Inc., 1997, "Laboratory Analysis of Soil Hydraulic Properties of Tennessee Valley Authority Soil Samples," Letter Report, December 30, 1997.
- Domenico, P. A., and F. W. Schwartz, 1990, Physical and Chemical Hydrogeology, John Wiley & Sons, Inc., New York, New York.
- ESC, 1985, "Progress Report, Environmental Site Assessment, Federal Laboratories, Inc., Saltsburg, Pennsylvania," Project No. 85-103A, 2 volumes, Earth Sciences Consultants, Inc., Pittsburgh, Pennsylvania.
- ESC, 1992a, "Summary of Site Characterization Studies, Federal Laboratories, Saltsburg, Pennsylvania," Technical Report, Earth Sciences Consultants, Inc., Pittsburgh, Pennsylvania,

- ESC, 1992b, "Removal Site Evaluation/Feasibility Study," Technical Report, Earth Sciences Consultants, Inc., Pittsburgh, Pennsylvania.
- Fenneman, N. M., 1938, "Physiography of the Eastern United States," McGraw-Hill Book Company, Inc., New York and London.
- Ferm, J. C., "Allegheny Deltaic Deposits," Society of Economic Paleontologists and Mineralogists, Special paper 15, 250 p., 1970.
- Francis, R. M., 1981, "Hydrogeological properties of a fractured porous aquifer, Winter River Basin, Prince Edward Island," M.S. Thesis, University of Waterloo, Waterloo, Ontario.
- Freeze, R. A., and J. A. Cherry, 1979, Groundwater, Prentice-Hall, Inc., New Jersey.
- Gelhar, L. W., C. Welty, and K. R. Rehfeldt, 1992, "A Critical Review of Data on Field-Scale Dispersion in Aquifers," *Water Resources Research*, 28 (7): 1955-1974.
- Golder Associates, 1998, "RIP Theory , Manual, and User's Guide," <http://www.golder.com/rip>
- Harrison, B., E. A. Sudicky, and J. A. Cherry, 1992, "Numerical analysis of solute migration through fractured clayey deposits into underlying aquifers," *Water Resources Research*, 28(2): 5515-526.
- Howard, P. H., R. S. Boethling, W. F. Jarvis, W. M. Meylan, and E. M. Michalenko, 1991, Handbook of environmental degradation rates, CRC Press LLC, Boca Raton, Florida.
- Keller, A. A., 1996, "Single and multiphase flow and transport in fractured porous media," <http://www.esm.ucsb.edu/~keller/>
- Keroher, G. C., and 14 others, 1966, "Lexicon of Geologic Names of the United States for 1936-1960," Bulletin 1200, U.S. Geological Survey.
- Kueper, B. H., and D. B. McWhorter, 1991, "The behavior of dense, nonaqueous phase liquids in fractured clay and rock," *Ground Water*, 29(5): 716-728.
- Lyman, W. J., W. F. Reehl, and D. H. Rosenblatt, 1982, Handbook of chemical property estimation methods, McGraw-Hill, Inc., New York.
- Meckel, L. D., 1970, "Paleozoic Alluvial Deposition in the Central Appalachians: A Summary," in *Studies of Appalachian Geology: Central and Southern*, ed. G. W. Fisher, F. J. Pettijohn, J. C. Reed, Jr., and K. N. Weaver, Interscience Publishers, pp 49-67.
- Nelson, R. A., 1985, Geologic Analysis of Naturally Fractured Reservoirs, Gulf Publishing Company, Houston, Texas.



- Pankow, J. F., and J. A. Cherry, 1996, Dense Chlorinated Solvents and other DNAPLs in Groundwater, Waterloo Press, Portland, Oregon.
- Parker, B. L., D. B. McWhorter, and J. A. Cherry, 1997, "Diffusive loss of non-aqueous phase solvents from idealized fracture networks in geologic media," *Ground Water*, 35(6): 1077-1088.
- PTGS, "Pittsburgh Low Plateau Section - Appalachian Plateaus Province," Pennsylvania Topographic & Geologic Survey, <http://www.dcnr.state.pa.us/topogeo/map13/13plps.htm>, 1998.
- Rice, C. L., J. K. Hiatt, and E. D. Koozmin, 1994, "Glossary of Pennsylvanian Stratigraphic Names, Central Appalachian Basin," Geological Society of America Special Paper 294.
- Slough, K. J., E. A. Sudicky, and P. A. Forsyth, 1999, "Importance of rock matrix entry pressure on DNAPL migration in fractured geologic materials," *Ground Water*, 37(2): 237-244.
- Snow, D. T., 1968, "Rock fracture spacings, openings, and porosities," *J. Soil Mechanics and Foundations Division, Proceedings of the American Society of Civil Engineers*, 94(SM1): 73-91.
- Snow, D. T., 1970, "The frequency and apertures of fractures in rock," *J. Rock Mechanics and Mineral Science*, 7: 23-40.
- Sudicky, E. A., and R. G. McLaren, 1992, "The Laplace transform Galerkin technique for large-scale transport in discretely fractured porous formations," *Water Resources Research*, 28(2): 499-514.
- Sudicky, E. A., and R. G. McLaren, 1998, "FRACTRAN User's Guide: An efficient simulator for two-dimensional, saturated groundwater flow and solute transport in porous or discretely-fractured porous formations," University of Waterloo, Canada.
- Theis, C. V., 1935, "The Relationship Between the Lowering of the Piezometer Surface and the Rate and Duration of Discharge of a Well Using Groundwater Storage," *Transactions of the American Geophysical Union*, 16:519-524.
- Van Golf-Racht, T. D., 1982, Fundamentals of fractured reservoir engineering, Elsevier Scientific Publishing Company, Amsterdam.
- Wanless, H. R., 1939, "Pennsylvanian Correlations in the Eastern Interior and Appalachian Coal Fields," Geological Society of America Special Paper 17.
- Williams, D. R., and T. A. McElroy, 1997, "Water-Resources Data for Indiana County, Pennsylvania," Open-File Report 90-384, U.S. Geological Survey.

## Supplement F-1

### Bedrock Fracture Aperture Estimates

The fracture aperture data presented in the table below were estimated from the uncensored borehole flowmeter hydraulic conductivity (K) measurements presented in Appendix E. The relationship between fracture aperture ( $b$ ) and K given in Equation 2.2 (Section 2) of this report were used for these calculations. Other parameters used in the calculation include ambient groundwater density and viscosity values of  $1000 \text{ kg/m}^3$  and  $0.00114 \text{ kg/m}\cdot\text{s}$ , respectively, and a gravitational constant of  $9.8 \text{ m/s}^2$ .

$K$ (f/d)	$K$ (m/s)	$b$ (m)	$\ln b$
0.088	3.115E-06	5.10E-04	-9.884
0.177	6.229E-06	6.42E-04	-9.653
0.198	7.001E-06	6.68E-04	-9.614
0.198	7.001E-06	6.68E-04	-9.614
0.348	1.226E-05	8.05E-04	-9.427
0.364	1.283E-05	8.18E-04	-9.412
0.375	1.324E-05	8.26E-04	-9.402
0.379	1.338E-05	8.29E-04	-9.398
0.418	1.475E-05	8.56E-04	-9.365
0.485	1.713E-05	9.00E-04	-9.316
0.488	1.723E-05	9.02E-04	-9.314
0.496	1.750E-05	9.07E-04	-9.308
0.597	2.106E-05	9.64E-04	-9.247
0.747	2.635E-05	1.04E-03	-9.172
0.752	2.655E-05	1.04E-03	-9.170
0.752	2.655E-05	1.04E-03	-9.170
0.760	2.681E-05	1.05E-03	-9.166
0.840	2.965E-05	1.08E-03	-9.133
0.876	3.090E-05	1.10E-03	-9.119
0.979	3.456E-05	1.14E-03	-9.082
1.087	3.835E-05	1.18E-03	-9.047
1.257	4.434E-05	1.24E-03	-8.999
1.276	4.504E-05	1.24E-03	-8.993
1.412	4.984E-05	1.28E-03	-8.960
1.582	5.582E-05	1.33E-03	-8.922
1.588	5.605E-05	1.34E-03	-8.920
1.923	6.784E-05	1.42E-03	-8.857
1.986	7.008E-05	1.44E-03	-8.846
2.180	7.692E-05	1.48E-03	-8.815
2.225	7.851E-05	1.50E-03	-8.808

<b>K</b> <b>(f/d)</b>	<b>K</b> <b>(m/s)</b>	<b>b</b> <b>(m)</b>	<b>ln b</b>
2.279	8.042E-05	1.51E-03	-8.800
2.685	9.475E-05	1.59E-03	-8.745
2.713	9.574E-05	1.60E-03	-8.742
2.768	9.766E-05	1.61E-03	-8.735
2.876	1.015E-04	1.63E-03	-8.723
2.877	1.015E-04	1.63E-03	-8.722
2.900	1.023E-04	1.63E-03	-8.720
2.985	1.053E-04	1.65E-03	-8.710
3.085	1.088E-04	1.67E-03	-8.699
3.428	1.210E-04	1.73E-03	-8.664
3.684	1.300E-04	1.77E-03	-8.640
3.733	1.317E-04	1.78E-03	-8.636
4.518	1.594E-04	1.89E-03	-8.572
5.589	1.972E-04	2.03E-03	-8.501
6.882	2.428E-04	2.18E-03	-8.432
6.951	2.453E-04	2.19E-03	-8.428
7.021	2.477E-04	2.19E-03	-8.425
7.841	2.767E-04	2.28E-03	-8.388
8.215	2.899E-04	2.31E-03	-8.373
10.219	3.606E-04	2.49E-03	-8.300
11.369	4.012E-04	2.58E-03	-8.264
11.400	4.023E-04	2.58E-03	-8.263
11.752	4.147E-04	2.60E-03	-8.253
13.625	4.808E-04	2.74E-03	-8.204
15.589	5.501E-04	2.86E-03	-8.159
16.225	5.725E-04	2.90E-03	-8.146
17.549	6.193E-04	2.98E-03	-8.120
21.149	7.463E-04	3.17E-03	-8.058
22.303	7.870E-04	3.22E-03	-8.040
23.774	8.389E-04	3.29E-03	-8.019
24.260	8.561E-04	3.32E-03	-8.012
26.332	9.292E-04	3.41E-03	-7.984
26.693	9.419E-04	3.42E-03	-7.980
26.884	9.487E-04	3.43E-03	-7.978
30.725	1.084E-03	3.59E-03	-7.933
31.365	1.107E-03	3.61E-03	-7.926
41.045	1.448E-03	3.95E-03	-7.836
47.725	1.684E-03	4.15E-03	-7.786
74.658	2.634E-03	4.82E-03	-7.637
120.677	4.258E-03	5.66E-03	-7.477
165.722	5.848E-03	6.29E-03	-7.371
241.909	8.536E-03	7.14E-03	-7.245
335.058	1.182E-02	7.95E-03	-7.137
561.396	1.981E-02	9.45E-03	-6.965
mean =			-8.606
variance =			0.406

## Supplement F-2 DNAPL Entry Calculations

In general, in order for pooled DNAPL to enter a fracture, the capillary pressure ( $p_c$ ) at the base of the pool must exceed the entry pressure ( $p_e$ ) of the fracture. Assuming the DNAPL is non-wetting with respect to water and that the system is in hydrostatic equilibrium, the capillary pressure at the base of the pool is given by [Pankow and Cherry, 1996],

$$p_c = (\rho_{nw} - \rho_w)gh \quad (1)$$

where  $\rho_{nw}$  is the non-wetting phase (DNAPL) density,  $\rho_w$  is the wetting phase (water) density,  $g$  is the gravitational constant, and  $h$  is the DNAPL pool height. The entry pressure,  $p_e$ , of a rough-walled fracture is approximated by [Kueper and McWhorter, 1991],

$$p_e = 2\sigma \cos \theta / b \quad (2)$$

where  $\sigma$  is the interfacial tension between the DNAPL and water,  $\theta$  is the contact angle, and  $b$  is the fracture aperture. The minimum pool height,  $H_o$ , producing entry into a fracture can be found by equating (1) and (2):

$$H_o = 2\sigma \cos \theta / [(\rho_{nw} - \rho_w)gb] \quad (3)$$

For purposes of this cursory examination of fracture entry conditions associated with the CNS tear gas DNAPL, we assume the fluid properties of CF (CF) listed below for the DNAPL:

- CF density,  $\rho_{nw} = 1.47 \text{ g/cm}^3$
- CF interfacial tension,  $\sigma = 32.8 \text{ dynes/cm}$

Other parameters used in the calculations include water density ( $1.00 \text{ g/cm}^3$ ) and the gravitational constant ( $980 \text{ cm/s}^2$ ). It is further assumed that water is perfectly wetting with respect to CF such that  $\cos \theta = 0$ . Estimates of the minimum pool heights required for entry into fractures in the size range observed at the Area 15A site are presented in the table below.

**Table F-2.1 Minimum Pool Heights Required for DNAPL Entry**

$b$ (m)	$\ln b$	$H_o$ (cm)	Relative Aperture Size of Observed Fractures
5.1E-05	-9.88	27.9	minimum
5.7E-05	-9.77	25.0	≈5 percentile
1.8E-04	-8.61	7.9	mean
9.4E-04	-6.96	1.5	maximum

Estimates of the time required to drain the contents of a 55-gallon drum of CNS tear gas DNAPL through a single fracture,  $t^*$ , are computed for the observed fracture aperture size range. These estimates are only crude approximations for purposes of gauging how long the initial downward flow and redistribution of tear gas DNAPLs may last following container failure. We assume steady flow of DNAPL through a single vertical fracture under the mean ambient hydraulic gradient of 30%. The flow rate,  $Q_f$ , through a fracture is given by [Van Golf-Racht, 1982],

$$Q_f = A \rho_{nw} g b^2 J_{nw} / (12 \mu) \quad (4)$$

where  $A$  is the cross-sectional area of the fracture,  $J_z$  is the equivalent DNAPL pressure gradient,  $\mu$  is absolute fluid viscosity (equal to 50.11 kg/(m\*d) for CF), and other terms are as previously defined.  $A$  is assumed equal to the fracture aperture,  $b$ , times a one meter unit width.  $J_{nw}$  is the product of the ambient hydraulic gradient,  $J_w$ , times the fluid density ratio,  $\rho_w/\rho_{nw}$ . Estimates are conservative since the density gradient created by the DNAPL is ignored. Table F-2.2 presents estimates of  $t^*$  for the range of fracture apertures observed at the site.

**Table F-2.2 Estimated DNAPL Flow Rates and Drainage Times**

$b$ (m)	$\ln b$	$Q_f$ (m <sup>3</sup> /d)	$t^*$ (d)	Relative Aperture Size of Observed Fractures
5.1E-05	-9.88	0.0049	42.8	minimum
5.7E-05	-9.77	0.0068	30.6	≈5 percentile
1.8E-04	-8.61	0.2142	1.0	mean
9.4E-04	-6.96	30.51	0.01	maximum

### Supplement F-3

#### Parameter Estimates for Container Failure Distribution

The mean and standard deviation of the Area 15A drum failure distribution are estimated from the historical information regarding the disposal site. Since we are approximating the container failure distribution as a normal probability density function, it is convenient to arbitrarily define upper and lower end points of the distribution in terms of some number of standard deviations ( $\sigma$ ) from the mean ( $\mu$ ). For this purpose, we arbitrarily assumed end points at  $\pm 3\sigma$  from the mean which encompasses approximately 99.86% of the region beneath the normal curve. The normal probability density function is defined by [Benjamin and Cornell, 1970],

$$f(x) = (e^{-1/2u}) / (\sigma \sqrt{2\pi}), \quad (1)$$

where,

$$u = (x - \mu) / \sigma \quad (2)$$

The cumulative probability distribution function is given as,

$$F(u) = (1 / \sqrt{2\pi}) \int e^{-1/2u} du \quad (3)$$

where the integral is evaluated from negative infinity to  $u$ . Referring to Figure 3-2(a), we arbitrarily define the lower end point of the distribution (i.e.,  $-3\sigma$ ) as year 1948, the assumed year containers were buried. We also know that by 1985 approximately 90% of the containers had failed which corresponds to 90% of the total area under the normal curve. Thus, we know that for  $x = 37$  years (i.e.,  $1985 - 1948 = 37$ ),  $F(u) = 0.90$ , and from standard probability tables [Benjamin and Cornell, 1970] we find the corresponding value to  $u = 1.28$ . From equation (2), we have,

$$\mu = 37 - 1.28\sigma \quad (4)$$

We also know that for  $x = 3\sigma$ ,  $F(u) \approx 0.5$  and  $u \approx 0.00$ , and from equation (2),

$$\mu = 3\sigma \quad (5)$$

The characteristics of the container failure distribution can be estimated from equations (4) and (5) to obtain,  $\sigma = 8.64$  years and  $\mu = 25.94$  years. In terms of calendar years,  $\mu \approx 1948 + 26 = 1974$ .

**APPENDIX G**  
**REMEDIATION STRATEGY SELECTION**

**REMEDIAL STRATEGIES FOR  
CNS TEAR GAS LANDFILL  
AREA 15A FEDERAL LABORATORIES PLANT NO. 3  
SALTSBURG, PENNSYLVANIA**

*Prepared for*  
**U.S. ARMY ENVIRONMENTAL CENTER**  
*Aberdeen Proving Ground, Maryland 21010-5401*

*Prepared by*  
**Tennessee Valley Authority**  
**Environmental Research Center**  
*Muscle Shoals, Alabama 35662-1010*

**December 1998**

**TVA Contract No. RG-99802V**



## EXECUTIVE SUMMARY

This report summarizes the results of an investigation of remedial strategy alternatives for a CNS tear gas landfill at Area 15A, Federal Laboratories Plant No. 3 near Saltsburg, Pennsylvania. The study of remedial strategies is part of a larger study aimed at determining the fate and effect of the CNS tear gas components. An estimated 300 to 1,700 55-gallon drums of CNS tear gas were buried at Area 15A sometime during the late 1940s. Contamination consistent with CNS tear gas has been detected in groundwater near the site, as well as in surface water downgradient of the site. Among the three tear gas components (chloroform, chloropicrin, and phenacyl chloride), chloroform is the most persistent at the site and is the only one that has been detected in surface water. Due to the high cost and short-term risks associated with *ex situ* remedial strategies, this investigation focused on *in situ* treatments. Strategies for remediating the soil in the tear gas drum burial area were considered, as were strategies for remediating the groundwater. Although most of the tear gas components are believed to have moved down below the soil, soil remediation was considered since the information derived from the study may be useful at other sites contaminated with CNS tear gas.

The complex geology and soil properties of the site make it a poor candidate for active remediation. The soil in the drum burial area is poorly suited for many remedial technologies due to its low permeability. And since contaminants are denser than water, strategies that mobilize the contaminants in the soil may risk speeding their downward movement into the underlying bedrock. Contaminants present in the bedrock move through a complex network of discrete fractures with concurrent diffusion into the adjacent porous rock matrix. While active remedial methods may efficiently treat contaminants within the fractures, contamination in the rock matrix is largely inaccessible to treatment due to its relatively low permeability.

For this investigation, previous investigations and feasibility studies of Area 15A, as well as groundwater monitoring data, were reviewed. Other sources of information used in

this study included chemical reference manuals, recently published information dealing with the remediation of chlorinated solvents, remediation technology screening matrices, proceedings from conferences involving remediation of chlorinated and recalcitrant compounds, and direct communication with researchers and vendors involved in remediation of chlorinated solvents. Review of literature revealed that studies involving chloroform remediation are scarce. Likewise, reports of successes involving remediation of chlorinated solvents in fractured bedrock are also scarce. Sources indicated that pump and treat technologies are not likely to be successful in remediating chlorinated solvents in fractured bedrock. Plume containment, however, can be achieved in fractured bedrock.

For remediating the groundwater at Area 15A, the following two strategies are the only practical alternatives:

- Monitored Natural Attenuation
- Plume containment using extraction wells on the outer edge of the plume near the location of surface discharge

Analysis of groundwater revealed that some natural attenuation is taking place. High concentrations of dichloromethane (the breakdown product of reductive dechlorination of chloroform) in groundwater about 500 feet downgradient of the landfill support this conclusion. Also phosgene, the oxidative degradation product of chloroform and chloropicrin, has been detected in groundwater. High levels of degradation products of phenacyl chloride have also been detected in groundwater. In view of the strong evidence of degradation of the tear gas components, aggressive chemical treatments are not recommended as they could destroy microorganisms responsible for degradation. To defend a natural attenuation strategy, an assessment of the risks associated with the contamination of surface water needs to be made. This assessment also requires a better quantification of the amount of CNS tear gas-derived material that is reaching surface water. Recent surface water monitoring indicates that low levels of only chloroform are reaching surface water. A more thorough investigation of the seep water downgradient of the site is needed to verify that the current seep sampling is capturing the contamination

originating from the landfill. Likewise, a better delineation of the contaminant plume is needed in order to place monitoring wells required for verifying predicted natural attenuation.

For remediating the soil in the drum burial area, the following strategies are recommended:

- *In situ* chemical/biological treatment involving the addition of ammonium hydroxide and methanol through a surface infiltration/irrigation system. Groundwater and amendments would be extracted for recycling using horizontal wells positioned in the soil-bedrock interface.
- Hot air injection and base addition using a large diameter vertical mixing auger with soil vapor extraction (SVE) for capturing volatile organic compounds (VOCs).

To ascertain the landfill's amenability to bioremediation, laboratory studies were conducted to determine the microbial health and buffering capacity of the contaminated soil from the tear gas drum burial area. Microbial populations were found to be quite low. This was due to the low pH of the soil and toxicity of the contaminants. The low pH of the soil (around 4.0) was found to be adjustable to a pH of 6.8 with the addition of around two pounds of either agricultural limestone or ammonium hydroxide per cubic yard of soil. The low pH and high chloride content of the landfill soil indicate that dechlorination of the compounds is taking place.

A small treatability study was conducted involving the addition of ammonium hydroxide to the contaminated soil to hydrolyze chloropicrin and phenacyl chloride. There was no increase in hydrolysis compared to the untreated controls. However, there was some degradation of all three compounds in both the treated and untreated soil. To determine the effectiveness of the chemical/biological treatment strategy and to select the proper amendments, more treatability studies would be required.

The strategy involving soil mixing, hot air injection, base addition, and SVE is technically feasible but requires some treatability testing to properly size the equipment, to determine the most suitable base, and to determine the most cost-effective levels of heat input. The benefit of both soil treatment strategies must be based on their value toward the long-term cleanup goals for the groundwater. A hydrogeologic modeling study of the fractured bedrock aquifer revealed that the time required to restore the groundwater would not be decreased significantly by the treatment of the soil in the landfill area. The hydrogeologic modeling study is described in detail in Appendix F of the Tear Gas Fate and Effects Study Report.

## TABLE OF CONTENTS

SECTION NUMBER	TITLE	PAGE NUMBER
1.0	INTRODUCTION	1
1.1	Introduction	1
1.2	Background	1
2.0	SITE DESCRIPTION	3
2.1	Site Location and Setting	3
2.2	Climate	5
2.3	Regional and Local Geology	5
2.4	Topography	7
2.5	Soil Type	7
2.6	Surface Waters	8
2.7	Groundwater	9
2.8	Contaminant Profile	11
2.8.1	Soil Contamination	11
2.8.2	Groundwater Contamination	11
2.8.3	Surface Water Contamination	16
2.9	Regulatory Actions	16
2.10	Current Response to Regulatory Action	17
2.11	Focus of Remedial Strategies	18
3.0	CONTAMINANT PERSPECTIVES	19
3.1	Presumptive Remedies	21
3.2	Data Requirements for Soil	22
3.3	Data Requirements for Groundwater	27
3.4	Data Requirements for Off-Gases	28
3.5	Properties and Behavior of CNS Compounds	29
3.5.1	Chloroform	29
3.5.2	Chloropicrin	31
3.5.3	Phenacyl Chloride	33
4.0	TREATMENT PERSPECTIVES	35
4.1	Soil Treatment Technologies	36
4.2	Groundwater Treatment Technologies	39
4.3	Containment Methods	43

## TABLE OF CONTENTS (Continued)

SECTION NUMBER	TITLE	PAGE NUMBER
5.0	TECHNOLOGY PROFILES	44
5.1	Technologies Rejected	44
5.2	Summary of Similar Remedial Actions	46
5.3	Technologies Considered	47
5.3.1	<i>In situ</i> Biological Treatments	49
5.3.2	<i>In situ</i> Chemical Treatments	54
5.3.3	<i>In situ</i> Thermal Treatment	56
5.4	Groundwater Treatment Technologies	57
5.4.1	Containment Methods	57
5.4.2	Monitored Natural Attenuation	58
5.5	Additional Site Characterization Recommendations	60
6.0	SUMMARY AND RECOMMENDATIONS	62
7.0	REFERENCES	65

## LIST OF TABLES

TABLE NUMBER	TITLE	PAGE NUMBER
3-1	Physical Properties of Area 15A Uncontaminated Soils	24
3-2	Physical Properties of Contaminated Area 15A Soil	24
3-3	Hydraulic Properties of Uncontaminated Area 15A Soil	26
3-4	Individual and Mixture Solubilities of CNS Components	30
3-5	Chloroform Physical and Chemical Properties	30
3-6	Chloropicrin Chemical and Physical Properties	32
3-7	Phenacyl Chloride Chemical and Physical Properties	34
4-1	Soil Treatment Technology Descriptions	37
4-2	Comparison of Soil Treatment Technologies	38
4-3	Groundwater Treatment Technologies	41
5-1	Treatment Technologies Rejected	45
5-2	<i>In situ</i> Soil Treatment Technologies Screening Matrix	48

## LIST OF FIGURES

FIGURE NUMBER	FIGURE TITLE	PAGE NUMBER
2-1	Location of Federal Laboratories Plant No. 3	4
2-2	Surface Drainage in the Vicinity of Area 15A	6
2-3	Generalized Hydrogeologic Profile Through Disposal Site	10
2-4	Temporal Plots of Chloroform Contamination in MWS-8 and MWS-5A	13
2-5	Temporal Plot of Chloropicrin Contamination in MWS-8 and MWS-5A	14
5-1	Conceptual Schematic for Chemical/Biological Injection and Recovery System	52

## SECTION 1.0

### INTRODUCTION

#### 1.1 Introduction

The United States Army Environmental Center (USAEC) contracted with Tennessee Valley Authority (TVA) to conduct a scientific study of the fate, transport, and effects of CNS tear gas in soils. The goal of this study was to obtain basic information about the behavior of soil-borne CNS tear gas components that could be used in modeling their behavior in soil and groundwater. A landfill used to dispose of several hundred drums of CNS tear gas after World War II was selected by the U.S. Congress as the focus of this study. Information obtained from the fate, transport, and effects study was used in hydrogeologic models to predict the fate and transport of the CNS tear gas components placed in the landfill. This information, additional published information, and discussions with knowledgeable individuals were used to identify and evaluate the technical merits of remedial options for the landfill site. Factors that influence remedial technology selection, such as properties of the contaminants, site hydrogeology, and regulatory concerns, are also discussed.

#### 1.2 Background

CNS tear gas consists of a mixture of 2-chloroacetophenone (CN), chloropicrin, and chloroform with the following approximate composition: 24% CN, 38% chloropicrin, and 38% chloroform. CN, also known as phenacyl chloride, is a strong lachrymator. Chloropicrin is a vomitory agent and chloroform functions as a solvent for phenacyl chloride which would otherwise exist in solid form. Due to differing properties and characteristics, these compounds separate in the environment and may require different means for extraction or remediation.



The site selected for this study is the Federal Laboratories Plant No. 3 in Saltsburg, Pennsylvania. The Saltsburg site was first used during World War II. In the months before the United States' official entry into World War II, the Army's Chemical Warfare Service (CWS) identified three sites for the construction of new manufacturing facilities. These three facilities were to be owned and operated by private contractors for the manufacture and loading of incendiary bombs. One of the three facilities was located in Saltsburg, Pennsylvania, and the operator of this facility was Federal Laboratories, Inc. The Saltsburg facility was designated as Plant No. 3 because it was the third facility that Federal Laboratories operated in western Pennsylvania. From December 1941 through the end of the Vietnam conflict, Plant No. 3 was used to manufacture a wide variety of products for the military, including incendiary bombs, tear gas, vomit gas, munitions, numerous other pyrotechnic weapons, and non-lethal chemical weapons.

Following World War II, there was a surplus of the CNS material. Disposal of surplus CNS materials involved several private companies, including the Federal Laboratories. Although open burning was commonly used to dispose of surplus material at the Federal Laboratories site, some 300 to 1,700 drums of CNS were buried at the plant site. Several environmentally contaminated areas were identified at the Federal Laboratories site during an inspection by the U.S. Environmental Protection Agency Region III Field Investigation Team in 1983 and 1984. The burial location for the CNS tear gas drums was designated as Area 15A. The resulting environmental contamination from Area 15A is now the subject of an environmental investigation being conducted by TransTechnology Corporation, the present owner of Plant No. 3, and the successor-in-interest to Federal Laboratories.

## SECTION 2.0

### SITE DESCRIPTION

#### 2.1 Site Location and Setting

Federal Laboratories Plant No. 3 is located in Conemaugh Township, Indiana County, Pennsylvania. The facility is approximately 3 miles east of the town of Saltsburg and 1-1/2 miles north of the town of Tunnelton (Figure 2-1). The facility is approximately 2 miles north of the Conemaugh River. Manufacturing activities at the facility have occurred on approximately 35 acres adjacent to State Road 3003, commonly referred to as Tunnelton Road. Federal Laboratories Plant No. 3 is located on a hillside which generally slopes to the west-southwest. Area 15A is located in the western portion of the site and is approximately 1,000 feet east of Elders Run, a tributary of the Conemaugh River. Tributary B of Elders Run borders the western edge of the property and is about 400 feet west of Area 15A (Figure 2-2).

Published reports claim that 300 to 1,700 55-gallon drums of CNS tear gas that were shipped to Federal Laboratories after World War II were eventually buried in what is now known as Area 15A. The area is approximately 200 feet wide and 550 feet long. Photographs of the burial site before backfilling indicate that 1,700 is a good approximation of the number of drums buried.<sup>Ref. 1</sup>

It is evident that the buried drums are leaking. Test pits in the burial area have revealed rusted and deteriorated drums. It is estimated that 90% of the buried CNS has been released to the subsurface environment.<sup>Ref. 2</sup> Contamination consistent with CNS has been detected in groundwater at Area 15A, as well as in surface water draining into Tributary B of Elders Run (Figure 2-2). It is not believed, however, that contamination has migrated to any municipal or private

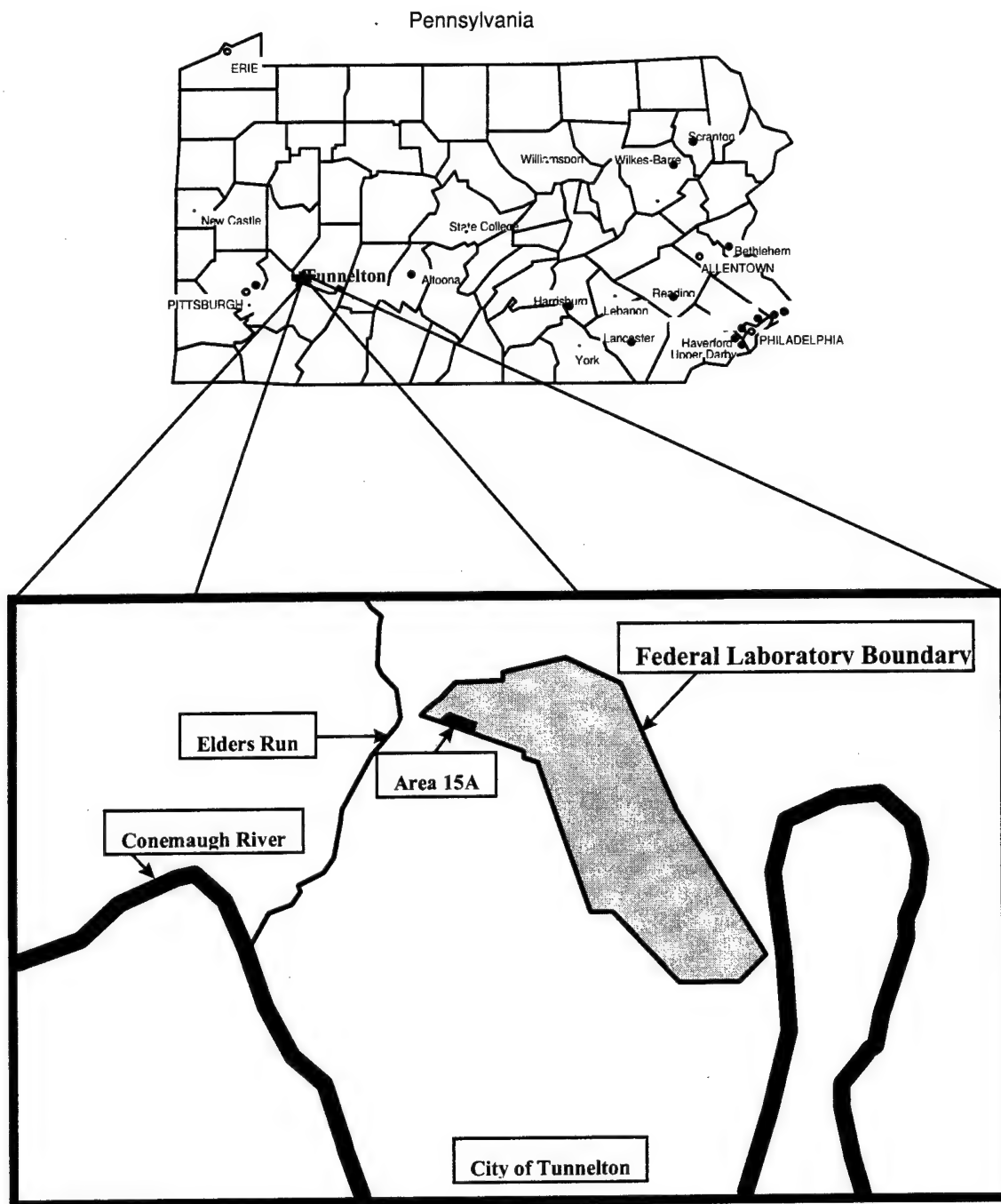


**Figure 2-1**  
**Location of Federal Laboratories Plant No. 3**

water supplies. Chloroform is the only contaminant associated with the CNS tear gas that has been detected in Tributary B near Area 15A. Chloroform and chloropicrin are highly volatile and have distinctive odors recognizable at relatively low concentrations.

## **2.2 Climate**

Indiana County has a continental climate with warm humid summers and cold winters. Prevailing winds from the west and southwest bring most of the major pressure systems affecting the area. The average wind direction is from the southwest (south 72° west).

Regional precipitation data (1962 to 1992) indicate an average annual precipitation of 36.4 inches. The maximum monthly precipitation rate was 11.05 inches (November 1985). The minimum monthly precipitation was 0.16 inch (October 1963). Annual precipitation for Tunnelton ranges from 40 to 44 inches. Temperature data indicate an annual average temperature of 52°F. Monthly highs average 77°F in July and monthly lows average 11°F in January.<sup>Ref. 3</sup>

## **2.3 Regional and Local Geology**

The Federal Laboratories Plant No. 3 is located within the Pittsburgh Plateaus Section of the Appalachian Plateau Physiographic Province. Geologic strata under the facility belong to the Pennsylvanian Age Glenshaw Formation of the Conemaugh Group. The Ames Limestone and Harlem (Friendsville) Coal form the upper boundary of the Glenshaw Formation while the Upper Freeport Coal defines its base. Water-bearing zones within the Glenshaw Formation include the Saltsburg, Buffalo, and Mahoning Sandstones.

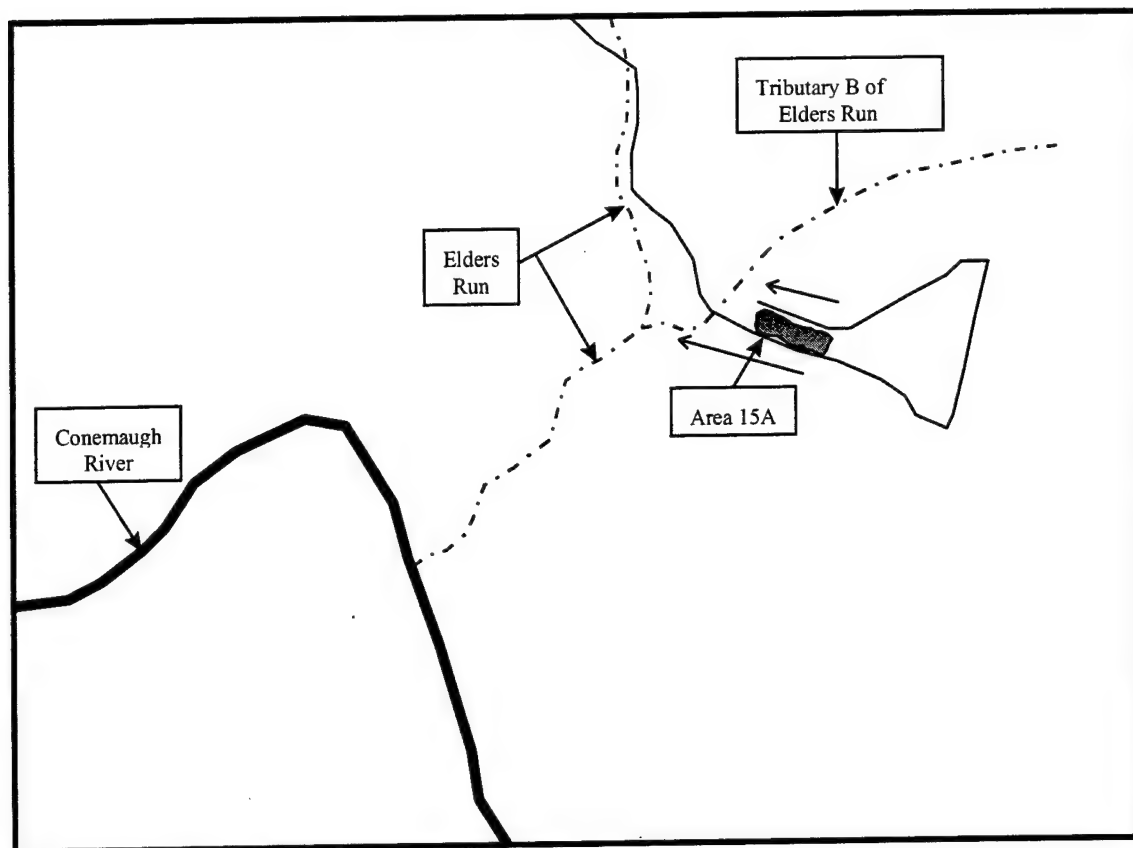


**Figure 2-2**  
**Surface Drainage in the Vicinity of Area 15A**

These units are subject to stratigraphic variation, both laterally and vertically, and consist of cyclic sequences of sedimentary rocks. Structural contours, based on the elevation of the Upper Freeport Coal Seam, indicate that regional geologic structures consist of a series of northeast-southwest trending anticlines and synclines. Area 15A is located on the southwestern flank of the Jacksonville Anticline which plunges gently to the southwest in this area.

## **2.4 Topography**

The entire Federal Laboratories facility is located on a hillside which generally slopes to the west-southwest (Figure 2-2).

Surface drainage from the facility is intercepted by three unnamed tributaries:

- Tributary A of Elders Run which flows north to south through the central portion of the facility collects the majority of the drainage from the site.
- Tributary B of Elders Run drains the westernmost portion of the property adjacent to Area 15A.
- A tributary draining the southeastern portion of the facility to the Conemaugh River.

## **2.5 Soil Type**

Indiana County soil survey maps indicate that the former disposal areas are located in soils of the Brinkerton, Gilpin, and Wharton Series. Soil identification tests conducted during an environmental site assessment indicate Area 15A contains soils of the Wharton Series. The Wharton Series is typically located on gently sloping broad hilltops and benches. The series consists of moderately well-drained residual soils developed from shale.

Other soil types that could be present are the Brinkerton Series which is generally located in gently sloping valleys and consists of poorly drained soils developed from materials eroded from adjacent uplands and the Gilpin Series which consists of moderately deep, well-drained soils developed from shale and sandstone bedrock.

## **2.6 Surface Waters**

The Federal Laboratories site has three distinct drainage basins. Drainage Basin I comprises the northwestern portion of the Federal Laboratories property and is drained by Tributary B of Elders Run. Basin I has an approximate surface area of 150 acres and contains Area 15A. Drainage Basin II is oriented north to south through the approximate center of the property and receives the majority of the surface drainage from the Federal Laboratories site. Basin II has an approximate surface area of 726 acres and is drained by Tributary A of Elders Run. Drainage Basin III drains into the unnamed stream that flows into the Conemaugh River. Basin III has an approximate surface area of 393 acres. Discharge from Basin III is generally limited to a portion of the runoff from Area 17 in the southeastern part of the Federal Laboratories site.

An impoundment located north of the facility's operations area collects the majority of drainage from this area of the site. This impoundment has been present for many years and currently is used to supply water to a firewater storage tank and non-potable water system.

## 2.7 Groundwater

Geologic information obtained from site investigations identified the Saltsburg Sandstone as the first continuous water-bearing zone beneath the Federal Laboratories facility.<sup>Ref. 2</sup> The Buffalo Sandstone was identified as the first water-bearing zone underlying the Saltsburg Sandstone (Figure 2-3).

Under the eastern section of the facility, groundwater associated with the Saltsburg Sandstone generally flows from northeast to southwest. Groundwater flow generally follows local topography, but may also be influenced by geologic structure. Potentiometric surface contours steepen in the vicinity of the unnamed tributary to Elders Run which flows through the northwestern portion of the site's property. In the western portion of the site near Area 15A, groundwater generally flows from northeast to southwest.

Groundwater flow direction within the Buffalo Sandstone is to the southeast in the eastern section of the Federal Laboratories site following structural trends. The western section of the site adjacent to Study Area 15A is located along the northwestern flank of the Jacksonville Anticline. Groundwater flow within the Buffalo Sandstone in this area is nearly east-west, reflecting this structural relationship.



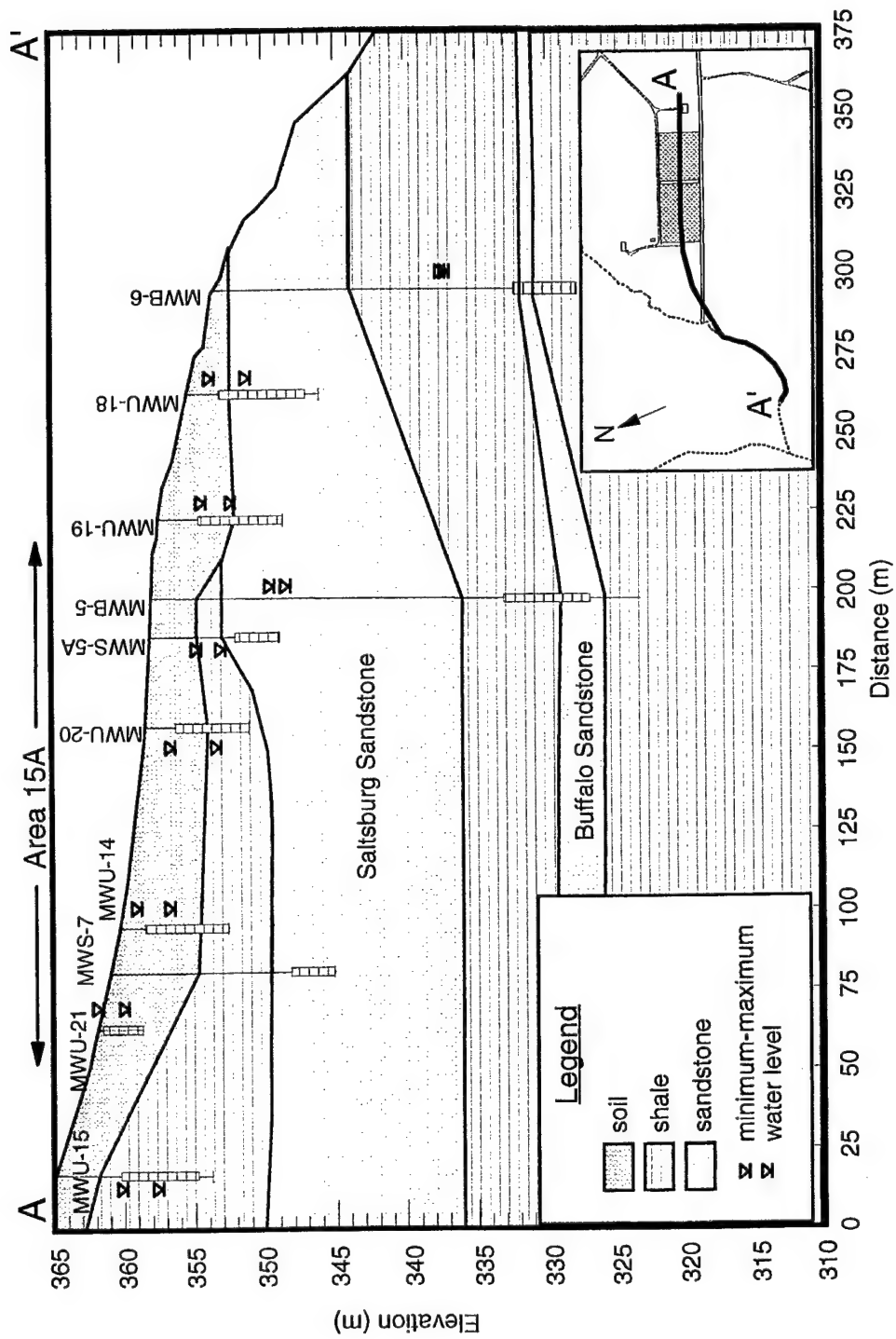


Figure 2-3 Generalized Hydrogeologic Profile Through Disposal Site

## **2.8 Contaminant Profile**

### **2.8.1 Soil Contamination**

In November 1997, samples were collected from Area 15A overburden soils. A soil sample taken from a depth 6 to 9.5 feet had the following concentrations of tear gas compounds:

Chloroform (mg/kg)	Chloropicrin (mg/kg)	Phenacyl Chloride (mg/kg)
25.8	23.4	31.4

Compared to the original formulation of the CNS tear gas (38% chloropicrin, 38% chloroform, and 24% phenacyl chloride), the phenacyl chloride concentration in this soil sample is high relative to the other two components. This may be a reflection of its lower mobility and higher tendency to be adsorbed to the soil. Despite the volatility of the chloroform and chloropicrin and their distinct odors, no odors were detected at ground level during the November 1997 sampling event. However, the sample with contaminant concentrations listed above had a distinctive odor indicating that chloroform and chloropicrin were present.

### **2.8.2 Groundwater Contamination**

The horizontal extent of groundwater contamination within the Saltsburg Sandstone in the vicinity of Area 15A is defined.<sup>Ref. 4</sup> Contaminant migration is to the west-southwest. Wells located upgradient of Area 15A contain no VOCs or only minor amounts of chloroform.

Wells located downgradient of the tear gas landfill, in the west and southwest, contain CNS contaminants. Samples collected from 1985 through 1992 in wells closest to the drum burial area revealed that the concentrations of chloroform, chloropicrin, and phenacyl chloride remained relatively constant over this time

period.<sup>Ref. 4</sup> More recent historical data is available from well MWS 8, located near the western boundary of the landfill. Samples taken in April 1986 and in June 1997 exhibited chloroform concentrations, respectively, of 190 and 200 mg/l. The near constant level of chloroform in the groundwater near the landfill indicates that chloroform in the bedrock is being solubilized by the groundwater at a steady rate. The same well has shown an average concentration of chloropicrin of 23.0 mg/l from May 1985 to June 1997. Phenacyl chloride concentration in MWS 8 has averaged 8.5 mg/l over the same time period.

The concentrations of chloroform over time in wells MWS-8 and MWS-5A are shown in Figure 2-4. Chloropicrin concentrations over time in the same wells is shown in Figure 2-5. The concentrations equivalent to 1% of the effective mixture solubilities of the two compounds are also shown in the plots. The effective mixture solubility is the amount of each component that is expected to dissolve in water when the mixture comes into contact with water. As a general rule, if concentrations of a DNAPL in groundwater exceed 1% of the effective solubility, then free-phase product is most likely present (see Figure 2-4 and 2-5). In borehole flowmeter tests conducted at the site in 1997, some synthetic components of the flowmeter assembly were damaged from solvent attack, suggesting the presence of residual product. The mixture solubility is discussed in more detail in Section 3.5 Properties and Behavior of CNS Compounds. The zero values in Figure 2-4 and 2-5 mean that there was no data for that particular date or the value was below the Method Detection Limit. Since Method Detection Limits were often very high for chloropicrin (10,000 µg/l to 100,000 µg/l), zero values do not represent an absence of chloropicrin.

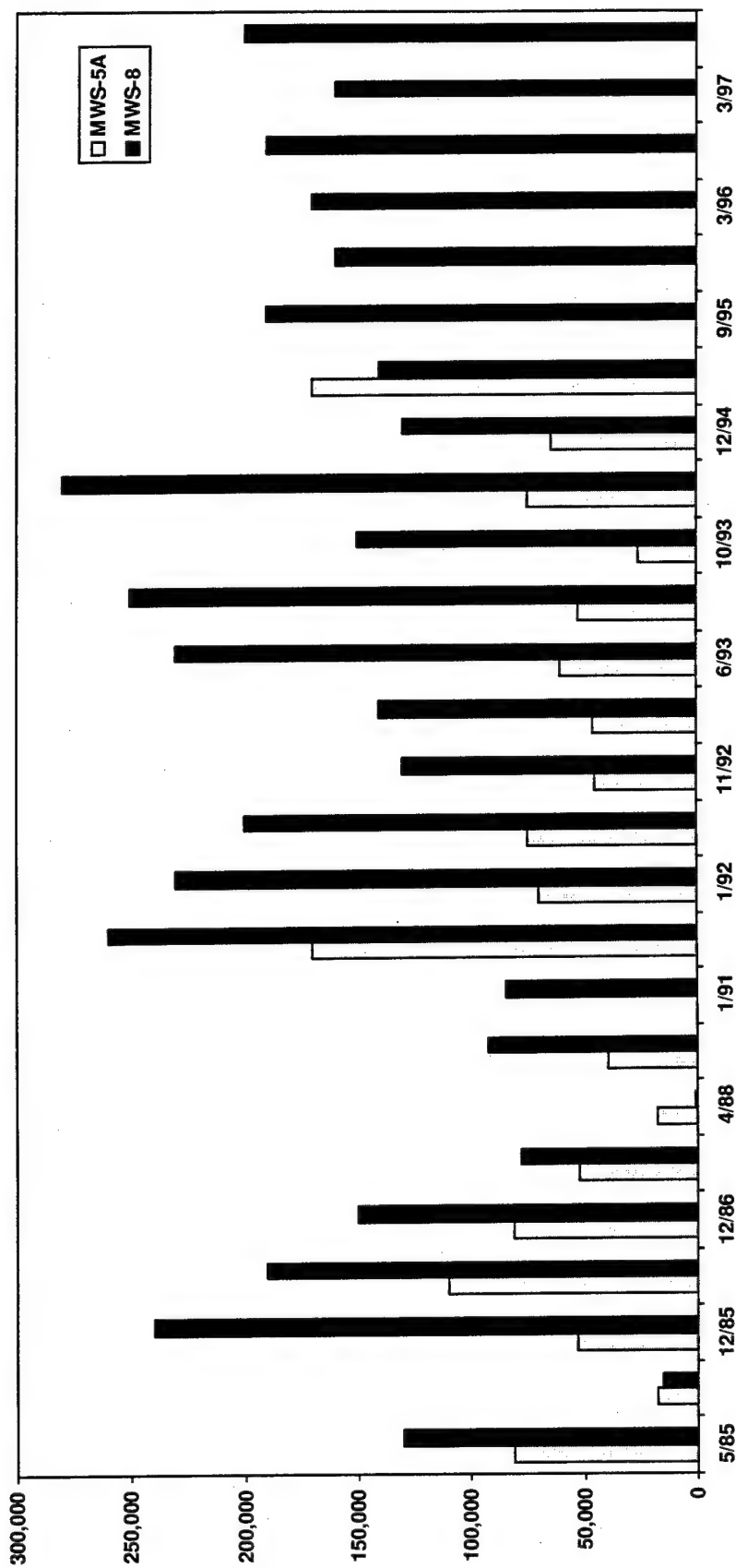


**Figure 2-4**  
Temporal Plots of Chloroform Contamination in MWS-8 and MWS-5A

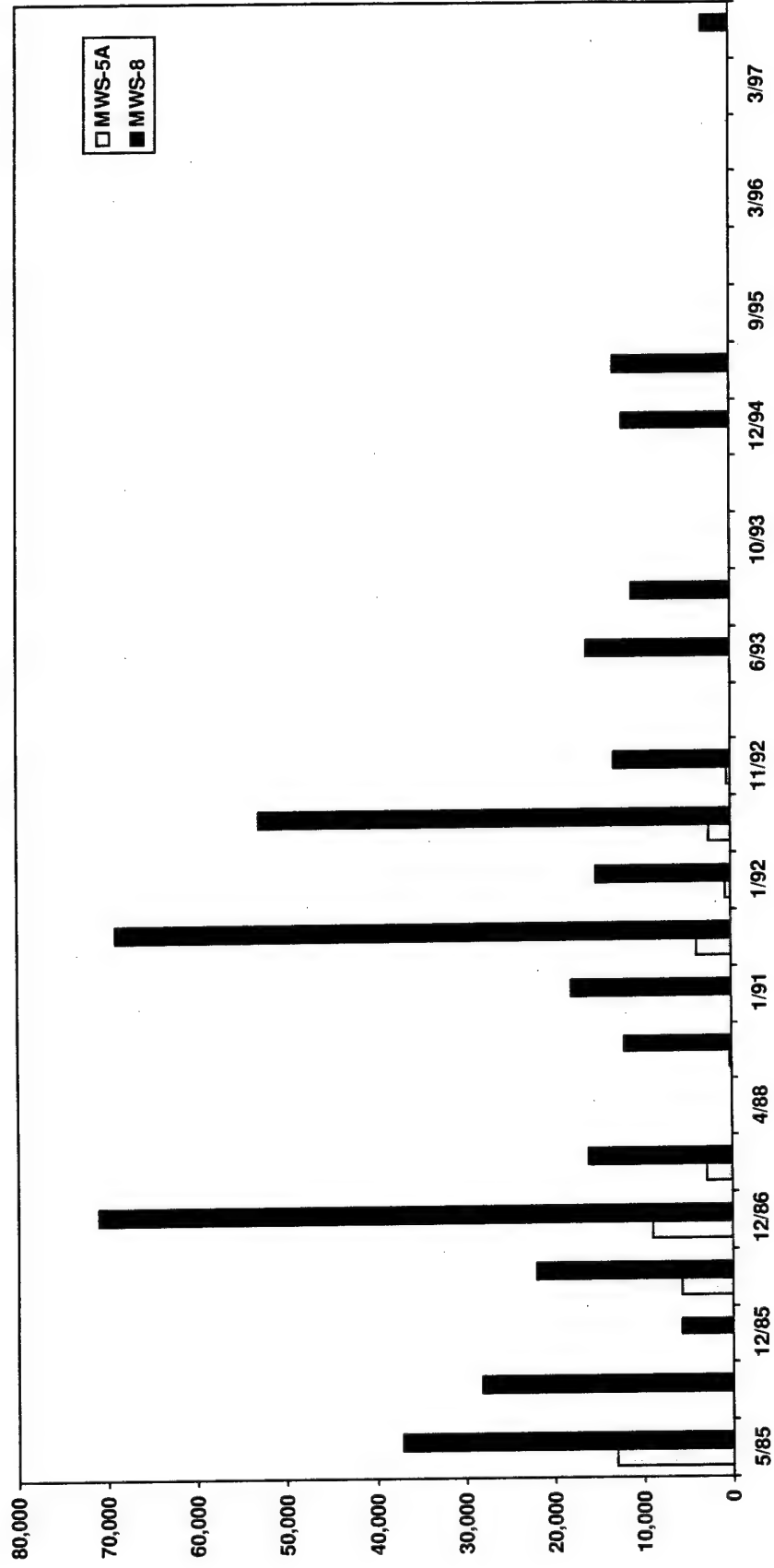


**Figure 2-5**  
Temporal Plot of Chloropicrin Contamination in MWS-8 and MWS-5A

The maximum concentrations of the three compounds found in wells downgradient of the landfill between 1995 and 1997 were as follows:

- 36 mg/l phenacyl chloride, well MWS-8<sup>Ref. 5</sup>
- 680 mg/l chloroform, well MWU-20<sup>Ref. 6</sup>
- 53 mg/l chloropicrin, well MWU-20<sup>Ref. 6</sup>

Groundwater flow in the vicinity of these wells is to the west-southwest toward the stream valley of Elders Run. The Saltsburg Sandstone outcrops along these valley walls at an approximate elevation of 1,130 feet, thus delineating the extent of contaminant migration to the west of Area 15A.<sup>Ref. 4</sup>

The vertical extent of contaminant migration appears to be generally limited to the Saltsburg Sandstone in the vicinity of Area 15A, although sampling below the Saltsburg has been limited to just three wells completed in the underlying Buffalo Sandstone. Only twice have VOCs been detected in Buffalo Sandstone monitoring wells near Area 15A. Low concentrations of chloroform (7 and 16 µg/l) were detected in this formation on two occasions from October 1987 through July 1992.

In summary, groundwater contamination in the vicinity of Area 15A appears to be primarily limited to the Saltsburg Sandstone. Groundwater related to the Buffalo Sandstone formation has been largely unaffected. Groundwater from the Saltsburg Sandstone appears to discharge to the surface as an intermittent seep or seeps which flow into Tributary B of Elders Run. A water supply inventory conducted in 1985 indicates that no domestic water supply wells exist within the contaminated water-bearing zones defined at the facility.

### **2.8.3 Surface Water Contamination**

Chloroform has been detected in seeps which drain into Tributary B of Elders Run (see Figure 2-2). During the July 1997 sampling event, chloroform was detected at a concentration of 900 µg/l. Chloroform has been detected only once in Elders Run. In 1985, a sample taken from Elders Run had a chloroform concentration of 14 µg/l. Neither chloropicrin nor phenacyl chloride has been detected in any surface water samples since 1985. <sup>Ref. 5, 6</sup>

### **2.9 Regulatory Actions**

In 1983 and 1984, the U.S. EPA Region III field investigation team identified several areas of soil and groundwater contamination at the Federal Laboratories facility near Saltsburg. In response to these findings, Earth Sciences Consultants, Inc., was retained to conduct a series of focused environmental investigations at the facility. During the investigations conducted in 1985 and 1986, one water sample from Elders Run had a very low concentration of chloroform. In a subsequent investigation conducted in 1991, low levels of chloroform were found in water collected from a seep downgradient of Area 15A and in water collected from Tributary B of Elders Run. The detection of chloroform in surface waters and groundwater outside of the Federal Laboratories property became the impetus for regulatory action by the Pennsylvania Department of Environmental Resources (PADER).

An Interim Monitoring Program (IMP) that requires quarterly sampling of groundwater and surface water and measurement of hydraulic heads in the upper (Saltsburg Sandstone), middle, and lower (Buffalo Sandstone) water-bearing zones was implemented in 1995.

## 2.10 Current Response to Regulatory Action

In response to PADER's concern regarding the offsite migration of chloroform, TransTechnology Corporation is currently developing a remedial strategy aimed at preventing CNS contaminants from reaching Elders Run. The strategy proposed by TransTechnology Corporation is referred to as a targeted pump and treat system. This involves an array of extraction wells oriented north-south that intercept groundwater from the uppermost aquifer (Saltsburg Sandstone) before it reaches discharge seeps. An *ex situ* treatment system is proposed to either degrade the contaminants in the liquid phase or remove them from the water and treat them as a vapor. A key element of the strategy is positioning of extraction wells downgradient of the contaminant source and near the point of surface discharge, the seeps. At this location, the concentration of contaminants in groundwater should be much lower than near the source, thus reducing the size and complexity of the water or off-gas treatment system. The location of the proposed targeted pump and treat system is on property adjacent to the Federal Laboratories boundary.

To design the targeted pump and treat system, a groundwater investigation was conducted in 1998 to determine the extent of the contaminant plume in the vicinity of the proposed extraction wells. The investigation entailed the installation of five upper zone and two middle zone wells southwest of Area 15A on the adjacent property. Results of the investigation revealed that the plume has a more southerly component than predicted. The implication is that the array of extraction wells will need to extend farther south than originally anticipated. At the time of this writing, TransTechnology is awaiting a response from PADER regarding the results of the groundwater investigation.



## 2.11 Focus of Remedial Strategies

This investigation of remedial strategies is focused on soil within the drum burial area of Area 15A. Despite the fact that the majority of the tear gas is no longer in drums and has infiltrated the fractured bedrock below, it is prudent to consider remediating the source for two reasons: 1) the remediation of the source area may shorten the required duration of the targeted pump and treat activities, and 2) the alternatives considered for the tear gas landfill may be applicable to other sites at Federal Laboratories or other military sites with CNS tear gas contamination.

*In situ* technologies for remediating the tear gas landfill area will also be examined in this study. In a previous evaluation of remedial alternatives for Area 15A, an *in situ* chemical/biological approach was selected based on relative performance and cost.<sup>Ref. 3</sup> The previous study provides no details of the chemical/biological technologies involved. This study considers many state-of-the-art chemical oxidative and reductive technologies, as well as biological approaches that have merit.

### SECTION 3.0 CONTAMINANT PERSPECTIVES

Information related to the properties and concentrations of chemical contaminants and their distribution within soil and bedrock at the site is essential for evaluation and selection of treatment technologies. For the purpose of screening potential technologies, the CNS tear gas compounds can be placed into one of two classes of chemicals. Chloroform and chloropicrin are considered halogenated volatile organic compounds and phenacyl chloride is a halogenated semi-volatile organic compound. Subsurface contamination by these compounds can exist in four phases:

- Gaseous phase - present as vapors in the unsaturated zone.
- Solid phase - present in liquid or solid form and adsorbed on soil particles in both the saturated and unsaturated zone.
- Aqueous phase - dissolved into pore water or groundwater according to solubility.
- Immiscible phase - present as dense, non-aqueous phase liquids (DNAPLs).

Transport of DNAPL within the bedrock aquifer will be controlled by the aperture size, orientation, and connectivity of fractures and by prevailing hydraulic gradients. Shallow fluid movement in the bedrock will occur primarily through a relatively sparse network of hydraulically active fractures as indicated by flowmeter testing. Only limited flow is expected in the Sandstone-shale rock matrix due to its low hydraulic conductivity. On entering fractures, the relatively soluble DNAPL compounds, such as chloroform, may dissolve and subsequently diffuse into (and out of) the rock matrix as they are transported with ambient groundwater. Migrating DNAPL may also become disconnected or trapped by capillary forces in narrow fractures forming zones of residual product. These regions of residual product and rock matrix contamination result in persistent sources of dissolved-phase contamination within the bedrock and are important

factors in the fate and transport of the tear gas contaminants.

Limited upward diffusion of volatile contaminants may also occur through the soil vadose zone above the drum-burial zone. Volatile losses are most likely for chloroform and, to a lesser extent, chloropicrin and chloroacetophenone. Overall vapor losses are expected to be small since the vapor densities of these compounds (which range from approximately 4.1 to 5.7) greatly exceed that of ambient air indicating a tendency for vapors to sink rather rise in the vadose zone. Vapor losses may be enhanced by seasonal water table fluctuations which may force vapors to the surface as rising water displaces soil vapors.

Seismic and electrical resistivity techniques for locating DNAPL have recently been tested. The seismic reflection survey technique is based on the attenuation of seismic signals due to the presence of DNAPL. In tests involving fractured bedrock, seismic reflection was able to locate large fractures (void space) in bedrock, but was not able to determine if the fractures contained DNAPL. The accuracy of the depth estimates also decreased with increasing depth. The estimated cost for a seismic survey is \$100,000.<sup>Ref. 7</sup> A less expensive technique for locating fractures is called fracture trace analysis and involves the use of high resolution aerial photographs and stereo imaging. Fracture trace analysis can be used to help position extraction wells as it can locate zones of high groundwater flow associated with fractures.

The surface-to-borehole resistivity method is based on the ability to image contaminants due to their higher electrical resistance. This technology has been used successfully to find LNAPL but was not effective for finding DNAPL.

Partitioning interwell tracer tests (PITT) have been used to verify the degradation of DNAPL. PITT technology involves the injection and retrieval of a tracer (alcohol or solvent) in groundwater wells. The tracer combines with DNAPL and

the amount of DNAPL present is estimated based on the loss of tracer. This technique has been approved to validate DNAPL degradation in porous media. In fractured media, the presence of preferential flow paths render PITT technology unusable.

### 3.1 Presumptive Remedies

A presumptive remedy is a technology that EPA believes will generally be the most appropriate remedy for a specific type of site. EPA is establishing presumptive remedies to accelerate the assessment of technologies by focusing the feasibility study. EPA expects that a presumptive remedy, when available, will be used for all CERCLA sites except under unusual conditions. Accordingly, EPA has determined that the site characterization data collection effort and the detailed analyses can be limited to the presumptive remedy, thereby streamlining the feasibility study. There are currently seven published presumptive remedy documents. Three that may be applicable to the types of contaminants at Area 15A are as follows:<sup>Ref. 8, 9, 10</sup>

- *Presumptive Response Strategy and Ex-Situ Treatment Technologies for Contaminated Groundwater at CERCLA Sites. Final Guidance* (EPA, 1996). EPA Document No. 540-R-96-023.
- *User Guide to the VOC's in Soils. Presumptive Remedy* (EPA, 1996). EPA Document 540-F-96-008.
- *Presumptive Remedies: Site Characterization and Technology Selection for CERCLA Sites With Volatile Organic Compounds in Soils* (EPA, 1993). EPA Document No. 540-F-93-048.

Soil vapor extraction (SVE), thermal desorption, and incineration are the presumptive remedies for Superfund sites with VOC-contaminated soil where the site characteristics meet certain criteria.<sup>Ref. 10</sup> Hydraulic conductivity of the soil in the tear gas drum burial area (ranging from  $7.0 \times 10^{-9}$  to  $5.0 \times 10^{-6}$  cm/sec) is less than ideal for treatment by SVE. EPA's guide for VOCs in soils<sup>Ref. 9</sup> suggests that soil permeability should be greater than  $10^{-6}$  cm/sec to be suitable for treatment by SVE. The high costs and short-term risks associated with the *ex situ* treatments, thermal desorption or incineration, make them unsuitable options for Area 15A. Remedies involving excavation and treatment of soil were rejected in the previous feasibility study.<sup>Ref. 3</sup> A more detailed description of remedial alternatives and their suitability is given in Section 4 - Treatment Perspectives.

### 3.2 Data Requirements for Soil

Site soil conditions frequently limit the selection of treatment processes. Some characteristics, such as pH and moisture, may be adjustable. However, other characteristics, such as soil particle size and organic matter content, may restrict treatment options. Below is a list of soil properties and characteristics that must be considered when selecting a treatment technology.

- Soil particle size distribution
- Soil homogeneity
- Bulk density
- Soil permeability
- Soil moisture
- Soil pH
- Humic content or organic matter content
- Total organic carbon (TOC)
- Availability of electron acceptors (i.e., oxygen, nitrate, iron, manganese, and sulfate)

Soil particle size distribution is an important factor for many soil treatment technologies. In general, coarse, unconsolidated soils are easiest of all types to

treat. Soil with high percentages of clay are difficult to treat by thermal desorption because of their tendency to cake. High silt and clay content are generally associated with low permeability soils, thus lowering the efficiency of vapor extraction processes or injection processes.

Soil homogeneity is desirable for obtaining uniform treatment by methods dependent on subsurface flow of gases or liquids. SVE and *in situ* treatments involving the addition of oxidizers or addition of materials for enhancing biodegradation of contaminants will perform better in a more homogeneous soil.

Soil permeability is the primary controlling factor of *in situ* treatment. The time required to move nutrients or other additives to the soil is highly dependent on permeability. High moisture content can hinder vacuum extraction processes but can be desirable for biodegradation processes. Extreme pH can deter biological activity. Most microbes favor a near neutral pH.

Physical characteristics of Area 15A soils are shown in Table 3-1. Soils identified as coming from Areas 1 and 2 were sampled near the western border of the tear gas landfill. Area 3 was near the eastern border of the landfill. The exact location of samples and details of the soil sampling are provided in Appendix A of this Tear Gas Fate and Effects Study report.

The organic carbon fraction for the Area 3 sample at a depth of 6 to 8 feet is considered anomalously high due to its close proximity to the contaminated zone. The average pH for the soil, 5.13, is typical for soils in the area.

Table 3-2 lists the properties of the one sample of contaminated soil taken from the tear gas landfill overburden. With the exception of pH, the physical properties of the contaminated soil are similar to those of the uncontaminated soil. The

**Table 3-1**  
**Physical Properties of Area 15A Uncontaminated Soils**

<b>Soil Identification</b>	<b>Sand (%)</b>	<b>Silt (%)</b>	<b>Clay (%)</b>	<b>Organic Carbon (%)</b>	<b>pH</b>	<b>Soil Texture</b>
Area 1 (6" - 2')	18.2	57.7	24.1	0.62	5.72	silt loam
Area 1 (2' - 4')	33.6	39.4	27.0	0.23	5.01	loam
Area 2 (6" - 2')	48.3	34.0	17.7	0.34	4.94	loam
Area 2 (2' - 4')	43.6	34.1	22.0	0.22	4.96	loam
Area 2 (4' - 6')	56.6	24.5	18.9	0.18	4.78	sandy loam
Area 3 (0' - 3')	14.1	56.2	29.7	0.74	4.94	silty clay loam
Area 3 (3' - 6')	8.2	61.0	30.8	0.62	5.38	silty clay loam
Area 3 (6' - 8')	11.8	59.1	29.1	3.85	5.27	silty clay loam
Averages	29.3	45.8	24.9	0.42*	5.13	

\*Average excluding Area 3 (6' - 8')

**Table 3-2**  
**Physical Properties of Contaminated Area 15A Soil**

<b>Soil Identification</b>	<b>Sand (%)</b>	<b>Silt (%)</b>	<b>Clay (%)</b>	<b>Soil Texture</b>	<b>Organic Carbon (%)</b>	<b>pH</b>
Area 15A (6' - 9.5')	19	48.7	32.3	Silty clay loam	0.48	3.89
<b>Soil Identification</b>	<b>Moisture (%)</b>	<b>Bulk Density (g/cm<sup>3</sup>)</b>	<b>Particle Density (g/cm<sup>3</sup>)</b>	<b>Soil Porosity (%)</b>	<b>Soil-Gas Diffusion (m<sup>2</sup>/d)</b>	
Area 15A (6' - 9.5')	11.6	1.67	2.56	34.8	1.8	

contaminated soil is more acidic (3.89 vs 5.13) than the uncontaminated soil. This supports the assertion from previous reports that chloroform and chloropicrin have decomposed to carbon dioxide and hydrochloric acid.<sup>Ref. 2, 11</sup>

All of the soil physical properties were measured by TVA. The Soil-Gas Diffusion coefficient was calculated from:

$$D_G = \frac{a^{10/3}}{\phi^2} D_G^{\text{air}}$$

where  $D_G^{\text{air}}$  is assumed to be 0.43 m<sup>2</sup>/d,  $\phi$  is the soil porosity, and  $a$  is the difference in soil porosity and water content.

Table 3-3 lists the laboratory results of the analyses of hydraulic properties of the uncontaminated Area 15A soils. The average calculated porosity was 34.4%. The hydraulic conductivity from falling head permeameter tests ranged from  $7 \times 10^{-9}$  to  $5 \times 10^{-6}$  cm/s and averaged about  $10^{-6}$  cm/s.

Based on the physical and hydraulic properties of the Area 15A soils, the three parameters that will have the greatest impact on the treatability of the soil are pH, hydraulic conductivity, and organic carbon content. The pH of the soil is less than ideal for microbial activity. The organic carbon content is relatively low for agricultural purposes but is high enough to reduce the effectiveness of some remedial technologies (e.g., chemical oxidation or reduction).<sup>Ref. 12</sup> The hydraulic conductivity is relatively low and thus will reduce the effectiveness of remedial strategies involving the movement of liquid or gases into or out of the soil matrix.



**Table 3-3**  
**Hydraulic Properties of Uncontaminated Area 15A Soil**

Sample ID	Ground Elevation (m-msl)	Sample Interval (m)	Initial Moisture Content		Dry Bulk Density (g/cm <sup>3</sup> )	Wet Bulk Density (g/cm <sup>3</sup> )	Calculated Porosity (%)	K <sub>sat</sub> (cm/s)
			Gravimetric (%)	Volumetric (%)				
A	364.85	2.3 to 3.4	19.4	33.2	1.71	2.04	35.5	2.7E-08
B	359.85	2.1 to 3.4	18.1	32.2	1.78	2.10	32.9	7.0E-09
C	357.57	2.3 to 3.5	16.6	29.3	1.77	2.06	33.3	7.8E-08
D	357.02	1.8 to 3	14.6	27.2	1.86	2.13	29.9	8.6E-09
E	357.66	1.8 to 3	15.4	25.8	1.67	1.93	36.8	2.9E-07
F	360.43	1.8 to 3	8.4	13.7	1.64	1.78	38.1	5.2E-06
Averages:			15.4	26.9	1.74	2.01	34.4	9.4E-07

### 3.3 Data Requirements for Groundwater

Groundwater quality parameters that can affect its treatability are pH, TOC, biochemical oxygen demand (BOD), and chemical oxygen demand (COD). As with soil, the pH of groundwater can affect microbial health and biodegradation.

Chemical oxidation and reduction processes are also affected by pH. Redox potential helps to define the oxidation-reduction equilibrium in aqueous systems. Certain halogenated organic compounds are more easily degraded under reducing or anaerobic conditions.

BOD, COD, and TOC measurements of contaminated water, as in soils, provide indications, respectively, of the biodegradable, chemically oxidizable, or combustible fractions of the organic contamination.

Suspended solids can cause clogging of treatment systems and may make it necessary to pretreat groundwater. Major anions (chloride, sulfate, phosphate, and nitrate) and cations (calcium, magnesium, sodium, and potassium) are important for evaluating the *in situ* geochemical interactions, contaminant migration, and contaminant speciation.

Many of the parameters that can be useful for determining the treatability of groundwater at Area 15A are not routinely measured. The groundwater interim monitoring program deals only with organic contaminants. Previous investigations of the site, however, have reported values for TOC, total organic halogen, and pH.<sup>Ref. 4</sup>

Two detailed studies of Area 15A groundwater chemistry have been conducted. A groundwater treatability study conducted in 1987 concluded that indigenous organisms at the site were capable of degrading the contaminants but were

inhibited by either low pH or toxicity of some of the contaminants.<sup>Ref. 3</sup> These findings supported Castro's assertion that low pH has impeded degradation of the contaminants.<sup>Ref. 11</sup> Also in this study, sewage treatment plant organisms were added to the groundwater to enhance biodegradation. The conclusion of the study was that either neutralization or dilution of the groundwater provided conditions suitable for microbial growth.

Earth Sciences Consultants, Incorporated, measured several groundwater parameters in their environmental site assessment reported in 1985.<sup>Ref. 2</sup> The important findings of this assessment were that groundwater from two middle zone monitoring wells, MWS-5A and MWS-8, had lower pH, higher specific conductance, and higher chloride levels than all other wells tested. These were all attributed to decomposition of CNS tear gas. MWS-5A also had high iron levels believed to be from drum deterioration. Also in MWS-5A benzene, carbon tetrachloride, chloroform, and methylene chloride were found. All of these compounds were said to be constituents or potential breakdown products of CNS tear gas.

In addition to chemical parameters, geologic and hydrologic information is important for designing, operating, and monitoring groundwater remediation. The hydrogeology of Area 15A is discussed in detail in Appendices F and G of the Tear Gas Fate and Effects Study report.

### **3.4 Data Requirements for Off-Gases**

An estimate of the emissions from a site during treatment may be necessary. Emissions of VOCs and particulate matter during site disturbances, such as excavation or even tilling operations, can be orders of magnitude higher than from undisturbed soil. Emissions from SVE or *ex situ* thermal processes can be estimated based on soil contaminant concentrations and throughput.

### 3.5 Properties and Behavior of CNS Compounds

The three components of CNS tear gas have different physical and chemical properties and are expected to separate or fractionate and behave differently in the environment. Sampling and analysis of soil and groundwater in the tear gas drum burial area have verified this. Due to phenacyl chlorides' low solubility in water, measured concentrations in groundwater are much lower than the other two compounds. Also, chloroform, the least biodegradable of the three compounds, is found in the highest concentrations in the groundwater downgradient of the landfill and at low concentrations in Tributary B. Table 3-4 lists the CNS component water solubilities, the effective mixture solubilities, and the information used to calculate the effective mixture solubilities of the components. The effective mixture solubility is the amount of each component that can be expected to go into solution when the DNAPL dissolves into water.

#### 3.5.1 Chloroform

Chloroform accounts for 38% of the original tear gas mixture. It is a halogenated VOC with the chemical formula  $\text{CHCl}_3$ . It is also referred to as trichloromethane. In CNS tear gas, chloroform served as a solvent for phenacyl chloride which would otherwise have been a solid. Table 3-5 lists chloroform's chemical and physical properties.

Of the three tear gas components, chloroform is the most volatile and the most soluble in water. Since it is denser than water, it will move downward under the force of gravity. Hydrolysis is not a significant fate process. The half-life for hydrolysis of chloroform is 3,500 years.<sup>Ref. 13</sup> It will also volatilize fairly rapidly from surface water. Dilute concentrations of chloroform are not expected to

**Table 3-4**  
**Individual and Mixture Solubilities of CNS Components**

Component	Mol Wt (gm/mol)	Weight Fraction	Mole Fraction	Activity Coefficient	Water Solubility (mg/l)	Effective Mixture Solubility (mg/l)
Phenacyl chloride	154.6	0.24	0.22	1.5739	500	173
Chloroform	119.4	0.38	0.452	0.9162	8,200	3,393
Chloropicrin	164.4	0.38	0.328	1.8158	1,500	893

**Table 3-5**  
**Chloroform Physical and Chemical Properties**

Parameter	Value
Physical description	Clear colorless liquid
Molecular weight	119.38
Density	1.485 @ 20°C <sup>Ref. 14</sup>
Melting point	-63.5°C
Boiling point	61.2°C
Log K <sub>ow</sub> – Coefficient of octanol/water partition	1.98 (Verschuere, 1983) <sup>Ref. 15</sup>
Log K <sub>oc</sub> – Coefficient of organic carbon partition	1.64 (Montgomery and Welkom, 1990) <sup>Ref. 16</sup> (2.58 based on TVA's K <sub>D</sub> of 1.84 and 0.48% soil carbon)
Soil sorption coefficient - K <sub>D</sub>	1.84 (measured by TVA)
Water solubility	8,000 mg/l (Montgomery and Welkom, 1990)
Viscosity	0.58 cP <sup>Ref. 17</sup>
Vapor pressure	100 mm Hg @ 10.4°C <sup>Ref. 18</sup> 200 mm Hg @ 25.9°C <sup>Ref. 18</sup>
Vapor density	1.05 g/l at 25°C (calculated from vapor pressure)
Henry's law constant	0.003 atm m <sup>3</sup> /mol or 0.13 dimensionless <sup>Ref. 16</sup>

persist in agitated bodies of water due to evaporation.<sup>Ref. 19</sup> It does not have a strong tendency to become bound by the soil or organic matter, consequently, chloroform is considered a relatively mobile compound.

Because of the electronegative character of halogen substituents, polyhalogenated compounds often behave as electron acceptors (oxidizers) and are reduced.<sup>Ref. 20</sup> Reductive dechlorination of chloroform can be accomplished by methanogens (anaerobic bacteria) and by the bacteria *Pseudomonas sp.*<sup>Ref. 21</sup> The end product is methane. The bacteria *Pseudomonas sp* can also oxidize chloroform using the enzyme toluene dioxygenase.<sup>Ref. 22</sup> Until recently, chloroform was not considered amenable to degradation by aerobic organisms. C.E. Castro has shown, however, that chloroform is readily oxidized by soil methylotrophs to carbon dioxide. The responsible organism is *Methylosinus trichosporium-Ob-3b*. The oxidation is accomplished by the enzyme methane monooxygenase and, in pure culture, the oxidation has a half life of about 0.5 hours.<sup>Ref. 23</sup> Anaerobic reduction processes, on the other hand, require several days or weeks.<sup>Ref. 23</sup>

### 3.5.2 Chloropicrin

Like chloroform, chloropicrin makes up 38% of the original tear gas mixture. It is a vomitory agent and can be classified as a halogenated VOC. Its chemical formula is  $\text{Cl}_3\text{CNO}_2$ . Table 3-6 lists its chemical and physical properties.

Chloropicrin is less soluble in water and more dense than chloroform. It is also less volatile. Like chloroform, chloropicrin does not have a strong tendency to sorb onto soil particles.<sup>Ref. 3</sup> Chloropicrin is a highly reactive compound since it is degraded several ways, biotically and abiotically. It is hydrolyzed by base. Hydroxyl groups bonded to clays can react with chloropicrin and remove the chlorine atoms and the nitro group from the carbon atom. It is reduced abiotically

**Table 3-6**  
**Chloropicrin Chemical and Physical Properties**

Parameter	Value
Physical description	Slightly oily liquid, intense odor
Molecular weight	164.39
Density	1.66 g/ml @ 20°C <sup>Ref. 14</sup>
Melting point	-69.2°C
Boiling point	112°C
Log K <sub>OW</sub> – Coefficient of octanol/water partition	1.56 (Verschueren, 1983) <sup>Ref. 15</sup>
Log K <sub>OC</sub> – Coefficient of organic carbon partition	2.59 (based on TVA's K <sub>D</sub> of 1.87 and 0.48% soil carbon)
Soil sorption coefficient - K <sub>D</sub>	1.87 (measured by TVA)
Water solubility	2,272 mg/l @ 0°C <sup>Ref. 14</sup> 1.621 g/l @ 25°C <sup>Ref. 14</sup>
Viscosity	1.02 cP (measured by TVA)
Vapor pressure	23.8 mm Hg @ 25°C <sup>Ref. 24</sup>
Vapor density	0.15 g/l @ 20°C (calculated from vapor pressure)
Henry's law constant	0.10 <sup>Ref. 24</sup>

by iron and this process has inevitably occurred at Area 15A.<sup>Ref. 11</sup> Chloropicrin is rapidly dehalogenated by several species of *Pseudomonas*. The enzyme cytochrome P-450 is responsible for the dehalogenation. The dehalogenation can take place under aerobic or reducing conditions.<sup>Ref. 25, 26, 27</sup> Methanogenic bacteria may also reduce chloropicrin<sup>Ref. 28</sup> at Area 15A at depths where anaerobic conditions exist.

### 3.5.3 Phenacyl Chloride

Phenacyl chloride (2-chloroacetophenone) is a strong lacrimator (tear-causing agent) which accounts for 24% of the original tear gas mixture. It is practically insoluble in water but soluble in alcohol. It is a halogenated, semi-volatile organic compound (SVOC) and is a solid at room temperature. Table 3-7 lists its chemical and physical properties.

Phenacyl chloride is not likely to volatilize unless it is in solution with chloroform. Since it is barely soluble in water and is adsorbed onto organic matter in soil, it is the least mobile of the three compounds.

Like chloropicrin, phenacyl chloride is extremely sensitive to hydrolysis by nucleophilic reagents (electron rich reagents such as bases). It can also be reduced or oxidized. All three reactions can proceed by biotic or abiotic means.<sup>Ref. 23</sup> Microbial conversions of phenacyl chloride have not been documented. However, phenacyl chloride contains an aromatic ring and several species of bacteria are known to attack such ring structures by an oxidative process.<sup>Ref. 29</sup> The presence of benzene, ethyl benzene, benzaldehyde, and benzoyl chloride in groundwater downgradient of Area 15A indicate that some degradation of phenacyl chloride has taken place.<sup>Ref. 2, 30</sup> The dominant reaction should be hydrolysis by the hydroxyl radical.



**Table 3-7**  
**Phenacyl Chloride Chemical and Physical Properties**

Parameter	Value
Physical description	White to yellow powder or colorless to gray crystalline solid
Molecular weight	156.4
Density	1.34 g/ml @ 15°C <sup>Ref. 14</sup>
Melting point	54°C
Boiling point	245°C
Log K <sub>OW</sub> —Coefficient of octanol/water partition	2.08 <sup>Ref. 31</sup>
Log K <sub>OC</sub> —Coefficient of organic carbon partition	2.85 (based TVA's K <sub>D</sub> of 3.43 and 0.48% soil carbon)
Soil sorption coefficient - K <sub>D</sub>	3.43 (measured by TVA)
Water solubility	<1,000 mg/l @ 20°C <sup>Ref. 32</sup> Apparent solubility 0.5 g/l
Viscosity	Solid
Vapor pressure	0.0054 mm Hg @ 20°C <sup>Ref. 33</sup>
Vapor density	4.56 x 10 <sup>-3</sup> g/l @ 20°C (calculated from vapor pressure)
Henry's law constant	<9.12 x 10 <sup>-5</sup> (calculated on the basis of solubility =0.5 g/l)

## SECTION 4.0

### TREATMENT PERSPECTIVES

There are three primary strategies for remediating contaminated sites:

- Destruction or alteration of the contaminants,
- Extraction, and
- Immobilization.

Treatment technologies capable of destroying the contaminants are thermal, biological, and chemical treatment methods. These treatments can be applied *in situ* or *ex situ* to the contaminated soil.

Treatment technologies normally used for extracting contaminants include thermal desorption, soil washing, and solvent extraction. These three *ex situ* processes require excavation of the soil. Soil vapor extraction (SVE) is an *in situ* process. There are several technologies for extracting contaminants from groundwater including: phase separation, carbon absorption, air stripping, ion exchange, and combinations of these.

Immobilization technologies include stabilization, solidification, and containment technologies such as placement in a secure landfill, construction of a slurry wall, and installation of a low permeability cap.

In many remedial actions, more than one of the methods described above may be necessary. For soil contamination, for example, it is common to excavate and treat or stabilize the most highly contaminated soil and then place a low permeability cap over the less contaminated soil. VOCs are often extracted with SVE, then the residual organic compounds are treated biologically using bioventing. A very thorough discussion of remedial technologies is available

from the U.S. Army Environmental Center.<sup>Ref. 34</sup> Only those treatment technologies that have potential for use with CNS tear gas compounds at Area 15A are described in detail herein.

#### 4.1 Soil Treatment Technologies

Table 4-1 gives a brief description of soil treatment technologies that can potentially be used at Area 15A. Table 4-2 lists the advantages and disadvantages of these treatments in terms of their technical feasibility, short- and long-term risks, and cost.

When dealing with organic contaminants in soil, *ex situ* treatment technologies involve excavation of the soil and destruction of the contaminants (e.g., incineration), extraction of contaminants (e.g., thermal desorption), or stabilization and landfilling of the soil (Table 4-2). In a previous feasibility study,<sup>Ref. 3</sup> excavation followed by treatment of soil was evaluated for the tear gas drum burial area of Area 15A. Both onsite and offsite landfill disposal scenarios were considered and rejected due to the short-term risks associated with excavation and the high cost. The estimated soil volume was 33,400 cubic yards and the estimated costs were about \$15M for offsite treatment and disposal and about \$14M for onsite treatment and disposal. This yields a unit cost of \$420 to \$450 per cubic yard of soil which is comparable to other estimates. The published cost-range for excavation, retrieval, and landfilling of contaminated soil is from \$405 to \$690 per cubic yard.<sup>Ref. 34</sup>

*Ex situ* treatment of soil is not recommended due to the short-term risks and high costs. The five *in situ* treatments listed in Tables 4-1 and 4-2 will be discussed in more detail in Section 5.2 - Technologies Considered. *Ex situ* soil treatments are not recommended for Area 15A; however, *ex situ* groundwater treatment may be necessary to provide the most effective removal of CNS contaminants.

**Table 4-1**  
**Soil Treatment Technology Descriptions**

<b>Technology</b>	<b>Description</b>
<b><i>Ex situ</i> Soil Treatment Technologies</b>	
Landfill Disposal	This involves excavation and treatment (depending on the contaminants involved) and disposal in an approved RCRA landfill.
Thermal Desorption	<i>Ex situ</i> process where VOCs and SVOCs are removed by heating the soil. A carrier gas or vacuum system transports contaminants to the gas treatment system.
Incineration	High temperatures (900-1,200°C) are used to combust organic constituents in the soil in the presence of oxygen.
<b><i>In situ</i> Soil Treatment Technologies</b>	
Enhanced Bioremediation	The activity of naturally occurring microbes is stimulated by circulating water-based solutions through the contaminated soil. Nutrients, oxygen, pH adjusters, and other additives are used to enhance biodegradation and desorption of contaminants.
Chemical Treatment	Involves the addition of water-based additives to either oxidize or reduce contaminants. Typical oxidizers used are ozone, peroxide, or potassium permanganate. The most common reducing agent is sodium dithionite.
Natural Attenuation	Natural subsurface processes such as dilution, volatilization, biodegradation, adsorption, and chemical reactions with subsurface materials are allowed to reduce contaminant levels to acceptable levels.
Soil Vapor Extraction	Vacuum is applied through extraction wells to create a pressure/concentration gradient that induces gas-phase volatiles to diffuse through the soil to the extraction wells.
Thermally Enhanced SVE	Electrical resistance heating, electromagnetic heating, hot air, or steam is used to increase the volatilization of SVOCs and VOCs to facilitate extraction.

**Table 4-2**  
**Comparison of Soil Treatment Technologies**

Treatment	Short-Term Risk	Long-Term Risk	Stage of Development	Relative Cost*
<b>Ex situ Soil Treatment Methods</b>				
Landfill Disposal	High	Low	Fully developed	High (\$405-\$690/cu yd)
Thermal Desorption	High	Low	Fully developed	High (\$60-\$450/cu yd)
Incineration	High	Low	Fully developed	High (\$200-\$1,000/ton)
<b>In situ Soil Treatment Methods</b>				
Enhanced Bioremediation	Low	Medium	Treatability studies required	Low (\$20-\$80/cu yd)
Chemical Oxidation/Reduction	Low	Medium	Few vendors available	Medium
Natural Attenuation	Low	High	Modeling required	Low
SVE	Low	Low	Fully developed	Low (\$10-\$40/cu yd)
Thermally Enhanced SVE	Low	Low	Pilot scale	Medium (\$25-\$100/cu yd)

\*Costs taken from Reference 34. Cubic yard of soil is assumed to weigh 1.5 tons.

## 4.2 Groundwater Treatment Technologies

There are many *in situ* and *ex situ* treatment technologies for groundwater. The discussion of these technologies will be limited to those technologies or approaches that are suitable for Area 15A. Area 15A has hydrogeologic characteristics that make the site a poor candidate for groundwater treatment. The drums of tear gas were buried on top of bedrock in a clayey soil with relatively low permeability (ranging from  $7.0 \times 10^{-9}$  cm/sec to  $5.0 \times 10^{-6}$  cm/sec). Groundwater flow measurements reveal that shallow groundwater movement in the Saltsburg Sandstone is dominated by a few thin preferential flow zones.<sup>Ref. 35</sup> Hydraulic conductivity in these thin zones was as high as 0.2 cm/sec. Past experience with fractured bedrock sites indicates that cleanup times can be extremely long because contaminants diffuse slowly from the rock matrix.

A committee assembled by the National Research Council to discuss alternatives to groundwater cleanup concluded that fractured media were the most difficult to remediate.<sup>Ref. 36</sup> A summary of 42 pump and treat systems in fractured media revealed that none of the systems have achieved cleanup goals equivalent to drinking water standards. Containment of the contamination, however, was considered possible at the sites.

In response to the State's concerns regarding detection of chloroform in the seeps west of Area 15A, TransTechnology Corporation has proposed a groundwater containment strategy. The containment strategy, referred to as a targeted pump and treat, involves a row of groundwater extraction wells placed downgradient of Area 15A on adjacent property.

Table 4-3 lists groundwater treatment technologies that can augment or be incorporated into the TransTechnology Corporation-proposed pump and treat system.

The complex geology of Area 15A does not favor any type of groundwater treatment; however, the *in situ* processes listed above can be positioned upgradient from the proposed extraction wells in an effort to reduce contaminant concentrations. In the most recent groundwater investigations, methylene chloride,  $\text{CH}_2\text{Cl}_2$  (dichloromethane), was detected at fairly high concentrations, indicating that some reduction of chloroform is taking place.<sup>Ref. 30</sup> Ethyl benzene and benzene were also detected indicating that phenacyl chloride is also being degraded. The levels of benzene and ethyl benzene were an order of magnitude higher than levels of phenacyl chloride in groundwater. Chloropicrin was not detected in the most recent groundwater investigation, however, the Method Detection Limits were so high (100 to 500,000  $\mu\text{g/l}$ ) that the absence of chloropicrin cannot be confirmed.

If the groundwater being extracted fails to meet discharge standards, it has to be treated by an *ex situ* process or recycled by injection into upgradient wells or other delivery systems where additives are introduced. The drinking water maximum contaminant level for chloroform is 0.10 mg/l. Recycling of contaminated groundwater raises several environmental issues that must be addressed in the system design. The primary issue is the containment of additives and groundwater within the treatment area. Also, the toxicity and persistence of additives and degradation by-products must be considered. For example, nitrate is an alternative electron acceptor for enhancing anaerobic biodegradation; however, injection of nitrate into groundwater is prohibited in many states because it is regulated through drinking water standards.

**Table 4-3**  
**Groundwater Treatment Technologies**

<b>Technology</b>	<b>Description</b>
<b><i>In situ</i> Groundwater Treatment Technologies</b>	
Co-Metabolic Treatment	Injection of liquids or gases (e.g., toluene, methane, or methanol) to enhance the rate of methanotrophic degradation of organic contaminants.
Enhanced Biodegradation	The rate of biodegradation of organic contaminants is enhanced by providing nutrients, electron acceptors, and competent degrading microorganisms.
Natural Attenuation	Natural subsurface processes such as dilution, volatilization, biodegradation, adsorption, and chemical reactions with subsurface materials are allowed to reduce contaminant levels.
Chemical Oxidation	Strong oxidizers are injected in the groundwater to oxidize organic contaminants.
<b><i>Ex-Situ</i> Groundwater Treatment Technologies</b>	
Air Stripping	Volatile organics are partitioned away from groundwater by increasing the surface area of groundwater exposed to air.
Sprinkler Irrigation	Groundwater is distributed through a sprinkler irrigation system to volatilize contaminants.
Granulated Activated Carbon Adsorption	Groundwater is passed through columns containing activated carbon to which organic contaminants are adsorbed.
Ozonation	Contaminated water and ozone are passed through a packed bed reactor containing activated carbon which acts as a catalyst as contaminants are oxidized by oxygen radicals.



Enhanced biodegradation is normally applied to non-halogenated VOCs and SVOCs. Co-metabolic treatment is still being developed. Chemical oxidation is also a relatively new technology. Hydrogen peroxide and potassium permanganate have been used to oxidize two-carbon halogenated compounds like trichloroethylene.<sup>Ref. 37, 38, 39, 40</sup> In a study involving the use of several oxidizers for treating contaminated groundwater, ozone was found to be effective for oxidizing chloroform while hydrogen peroxide was not.<sup>Ref. 41</sup> Potassium permanganate is not considered effective for oxidizing chloroform.<sup>Ref. 42</sup>

*In situ* treatment of groundwater may be feasible at sites where a contaminant plume is well defined and the subsurface media are amenable to treatment. In fractured bedrock, the treatment times are likely to be extremely long. Simulations of natural attenuation in the bedrock beneath Area 15A (modeling work is summarized in Appendix F of this document) predict that it may take in excess of 200 years for the CNS constituents to be naturally flushed out of the bedrock. Given this timeframe for DNAPLs to diffuse out of the bedrock, it is difficult to justify any groundwater treatment strategies.

The *ex situ* treatments listed in Table 4-3 can be used in conjunction with a targeted pump and treat system to remove chloroform from the extracted groundwater. Since federal clean air regulations have not been promulgated for off-gases from groundwater remediation processes, VOCs removed by air stripping can probably be vented to the atmosphere. However, carbon adsorption could be used to adsorb and dispose of the chloroform and chloropicrin since both are air strippable.<sup>Ref. 43</sup> Biofilters that can degrade VOCs will have advantages over carbon adsorption in that they are less expensive to operate and they degrade the contaminants eliminating the need for waste disposal. Sprinkler irrigation may be considered environmentally acceptable if the concentrations of contaminants in the groundwater are low enough for all of the contaminants to volatilize before reaching the ground

### 4.3 Containment Methods

There are several ways to prevent the movement of contaminants in soil and groundwater:

- Low permeability cap,
- Slurry walls,
- *In situ* solidification or vitrification, and
- Groundwater pumping.

For a variety of reasons, only groundwater pumping will be considered for Area 15A. Capping of the site or the use of slurry walls is not considered feasible because of the high hydraulic conductivity of the Saltsburg Sandstone beneath the site. *In situ* vitrification is a developing technology involving the heating of the soil using electrical current. It is relatively expensive (\$300-\$450 per ton) and has not been conducted commercially. Solidification, which refers to the mixing of cementitious materials using an auger, is normally only used for inorganic contaminants and is ineffective against VOCs.

As proposed by TransTechnology Corporation and described in Section 5, groundwater pumping can be used to reduce or intercept the contaminant plume.

## SECTION 5.0

### TECHNOLOGY PROFILES

Many of the common methods for treating VOCs will not be effective at Area 15A because most of the tear gas originally buried at the site has migrated into the underlying bedrock. The potential risks from human exposure to the compounds make *ex situ* soil processes undesirable. The following section lists the technologies being rejected from this evaluation and the reasons for their rejection.

#### 5.1 Technologies Rejected

Table 5-1 lists the technologies for treating soil that were rejected from this evaluation and the basis for rejection of each.

Technologies involving the excavation and treatment of soil were rejected because of the high cost and risks. In addition to the hazards associated with exposure to tear gas compounds, phosgene, an extremely toxic compound, is a possible degradation product of both chloroform and chloropicrin. It is an insidious poison because it is not irritating immediately, even when fatal concentrations are inhaled.<sup>Ref. 14</sup>

Capping and barrier walls are not feasible at Area 15A because the fractured bedrock provides no barrier to lateral or downward movement of contaminants. Capping would retard the downward movement of contaminants in the soil overburden; however, most of the contaminants have already reached bedrock. The preferential flow zones in the bedrock are impossible to isolate using a low-permeability cover. Reactive barrier walls have been used effectively to reduce chlorinated solvents in groundwater passing through the wall. To effectively treat all the contaminated groundwater, the wall must be keyed into an

**Table 5-1**  
**Treatment Technologies Rejected**

<b>Technology</b>	<b>Reason for Rejection</b>
Incineration	High cost and high short-term risk
Thermal Desorption	High cost and high short-term risk
Landfilling	High cost and high short-term risk
<i>Ex situ</i> Bioremediation	High operating and maintenance cost and short-term risk
<i>Ex situ</i> Chemical Treatment	Short-term risk
<i>Ex situ</i> Chemical Extraction	Relatively high cost and short-term risk
<i>In situ</i> Solidification	High cost and limited effectiveness for contaminants of concern
Capping	Site hydrogeology not suitable for technology
Barrier Walls	Site hydrogeology not suitable for technology
<i>In situ</i> Vitrification	High cost and technology unproven on the scale required for Area 15A

aquitard or confining clay layer. The lack of these barriers to downward flow make Area 15A unsuitable for this type of containment.

Vertical flow in the bedrock at Area 15A was estimated by transport simulations. The results of these simulations are summarized in Section 4 of this final report of the Tear Gas Fate and Effects Study. A detailed report of the fractured bedrock modeling work is provided in Appendix F.

One other aspect of Area 15A that makes it poorly suited for many technologies is the shape and size of the area of contaminated soil. The soil overburden in the tear gas landfill area is 10 to 12 feet thick and covers an area of approximately two acres. This broad shallow area is not well suited for *in situ* technologies involving the delivery of additives using vertical wells. The sheer volume of soil (roughly 34,000 cubic yards) is such that many treatments are prohibitively expensive. At a typical cost of \$30 per cubic yard (average for bioventing or soil vapor extraction),<sup>Ref. 34</sup> the total price tag for remediating the soil overburden at Area 15A would be over \$1 million.

## **5.2 Summary of Similar Remedial Actions**

There are no reports of remedial actions involving CNS tear gas constituents. There are also few successful remedial actions involving DNAPLs in fractured media. One successful cleanup of perchloroethylene (PCE) in bedrock used pneumatic fracturing, vacuum dewatering, hot air injection, and vapor extraction.<sup>Ref. 44</sup> One hundred wells were used to remove PCE from beneath a building in an urban setting. The cleanup involved only 500 gallons of PCE. The account of the remedial action did not provide a cost for the removal of PCE; however, the description of the operation implied that it was relatively expensive.

Another cleanup involving a mixture of chlorinated solvents, including chloroform in fractured bedrock, has been ongoing for 10 years. Like the PCE cleanup mentioned above, it involves vapor extraction; however, it is being done by air stripping the extracted groundwater. An estimated 92,000 pounds of VOCs had been removed in the first six years of operation. The operation had successfully contained the plume after several years of operation, but had not decreased the size of the plume. Capital costs for the operation were \$8M and annual operating costs were \$588K.

Neither of these remedial actions provide information that support active remediation of the bedrock aquifer at Area 15A.

### 5.3 Technologies Considered

*In situ* technologies can be divided into three categories: biological, physical/chemical, and thermal treatment. Many of the technologies require similar hardware, however, the types and volumes of additives vary. Table 5-2 lists all of the *in situ* technologies for the soil at Area 15A that were considered in this evaluation. The relative applicability, availability, cleanup time, and cost of the technologies are also provided.

The ratings for applicability take into account the site-specific limitations. For example, SVE is normally recommended for remediating VOCs. However, the assumed low permeability of the soil makes this technology less applicable at Area 15A.

Availability refers to the number of vendors that can design, construct, and maintain a technology. A rating of 1 means that there are at least five vendors, 2 means that there are three to five vendors, and 3 means that there are fewer than 3 vendors for the technology.

Table 5-2

*In situ* Soil Treatment Technologies Screening Matrix

Technology	Applicability	Availability	Cost	Cleanup Time
<b><i>In situ</i> Biological Treatment</b>				
Bioventing	3	1	1	3
Enhanced aerobic bioremediation <sup>I</sup>	2	2	2	3
Anaerobic bioremediation	2	3	2	3
Enhanced biological/chemical degradation	2	2	2	2
Monitored natural attenuation	1	1	1	3
<b><i>In situ</i> Physical/Chemical Treatment</b>				
Electrokinetic extraction	3	3	3	3
Extraction aided by fracturing	2	3	2	2
Soil flushing	3	1	3	3
Soil vapor extraction	3	1	1	2
Chemical oxidation	2	3	2	2
Chemical reduction	2	3	2	2
<b><i>In situ</i> Thermal Treatment</b>				
Thermally enhanced SVE <sup>II</sup>	2	3	2	1

Ratings: 1=better, 2=average, 3=worse

(I) Additives include air sparging, magnesium peroxide, ozone, and hydrogen peroxide

(II) Heating done by injecting hot air or by injecting hot air while mixing soil with an auger

A thorough review of available literature and discussions with vendors revealed that very little field work has been done with the particular contaminants found at Area 15A. A number of demonstrations and full-scale remedial actions have involved DNAPLs and halogenated organic compounds; however, the preponderance of these activities has involved two-carbon chlorinated compounds such as trichloroethylene. Generally, the heavily chlorinated compounds are not amenable to biodegradation and the single-carbon chlorinated compounds are more difficult to oxidize than the two-carbon chlorinated compounds. Only one vendor has claimed to have an oxidizing agent capable of oxidizing chloroform *in situ*. This company uses ozone as the oxidizer and delivers it to the soil by injecting it into groundwater beneath the contaminated soil.

#### 5.3.1 *In situ* Biological Treatments

**Monitored Natural Attenuation:** Among the *in situ* biological treatment alternatives considered, monitored natural attenuation has the highest rating in terms of applicability (Table 5-2). There are several reasons for this high rating. In the current setting, the tear gas components pose little risk to the environment. Deed restrictions and institutional controls can prevent human exposure to the landfill area. Offsite migration is a concern; however, the low concentrations and volatility of chloroform are such that it is unlikely to persist in surface water. The remaining two compounds are not being detected in seep water. Exploratory trench investigations in 1985 revealed that 90% of the drums had deteriorated.<sup>Ref. 2</sup> A second investigation in 1995 found no intact drums.<sup>Ref. 43</sup> Using the assumption that 90% of the drums were deteriorated by 1985, the modeling described herein estimates that by the year 2000, there will be no tear gas within drums. In view of the difficulty associated with remediating contaminants diffused into the bedrock matrix, natural attenuation merits consideration. Further characterization of the seeps downgradient of Area 15A is needed to quantify the amount of CNS-derived



contaminants reaching surface water and to assess the risk of this surface water contamination.

**Bioventing:** Bioventing is often used in conjunction with soil vapor extraction. Bioventing provides oxygen for biodegradation of compounds that remain after SVE. Bioventing is most effective on nonhalogenated hydrocarbons. To be effective on chlorinated compounds, a co-metabolite must be present. At Area 15A, a co-metabolite such as methane must be added since all the contaminants are chlorinated. Even if a co-metabolite were supplied, microbial activity will be impeded by the acid pH in the contaminated zone. Also, the low permeability of the soil will impede air movement. For these reasons, bioventing is not considered a viable alternative for remediating the soil in the tear gas drum burial area.

**Enhanced Aerobic Bioremediation:** Contaminants can be degraded by stimulating indigenous microbes or by adding microbes to the soil that have been acclimated (grown in the presence of a chemical similar to the contaminant). Nutrients, oxygen, and other additives are generally mixed with groundwater or uncontaminated water and injected or allowed to infiltrate from the surface. An alternate oxygen source such as hydrogen peroxide can also be added to the soil. The rate of hydrogen peroxide addition for bioremediation is much lower than for chemical oxidation. Hydrogen peroxide has not been proven effective for oxidizing chloroform, the primary contaminant. Based on the assumed hydraulic conductivity of disposal area soils, the shallow overburden is better suited for an infiltration gallery than injection wells (see Appendix G - Evaluation of Injection Recovery Alternatives).

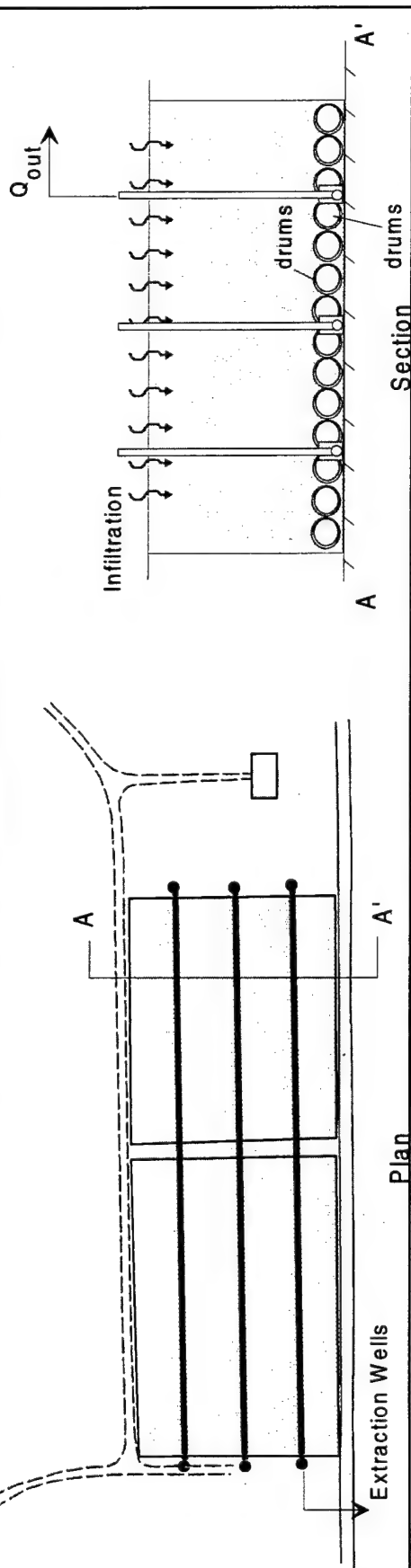
With the assumed low permeability of the soil overburden and relatively high permeability of the Saltsburg Sandstone, a properly designed monitoring and groundwater recycling system is required for *in situ* treatment of the tear gas drum

burial area. Simulations performed and reported herein, which included a number of injection/recovery alternatives, revealed that an infiltration gallery with horizontal recovery wells was superior to systems involving trenches or vertical recovery wells. A detailed discussion of the modeling work performed to select the optimum system of injection/recovery for *in situ* soil treatment is given in Appendix G of this report. Schematics of the two systems which provided the most efficient delivery and recovery of amendments are shown in Figure 5-1. The simulations indicate that, depending on the alternative considered, significant time may be required to move water and amendments through the soil due to its assumed low permeability. The use of shallow vertical injection wells can reduce the time required to fill the pore space. However, injection well spacing might make this alternative infeasible. Tilling the upper two to three feet of soil increases the liquid storage capacity of the upper portion of the soil overburden, but does not significantly reduce time required to fill soil pores with water and amendments.

**Enhanced Anaerobic Bioremediation:** Anaerobic remediation can be stimulated with the same system hardware as that described for aerobic remediation. Even though heavily chlorinated compounds are often easier to reduce than to oxidize,<sup>Ref. 20</sup> it is difficult to achieve anaerobic conditions in the field. Also, anaerobic microbial reduction is a much slower process than microbial oxidation.<sup>Ref. 21</sup> In view of the limited number of documented remedial actions involving *in situ* anaerobic degradation, anaerobic approaches are ranked below aerobic approaches. However, since there is evidence of reductive dechlorination of chloroform in the groundwater (high concentration of methylene chloride in wells 200 to 600 feet downgradient of the tear gas landfill area), treatability studies may be warranted for determining the suitability of enhancing anaerobic processes.

### Longitudinal Horizontal Extraction Wells/Infiltration Gallery (Scenario 6a)

(Scenario 6a)



### Latitudinal Horizontal Extraction Wells/Infiltration Gallery (Scenario 6b)

(Scenario 6b)

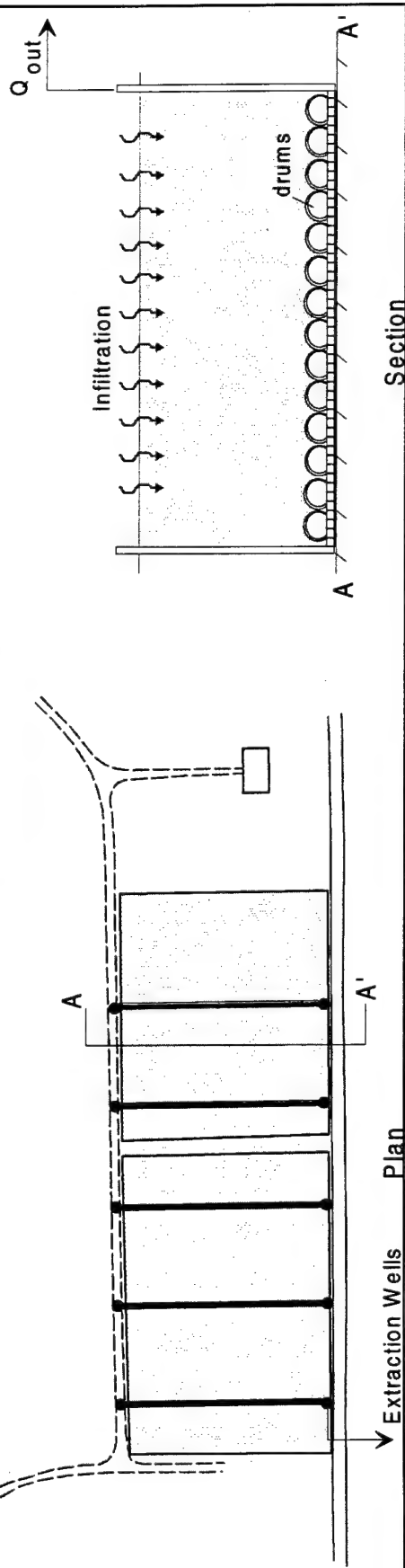


Figure 5-1 Conceptual Schematics for Chemical/Biological Injection and Recovery Systems

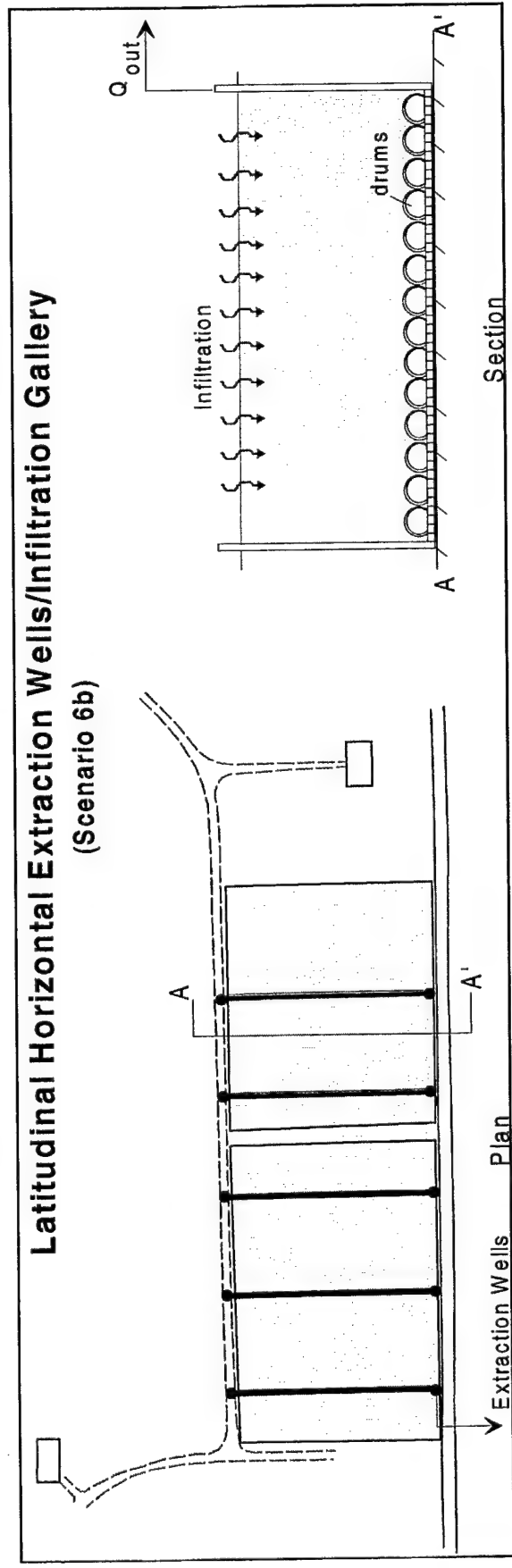
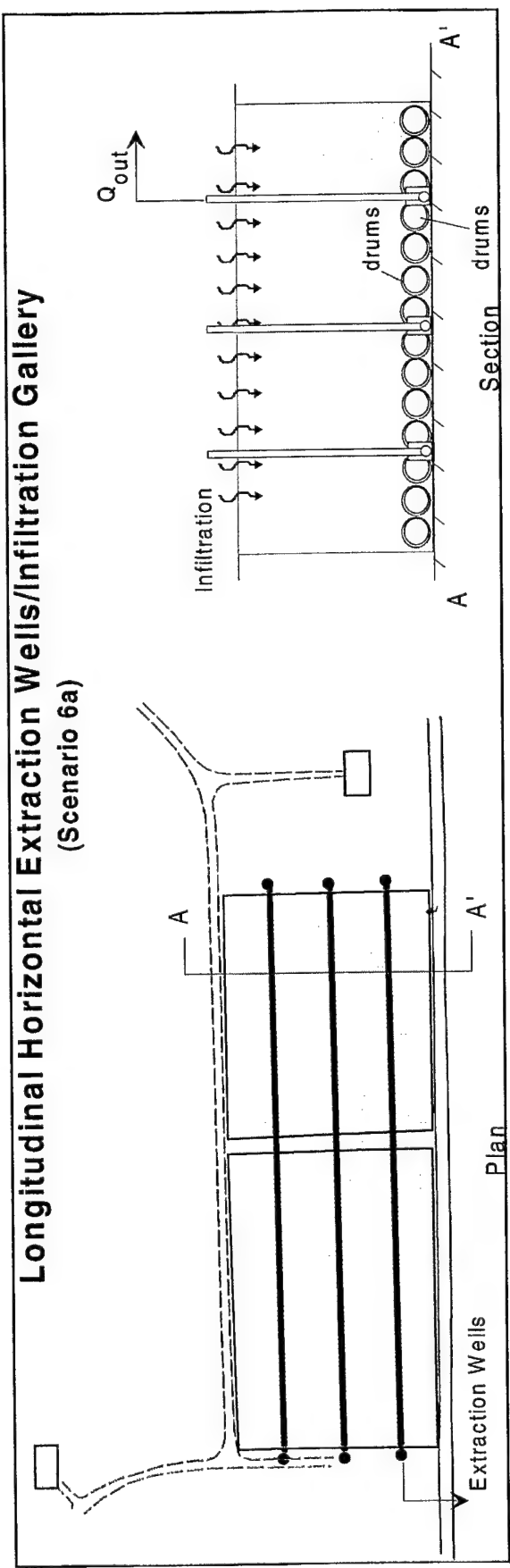


Figure 5-1 Conceptual Schematics for Chemical/Biological Injection and Recovery Systems

**Enhanced Biological/Chemical Degradation:** Among the *in situ* degradation processes, a combination of biological and chemical degradation is considered the optimal approach for several reasons.<sup>Ref. 12</sup> Chloropicrin and phenacyl chloride are both easily hydrolyzed by bases. This abiotic process may proceed rapidly if the pH of the soil being treated can be raised above neutral. A near neutral pH is also required for optimal microbial growth. A sample of contaminated soil taken from Area 15A in 1997 exhibited a pH of around 4. Buffering tests determined that around 3.7 pounds of agricultural limestone or 2 pounds of ammonium hydroxide per cubic yard of soil will raise the pH from 4 to 7. A report describing the buffering tests is provided in Supplement 1 to this Remedial Strategies Report.

The most rapid microbial degradation of chloroform involves oxygen insertion by soil methylotrophs or nitrifiers. The organism *Methylosinus trichosporium-Ob-3b* has been shown to oxidize chloroform with a reaction half-life of about 0.5 hour.<sup>Ref. 22</sup> By using ammonium hydroxide as the base, chloropicrin and phenacyl chloride can be hydrolyzed while the growth of nitrifying bacteria is enhanced. The growth of methylotrophs can be stimulated by the addition of methanol. Methanol is the preferred substrate for enhancing growth of methylotrophs because these bacteria metabolize methanol. Also, methanol is soluble in water and chloroform and can serve as a carrier for ammonia and ammonium hydroxide.

The preferred approach for *in situ* degradation of contaminants in the drum burial area is the addition of ammonium hydroxide followed by the addition of methanol. Lime or another base may be substituted for ammonium hydroxide, however, these materials are inferior in terms of their ability to penetrate the soil. Methane may be substituted for methanol, but it is inferior since it is not as soluble in water. Propanol can also be used, but is more expensive than methanol, is not as good a solvent, and is not as readily metabolized by the methylotrophs.<sup>Ref. 45</sup>

### 5.3.2 *In situ* Chemical Treatments

Many of the *in situ* physical/chemical treatments listed in Table 5-2 have limited applicability at Area 15A. Electrokinetic extraction involves the passing of current through the soil to move ions in saturated soil pore space by electro-osmotic forces or by electromigration. This is a developing technology primarily used to remove metals and has not been successfully demonstrated full-scale.

**Extraction Aided by Fracturing:** The use of high pressure air (or other fracturing methods) is an option for increasing the permeability of the soil overburden, thus enhancing the performance of SVE or other technologies involving the delivery of additives to contaminated soil. There are currently few vendors for the technology. Area 15A is not well suited for this technology because of the risks associated with exacerbating DNAPL migration into the underlying bedrock. Also, the depth of the soil overburden is such that the soil might be more easily loosened by tillage equipment or a large-diameter auger.

**Soil Flushing:** Soil flushing involves the use of water or a mixture of water and surfactants or co-solvents to remove contaminants from soil. The extracting fluid and contaminants must be recovered and treated to destroy or dispose of contaminants. This technology is in the developing phases in the United States. The target contaminants are inorganics, however, the technology can be used for VOCs and SVOCs. Field treatability studies are required to determine the suitability of the technology. As with other technologies at Area 15A, the risk of mobilizing and driving the DNAPLs downward is a major concern. The injection and recovery system for soil flushing would be similar to that used for *in situ* chemical/biological treatment. Strategies that degrade contaminants *in situ* will be less risky and relatively inexpensive compared to technologies that merely extract the contaminants. Consequently, soil flushing is not recommended for Area 15A.

**Soil Vapor Extraction:** SVE is EPA's presumptive remedy for VOC-contaminated soil. It involves placing a vacuum on the soil and passing air through the soil to remove volatile compounds. It is preferred over other technologies because of its low cost. There are three reasons why SVE is not considered the best strategy for Area 15A: 1) the high clay and silt content of the soil make it difficult to treat, 2) the adsorptive tendencies of phenacyl chloride make it unsuitable for SVE, and 3) the contaminants will not be degraded *in situ* and will require treatment or adsorption on activated carbon.

**Chemical Oxidation:** Chemical oxidation would be accomplished in a manner similar to enhanced aerobic biodegradation. The difference is that a strong oxidizing agent is injected instead of nutrients. Aerobic biodegradation can also be stimulated using an oxidizing agent, however, the amount and concentration are sufficient only to supply oxygen for microbes. There have been a number of laboratory and field studies involving chemical oxidation of chlorinated hydrocarbons. Most of this work has involved trichloroethylene (TCE) or mixtures of solvents that contained little or no chloroform. Vendors and researchers have stated that chloroform is one of the more difficult compounds to oxidize because it has only single bonds and no carbon-to-carbon double bond as does TCE.<sup>Ref. 46</sup> Among the agents commonly used to oxidize organic compounds, ozone is the only one that has been shown to be effective against chloroform. Hydrogen peroxide and potassium permanganate are not effective for oxidizing chloroform.<sup>Ref. 41, 42</sup>

There are four reasons that oxidation by ozone is not the preferred strategy for Area 15A: 1) ozone is a relatively expensive additive, 2) the sterilizing effect of ozone could destroy microbes and their associated biodegradation, 3) ozone requirements will be large since much of the ozone will be consumed by soil humic acids, and 4) chemical oxidation of chloroform yields phosgene.

**Chemical Reduction:** Reducing agents like sodium dithionite can be used to initiate the reduction of CNS compounds by producing sulfoxylate anion radicals ( $\text{SO}_2^-$ ). Like the oxidizing agents, reducing agents can be scavenged by humic acids and transition metal salts. Also, the oxidative capacity of the site will be diminished. Both chemical oxidation and reduction are developing technologies. Neither is listed among *in situ* technologies in the Federal Remediation Technologies Roundtable's screening matrix.<sup>Ref. 34</sup>

### 5.3.3 *In situ* Thermal Treatment

Thermally enhanced SVE is a technology that should be considered for Area 15A because of low soil permeability. One reported success involving DNAPLs in fractured bedrock used a combination of pneumatic fracturing, vacuum extraction, and hot air injection.<sup>Ref. 44</sup> This was done on a less broad, but deeper, plume than that at Area 15A. Also, there was much less contaminant, about 500 gallons versus the possible 15,000-85,000 gallons at Area 15A. The cost per pound of DNAPL removed was quite high, but the urban setting and high value of the land justified the high cost.

A more simple method for treating Area 15A would involve the use of a large-diameter vertical auger for mixing the soil and injecting hot air. A shroud and vapor recovery system will be required to capture volatile contaminants. Like other extraction methods, this strategy has the problems associated with disposal or treatment of the contaminants. The main advantage is that this approach is fairly simple and can be accomplished in a relatively short time. In bench-scale studies using a vertical auger to mix and inject 100°C-air, 99% removal of chloroform was achieved when combined with SVE.<sup>Ref. 47</sup> Eighty-five percent of the chloroform was removed with hot air only. An estimated cost of \$75 per cubic yard was given for the combination of mixing, hot air injection, and SVE. This setup can also be



used to mix a base with the soil to hydrolyze the chloropicrin and phenacyl chloride. The addition of base would raise the cost of the treatment to around \$100 per cubic yard. The results of this bench-scale study are promising, however, it should be noted that an unrealistic amount of hot air was used in the tests. About 2,000 soil-pore volumes of hot air were passed through the soil.

#### 5.4 Groundwater Treatment Technologies

The fractured bedrock beneath Area 15A makes it unsuitable for groundwater pump and treat technologies. A thorough study of ongoing pump and treat operations concluded that all of the pump and treat systems in fractured bedrock were unlikely to achieve drinking water standards in a reasonable timeframe, but were capable of containing the contaminant plume.<sup>Ref. 36</sup> In Section 4 - Treatment Perspectives, *in situ* and *ex situ* groundwater treatment technologies are mentioned. Because of the long time required for the CNS tear gas compounds to diffuse out of the bedrock (50 years based on fractured bedrock simulations reported herein), *in situ* groundwater treatment technologies are not recommended for Area 15A. Containment of the contaminants, however, may be a viable alternative if monitored natural attenuation is deemed unacceptable by the state.

##### 5.4.1 Containment Methods

The fractured bedrock beneath the tear gas drum burial area makes it impractical to use a cap or barrier walls to contain the contaminants. The only practical way to prevent the offsite movement of contaminants is by groundwater extraction. The approach being proposed by TransTechnology Corporation is to intercept contaminants before they exit the ground using an array of extraction wells. Extraction of groundwater from near the edge of the plume is proposed instead of from the center of the plume to take advantage of natural degradation processes.

The highest concentration of chloroform in the area of the proposed extraction wells was 12 mg/l.<sup>Ref. 30</sup> Another well around 300 feet due south of the landfill (MWU-29) had a concentration of 730 mg/l. This is about four times higher than the average concentration of chloroform (161 mg/l) from monitoring well MWS-8, which is less than 100 feet west of the landfill. MWS-8 has previously shown the highest levels of chloroform among all wells included in the monitoring program.

This high concentration of chloroform in MWU-29 raises concern because it indicates that the movement of CNS contaminants from the landfill may be in a more southerly direction than previously presumed. Previous investigations have concluded that the contaminants are moving westerly and are primarily confined to the uppermost water-bearing stratum, the Saltsburg Sandstone (see Figure 2-3 of this appendix). The high chloroform level of MWU-29 could be a reflection of the heterogeneous nature of fractured bedrock contamination. It is possible that the seep sampling done as part of the quarterly monitoring program may not be capturing the discharge of CNS-contaminated groundwater. To design the targeted pump and treat system and to determine if monitored natural attenuation is a viable alternative, a better delineation of the contaminant plume is required. Also, the actual sources of groundwater discharge, the seeps hydraulically connected to the CNS source, need to be located and sampled to determine the quantity of CNS-derived contaminants that are leaving the site. Without this information, a targeted pump and treat system cannot be designed nor can monitored natural attenuation be justified.

#### **5.4.2 Monitored Natural Attenuation**

Monitored natural attenuation requires predictive analysis to demonstrate that natural processes will reduce contaminant concentrations below risk-based standards before potential exposure pathways are completed. The term “monitored” is used in this report to signify that long-term monitoring must be

conducted to confirm that degradation is proceeding at rates consistent with cleanup objectives. Monitored natural attenuation has been selected at Superfund sites, for example, where removal of DNAPLs was determined to be technically impractical or where it was determined that active remedial measures will not significantly shorten remediation timeframes.<sup>Ref. 34</sup>

Active remediation of Area 15A may not appreciably shorten the treatment time because the contaminants are diffused into bedrock. Simulations of natural attenuation of the bedrock aquifer, reported herein, indicate that a period of around 50 years will be required for the chloroform levels to fall below the action level of  $10^{-4}$  g/l. It is also estimated that by the year 2000, all of the drums of CNS tear gas will have deteriorated, allowing all of the tear gas to migrate into the bedrock. These facts make it difficult to promote a remedial strategy involving the treatment of soil in the tear gas landfill area.

To justify natural attenuation, degradation of contaminants must be verified. There are several characteristics of Area 15A that indicate natural attenuation is occurring. These include: 1) at a distance of 400 feet from the source area, phenacyl chloride concentrations are much lower than concentrations of its degradative by-product, benzene; 2) at a distance of 400 to 600 feet downgradient of the source area, methylene chloride is present at high levels indicating that chloroform is being reduced; 3) concentrations of the tear gas components in seep water is much lower than that predicted by fractured bedrock simulations assuming no degradation; 4) the soil in the landfill area is acidic ( $\text{pH} = 4$ ) due to the buildup of hydrochloric acid; 5) phosgene, the oxidative breakdown product of chloroform and chloropicrin has been detected in groundwater near the landfill; and 6) breakdown products of phenacyl chloride, benzoyl chloride, and benzaldehyde have been detected in groundwater near the landfill.

Fractured media simulations based on the assumption that no degradation is taking place yield concentrations of tear gas in the seeps that are much higher than what has been reported. Aerobic mineralization and degradation rate studies reported in the main body of this report suggest that the degradation half-lives of chloroform, chloropicrin, and phenacyl chloride are respectively, 277, 0.21, and 5.6 days. Using a biodegradation half-life of 277 days in the fractured media, modeling yields estimates of chloroform concentration that are similar to what has been measured in the field. Chloroform concentrations in seep water are around 20 to 900 ug/l, concentrations compatible with the model.

## **5.5 Additional Site Characterization Recommendations**

To support natural attenuation as a remedial strategy or to properly design a plume containment strategy, the southwestern extent of groundwater contamination needs to be located. Also, the amount of CNS-derived contaminants that are leaving the site via the wet-weather seeps needs to be better defined.

In 1998, six new monitoring wells were installed to the south and west of the tear gas landfill. These wells are numbered 28 through 32 and their location is shown in Figure 2-10 of Appendix F. Well MWU-28, 800 feet due south of the landfill, was free of CNS contaminants. The well farthest to the southwest, MWU-30, had detectable levels of tear gas contaminants. MWU-28 and MWU-30 are about 1,000 feet apart and the only well between them, MWU-29, had the highest levels of chloroform. MSU-29, however, is much closer to the landfill than either MSU-28 or MSU-30. To estimate the southwestern limit of the plume, an upper zone well needs to be installed southwest of well MWU-30 and one or more wells need to be installed between MWU-30 and MWU-28.

Characterization of the seeps has been made difficult by their intermittent flow. Frequently during quarterly sampling events the seeps have had no flow and could

not be sampled. Improvements are recommended in characterizing both the seep flows and water quality. Installation of weirs or other flow monitoring systems (e.g., Parshall flumes) at two sites on Tributary B are recommended: one above the seep area and one below the seeps. Continuous data recorders should be installed at each location in order to estimate the Saltsburg seep contribution to flow. One will need to examine the expected range of flows before selecting the weir or other flow monitoring system design. Seep water quality samples should be collected as close as possible to the point of seep emergence in order to prevent volatile losses. Sampling should be conducted over the full range of seasonal flows. These measurements will also allow validation of natural attenuation predictions.

## SECTION 6.0

### SUMMARY AND RECOMMENDATIONS

The remedial strategy recommendations are based on a thorough study of the developed and developing technologies applicable to CNS tear gas contaminants. A primary goal was to develop a strategy for remediating Area 15A soil. However, bedrock aquifer simulations indicate that soil remediation may not appreciably shorten the time required for natural restoration of the aquifer. The remedial strategy recommendations, as well as the simulations done as a part of the tear gas fate and effects study, are based on many assumptions. For example, the exact number of drums buried was assumed to be 1,700. Physical properties of the soil in the landfill are assumed to be similar to those of the undisturbed soils adjacent to the landfill. Groundwater characterization is limited primarily to the uppermost water-bearing stratum. The assumption that Buffalo Sandstone has not been contaminated by CNS tear gas is based on a limited number of wells.

Additional site characterization is recommended to better understand groundwater flow at the site and to verify the degradation of the tear gas components. The actual path of contaminant migration needs to be determined. It is possible that higher concentrations of chloroform are reaching the ground surface from other seeps. A more thorough and widespread sampling of seep discharges is necessary to accurately estimate the discharge of tear gas components to surface water.

To properly design the pump and treat system, an accurate characterization of the vertical and horizontal extent of contamination is needed. The complex geology of the fractured bedrock makes it very difficult to pinpoint the location of the contaminants. From the concentration of contaminants measured in groundwater, it can be surmised that free phase DNAPL exists in pockets in the bedrock.

A geophysical survey of the landfill area is needed to determine the extent and connectivity of voids resulting from the deterioration of drums. This has important implications regarding the design of an injection and recovery system.

For remediating the soil overburden, the following strategies should be considered:

- *In situ* chemical/biological treatment
- Hot air injection and base addition using a large diameter mixing auger and SVE for capturing VOCs

For remediating the groundwater, the following two strategies are recommended:

- Monitored natural attenuation
- Plume containment using extraction wells on the outer edge of the plume near the wet weather seeps

***In situ* Chemical/Biological Treatment:** The preferred additives for the *in situ* chemical/biological treatment are ammonium hydroxide to promote hydrolysis and methanol to promote growth of methylotrophs. Alternative additives are agricultural limestone, methane, and propanol. The most efficient delivery system involves an infiltration gallery and horizontal extraction wells. The area would not be protected from precipitation, however, the concentration of additives being applied would be adjusted to account for dilution by precipitation. Extracted groundwater would be monitored to ascertain the performance of the operation and would be reinjected or allowed to infiltrate. The cheapest form of ammonium hydroxide would be fertilizer-grade aqueous ammonia which is 24% ammonia. Because of its volatility, aqueous ammonia must be injected a few inches below the ground surface using buried drip irrigation tubing. To increase the liquid-holding capacity of the soil, it should be tilled to the greatest depth possible. The cost of this remedial action will be

approximately \$500,000. About two-fifths of this cost is for installation of horizontal wells.

**Soil Mixing:** The strategy involving soil mixing, base injection, hot air injection, and SVE would be similar in cost to the chemical/biological degradation treatment. It ranks behind the chemical/biological degradation because some contaminant will need to be treated as an off-gas.

**Natural Attenuation:** Monitored natural attenuation is the preferred treatment for groundwater if the potential risk from surface contamination is acceptable. A better delineation of the plume is required as is the quantification of surface discharge of the tear gas constituents and breakdown products.

**Targeted Pump and Treat:** If plume containment is ultimately selected as the treatment strategy, the extent of the plume must be determined and serious consideration should be given to air stripping and venting of volatile compounds. If VOCs require treatment, biofiltration should be considered as it is less expensive than carbon adsorption.



## SECTION 7.0

### REFERENCES

1. Personal correspondence with Jeffrey Forgang, Director of Environmental Affairs. April 1998. TransTechnology Corporation, Liberty Corner, NJ.
2. Earth Sciences Consultants, Inc. "*Environmental Site Assessment: Federal Laboratories, Inc., Saltsburg, PA.*" 1985. Project No. 85-103A. Volume 1 of 2. Earth Sciences Consultants, Incorporated, Pittsburgh, PA.
3. Earth Sciences Consultants, Inc. "*Removal Site Evaluation/Feasibility Study--Federal Laboratories Facility, Saltsburg, PA.*" October 1992. Project No. 5103D.
4. Earth Sciences Consultants, Inc. "*Summary of Site Characterization Studies.*" October 1992.
5. Conestoga-Rovers & Associates. "*Groundwater Monitoring Report: 1995 Quarterly Monitoring and 1995 Monthly Seep Sampling.*" February 1996. Reference No. 6099 (15).
6. Conestoga-Rovers & Associates. "*Interim Monitoring Program Second Quarter 1997 Sampling Event.*" April 1998. Reference No. 6099 (25).
7. Personal Correspondence with Nate Sinclair. 1998. Naval Facilities Engineering Service Center, Port Hueneme, CA.
8. EPA. "*Presumptive Response Strategy and Ex-Situ Treatment Technologies for Contaminated Groundwater at CERCLA Sites. Final Guidance.*" 1996. EPA Document No. 540-R-96-023.
9. EPA. "*User Guide to the VOC's in Soils. Presumptive Remedy.*" 1996. EPA Document No. 540-F-96-008.
10. EPA. "*Presumptive Remedies: Site Characterization and Technology Selection for CERCLA Sites With Volatile Organic Compounds in Soils.*" 1993. EPA Document No. 540-F-93-048.
11. Castro C. E. "*Chemical and Microbiological Transformation at Area 15A.*" 1986. Report to Alan E. Opel, TransTechnology Corporation. Provided in Appendix C of Reference 5.
12. Castro, C. E. "*The Remediation of Area 15A.*" 1998. Letter Report Prepared for the Tennessee Valley Authority Under Contract Number: 99RE6-245326.

13. Mabrey, W., and T. Mill. "*Critical Review of Hydrolysis of Organic Compounds in Water Under Environmental Conditions.*" 1978. J. Phys, Chem. Ref. Data. 7:383-415.
14. Dilling, W. L., N. B. Tefertiller, and G. J. Kallos. "*Evaporation Rates and Reactivities of Methylene Chloride, Chloroform, 1,1,1-Trichloroethane, Trichloroethylene, Tetrachloroethylene, and Other Chlorinated Compounds in Dilute Aqueous Solutions.*" 1975. Environmental Science and Technology. Volume 9, No. 9.
15. "*The Merck Index, 10<sup>th</sup> Edition.*" 1983. ISBN Number 911910-27-1. Merck & Company, Inc., Rahway, NJ.
16. Verschueren. "*Handbook of Environmental Data on Organic Chemicals.*" 1983. Van Nostrand Reinhold Co., New York.
17. Montgomery, J. H., and L. M. Welkom. "*Groundwater Chemicals Desk Reference.*" 1990. Lewis Publishers, Inc., 121 South Main Street, Chelsea, MI.
18. EPA. "*Locating and Estimating Air Emissions From Sources of Chloroform*" March 1984. EPA-450/4-84/007c.
19. Grayson, M., ed. "*Kirk-Othmer Encyclopedia of Chemical Technology Third Edition.*". 1980. Volume II. John Wiley and Sons, New York, NY.
20. Vogel, T. M., C. S. Criddle, and P. L. McCarty. "*Transformations of Halogenated Aliphatic Compounds.*" 1987. Environmental Science and Technology. Vol. 21, No. 8.
21. Castro, C. E. "'Environmental Dehalogenation: Chemistry and Mechanism.'" 1998. Rev Environ Contam Toxicol 155:1-67. Springer-Verlag.
22. McClay, K, B. G. Fox, and R. J. Steffan. "*Chloroform Mineralization by Toluene Oxidizing Bacteria.*" 1996. Applied and Environmental Microbiology. Vol. 62, pp. 2716-2722.
23. Barnicki, E. W., and C. E. Castro. "Biodehalogenation: Rapid Oxidative Metabolism of Mono- and Polyhalomethanes by Methylosinus Trichosporium OB-3b." 1994. Environmental Toxicology and Chemistry, Vol. 13, pp. 241-245.
24. Howard, P. H., ed. "*Handbook of Environmental Fate and Exposure Data for Organic Chemicals.*" 1991. Lewis Publishers, Chelsea, MI.
25. Castro, C. E., R. E. Wade, and N. O. Belser. 1983. J. Agric. Food Chem. 31, 1184.
26. Castro, C. E., R. E. Wade, and N. O. Belser. 1985. Biochemistry. 24, 204.

27. Castro, C. E., W. H. Yokoyama, and N. O. Belser. 1988. J. Agric. Food Chem. 36, 915.
28. Castro, C. E., M. C. Helvenston, and N. O. Belser. "Biodehalogenation, Reductive Dehalogenation by *Methanobacterium Thermoautotrophicum*. Comparison With Nickel(1)octaethylisbacteriochlorin Anion, An F-430 Model." 1994. Environ. Toxicol. And Chem. 13, 429-433.
29. Gibson, D. T. "Microbial Degradation of Organic Compound." 1984. Marcel Dekkar, Inc., New York, NY.
30. Forgang, J. A. "Interim Data Presentation, Area 15A Offsite Investigation Program." 1998. Report submitted to F. Baldassare, Pennsylvania Department of Environmental Resources.
31. ICSC, Commission of the European Union, Luxembourg. 1998.
32. Radian Corporation, August 29, 1991.
33. EPA, Technology Transfer Network, United Air Toxics  
Website <http://www.epa.gov/ttnuatw1/hlthef/chlo-phe.html>.
34. USAEC. "Remediation Technologies Screening Matrix and Reference Guide." 1997. Federal Remediation Technologies Roundtable. USAEC/SFIM-AEC-ET-CR-97053.
35. Boggs, J. M., and H. E. Julian. "Demonstration of the Electromagnetic Borehole Flowmeter at Federal Laboratories Area 15A, Saltsburg, Pennsylvania." 1998. TVA Publication Number WR98-1-520-200. Engineering Laboratory, Norris, TN.
36. National Academy of Sciences. "Alternatives to Groundwater Cleanup". 1994. ISBN 0-309-04994-6.
37. Jerome, K. M., B. B. Looney, and J. Wilson. "Field Demonstration of In situ Fenton's Destruction of DNAPLs." 1998. Physical, Chemical and Thermal Technologies: Remediation of Chlorinated and Recalcitrant Compounds. pp. 353-358. Batelle Memorial Institute. Columbus, OH.
38. Tratnyek, P. G., T. L. Johnson, S. D. Warner, H. S. Clarke, and J. A. Baker. "In situ Treatment of Organics by Sequential Reduction and Oxidation." 1998. Physical, Chemical, and Thermal Technologies: Remediation of Chlorinated and Recalcitrant Compounds. pp. 371-376. Batelle Memorial Institute. Columbus, OH.

39. McKay, D. A. Hewitt, S. Reitsma, J. LaChance, and R. Baker. *"In situ Oxidation of Trichloroethylene Using Potassium Permanganate: Part 2. Pilot Study."* 1998. Physical, Chemical, and Thermal Technologies: Remediation of Chlorinated and Recalcitrant Compounds. pp. 377-382. Batelle Memorial Institute. Columbus, OH.
40. LaChance, J. C., S. Reitsma, D. McKay, and R. Baker. *"In situ Oxidation of Trichloroethylene Using Potassium Permanganate: Part 1. Theory and Design."* 1998. Physical, Chemical, and Thermal Technologies: Remediation of Chlorinated and Recalcitrant Compounds. pp. 397-402. Batelle Memorial Institute. Columbus, OH.
41. Simovic, L., and J. P. Jones. *"Removal of Organic Micropollutants From Contaminated Groundwater by Oxidation and Stripping."* 1987. Water Pollution Research Journal Canada. Volume 22, No. 1, pp. 187-196.
42. Remediation Information Management System. 1999. Abstract Regarding CAIROX Potassium Permanganate Technology for Oxidizing Halogenated Organic Compounds. Carus Chemical Company.
43. Forgang, J. A., and K. R. McIntosh. *"Case Study: Fate, Transport, and Remediation of Tear Gas Chemicals in Groundwater."* 1996. Proceedings of the Twenty-Eighth Mid-Atlantic Industrial and Hazardous Waste Conference. Technomic Publishing Company, Inc., Lancaster, PA.
44. Dorrlor, R. C., W. S. Pendexter, and K. J. Mathys. *"Remediating DNAPLs: It Can Be Done."* April 1998. Soil and Groundwater Cleanup.
45. Correspondence with Dan Bryant. June 1998. Geo-Cleanse<sup>TM</sup> International, Inc., Kenilworth, NJ.
46. Day, S. R., and L. Moos. *"A Comparison of In situ Soil Mixing Treatments."* 1998. Physical, Chemical, and Thermal Technologies: Remediation of Chlorinated and Recalcitrant Compounds. pp. 19-24. Batelle Memorial Institute. Columbus, OH.

**Supplement 1**  
**Tear Gas Fate and Effects Study**  
**Interim Progress Report (Soil Neutralization)**

**SUMMARY**

**SMP SINGLE-BUFFER METHOD FOR DETERMINING LIME REQUIREMENT**

The Shoemaker, McLean, and Pratt (SMP) single-buffer method was used to determine an application rate for pH adjustment of the CNS tear gas-contaminated soil.<sup>48</sup> Equipment and reagents were prepared as outlined in the procedure. The pH meter was calibrated before and after readings and showed stability throughout the test (data not shown). A supply of the previously autoclaved soil was dried and passed through a 0.065-inch screen. For pH readings, the soil was mixed with 0.01 M CaCl<sub>2</sub>. Triplicate determinations were made. The final pH value after addition of SMP buffer was 6.88. The corresponding lime requirements were read from the soil-buffer pH table. Estimates in the soil-buffer table are reported on the basis of metric tons/ha for the surface 20 cm of soil. Table 1 is an excerpt of a portion of the soil-buffer table for the value of pH 6.8 only. The table provides lime requirements for soil-buffer values over the range from pH 4.8 to 6.8.

An estimate of the gCaCO<sub>3</sub> requirement per cm<sup>3</sup> of soil to neutralize to around pH 6.8-7.0

$$\text{is } \frac{2.4 \frac{\text{metric tons}}{\text{ha}} \cdot \frac{\text{ha}}{10^8 \text{ cm}^2} \cdot \frac{10^6 \text{ g}}{\text{metric tons}}}{20 \text{ cm}} = 1.2 \times 10^{-3} \text{ g / cm}^3.$$

(The requirement in pounds CaCO<sub>3</sub> per yd<sup>3</sup> of soil is

$$\frac{2.4 \frac{\text{metric tons}}{\text{ha}} \cdot \frac{\text{ha}}{11959.9 \text{ yd}^2} \cdot \frac{2204.6 \text{ pounds}}{\text{metric tons}}}{20 \text{ cm} \cdot \frac{0.01094 \text{ yd}}{\text{cm}}} = \frac{2.0 \text{ pounds}}{\text{yd}^3}.)$$

**Table 1**

**Excerpt from Soil-Buffer pH Table for Evaluation of SMP Single-Buffer Method  
Showing Results for SMP Soil-Buffer Value of 6.8 Only**

<b>Desired pH</b>					
	7.0	7.0	6.5	6.0	5.2
	Mineral soils				Organic soils
	Amendment to reach desired pH (metric tons/ha)				
<b>Soil-buffer pH 6.8</b>	<b>Pure CaCO<sub>3</sub></b>	<b>Ag-Ground limestone</b>			
	2.4	3.2	2.7	2.3	1.5

#### SOIL NEUTRALIZATION CURVE ( $\text{CaCO}_3$ )

The validity of the lime requirement estimate for soil neutralization was confirmed in the following manner. Six 30-g soil samples of the dried, autoclaved soil were weighed and numbered samples 1 through 6.  $\text{CaCO}_3$  was added directly to respective soil samples 1 through 6 resulting in 0.0008, 0.0012, 0.0027, 0.0050, 0.0101, and 0.0150 g  $\text{CaCO}_3$  per g (or  $\text{cm}^3$ ) soil. Sufficient 0.01 M  $\text{CaCl}_2$  was added to bring the soil moisture to approximately 20%. The soil samples were incubated for 16 days. During this period, the soil was allowed to dry, then remoistened three times to simulate field wet-dry periods. When the final pH was determined, a 10-g portion from each soil sample was mixed with 10 ml of water and another 10-g portion with 10 ml 0.01M  $\text{CaCl}_2$ . There was little difference between readings with water and with 0.01M  $\text{CaCl}_2$ . Figure 1 depicts the titration curve of soil samples mixed with water for pH determinations.

Extrapolation of the initial portion of the titration curve results in an estimate of 0.0022 g  $\text{CaCO}_3/\text{g}$  soil (3.7 pounds/ $\text{yd}^3$ ) for adjusting the soil pH to 6.8. This estimate is relatively close to the SMP single-buffer method result of 0.0012 g/ $\text{cm}^3$  (2 pounds/ $\text{yd}^3$ ).

#### SOIL NEUTRALIZATION CURVE ( $\text{NH}_4\text{OH}$ )

An additional determination of the amount of  $\text{NH}_4\text{OH}$  required to adjust the soil to pH 6.8 was made. To determine the amounts of  $\text{NH}_4\text{OH}$  to add to soil for the test, it was assumed that the two bases will display similar strengths for neutralizing the soil. Two 30-g soil samples of the dried, autoclaved soil were weighed and solutions of  $\text{NH}_4\text{OH}$  were prepared in such a way as to provide 0.0216 and 0.0361 g  $\text{NH}_4\text{OH}$  per 30 g (or  $\text{cm}^3$ ) soil and sufficient liquid to bring the soil moisture to approximately 20%. The soil samples were incubated as described for  $\text{CaCO}_3$  tests above. Figure 2 depicts the titration curve of soil samples mixed with water for pH determinations.

**Figure 1**  
**Titration Curve of CNS-Contaminated Soil With  $\text{CaCO}_3$**

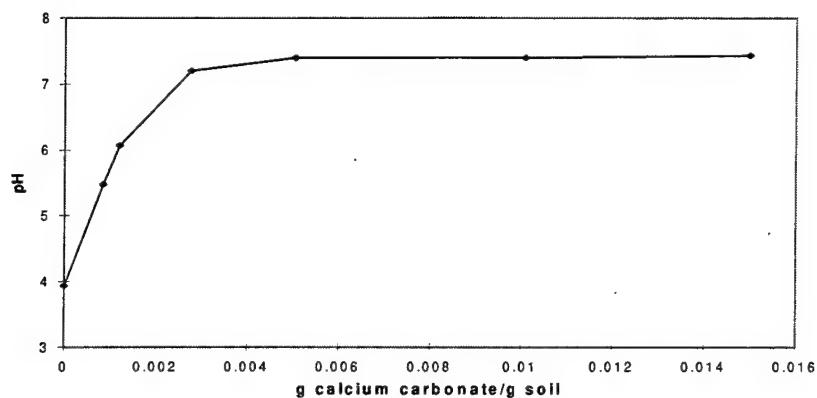
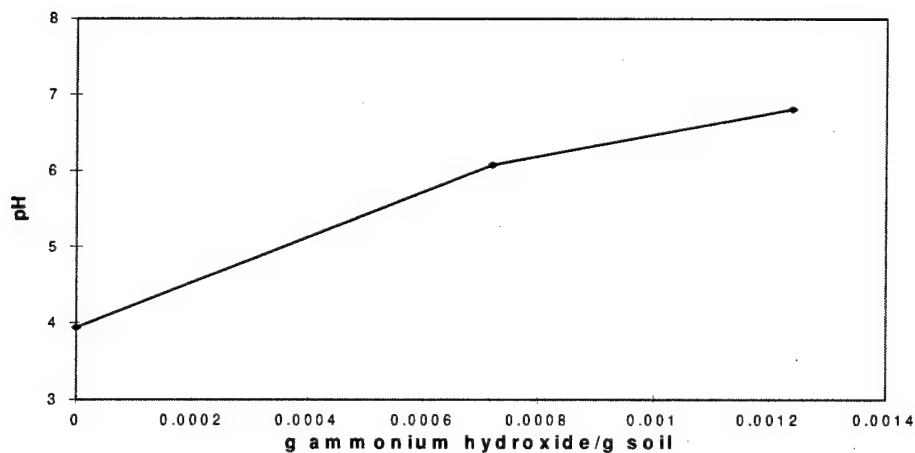


**Figure 2**  
**Titration Curve of CNS-Contaminated Soil With  $\text{NH}_4\text{OH}$**





Extrapolation of the titration curve results in an estimate of  $1.2 \times 10^{-3}$  g  $\text{NH}_4\text{OH}$ /g soil (2 pounds/yd<sup>3</sup>) for adjusting the soil pH to 6.8.

## RESULTS AND DISCUSSION

The amount of ammonia to achieve a pH of 6.8 in the CNS contaminated soil was determined to be  $1.2 \times 10^{-3}$  g  $\text{NH}_4\text{OH}$ /g soil (2 pounds  $\text{NH}_4\text{OH}$ /yd<sup>3</sup>) or  $4.8 \times 10^{-4}$  g N/g soil (0.8 pounds N/yd<sup>3</sup>). The rate is based on a soil depth of 20 cm.

A near-neutral pH is optimum for bacterial growth and activity. Additionally, a typical N application rate for successful microbial growth is a carbon to nitrogen ratio of 100:10. The components found in the contaminated soil (25.8 mg/kg CF, 23.4 mg/kg CP, and 31.4 mg/kg CN) account for a total of 23.8 mg C/kg soil ( $2.38 \times 10^{-5}$  g C/g soil). If CNS components are the only source of carbon in the soil, then a C:N ratio of 100:2017 will result from the addition of  $4.8 \times 10^{-4}$  g N/g soil. However, the soil organic carbon is reported to be 0.48% ( $4.8 \times 10^{-3}$  g C/g soil). Assuming the latter soil carbon concentration of  $4.8 \times 10^{-3}$  g C/g soil, application of N at the rate to achieve a pH of 6.8,  $4.8 \times 10^{-4}$  g N/g soil, will result in a C:N of 100:10. Fortuitously, the amount of  $\text{NH}_4\text{OH}$  for neutralization is also that needed for the C:N of 100:10.

**APPENDIX H**  
**INJECTION AND RECOVERY SYSTEM DESIGN**

**DRAFT**

April 29, 1999

EVALUATION OF INJECTION AND RECOVERY ALTERNATIVES FOR  
AREA 15A CONTAMINANT SOURCE  
FEDERAL LABORATORIES FACILITY NO. 3  
SALTSBURG, PENNSYLVANIA

*Prepared for*

U.S Army Environmental Center  
*Aberdeen Proving Ground, Maryland*

*Prepared by*

Tennessee Valley Authority  
Environmental Research Center  
*Muscle Shoals, Alabama*

April 1999

TVA Contract No. RG-99802V  
Report No.

## Table of Contents

List of Figures .....	iii
List of Tables .....	iv
Acronyms and Abbreviations .....	vi
Executive Summary .....	vii
1. Introduction.....	1
1.1 Background .....	1
1.2 Purpose and Scope .....	2
2. Site Location and Setting .....	4
3. Physiography and Depositional Environment .....	7
3.1 Physiography.....	7
3.2 Depositional Environment .....	9
4. Geology.....	12
4.1 Bedrock.....	12
4.2 Soils .....	16
4.3 Local Coal Mines.....	18
5. Hydrostratigraphy .....	20
6. Groundwater Recharge .....	27
6.1 Overview.....	27
6.2 Water Balance (HELP) Model Description .....	27
6.3 Water Balance (HELP) Model Set-Up.....	28
6.4 Water Balance (HELP) Results.....	29
7. Soil and Bedrock Hydraulic Properties.....	30
7.1 Soil Hydraulic Properties.....	30
7.2 Bedrock Hydraulic Properties.....	31
8. Injection-Recovery System Simulations.....	34
8.1 Model Selection (MODFLOW and MT3DMS) .....	34
8.2 Conceptual Model.....	35
8.3 Model Set-Up.....	35
8.4 Remediation Alternatives.....	40

8.5 Flow Model Results .....	46
8.6 Transport Model Results.....	56
9. Conclusions and Recommendations .....	58
9.1 Conclusions.....	58
9.2 Recommendations.....	59
10. References.....	62

## List of Figures

2-1 Site Location Map.....	5
2-2 Topography in the Vicinity of Area 15A (Contours in ft-msl).....	6
3-1 Regional Physiography Maps (Adapted from Pennsylvania Department of Conservation and Natural Resources Maps 13 and 64) .....	8
4-1 Structural Map of the Region Surrounding Area 15A Using Base of the Upper Freeport Coal as Lithologic Marker (Adapted from Williams and McElroy, 1997) .....	14
4-2 Top of Bedrock in the Vicinity of Area 15A (Contours in m-msl).....	15
4-3 Soil Sampling Map for (a) May 1997 and (b) November 1997.....	17
4-4 Approximate Aerial Extent of the Upper Freeport Coal Underground Tunnel System for the Abandoned Watson Mine in the Vicinity of Area 15A .....	19
5-1 Temporal Plots of Groundwater Levels at Wells Developed in the Saltsburg Sandstone .....	21
5-2 Potentiometric Maps for the Saltsburg Sandstone During (a) March 1997 - Wet Period, and (b) December 1998 - Dry Period (Contours in m-msl).....	22
5-3 Continuous Groundwater Levels Versus Precipitation at Wells MWU-15, MWU-19, MWU-20, and OWP-15 for the Period December 1997 through July 1998 (Dashed Lines Indicate Artificially Generated Data).....	24
5-4 Temporal Plots of Groundwater Levels at Wells Developed in the Buffalo Sandstone.....	25
5-5 Potentiometric Maps for the Buffalo Sandstone During (a) March 1997 - Wet Period, and (b) December 1998 - Dry Period (Contours in m-msl) .....	26

8-1	Domain, Initial Grid System, and Boundary Conditions for MODFLOW and MT3DMS Model Simulations .....	36
8-2	East-West Cross Section of Model at y=3240 m Showing Layering Scheme Used in Model Simulations.....	38
8-3	Conceptual Schematics for Remediation Scenarios 2 and 3.....	42
8-4	Conceptual Schematics for Remediation Scenarios 4 and 5.....	43
8-5	Conceptual Schematics for Remediation Scenarios 6a and 6b .....	44
8-6	Calibrated Flow Model Results: (a) Equipotential Surface Map (Contours in m-msl) and (b) Comparison of Predicted and Observed Heads.....	47
8-7	Directional Vectors from Flow Model Simulation of Scenario (Base Case).....	49
8-8	Potentiometric Heads at Depth of 1 to 1.5 m from Flow Model Simulations of Scenarios 2 - 6.....	50
8-9	East-West Cross Section of Model at y = 3240 m Illustrating Pathline Predictions (Particle Tracking) for Scenario 6b.....	51
8-10	Potentiometric Heads for Scenario 6b Along East-West Cross Section of Model at y = 3240 m.....	53
8-11	Comparison of Flow Model Simulations: (Top) Cumulative Pore Volume Fraction Versus Time, and (Bottom) Influx Reaching Withdrawal.....	54
8-12	Transport Predictions for Scenario 6b After One, Three, and Five Years. Plot is Oriented Along East-West Cross Section of Model at y = 3240 m.....	57

### List of Tables

4-1	Results of Laboratory Analyses for Soil Physical Properties .....	16
6-1	Soil Properties Used in the HELP Simulation.....	29
6-2	Average Annual Totals for 20-yr Simulation .....	29
7-1	Results of Laboratory Analyses for Soil Hydraulic Properties.....	30
7-2	Transmissivity and Hydraulic Conductivity Values of Upper Zone Wells from Constant Rate Pumping Test.....	32
8-1	Layer Hydraulic Properties for MODFLOW/MT3DMS Simulations.....	39

8-2	Remedial Scenarios Considered in Model Simulations.....	41
8-3	Predicted Steady-State Influx Reaching Withdrawal System and Cumulative Yearly Pore Volume Fraction from Flow Model Simulations.....	55

## Acronyms and Abbreviations

CNS	Mixture of 2-Chloroacetophenone (CN), Chloroform (CF), and Chloropicrin (CP)
CRA	Conestoga-Rovers & Associates
DNAPL	Dense, Non-aqueous Phase Liquid
CN	2-Chloroacetophenone
CF	Chloroform
CP	Chloropicrin
MCL	Maximum Concentration Limit
MSL	Mean Sea Level
ESC	Environmental Sciences Consultants, Inc.
UF	Upper Freeport
TOC	Total Organic Carbon
K	Hydraulic Conductivity
$K_h$	Horizontal Hydraulic Conductivity
$K_v$	Vertical Hydraulic Conductivity
$K_{sat}$	Saturated Hydraulic Conductivity
CJSL	Cooper Jacob Straight-Line
T	Transmissivity
USEPA	U.S. Environmental Protection Agency



## Executive Summary

A numerical modeling analysis has been performed to quantitatively evaluate aqueous treatment agent injection and recovery alternatives for the drum burial zone of the Area 15A CNS tear gas disposal site. The site is characterized by a thin layer of residual silty/sandy clay soil averaging approximately 3 m in thickness in the drum disposal area. Fractured and interbedded sandstones, shales, and thin coal seams of the Glenshaw Formation lie below the soil overburden. Groundwater originating at the site as incident precipitation migrates downward through the drum burial zone into the underlying bedrock. Subsequent groundwater movement in the bedrock is both downward and southwesterly, occurring primarily in a sparse network of hydraulically active fractures with only limited flow in the low permeability rock matrix. Groundwater ultimately discharges along bedrock outcrops forming surface seeps located less than 200 m west of Area 15A.

The scenarios considered for active remediation are relegated to the soil and shallow bedrock horizon of the contaminant source area defined by previous site investigations. In comparing injection and recovery scenarios, an emphasis is placed on potential designs meeting the following criteria: hydraulic efficiency and minimization of offsite contaminant migration; effective delivery of aqueous treatment agents to reduce contaminant concentrations; and the resultant project lifetime. The conceptual model used for numerical simulations relies on historical characterization information and more recent data collected for this study.

In addition to a base case alternative, five different types of engineered delivery/recovery systems have been simulated to obtain a relative comparison of optimal source control measures. All of these alternatives include vertical wells, horizontal wells, or trenches for fluid recovery. Additionally, injection of aqueous agents to augment contaminant degradation are included as shallow injection wells or infiltration galleries.

Results of flow model simulations indicate that the use of shallow injection wells for delivery of an aqueous agent to the site disposal area is limited by the assumed hydraulic conductivity of the disposal area ( $5 \times 10^{-6}$  cm/s). An infiltration gallery scheme is preferred since it allows higher influx rates and provides more uniform distribution through the soil zone of the disposal area. Of all scenarios evaluated, model simulation results indicate that horizontal extraction wells installed at the base of the disposal area provide the most effective capture of

both existing contaminants within the soil horizon and aqueous treatment agents added via an infiltration gallery. The optimal solution includes horizontal wells oriented perpendicular to the natural (westerly) hydraulic gradient. Flow model predictions indicate that over 80 percent of influx through a simulated infiltration gallery is extracted by horizontal wells in this alternative. Additionally, 1.3 pore volumes per year of groundwater are displaced through soil within confines of the disposal area under the optimal scenario. This is an order of magnitude greater than alternatives relying on vertical wells or trench systems for groundwater extraction.

Transport simulation results for scenarios adopting vertical extraction wells and trenches indicate poor removal of existing contaminants and a strong potential for aqueous agents to escape through the bottom of the disposal area. Additionally, insufficient lateral dispersion of aqueous agents is afforded by trench systems or linear injection methods. Transport simulation results for the horizontal well scenario are optimal with regard to relatively rapid vertical migration of an infiltrating solution and subsequent behavior of the resulting plume. Aqueous agents may be well distributed throughout the soil zone, but will remain within the confines of the disposal area. Predicted concentrations of an aqueous agent entering the underlying Saltsburg Sandstone approach only five percent of initial concentrations after five years.

# **1. Introduction**

## **1.1 Background**

The Army Environmental Center contracted with TVA Resource Management to conduct a scientific study of the fate, transport, and effects of CNS tear gas in soils. The goal of this study was to obtain basic information regarding the behavior of soil-borne CNS tear gas components for use in predicting their transport and fate in soil and groundwater. A CNS tear gas disposal facility operated by the U.S. Army following World War II near Saltsburg, Pennsylvania, was selected as the study site. The original project goal was expanded to include development of a remedial strategy for the disposal facility, known as Area 15A, now owned by TransTechnology Corporation.

CNS tear gas is composed of chloroform (CF), chloropicrin (CP), and 2-chloroacetophenone (CN) in relative proportions of 38%, 38%, and 24%, respectively. CF and CP are dense nonaqueous phase liquids (DNAPLs). CF serves as a solvent for CN which is a solid at standard temperature and pressure. The migration behavior of DNAPLs in the subsurface is complex and is strongly affected by the density gradient they create by virtue of their higher density compared with water. Unlike neutrally buoyant compounds, their migration is often influenced as much by geologic conditions as by ambient groundwater movement. Because of their complex migration behavior, characterizing the subsurface spatial distribution of DNAPLs is problematic. Care must be taken in exploratory drilling and well installation not to create pathways for further downward migration of DNAPL contaminants. For this reason, there has been no characterization of the CNS contaminant plumes directly beneath Area 15A.

In general, the Area 15A site is mantled by relatively thin soil that is underlain by fractured sandstone and shale bedrock. Some 300 to 1700 metal drums containing CNS tear gas were buried in the soil sometime in the late 1940s. Subsequent corrosion of the metal containers has lead to contamination of both the soil and underlying bedrock aquifer. The focus of remedial strategies development in the present study has been on restoration of the contaminated soil overburden. Severe technical difficulties associated with treatment or removal of DNAPL contaminants in fractured porous media render active remediation of the bedrock aquifer infeasible from a practical standpoint.

An important issue at Area 15A is whether overburden remediation will significantly reduce the overall time required for natural restoration of remaining contamination within the bedrock aquifer in the site vicinity. The prediction of natural attenuation of site contaminants is more complex than a predictive analysis of relatively shallow remediation alternatives since it includes realizations of the deeper fracture flow system. Hence, the natural restoration of Area 15A is simulated separately using a model that accounts for fracture flow and transport within bedrock media as described in Appendix F.

An assessment of remedial strategy alternatives for Area 15A is provided in Appendix H. As described in Appendix H, strategies with good feasibility for remediating soil within the drum burial area include in situ chemical/biological treatment involving the delivery of ammonium hydroxide and methanol, and hot air injection with base addition using a large diameter mixing auger and soil vapor extraction. Assuming that some type of source remediation will be required for Area 15A, it is advantageous to evaluate potential treatment scenarios given hydrogeologic constraints of the site. A critical component in such an evaluation is determination of an injection and recovery strategy that will provide optimal delivery of treatment agents to CNS contaminants while maintaining hydrodynamic isolation of the source area. This report describes the systematic analysis of aqueous treatment agent injection and recovery scenarios using model simulations of shallow groundwater flow and transport.

## **1.2 Purpose and Scope**

The primary objective of this study is a quantitative evaluation of aqueous treatment agent injection and recovery alternatives for the contaminant source area of Area 15A using groundwater flow and transport model predictions. This report discusses the results of model simulations for conditions of active remediation. The scenarios considered for active remediation are relegated to the soil and shallow bedrock horizon of the contaminant source area defined by previous site investigations. Simulations were run using the respective flow and transport models MODFLOW and MT3DMS.

Controlling subsurface fluids is among the highest priorities in managing sites with in situ contamination. In comparing injection and recovery scenarios, an emphasis is placed on potential designs emphasizing hydraulic efficiency and minimization of offsite contaminant migration (capture zone); effective delivery of aqueous treatment agents to reduce contaminant

concentrations (pore volume); and relatively short time requirements. Probably the most common system used to recover fluids at a contaminated site is a vertical well. However, this system is by no means the most effective in every situation. Therefore, this study includes alternatives to conventional applications of vertical wells that may improve performance and reduce project lifetime. The conceptual model used for numerical simulations relies on historical characterization information and more recent data collected for this study.

## 2. Site Location and Setting

The Federal Laboratories facility is located in Conemaugh Township, Indiana County, Pennsylvania. Historical operations of the Federal Laboratory are described in previous site investigation reports by Earth Sciences Consultants, Inc. (ESC) (ESC, 1985 and ESC, 1992a,b). The facility is approximately 4.5 km east of the town of Saltsburg and 2.0 km north of the town of Tunnelton (Figure 2-1). Manufacturing activities currently exist on 14.2 ha adjacent to State Route 3003 (Tunnelton Road).

Area 15A resides on the western portion of the Federal Laboratories property within a 60.7-ha area referred to as Drainage Basin I (ESC, 1992a,b; Figure 2-4). The site is topographically situated in the uplands along the north side of the Conemaugh River. In the immediate vicinity of the disposal site, the land surface slopes gently to the west toward Elders Run, a tributary to the Conemaugh River.

According to ESC (1992a,b), the approximate contaminated surface area of Area 15A is 1.52 ha. Based on surface geophysical investigations, test pits, borings, and monitoring wells, the contaminant source area (~1 ha) is depicted by rectangles with approximate overall dimensions of 61 m by 168 m (Figure 2-2). As shown in Figure 2-2, Area 15A is bounded on the immediate NW by Tributary B, and Tributary A is located approximately 240 m east of the site. A public gravel road is proximal to the southern boundary of the site, and a small gravel roadway provides access to the site from the east. The ground surface of Area 15A is grassed, and elevation ranges from approximately 1170 to 1200 ft-msl (3 to 4 percent westerly slope). Just west and south of the site the ground elevation declines steeply toward Elders Run and the Conemaugh River.

Surface geophysical investigations, test pits, and interviews with plant personnel were used to estimate the approximate extent and alignment of buried drums in Area 15A. Drums were judged to be lying on their sides in rows oriented NE-SW, perpendicular to the gravel roadway south of the site. The conditions of the drums (55-gallon; heavy gauge steel) ranged from slightly to extremely deteriorated. The occurrence of aqueous fluids in the eleven drums investigated and stained soil adjacent to the drums indicate leakage over time. Data from test pits suggest that CNS comprises about ten percent of the total volume of drums investigated. Consequently, the vast majority of CNS originally in the drums at the time of burial has leaked into the adjacent soils (ESC, 1985). This has been confirmed by soil sampling at the site.

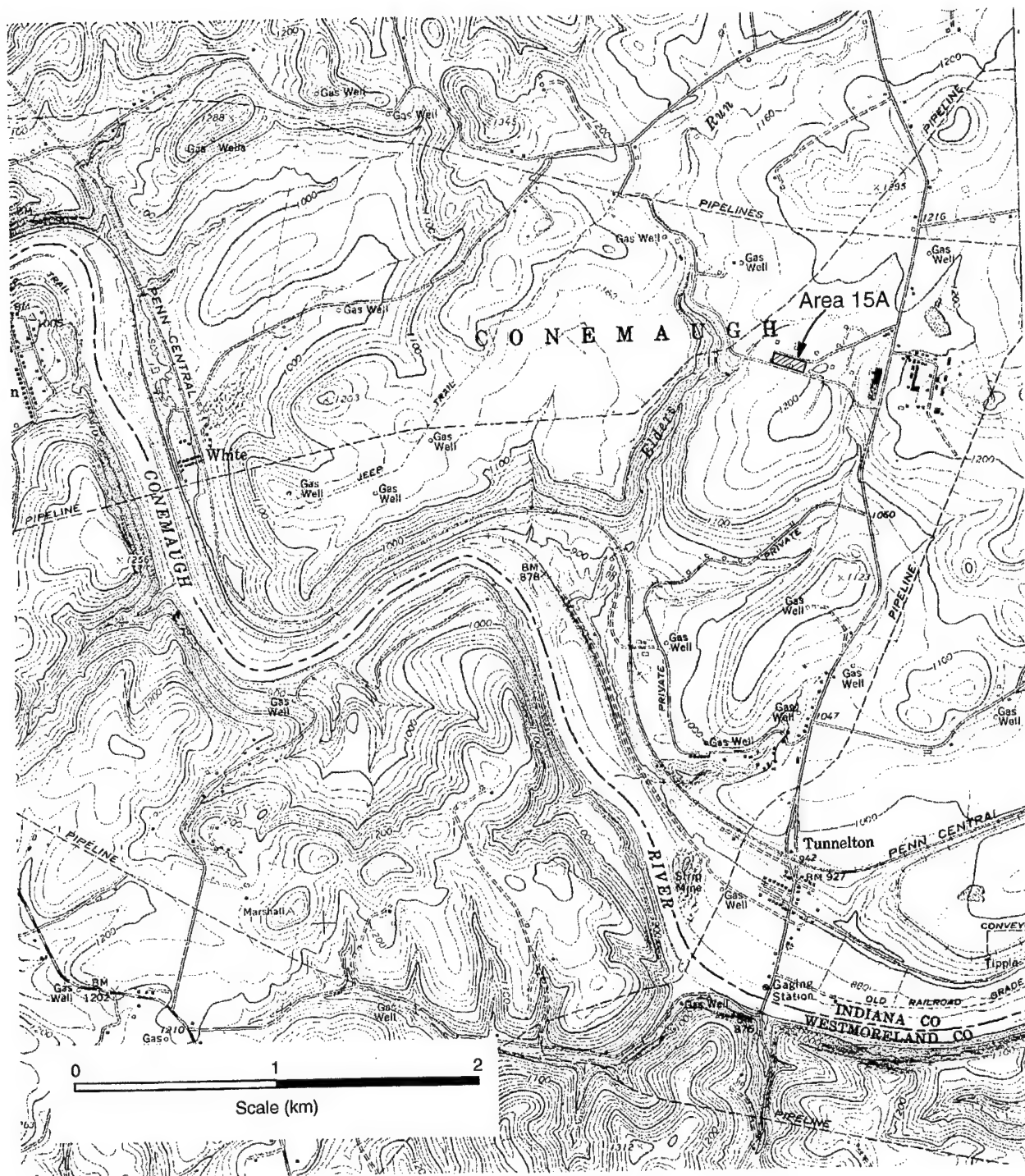


Figure 2-1 Site Location Map

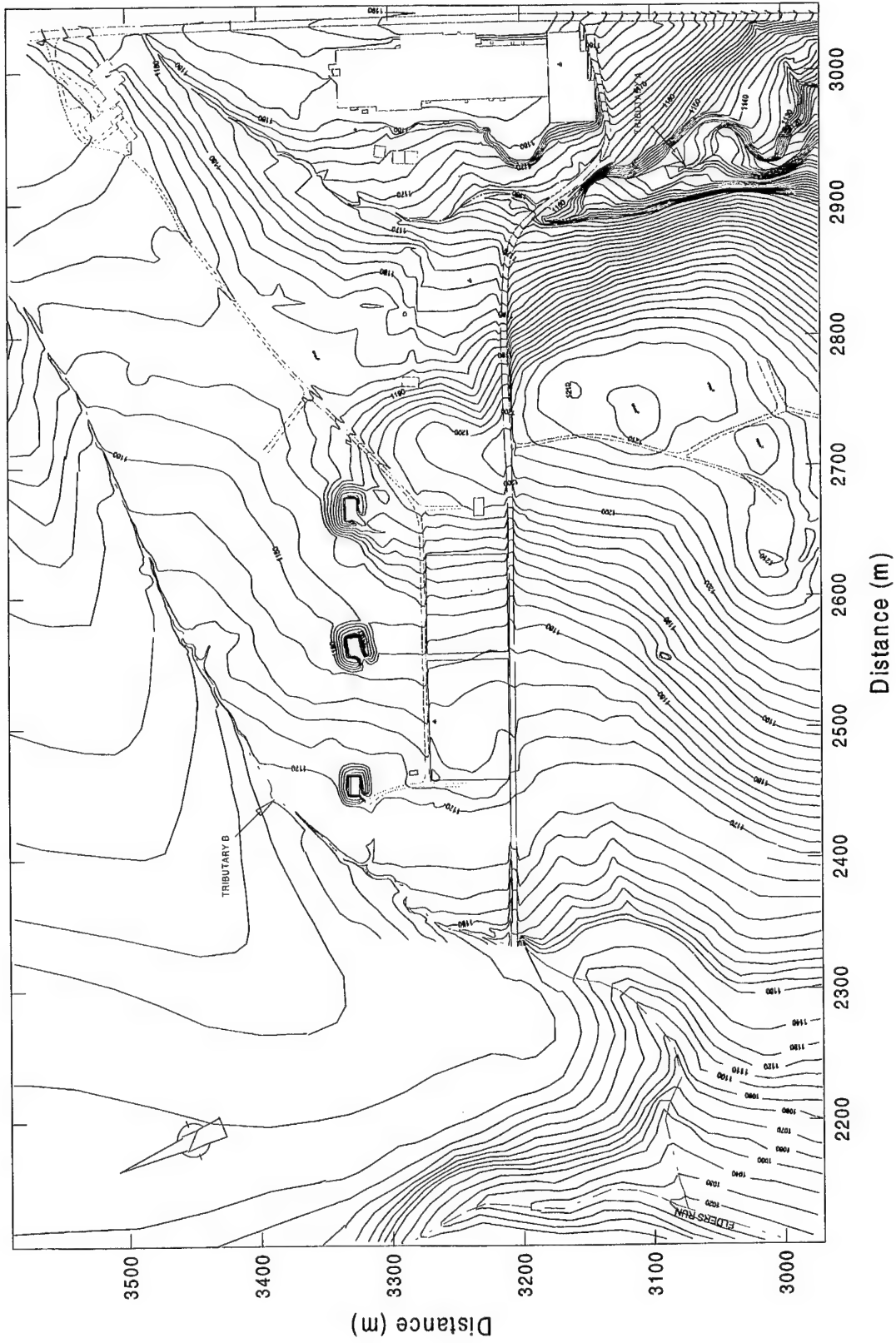


Figure 2-2 Topography in the Vicinity of Area 15A (Contours in ft-msl)



### 3. Physiography and Depositional Environment

#### 3.1 Physiography

The site resides in the Pittsburgh Low Plateau Section of the Appalachian Plateaus Physiographic Province within the Appalachian basin (Figure 3-1). The study site resides in the unglaciated section of the Appalachian Plateaus Province. Historically, this section has been referred to as the Unglaciated Allegheny Plateau Section (Fenneman, 1938). The Appalachian Plateaus Physiographic Province extends over more than one-half of Pennsylvania. The province is bounded on the east and southeast by the Valley and Ridge Province and by a narrow strip of the Central Lowland Province in Erie County, Pennsylvania. The Appalachian Plateaus Province is underlain by rocks that are continuous with those of the Valley and Ridge Province. In the Appalachian Plateaus the layered rocks are nearly flat-lying or gently tilted and warped rather than being intensively folded and faulted. The eastern boundary of the Appalachian Plateaus is marked by a prominent southeast-facing scarp called the Allegheny Front in Pennsylvania. A northward-facing erosional escarpment forms the boundary between the Appalachian Plateaus and the Central Lowland Provinces. The altitude of the Appalachian Plateaus Province is higher than that of the Valley and Ridge Province as well as the Central Lowland Province.

The Pittsburgh Low Plateau Section consists of a smooth, undulating upland surface that is maturely dissected by numerous, narrow, relatively shallow valleys. The uplands are developed on rocks containing the bulk of the significant bituminous coal in Pennsylvania. The landscape reflects this by the presence of some operating surface and subsurface mines, many old stripping areas, and many reclaimed stripping areas (PTGS, 1998). Ground surface elevations in the Pittsburgh Low Plateau Section range from 200 to 520 m-msl. Local relief between valley bottoms and upland surfaces may be as much as 120 m. Valley sides are usually moderately steep except in the upper reaches of streams where the side slopes are fairly gentle. Ground surface elevations in the vicinity of the site range from about 270 to 340 m-msl (Figures 2-1 and 2-2).

Geologic structure in this section of the Appalachian Plateaus Province consists of a series of NE-SW trending anticlines and synclines which resulted from compressional forces from the southeast during episodic mountain building. The intensity of structural deformation decreases progressively to the west from the Appalachian structural front. Hence, the rocks of

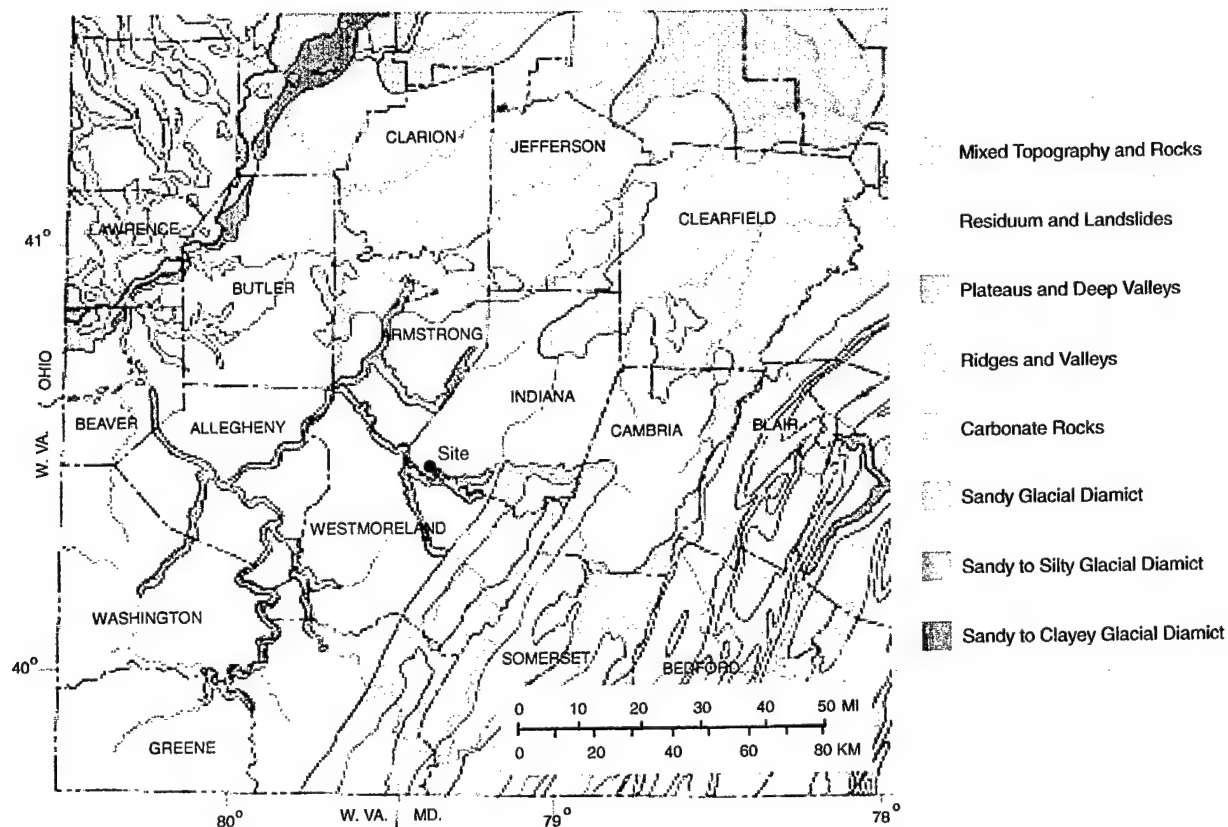
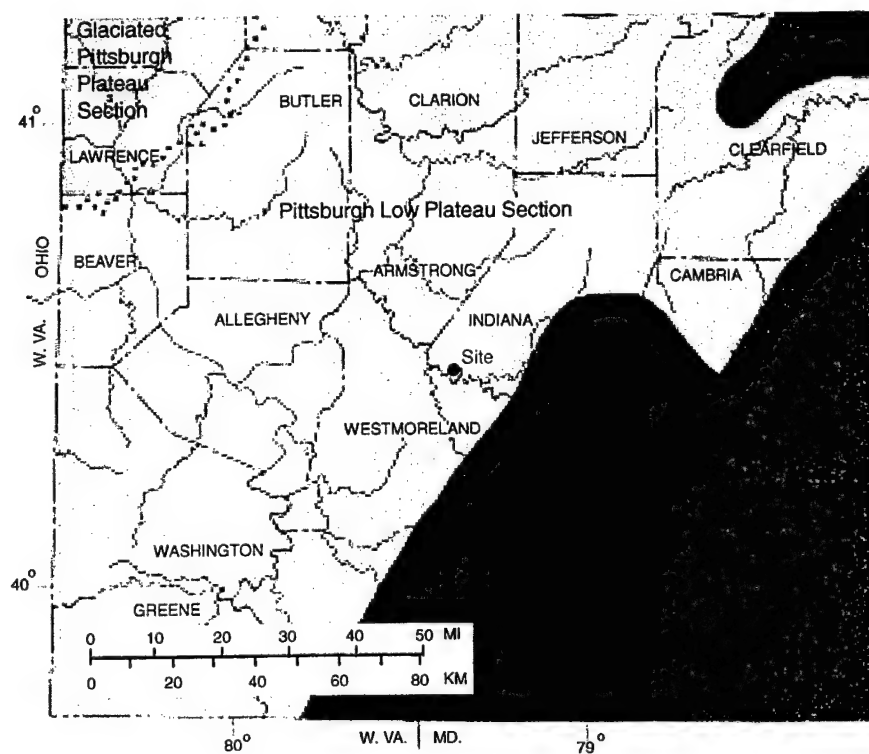


Figure 3-1 Regional Physiography Maps (Adapted from Pennsylvania Department of Conservation and Natural Resources Maps 13 and 64)

the Appalachian Plateaus are characterized by the general absence of thrust faults intersecting the surface and by gentle, approximately symmetric surface folds (Colton, 1970).

### **3.2 Depositional Environment**

The Appalachian Basin is an oblong sedimentary basin extending from the Canadian shield southwestward to Alabama, approximately parallel to the Atlantic coastline. This basin is an elongated down-warped segment of the earth's crust in which a great thickness of sediment accumulated, mostly from shallow marine deposition of tectonic source sediments during long periods throughout the Paleozoic era. To some extent concurrently with deposition, but largely after the bulk of sediments had been deposited, the mass of sedimentary rock was uplifted and deformed. Finally, erosional processes [e.g., removal of the Schooley Peneplain (Fenneman, 1938)] which are still active, created the present topography (Colton, 1970).

The study site resides on the western margin of the Appalachian geosyncline, a narrow zone of maximum subsidence oriented NE-SW within the Appalachian Basin. The western margin is a transitional zone of the geosyncline to a broad stable platform area (foreland). Thick wedges of nonmarine clastics were deposited at three times during the filling of the Appalachian geosyncline, once in the late Ordovician and early Silurian, and twice in the late Devonian through Pennsylvanian. Each sequence is associated with a major source area orogeny (mountain building episode of the Appalachians) and terminated a period of widespread marine deposition. These thick, dominantly alluvial accumulations of lithologies, ranging from conglomerate to coal, thin markedly away from the source and intertongue basinward (W-NW) with shallow marine sections. Lithologically, Pennsylvanian formations show similar regional patterns. The clastics are coarsest in the eastern areas and become progressively finer to the W-NW. In the westernmost areas, shale predominates over sandstone. The Pennsylvanian sequence originally constituted a much thicker and more extensive wedge of clastic rocks, much of which has been removed since Paleozoic time (Meckel, 1970).

The alluvial wedge was formed in three phases. There was (a) an initial period of regional regression during which continental environments replaced marine environments; followed by (b) a period of maximum nonmarine regression; and (c) a final period of regional transgression during which the marine encroached back across the basin.

During regional regression, the rate of terrestrial deposition exceeded the rate of subsidence and there was a westward progradation of the coastal plain. Therefore, the transitional marine-nonmarine contact rose in the stratigraphic section to the west.

Alluvial deposition extended into the basin from the southeast during maximum regression. The rates of subsidence and deposition were approximately equal. Local transgressions and regressions occurred at this time in the distal part of the basin by epeirogenic episodes.

During regional transgression, the rate of subsidence exceeded the rate of deposition and marine deposition advanced easterly (Meckel, 1970).

A second depositional system, intermittent during Pennsylvanian time, contributed small volumes of material to the Appalachian Basin. This system originated in a stable northern (cratonic) source which bounded the basin to the north. Fluvial material was dispersed S-SW across the relatively stable, slowly subsiding northern margin of the depositional basin. The material either reworked with sediments from the eastern tectonic source or was removed by erosion along the northern margin of the basin.

The uppermost sequence of rocks at the site belong to the Conemaugh Formation. Approximately 120 to 150 m thick, the Conemaugh was deposited in late Paleozoic time, primarily during the Upper Pennsylvanian Period (290 to 300 Ma). During this interval, the Appalachian Orogeny (Revolution) occurred intermittently with periods of widespread alluvial deposition from the E-SE. Regionally, the sediments represent a variety of depositional environments, all of which are elements of a broad coastal plain flanking a marine embayment. Along the western margin of the geosyncline (Foreland), the sediments are low-gradient deltaic and intertidal planes derived from a broad emergent alluvial apron. According to Meckel (1970), the depositional pattern of the tectonically derived sediments is one of thick alluvial clastics in the east which thin and intertongue westward with thinner time-equivalent marine strata.

The Conemaugh Formation coincides with the Llewellyn Formation in the Upper Pennsylvanian stratigraphic column and includes equivalent strata. The Llewellyn is mainly characterized by cyclic repetitions of interbedded sandstone, shale, and coal. The upper part of the Llewellyn also contains several thin limestone beds, one of which--the marine Mill Creek Limestone--is generally correlated with the Ames Limestone (middle of the Conemaugh Group, top of the Glenshaw Formation). Recently discovered caliche in several seatrock and non-

seatrock soils above the Mill Creek Limestone is the first demonstration that calcitic soils common in the middle and upper Conemaugh Group of western Pennsylvania also occur in the Northern Anthracite Region. Meckel (1970) indicates that paleocurrents (which affect sediment dispersal) during deposition of the Llewellyn were predominantly northerly.

Facies of the arenaceous upper bedrocks at the site suggest basal lacustrine and flood plain deposition accompanied by episodic progradation by meandering stream deposits. The source of the sediment was probably a combination of clastics from both the tectonic source to the east and cratonic sources to the north. The light gray to dark gray mudrocks (shales and siltstones) and sandstones are highly carbonaceous and suggest deposition in an anoxic environment with little water circulation. Low granularity also implies deposition via turbidity currents or geostrophic flows. Such conditions are indicative of ancient lacustrine facies. However, paleontologic studies to distinguish fossils as marine or non-marine are lacking. Observations of fissility and thin bedding in the mudrock cores suggest a fresh water depositional environment. There were likely periods of emergence during deposition of the site upper bedrocks since thin coal seams were produced by autochthonous swamp deposits. The site setting during periods of basal rock deposition, therefore, may be described as a subaerial swamp bordering the lacustrine basin during low water periods.

The presence of thin conglomerate (rounded gravel) beds and clasts (i.e., rip-up and detrital) in the upper bedrocks at the site also indicate time intervals of relatively fast moving waters (fluvial activity) across the site during pluvial times. Lithologic evidence of progradation and/or fluvial activity is also displayed by large lateral facies variations and bedding (i.e., thin to massive). The source of conglomerate containing sediment is likely cratonic material originating from the north. Ferm's (1970) depositional model for Pennsylvanian rocks in Indiana County is one of an actively prograding delta wedge from the north. This model is supported, to some degree, by fluvial strata in upper bedrocks at the site. It is possible that fluvial-dominated deltaic deposits from the north periodically drowned and reworked swampy flood plain and lacustrine sediments at the site during several periods. However, the position of the site relative to the vertical and lateral facies of the prograding delta is undetermined.

## 4. Geology

### 4.1 Bedrock

The primary geologic unit of interest relative to Area 15A is the Pennsylvanian Age Glenshaw Formation of the Conemaugh Group. It is the uppermost lithologic unit at Area 15A. The Glenshaw is comprised of a sequence of interbedded sandstone, shale, and thin coal units. The top of the Upper Freeport Coal marks the base of the Conemaugh Group and Glenshaw Formation.

Based on a review of the site assessment literature, ESC (1985) was the first to delineate stratigraphic units of interest beneath the site. Typical of strata within this geologic sequence, the arenaceous members of the Glenshaw are described by ESC (1985) as fine- to medium-grained, micaceous, thin to massively bedded, and commonly displaying large lateral facies variation. Argillaceous strata are depicted as fissile and typically thin bedded. Coal seams are thin and discontinuous or may be represented by bony coal, possibly the Brush Creek Coal horizon. ESC (1985) indicates that the lithologic units of interest beneath the site are, from youngest to oldest, the Saltsburg Sandstone, Buffalo Sandstone, Brush Creek Coal, Mahoning Coal, Mahoning Sandstone, and Upper Freeport Coal. This stratigraphic description has been echoed in subsequent reports (ESC, 1992a, b) dealing with Federal Laboratories site investigations.

The names of many stratigraphic units, particularly coal-beds and sandstone units, have arisen from local nomenclature, particularly by coal companies. The names have been taken from geographic locations within relatively small mining districts or within coherent drainage basins. Rice et al. (1994) provide a comprehensive glossary for the central Appalachian Basin which expands on older stratigraphic glossaries and includes the joint SEAMS database of the University of Kentucky's Energy Center for Applied Energy Research and the Kentucky Geological Survey. Informal rock units contained in the glossary and present at the site include the Buffalo and Saltsburg Sandstones. According to the glossary of Rice et al. (1994), the Saltsburg Sandstone is exposed along Conemaugh and Loyalhanna Rivers near Saltsburg, Indiana County, Pennsylvania; in Conemaugh Formation between Harlem Coal or Pittsburgh Redbeds (above) and Upper Bakerstown Coal (Keroher et al., 1966). The Buffalo Sandstone is a massive sandstone member cropping out in Buffalo Creek, Buffalo Township, eastern Butler

County, Pennsylvania; in lower part of Conemaugh Formation between Cambridge or Meyersdale limestone (above) and Brush Creek limestone (Wanless, 1939).

The glossary of Rice et al. (1994) indicates that the original designation of lithologic units at the site by ESC (1985) may be the result of convenience rather than true stratigraphic identity since these formations exhibit significant lateral facies variability. Regardless, this nomenclature is sufficient for purposes of lithologic description, and the stratigraphic time correlation is approximately correct. For the sake of continuity, therefore, this report will adhere to the lithologic nomenclature prescribed by ancestral investigation reports.

Based on geologic logs for monitoring wells in the site vicinity, it appears that shale or saptolite lies directly below the eastern two-thirds of the disposal area, with the Saltsburg Sandstone directly underlying the remaining area. According to ESC (1992a), the Saltsburg Sandstone outcrops along tributary B at an approximate elevation of 344.4 m-msl. The Saltsburg is a fine- to medium-grained sandstone containing fissile shale sequences and very thin coal seams. Thickness is on the order of 15 m or less in the site vicinity. A predominantly shale zone some 6 to 12 m thick separates the Saltsburg Sandstone from the underlying Buffalo Sandstone. The Buffalo consists of gray shaly sandstone and ranges from one to four m in thickness. To our knowledge, no subsurface investigations have been performed below the Buffalo Sandstone at Area 15A.

Figure 4-1, adapted from Williams and McElroy (1997), depicts the shallow geologic structure near Area 15A constructed from well and boring logs in the area. The elevation contours in the figure represent the base of the Upper Freeport (UF) Coal, an excellent marker bed residing at the base of Glenshaw Formation. As shown in Figure 4-1, Area 15A resides on the western flank of the Jacksonville Anticline which plunges gently (about three percent near the site) to the southwest. Geologic strata directly beneath Area 15A dip gently to the northwest.

Figure 4-2 shows the top of bedrock in the vicinity of Area 15A as determined from drilling at the site which is supplemented with best estimates of bedrock elevations along streams and extreme boundaries of the model. As shown in Figure 4-2, bedrock elevations near Area 15A range from over 365 m-msl (at the hill south of the site) to less than 310 m-msl (in the stream channel of Elders Run). Bedrock elevations extend from 360 to 355 m-msl, east to west, beneath the disposal area.



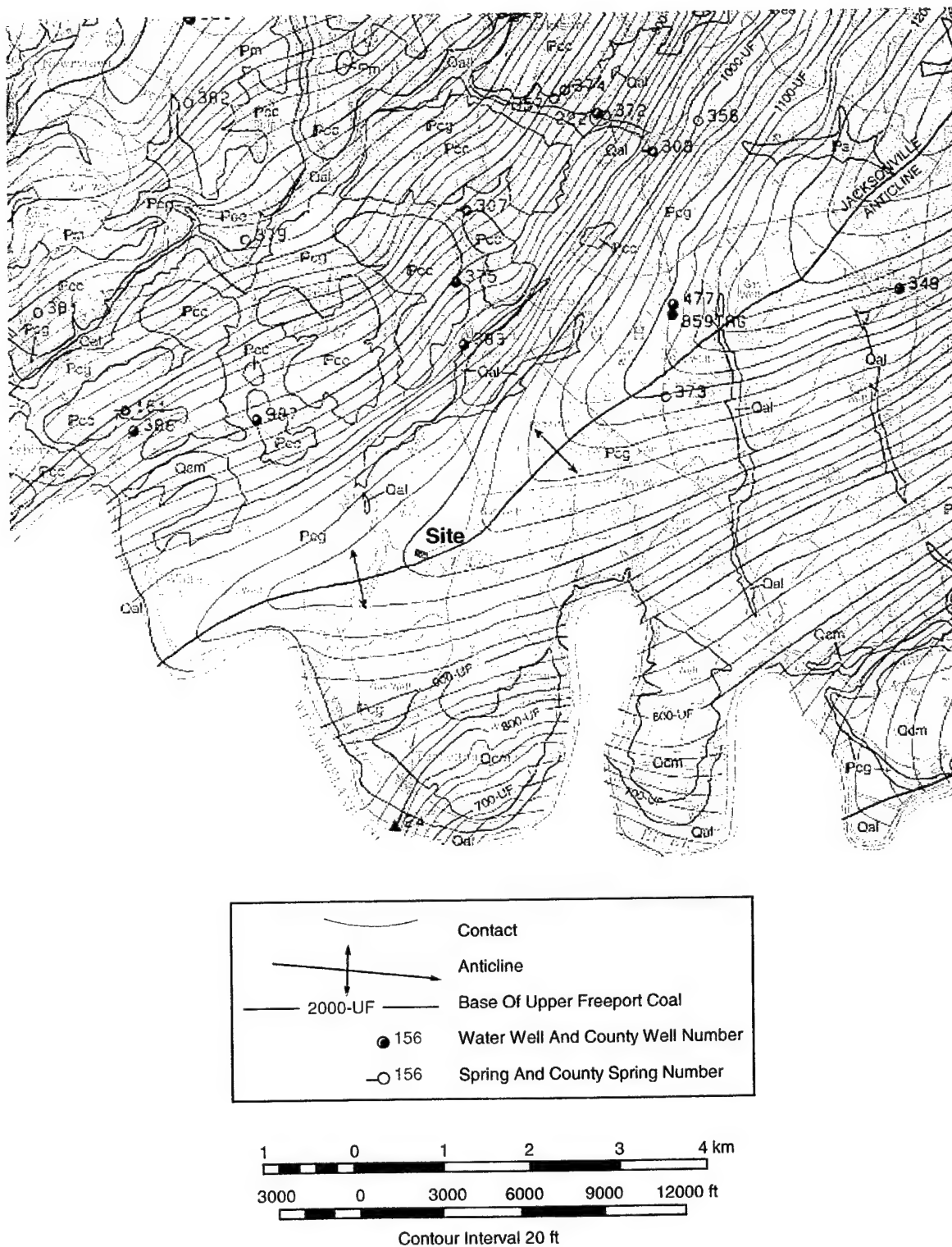


Figure 4-1 Structural Map of the Region Surrounding Area 15A Using Base of the Upper Freeport Coal as Lithologic Marker (Adapted from Williams and McElroy, 1997)



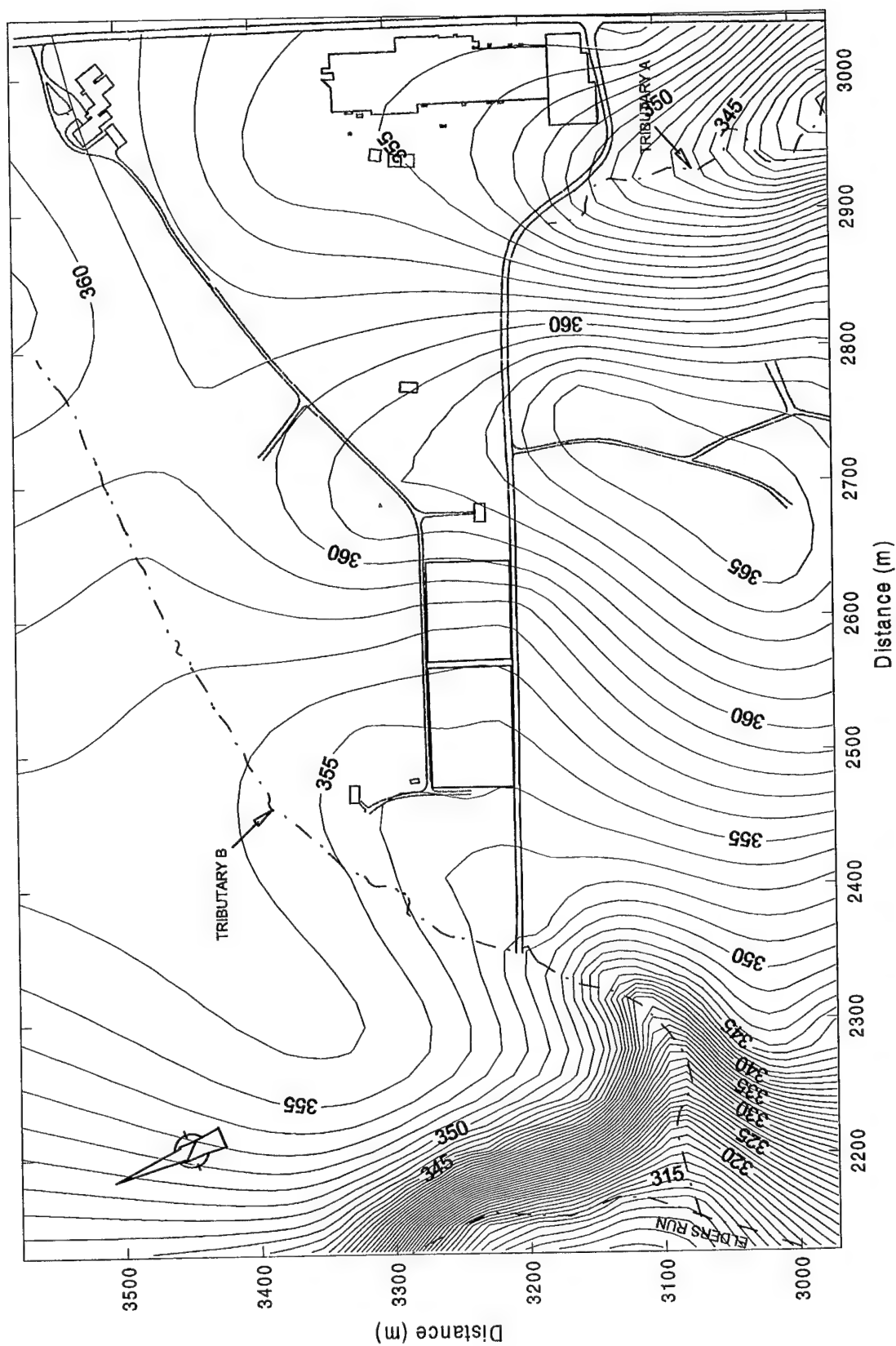


Figure 4-2 Top of Bedrock in the Vicinity of Area 15A (Contours in m-MSL)

## 4.2 Soils

A generalized hydrostratigraphic section through the Area 15A site is presented in Appendix F, Figure 3-1a. The unconsolidated soil overburden beneath the site is derived from weathering of the underlying shale and sandstone bedrock. Five test pits in Area 15A indicated silty clay soil thickness ranging from 1.1 to 2.4 m (ESC, 1985). However, well installation and soil borings suggest that soil thickness ranges from about 2.7 to 3.4 m within the immediate vicinity of the disposal area. Shallower soil depths occur on the eastern side of the site gradually increasing in depth to the west.

In May 1997, eight soil samples were collected from four areas in the vicinity of the Area 15A disposal site (Figure 4-3a) and analyzed for selected properties by TVA's Environmental Research Center. As shown in Table 4-1, residual soils are primarily silty to sandy clay with occasional weathered rock fragments. Total organic carbon (TOC) and pH of the soil samples average 0.42 percent and 5.13, respectively. The TOC of soil sample 8 is considered anomalously high due to its sampling location within the contaminated source.

**Table 4-1**  
**Results of Laboratory Analyses for Soil Physical Properties**

Sample ID	Sample Interval (m)	Grain Size			Organic Carbon (%)	pH	Classification
		Sand (%)	Silt (%)	Clay (%)			
1	0.2 to 0.6	18.2	57.7	24.1	0.62	5.72	silt loam
2	0.6 to 1.2	33.6	39.4	27.0	0.23	5.01	loam
3	0.2 to 0.6	48.3	34.0	17.7	0.34	4.94	loam
4	0.6 to 1.2	43.9	34.1	22.0	0.22	4.96	loam
5	1.2 to 1.8	56.6	24.5	18.9	0.18	4.78	sandy loam
6	0.0 to 0.9	14.1	56.2	29.7	0.74	4.94	silty clay loam
7	0.9 to 1.8	8.2	61.0	30.8	0.62	5.38	silty clay loam
8	1.8 to 2.4	11.8	59.1	29.1	3.85	5.27	silty clay loam
Averages:		29.3	45.8	24.9	0.42*	5.13	

\*Average Excluding Sample 8



### 4.3 Local Coal Mines

Figure 4-4 shows the approximate aerial extent of the Upper Freeport Coal underground tunnel system for the abandoned Watson Mine in the vicinity of Area 15A. This figure is based on a plat obtained from the Pennsylvania Department of Environmental Protection's District Mining Office in McMurray, Pennsylvania. Figure 4 from ESC (1985) indicates that the abandoned underground tunnel system extends beneath Area 15A at a depth of about 55 m below ground surface (ESC, 1992a). The representation of the tunnel system in Figure 4-4 is slightly different from that of ESC (1985) and indicates that mining excavations may be limited to the southern boundary of Area 15A. Both figures, however, indicate that the abandoned tunnel system resides below the contaminated horizons of Area 15A.

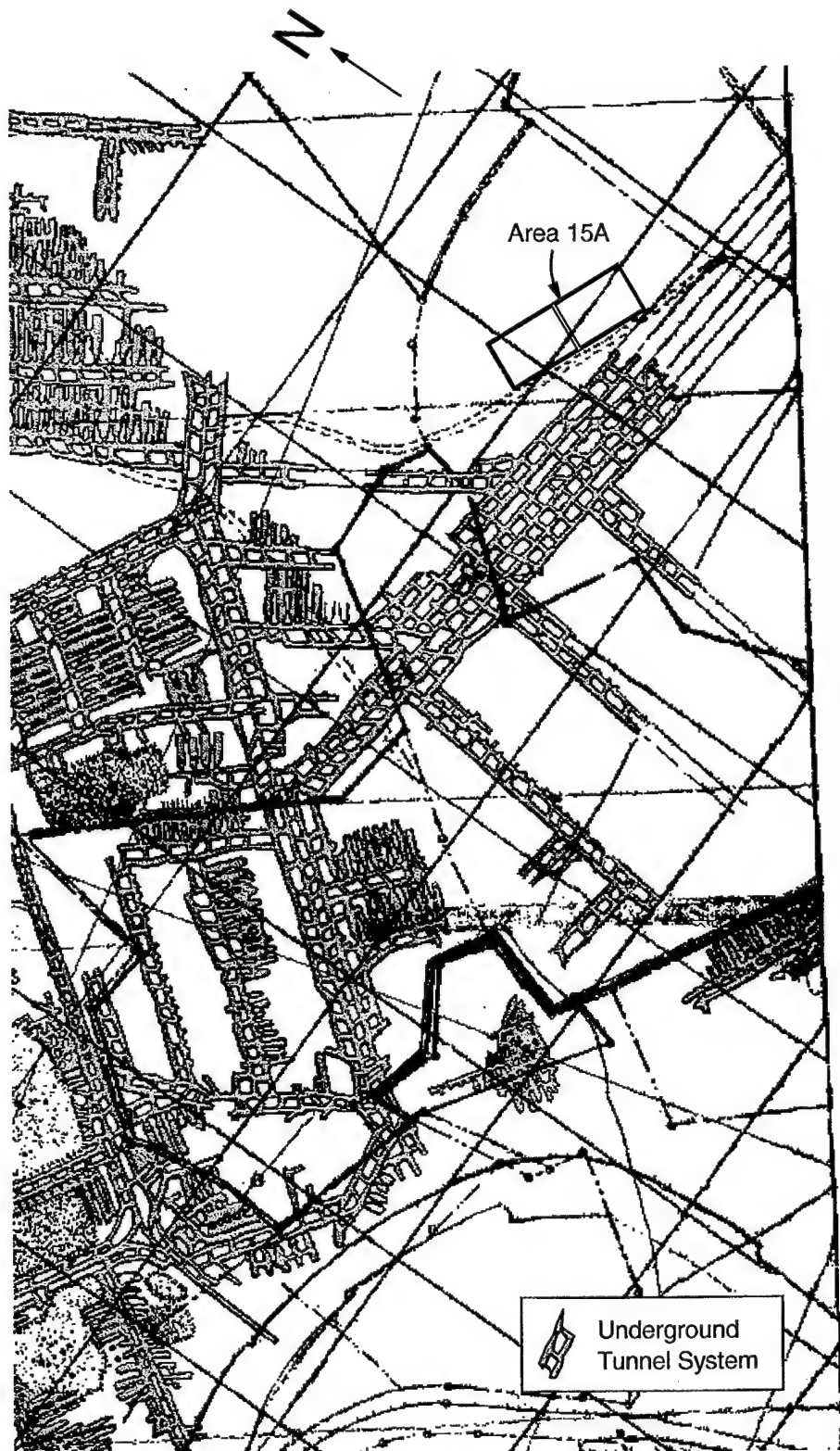


Figure 4-4 Approximate Aerial Extent of the Upper Freeport Coal Underground Tunnel System for the Abandoned Watson Mine in the Vicinity of Area 15A

## 5. Hydrostratigraphy

Aquifers within the Glenshaw include (in order of increasing depth) the Saltsburg Sandstone, Buffalo Sandstone, and Mahoning Sandstone (ESC, 1985). Although considered an aquifer in the site region, the water-bearing capacity of the Buffalo is locally doubtful.

It is expected that the potentiometric surface within the soil horizon at the site generally follows topographic trends. Only one soil well, OWP-15, has been installed at Area 15A. Groundwater level measurements at site wells indicate that soil groundwater levels (Figure 5-1) follow temporal trends that are very similar to shallow bedrock (MWS wells) at the site. According to ESC (1985), high and low chroma mottling (alternating oxidizing and reducing conditions) of the soil observed during test pit investigations suggests the occurrence of a fluctuating seasonal perched water table. The fluctuation of groundwater levels is supported by water level data from OWP-15 which indicate groundwater levels ranging from 0.70 m to more than 2.43 m below ground surface at the site. During dry periods (e.g., 12/98), groundwater levels may reside below the top of bedrock beneath all, or parts, of the disposal site. It is possible that perched groundwater conditions can occur in soil horizons underlain by relatively permeable bedrock fractures, or in relatively transmissive soil zones resulting from drum corrosion. However, there have been no quantitative field measurements to assess this situation.

Of interest in Figure 5-1 is the strong correlation in groundwater level measurements between well OWP-15 and MWS-9. Well MWS-9, a shallow bedrock well over 35 m north of the disposal area (Figure 4-3), has exhibited anomalous groundwater levels since its installation. It has been described as occasionally artesian by some field investigators. Based on groundwater level observations shown in Figure 5-1, it is likely that well MWS-9 intersects a transmissive vertical or horizontal fracture interval that is well interconnected with the disposal facility.

Groundwater levels of shallow bedrock wells MWU-14 through MWU-21 are shown in Figure 5-1. This plot indicates nothing remarkable, and the general trend in hydraulic gradients is from east to west across the site as shown in Figure 5-2. Based on groundwater level measurements at wells MWU-15 and MWU-16, the average horizontal gradient in the upper bedrock ranges from about 2.2 to 2.6 percent across the disposal site. Depending on cumulative recharge and seasonal conditions, groundwater levels can vary significantly at the site. Figure 5-2 depicts the potentiometric surface in the Saltsburg Sandstone for extreme high and

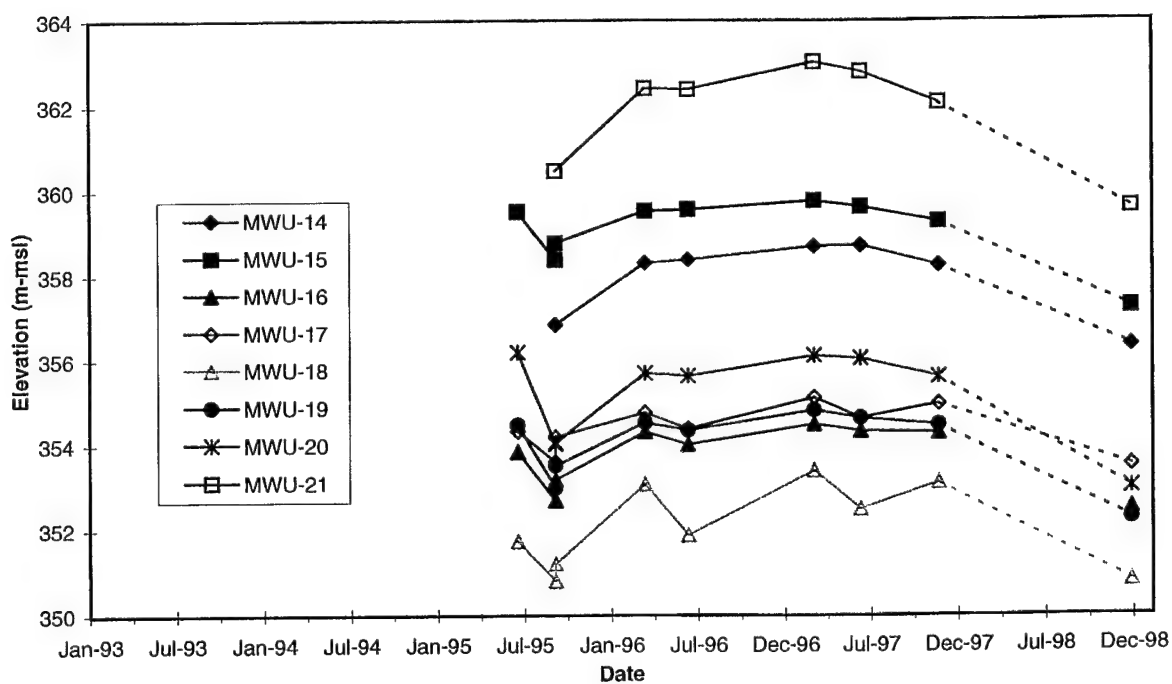
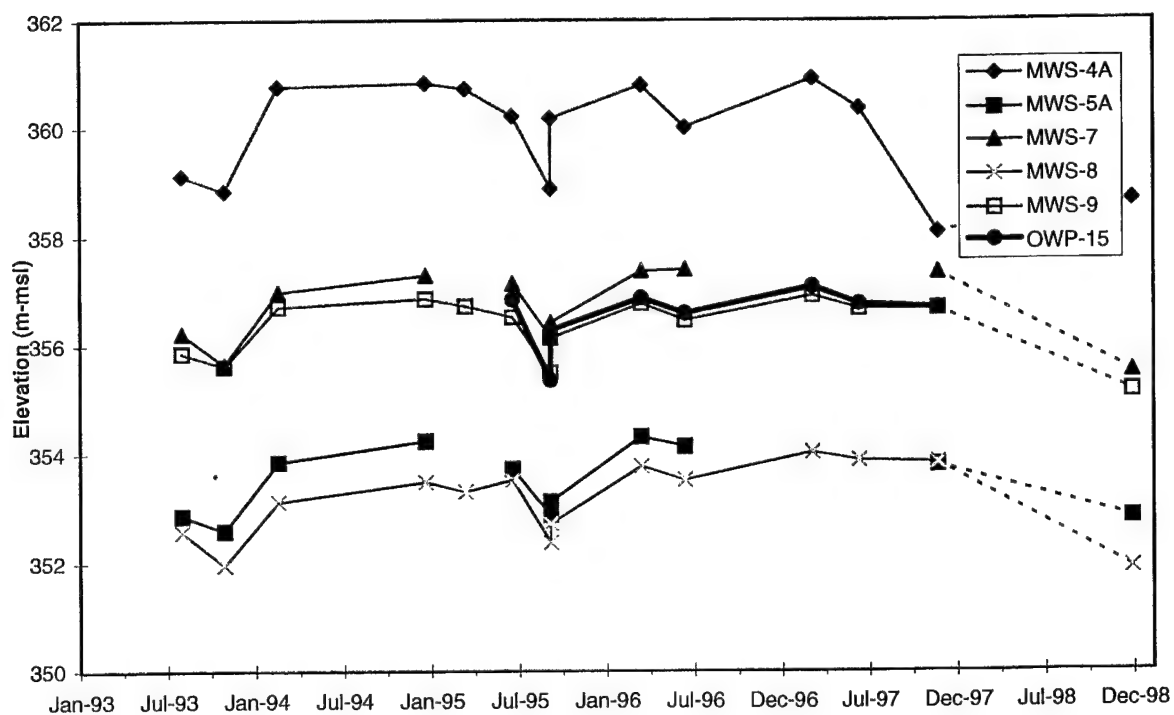


Figure 5-1 Temporal Plots of Groundwater Levels at Wells Developed in the Saltsburg Sandstone

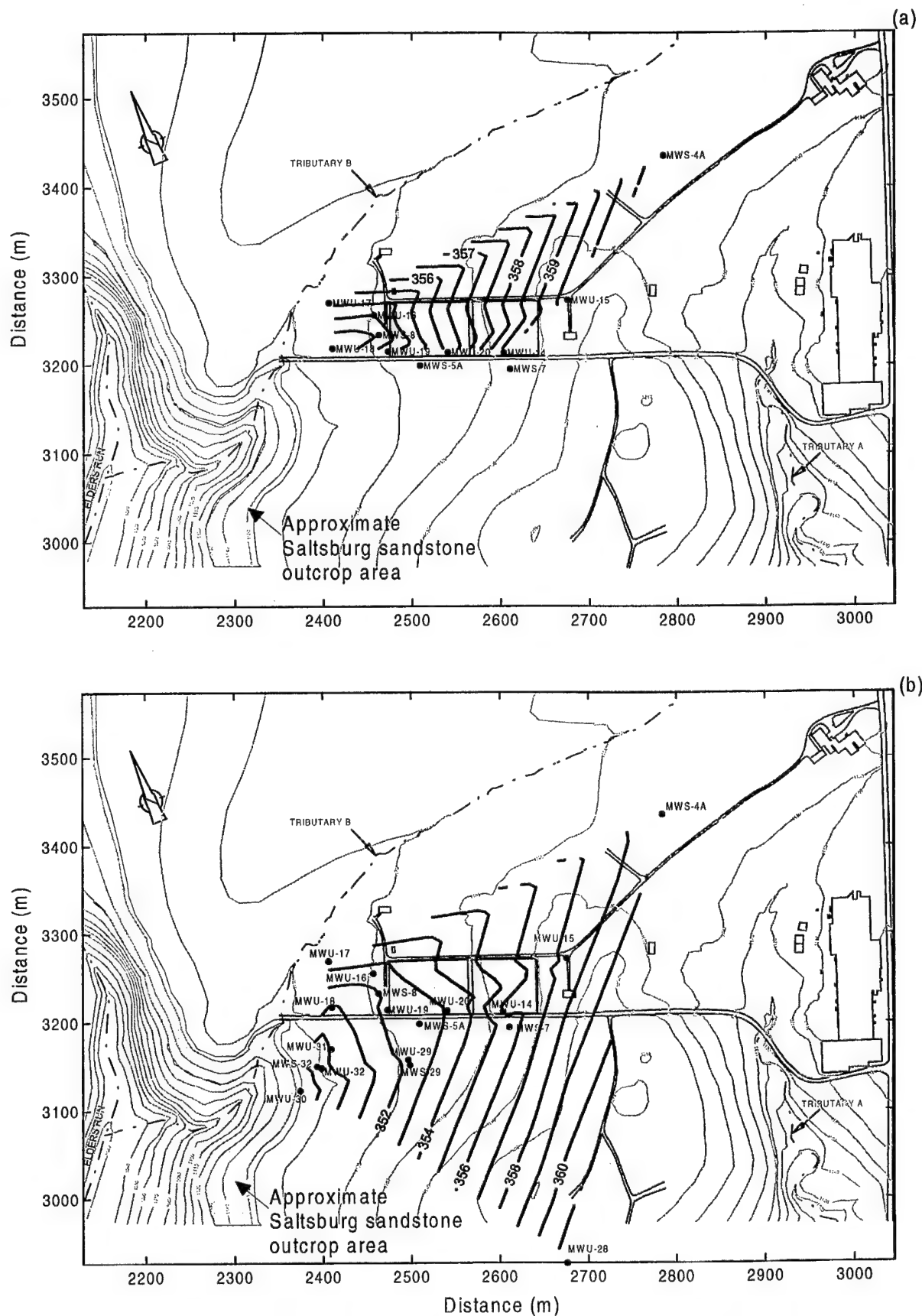


Figure 5-2 Potentiometric Maps for the Saltsburg Sandstone During (a) March 1997 - Wet Period, and (b) December 1998 - Dry Period (Contours in m-msl)



low groundwater stages of March 1997 and December 1998, respectively. As shown in the figure, hydraulic gradients and general trends in the potentiometric surface exhibit only minor differences.

Continuous precipitation and groundwater level measurements from selected wells at the site are shown in Figure 5-3. Based on the period of measurement (12/97 - 7/98), it can be inferred from Figure 5-3 that there is little variability between groundwater levels of soil well OWP-15 and shallow bedrock wells (MWU-15, MWU-19, and MWU-20) in response to precipitation events.

Figure 5-4 shows groundwater levels collected at wells MWB-4, MWB-5, and MWB-6 (Buffalo Sandstone wells) since 1993. With little exception, potentiometric levels in these site wells exhibit little temporal variability. Figures 5-2 and 5-5 show the potentiometric surface of the upper Saltsburg Sandstone and the Buffalo Sandstone for periods of high (3/97) and low (12/98) groundwater conditions. The gradient of the potentiometric surface in the Saltsburg is approximately 2 to 3 percent to the W-SW, whereas that of the Buffalo ranges from 16 to 19 percent W-SW. A roughly east-to-west direction of groundwater movement across the disposal site is indicated by both potentiometric maps. Based on the prevailing horizontal hydraulic gradients in these aquifers and on geologic considerations, it appears that groundwater originating on-site, or passing beneath the site from areas to the west, ultimately discharges at the aquifer outcrop areas west of the site.

The vertical component of the hydraulic gradient at the site is downward. This is evident in comparisons of the potentiometric surfaces for the Saltsburg and Buffalo aquifers (Figures 5-1 and 5-4) and in comparisons of the water levels in staged monitoring wells such as MWS-5A and MWB-5. The magnitude of the hydraulic gradient between the two aquifers ranges from approximately 20 to 30 percent based on this well pair. The relatively vertical hydraulic gradient at the site is probably produced by poor vertical hydraulic interconnectivity between the Saltsburg and Buffalo Sandstones. This suggests that the shale zone separating the Saltsburg and Buffalo Sandstones may be expected to exhibit low vertical hydraulic conductivity. The presence of the abandoned mine in the Upper Freeport Coal seam, some 55 m below the site, may also contribute to the downward hydraulic gradient.

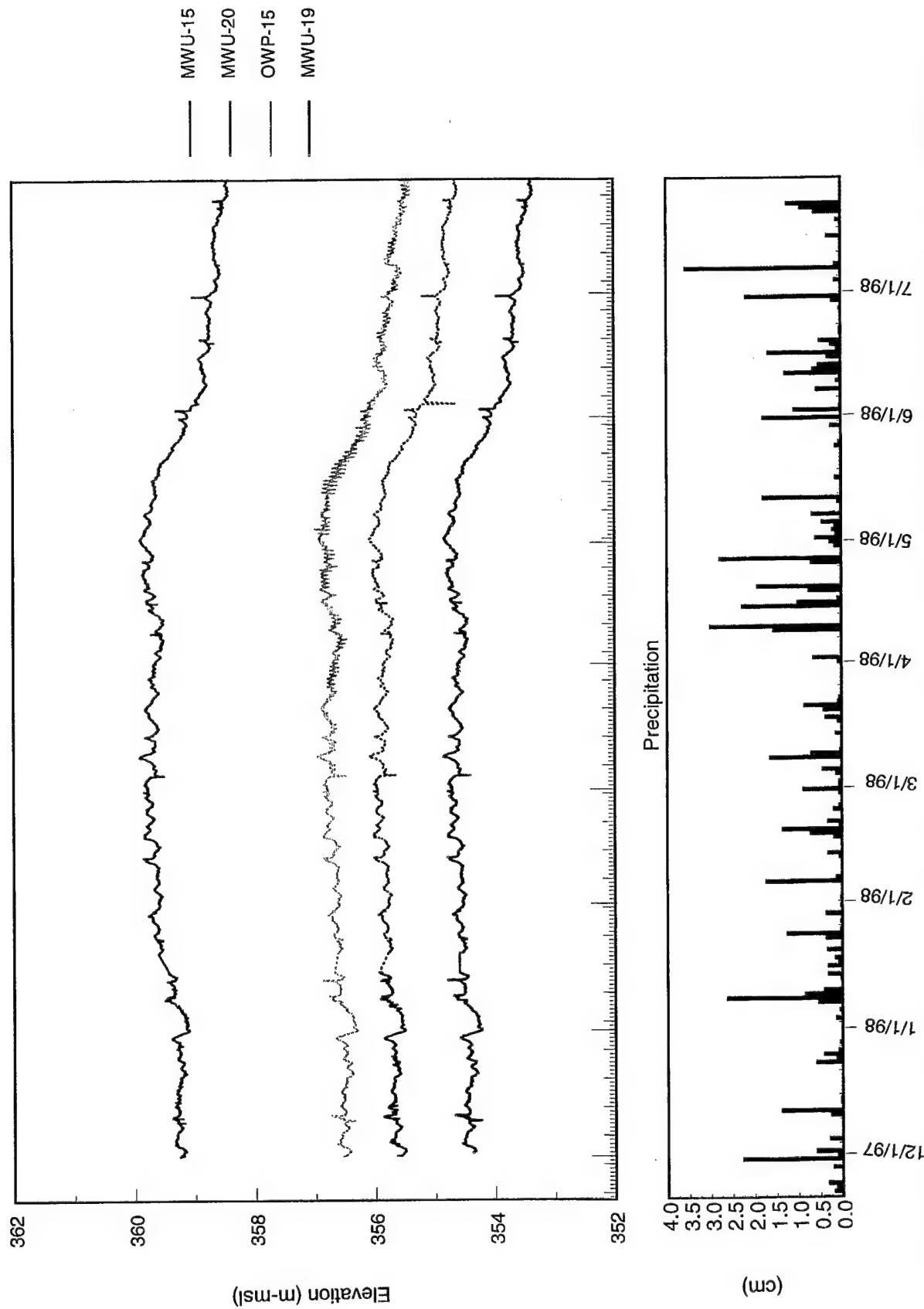


Figure 5-3 Continuous Groundwater Levels Versus Precipitation at Wells MWU-15, MWU-20, OWP-15, and MWU-19 for the Period December 1997 through July 1998 (Dashed Lines Indicate Artificially Generated Data)

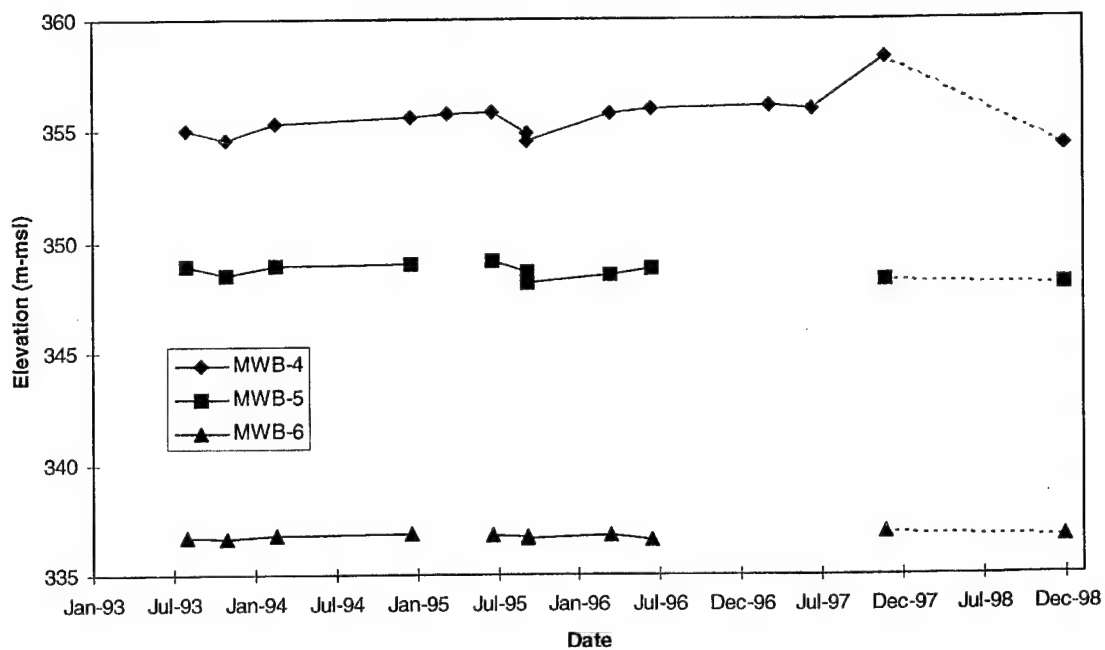


Figure 5-4 Temporal Plots of Groundwater Levels at Wells Developed in the Buffalo Sandstone

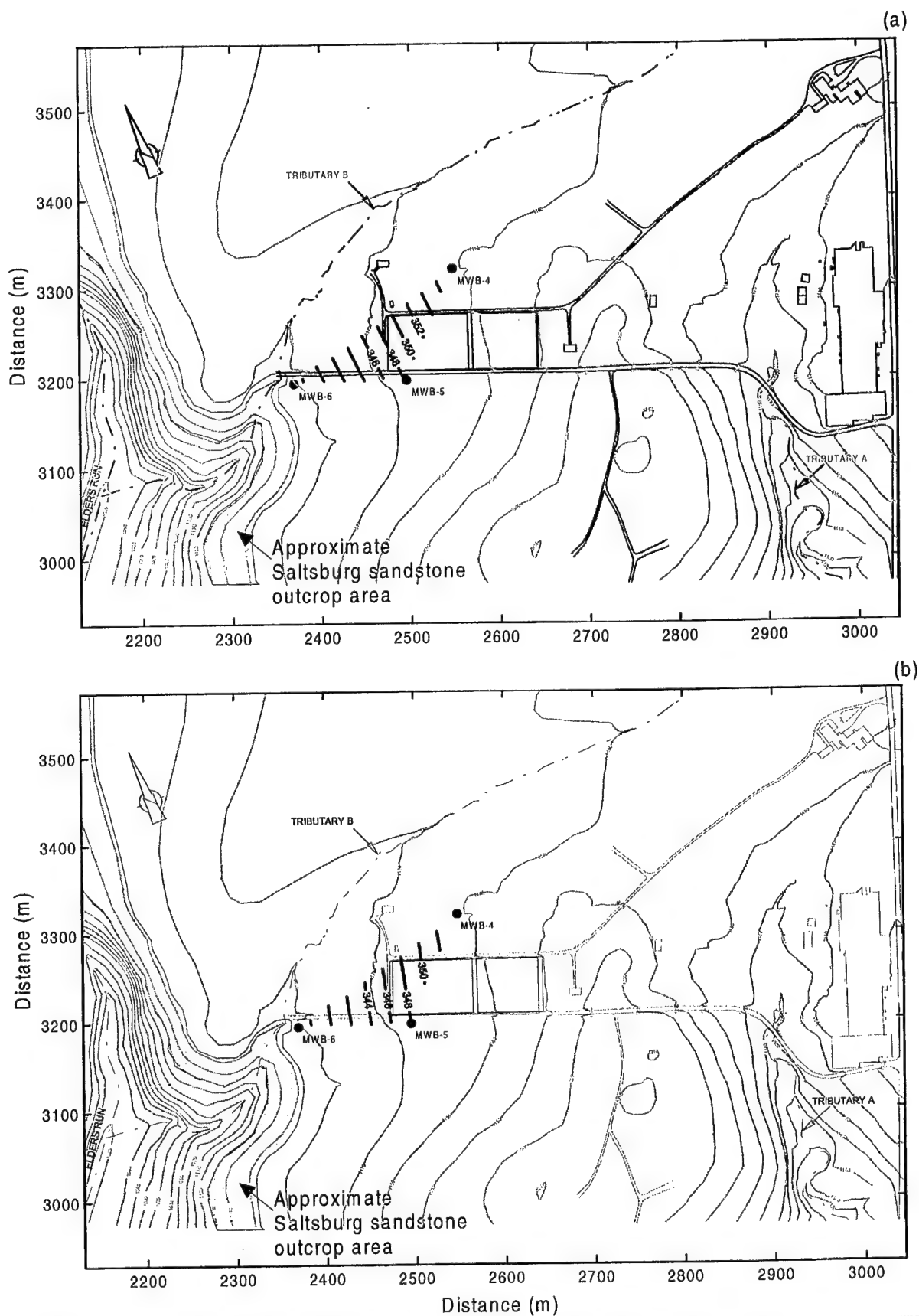


Figure 5-5 Potentiometric Maps for the Buffalo Sandstone During (a) March 1997 - Wet Period, and (b) December 1998 - Dry Period (Contours in m-msl)

## **6. Groundwater Recharge**

### **6.1 Overview**

Model simulations conducted for Area 15A inherently require input to define recharge boundary conditions. Therefore, some knowledge of the amount of natural recharge to the site aquifer is mandatory. According to ESC (1992b), the average 24-hr rainfall for the 2-yr and 25-yr storm events in Indiana County, Pennsylvania, are estimated to be 7 and 11.4 cm, respectively. Assuming these are Brinkerton surface soils, runoff calculations are 2.3 and 5.6 cm respectively, for 2-yr and 25-yr storm events. ESC (1992b) suggests that the remaining 80 percent of precipitation infiltrates and 20 percent is lost to evapotranspiration. Therefore, the respective recharge estimates for the 2-yr and 25-yr storm events are 3.8 and 4.7 cm. Based on 60 percent flow-duration data, Bloyd (1974) suggests that recharge in the Allegheny River basin is less than 18 percent of average annual precipitation, or less than 19.2 cm/yr.

There are various analytical and numerical techniques that can be used to estimate natural groundwater recharge based on historical meteorological data, soil properties, evapotranspiration, and other associated data/processes. Development of a water balance for the recharge area of an aquifer is a useful means for determining groundwater recharge. An advantage of the water balance method is that the aquifer does not have to be in dynamic equilibrium in order to use it, and many of the parameters (e.g., precipitation and soil properties) used for the hydrologic budget are directly measured. The Hydrologic Evaluation of Landfill Performance (HELP - Version 3) model (Schroeder et al., 1994) has been applied to estimate the natural recharge rate for the Area 15A site.

### **6.2 Water Balance (HELP) Model Description**

The HELP model is a quasi-two-dimensional, deterministic water routing model for determining water balances. The model was adapted from the Hydrologic Simulation Model for Estimating Percolation at Solid Waste Disposal Sites (HSSWDS) of the U.S. Environmental Protection Agency (Perrier and Gibson, 1980) and various other models including the U.S. Department of Agriculture's Chemical Runoff and Erosion from Agricultural Management Systems (CREAMS) model (Knisel, 1980), the Simulator for Water Resources in Rural Basins (SWRRP) model (Arnold et al., 1989), the Snow Accumulation and Ablation (SNOW-17) model (Anderson, 1973), and the synthetic weather generator (WGEN) model (Richardson and Wright, 1984).

HELP routes infiltration through three layer types: vertical percolation, lateral percolation, and barrier soil. In a vertical percolation layer, flow can be downward due to gravity or upward due to evapotranspiration. Capillary forces are neglected, and a downward hydraulic gradient of unity is assumed. In a lateral percolation layer, both lateral drainage and vertical percolation can occur. Lateral drainage can occur only if a drain plane is specified by the user. In a barrier soil layer, which is assigned a permeability low enough to restrict vertical flow in the layers above it, only vertical percolation can occur. However, the downward hydraulic gradient can exceed unity when a saturated mound forms. HELP estimates the unsaturated hydraulic conductivity with a two-step process. In the first step, the pore-size distribution index for the Brooks-Corey equation (Brooks and Corey, 1964) is calculated. In the second step, the distribution index and the power function of Campbell (1974) are used to calculate the unsaturated hydraulic conductivity.

Input requirements of the HELP model include daily meteorological data, soil characteristics, and dimensional/design specifications. Daily meteorological data necessary for HELP simulations consists of precipitation, temperature, solar radiation, humidity, and wind speed. The soil requirements include porosity, field capacity, wilting point, saturated hydraulic conductivity, evaporative depth, and initial moisture content. The dimensional specifications include: number, type, and thickness of layers; layer and ground surface slopes; and Soil Conservation Service (SCS) runoff curve numbers.

### **6.3 Water Balance (HELP) Model Set-Up**

The HELP model for Area 15A is configured as soil layers. The uppermost horizon is a fine sandy loam topsoil (0.15 m thick) that is designated as a vertical percolation layer. This is underlain by a second soil layer (2.9 m thick) which is also a vertical percolation layer referred to as Saltsburg Soil. Table 6-1 describes the properties of the soils used in the HELP simulation. Implicit in the model is a 3.3 percent slope for all model layers, and an SCS Runoff Curve Number of 75. The vegetation class is excellent grass and the evaporative depth is 20.3 cm.

**Table 6-1**  
**Soil Properties Used in the HELP Simulation**

Soil Type	Porosity	Field Capacity	Wilting Point	Initial Moisture Content (%)	Hydraulic Conductivity (cm/s)
Top Soil	.47	.22	.10	.27	$5.2 \times 10^{-3}$
Saltsburg Soil	.34	.13	.06	.15	$1.0 \times 10^{-6}$

Precipitation data are synthetically generated using a WGEN subroutine and statistical coefficients developed from monthly summaries (1975 to 1998). Monthly data were obtained from the Westmoreland County Airport in Latrobe, Pennsylvania. Daily solar radiation, wind speed, and relative humidity were also generated using WGEN. However, these data are based on latitude (40.44 degrees) and daily precipitation reports from Pittsburgh, Pennsylvania.

#### 6.4 Water Balance (HELP) Results

Table 6-2 provides the average annual totals of water balance components for the 20-yr HELP simulation. In general, approximately 79% of precipitation at the site is removed by evapotranspiration and runoff. Of the remaining precipitation, 12.6 percent percolates through the 3-m soil horizon. This is equivalent to a net average annual recharge rate of 11.6 cm (4.55 in.).

**Table 6-2**  
**Average Annual Totals for 20-yr Simulation**

	Average	Std. Dev.	%
Precipitation	91.8	12.3	100
Runoff	16	6.8	17.5
Evapotranspiration	56.1	6.8	61.1
Percolation Through Saltsburg Soil	11.6	9.5	12.6

## 7. Soil and Bedrock Hydraulic Properties

### 7.1 Soil Hydraulic Properties

As previously mentioned, residual soils at the site are primarily silty to sandy clay with occasional weathered rock fragments. It is expected that the soil/bedrock interface is gradational at many locations. Previous site investigation reports do not indicate measurements of soil hydraulic properties. Hence, soil samples were obtained as part of this study to gauge hydraulic properties necessary to support numerical modeling. At the request of the site owner, and for Health and Safety reasons, soil samples were collected outside of the designated disposal area. Hence, these results are not representative of soils used to backfill the disposal area.

In November 1997, six soil samples were collected from the perimeter of the Area 15A disposal site (Figure 4-3b) and analyzed for specific hydraulic properties by D.B. Stephens & Associates (1997). Soil samples were recompacted in the laboratory. As shown in Table 7-1, saturated hydraulic conductivity ( $K_{sat}$ ) of the soil samples from falling head permeameter tests ranges from  $7 \times 10^{-9}$  to  $5 \times 10^{-6}$  cm/s, with an average of  $10^{-6}$  cm/s. The average calculated porosity of the samples is 34.4 percent.

Table 7-1

Results of Laboratory Analyses for Soil Hydraulic Properties

Sample ID	Ground Elevation (m-msl)	Sample Interval (m)	Initial Moisture Content		Dry Bulk Density (g/cm <sup>3</sup> )	Wet Bulk Density (g/cm <sup>3</sup> )	Calculated Porosity (%)	$K_{sat}$ (cm/s)
			Gravimetric (%)	Volumetric (%)				
A	364.85	2.3 to 3.4	19.4	33.2	1.71	2.04	35.5	2.7E-08
B	359.85	2.1 to 3.4	18.1	32.2	1.78	2.10	32.9	7.0E-09
C	357.57	2.3 to 3.5	16.6	29.3	1.77	2.06	33.3	7.8E-08
D	357.02	1.8 to 3	14.6	27.2	1.86	2.13	29.9	8.6E-09
E	357.66	1.8 to 3	15.4	25.8	1.67	1.93	36.8	2.9E-07
F	360.43	1.8 to 3	8.4	13.7	1.64	1.78	38.1	5.2E-06
Averages:			15.4	26.9	1.74	2.01	34.4	9.4E-07



## 7.2 Bedrock Hydraulic Properties

Bedrock hydraulic properties (i.e., mean K, matrix K, and fracture K), fracture orientation, density, and dimensions have been estimated or inferred from borehole flowmeter testing, geologic core logs, and reports regarding regional geologic structure. Site-specific fracture data are limited to horizontal fractures since all test wells and core holes completed to date have been vertically oriented.

To our knowledge, the first on-site pumping test at Area 15A was conducted in June 1985 by CRA (1995). Prior to a step test, a constant rate pumping test was conducted for a period of seven hours. This was followed by a recovery period of 43 hours. Well MWS-8 was pumped at an initial flow rate of 15.1 L/min for 30 minutes. Following a brief (6 min) shut down due to pump malfunction, pumping resumed at an average flow rate of 17 L/min. Fifteen observation wells at the site were monitored before, during, and after (recovery) pumping.

Drawdown during the pumping test was relatively symmetrical, indicating approximately radial groundwater flow to the pumping well. All upper zone observation wells monitored during the test responded to pumping at MWS-8 except for wells MWU-20 (questionable response), MWU-15, and MWS-4A. The latter are the most remote of the upper zone wells monitored and are located at distances of 80, 215, and 380 m, respectively, from MWS-8. Table 7-2 shows transmissivity and hydraulic conductivity values estimated for the upper zone based on the Theis (1935) method of analysis by CRA (1995), and the Cooper-Jacob Straight-Line analysis (Cooper and Jacob, 1946) by the authors.

As shown in Table 7-2, the geometric mean K estimates ( $1.7 \times 10^{-3}$  and  $8.4 \times 10^{-3}$  cm/s) differ by a factor of about five. The results of single-well pumping tests conducted during borehole flowmeter measurements at the site (Appendix E; Table 5-2) indicate mean and geometric mean K values of  $1.5 \times 10^{-5}$  and  $8 \times 10^{-6}$  cm/s, respectively, for shallow bedrock.

Due to constraints imposed by existing well designs, flowmeter testing of site bedrock (Appendix E) has been limited to the lower meter or less of soil overburden and the upper 3 to 6 m of sandstone and shale associated with the Saltsburg Formation. In general, flowmeter test results indicate that a few thin flow zones dominate shallow groundwater movement. This is common in fractured sedimentary rock aquifers in which groundwater moves preferentially through a few hydraulically active fractures with only minor flow through the porous rock matrix.

**Table 7-2**  
**Transmissivity and Hydraulic Conductivity Values of Upper Zone**  
**Wells from Constant Rate Pumping Test**

Well	Well Type	CJSL Analyses <sup>1</sup>		Theis Analyses <sup>2</sup>	
		T (m <sup>2</sup> /d)	K (cm/s)	T (m <sup>2</sup> /d)	K (cm/s)
MWS-8	Pumping	1.9	4.6E-04		
MWS-5A	Observation	2.7	7.0E-04	5.0	5.8E-03
MWS-9	Observation	17.7	4.4E-03		
MWU-16	Observation	13.2	3.3E-03	4.1	4.7E-03
MWU-17	Observation	5.8	1.1E-03	16.6	1.9E-02
MWU-18	Observation	2.4	4.5E-04	5.7	6.6E-03
MWU-19	Observation	5.8	1.1E-03	9.9	1.2E-02
MWU-20	Observation	9.1	2.0E-03		
OWP-15	Observation	28.4	2.2E-02		
Mean:		9.7	3.9E-03	8.3	9.6E-03
Geometric Mean:		6.6	1.7-03	7.2	8.4E-03

<sup>1</sup>Cooper-Jacob Straight-Line Analyses

<sup>2</sup>Theis Method of Analyses

Flow profiles for the shallow test wells typically indicate two preferential flow zones. The shallowest of these features lies within the upper bedrock and/or in the lower part of the soil overburden near the soil/bedrock interface. A transitional zone of variably-weathered bedrock undoubtedly exists between unconsolidated soils and competent bedrock. However, this cannot be confirmed with available geologic logs. Some 2.4 to 3.6 m below the upper fracture zone, another preferential flow zone was observed at most test sites. Based on geologic logs, this zone may represent a bedding fracture.

A total of 165 discrete horizontal hydraulic conductivity ( $K_h$ ) estimates were obtained during eight flowmeter tests (Appendix E) in shallow bedrock at Area 15A.  $K_h$  estimates ranged from  $1.4 \times 10^{-5}$  to 0.2 cm/s. Visual inspection reveals no major differences between the overall magnitude of K data for the sandstones and shales. Data exhibit a mean log  $K_h$  of 0.61 and

standard deviation of 0.83. Based on a summary of flowmeter measurements, the geometric mean  $K_h$  for the Saltsburg Sandstone is approximately  $5 \times 10^{-4}$  cm/s. Considering that flowmeter measurements relate to active fracture intervals in the Saltsburg Sandstone, this is a more realistic estimate of the effective horizontal  $K$  for shallow bedrock at the site.

The hydraulic conductivity of the unfractured matrix of sandstone and shale is generally well below the measurement threshold of the flowmeter. That is to say, the matrix  $K$  values for shales rarely exceed  $10^{-7}$  cm/s, while values less than  $10^{-5}$  cm/s are typical of sandstones (Freeze and Cherry, 1979). Therefore, the measured hydraulic conductivities for the sandstone and shale bedrock can largely be attributed to fractures. Since all of the test wells are vertically oriented, we can infer that the measured  $K$  values are primarily associated with horizontal fractures intersected by the wells. However, vertical fracture sets undoubtedly exist at the site as a result of past tectonic activity. The anticlinal structure of the bedrock underlying Area 15A suggests the likelihood of vertical tension fracture sets. However, this cannot be confirmed with data derived from vertical wells.

Rock matrix  $K$  at the site has not been specifically measured. However, a literature survey of matrix properties for sandstones and shales are summarized in Appendix F. Bedrock matrix hydraulic conductivity was adjusted within the limits of the literature estimates during initial fracture flow model calibrations resulting in calibrated values of  $10^{-7}$  cm/s for both  $K_h$  and  $K_v$ .

## 8. Injection-Recovery System Simulations

### 8.1 Model Selection (MODFLOW and MT3DMS)

In numerical modeling, large changes in aquifer properties can produce inaccurate numerical solutions whose errors can easily go undetected. Performing accurate mass balances and sensitivity analyses on the temporal and spatial discretization enhances detection of these problems. Numerical simulations involving three-dimensional steady-state groundwater flow and transport modeling of the saturated overburden and shallow bedrock have been conducted using MODFLOW (McDonald and Harbaugh, 1984) and MT3DMS (Zheng and Wang, 1998), respectively. Both of these models have been thoroughly validated and provide global mass balance information.

Currently, MODFLOW is the most widely used groundwater flow code in the United States. MODFLOW is a three-dimensional, block-centered finite difference model. Several numerical methods have been developed to solve the finite difference equations in MODFLOW. Three standard solvers are the Slice-Successive Over-relaxation (SSOR) package, Strongly Implicit Procedure (SIP), and Preconditioned Conjugate-Gradient (PCG2) package (Hill, 1990). The numerical method used for Area 15A simulations is the WHS solver (Adams, 1998). The WHS solver uses a bi-conjugate gradient algorithm to solve the partial differential equations relating to groundwater flow. This solver offers an advantage of several stabilizing and pre-conditioning procedures to optimize it for groundwater systems and finite-difference matrices.

In comparing various site remediation alternatives, initial estimates of advective travel time are made using MODPATH (Pollock, 1989). MODPATH is a semi-analytical particle tracking scheme that utilizes output from MODFLOW to compute the directional velocity of groundwater along flow paths.

MT3DMS is the next-generation of the modular three-dimensional transport model MT3D (Zheng, 1990) for simulation of advection, dispersion, and chemical reactions in groundwater systems. MT3DMS is designed to couple with the output from MODFLOW and offers five options to solve the transport equation. Three of these options are based on the Method of Characteristics (MOC); the fourth option on an upstream, finite difference method; and the final method employs a total variation diminishing (TVD) scheme. The explicit upstream finite difference option of MT3DMS was used for Area 15A numerical predictions

coupled with a new implicit generalized conjugate gradient solver. The resulting numerical solutions are stable.

## **8.2 Conceptual Model**

The conceptual model used for numerical simulations relies on historical characterization information and more recent data collected for this study. The conceptual model for Area 15A includes an upper recharge boundary of 11.6 cm/yr distributed uniformly over the model domain. The net annual recharge value of 11.6 cm/yr is based on HELP model simulations described above. Additionally, flow model calibration and zero mass balance discrepancies support this net annual recharge value.

Steady-state conditions are assumed for the flow model since inadequate data exists to support transient simulations. The upper horizon of the model consists of a relatively thin mantle of soil overlying shallow fractured bedrock (Saltsburg Sandstone). The lower horizon of Saltsburg Sandstone is represented as equivalent porous media. Results from laboratory permeameter tests, single-well pumping tests, and flowmeter surveys provide the information necessary to develop the hydraulic structure for the model. Average surface and groundwater elevations from on-site measurements are used to establish constant head boundaries for the model and for flow calibration purposes. The thickness of a model layer varies according to the results of well installation, boring logs, and test pits at the site. Gridding of the model is dependent on the remediation system being simulated.

Transport simulations are performed for constant source terms of unity since we are primarily interested in an evaluation of the delivery of aqueous treatment agents to reduce contaminant concentrations. The transport model is conservative in that chemical reactions are not considered (i.e., no sorption or biodegradation). Hence, transport of an aqueous agent additive occurs via advection and dispersion only.

## **8.3 Model Set-Up**

Figure 8-1 shows the model domain, initial grid system, and boundary conditions for the MODFLOW and MT3DMS numerical applications. The model follows the Federal Laboratories coordinate system with maps oriented northerly. This allows full model proportioning and importing of digital maps with a high degree of accuracy.



Since our simulations focus on the interior of the model domain, the constant head boundaries are set far from the area of interest. This prevents imposed stresses to the interior part of the system from reaching the model boundaries. Preliminary model simulations were conducted to gauge the drawdown effects of interior pumping wells at boundaries. Based on trial and error simulations, the resulting scale of 610 m by 914 m in the horizontal minimizes stresses to model boundaries (Figure 8-1).

Constant head boundaries for the model are based on average surface and groundwater elevations from on-site measurements. In areas where groundwater data were absent, constant head boundaries were extrapolated from average site measurements using topographic and top of bedrock information. Average groundwater level measurements at site wells are also used in final calibration of the flow model.

The longitudinal axis of the model grid is oriented along the groundwater flow path. The finite difference grid is initially discretized into horizontal cells, 15.2 m by 15.2 m, within the active model domain. For all simulations, grid resolution within the disposal area is higher than the surrounding domain since this dimension is a function of the expected curvature of the potentiometric surface. The largest horizontal grid dimension within the disposal area (Figure 8-1) is 3.8 m.

Figure 8-2 illustrates the layering scheme used in the model. The base model is subdivided into three layers. The uppermost layer represents soil, and the lower layers depict the Saltsburg Sandstone. Depending on the remediation scenario being modeled, subsequent simulations included refinement of this layering system. The use of upper and lower variable boundaries results in variable layer thicknesses. The upper (top) model boundary is variable, with the elevations equivalent to ground surface, as shown in Figure 8-2. The top-of-ground data for model input was obtained from existing topographic maps of the site (ESC, 1992a, b). The soil/bedrock interface of the model is also variable. This interface represents top-of-rock as determined from drilling at the site that was supplemented with best estimates of bedrock elevations along streams and extreme boundaries of the model. The bottom boundary of the model (Figure 8-2) is based on an assumed thickness of the Saltsburg Sandstone that averages about 15 m. No vertical flow is permitted across the bottom boundary.

Section 7.1 describes characterization studies conducted at the site, results of these studies, and interpretation of the results. Hydraulic properties for various model layers are

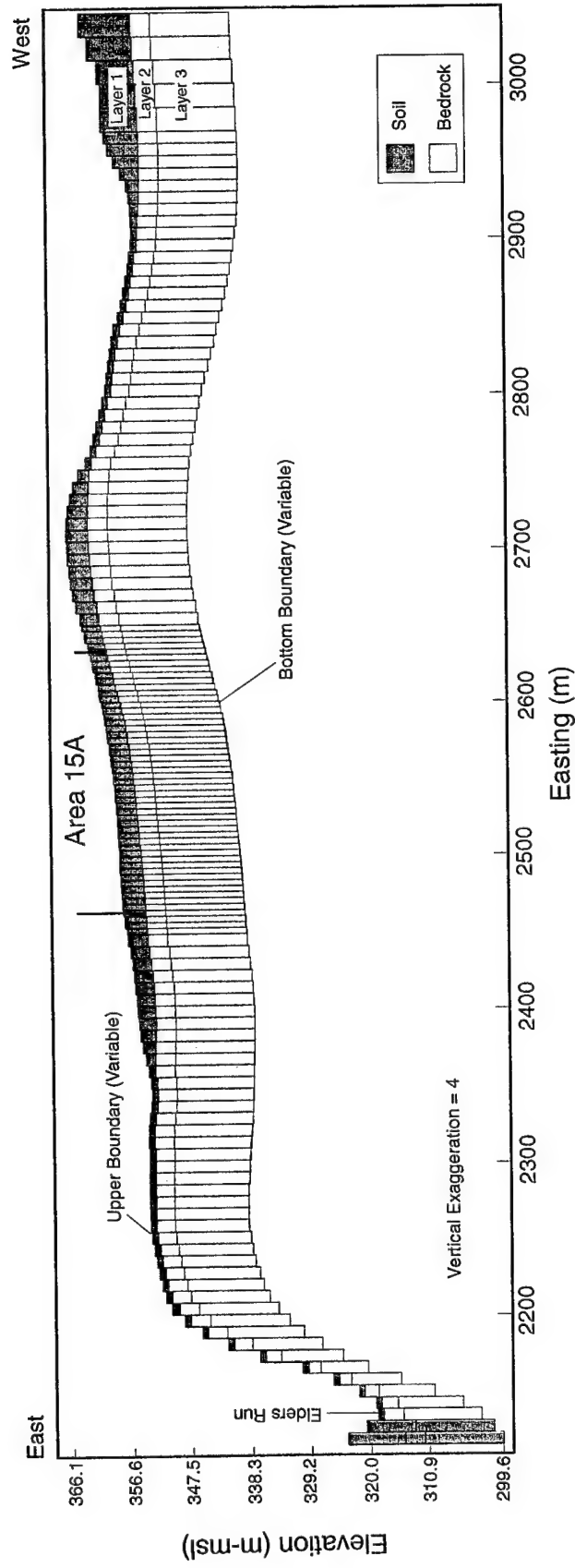


Figure 8-2 East-West Cross Section of Model at  $y=3240$  m Showing Layering Scheme Used in Model Simulations



shown in Table 8-1. Based on laboratory permeameter tests of soil samples, and noting that samples were recompacted, it is likely that site soils are best characterized as silty to sandy clays with  $K_h$  values averaging about  $10^{-6}$  cm/s (Table 7-1). From a summary of flowmeter measurements, the geometric mean  $K_h$  for the Saltsburg Sandstone is approximately  $5 \times 10^{-4}$  cm/s. The values of vertical hydraulic conductivity ( $K_v$ ) for soil and bedrock at the site are based on initial flow model runs. Variations of  $K_v$  were conducted using the fixed recharge value of 11.6 cm/yr until model predictions approximated hydraulic heads and gradients from field measurements. The resulting  $K_v$  value of  $10^{-7}$  cm/s for site soils (Table 8-1) agrees well with the geometric mean of permeameter test results. For fine textured soils such as those at the site, the ratio of horizontal to vertical hydraulic conductivity is expected to be about an order of magnitude. The  $K_v$  of the underlying Saltsburg Sandstone,  $10^{-6}$  cm/s, is derived solely from flow model calibration.

Essentially no hydraulic characterization has been conducted for soils within the immediate disposal area of Area 15A. In assigning K values to soils within the immediate disposal area, a conservative assumption is that K values are higher than those of the surrounding site soils. Soils within the disposal area of Area 15A have been excavated and redeposited, likely with limited compaction. It is likely that drum corrosion has resulted in stoping of soil into remaining void spaces. Although a somewhat arbitrary designation, the uniform  $K_v$  and  $K_h$  value of  $5 \times 10^{-6}$  cm/s (Table 8-1) for disposal area soil provides reasonable flow model calibration.

**Table 8-1**  
**Layer Hydraulic Properties for MODFLOW/MT3DMS Simulations**

Layer	#	Media	$K_h$ (cm/s)	$K_v$ (cm/s)	$\theta$	$\theta_{eff}$	$S_s$ (m <sup>-1</sup> )	$S_y$
upper	1	soil	1.E-06	1.E-07	0.34	0.05	3.0E-05	0.10
disposal area	1	soil	5.E-06	5.E-06	0.34	0.05	3.0E-05	0.10
middle	2	bedrock	5.E-04	1.E-06	0.17	0.05	3.0E-07	0.05
lower	3	bedrock	5.E-04	1.E-06	0.17	0.05	3.0E-07	0.05

Additional parameters for the flow and transport model (Table 8-1) include constant specific storage and specific yield parameters of  $3 \times 10^{-5} \text{ m}^{-1}$  and 0.1, respectively, for soils. Bedrock specific storage and specific yield parameters are also constant at  $3 \times 10^{-7} \text{ m}^{-1}$  and 0.05, respectively. The respective total and effective porosity values for soil are 0.34 and 0.05, based on laboratory measurements (Table 7-1). Based on a review of the literature for sandstones and shales similar to those underlying the site (Appendix F), effective porosity for the Saltsburg Sandstone is 0.05.

The longitudinal and horizontal transverse dispersivities for the model are constant and within the order of grid spacing at 1.5 m (5 ft). The vertical transverse dispersivity is 0.15 m (0.5 ft). These values are within the range of dispersivity for the model scale compared to dispersivity estimates reported by Gelhar et al. (1992). Molecular diffusion is considered negligible for all model runs.

#### **8.4 Remediation Alternatives**

In addition to a base case, no action alternative, five different types of engineered delivery/recovery systems have been simulated to obtain a relative comparison of optimal source control measures. All of the engineered remedial alternatives included in this evaluation involve some type of hydraulic control (i.e., trench, vertical well, or horizontal well) for the recovery of fluids. Additionally, injection of aqueous agents to augment contaminant degradation are included as shallow injection wells or an infiltration gallery. The infiltration gallery is envisioned to be a network of porous lines or tubes that are buried beneath the soil frost line to prevent freezing. Burial of the feed system also dampens the volatilization of treatment agents (e.g., ammonia/methanol). Hydraulic efficiency and minimization of off-site contaminant migration is accentuated in this assessment. Transport simulations are considered qualitative expectations of a given delivery system due to an assumption of conservative (no attenuation or degradation) movement. Given that these are idealized remedial concepts that require several critical assumptions (e.g., disposal area soil K values), results are viewed in a relative fashion. Final design and numerical simulation of the remediation system for Area 15A should rely on additional site characterization data.

For the simulation of each remedial alternative, the maximum amount of water possible is delivered to the disposal area (via infiltration gallery or injection wells), but is maintained below ground surface. In all cases, this involved trial and error simulations for calibration.

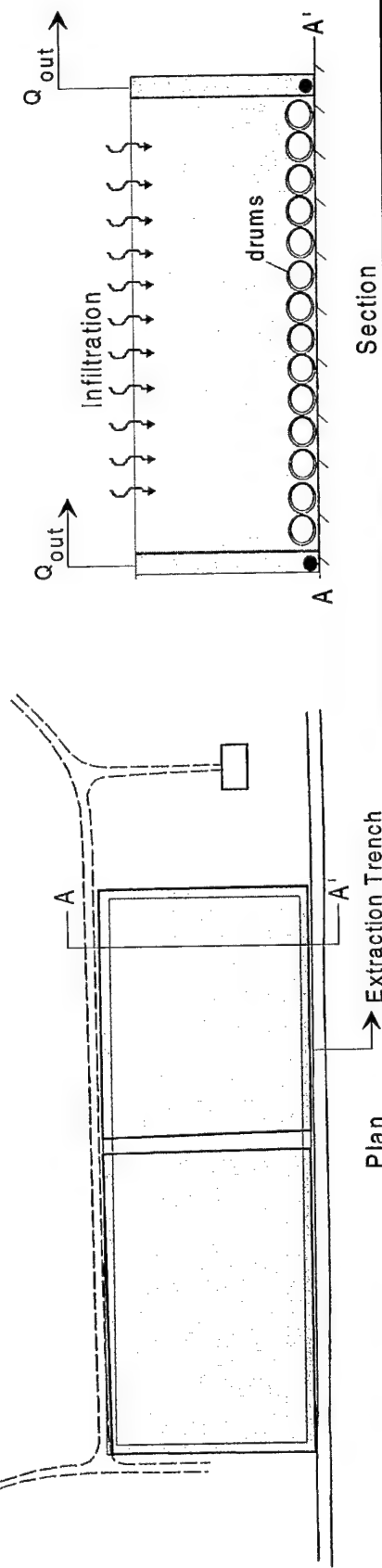
Table 8-2 lists the scenarios contemplated for site remediation. Figures 8-3 through 8-5 provide conceptual schematics of the systems:

**Table 8-2**  
**Remedial Scenarios Considered in Model Simulations**

<i>Scenario 1</i>	Base Case (No Remedial Controls)
<i>Scenario 2</i>	Perimeter Extraction Trench/Infiltration Gallery
<i>Scenario 3</i>	Extraction Trench/Injection Trench
<i>Scenario 4a</i>	Vertical Extraction Wells/Injection Wells
<i>Scenario 4b</i>	Vertical Extraction Wells/Infiltration Gallery
<i>Scenario 5</i>	Extraction Trench/Injection Wells
<i>Scenario 6a</i>	Longitudinal Horizontal Extraction Wells/Infiltration Gallery
<i>Scenario 6b</i>	Latitudinal Horizontal Extraction Wells/Infiltration Gallery

- *Scenario 1* (base case) includes no hydrodynamic remediation but is included to depict results of the calibrated numerical model. The steady-state potentiometric heads from this simulation serve as initial head conditions for subsequent model runs of all remedial scenarios.
- *Scenario 2* involves the extraction of contaminated groundwater using a trench (french drain) surrounding the entire perimeter of the disposal area (Figure 8-3). For Scenario 2, it is assumed that the narrow trench width (~1m) makes it improbable to excavate bedrock material. Hence, the trench is founded on the top of bedrock beneath the disposal area. In practice, we expect such trenches to contain highly permeable media (e.g., coarse sand or

### Extraction Trench/Infiltration Gallery (Scenario 2)



### Extraction Trench/Injection Trench (Scenario 3)

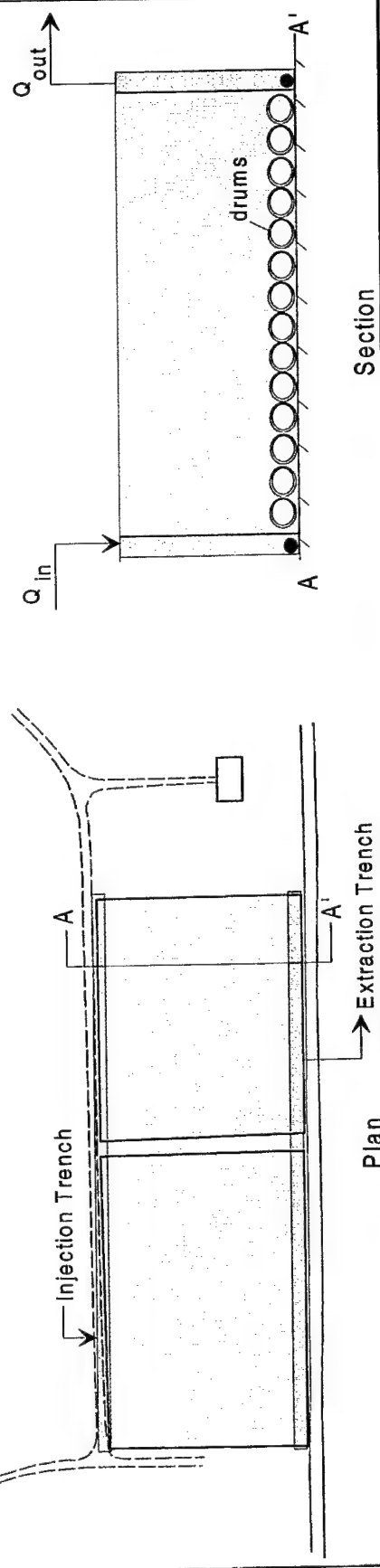
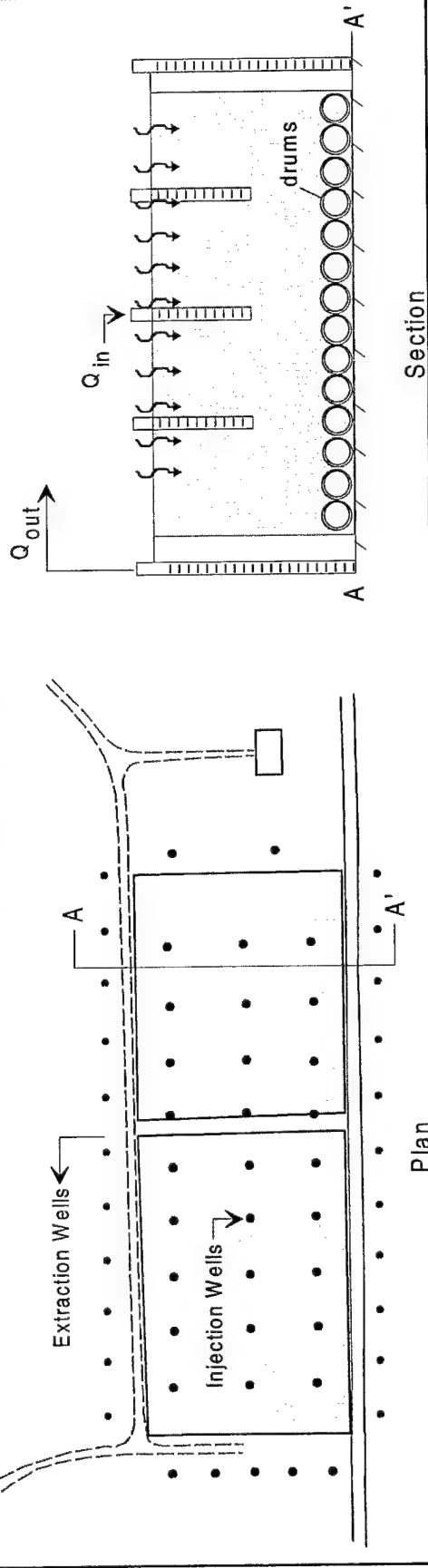


Figure 8-3 Conceptual Schematics for Remediation Scenarios 2 and 3

# Vertical Extraction Wells/Injection Wells or Infiltration Gallery

(Scenario 4a & b)



# Extraction Trench/Injection Wells

(Scenario 5)

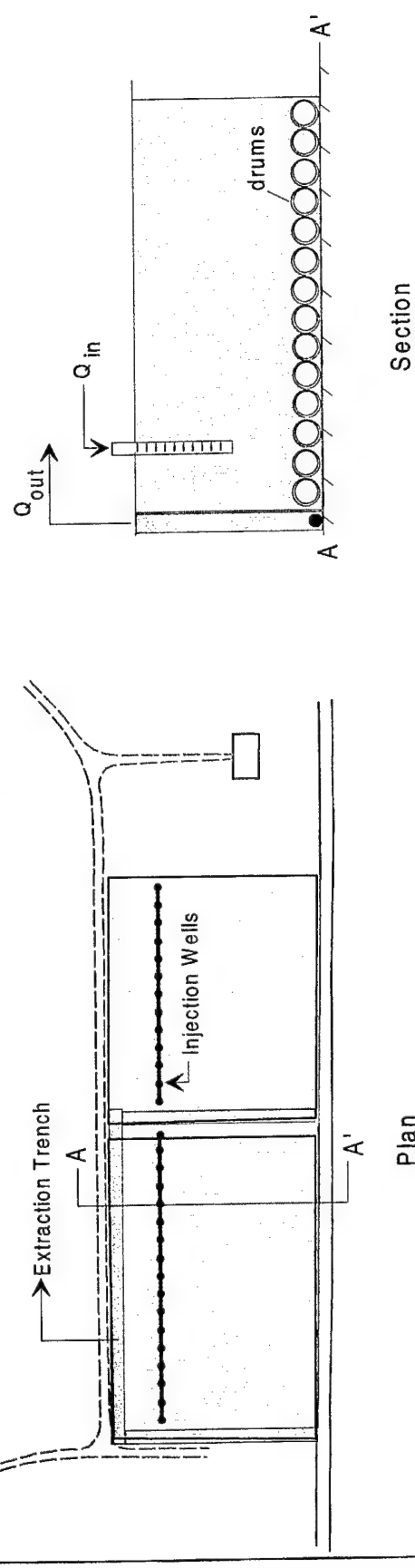


Figure 8-4 Conceptual Schematics for Remediation Scenarios 4 and 5

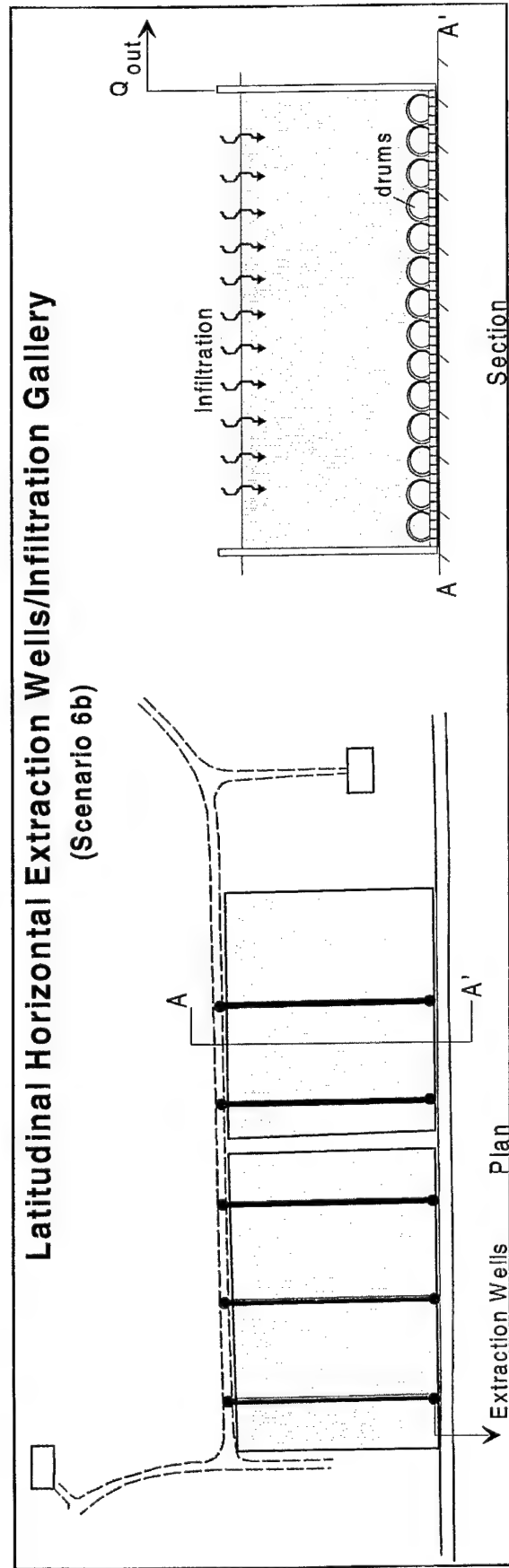
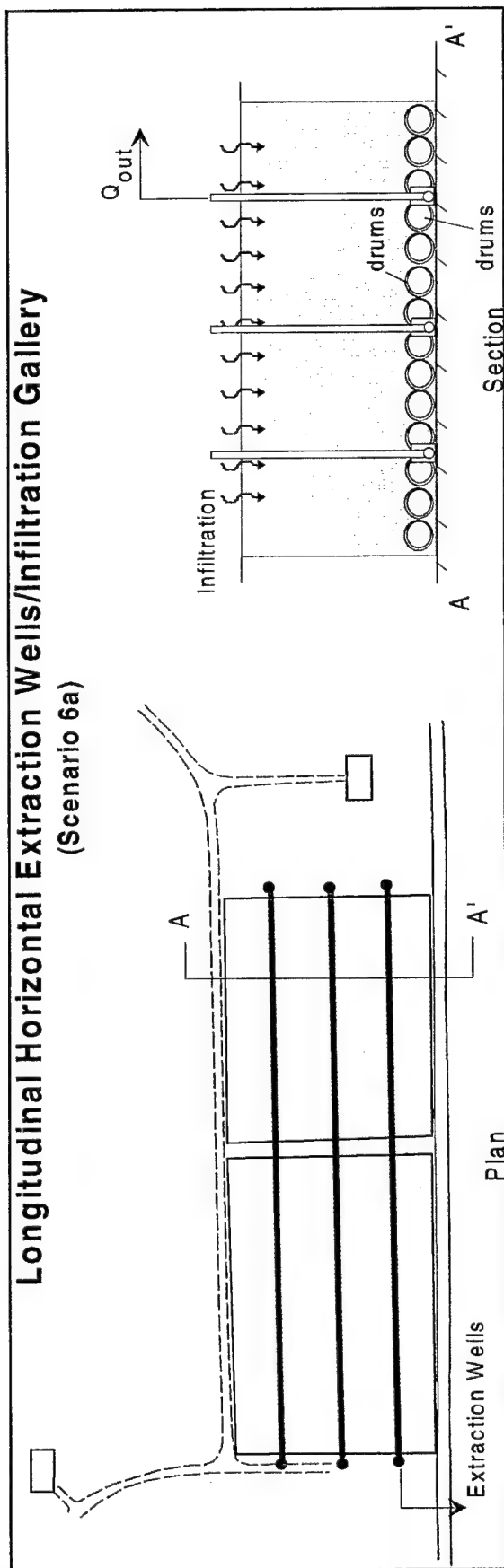


Figure 8-5 Conceptual Schematics for Remediation Scenarios 6a and 6b

gravel) overlaying perforated collection pipes. Groundwater removal rates from occasional standpipes are used to keep levels as low as possible. For the flow model simulation, constant head boundaries are applied along each trench to maintain groundwater levels equivalent to the top of bedrock (trench bottoms). It is assumed that the trenches are filled with coarse sand/small gravel with a uniform K of 0.1 cm/s. Scenario 2 includes higher resolution gridding in the horizontal along trench positions. A calibrated recharge rate of 25.4 cm/yr simulates the infiltration gallery within the disposal area.

- *Scenario 3* entails the extraction of contaminated groundwater using a trench (french drain) located on the southern side of the disposal area and injection into a trench located on the northern side of the disposal area (Figure 8-3). As in Scenario 2, the trenches are founded on the top of bedrock beneath the disposal area, and constant head boundaries are applied along each trench to maintain groundwater levels equivalent to the top of bedrock (trench bottoms). It is assumed that the trenches are filled with coarse sand/small gravel with a uniform K of 0.1 cm/s. Scenario 3 includes higher resolution gridding in the horizontal along both trench positions as compared to Scenario 2. The soil and Saltsburg Sandstone horizons are subdivided into 4 and 3 layers, respectively. A calibrated recharge rate of 25.4 cm/yr is to simulate the infiltration gallery within the disposal area.
- *Scenario 4* includes the extraction of contaminated groundwater using 29 vertical withdrawal wells located around the perimeter of the disposal area (Figure 8-4). The wells extend to the top of bedrock beneath the disposal area, and a pumping rate of 0.076 L/min for each well (total of 2.1 L/min) is used to maintain groundwater levels near the top of bedrock. Scenario 4 includes higher resolution gridding in the horizontal along well locations. The soil and Saltsburg Sandstone horizons are subdivided into 6 and 5 layers, respectively. Both shallow vertical injection wells (Scenario 4a) and an infiltration gallery (Scenario 4b) are simulated for the aqueous delivery system. There are 27 vertical wells, each developed to a depth of less than 1 m, to simulate the first delivery scheme. Injection rates are 0.076 L/min at each well (equivalent to well extraction rate). A calibrated recharge rate of 25.4 cm/yr simulates the infiltration gallery within the disposal area.

- Scenario 5* is a simulation of the conceptual remediation plan proposed by ESC (1992b) with the exception that Saltsburg Sandstone recovery wells are not included in the system. The extraction of contaminated groundwater involves a trench (french drain) located as shown in Figure 8-4. Unlike previous scenarios, the trenches are assumed to extend one meter below bedrock, and constant head boundaries are applied along each trench to maintain groundwater levels equivalent to the trench bottoms (~1 m into the Saltsburg Sandstone). It is assumed that the trenches are filled with small gravel possessing a uniform K of 0.18 cm/s. Scenario 5 includes higher resolution gridding in the horizontal along all trench positions. The soil and Saltsburg Sandstone horizons are subdivided into 6 and 5 layers, respectively. A single string of injection wells, located as shown in Figure 8-4, are assumed to deliver aqueous treatment agents to the contaminated soils at the site. Simulation of the delivery wells was conducted using constant heads varying from about 357 to 361 m-msl (0.5 m below ground surface) along the line of injection wells.
- Scenario 6* represents the extraction of contaminated groundwater using a horizontal well system beneath the disposal area. Two configurations of horizontal wells are considered (Figure 8-5). Wells are installed in the longitudinal direction (E-W) for Scenario 6a. Wells are installed in the latitudinal direction (N-S) for Scenario 6b. For both conditions, the horizontal wells are assumed to be installed using trenching methods. The parallel spacing of horizontal wells is about 21 and 30 m for Scenarios 6a and 6b, respectively. This spacing is better than optimum based on drainage estimates using the methods of Joshi (1991). The wells are surrounded by 0.3 m of gravel-pack with an effective K of 0.1 cm/s. The well extraction rate is 2.3 L/min. Scenario 6 includes higher resolution gridding in the horizontal along all horizontal wells. The soil and Saltsburg Sandstone horizons are subdivided into 6 and 5 layers, respectively. A calibrated recharge rate of 50.8 cm/yr, double that achieved in previous scenarios, simulates the infiltration gallery within the disposal area.

## 8.5 Flow Model Results

Figure 8-6a displays the resulting equipotential surface from the calibrated flow model (Base Case - Scenario 1). Groundwater movement in the vicinity of Area 15A is westerly towards Tributary B and Elders Run. A plot of predicted heads versus observed (field measured)



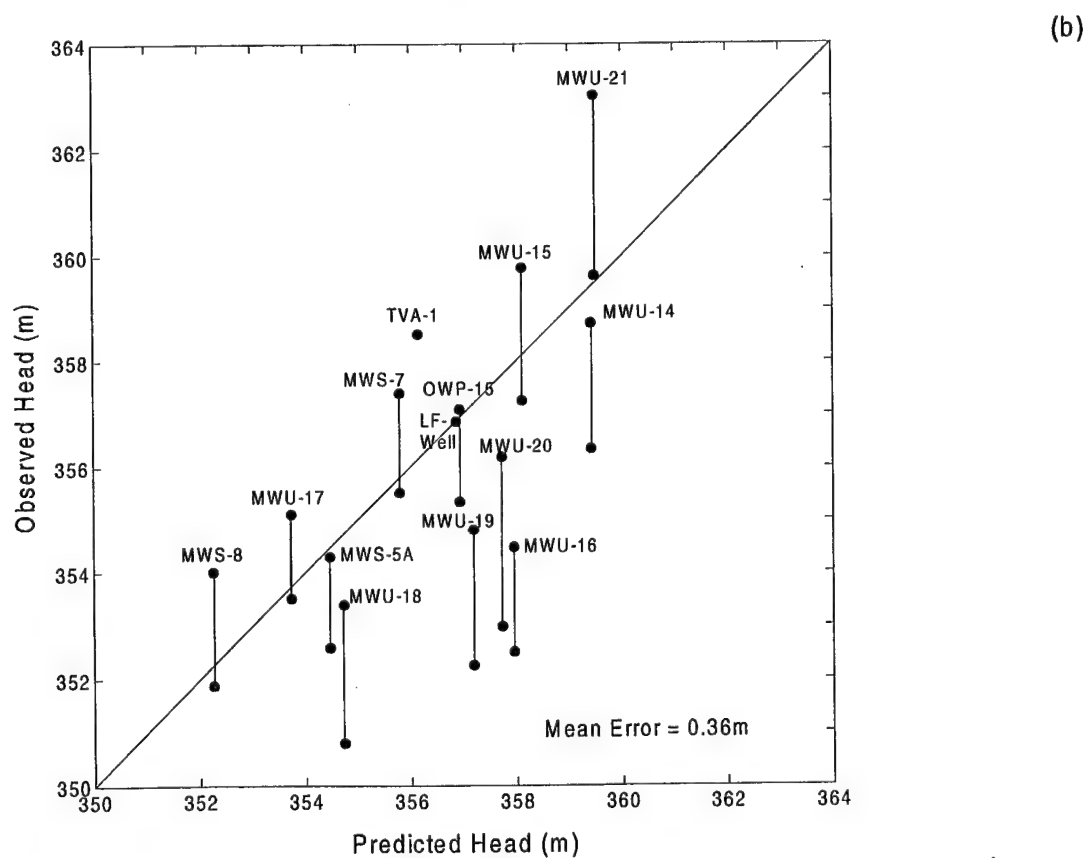
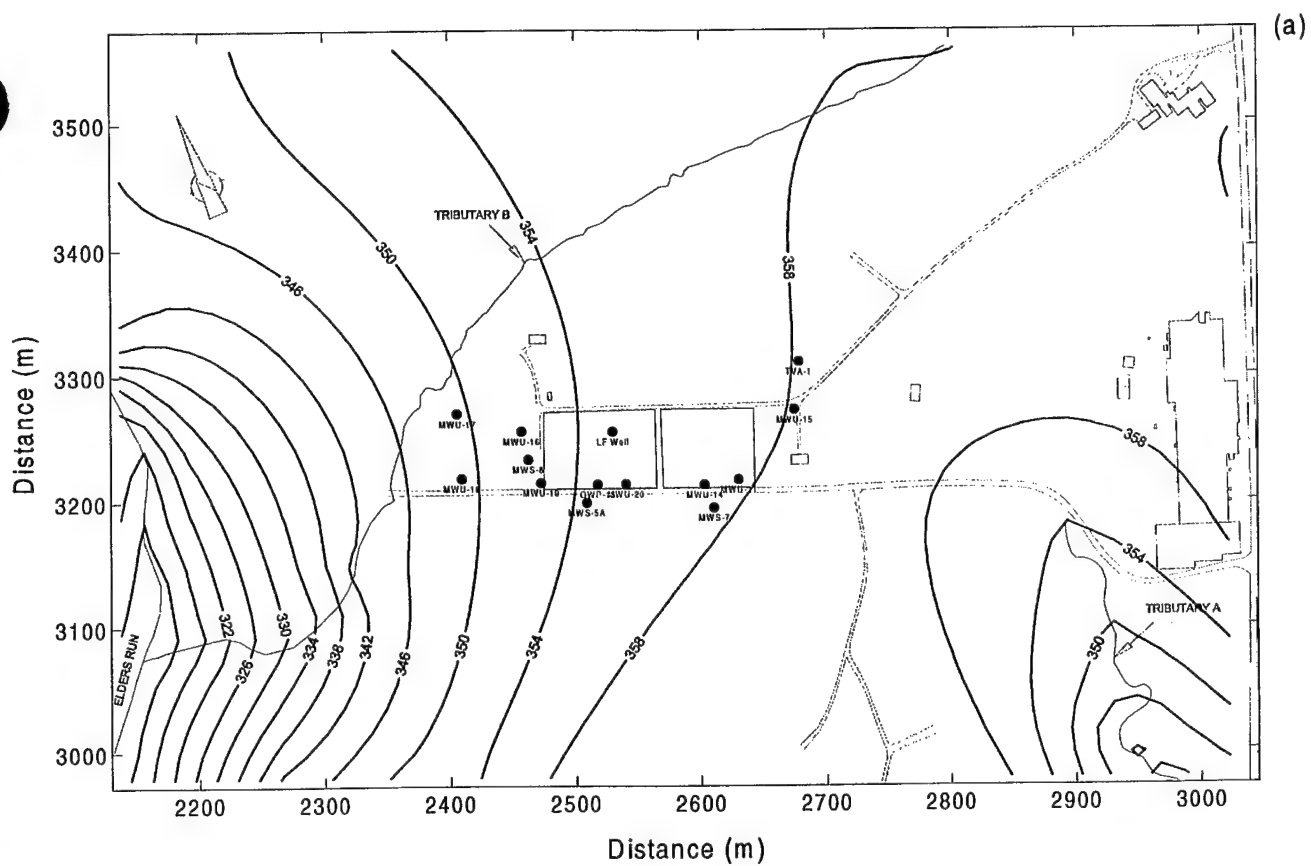


Figure 8-6 Calibrated Flow Model Results: (a) Equipotential Surface Map (Contours in m-msl) and (b) Comparison of Predicted and Observed Heads

heads from observation wells at the site is shown in Figure 8-6b. The mean error for flow calibration is the summation of differences between calculated and observed heads for each observation well divided by the total number of observation wells. The resulting mean error for the calibrated flow model is 0.36 m, which is sufficient considering the scale of the model. Volumetric budget information for the flow model shows zero percent discrepancy.

Figure 8-7 shows directional vectors for an E-W model transect along  $y = 3240$  m (centroid of disposal area) and is provided to illustrate predicted groundwater flow directions beneath the site. As shown in the figure, groundwater movement is essentially vertical from the soil zone (layer 1) and becomes near horizontal to strictly horizontal in the Saltsburg Sandstone (layers 2 and 3). Although the Saltsburg Sandstone is represented as an equivalent porous medium in these model simulations, results indicate that the relatively high  $K_h$  of this bedrock unit significantly influences shallow groundwater movement.

In general, the use of shallow injection wells for delivery of an aqueous agent to the site disposal area is limited by the assumed  $K$  of the disposal area ( $5 \times 10^{-6}$  cm/s). The infiltration gallery scheme provides better results (i.e., allows more influx and better flow distribution) due to distribution over the entire surface of the disposal area. For example, 27 equally-spaced wells were used in Scenario 4a, but the infiltration gallery of Scenario 4b allows more artificial recharge to the disposal area. Although the results of Scenario 4a can be improved by the addition of many more shallow injection wells, it is anticipated that this is cost prohibitive relative to the installation of a shallow infiltration gallery.

Figure 8-8 depicts predicted potentiometric heads in the soil horizon at a depth of 1 to 1.5 m for all remediation scenarios. Scenarios 2, 3, and 4 show similar trends in predicted heads. Additionally, capture zones for these scenarios are similar, and MODPATH predictions indicate that advective groundwater movement through the central portion of the disposal area (soil horizon) remains downward to the Saltsburg Sandstone and subsequently downgradient of the site. The predicted capture in Scenario 5 is a significant improvement over Scenarios 2, 3, and 4 due primarily to the trenches being rooted into the shallow bedrock. However, model simulations indicate that Scenario 6 (horizontal wells) provides the most effective capture of both existing contaminants within the soil horizon and aqueous treatment agents (artificial recharge) added via an infiltration gallery. Figure 8-9 illustrates Scenario 6b MODPATH predictions for an E-W model transect along  $y = 3240$  m, the approximate center of the disposal area. The

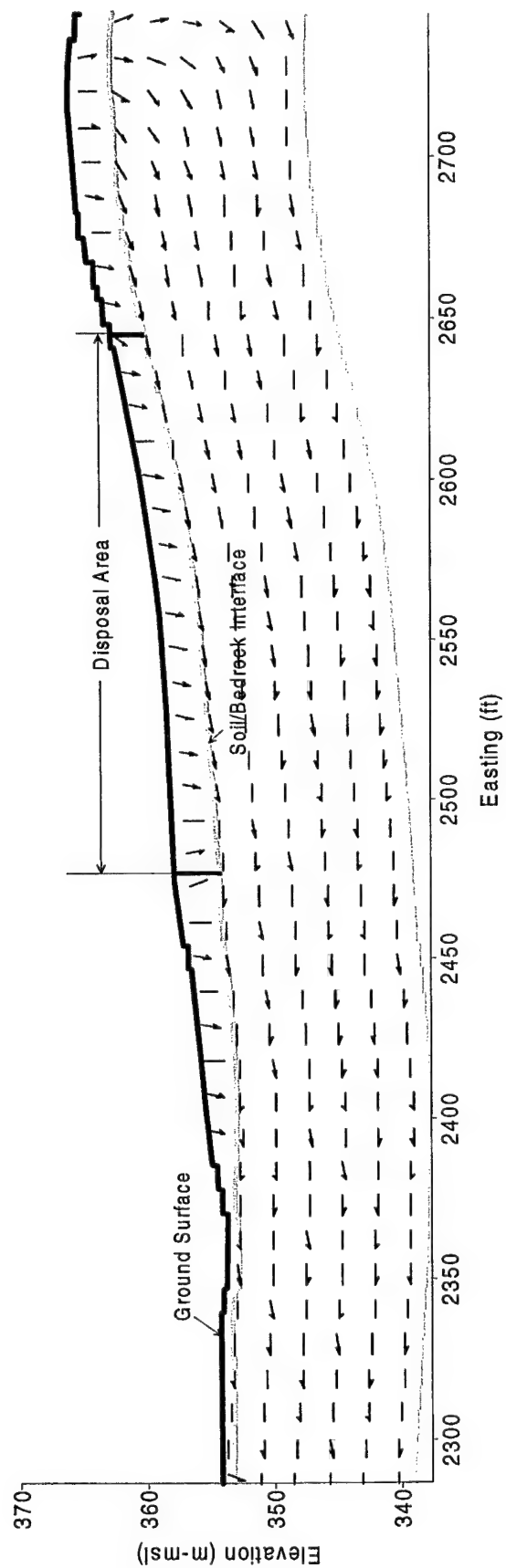


Figure 8-7 Directional Vectors From Flow Model Simulation of Scenario (Base Case)

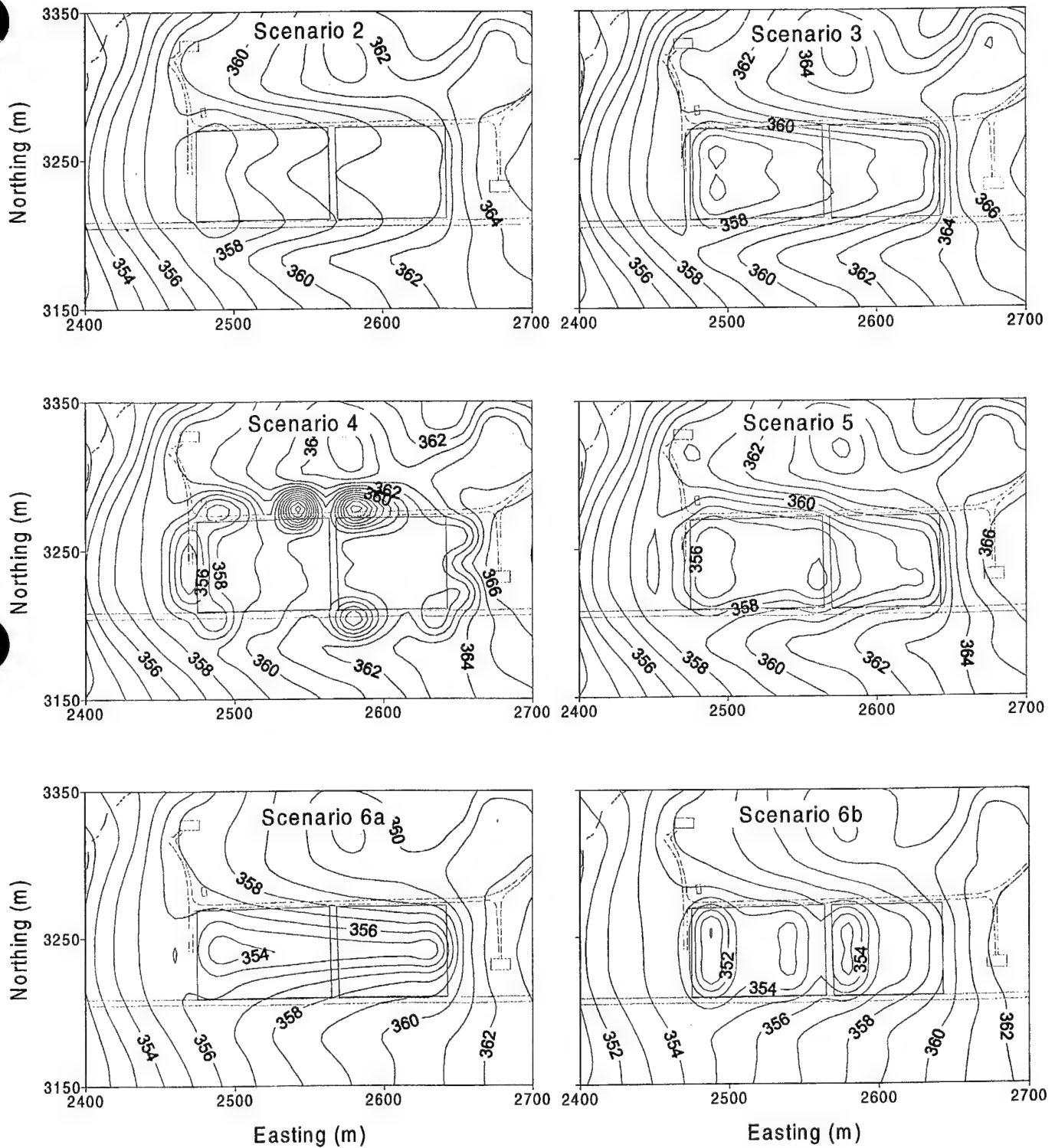


Figure 8-8 Potentiometric Heads at Depth of 1 to 1.5 m from Flow Model Simulations of Scenarios 2 - 6

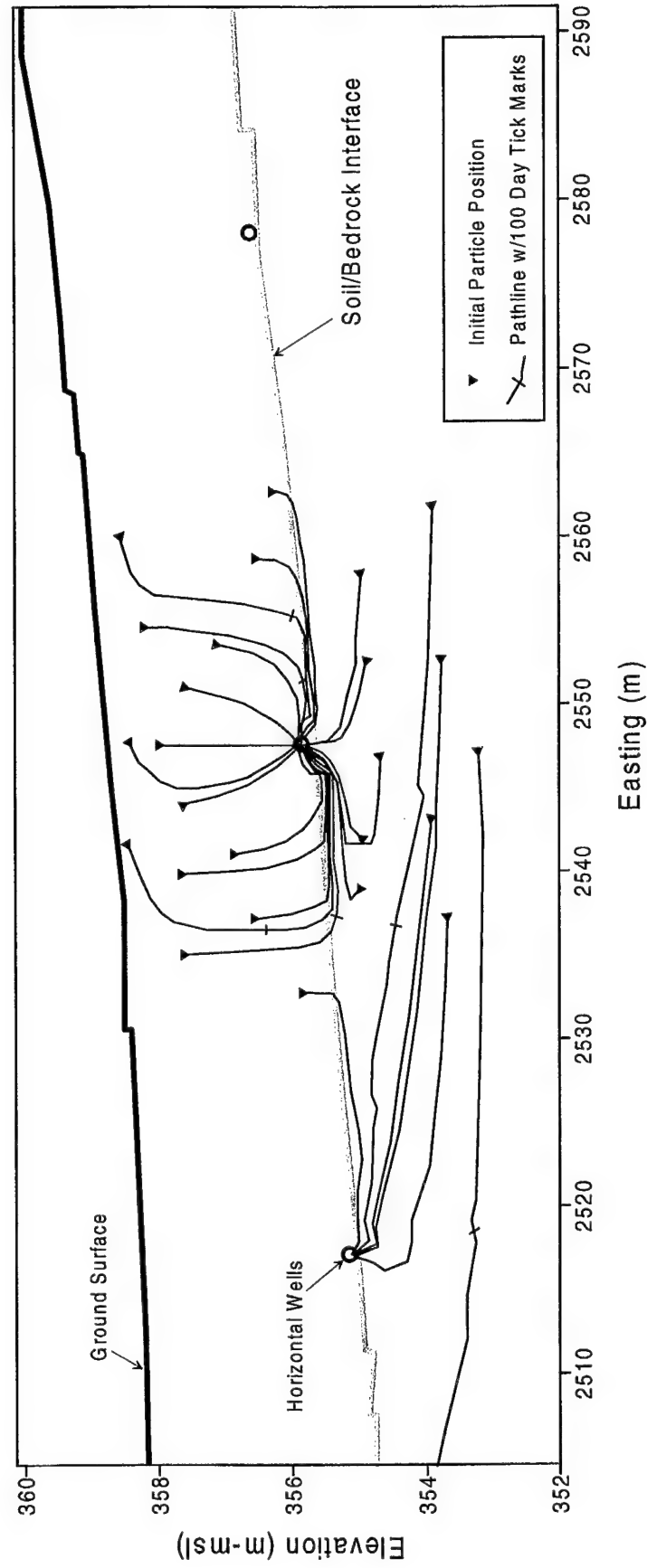


Figure 8-9 East-West Cross Section of Model at  $y = 3240$  m Illustrating Pathline Predictions (Particle Tracking) for Scenario 6b

horizontal well arrangement is successful in capturing theoretical particles located within the soil horizon. Figure 8-9 also suggests that the horizontal well system may provide some benefit in remediation of the shallow Saltsburg Sandstone; however, this is primarily an artifact of the model configuration. In reality, this is completely dependent on the interconnection of fractures with basal soils of the disposal area.

Both horizontal well configurations (Scenarios 6a and b) provide similar predictions with regard to groundwater extraction and capture zone. However, Scenario 6b is considered the optimal solution because of its orientation. Figure 8-10 shows predicted steady-state heads for Scenario 6b along the E-W model transect ( $y = 3240$  m). In general, a horizontal well drains the largest volume if placed normal to plane of maximum permeability (USEPA, 1994). At Area 15A, site constraints and natural hydraulic gradients (westerly) suggest alignment of horizontal wells perpendicular to groundwater flow (N-S). In addition to added redundancy in the extraction system, this alignment allows adjustment to individual well extraction rates for increased control in the engineered hydrodynamics of the remediation system.

Using zone budget predictions from MODFLOW, the influx delivered through injection wells or an infiltration gallery can be expressed as a percentage of groundwater withdrawal (extraction) for any given scenario. Table 8-3 and Figure 8-11 depict these predictions for Scenarios 2 through 6. Overall, less than five percent of influx is removed by the extraction systems identified by Scenarios 3 and 4. Scenarios 2 and 5 show some comparative increase in influx extraction, but Scenarios 6a and b, in particular Scenario 6b, is by far the most efficient system for fluid recovery. Both Scenario 6a and 6b indicate  $> 80\%$  efficiency rates in recovery of artificial recharge.

To assist in future treatability studies, Table 8-3 and Figure 8-11 also illustrate predicted annual pore water displacement through the soil zone of the disposal area. One pore volume is equivalent to approximately  $10,700 \text{ m}^3$ , and ten years is arbitrarily selected as the event horizon. As indicated in Table 8-3 and Figure 8-11, Scenarios 3 and 5 are estimated to require eight years for displacement of a single pore volume of an aqueous treatment agent. This is little improvement over natural conditions (Scenario 1 - Base Case). Comparable simulations for Scenarios 2 and 4 indicate some improvement in the time for one pore volume to flush through the disposal area. Scenario 6b stands out as the most efficient system for moving fluid through

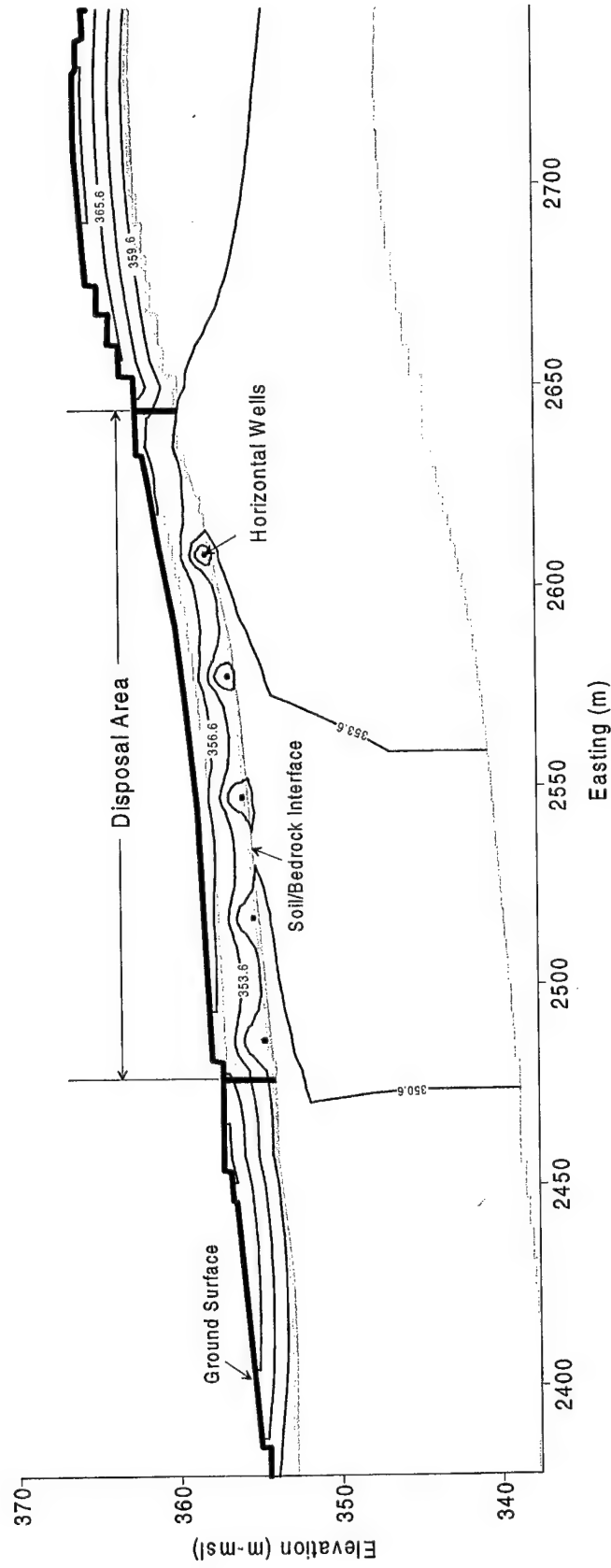


Figure 8-10 Potentiometric Heads for Scenario 6b Along East-West Cross Section of Model at  $y = 3240$  m

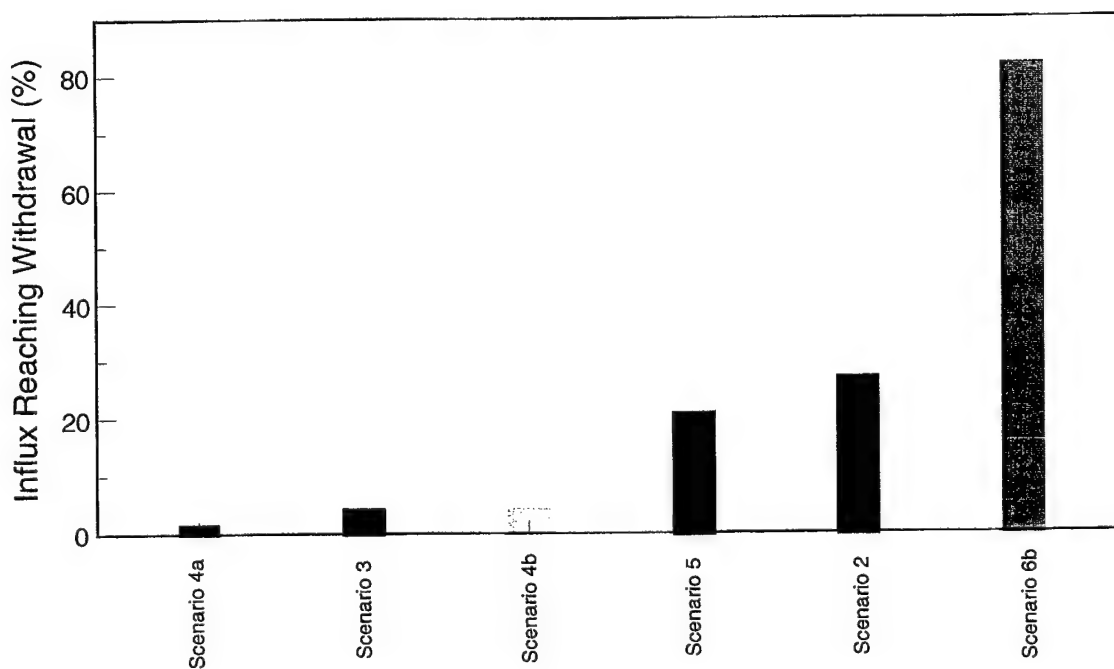
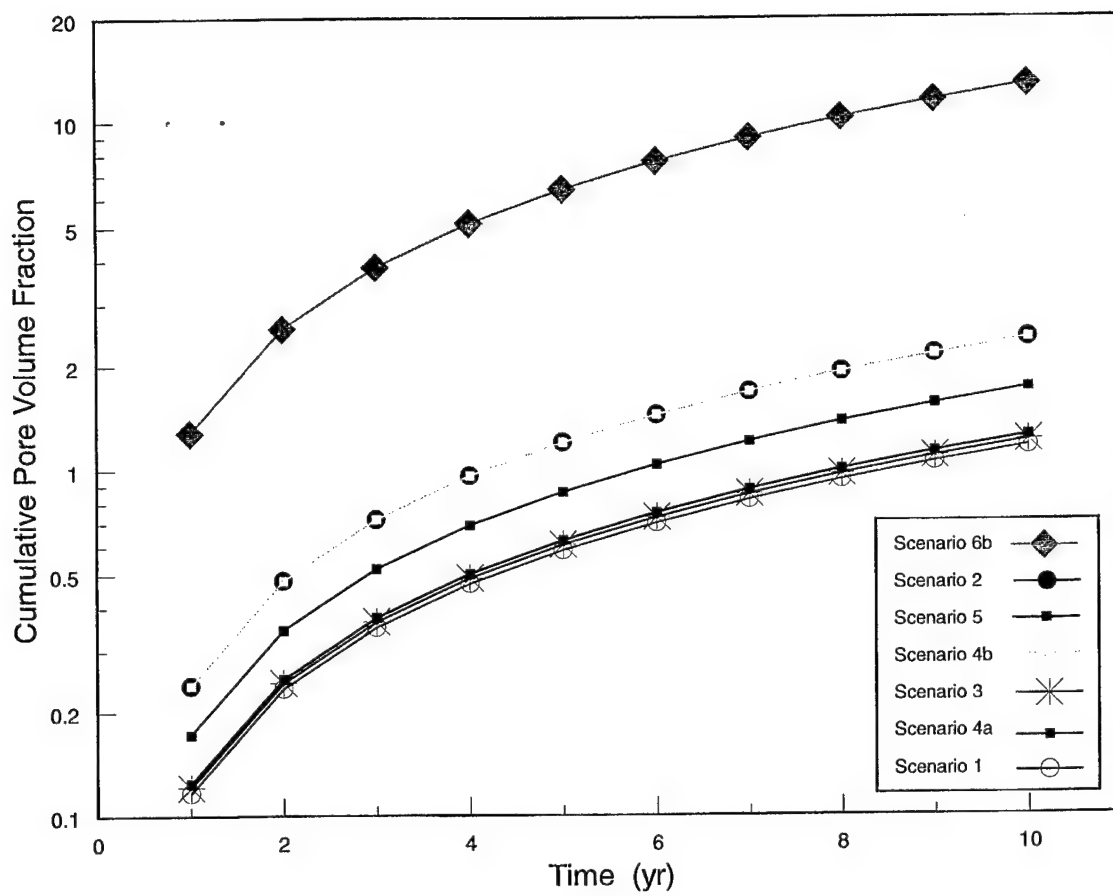


Figure 8-11 Comparison of Flow Model Simulations: (Top) Cumulative Pore Volume Fraction Versus Time, and (Bottom) Influx Reaching Withdrawal



Table 8-3

**Predicted Steady-State Influx Reaching Withdrawal System and Cumulative Yearly Pore Volume Fraction from Flow Model Simulations**

	Description	Influx Reaching Withdrawal (%)	Cumulative Yearly Pore Volume Fraction									
			1	2	3	4	5	6	7	8	9	10
<i>Scenario 2</i>	Perimeter Extraction	27.4	0.2	0.5	0.7	1.0	1.2	1.4	1.7	1.9	2.2	2.4
	Trench/Infiltration Gallery											
<i>Scenario 3</i>	Extraction Trench/Injection	4.6	0.1	0.2	0.4	0.5	0.6	0.7	0.9	1.0	1.1	1.2
	Trench											
<i>Scenario 4a</i>	Vertical Extraction	2.1	0.2	0.3	0.5	0.7	0.9	1.0	1.2	1.4	1.6	1.7
	Wells/Injection Wells											
<i>Scenario 4b</i>	Vertical Extraction	4.6	0.2	0.5	0.7	1.0	1.2	1.4	1.7	1.9	2.2	2.4
	Wells/Infiltration Gallery											
<i>Scenario 5</i>	Extraction Trench/Injection	21.2	0.1	0.3	0.4	0.5	0.6	0.8	0.9	1.0	1.1	1.3
	Wells											
<i>Scenario 6b</i>	Latitudinal Horizontal	83.0	1.3	2.6	3.8	5.1	6.4	7.7	9.0	10.2	11.5	12.8
	Extraction Wells/Infiltration Gallery											

the disposal area. For this case, it is estimated that 1.3 pore volumes per year may be cycled through the contaminated soil zone of Area 15A.

Additional flow model simulations of Scenario 6b were conducted to examine the sensitivity of soil K within the disposal area to annual pore volume displacement. As expected, results indicate that increases in soil K lead to advective increases in vertical groundwater movement. This can also allow increases in artificial recharge rates, whether by injection wells or an infiltration gallery. Significant differences are not observed in model results unless K augmentation is applied to soil depths in excess of one meter. Increasing the hydraulic conductivity of disposal area soils can be accomplished using methods such as induced fracturing or mechanical tilling. However, a full examination of the potential for atmospheric releases of CNS vapors and enhanced vertical contaminant migration should be fully examined before implementation of such activities.

## 8.6 Transport Model Results

Transport simulation results for Scenario 2 indicate poor removal of existing contaminants and aqueous agents exiting the bottom of the disposal area at about 30 percent of initial concentrations after five years. Scenario 3 transport results show extremely poor lateral spreading of aqueous treatment agents, with the majority of fluid escaping the bottom of the injection trench. Although the lateral dispersion of aqueous agents is good for Scenario 4, especially the injection well formulation of Scenario 4b, vertical migration is not arrested by the extraction wells. Hence, the vast majority of existing contaminants and aqueous treatment agents egress to the Saltsburg Sandstone. Transport results for Scenario 5 indicate poor transverse dispersion of aqueous treatment agents from the line of injection wells after a five-year simulation period. However, the extraction trenches are effective in capturing the majority of influx to the disposal area. After five years, predicted concentrations of aqueous agents leaving the site are approximately ten percent of initial values.

It is not surprising that transport simulation results for Scenario 6b are optimal with regard to rapid vertical migration of an infiltrating solution and subsequent behavior of the resulting plume. The horizontal wells at the base of the disposal area are effective in preventing vertical movement of aqueous agents and soil zone contaminants into the Saltsburg Sandstone. Figure 8-12 shows the transport results of Scenario 6b for simulation times of 1, 3, and 5 years along the E-W model transect ( $y = 3240$  m). As shown in the figure, concentrations of conservative aqueous agents are well distributed after a simulation period of one year. Additionally, the majority of aqueous agent added at ground surface (infiltration due to artificial recharge of 50.8 cm/yr) remains within the confines of the disposal area. Due to hydrodynamic dispersion, predicted concentrations of the aqueous agent entering the underlying Saltsburg Sandstone approach only five percent of initial concentrations after five years.

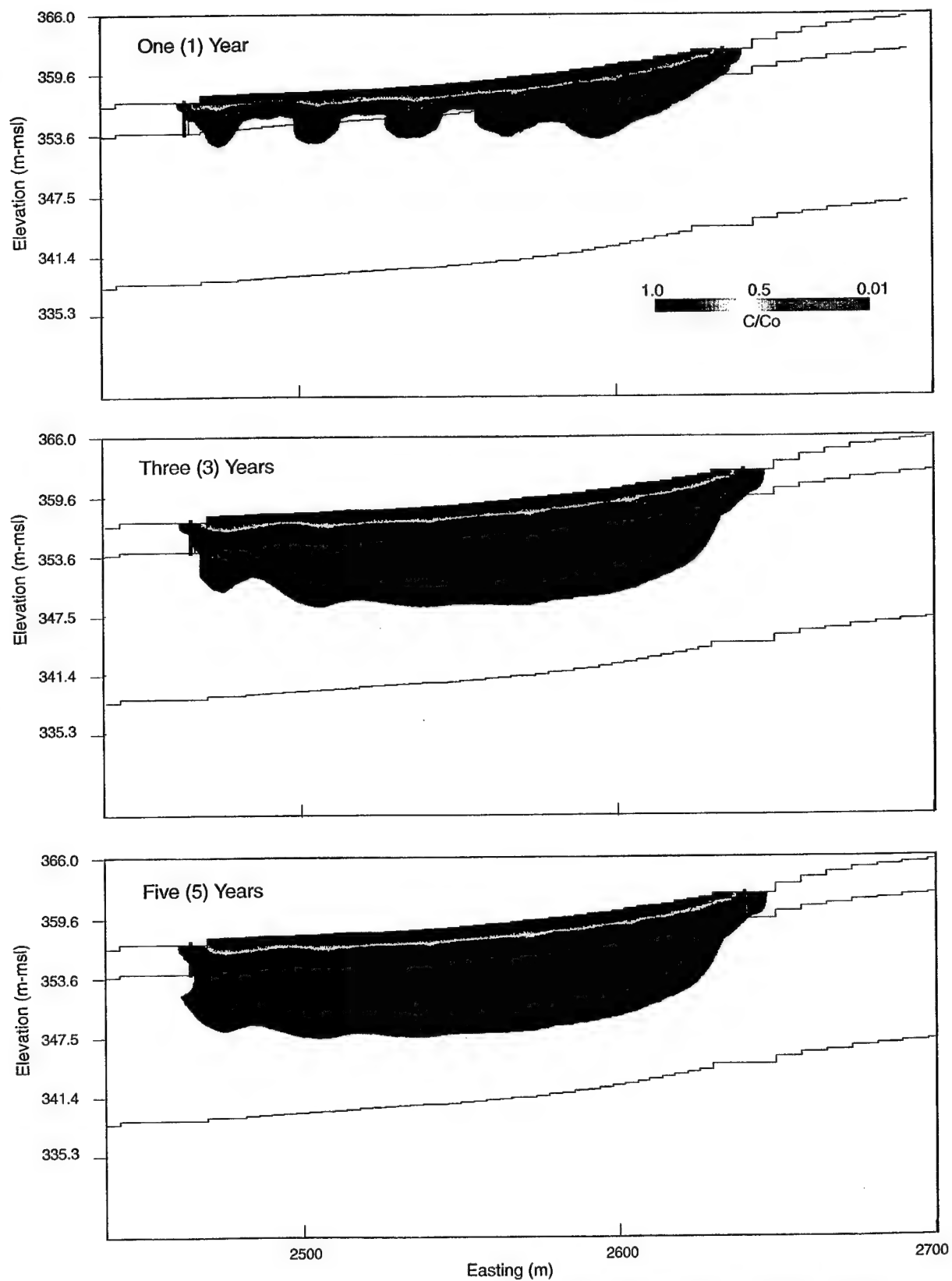


Figure 8-12 Transport Predictions for Scenario 6b After One, Three, and Five Years.  
Plot is Oriented Along East-West Cross Section of Model at  $y = 3240$  m

## 9. Conclusions and Recommendations

### 9.1 Conclusions

The three-dimensional model developed for the systematic analysis of aqueous treatment agent injection and recovery scenarios provides reasonable representations of the hydrogeologic system present at Area 15A. The predicted hydraulic head field of the calibrated flow model is in agreement with observed heads of site monitoring wells in the shallow groundwater system.

In general, the effectiveness of shallow injection wells for delivery of an aqueous agent to the site disposal area is limited by the assumed  $K$  of the disposal area ( $5 \times 10^{-6}$  cm/s). Although simulation results for injection well scenarios show improvements with the addition of many more shallow injection wells, it is anticipated that this is cost prohibitive relative to the installation of a shallow infiltration gallery. An infiltration gallery scheme is preferred since it allows higher influx rates and provides more uniform distribution through the soil zone of the disposal area. Model simulations also suggest that increases in artificial recharge rates can be obtained by increasing the hydraulic conductivity of disposal area soils using methods such as induced fracturing or mechanical tilling. However, due to the potential for atmospheric releases of CNS vapors and enhanced vertical contaminant migration, careful examination of all site factors and remedial components is warranted.

Of all scenarios evaluated, horizontal extraction wells installed at the base of the disposal area provide the most effective capture of both existing contaminants within the soil horizon and aqueous treatment agents added via an infiltration gallery. Scenario 6b is considered the optimal scenario because horizontal wells are orientated perpendicular to the natural hydraulic gradient. In addition to added redundancy in the extraction system, this alignment allows adjustment to individual well extraction rates for increased control in the engineered hydrodynamics of the remediation system. Flow model predictions indicate that over 80 percent of influx through a simulated infiltration gallery is extracted by horizontal wells in Scenario 6. This is at least twice as effective as other alternatives considered in model simulations. Additionally, 1.3 pore volumes of groundwater per year are displaced through soil within confines of the disposal area under Scenario 6. This is an order of magnitude greater than alternatives relying on vertical wells or trench systems for groundwater extraction.

Transport simulation results for scenarios adopting vertical extraction wells and trenches indicate poor removal of existing contaminants and a strong potential for aqueous agents to escape through the bottom of the disposal area. Additionally, insufficient lateral dispersion of aqueous agents is obtained using trench systems or linear injection methods. Transport simulation results for the Scenario 6b are optimal with regard to relatively rapid vertical migration of an infiltrating solution and subsequent behavior of the resulting plume. The horizontal wells located along the base of the disposal area are effective in preventing vertical movement of aqueous agents and soil zone contaminants into the underlying Saltsburg Sandstone. Concentrations of conservative aqueous agents are well distributed throughout the soil zone, but remain within the confines of the disposal area. Predicted concentrations of an aqueous agent entering the underlying Saltsburg Sandstone approach only five percent of initial concentrations after five years.

## 9.2 Recommendations

Shallow groundwater flow and transport simulations for Area 15A strongly indicate that a scenario based on horizontal extraction wells oriented north-south (coupled with an infiltration gallery) is optimal with regard to hydrodynamic isolation of the site disposal area and delivery of treatment agents. Cost is a critical factor when considering the application of horizontal wells and can range widely depending on the installation method, site geology, well materials, vertical depth, and well length. A primary benefit of horizontal well applications versus conventional vertical wells is a shorter project lifetime. The time constituent of a project can translate to significant cost in terms of facility operation and maintenance.

Fortunately, the soil zone of the disposal area is relatively thin, less than 3 m. Hence, the site is a prime candidate for installation of horizontal wells using a "one-pass" trenching method. Although, this is not the only method available for horizontal well installation, it should be considered for the Area 15A site. The technique relies on specialized trenching equipment that excavates a trench, supports the side-walls, inserts well pipe in the trench, and then backfills the trench with selected media, all in one step. Cost estimates were solicited from contractors experienced in these applications for installation of 15.2-cm diameter wells as in Scenario 6b. Prices for horizontal well installation at Area 15A using this method are expected to range from

\$100,000 to \$200,000 including all materials, mobilization/demobilization, and decontamination. Directional drilling of horizontal wells is anticipated to be significantly more expensive.

Additional site characterization is recommended to verify some of the more conjectural premises of this study. The lack of data within the confines of the disposal area is currently the most serious limitation to model accuracy. Sampling and analysis of soils from within the disposal area is highly recommended to gauge their hydraulic and physical properties. These data are necessary prior to final design of any remedial system for Area 15A. Although not essential for developing an injection/recovery system for Area 15A, additional field characterization studies that would be helpful for improving our understanding of the groundwater flow system at Area 15A include:

- *Installation of shallow wells/piezometers within the drum disposal area and monitoring of hydraulic heads.* Other than well OWP-15, no permanent monitoring wells have been established within the drum disposal area. Previous studies (ESC, 1985) have suggested that perched groundwater conditions may exist within the disposal area. Additional groundwater level data from the interior of the disposal area will resolve this issue. Examination of groundwater levels within the disposal area relative to shallow wells developed in the Saltsburg Sandstone will also provide some impression of transient wetting front movement from precipitation events.
- *A geophysical survey of the drum disposal area.* Assuming that the majority of drums buried at the site have corroded, voids should be present within this soil horizon. Depending on the dimensions and interconnectivity of relic openings, a relatively transmissive zone may reside within basal soils of the drum disposal area. This has important implications with regard to design and effectiveness of an injection/recovery system targeted at the drum disposal area.
- *Soil sampling within the disposal area to quantify contaminant concentrations and residual DNAPL.* The prevailing assertion is that approximately ninety percent of DNAPL product has leaked from buried drums. This is predicated on test pits that were not advanced below the buried drums. Additional soil sampling to gauge residual DNAPL product and CNS concentrations will provide verification of current presumptions regarding the contaminant source.
- *Identification and continuous water quality monitoring of seeps before, during, and after precipitation events.* Currently, the results of water quality monitoring of discharge seeps is

based on limited sampling events. However, it is probable that contaminant concentrations are highly variable due to episodic releases. Precipitation events and groundwater stage are probably two of the most important factors related to seep discharge. Therefore, continuous monitoring across rainfall events will provide temporal characterization of contaminant concentrations. Such data will support a natural attenuation strategy and risk assessment for Area 15A.

- *Continuous flow and water quality monitoring of Tributary B before, during, and after precipitation events.* Currently, the results of water quality monitoring of Tributary B is based on limited sampling events. As with seep discharge, it is probable that contaminant concentrations are highly variable due to episodic releases that are governed by precipitation events and ambient groundwater levels. Continuous streamflow monitoring across rainfall events provides temporal characterization of contaminant concentrations. Such data will support a natural attenuation strategy and risk assessment for Area 15A. Additionally, continuous flow monitoring, accompanied by precipitation and groundwater level measurements, will allow accurate water balance estimates. In conjunction with water quality monitoring, such data allow quantitative mass flux predictions to downstream receptors.

## 10. References

- Adams, J., "The WHS Solver: A new Bi-CGSTAB Solver for MODFLOW," Waterloo Hydrogeologic, Inc., Waterloo, Ontario, May 1998.
- Anderson, Eric A., "National Weather Service River Forecast System -- Snow Accumulation and Ablation Model," NOAA Technical Memorandum NWS HYDRO-17, U.S. Dept. of Commerce, Silver Spring, Maryland, 217p., 1973.
- Arnold, J. G., J. R. Williams, A. D. Adams, and N. B. Sammons, "SWRRB, A Simulator for Water Resources in Rural Basins," Agricultural Research Services, USDA, Texas A&M Press, College Station, Texas, 1989.
- Bloyd, R. M. Jr., "Summary Appraisals of the Nation's Ground-water Resources - Ohio Region," United States Geological Survey, Professional Paper 813-A, U.S. Government Printing Office, 1974.
- Brooks, R. H., and A. T. Corey, "Hydraulic Properties of Porous Media," Hydrology Paper 3, Colorado State University, Fort Collins, Colorado, 1964.
- Campbell, S. G., "A Simple Method for Determining Unsaturated Hydraulic Conductivity from Moisture Retention Data," *Soil Science*, 117(6):311-314, 1974.
- Colton, G. W., "The Appalachian Basin - Its Depositional Sequences and Their Geologic Relationships," in *Studies of Appalachian Geology: Central and Southern*, ed. G. W. Fisher, F. J. Pettijohn, J. C. Reed, Jr., and K. N. Weaver, Interscience Publishers, pp 5-47, 1970.
- Cooper, H. H. Jr., and C. E. Jacob, "A Generalized Graphical Method for Evaluations of Formation Constants and Summarizing Well Field History," Transactions of the American Geophysical Union, 27:526-534, 1946.
- CRA, "Area 15A Groundwater Pumping Evaluation, Federal Laboratories, Saltsburg, Pennsylvania," Ref. No. 6099 (13), Conestoga-Rovers & Associates, Niagara Falls, New York, November 1995.
- D. B. Stephens & Associates, Inc., "Laboratory Analysis of Soil Hydraulic Properties of Tennessee Valley Authority Soil Samples," Letter Report, December 30, 1997.
- ESC, "Progress Report, Environmental Site Assessment, Federal Laboratories, Inc., Saltsburg, Pennsylvania," Project No. 85-103A, 2 volumes, Earth Sciences Consultants, Inc., Pittsburgh, Pennsylvania, July 1985.



- ESC, "Summary of Site Characterization Studies, Federal Laboratories, Saltsburg, Pennsylvania," Technical Report, Earth Sciences Consultants, Inc., Pittsburgh, Pennsylvania, 1992a.
- ESC, "Removal Site Evaluation/Feasibility Study," Technical Report, Earth Sciences Consultants, Inc., Pittsburgh, Pennsylvania, 1992b.
- Fenneman, N. M., "Physiography of the Eastern United States," McGraw-Hill Book Company, Inc., New York and London, 1938.
- Ferm, J. C., "Allegheny Deltaic Deposits," Society of Economic Paleontologists and Mineralogists, Special paper 15, 250 p., 1970.
- Flint, N. K., "Geology and Mineral Resources of Southern Somerset County, Pennsylvania," Pennsylvania Geological Survey (4<sup>th</sup> ser.) County Report C56A, 1965.
- Freeze, R. A., and J. A. Cherry, Groundwater, Prentice-Hall, Inc., New Jersey, 600 pp, 1979.
- Gelhar, L. W., C. Welty, and K. R. Rehfeldt, "A Critical Review of Data on Field-Scale Dispersion in Aquifers," Water Resources Research, Vol. 28, No. 7, pp 1955-74, 1992.
- Hill, M. C., "Preconditioned Conjugate-Gradient 2 (PCG2), A Computer Program for Solving Ground-Water Flow Equations," Water-Resources Investigations Report 90-4048, U.S. Geological Survey, 1990.
- Joshi, S. D., "Horizontal Well Technology," PennWell Books, PennWell Publishing Company, Tulsa, Oklahoma, 1991.
- Keroher, G. C. and 14 others, "Lexicon of Geologic Names of the United States for 1936-1960," Bulletin 1200, U.S. Geological Survey, 1966.
- Knisel, W. G., Editor, CREAMS. A Field Scale Model for Chemical Runoff and Erosion from Agricultural Management Systems, Vols. I, II, and III, Draft Copy, USDA-SEA, AR, Cons. Res. Report 24, 643 pp, 1980.
- McDonald, M. G., and A. W. Harbaugh, "A Modular Three-Dimensional Finite-Difference Ground-Water Flow Model," U.S. Geological Survey, 1984.
- Meckel, L. D., "Paleozoic Alluvial Deposition in the Central Appalachians: A Summary," in *Studies of Appalachian Geology: Central and Southern*, ed. G. W. Fisher, F. J. Pettijohn, J. C. Reed, Jr., and K. N. Weaver, Interscience Publishers, pp 49-67, 1970.
- Pollock, D. W., "Documentation of Computer Programs to Compute and Display Pathlines Using Results from the U.S. Geological Survey Modular Three-Dimensional Finite-Difference Ground-Water Flow Model," Open File Report 89-381, U.S. Geological Survey, 1989.

- Perrier, E. R., and A. C. Gibson, "Hydrologic Simulation on Solid Waste Disposal Sites," Technical Resource Document, EPA-SW-868, U.S. Environmental Protection Agency, Cincinnati, Ohio, 1980.
- PTGS, "Pittsburgh Low Plateau Section - Appalachian Plateaus Province," Pennsylvania Topographic & Geologic Survey, 1998.  
<http://www.dcnr.state.pa.us/topogeo/map13/13plps.htm>
- Rice, C. L., J. K. Hiatt, and E. D. Koozmin, "Glossary of Pennsylvanian Stratigraphic Names, Central Appalachian Basin," Geological Society of America Special Paper 294, 1994.
- Richardson, C. W., and D. A. Wright, "WGEN: A Model for Generating Daily Weather Variables," ARS-8, Agricultural Research Service, USDA, 1984.
- Schroeder, P. R., T. S. Dozier, P. A. Zappi, B. M. McEnroe, J. W. Sjostrom, and R. L. Peyton, "The Hydrologic Evaluation of Landfill Performance (HELP) Model: Engineering Documentation for Version 3," EPA/600/R-94/168b, Office of Research and Development, Washington, DC, September 1994.
- Theis, C. V., "The Relationship Between the Lowering of the Piezometer Surface and the Rate and Duration of Discharge of a Well Using Groundwater Storage," Transactions of the American Geophysical Union, 16:519-524, 1935.
- USEPA, "Manual - Alternative Methods for Fluid Delivery and Recovery," EPA/625/R-94/003, U.S. Environmental Protection Agency, Office of Research and Development, Washington, DC, September 1994.
- Wanless, H. R., "Pennsylvanian Correlations in the Eastern Interior and Appalachian Coal Fields," Geological Society of America Special Paper 17, 1939.
- Williams, D. R., and T. A. McElroy, "Water-Resources Data for Indiana County, Pennsylvania," Open-File Report 90-384, U. S. Geological Survey, 1997.
- Zheng, C., "MT3D - A Modular Three-Dimensional Transport Model for Simulation of Advection, Dispersion, and Chemical Reactions of Contaminants in Groundwater Systems," S. S. Papadopoulos & Associates, Inc., 1990.
- Zheng and Wang, C., "MT3DMS - A Modular Three-Dimensional Multispecies Transport Model for Simulation of Advection, Dispersion, and Chemical Reactions of Contaminants in Groundwater Systems," Documentation and Users Guide, Departments of Geology and Mathematics, University of Alabama, Tuscaloosa, Alabama, 1998.